

Identification of Peroxisome Proliferator-Activated Receptor Alpha (PPAR α)-Dependent Genes Involved in Peroxisome Proliferator-Induced Hepatocarcinogenesis

LEUNG Wan-chi

**A Thesis Submitted in Partial Fulfillment
of the Requirements for the Degree of
Master of Philosophy
in
Environmental Science Programme**

© The Chinese University of Hong Kong

Nov 2005



Thesis Committee

Professor C.C.Wan (Chair)

Professor S.S.T. Lee (Thesis Supervisor)

Professor C.C. Wan (Committee Member)

Professor Y.Y. Ho (Committee Member)

Professor T. Pineau (External Examier)

Abstract

Peroxisome proliferator-activated receptors (PPARs) are the members of the steroid/retinoid nuclear receptor family. PPARs include three isoforms: α , δ/β , and γ . PPAR α is the isoform responsible for lipid metabolism and peroxisome proliferator (PP)-induced pleiotropic responses and hepatocarcinogenesis. Short-term (2 weeks) administration of PP causes peroxisome proliferation, hepatomegaly and induction of gene expressions that involved in fatty acid β -oxidation. Long-term (11 months) administration of PP causes hepatocarcinogenesis. PP is a group of chemicals include some plasticizers such as DEHP di(2-ethylhexyl)phthalate) and hyperlipidemic drugs such as clofibrate and Wy-14,643. As humans are exposed to peroxisome proliferators chronically, the long-term effect of peroxisome proliferators on human should be identified.

In my study, Wy-14,643 compound was selected as 100% hepatocarcinogenic effect was observed after long-term treatment. PPAR α wild-type and PPAR α (-/-) mice were fed with a control or a 0.1% Wy-14,643 diet for 11 months in order to find out the genes that are PPAR α dependent and Wy-14,643 responsive. In order to study the time-dependent liver damage and genes expression that are induced by Wy-14,643, 24 hours gavage feeding, 1 week, 2 weeks and 6 months feeding experiments were also performed.

Hepatomegaly was observed in the PPAR α (+/+) fed with 0.1% Wy-14,643 after 1 week treatment and the level of liver enlargement was increased with prolonged period of treatment. The relative organ weights of white fat, brown fat and spleen in the 0.1% Wy-14,643 fed PPAR α mice were lower compared to their controls. Serum cholesterol and triglyceride levels were also measured for different time points. Serum cholesterol level was significantly higher in 0.1% Wy-14,643 fed PPAR α (+/+) mice at 11 months treatment. Time-dependent decrease in serum triglyceride level was observed in PPAR α (+/+) mice fed with 0.1% Wy-14,643. The time-dependent decrease was started at 24 hours gavage feeding and continued to 11 months treatment.

Histology was performed to study the liver damage that induced by Wy-14,643 after chronic exposure. Irregular hepatocytes arrangement, enlarged sinusoidal spaces and trabecular cell clusters were observed in PPAR α (+/+) mice fed with 0.1% Wy-14,643. In PPAR α (-/-) mice, with the disruption of PPAR α gene, lipid accumulation was found in both control and 0.1% Wy-14,643 treatment group started at 24 hours gavage feeding.

After 11 months feeding experiment, fluorescent differential display was employed to screen out the genes in liver that are PPAR α -dependent and Wy-14,643 responsive as fluorescent differential display is able to compare several treatment groups at the same time. A total of eleven fluoroDD gels were performed and

seventeen PPAR α -dependent and Wy-14,643 responsive genes were confirmed in this project. They include peroxisomal delta 3, delta 2-enoyl-Coenzyme A isomerase, mouse cysteine sulfinic acid decarboxylase, mouse acetyl-Coenzyme A dehydrogenase, medium chain, peroxisome biogenesis factor 16, mouse Cyp4a14, mouse peroxisomal bifunctional enzyme, mouse Cyp4a10, very-long-chain acyl-CoA synthetase, mouse peroxisomal acyl-CoA oxidase, mouse hydroxysteroid (17-beta) dehydrogenase 11, mouse adipose differentiation related protein and mouse carnitine O-octanoyltransferase were confirmed to be up-regulated by 0.1% Wy-14,643 and PPAR α -dependent. Mouse apolipoprotein A-V, mouse UDP-glucuronosyltransferase 2 family member 5, mouse serine protease inhibitor 1-1, mouse major urinary protein II and mouse carboxyesterase were confirmed to be down-regulated by 0.1% Wy-14,643 and PPAR α dependent.

Temporal expression of all the seventeen genes (except mouse apolipoprotein A-V) was also performed to observe the time-dependent changes of these genes expression. Up-regulation of mouse peroxisomal delta 3, delta 2-enoyl-Coenzyme A isomerase, mouse acetyl-Coenzyme A dehydrogenase, medium chain, peroxisome biogenesis factor 16, mouse Cyp4a14, mouse peroxisomal bifunctional enzyme, mouse Cyp4a10, very-long-chain acyl-CoA synthetase, mouse peroxisomal acyl-CoA oxidase, mouse hydroxysteroid (17-beta) dehydrogenase 11, mouse adipose differentiation

related protein and mouse carnitine O-octanoyltransferase were started at 24 hours and persisted to 11 months treatment while up-regulation of mouse cysteine sulfinic acid decarboxylase was started at 1 week and persisted to 11 months. Down-regulation of mouse serine protease inhibitor 1-1, mouse major urinary protein II and mouse carboxyesterase was started at 1 week and continued to 11 months. Mouse UDP-glucuronosyltransferase 2 family member 5 was down-regulated at 2 weeks and persisted to 11 months.

Based on the genes identified, oxidative stress is suggested to be the mechanism of PP-induced hepatocarcinogenesis. However, we still not know whether other mechanisms are involved in the PP-induced hepatocarcinogenesis. It is suggested that PP-induced hepatocarcinogenesis is due to the combined effect of oxidative stress and inhibition of apoptosis and increase in cell replication. Further studies are necessary to find out the relationship of different mechanisms and the chronic effect of peroxisome proliferators on humans.

摘 要

過氧化物酶增殖因數啓動受體 (PPARs) 是類固醇/維生素 A 核受體家族的成員。PPARs 有三種亞型， α 、 δ/β 和 γ 。其中 PPAR α 是參與脂肪代謝、過氧化物酶增殖因數 (PP) 誘導的多向應答以及肝臟腫瘤發生的主要亞型。短期 (2 周) 的 PP 處理會引發過氧化物酶體增殖，肝腫大以及誘發參與脂肪酸 β 氧化的基因的表達。長期 (11 個月) 的 PP 處理會導致肝臟腫瘤的發生。PP 是一類化學藥品包括一些可塑劑例如 DEHP 和高脂血藥物例如安妥明和 Wy-14,643。由於人類暴露於充滿過氧化物酶增殖因數的環境中，所以有必要研究過氧化物酶增殖因數對人類長期的影響。

在本研究中，主要研究 Wy-14,643 化合物的作用，因為目前已知 Wy-14,643 的長期處理必然會引發肝臟腫瘤。用含有 0.1% Wy-14,643 的飼料和不含有 Wy-14,643 的常用飼料喂養 PPAR α 野生型和 PPAR α 敲除的小鼠，從而分離 PPAR α 依賴以及 Wy-14,643 誘導的基因。爲了研究肝臟損傷的時間性以及 Wy-14,643 誘導的基因表達，分別在喂養 24 小時、1 周、2 周以及 6 個月收集樣品進行試驗。

PPAR α 野生型的小鼠，在用含有 0.1% Wy-14,643 的飼料喂養 1 周後，發生肝腫大；隨著喂養時間的增加，肝腫大的程度也增加。同時，0.1% Wy-14,643 喂養的 PPAR α 野生小鼠，白脂肪、棕脂肪以及脾臟的重量比正常喂養的 PPAR α 野生小鼠要輕。本研究也檢測了不同時間點的小鼠血清中膽固醇和甘油三酯的水平。0.1% Wy-14,643 喂養了 11 個月

的 PPAR α 野生小鼠的血清中的膽固醇水平顯著的升高。而在 0.1% Wy-14,643 喂養的 PPAR α 野生小鼠中，從 24 小時起，血清中甘油三酯的水平隨著時間延長而降低。

採用組織學的方法，本研究檢測了長期 Wy-14,643 處理下，小鼠的肝臟損傷。在 0.1% Wy-14,643 喂養的 PPAR α 野生小鼠中，觀察到肝實質細胞的不規則排列，竇狀隙擴大以及橫紋細胞簇。而在 PPAR α 敲除小鼠中，由於缺失了 PPAR α 基因，不管是餵食常用飼料或者含有 0.1% Wy-14,643 的飼料，從 24 小時起，都觀察到脂肪堆積的情況。

在喂養了 11 個月後，採用熒光差異顯示 (FluoroDD) 技術從小鼠的肝臟中篩選 PPAR α 依賴以及 Wy-14,643 誘導的基因。採用此技術是因為熒光差異顯示技術可以同時比較不用喂養組別的樣品。本研究從 11 塊 FluoroDD 膠中分離到 17 個 PPAR α 依賴及 Wy-14,643 誘導的基因。其中包括：過氧化物 Δ -3, Δ -2-烯酰輔酶 A 異構酶，小鼠半胱次磺酸脫羧酶，小鼠乙酰輔酶 A 脫氫酶，過氧化物生物合成因子 16，小鼠細胞色素 4a14，小鼠過氧化物雙功能酶，小鼠細胞色素 4a10，超長鏈酰基輔酶 A 合成酶，小鼠過氧代物酰基輔酶 A 氧化酶，小鼠輕基類固醇 (17- β) 脫氫酶 11，小鼠脂肪分其化相關蛋白和小鼠肉碱 O-辛酰輕移酶是 PPAR α 依賴以及 Wy-14,643 誘導上調的；而小鼠載脂蛋白 A-V，小鼠 UDP-葡萄糖醛酸轉移酶 2 家族成員 5，小鼠絲氨酸蛋白酶抑制因子 1-1，小鼠主要尿蛋白 II 和小鼠羧酶酯酶是 PPAR α 依賴以及 Wy-14,643 誘導下調的。

除了小鼠載脂蛋白 A-V，本研究檢測了所有 16 個基因隨 Wy-14,643 處

理時間的表達水平變化。過氧化物 Δ -3, Δ -2-烯酰輔酶 A 異構酶, 小鼠乙酰輔酶 A 脫氫酶, 過氧化物生物合成因子 16, 小鼠細胞色素 4a14, 小鼠過氧化物雙功能酶, 小鼠細胞色素 4a10, 超長鏈酰基輔酶 A 合成酶, 小鼠過氧代物酰基輔酶 A 氧化酶, 小鼠輕基類固醇 (17- β) 脫氫酶 11, 小鼠脂肪分其化相關蛋白和小鼠肉碱 O-辛酰輕移的表達水平從 Wy-14,643 處理 24 小時開始升高, 一直持續到 11 個月; 而小鼠半胱次礦酸脫羧酶的上調從 1 周持續到 11 個月。小鼠絲氨酸蛋白酶抑制因子 1-1, 小鼠主要尿蛋白 II 和小鼠羧酶酯酶表達水平的降低從 1 周開始, 直至 11 個月; 小鼠 UDP-葡萄糖醛酸轉移酶 2 家族成員 5 的下調從 2 周到 11 個月。

基於鑒定的基因, PP 誘導的肝臟腫瘤發生的機制可能是由於氧化作用。而然, 我們不能確定是否還有其他機制參與 PP 誘導的肝臟腫瘤發生。本研究顯示, PP 誘導的肝臟腫瘤發生是氧化壓力、細胞調亡被抑止和細胞複製的增加的綜合作用。我們需要進行更深入的研究來檢測不同機制之間的關係及過氧化物酶增殖因數對人體的長期效應。

Acknowledgements

I would like to give my special thanks for my supervisor, Prof. Lee Sau-Tuen Susanna, for her support throughout these years. Her critical advice guidance on my project will be very useful in my future.

I would like to express my gratitude to Prof. Cheung Wing-Tai for his advise on my project and Prof. Chan Woo-Yee Woody for providing training on histology.

I am grateful to my colleagues Ms. Chen Ka-Pik, Ms. Li Sui-Mui, Ms. Lo Kam-Chun, Mr. Ng Lui, Ms. Sreedevi Avasarala and Ms. Sun Yan for their support and valuable advice in my research. Technical support from Mr. Kam Yiu-Wing and Mr. Chui Shun-Keung is also important for my project. I would also want to give my thanks for Ms. Chan Pui-Ting, Ms. Yuen Yee-Lok and Ms. Yau Wing-Yiu for their kind help.

Last but not least, I am extremely thankful to my parents and sisters for their support and encouragement during these years.

TABLE OF CONTENTS

	Page
Abstract	i
Abstract (Chinese Version)	v
Acknowledgements	viii
Tables of Contents	ix
List of Abbreviations	xxx
List of Figures	xxxiii
List of Tables	xlii
Chapter 1 Literature review	1
1.1 Peroxisome proliferator activator receptors	1
1.2 Peroxisome proliferators	6
1.2.1 Hepatomegaly	9
1.2.2 Peroxisome proliferation	11
1.2.3 Target genes regulation	12
1.2.4 Hypolipidemic effect	16
1.2.5 Hepatocarcinogenesis	18
1.3 Mode of actions	20
1.3.1 Oxidative stress	21
1.3.2 Inhibition of apoptosis	22
1.3.2 Increase in cell replication	22
1.3.4 Alterations in cell cycle control	23
1.4 Objectives	23
Chapter 2 Materials and Methods	25
2.1 Animal tail-genotyping	25
2.1.1 Materials	25
2.1.2 Methods	28
2.2 Animal treatment	29
2.2.1 Materials	29
2.2.2 Methods	29

	Page
2.3 Serum cholesterol and tryiglyceride analysis	30
2.3.1 Materials	31
2.3.2 Methods	31
2.3.2.1 Serum preparation	31
2.3.2.2 Serum cholesterol analysis	31
2.3.2.3 Serum triglyceride analysis	32
2.4 Histological analysis	32
2.4.1 Materials	32
2.4.2 Methods	33
2.5 Total RNA isolation	34
2.5.1 Materials	34
2.5.2 Methods	34
2.6 DNase I treatment of total liver RNA	37
2.6.1 Materials	37
2.6.2 Methods	37
2.7 Reverse transcription (RT) of mRNA and non- fluorescent PCR (non-fluoroDD PCR)	38
2.7.1 Materials	43
2.7.2 Methods	43
2.8 Reverse transcription (RT) of mRNA and fluorescent PCR (fluoroDD PCR)	44
2.8.1 Materials	44
2.8.2 Method	44
2.9 Fluorescent differential display (fluoroDD)	45
2.9.1 Materials	45
2.9.2 Methods	45
2.9.2.1 FluoroDD gel preparation	45
2.9.2.2 Sample preparation and electrophoresis	45
2.10 Excision of differentially expressed cDNA fragments	46
2.10.1 Materials	46
2.10.2 Methods	46
2.11 Reamplification of differentially expressed cDNA fragments	48
2.11.1 Materials	48
2.11.2 Methods	50
2.12 Subcloning of reamplified cDNA fragmens	50
2.12.1 Materials	53

	Page
2.12.2 Methods	53
2.12.2.1 Ligation	53
2.12.2.2 Transformation	53
2.12.2.3 Phenol-choloroform extraction	54
2.12.2.4 Confirmation of insert size by <i>EcoRI</i> digestion	54
2.12.2.5 Mini-preparation of plasmid DNA from recombinant clones	55
2.13 Sequencing of subcloned cDNA fragments	55
2.13.1 Materials	56
2.13.2 Methods	56
2.13.2.1 Sequencing of fluoroDD cDNA fragments	56
2.13.2.2 Blast search against computer database	57
2.14 Northern blot analysis of sequenced cDNA fragments	57
2.14.1 Materials	58
2.14.2 Methods	58
2.14.2.1 Formaldehyde agarose gel electrophoresis of total RNA	58
2.14.2.2 Preparation of DIG-labeled RNA probes for hybridization	59
2.14.2.3 Preparation of PCR DIG-labeled cDNA probes for hybridization	60
2.14.2.4 Hybridization and colour development	60
Chapter 3 Results	62
3.1 Confirmation of genotypes by PCR	62
3.2 Body weight changes	62
3.3 Organ weight changes	67
3.4 Serum cholesterol and triglyceride levels	70
3.5 Liver histology	78
3.6 Reverse transcription (RT) of mRNA and non-fluorescent PCR (non-flurroDD PCR)	114
3.7 Reverse transcription (RT) of mRNA and fluorescent PCR (fluoroDD PCR)	125
3.8 Reamplification of fluorescent differential display (FDD) fragments	138
3.9 Subcloning of reamplified FDD fragments	162

	Page
3.10 Sequencing of subcloned cDNA fragments	176
3.11 Northern blot analysis of sequenced cDNA fragments	195
Chapter 4 Discussion	250
4.1 Body weight changes	250
4.2 Organ weight changes	251
4.3 Serum cholesterol and triglyceride levels	253
4.4 Liver histology	254
4.5 Functions and roles of identified PPAR α -dependent and Wy-14,643-responsive genes	255
4.6 Mechanism of PP-induced hepatocarcinogenesis	270
Chapter 5 Conclusions	274
References	276
Appendix A Tables of preparation of reaction mix	285
Table A1. Preparation of animal tail genotyping PCR reaction	285
Table A2. Preparation of DNase I treatment	285
Table A3. Preparation of reverse transcription of non-fluoroDD and fluoroDD	285
Table A4. Preparation of non-fluoroDD and fluoroDD RT-PCR	286
Table A5. Preparation of reamplification of differentially expressed cDNA fragments	286
Table A6. Preparation of PCR reaction for DNA sequencing	286
Table A7. Preparation of PCR reaction for RNA probe	287
Table A8. Preparation of PCR reaction for cDNA probe	287
Appendix B DNA sequences and sequencing alignments of FluoroDD Fragments	288
B 1.1: DNA sequence of cDNA subclone <u>AA1#2</u> (AP1 & ARP2) using <u>M13 forward (-20) primer</u>	288

	Page
B 1.2: Sequencing alignment of cDNA subclone AA1#2 with mouse peroxisomal delta 3, delta 2-enoyl-Coenzyme A isomerase (Peci) by BLAST searching against the National Center for Biotechnology Information database	288
B 1.3: Summary of sequence alignment of cDNA subclone <u>AA1#2</u> with <u>mouse Peci</u>	288
B 2.1: DNA sequence of cDNA subclone <u>AA1#3</u> (AP1 & ARP2) using <u>M13 forward (-20) primer</u>	289
B 2.2: Sequencing alignment of cDNA subclone AA1#3 with mouse peroxisomal delta 3, delta 2-enoyl-Coenzyme A isomerase (Peci) by BLAST searching against the National Center for Biotechnology Information database	289
B 2.3: Summary of sequence alignment of cDNA subclone <u>AA1#3</u> with <u>mouse Peci</u>	289
B 3.1: DNA sequence of cDNA subclone <u>AA1#4</u> (AP1 & ARP2) using <u>M13 reverse primer</u>	290
B 3.2: Sequencing alignment of cDNA subclone AA1#4 with mouse peroxisomal delta 3, delta 2-enoyl-Coenzyme A isomerase (Peci) by BLAST searching against the National Center for Biotechnology Information database	290
B 3.3: Summary of sequence alignment of cDNA subclone <u>AA1#4</u> with <u>mouse Peci</u>	290
B 4.1: DNA sequence of cDNA subclone <u>AA1#20</u> (AP1 & ARP2) using <u>M13 forward (-20) primer</u>	291
B 4.2: Sequencing alignment of cDNA subclone AA1#20 with mouse peroxisomal delta 3, delta 2- enoyl-Coenzyme A isomerase (Peci) by BLAST searching against the National Center for Biotechnology Information database	291
B 4.3: Summary of sequence alignment of cDNA subclone <u>AA1#20</u> with <u>mouse Peci</u>	291
B 5.1: DNA sequence of cDNA subclone <u>AA4#1</u> (AP1 & ARP2) using <u>M13 forward (-20) primer</u>	292
B 5.2: Sequencing alignment of cDNA subclone AA4#1 with mouse apolipoprotein A-V (Apoa5) by BLAST searching against the National Center for Biotechnology Information database	292

	Page
B 5.3: Summary of sequence alignment of cDNA subclone <u>AA4#1</u> with <u>mouse ApoA5</u>	292
B 6.1: DNA sequence of cDNA subclone <u>AA4#9</u> (AP1 & ARP2) using <u>M13 reverse primer</u>	293
B 6.2: Sequencing alignment of cDNA subclone AA4#9 with mouse apolipoprotein A-V (ApoA5) by BLAST searching against the National Center for Biotechnology Information database	293
B 6.3: Summary of sequence alignment of cDNA subclone <u>AA4#9</u> with <u>mouse ApoA5</u>	293
B 7.1: DNA sequence of cDNA subclone <u>AA5#5</u> (AP1 & ARP2) using <u>M13 forward (-20) primer</u>	294
B 7.2: Sequencing alignment of cDNA subclone AA5#5 with mouse mitochondrion by BLAST searching against the National Center for Biotechnology Information database	294
B 7.3: Summary of sequence alignment of cDNA subclone <u>AA5#5</u> with <u>mouse mitochondrion</u>	294
B 8.1: DNA sequence of cDNA subclone <u>AA6#1</u> (AP1 & ARP2) using <u>M13 forward (-20) primer</u>	295
B 8.2: Sequencing alignment of cDNA subclone AA6#1 with mouse mitochondrion by BLAST searching against the National Center for Biotechnology Information database	295
B 8.3: Summary of sequence alignment of cDNA subclone <u>AA6#1</u> with <u>mouse mitochondrion</u>	295
B 9.1: DNA sequence of cDNA subclone <u>AA6#9</u> (AP1 & ARP2) using <u>M13 reverse primer</u>	296
B 9.2: Sequencing alignment of cDNA subclone AA6#9 with mouse mitochondrion by BLAST searching against the National Center for Biotechnology Information database	296
B 9.3: Summary of sequence alignment of cDNA subclone <u>AA6#9</u> with <u>mouse mitochondrion</u>	296
B 10.1: DNA sequence of cDNA subclone <u>AA7#3</u> (AP1 & ARP2) using <u>M13 forward (-20) primer</u>	297
B 10.2: Sequencing alignment of cDNA subclone AA7#3 with mouse mitochondrion by BLAST searching against the National Center for Biotechnology Information database	297

	Page
B 10.3: Summary of sequence alignment of cDNA subclone <u>AA7#3</u> with <u>mouse mitochondrion</u>	297
B 11.1: DNA sequence of cDNA subclone <u>AA7#5</u> (AP1 & ARP2) using <u>M13 reverse primer</u>	298
B 11.2: Sequencing alignment of cDNA subclone AA7#5 with mouse mitochondrion by BLAST searching against the National Center for Biotechnology Information database	298
B 11.3: Summary of sequence alignment of cDNA subclone <u>AA7#5</u> with <u>mouse mitochondrion</u>	298
B 12.1: DNA sequence of cDNA subclone <u>AA10#1</u> (AP1 & ARP2) using <u>M13 forward (-20) primer</u>	299
B 12.2: Sequencing alignment of cDNA subclone AA10#1 with mouse cysteine sulfinic acid decarboxylase (Csad) by BLAST searching against the National Center for Biotechnology Information database	299
B 12.3: Summary of sequence alignment of cDNA subclone <u>AA10#1</u> with <u>mouse Csad</u>	299
B 13.1: DNA sequence of cDNA subclone <u>AA10#1</u> (AP1 & ARP2) using <u>M13 reverse primer</u>	300
B 13.2: Sequencing alignment of cDNA subclone AA10#1 with mouse cysteine sulfinic acid decarboxylase (Csad) by BLAST searching against the National Center for Biotechnology Information database	300
B 13.3: Summary of sequence alignment of cDNA subclone <u>AA10#1</u> with <u>mouse Csad</u>	300
B 14.1: DNA sequence of cDNA subclone <u>AA12#4</u> (AP1 & ARP2) using <u>M13 forward (-20) primer</u>	301
B 14.2: Sequencing alignment of cDNA subclone AA12#4 with mouse acetyl-coenzyme A dehydrogenase, medium chain (MCAD) by BLAST searching against the National Center for Biotechnology Information database	301
B 14.3: Summary of sequence alignment of cDNA subclone <u>AA12#4</u> with <u>mouse MCAD</u>	301
B 15.1: DNA sequence of cDNA subclone <u>AA12#4</u> (AP1 & ARP2) using <u>M13 reverse primer</u>	302

	Page
B 15.2: Sequencing alignment of cDNA subclone AA12#4 with mouse acetyl-coenzyme A dehydrogenase, medium chain (MCAD) by BLAST searching against the National Center for Biotechnology Information database	302
B 15.3: Summary of sequence alignment of cDNA subclone <u>AA12#4</u> with <u>mouse MCAD</u>	302
B 16.1: DNA sequence of cDNA subclone <u>AB7#2</u> (AP3 & ARP3) using <u>M13 forward (-20) primer</u>	303
B 16.2: Sequencing alignment of cDNA subclone AB7#2 with mouse UDP-glucuronosyltransferase 2 family, member 5 (UGT2b5) by BLAST searching against the National Center for Biotechnology Information database	303
B 16.3: Summary of sequence alignment of cDNA subclone <u>AB7#2</u> with <u>mouse UGT2b5</u>	303
B 17.1: DNA sequence of cDNA subclone <u>AB7#8</u> (AP3 & ARP3) using <u>M13 reverse primer</u>	304
B 17.2: Sequencing alignment of cDNA subclone AB7#8 with mouse UDP-glucuronosyltransferase 2 family, member 5 (UGT2b5) by BLAST searching against the National Center for Biotechnology Information database	304
B 17.3: Summary of sequence alignment of cDNA subclone <u>AB7#8</u> with <u>mouse UGT2b5</u>	304
B 18.1: DNA sequence of cDNA subclone <u>AB17#16</u> (AP3 & ARP3) using <u>M13 reverse primer</u>	305
B 18.2: Sequencing alignment of cDNA subclone AB17#16 with mouse mitochondrion by BLAST searching against the National Center for Biotechnology Information database	305
B 18.3: Summary of sequence alignment of cDNA subclone <u>AB17#16</u> with <u>mouse mitochondrion</u>	305
B 19.1: DNA sequence of cDNA subclone <u>AB18#4</u> (AP3 & ARP3) using <u>M13 forward (-20) primer</u>	306
B 19.2: Sequencing alignment of cDNA subclone AB18#4 with mouse mitochondrion by BLAST searching against the National Center for Biotechnology Information database	306

	Page
B 20.1: DNA sequence of cDNA subclone <u>AB18#4</u> (AP3 & ARP3) using <u>M13 reverse primer</u>	307
B 20.2: Sequencing alignment of cDNA subclone AB18#4 with mouse mitochondrion by BLAST searching against the National Center for Biotechnology Information database	307
B 20.3: Summary of sequence alignment of cDNA subclone <u>AB18#4</u> with <u>mouse mitochondrion</u>	307
B 21.1: DNA sequence of cDNA subclone <u>AB19#2</u> (AP3 & ARP3) using <u>M13 forward (-20) primer</u>	308
B 21.2: Sequencing alignment of cDNA subclone AB19#2 with mouse mitochondrion by BLAST searching against the National Center for Biotechnology Information database	308
B 21.3: Summary of sequence alignment of cDNA subclone <u>AB19#2</u> with <u>mouse mitochondrion</u>	308
B 22.1: DNA sequence of cDNA subclone <u>AB19#10</u> (AP3 & ARP3) using <u>M13 reverse primer</u>	309
B 22.2: Sequencing alignment of cDNA subclone AB19#10 with mouse mitochondrion by BLAST searching against the National Center for Biotechnology Information database	309
B 22.3: Summary of sequence alignment of cDNA subclone <u>AB19#10</u> with <u>mouse mitochondrion</u>	309
B 23.1: DNA sequence of cDNA subclone <u>AB22#9</u> (AP3 & ARP3) using <u>M13 forward (-20) primer</u>	310
B 23.2: Sequencing alignment of cDNA subclone AB22#9 with mouse peroxisome biogenesis factor 16 (Pex16) by BLAST searching against the National Center for Biotechnology Information database	310
B 23.3: Summary of sequence alignment of cDNA subclone <u>AB22#9</u> with <u>mouse Pex16</u>	310
B 24.1: DNA sequence of cDNA subclone <u>AB22#9</u> (AP3 & ARP3) using <u>M13 reverse primer</u>	311
B 24.2: Sequencing alignment of cDNA subclone AB22#9 with mouse peroxisome biogenesis factor 16 (Pex16) by BLAST searching against the National Center for Biotechnology Information database	311

	Page
B 24.3: Summary of sequence alignment of cDNA subclone <u>AB22#9</u> with <u>mouse Pex16</u>	311
B 25.1: DNA sequence of cDNA subclone <u>AB24#9</u> (AP3 & ARP3) using <u>M13 forward (-20) primer</u>	312
B 25.2: Sequencing alignment of cDNA subclone AB24#9 with mouse Cyp4a14 by BLAST searching against the National Center for Biotechnology Information database	312
B 25.3: Summary of sequence alignment of cDNA subclone <u>AB24#9</u> with <u>mouse Cyp4a14</u>	312
B 26.1: DNA sequence of cDNA subclone <u>AB24#9</u> (AP3 & ARP3) using <u>M13 reverse primer</u>	313
B 26.2: Sequencing alignment of cDNA subclone AB24#9 with mouse Cyp4a14 by BLAST searching against the National Center for Biotechnology Information database	313
B 26.3: Summary of sequence alignment of cDNA subclone <u>AB24#9</u> with <u>mouse Cyp4a14</u>	313
B 27.1: DNA sequence of cDNA subclone <u>AB25#6</u> (AP3 & ARP3) using <u>M13 forward (-20) primer</u>	314
B 27.2: Sequencing alignment of cDNA subclone AB25#6 with mouse Cyp4a14 by BLAST searching against the National Center for Biotechnology Information database	314
B 27.3: Summary of sequence alignment of cDNA subclone <u>AB25#6</u> with <u>mouse Cyp4a14</u>	314
B 28.1: DNA sequence of cDNA subclone <u>AB26#17</u> (AP3 & ARP3) using <u>M13 forward (-20) primer</u>	315
B 28.2: Sequencing alignment of cDNA subclone AB26#17 with mouse Cyp4a14 by BLAST searching against the National Center for Biotechnology Information database	315
B 28.3: Summary of sequence alignment of cDNA subclone <u>AB26#17</u> with <u>mouse Cyp4a14</u>	315
B 29.1: DNA sequence of cDNA subclone <u>AB26#30</u> (AP3 & ARP3) using <u>M13 reverse primer</u>	316
B 29.2: Sequencing alignment of cDNA subclone AB26#30 with mouse Cyp4a14 by BLAST searching against the National Center for Biotechnology Information database	316

	Page
B 29.3: Summary of sequence alignment of cDNA subclone <u>AB26#30</u> with <u>mouse Cyp4a14</u>	316
B 30.1: DNA sequence of cDNA subclone <u>AB29#7</u> (AP3 & ARP3) using <u>M13 forward (-20) primer</u>	317
B 30.2: Sequencing alignment of cDNA subclone AB29#7 with mouse catalase by BLAST searching against the National Center for Biotechnology Information database	317
B 30.3: Summary of sequence alignment of cDNA subclone <u>AB29#7</u> with <u>mouse catalase</u>	317
B 31.1: DNA sequence of cDNA subclone <u>AC1#1</u> (AP2 & ARP19) using <u>M13 forward (-20) primer</u>	318
B 31.2: Sequencing alignment of cDNA subclone AC1#1 with mouse serine (or cysteine) proteinase inhibitor (SPI) by BLAST searching against the National Center for Biotechnology Information database	318
B 31.3: Summary of sequence alignment of cDNA subclone <u>AC1#1</u> with <u>mouse SPI</u>	318
B 32.1: DNA sequence of cDNA subclone <u>AC1#1</u> (AP2 & ARP19) using <u>M13 reverse primer</u>	319
B 32.2: Sequencing alignment of cDNA subclone AC1#1 with mouse serine (or cysteine) proteinase inhibitor (SPI) by BLAST searching against the National Center for Biotechnology Information database	319
B 32.3: Summary of sequence alignment of cDNA subclone <u>AC1#1</u> with <u>mouse SPI</u>	319
B 33.1: DNA sequence of cDNA subclone <u>AC1#2</u> (AP2& ARP19) using <u>M13 forward (-20) primer</u>	320
B 33.2: Sequencing alignment of cDNA subclone AC1#2 with mouse serine (or cysteine) proteinase inhibitor (SPI) by BLAST searching against the National Center for Biotechnology Information database	320
B 33.3: Summary of sequence alignment of cDNA subclone <u>AC1#2</u> with <u>mouse SPI</u>	320
B 34.1: DNA sequence of cDNA subclone <u>AC1#2</u> (AP2& ARP19) using <u>M13 reverse primer</u>	321

	Page
B 34.2: Sequencing alignment of cDNA subclone AC1#2 with mouse serine (or cysteine) proteinase inhibitor (SPI) by BLAST searching against the National Center for Biotechnology Information database	321
B 34.3: Summary of sequence alignment of cDNA subclone <u>AC1#2</u> with <u>mouse SPI</u>	321
B 35.1: DNA sequence of cDNA subclone <u>AC2#2</u> (AP2 & ARP19) using <u>M13 reverse primer</u>	322
B 35.2: Sequencing alignment of cDNA subclone AC2#2 with mouse bifunctional enzyme (PBFE) by BLAST searching against the National Center for Biotechnology Information database	322
B 35.3: Summary of sequence alignment of cDNA subclone <u>AC2#2</u> with <u>mouse PBFE</u>	322
B 36.1: DNA sequence of cDNA subclone <u>AC2#5</u> (AP2 & ARP19) using <u>M13 reverse primer</u>	323
B 36.2: Sequencing alignment of cDNA subclone AC2#5 with mouse catalase by BLAST searching against the National Center for Biotechnology Information database	323
B 36.3: Summary of sequence alignment of cDNA subclone <u>AC2#5</u> with <u>mouse catalase</u>	323
B 37.1: DNA sequence of cDNA subclone <u>AC2#6</u> (AP2 & ARP19) using <u>M13 forward (-20) primer</u>	324
B 37.2: Sequencing alignment of cDNA subclone AC2#6 with mouse serine (or cysteine) proteinase inhibitor (SPI) by BLAST searching against the National Center for Biotechnology Information database	324
B 37.3: Summary of sequence alignment of cDNA subclone <u>AC2#6</u> with <u>mouse SPI</u>	324
B 38.1: DNA sequence of cDNA subclone <u>AC4#3</u> (AP2 & ARP19) using <u>M13 forward (-20) primer</u>	325
B 38.2: Sequencing alignment of cDNA subclone AC4#3 with mouse Cyp2a5 by BLAST searching against the National Center for Biotechnology Information database	325
B 38.3: Summary of sequence alignment of cDNA subclone <u>AC4#3</u> with <u>mouse Cyp2a5</u>	325

	Page
B 39.1: DNA sequence of cDNA subclone <u>AC4#3</u> (AP2 & ARP19) using <u>M13 reverse primer</u>	326
B 39.2: Sequencing alignment of cDNA subclone AC4#3 with mouse serine (or cysteine) proteinase inhibitor (SPI) by BLAST searching against the National Center for Biotechnology Information database	326
B 39.3: Summary of sequence alignment of cDNA subclone <u>AC4#3</u> with <u>mouse SPI</u>	326
B 40.1: DNA sequence of cDNA subclone <u>AC7#5</u> (AP2& ARP19) using <u>M13 forward (-20) primer</u>	327
B 40.2: Sequencing alignment of cDNA subclone AC7#5 with mouse serine (or cysteine) proteinase inhibitor (SPI) by BLAST searching against the National Center for Biotechnology Information database	327
B 40.3: Summary of sequence alignment of cDNA subclone <u>AC7#5</u> with <u>mouse SPI</u>	327
B 41.1: DNA sequence of cDNA subclone <u>AD6#4</u> (AP2 & ARP18) using <u>M13 reverse primer</u>	328
B 41.2: Sequencing alignment of cDNA subclone AD6#4 with mouse N-terminal Asn amidase (NtanI) by BLAST searching against the National Center for Biotechnology Information database	328
B 41.3: Summary of sequence alignment of cDNA subclone <u>AD6#4</u> with <u>mouse NtanI</u>	328
B 42.1: DNA sequence of cDNA subclone <u>AD6#10</u> (AP2 & ARP18) using <u>M13 forward (-20) primer</u>	329
B 42.2: Sequencing alignment of cDNA subclone AD6#10 with mouse Cyp4a10 by BLAST searching against the National Center for Biotechnology Information database	329
B 42.3: Summary of sequence alignment of cDNA subclone <u>AD6#10</u> with <u>mouse Cyp4a10</u>	329
B 43.1: DNA sequence of cDNA subclone <u>AD6#10</u> (AP2 & ARP18) using <u>M13 reverse primer</u>	330
B 43.2: Sequencing alignment of cDNA subclone AD6#10 with mouse Cyp4a10 by BLAST searching against the National Center for Biotechnology Information database	330

	Page
B 43.3: Summary of sequence alignment of cDNA subclone <u>AD6#10</u> with <u>mouse Cyp4a10</u>	330
B 44.1: DNA sequence of cDNA subclone <u>AD8#2</u> (AP2 & ARP18) using <u>M13 forward (-20) primer</u>	331
B 44.2: Sequencing alignment of cDNA subclone AD8#2 with mouse Cyp4a10 by BLAST searching against the National Center for Biotechnology Information database	331
B 44.3: Summary of sequence alignment of cDNA subclone <u>AD8#2</u> with <u>mouse Cyp4a10</u>	331
B 45.1: DNA sequence of cDNA subclone <u>AD8#7</u> (AP2 & ARP18) using <u>M13 reverse primer</u>	332
B 45.2: Sequencing alignment of cDNA subclone AD8#7 with mouse Cyp4a10 by BLAST searching against the National Center for Biotechnology Information database	332
B 45.3: Summary of sequence alignment of cDNA subclone <u>AD8#7</u> with <u>mouse Cyp4a10</u>	332
B 46.1: DNA sequence of cDNA subclone <u>AD9#2</u> (AP2 & ARP18) using <u>M13 forward (-20) primer</u>	333
B 46.2: Sequencing alignment of cDNA subclone AD9#2 with mouse Cyp4a10 by BLAST searching against the National Center for Biotechnology Information database	333
B 46.3: Summary of sequence alignment of cDNA subclone <u>AD9#2</u> with <u>mouse Cyp4a10</u>	333
B 47.1: DNA sequence of cDNA subclone <u>AD9#3</u> (AP2 & ARP18) using <u>M13 reverse primer</u>	334
B 47.2: Sequencing alignment of cDNA subclone AD9#3 with mouse Cyp4a10 by BLAST searching against the National Center for Biotechnology Information database	334
B 47.3: Summary of sequence alignment of cDNA subclone <u>AD9#3</u> with <u>mouse Cyp4a10</u>	334
B 48.1: DNA sequence of cDNA subclone <u>AF1#8</u> (AP10 & ARP13) using <u>M13 forward (-20) primer</u>	335

	Page
B 48.2: Sequencing alignment of cDNA subclone AF1#8 with mouse very-long-chain acyl-coA synthetase (VLACS) by BLAST searching against the National Center for Biotechnology Information database	335
B 48.3: Summary of sequence alignment of cDNA subclone <u>AF1#8</u> with <u>mouse VLACS</u>	335
B 49.1: DNA sequence of cDNA subclone <u>AF1#8</u> (AP10 & ARP13) using <u>M13 reverse primer</u>	336
B 49.2: Sequencing alignment of cDNA subclone AF1#8 with mouse very-long-chain acyl-coA synthetase (VLACS) by BLAST searching against the National Center for Biotechnology Information database	336
B 49.3: Summary of sequence alignment of cDNA subclone <u>AF1#8</u> with <u>mouse VLACS</u>	336
B 50.1: DNA sequence of cDNA subclone <u>AF21#5</u> (AP10 & ARP13) using <u>M13 reverse primer</u>	337
B 50.2: Sequencing alignment of cDNA subclone AF21#5 with mouse cell death-inducing DNA fragmentation factor, alpha subunit-like effector B (Cideb) by BLAST searching against the National Center for Biotechnology Information database	337
B 50.3: Summary of sequence alignment of cDNA subclone <u>AF21#5</u> with <u>mouse Cideb</u>	337
B 51.1: DNA sequence of cDNA subclone <u>AF25#6</u> (AP10 & ARP13) using <u>M13 forward (-20) primer</u>	338
B 51.2: Sequencing alignment of cDNA subclone AF25#6 with mouse major urinary protein 2 (MUP II) by BLAST searching against the National Center for Biotechnology Information database	338
B 51.3: Summary of sequence alignment of cDNA subclone <u>AF25#6</u> with <u>mouse MUP II</u>	338
B 52.1: DNA sequence of cDNA subclone <u>AF25#7</u> (AP10 & ARP13) using <u>M13 reverse primer</u>	339
B 52.2: Sequencing alignment of cDNA subclone AF25#7 with mouse major urinary protein 2 (MUP II) by BLAST searching against the National Center for Biotechnology Information database	339

	Page
B 52.3: Summary of sequence alignment of cDNA subclone <u>AF25#7</u> with <u>mouse MUP II</u>	339
B 53.1: DNA sequence of cDNA subclone <u>AF30#4</u> (AP10 & ARP13) using <u>M13 forward (-20) primer</u>	340
B 53.2: Sequencing alignment of cDNA subclone AF30#4 with mouse mRNA for suppressor of actin mutations (SAC1 gene) by BLAST searching against the National Center for Biotechnology Information database	340
B 53.3: Summary of sequence alignment of cDNA subclone <u>AF30#4</u> with <u>mouse SAC1</u>	340
B 54.1: DNA sequence of cDNA subclone <u>AF30#5</u> (AP10 & ARP13) using <u>M13 reverse primer</u>	341
B 54.2: Sequencing alignment of cDNA subclone AF30#5 with mouse mitochondrion by BLAST searching against the National Center for Biotechnology Information database	341
B 54.3: Summary of sequence alignment of cDNA subclone <u>AF30#5</u> with <u>mouse mitochondrion</u>	341
B 55.1: DNA sequence of cDNA subclone <u>AH1#6</u> (AP11 & ARP19) using <u>M13 forward (-20) primer</u>	342
B 55.2: Sequencing alignment of cDNA subclone AH1#6 with mouse EST by BLAST searching against the National Center for Biotechnology Information database	342
B 55.3: Summary of sequence alignment of cDNA subclone <u>AH1#6</u> with <u>mouse EST</u>	342
B 56.1: DNA sequence of cDNA subclone <u>AI1#5</u> (AP6 & ARP4) using <u>M13 forward (-20) primer</u>	343
B 56.2: Sequencing alignment of cDNA subclone AI1#5 with mouse serine (or cysteine) proteinase inhibitor (SPI) by BLAST searching against the National Center for Biotechnology Information database	343
B 56.3: Summary of sequence alignment of cDNA subclone <u>AI1#5</u> with <u>mouse SPI</u>	343
B 57.1: DNA sequence of cDNA subclone <u>AI1#5</u> (AP6 & ARP4) using <u>M13 reverse primer</u>	344

	Page
B 57.2: Sequencing alignment of cDNA subclone <u>AI1#5</u> with mouse serine (or cysteine) proteinase inhibitor (SPI) by BLAST searching against the National Center for Biotechnology Information database	344
B 57.3: Summary of sequence alignment of cDNA subclone <u>AI1#5</u> with <u>mouse SPI</u>	344
B 58.1: DNA sequence of cDNA subclone <u>AI18#6</u> (AP6 & ARP4) using <u>M13 forward (-20) primer</u>	345
B 58.2: Sequencing alignment of cDNA subclone <u>AI18#6</u> with mouse argininosuccinate lyase (Asl) by BLAST searching against the National Center for Biotechnology Information database	345
B 58.3: Summary of sequence alignment of cDNA subclone <u>AI18#6</u> with <u>mouse Asl</u>	345
B 59.1: DNA sequence of cDNA subclone <u>AI18#6</u> (AP6 & ARP4) using <u>M13 reverse primer</u>	346
B 59.2: Sequencing alignment of cDNA subclone <u>AI18#6</u> with mouse argininosuccinate lyase (Asl) by BLAST searching against the National Center for Biotechnology Information database	346
B 59.3: Summary of sequence alignment of cDNA subclone <u>AI18#6</u> with <u>mouse Asl</u>	346
B 60.1: DNA sequence of cDNA subclone <u>AJ1#4</u> (AP6 & ARP14) using <u>M13 forward (-20) primer</u>	347
B 60.2: Sequencing alignment of cDNA subclone <u>AJ1#4</u> with mouse carboxylesterase by BLAST searching against the National Center for Biotechnology Information database	347
B 60.3: Summary of sequence alignment of cDNA subclone <u>AJ1#4</u> with <u>mouse carboxylesterase</u>	347
B 61.1: DNA sequence of cDNA subclone <u>AJ1#5</u> (AP6 & ARP14) using <u>M13 reverse primer</u>	348
B 61.2: Sequencing alignment of cDNA subclone <u>AJ1#5</u> with mouse carboxylesterase by BLAST searching against the National Center for Biotechnology Information database	348
B 61.3: Summary of sequence alignment of cDNA subclone <u>AJ1#5</u> with <u>mouse carboxylesterase</u>	348

	Page
B 62.1: DNA sequence of cDNA subclone <u>AJ2#10</u> (AP6 & ARP14) using <u>M13 forward (-20) primer</u>	349
B 62.2: Sequencing alignment of cDNA subclone AJ2#10 with peroxisomal acyl-coA oxidase (AOX) by BLAST searching against the National Center for Biotechnology Information database	349
B 62.3: Summary of sequence alignment of cDNA subclone <u>AJ2#10</u> with <u>mouse AOX</u>	349
B 63.1: DNA sequence of cDNA subclone <u>AJ2#10</u> (AP6 & ARP14) using <u>M13 reverse primer</u>	350
B 63.2: Sequencing alignment of cDNA subclone AJ2#10 with peroxisomal acyl-coA oxidase (AOX) by BLAST searching against the National Center for Biotechnology Information database	350
B 63.3: Summary of sequence alignment of cDNA subclone <u>AJ2#10</u> with <u>mouse AOX</u>	350
B 64.1: DNA sequence of cDNA subclone <u>AJ9#1</u> (AP6 & ARP14) using <u>M13 forward (-20) primer</u>	351
B 64.2: Sequencing alignment of cDNA subclone AJ9#1 with mouse catalase by BLAST searching against the National Center for Biotechnology Information database	351
B 64.3: Summary of sequence alignment of cDNA subclone <u>AJ9#1</u> with <u>mouse catalase</u>	351
B 65.1: DNA sequence of cDNA subclone <u>AJ9#1</u> (AP6 & ARP14) using <u>M13 reverse primer</u>	352
B 65.2: Sequencing alignment of cDNA subclone AJ9#1 with mouse suppressor of actin mutations (SAC1 gene) by BLAST searching against the National Center for Biotechnology Information database	352
B 65.3: Summary of sequence alignment of cDNA subclone <u>AJ9#1</u> with <u>mouse SAC1</u>	352
B 66.1: DNA sequence of cDNA subclone <u>AL2#8</u> (AP7 & ARP15) using <u>M13 forward (-20) primer</u>	353

	Page
B 66.2: Sequencing alignment of cDNA subclone AL2#8 with mouse hydroxysteroid (17-beta) dehydrogenase 11 (Hsd17 β 11) by BLAST searching against the National Center for Biotechnology Information database	353
B 66.3: Summary of sequence alignment of cDNA subclone <u>AL2#8</u> with <u>mouse HSD17β11</u>	353
B 67.1: DNA sequence of cDNA subclone <u>AL3#3</u> (AP7& ARP15) using <u>M13 forward (-20) primer</u>	354
B 67.2: Sequencing alignment of cDNA subclone AL3#3 with mouse hydroxysteroid (17-beta) dehydrogenase 11 (Hsd17 β 11) by BLAST searching against the National Center for Biotechnology Information database	354
B 67.3: Summary of sequence alignment of cDNA subclone <u>AL3#3</u> with <u>mouse HSD17β11</u>	354
B 68.1: DNA sequence of cDNA subclone <u>AL3#3</u> (AP7& ARP15) using <u>M13 reverse primer</u>	355
B 68.2: Sequencing alignment of cDNA subclone AL3#3 with mouse hydroxysteroid (17-beta) dehydrogenase 11 (Hsd17 β 11) by BLAST searching against the National Center for Biotechnology Information database	355
B 68.3: Summary of sequence alignment of cDNA subclone <u>AL3#3</u> with <u>mouse HSD17β11</u>	355
B 69.1: DNA sequence of cDNA subclone <u>AO1#2</u> (AP5 & ARP10) using <u>M13 forward (-20) primer</u>	356
B 69.2: Sequencing alignment of cDNA subclone AO1#2 with mouse adipose differentiation related protein (ADFP) by BLAST searching against the National Center for Biotechnology Information database	356
B 69.3: Summary of sequence alignment of cDNA subclone <u>AO1#2</u> with <u>mouse ADFP</u>	356
B 70.1: DNA sequence of cDNA subclone <u>AO1#5</u> (AP5 & ARP10) using <u>M13 reverse primer</u>	357
B 70.2: Sequencing alignment of cDNA subclone AO1#5 with mouse carnitine O-octanoyltransferase (Crot) by BLAST searching against the National Center for Biotechnology Information database	357

	Page
B 70.3: Summary of sequence alignment of cDNA subclone <u>AO1#5</u> with <u>mouse Crot</u>	357
B 71.1: DNA sequence of cDNA subclone <u>AO2#6</u> (AP5 & ARP10) using <u>M13 forward (-20) primer</u>	358
B 71.2: Sequencing alignment of cDNA subclone AO2#6 with mouse RNase A family 4 (Rnase4) by BLAST searching against the National Center for Biotechnology Information database	358
B 71.3: Summary of sequence alignment of cDNA subclone <u>AO2#6</u> with <u>mouse Rnase4</u>	358
B 72.1: DNA sequence of cDNA subclone <u>AO2#6</u> (AP5 & ARP10) using <u>M13 reverse primer</u>	359
B 72.2: Sequencing alignment of cDNA subclone AO2#6 with mouse RNase A family 4 (Rnase4) by BLAST searching against the National Center for Biotechnology Information database	359
B 72.3: Summary of sequence alignment of cDNA subclone <u>AO2#6</u> with <u>mouse Rnase4</u>	359
B 73.1: DNA sequence of cDNA subclone <u>AO2#8</u> (AP5 & ARP10) using <u>M13 reverse primer</u>	360
B 73.2: Sequencing alignment of cDNA subclone AO2#8 with mouse carnitine O-octanoyltransferase (Crot) by BLAST searching against the National Center for Biotechnology Information database	360
B 73.3: Summary of sequence alignment of cDNA subclone <u>AO2#8</u> with <u>mouse Crot</u>	360
B 74.1: DNA sequence of cDNA subclone <u>AO8#2</u> (AP5 & ARP10) using <u>M13 forward (-20) primer</u>	361
B 74.2: Sequencing alignment of cDNA subclone AO8#2 with mouse RNase A family 4 (Rnase4) by BLAST searching against the National Center for Biotechnology Information database	361
B 74.3: Summary of sequence alignment of cDNA subclone <u>AO8#2</u> with <u>mouse Rnase4</u>	361
B 75.1: DNA sequence of cDNA subclone <u>AP4#4</u> (AP12 & ARP2) using <u>M13 forward (-20) primer</u>	362

	Page
B 75.2: Sequencing alignment of cDNA subclone AP4#4 with mouse mitochondrion by BLAST searching against the National Center for Biotechnology Information database	362
B 75.3: Summary of sequence alignment of cDNA subclone <u>AP4#4</u> with <u>mouse mitochondrion</u>	362
B 76.1: DNA sequence of cDNA subclone <u>AP4#4</u> (AP12 & ARP2) using <u>M13 reverse primer</u>	363
B 76.2: Sequencing alignment of cDNA subclone AP4#4 with mouse mitochondrion by BLAST searching against the National Center for Biotechnology Information database	363
B 76.3: Summary of sequence alignment of cDNA subclone <u>AP4#4</u> with <u>mouse mitochondrion</u>	363

List of Abbreviations

α 2U	α 2- urinary globulin
A	Absorbance
ADRP	Adipose differentiation related protein
ALDH	Aldehydehydrogenase
AP	Anchored primer
ApoA1	Apolipoprotein A-I
ApoA2	Apolipoprotein A-II
ApoA5	Apolipoprotein A-V
ApoAIII	Apolipoprotein C-III
ARP	Arbitrary primer
Asl	Argininosuccinate lyase
ATP	Adenosine triphosphate
ATT	α -1 antitrypsin
AOX	Acyl-CoA oxidase
BCIP	5-bromo-4-chloro-3-indolyl-phosphate
BLAST	Basic Local Alignment Search Tool
Bp	Basepair
BOX	Branched-chain acyl-CoA oxidase
bw	Body weight
CAT	Carnitine acetyltransferase
CAD	Coronary artery disease
cDNA	Complementary deoxyribonucleic acid
cm	Centimeter
Cideb	Cell death-inducing DNA fragmentation factor
CoA	Coenzyme A
Crot	Carnitine O-octanoyltransferase
CPT	Carnitine palmitoyltransferase
Csad	Cysteine sulfinic acid decarboxylase
CTL	Control diet
Cyp2a5	Cytochrome P450, family2, subfamily a, polypeptide 5
Cyp4a10	Cytochrome P450, family 4, subfamily a, polypeptide 10
Cyp4a14	Cytochrome P450, family 4, subfamily a, polypeptide 14
DBD	DNA-binding domain
DD	Differential display
DEHA	Di(2-ethylhexyl)adipate

DEHP	Di(2-ethylhexyl)phtalate
DNA	Deoxyribonucleic acid
DNTP	Deoxyribonucleotide-5-phosphate
DR-1	Direct repeat 1
DTT	Dothiothreitol
EPHX	Epoxide hydroxide
EDTA	Ethylenediaminetetraacetic acid
FDD	Fluorescent differential display
g	Gram
GAPDH	Glyceraldehyde-3-phosphate dehydrogenase
GDP	Glycerol-3-phosphate and adenosine-5'-adiphate
HDL	High density lipoprotein
H ₂ O ₂	Hydrogen peroxide
2-HPCL	2-hydroxyphtanoyl-CoA lyase
hr	Hours
Hsd17b11	Hydroxysteroid (17-beta) dehydrogenase 11
IPTG	Isopropyl-β-D-thiogalactoside
LBD	Ligand binding domain
LPL	Lipoprotein lipase
Kb	Kilobase
KO	Knockout
MCAD	Acetyl-coenzyme A dehydrogenase, medium chain
μl	Microlitre
μm	Micrometer
μM	Micromolar
μm	Micrometer
min	Minutes
mg/dl	Milligram/deci litre
ml	Millilitre
ml/g	Millilitre/gram
mM	Mililimolar
mo	Months
MUP II	Mouse major urinary protein II
NaCl	Sodium chloride
NBT	Nitroblue tetrazolium chloride
Ntanl	N-terminal Asn amidase
Ng	Nanogram
nm	Nanometer

orm 1	Orosomucoid 1
Oligo(dT)	Oligopolydeoxythymidine
PBFE	Peroxisomal bifunctional enzyme
PCR	Polymerase chain reaction
Peci	Peroxisomal delta3, delta2-enoyl-coenzyme A isomerase
Pex16	Peroxisome biogenesis factor 16
PP	Peroxisome proliferator
PPAR	Peroxisome proliferator-activated receptor
PPRE	Peroxisome proliferator responsive element
PUFA	Polyunsaturated fatty acid
RNA	Ribonucleic acid
Rnase 4	Ribonuclease 4
rpm	Round per minute
RT-PCR	Reverse transcription-polymerase chain reaction
RXR	Retinoid X receptors
Sac1 gene	Suppressor of actin mutations
SDS	Sodium dodecyl sulfate
sec	Second
Serpinf 2	Serine (or cysteine) proteinase inhibitor, clade F, member 2,
SPI	Serine (or cysteine) proteinase inhibitor, clade A, member 1a
Spi2	Serine (or cysteine) proteinase inhibitor, clade A, member 3K
SSC	Sodium chloride/sodium citrate buffer
TAG	Triacylglycerols
TMR	Tetramethylrhodamine
Tris-HCL	Tris (hydroxymethyl)aminomethane/hydrochloric acid
UGT2b5	UDP-glucuronosyltransferase 2 family member 5
V	Voltage
VLACS	Very long-chain acyl-CoA synthetase
VLDL	Very low density lipoprotein
VLFA	Very long-chain fatty acid
W	Watt
wk	Weeks
Wy	Wy-14,643 [4-chloro-6(2,3-xylindino)2-pyrimidinylthiolacetic acid]
Wy-14,643	4-chloro-6(2,3-xylindino)2-pyrimidinylthiolacetic acid
X-Gal	5-bromo-4-chloro-3-indolyl-D-thiogalactoside
8-OH-dG	8-Hydroxydeoxyguanosine

List of Figures

	Page
Figure 2.1.1	External morphology of 3 months old PPAR α (+/+) and PPAR α (-/-) male mice. 26
Figure 2.1.2	A schematic representation of PPAR α (+/+) and PPAR α (-/-) mouse genomic organization and the location of PCR primers designed for tail-genotyping. 27
Figure 2.4.1	Flowchart showing the steps for histological analysis. 35
Figure 2.5.2.1	Flowchart showing the steps for isolation of total RNA. 36
Figure 2.7.1	Sequences of 12 different 3'-oligo(dT ₁₂) anchored primers (APs). 39
Figure 2.7.2	Sequences of 20 different 5'-arbitrary primers (ARPs). 40
Figure 2.7.3	Sequences of 12 different 3'-tetramethylrhodamine-labeled oligo(dT ₁₂) anchored primers (TMR-APs). 41
Figure 2.7.4	A schematic diagram showing the synthesis of non-fluoroDD PCR. 42
Figure 2.11.1	A schematic diagram showing the reamplification of cDNA fragments. 49
Figure 2.12.1	The restriction map and multiple cloning site (MCS) of pT-Adv vector used for subcloning of reamplified cDNA fragments. 51
Figure 2.12.2	The restriction map and multiple cloning site (MCS) of PCR [®] II-TOPO [®] vector used for subcloning of reamplified cDNA fragments 52
Figure 3.1.1	Confirmation of genotypes of PPAR α (+/+) and PPAR α (-/-) mice used for (A) 24 hours, (B) 1 week and (C) 2 weeks treatment. 63
Figure 3.1.2	Confirmation of genotypes of PPAR α (+/+) and PPAR α (-/-) mice used for (A) 6 months and (B) 11 months treatment. 64
Figure 3.2.1	Effect 6 months of 0.1% Wy-14643 treatment on body weight change (%) in PPAR α (+/+) and PPAR α (-/-) mice. 65
Figure 3.2.2	Effect of 11 months 0.1% Wy-14643 treatment on body weight change (%) in PPAR α (+/+) and PPAR α (-/-) mice. 66
Figure 3.3.1	Effect of 24 hours, 1 week, 2 weeks, 6 months and 11 months 0.1% Wy-14643 treatment on (A) liver morphology and (B) liver weights of PPAR α (+/+) and PPAR α (-/-) mice. 68
Figure 3.3.2	Effect of 24 hours, 1 week, 2 weeks, 6 months and 11 months 0.1% Wy-14643 treatment on (A) white fat morphology and (B) white fat weights of PPAR α (+/+) and PPAR α (-/-) mice. 71

		Page
Figure 3.3.3	Effect of 24 hours, 1 week, 2 weeks, 6 months and 11 months 0.1% Wy-14643 treatment on (A) brown fat morphology and (B) brown fat weights of PPAR α (+/+) and PPAR α (-/-) mice.	73
Figure 3.3.4	Effect of 24 hours, 1 week, 2 weeks, 6 months and 11 months 0.1% Wy-14643 treatment on (A) spleen morphology and (B) spleen weights of PPAR α (+/+) and PPAR α (-/-) mice.	75
Figure 3.4.1	Effect of 24 hours, 1 week, 2 weeks, 6 months and 11 months 0.1% Wy-14643 treatment on serum cholesterol level of PPAR α (+/+) and PPAR α (-/-) mice.	79
Figure 3.4.2	Effect of 24 hours, 1 week, 2 weeks, 6 months and 11 months 0.1% Wy-14643 treatment on serum triglyceride level of PPAR α (+/+) and PPAR α (-/-) mice.	80
Figure 3.5.1	Hematoxylin and eosin staining of the central vein region (20X) of liver sections (5 μ m) taken from PPAR α (+/+) and PPAR α (-/-) mice after 24 hours gavage feeding with 1% methylcellulose (control vehicle) (panels A, B) or Wy-14,643 (50 mg/kg bw) (panels C, D) (n=3).	81
Figure 3.5.2	Hematoxylin and eosin staining of the central vein region (40X) of liver sections (5 μ m) taken from PPAR α (+/+) and PPAR α (-/-) mice after 24 hours gavage feeding with 1% methylcellulose (control vehicle) (panels A, B) or Wy-14,643 (50 mg/kg bw) (panels C, D) (n=3).	82
Figure 3.5.3	Hematoxylin and eosin staining of the middle zone (20X) of liver sections (5 μ m) taken from PPAR α (+/+) and PPAR α (-/-) mice after 24 hours gavage feeding with 1% methylcellulose (control vehicle) (panels A, B) or Wy-14,643 (50 mg/kg bw) (panels C, D) (n=3).	83
Figure 3.5.4	Hematoxylin and eosin staining of the middle zone (40X) of liver sections (5 μ m) taken from PPAR α (+/+) and PPAR α (-/-) mice after 24 hours gavage feeding with 1% methylcellulose (control vehicle) (panels A, B) or Wy-14,643 (50 mg/kg bw) (panels C, D) (n=3).	84
Figure 3.5.5	Hematoxylin and eosin staining of the portal vein region (20X) of liver sections (5 μ m) taken from PPAR α (+/+) and PPAR α (-/-) mice after 24 hours gavage feeding with 1% methylcellulose (control vehicle) (panels A, B) or Wy-14,643 (50 mg/kg bw) (panels C, D) (n=3).	85
Figure 3.5.6	Hematoxylin and eosin staining of the portal vein region (40X) of liver sections (5 μ m) taken from PPAR α (+/+) and PPAR α (-/-) mice after 24 hours gavage feeding with 1% methylcellulose (control vehicle) (panels A, B) or Wy-14,643 (50 mg/kg bw) (panels C, D) (n=3).	86

		Page
Figure 3.5.7	Hematoxylin and eosin staining of the central vein region (20X) of liver sections (5 μ m) taken from PPAR α (+/+) and PPAR α (-/-) mice after 1 week treatment with a 0.0% Wy-14,643 (control diet) (panels A, B) or a 0.1% Wy-14,643 diet (panels C, D) (n=3).	88
Figure 3.5.8	Hematoxylin and eosin staining of the central vein region (40X) of liver sections (5 μ m) taken from PPAR α (+/+) and PPAR α (-/-) mice after 1 week treatment with a 0.0% Wy-14,643 (control diet) (panels A, B) or a 0.1% Wy-14,643 diet (panels C, D) (n=3).	89
Figure 3.5.9	Hematoxylin and eosin staining of the middle zone (20X) of liver sections (5 μ m) taken from PPAR α (+/+) and PPAR α (-/-) mice after 1 week treatment with a 0.0% Wy-14,643 (control diet) (panels A, B) or a 0.1% Wy-14,643 diet (panels C, D) (n=3).	90
Figure 3.5.10	Hematoxylin and eosin staining of the middle zone (40X) of liver sections (5 μ m) taken from PPAR α (+/+) and PPAR α (-/-) mice after 1 week treatment with a 0.0% Wy-14,643 (control diet) (panels A, B) or a 0.1% Wy-14,643 diet (panels C, D) (n=3).	91
Figure 3.5.11	Hematoxylin and eosin staining of the portal vein region (20X) of liver sections (5 μ m) taken from PPAR α (+/+) and PPAR α (-/-) mice after 1 week treatment with a 0.0% Wy-14,643 (control diet) (panels A, B) or a 0.1% Wy-14,643 diet (panels C, D) (n=3).	92
Figure 3.5.12	Hematoxylin and eosin staining of the portal vein region (40X) of liver sections (5 μ m) taken from PPAR α (+/+) and PPAR α (-/-) mice after 1 week treatment with a 0.0% Wy-14,643 (control diet) (panels A, B) or a 0.1% Wy-14,643 diet (panels C, D) (n=3).	93
Figure 3.5.13	Hematoxylin and eosin staining of the central vein region (20X) of liver sections (5 μ m) taken from PPAR α (+/+) and PPAR α (-/-) mice after 2 weeks treatment with a 0.0% Wy-14,643 (control diet) (panels A, B) or a 0.1% Wy-14,643 diet (panels C, D) (n=3).	94
Figure 3.5.14	Hematoxylin and eosin staining of the central vein region (40X) of liver sections (5 μ m) taken from PPAR α (+/+) and PPAR α (-/-) mice after 2 weeks treatment with a 0.0% Wy-14,643 (control diet) (panels A, B) or a 0.1% Wy-14,643 diet (panels C, D) (n=3).	95
Figure 3.5.15	Hematoxylin and eosin staining of the middle zone (20X) of liver sections (5 μ m) taken from PPAR α (+/+) and PPAR α (-/-) mice after 2 weeks treatment with a 0.0% Wy-14,643 (control diet) (panels A, B) or a 0.1% Wy-14,643 diet (panels C, D) (n=3).	96

		Page
Figure 3.5.16	Hematoxylin and eosin staining of the middle zone (40X) of liver sections (5 μ m) taken from PPAR α (+/+) and PPAR α (-/-) mice after 2 weeks treatment with a 0.0% Wy-14,643 (control diet) (panels A, B) or a 0.1% Wy-14,643 diet (panels C, D) (n=3).	97
Figure 3.5.17	Hematoxylin and eosin staining of the portal vein region (20X) of liver sections (5 μ m) taken from PPAR α (+/+) and PPAR α (-/-) mice after 2 weeks treatment with a 0.0% Wy-14,643 (control diet) (panels A, B) or a 0.1% Wy-14,643 diet (panels C, D) (n=3).	98
Figure 3.5.18	Hematoxylin and eosin staining of the portal vein region (40X) of liver sections (5 μ m) taken from PPAR α (+/+) and PPAR α (-/-) mice after 2 weeks treatment with a 0.0% Wy-14,643 (control diet) (panels A, B) or a 0.1% Wy-14,643 diet (panels C, D) (n=3).	99
Figure 3.5.19	Hematoxylin and eosin staining of the central vein region (20X) of liver sections (5 μ m) taken from PPAR α (+/+) and PPAR α (-/-) mice after 6 months treatment with a 0.0% Wy-14,643 (control diet) (panels A, B) or a 0.1% Wy-14,643 diet (panels C, D) (n=3).	101
Figure 3.5.20	Hematoxylin and eosin staining of the central vein region (40X) of liver sections (5 μ m) taken from PPAR α (+/+) and PPAR α (-/-) mice after 6 months treatment with a 0.0% Wy-14,643 (control diet) (panels A, B) or a 0.1% Wy-14,643 diet (panels C, D) (n=3).	102
Figure 3.5.21	Hematoxylin and eosin staining of the middle zone (20X) of liver sections (5 μ m) taken from PPAR α (+/+) and PPAR α (-/-) mice after 6 months treatment with a 0.0% Wy-14,643 (control diet) (panels A, B) or a 0.1% Wy-14,643 diet (panels C, D) (n=3).	103
Figure 3.5.22	Hematoxylin and eosin staining of the middle zone (40X) of liver sections (5 μ m) taken from PPAR α (+/+) and PPAR α (-/-) mice after 6 months treatment with a 0.0% Wy-14,643 (control diet) (panels A, B) or a 0.1% Wy-14,643 diet (panels C, D) (n=3).	104
Figure 3.5.23	Hematoxylin and eosin staining of the portal vein region (20X) of liver sections (5 μ m) taken from PPAR α (+/+) and PPAR α (-/-) mice after 6 months treatment with a 0.0% Wy-14,643 (control diet) (panels A, B) or a 0.1% Wy-14,643 diet (panels C, D) (n=3).	105
Figure 3.5.24	Hematoxylin and eosin staining of the portal vein region (40X) of liver sections (5 μ m) taken from PPAR α (+/+) and PPAR α (-/-) mice after 6 months treatment with a 0.0% Wy-14,643 (control diet) (panels A, B) or a 0.1% Wy-14,643 diet (panels C, D) (n=3).	106

		Page
Figure 3.5.25	Hematoxylin and eosin staining of the central vein region (20X) of liver sections (5 μ m) taken from PPAR α (+/+) and PPAR α (-/-) mice after 11 months treatment with a 0.0% Wy-14,643 (control diet) (panels A, B) or a 0.1% Wy-14,643 diet (panels C, D) (n=3).	107
Figure 3.5.26	Hematoxylin and eosin staining of the central vein region (40X) of liver sections (5 μ m) taken from PPAR α (+/+) and PPAR α (-/-) mice after 11 treatment with a 0.0% Wy-14,643 (control diet) (panels A, B) or a 0.1% Wy-14,643 diet (panels C, D) (n=3).	108
Figure 3.5.27	Hematoxylin and eosin staining of the middle zone (20X) of liver sections (5 μ m) taken from PPAR α (+/+) and PPAR α (-/-) mice after 11 months treatment with a 0.0% Wy-14,643 (panels A, B) or a 0.1% Wy-14,643 diet (panels C, D) (n=3).	109
Figure 3.5.28	Hematoxylin and eosin staining of the middle zone (40X) of liver sections (5 μ m) taken from PPAR α (+/+) and PPAR α (-/-) mice after 11 months treatment with a 0.0% Wy-14,643 (panels A, B) or a 0.1% Wy-14,643 diet (panels C, D) (n=3).	110
Figure 3.5.29	Hematoxylin and eosin staining of the portal vein region (20X) of liver sections (5 μ m) taken from PPAR α (+/+) and PPAR α (-/-) mice after 11 months treatment with a 0.0% Wy-14,643 (control diet) (panels A, B) or a 0.1% Wy-14,643 diet (panels C, D) (n=3).	111
Figure 3.5.30	Hematoxylin and eosin staining of the portal vein region (40X) of liver sections (5 μ m) taken from PPAR α (+/+) and PPAR α (-/-) mice after 11 months treatment with a 0.0% Wy-14,643 (control diet) (panels A, B) or a 0.1% Wy-14,643 diet (panels C, D) (n=3).	112
Figure 3.5.31	Hematoxylin and eosin staining of liver sections (5 μ m) taken from PPAR α (+/+) after 11 months treatment with a 0.1% Wy-14,643 diet (10X: panels A, B, C; 40X: panels D, E, F).	113
Figure 3.6.1	Preliminary screening for differential display patterns using non-fluorescent AP1 in combinations with ARP2, ARP3, ARP6, ARP10, ARP16 and ARP20.	115
Figure 3.6.2	Preliminary screening for differential display patterns using non-fluorescent AP2 in combinations with ARP1, ARP3, ARP10, ARP12, ARP16, ARP18 and ARP19.	116
Figure 3.6.3	Preliminary screening for differential display patterns using non-fluorescent AP3 in combination with ARP3.	117
Figure 3.6.4	Preliminary screening for differential display patterns using non-fluorescent AP5 in combinations with ARP1, ARP2, ARP3, ARP10, ARP12 and ARP18.	118

	Page
Figure 3.6.5	Preliminary screening for differential display patterns using non-fluorescent AP6 in combinations with ARP1, ARP4, ARP5, ARP8, ARP12 and ARP14. 119
Figure 3.6.6	Preliminary screening for differential display patterns using non-fluorescent AP7 in combinations with ARP10 and ARP15. 120
Figure 3.6.7	Preliminary screening for differential display patterns using non-fluorescent AP10 in combinations with ARP1, ARP6, ARP10, ARP12, ARP13 and ARP16. 121
Figure 3.6.8	Preliminary screening for differential display patterns using non-fluorescent AP11 in combinations with ARP1, ARP3, ARP5, ARP8, ARP12, ARP17, ARP19 and ARP20. 122
Figure 3.6.9	Preliminary screening for differential display patterns using non-fluorescent AP12 in combinations with ARP2. 123
Figure 3.7.1	Fluorescent differential display of gel AA performed with AP1 and ARP2. 126
Figure 3.7.2	Fluorescent differential display of gel AB performed with AP3 and ARP3. 127
Figure 3.7.3	Fluorescent differential display of gel AC performed with AP2 and ARP19. 128
Figure 3.7.4	Fluorescent differential display of gel AD performed with AP2 and ARP18. 129
Figure 3.7.5	Fluorescent differential display of gel AF performed with AP10 and ARP13. 130
Figure 3.7.6	Fluorescent differential display of gel AH performed with AP11 and ARP19. 131
Figure 3.7.7	Fluorescent differential display of gel AI performed with AP6 and ARP4. 132
Figure 3.7.8	Fluorescent differential display of gel AJ performed with AP6 and ARP14. 133
Figure 3.7.9	Fluorescent differential display of gel AL performed with AP7 and ARP15. 134
Figure 3.7.10	Fluorescent differential display of gel AO performed with AP5 and ARP10. 135
Figure 3.7.11	Fluorescent differential display of gel AP performed with AP12 and ARP2. 136
Figure 3.8.1	Reamplification of cDNA fragments excised from fluoroDD gel AA (AP1 and ARP2). 150
Figure 3.8.2	Reamplification of cDNA fragments excised from fluoroDD gel AB (AP3 and ARP3) Part I. 152
Figure 3.8.3	Reamplification of cDNA fragments excised from fluoroDD gel AB (AP3 and ARP3) Part II. 153
Figure 3.8.4	Reamplification of cDNA fragments excised from fluoroDD gels AC (AP2 and ARP19) and AD (AP2 and ARP18). 155
Figure 3.8.5	Reamplification of cDNA fragments excised from fluoroDD gel AF (AP10 and ARP13). 156

	Page
Figure 3.8.6	Reamplification of cDNA fragments excised from fluoroDD gels AH (AP11 and ARP19) and AI (AP6 and ARP4). 158
Figure 3.8.7	Reamplification of cDNA fragments excised from fluoroDD gels AJ (AP6 and ARP14), AL (AP7 and ARP15), AO (AP5 and ARP10) and AP (AP12 and ARP2). 159
Figure 3.9.1	<i>EcoRI</i> digested cDNA fragments excised from gel AA (AP1 and ARP2). 163
Figure 3.9.2	<i>EcoRI</i> digested cDNA fragments excised from gel AB (AP3 and ARP3) Part I. 165
Figure 3.9.3	<i>EcoRI</i> digested cDNA fragments excised from gel AB (AP3 and ARP3) Part II. 166
Figure 3.9.4	<i>EcoRI</i> digested cDNA fragments excised from gel AC (AP2 and ARP19). 168
Figure 3.9.5	<i>EcoRI</i> digested cDNA fragments excised from gels AD (AP2 and ARP18) and AF (AP10 and ARP13). 169
Figure 3.9.6	<i>EcoRI</i> digested cDNA fragments excised from gels AH (AP11 and ARP19) and AI (AP6 and ARP4). 170
Figure 3.9.7	<i>EcoRI</i> digested cDNA fragments excised from gel AJ (AP6 and ARP14). 171
Figure 3.9.8	<i>EcoRI</i> digested cDNA fragments excised from gels AL (AP7 and ARP15), AO (AP5 and ARP10) and AP (AP12 and ARP2). 174
Figure 3.10.1	Frequency of cDNA fragments matched to the same gene (no. of cDNA / total no. of cDNA fragments successfully sequenced X 100%). 194
Figure 3.11.1	Confirmation of fluoroDD expression pattern of subclone AA1#2 (peroxisomal delta 3, delta 2-enoyl-coenzyme A isomerase) by Northern blot analysis. 197
Figure 3.11.2	Confirmation of fluoroDD expression pattern of subclone AA4#9 (apolipoprotein A-V) by Northern blot analysis. 198
Figure 3.11.3	Confirmation of fluoroDD expression pattern of subclone AA10#1 (cysteine sulfinic acid decarboxylase) by Northern blot analysis. 199
Figure 3.11.4	Confirmation of fluoroDD expression pattern of subclone AA12#4 (acetyl-Coenzyme A dehydrogenase, medium chain) by Northern blot analysis. 200
Figure 3.11.5	Confirmation of fluoroDD expression pattern of subclone AB7#2 (UDP-glucuronyltransferase 2b5) by Northern blot analysis. 203
Figure 3.11.6	Confirmation of fluoroDD expression pattern of subclone AB22#9 (peroxisome biogenesis factor 16) by Northern blot analysis. 204
Figure 3.11.7	Confirmation of fluoroDD expression pattern of subclone AB25#6 (cytochrome P450, family 4, subfamily a, polypeptide 14) by Northern blot analysis. 205

		Page
Figure 3.11.8	Confirmation of fluoroDD expression pattern of subclone AC1#2 (serine protease inhibitor) by Northern blot analysis.	207
Figure 3.11.9	Confirmation of fluoroDD expression pattern of subclone AC2#2 (peroxisomal bifunctional enzyme) by Northern blot analysis.	208
Figure 3.11.10	Confirmation of fluoroDD expression pattern of subclone AD8#2 (cytochrome P450, family 4, subfamily a, polypeptide 10) by Northern blot analysis.	209
Figure 3.11.11	Confirmation of fluoroDD expression pattern of subclone AF1#8 (very long chain acyl-CoA synthetase) by Northern blot analysis.	211
Figure 3.11.12	Confirmation of fluoroDD expression pattern of subclone AF25#7 (mouse major urinary protein II) by Northern blot analysis.	212
Figure 3.11.13	Confirmation of fluoroDD expression pattern of subclone AJ1#5 (carboxylesterase) by Northern blot analysis.	213
Figure 3.11.14	Confirmation of fluoroDD expression pattern of subclone AJ2#10 (peroxisomal acyl-CoA oxidase) by Northern blot analysis.	214
Figure 3.11.15	Confirmation of fluoroDD expression pattern of subclone AL3#3 [hydroxysteroid (17-beta) dehydrogenase 11] by Northern blot analysis.	216
Figure 3.11.16	Confirmation of fluoroDD expression pattern of subclone AO1#2 (adipose differentiation related protein, ADFP) by Northern blot analysis.	217
Figure 3.11.17	Confirmation of fluoroDD expression pattern of subclone AO2#8 (carnitine O-octanoyltransferase) by Northern blot analysis.	218
Figure 3.11.18.	Up-regulation of GAPDH was observed in PPAR α (+/+) mice fed with a 0.1% (w/w) Wy-14,643 diet for 11 months.	220
Figure 3.11.19.	Confirmation of fluoroDD expression pattern of mitochondria by Northern blot analysis.	221
Figure 3.11.20.	Confirmation of fluoroDD expression pattern of EST by Northern blot analysis.	222
Figure 3.11.21	Temporal expression of AA1#2 (peroxisomal delta 3, delta 2-enoyl-coenzyme A isomerase).	224
Figure 3.11.22	Temporal expression of AA10#1 (cysteine sulfinic acid decarboxylase).	227
Figure 3.11.23	Temporal expression of AA12#4 (acetyl-Coenzyme A dehydrogenase, medium chain).	228
Figure 3.11.24	Temporal expression of AB7#2 (UDP-glucuronosyltransferase 2b5).	229
Figure 3.11.25	Temporal expression of AB22#9 (peroxisome biogenesis factor 16).	232

		Page
Figure 3.11.26	Temporal expression of AB25#6 (cytochrome P450, family 4, subfamily a, polypeptide 14).	233
Figure 3.11.27	Temporal expression of AC1#2 (serine protease inhibitor).	234
Figure 3.11.28	Temporal expression of AC2#2 (peroxisomal bifunctional enzyme).	235
Figure 3.11.29	Temporal expression of AD8#2 (cytochrome P450, family 4, subfamily a, polypeptide 10).	236
Figure 3.11.30	Temporal expression of AF1#8 (very long chain acyl-CoA synthetase).	239
Figure 3.11.31	Temporal expression of AF25#7 (mouse major urinary protein II).	240
Figure 3.11.32	Temporal expression of AJ1#5 (carboxylesterase).	242
Figure 3.11.33	Temporal expression of AJ2#10 (peroxisomal acyl-CoA oxidase).	243
Figure 3.11.34	Temporal expression of AL3#3 (hydroxysteroid (17-beta) dehydrogenase 11).	244
Figure 3.11.35	Temporal expression of AO1#2 (adipose differentiation related protein).	247
Figure 3.11.36	Temporal expression of AO2#8 (carnitine O-octanoyltransferase).	248
Figure 4.5.1.1	Peroxisome β -oxidation systems, inducible and non-inducible.	262
Figure 4.6.1	Summary of PPAR α dependent and Wy-14,643 responsive genes caused oxidation stress.	271

List of Tables

	Page
Table 1.1.1	Tissue distribution and physiological role of PPAR α , β & γ in rodents 4
Table 1.2.1	Natural and synthetic PPAR α ligands 7
Table 1.2.3.1	List of PPAR α regulated genes in liver 14
Table 2.10.1	The expected differential expression patterns of cDNA fragments displayed on non-fluoroDD and fluoroDD gels. 47
Table 3.3.1	Effect of Wy-14,643 feeding on kidney, heart, brain, lung and testis weight change of 24 hours, 1 week, 2 weeks, 6 months and 11 months feeding experiment. 77
Table 3.6.1	Combinations of anchored primers (APs) and arbitrary primers (ARPs) used for non-fluoroDD RT-PCR 124
Table 3.7.1	Summary of cDNA fragments excised from gel AA (AP1 and ARP2) 137
Table 3.7.2	Summary of cDNA fragments excised from gel AB (AP3 and ARP3) Part I 139
Table 3.7.3	Summary of cDNA fragments excised from gel AB (AP3 and ARP3) Part II 140
Table 3.7.4	Summary of cDNA fragments excised from gel AC (AP2 and ARP19) 141
Table 3.7.5	Summary of cDNA fragments excised from gel AD (AP2 and ARP18) 142
Table 3.7.6	Summary of cDNA fragments excised from gel AF (AP10 and ARP13) Part I 143
Table 3.7.7	Summary of cDNA fragments excised from gel AF (AP10 and ARP13) Part II 144
Table 3.7.8	Summary of cDNA fragments excised from gel AH (AP11 and ARP19) 145
Table 3.7.9	Summary of cDNA fragments excised from gel AI (AP6 and ARP4) 146
Table 3.7.10	Summary of cDNA fragments excised from gels AJ (AP6 and ARP14) and AL (AP7 and ARP15) 147
Table 3.7.11	Summary of cDNA fragments excised from gels AO (AP5 and ARP10) and AP (AP12 and ARP2) 148
Table 3.8.1	Summary of reamplified cDNA fragments excised from gel AA (AP1 and ARP2) 151
Table 3.8.2	Summary of reamplified cDNA fragments excised from gel AB (AP3 and ARP3) 154
Table 3.8.3	Summary of reamplified cDNA fragments excised from gels AC (AP2 and ARP19), AD (AP2 and ARP18) and AF (AP10 and ARP13) 157
Table 3.8.4	Summary of reamplified cDNA fragments excised from gels AH (AP11 and ARP19), AI (AP6 and ARP4) and AJ (AP6 and ARP14) 160

	Page
Table 3.8.5	Summary of reamplified cDNA fragments excised from gels AL (AP7 and ARP15), AO (AP5 and ARP10) and AP (AP12 and ARP2) 161
Table 3.9.1	Summary of cDNA fragments subcloned from gel AA (AP1 and ARP2) 164
Table 3.9.2	Summary of cDNA fragments subcloned from gel AB (AP3 and ARP3) 167
Table 3.9.3	Summary of cDNA fragments subcloned from gels AC (AP2 and ARP19) and AD (AP2 and ARP18) 172
Table 3.9.4	Summary of cDNA fragments subcloned from gels AF (AP10 and ARP13), AH (AP11 and ARP19), AI (AP6 and ARP4) and AJ (AP6 and ARP14) 173
Table 3.9.5	Summary of cDNA fragments subcloned from gels AL (AP7 and ARP15), AO (AP5 and ARP10) and AP (AP12 and ARP2) 175
Table 3.10.1	DNA sequences of cDNA fragments subcloned from gel AA (AP1 and ARP2) part I 178
Table 3.10.2	DNA sequences of cDNA fragments subcloned from gel AA (AP1 and ARP2) part II 179
Table 3.10.3	DNA sequences of cDNA fragments subcloned from gel AB (AP3 and ARP3) part I 180
Table 3.10.4	DNA sequences of cDNA fragments subcloned from gel AB (AP3 and ARP3) part II 181
Table 3.10.5	DNA sequences of cDNA fragments subcloned from gel AB (AP3 and ARP3) part III 182
Table 3.10.6	DNA sequences of cDNA fragments subcloned from gel AC (AP2 and ARP19) part I 183
Table 3.10.7	DNA sequences of cDNA fragments subcloned from gel AC (AP2 and ARP 19) part II 184
Table 3.10.8	DNA sequences of cDNA fragments subcloned from gel AC (AP2 and ARP19) part III 185
Table 3.10.9	DNA sequences of cDNA fragments subcloned from gel AD (AP2 and ARP18) 186
Table 3.10.10	DNA sequences of cDNA fragments subcloned from gel AF (AP10 and ARP13) 187
Table 3.10.11	DNA sequences of cDNA fragments subcloned from gels AF (AP10 and ARP13) and AH (AP11 and ARP19) 188
Table 3.10.12	DNA sequences of cDNA fragments subcloned from gel AI (AP6 and ARP4) 189
Table 3.10.13	DNA sequences of cDNA fragments subcloned from gel AJ (AP6 and ARP14) 190
Table 3.10.14	DNA sequences of cDNA fragments subcloned from gel AL (AP7 and ARP15) 191
Table 3.10.15	DNA sequences of cDNA fragments subcloned from gel AO (AP5 and ARP10) 192
Table 3.10.16	DNA sequences of cDNA fragments subcloned from gel AP (AP12 and ARP2) 193

		Page
Table 3.11.1	Summary of Northern blot analysis of cDNA fragments subcloned from gel AA (AP1 and ARP2)	201
Table 3.11.2	Summary of Northern blot analysis of cDNA fragments subcloned from gel AB (AP3 and ARP3)	206
Table 3.11.3	Summary of Northern blot analysis of cDNA fragments subcloned from gels AC (AP2 and ARP19) and AD (AP2 and ARP18)	210
Table 3.11.4	Summary of Northern blot analysis of cDNA fragments subcloned from gels AF (AP10 and ARP19) and AJ (AP6 and ARP14)	215
Table 3.11.5	Summary of Northern blot analysis of cDNA fragments subcloned from gels AL (AP7 and ARP15) and AO (AP5 and ARP 10)	219
Table 3.11.6	Summary of Northern blot analysis on temporal expression patterns of cDNA fragments subcloned from gel AA (AP1 and ARP2)	225
Table 3.11.7	Summary of Northern blot analysis on temporal expression patterns of cDNA fragments subcloned from gel AB (AP3 and ARP3)	230
Table 3.11.8	Summary of Northern blot analysis on temporal expression patterns of cDNA fragments subcloned from gels AC (AP2 and ARP19) and AD (AP2 and ARP18)	237
Table 3.11.9	Summary of Northern blot analysis on temporal expression patterns of cDNA fragments subcloned from gel AF (AP10 and ARP 13)	241
Table 3.11.10	Summary of Northern blot analysis on temporal expression patterns of cDNA fragments subcloned from gels AJ (AP6 and ARP14) and AL (AP7 and ARP15)	245
Table 3.11.11	Summary of Northern blot analysis on temporal expression patterns of cDNA fragments subcloned from gel AO (AP5 and ARP10)	249
Table 4.5.1	List of PPAR α regulated genes in liver (with the genes identified in this project)	256

Chapter 1 Literature review

Peroxisome proliferator activated receptor (Aldridge *et al.*) was first cloned from mouse liver in 1990 (Issemann and Green, 1990). There are three isoforms: PPAR α , PPAR δ (also known as NUC1 and PPAR β), and PPAR γ . Among the three isoforms, PPAR α is involved in lipid metabolism (Dreyer *et al.*, 1993), short-term peroxisome proliferator-induced pleiotropic responses (Lee *et al.*, 1995) and long-term hepatocarcinogenesis (Peters *et al.*, 1997). Identification of the genes that regulated by PPAR α and affected by peroxisome proliferators can help us to understand more about the mechanism(s) of peroxisome proliferator-induced liver cancer. Monitoring the early expression of peroxisome proliferators-responsive and PPAR α -dependent genes can be useful to prevent the induction of cancer by new peroxisome proliferator chemical.

1.1 Peroxisome proliferator activator receptors

Peroxisome proliferator activated receptors (PPARs) are belonging to the large steroid/retinoid nuclear receptor family which has a common modular structure. It consists of six functional domains, defined as A and B (transactivation), C (DNA-binding), and D, E, and F (ligand-binding, dimerization and transactivation) (Motojima, 1993; Mangelsdorf *et al.*, 1995; Kota *et al.*, 2005). The A and B domains

are ligand-independent transcriptional activation domains (activation function-1) (Werman *et al.*, 1997; Kota *et al.*, 2005). They are active in some cell types and responsible for phosphorylation of PPAR. The C domain that is DNA-binding domain (DBD) consisting of two zinc finger DNA binding motifs. The DNA-binding domain promotes the binding of PPAR to the PPRE in the promoter region of target genes. The D domain is the docking region for cofactors. The E domain (LBD) is responsible for ligand specificity and activation of PPAR binding to the PPRE that increases the target gene expressions. Modulators of transcription such as coactivators and corepressors interact with ligand-dependent activation function 2 (AF-2), which located in the E/F domain .

PPARs heterodimerize with the retinoid X receptors (RXRs) and bind to the PPRE of target genes. *In vitro*, when the PPARs and RXRs present at high concentrations, they will heterodimerize, but stimulation by ligands are required at the lower concentrations of the receptors in cells (Forman *et al.*, 1997; Kliewer *et al.*, 1997). The heterodimer binds to a consensus motif named peroxisome proliferator response element (PPRE), which most commonly consisting of the hexad [A/G]GGTCA directly repeated with a one nucleotide spacer (DR-1 elements) (Kliewer *et al.*, 1992). It is reported that PPARs also bind other sites such as DR-2 elements (Everett *et al.*, 2000). PPAR-RXR heterodimers interacting at a PPRE can

respond to either PPs or the RXR ligand, 9-*cis*-retinoic acid. Some retinoids can activate the PPAR-RXR heterodimer through binding RXRs. They exhibit peroxisome proliferation and induction of the enzymes that involved in β -oxidation of fatty acids, which is induced by peroxisome proliferators. PPARs cannot bind to the PPREs of the target genes without interacting with the RXR to form the heterodimer (Gearing *et al.*, 1993; Keller *et al.*, 1993). PPRE is identified in the 5' upstream regions of several target genes and as an almost perfect direct repeat of the sequence TG(A/T)CCT separated by one base pair in the genes of the peroxisomal acyl CoA oxidase (AXO), bi-functional enzyme (PBFE), and thiolase, the microsomal CYP4A subfamily and the cytosolic L-FABP (Lee *et al.*, 1995).

To date, there are three major types of PPAR have been identified: PPAR α , PPAR β/δ and PPAR γ which perform different physiological functions based on their tissue-specific expression (Table 1.1.1). PPAR α is highly expressed in liver, kidney, muscle and fat body in rodents (Kliwer *et al.*, 1994; Braissant and Wahli, 1998). However, the level of PPAR α expression in humans is lower than in rodents (Palmer *et al.*, 1998) and higher levels in heart, kidney, skeletal muscle and large intestine kidney and muscle (Mukherjee *et al.*, 1997). PPAR α regulates the fatty acid metabolism through stimulating peroxisomal and mitochondrial β -oxidation and microsomal ω -oxidation. PPAR α also involves in detoxification of endogenous and

Table 1.1.1. Tissue distribution and physiological role of PPAR α , β & γ in rodents

Isoforms	Tissue distribution	Physiological role
α	Liver, kidney, muscle and adipose tissue	Lipid metabolism Regulation of inflammation Detoxification of endogenous and exogenous chemicals
β/δ	Expressed ubiquitously	Embryo implantation Decidualization
γ	Adipose tissue, spleen, intestine	Adipocyte differentiation Regulation of inflammation

exogenous active molecules, some of which may be PPAR ligands (Beck *et al.*, 1992) and down-regulates inflammatory responses (Devchand *et al.*, 1996; Staels *et al.*, 1998). PP-induced pleiotropic responses shown in recombinant adenovirus that expresses human and mouse PPAR α indicated that human PPAR α is functionally competent and is equally as dose-sensitive as mouse PPAR α in inducing peroxisome proliferation (Yu *et al.*, 2001). PPAR β/δ is ubiquitously expressed in both rodents and humans and it is expressed at low level in liver and kidney (Kliwer *et al.*, 1994; Braissant *et al.*, 1996). The physiological function of PPAR β/δ is not yet well defined, previous reports have mentioned that it is involved in embryo implantation and decidualization (Lim *et al.*, 1999). PPAR γ exists in two distinct isoforms PPAR γ 1 and PPAR γ 2, which PPAR γ 1 is expressed in liver but expressed in lower levels in adipose tissue and PPAR γ 2 is expressed in adipose tissue and is a potent regulator of adipocyte differentiation. It is also expressed in macrophages, fat-storing cells such as hepatic stellate cells, liver, lung, kidney, placenta and colon. The expression of PPAR γ in liver is at higher level in human when compared with that in rodent (Tugwood *et al.*, 1996). PPAR γ inhibits angiogenesis and inflammatory processes, plays a role in adipocyte differentiation and regulates adipocyte-specific gene expression (Tontonoz *et al.*, 1994; MacDougald and Lane, 1995).

PPAR α is qualitatively and quantitatively different between rodent and human.

The levels of PPAR α mRNA and DNA binding activity are considerably lower in human liver samples than in rat liver. There is sequence variation of the human PPAR α that results in a truncated protein incapable of binding DNA that makes up 10-40% of human PPAR mRNA in liver. It is reported that human liver contains a functionally active PPAR α , however, the human PPAR α is expressed only about 10% of that in mouse liver, and extracts from human liver contain little PPAR α that can bind to a PPRE (Palmer *et al.*, 1998). Sequence variant of PPAR (hPPAR6/29) that varies at three residues from the first cloned sequences is also found. This sequence variant can bind DNA but is not activated by PPAR ligands, which plays a role as dominant negative suppressor.

1.2 Peroxisome proliferators

Peroxisome proliferators (PPs) are the group of chemicals which stimulate proliferation of peroxisomes. They consist of a broad spectrum of chemicals with little structural similarity, except for the presence of an aromatic ring, carboxylic acid and aliphatic chain. Most peroxisome proliferators are amphipathic molecules containing a hydrophobic backbone (aliphatic or aromatic) linked to an acidic function, which is essential for ligand activity. (Corton *et al.*, 2000).

This group of chemicals (Table 1.2.1) include naturally occurring steroids such

Table 1.2.1. Natural and synthetic PPAR α ligands

Natural ligands	
Saturated fatty acids	Palmitic (16:0) Stearic (18:0)
Monounsaturated fatty acid	Palmitoleic (16:1) Oleic (18:1) Elaidic (20:1)
Polyunsaturated fatty acids	Linoleic (18:2, n-6) Arachidonic (20:4, n-3) Eicosapentaenoic (22:5, n-3) Docosahexaenoic (22:6, n-3)
Eicosanoids	Prostaglandins A1 Leukotriene B4
Synthetic ligands	
Plasticizers	DEHP DBP DEHA
Industrial solvent	Trichloroethylene
Herbicides	Lactofen Fomasafen Haloxypop
Hypolipidemic drugs	Clofibric acid Fibrates Wy-14,643

as dehydroepiandrosterone (DHEA) (Frenkel *et al.*, 1990), fatty acid such as including palmitic acid, oleic acid, linoleic acid and arachidonic acid (Gottlicher *et al.*, 1992) and ecosanoids (Forman *et al.*, 1997) such as the inflammatory mediator leukotriene B₄ (Devchand *et al.*, 1996).

PP also includes some synthetic compounds (Table 1.2.1) such as di(2-ethylhexyl)phthalate (DEHP) (Okita and Chance, 1984) which has been listed by the International Agency for Research on Cancer (IARC) and by the National Toxicology Program as a possible or reasonably anticipated human carcinogen because it induces dose-related increases in liver tumors in both sexes of rats and mice (IARC, 1982; Melnick, 2001) and di-(2-ethylhexylexyl)adipate (DEHA) (Bell, 1983). Hypolipidemic drugs such as clofibrate (Reddy and Qureshi, 1979), Wy-14,643 [4-chloro-6(2,3-xylidino)-2-pyrimidinyl-thio] acetic acid (Reddy and Krishnakantha, 1975) and nafenopin also have marked hepatomegalic and peroxisome-proliferative properties. Chronic nafenopin treatment developed hepatocellular carcinomas, some of which metastasized to the lungs in acatalasemic mice (Reddy *et al.*, 1976). Other synthetic peroxisome proliferators include herbicides such as lactofen (1'[carboethoxy]ethyl 5-[2-chloro-4-[trifluoro-methyl] phenoxy]-2-nitrobenzoate) which induces liver tumor in mice, pure and technical grade lactofen appear to induce murine liver tumors through a mechanism similar to epigenetic hepatocarcinogens of

the peroxisome proliferating type (Butler *et al.*, 1988), fomesafen that causes peroxisome-related tumours in the mouse, man is neither susceptible nor sensitive to this mechanism (Smith and Elcombe, 1989) and haloxyfop [2-(4-((3-chloro-5-(trifluoromethyl)-2-pyridinyl)oxy)phenoxy)propanoic acid] . Ingestion of haloxyfop by rats and/or mice (0.1-14 mg/kg/day for 2 to 4 weeks) resulted in significant dose-related PP as evidenced by hepatocellular hypertrophy, increased peroxisome volume density (VD) and induction of peroxisomal enzymes and CYP4A1 (Stott *et al.*, 1995). Trichloroethylene (TCE) is an industrial solvent and a widespread environmental contaminant and identified as a weak PP (Zhou and Waxman, 1998; Laughter *et al.*, 2004).

Peroxisome proliferators may activate PPARs by binding directly to the receptor or indirectly to generate PPAR ligands by perturbing lipid metabolism (Corton *et al.*, 2000). Peroxisome proliferators may act indirectly by increasing the level of the free fatty acids as some peroxisome proliferators can bind to liver fatty-binding protein and displace fatty acids such as oleic acid (Green, 1995).

1.2.1 Hepatomegaly

Treatment with PP results in rodents in pleiotropic responses, one of the morphological changes is hepatomegaly. A histological method utilizing the optical

dissector principle indicated that the hepatomegaly induced by the peroxisome proliferator gemfibrozil is a combination effect of hypertrophy and hyperplasia (Carthew *et al.*, 1998). Treatment with clofibrate, nafenopin, tiburic acid and Wy-14,643 produced a marked hepatomegaly in the mice. The increase in liver weight correlated well with the increase in total hepatic DNA and in the collective volume of hepatocyte peroxisomes (Moody and Reddy, 1978). Treatment with different peroxisome proliferators, including clofibrate, ciprofibrate, nafenopin, gemfibrozil, Wy-14,643, DEHP and DEHA at carcinogenic doses on male F-344 rats for 1 week shown a close correlation between relative liver weights and hepatocarcinogenicity ($r = 0.910$). (Takagi *et al.*, 1992). This suggested that the hepatomegaly may be an early biomarker for prediction of the potential hepatocarcinogenicity of peroxisome proliferators. A strong correlation between the animal thyroid status and both hepatocyte proliferation ($r^2 = 0.62$) and hepatocyte surface area ($r^2 = 0.83$) suggested that the thyroid status of the animal was important in PPAR α -mediated hepatocellular proliferation and liver cell enlargement (Wang *et al.*, 2004). Treatment with clofibrate and Wy-14,643 did not result in significant hepatomegaly in the PPAR α (-/-) mice when compare with the untreated PPAR α (+/+) mice (Lee *et al.*, 1995). This indicated that the PP-induced hepatomegaly is mediated by PPAR α .

1.2.2 Peroxisome proliferation

Peroxisome proliferation means the increase in both the sizes and the number of peroxisomes and is induced by peroxisome proliferators such as clofibrates and Wy-14,643. High fat diets, starvation and cold temperatures may also stimulate peroxisome proliferation (Gonzalez, 1997). Peroxisome proliferation has been reported to be strongly associated with but not causally to tumour formation (Green, 1995). Di(2-ethylhexyl) adipate (DEHA) is a strong peroxisome proliferator but weakly carcinogenic. It is reported that the peroxisome proliferator such as DEHA may only partially activate peroxisome proliferators-activated receptors (PPARs) while some chemicals may fully activate PPARs. Chemicals, which stimulate only part of the receptor's activity will cause peroxisome proliferation while complete activation is required to stimulate tumourigenesis. Peroxisome proliferation is also proposed as a biomarker of exposure to a variety of pollutants in the environmental pollution assessment (Cajaraville *et al.*, 2003).

It is suggested that the PP-induced peroxisome proliferation was due to the increase in rate of transcription of genes encoding peroxisomal fatty acid β -oxidation enzymes. The increase in level of mRNA of specific genes will lead to increase in expression of specific protein that will accumulate within smooth membrane channels and result in peroxisome proliferation (Dzhekova-Stojkova *et al.*, 2001).

PP-induced peroxisome proliferation is not observed in PPAR α (-/-) mice with the administration of classical peroxisome proliferators, clofibrate and Wy-14,643. It indicates that PPAR α is the major isoform required for mediating PP-induced peroxisome proliferations (Lee *et al.*, 1995). PPAR α -humanized mice shown induction of genes involved in peroxisomal and mitochondrial fatty acid metabolism and resultant decrease of serum triglycerides upon treatment with Wy-14,643. However, hepatocellular proliferation was not observed in PPAR α -humanized mice. This suggested that the PPAR α -mediated pathways controlling lipid metabolism are independent from those controlling the cell proliferation pathways (Cheung *et al.*, 2004).

1.2.3 Target genes regulation

Induction of enzymes that involved in peroxisomal and mitochondrial β -oxidation and microsomal ω -oxidation of fatty acids is observed after administration of peroxisome proliferators. For peroxisomal β -oxidation, induction of acyl coenzyme A (acyl-CoA) oxidase (AXO), bifunctional enzymes (PBFE) and 3-ketoacylCoA thiolase (thiolase) that located in the peroxisomal matrix are induced with the administration of peroxisome proliferators and they are direct targets of PPAR α (Desvergne and Wahli, 1999). The fold of induction of AXO, BIEN and

thiolase is about 10- to 30-fold, whereas catalase and urate oxidase activities are increased 2- to 3-fold (Reddy *et al.*, 1986; Nemali *et al.*, 1988; Nemali *et al.*, 1989).

Soluble epoxide hydrolase (sEPHX) is also induced in rat liver with the peroxisomal β -oxidation by peroxisome proliferators with 5- to 10-fold increase (Grant *et al.*, 1993). Dramatic increases in the activities of other peroxisomal enzymes, such as carnitine acetyltransferase and carnitine octanoyltransferase also occur in the livers. PPAR α further regulates the mitochondrial β -oxidation by modulating the expression of medium-chain acyl-CoA dehydrogenase (MCAD) gene (Desvergne and Wahli, 1999). The microsomal p450 4A family (Cyp4a1, 4a2 and 4a3) that involved in the ω -hydroxylation is induced upon the treatment with peroxisome proliferators and with 2- to 5-fold induction (Reddy and Mannaerts, 1994).

PPAR α also mediates the expressions of genes that involved in other metabolisms including biotransformation, ketogenesis, fatty acid activation, fatty acid binding and transport, lipoprotein metabolism, lipogenesis, inflammation, triglyceride clearance, gluconeogenesis, phospholipids secretion, cholesterol catabolism and amino acid metabolism (Mandard *et al.*, 2004) (Table 1.2.3.1).

There are sequence variations in PPAR target genes that alter the response to peroxisome proliferators. For example, human acyl-CoA oxidase promoter is

Table 1.2.3.1. List of PPAR α regulated genes in liver

Function of gene	Genes	
Amino acid metabolism	Alanine aminotransferase	
	Alanine glyoxylate transaminase	Cytosolic aspartate aminotransferase
	Arginase	Glutaminase
	Arginino-succinate lyase	Hydroxypyruvate/ glyoxylate reductase
	Arginino-succinate synthase	Mitochondrial aspartate aminotransferase
	Carbamoyl-phosphate synthase-I	Ornithine transcarbamoylase
Acute phase response	Alpha-1 acid glycoprotein/serine protease inhibitor	Fibrinogen
Bile acid metabolism	Cytochrome P450 7A1	
Bile salt transport	Na ⁺ taurocholate cotransporting polypeptide	
Biotransformation	Aldehyde dehydrogenase type 3	Glutathione-S-transferase alpha
	Cytochrome P450 2A5	Cytochrome P450 3A11
	Cytochrome P450 2C29	UDP-glycuronosyltransferase 1A9
	Cytosolic epoxide hydrolase	
Cell cycle	c-myc	Cyclin D1
Cell cycle regulation	G0/G1 switch gene 2	
Cellular proliferation	glucose-regulated protein-94	
Cholesterol metabolism	Cytochrome P450 12A1	Liver X receptor α
	Cytochrome P450 27A1	
Cholesterol transport	ABCA-a (via LXR α)	ABCG-8 (via LXR α)
	ABCG-5 (via LXR α)	
Desaturation of fatty acid	Delta-6-Desaturase	Stearoyl-CoA desaturase
	Delta-5-desaturase	
Fatty acid activation	Long-chain acyl-CoA synthetase	
Fatty acid binding/transport	Cytosolic fatty acid binding protein	
Fatty acid transport	Fatty acid transport protein-1	Fatty acid translocase
Fatty acid β -oxidation	Acyl-CoA oxidase	Medium-chain acyl-CoA dehydrogenase
	ATP-binding cassette half-transporter type 2	Long-chain acyl-CoA dehydrogenase
	ATP-binding cassette half-transporter type 3	Short-chain-specific 3-ketoacyl-CoA thiolase
	Bifunctional enzyme	Short-chain acyl-CoA
	Carnitine palmitoyl-transferase I	Sterol carrier protein-X
	Carnitine palmitoyl-transferase II	Thiolase B
	Dodecenoyl-CoA delta-isomerase	Very long chain acyl-CoA dehydrogenase
	Cytochrome P450 4A1	Cytochrome P450 4A10
	Cytochrome P450 4A3	Cytochrome P450 4A14
Fatty acid ω -hydroxylation	Cytochrome P450 4A6-Z	
Fatty acid synthesis	Malic enzyme	
Fatty acyl-CoA ester transport	Acyl-CoA binding protein	
Gluconeogenesis	Lactate dehydrogenase A4	

Table 1.2.3.1. List of PPAR α regulated genes in liver (con't)

Function of gene	Genes	
Glucose oxidation	Pyruvate dehydrogenase kinase isoform 4	
Heme biosynthesis	Coproporphyrinogen oxidase	
Hepatic sterol	Farnesoid X receptor/Bile acid receptor	
Hepatobiliary lipid transport	Multidrug resistance 2	
Hydrolysis of Acyl-CoA	Cytosolic acyl-CoA thioesterase-I	Peroxisomal acyl-CoA thioesterase 1A
	Cytosolic acyl-CoA thioesterase-II	Peroxisomal acyl-CoA thioesterase 1B
	Mitochondrial acyl-CoA thioesterase-I	Peroxisomal acyl-CoA thioesterase 2
Iron-binding protein	Lactoferrin	
Inflammation/ apoptosis	I κ B α	
Iron transport	Transferrin	
Ketogenesis	Mitochondrial HMG-CoA synthase	Mitochondrial HMG CoA synthase
Oxygen-free radical metabolism	Superoxide dimutase	
Plasma HDL metabolism	Apolipoprotein-AI	Apolipoprotein-AV
	Apolipoprotein-A I (via rev-erb α)	Apolipoprotein-CIII
	Apolipoprotein-AII	Phospholipid transfer protein
	Apolipoprotein-A IV	Scavenger receptor B-type I
Pheromone carrier	Alpha-2 urinary globulin/MUP-I	
Repressor of gene transcription	Rev-erb α	
ROS production	Uncoupling protein-2	
Triglyceride clearance	Lipoprotein lipase	
Steroid metabolism	11-beta-Hydroxysteroid dehydrogenase I	17-beta-hydroxysteroid dehydrogenase IV
Steroid hydroxylase	Cytochrome P450 2C11	Cytochrome P450 2C12
Vascular inflammation	Interleukin-6	Interleukin-6 receptor
	Interleukin-1 receptor-type 1	

differed from the rat sequence, which leads to the unresponsive of PPAR α in transfection studies. On the other hand, the apoAI promoter in humans is responsive to fibrates whereas it is unresponsive for rat promoter as it is differed at three nucleotides. It is reported that PPAR α is active in human liver as the human promoter has been shown to respond to fibrates in transgenic animals. This indicates that the responses to peroxisome proliferators between species differs quantitatively and qualitatively (Everett *et al.*, 2000).

1.2.4 Hypolipidemic effect

Numerous research suggested the causative relationship between dyslipidemia and coronary artery disease (CAD). Hypercholesterolemia (high LDL-cholesterol levels), hypoalphalipoproteinemia (low plasma HDL) and hypertriglyceridemia are considered as the risk factors (alone or combined) for CAD (Gervois *et al.*, 2000). Fibrates are the first efficient and widely used lipid-lowering drugs to be used for the treatment of dyslipidemia. High doses (300-1200 mg/day) of fibrates were suggested to achieve efficacious lipid-lowering activity in human (Berger and Moller, 2002). Clofibrate (ethyl- α -p-chlorophenoxyisobutyrate) is probably the most widely used hypolipidemic drug and believed to be low in toxicity (Havel and Kane, 1973).

PPAR α mediates the hypolipidemic action of hypolipidemic drugs (e.g. fibrate

and Wy-14,643) in the treatment of hypertriglyceridemia and hypoalphalipoproteinemia (low plasma HDL). The main effect of the hypolipidemic drugs is to lower the triglyceride and cholesterol levels in the plasma (Isseman and Green, 1990). The hypolipidemic effect of the peroxisome proliferators is the enhancement of catabolism of plasma triglyceride-rich lipoprotein due to a decrease in plasma apolipoprotein C-III through the suppression of the apolipoprotein C-III gene expression (Hertz *et al.*, 1995). Gene expression of the lipoprotein lipase, which is important in triglyceride metabolism, is also induced with the treatment of hypolipidemic drugs (Desvergne and Wahli, 1999; Yamazaki *et al.*, 2002). The induction of expression of lipoprotein lipase and increase accessibility of TG-rich lipoprotein particles for lipolysis due to reduced TG-rich lipoprotein apo C-III content will lead to the induction of lipoprotein lipolysis.

PPAR α also upregulates HDL that is inversely correlated with the incidence of CAD. It is suggested that HDL play a role from removing and recycling of cholesterol excess from peripheral tissues to liver. The upregulation of HDL is related to the changes in Apo A-I and Apo A-II. However, the responsive was of Apo A-I and Apo A-II in rodents and human are opposite with the application of peroxisome proliferators. Apo A-I and Apo A-II gene transcription is induced in human while their gene transcription is repressed in rodents (Gervois *et al.*, 2000).

Hepatic and cardiac lipid accumulation is observed in the PPAR α (-/-) mice as a result of specific inhibition of mitochondrial fatty acid import.

PPAR α , which also mediates the lipid metabolism, upregulates the gene expression of enzymes involved in conversion of fatty acids in acyl-CoA esters, fatty acid entry into mitochondria and peroxisomal and mitochondrial fatty acid catabolism (Gervois *et al.*, 2000). These results in the limitation of hepatic TG synthesis and very low density lipoprotein VLDL production.

1.2.5 Hepatocarcinogenesis

Long term administration (11 months) of Wy-14,643 leads to multiple hepatocellular neoplasms, including adenomas and carcinomas (Reddy and Qureshi, 1979; Peters *et al.*, 1997). The hepatocarcinogenicity of peroxisome proliferators must be nongenotoxic mechanisms as they will not cause DNA damage directly (von Daniken *et al.*, 1981). It is reported that there is correlation between the ability of a PP to bind to and/or activate PPAR α and the potency of the PP as an inducer of hepatocarcinogenesis. The strongest inducers of hepatocarcinogenesis, Wy-14,643, binds strongly to PPAR α and activates PPAR α to high levels. In contrast, bezafibrate is a relatively weak hepatocarcinogen and, binds and activates PPAR α weakly (Krey *et al.*, 1997).

The hepatocarcinogenesis induced by PPs is a multistage process consisting of hepatocellular hyperplasia and formation of altered hepatocellular foci, adenoma, and carcinoma. This process is reversible before the formation of carcinoma. The progression of PP-induced foci to hepatocellular adenomas requires continual exposure of PPs. Regression of the lesions (decrease proliferation and increase apoptosis) are observed after PP withdrawal (Marsman and Popp, 1994). After removal of nafenopin for five weeks, there is a 20% reduction in the number of hepatocytes in noninvolved tissue and 85% reduction of cells in foci, adenomas, and carcinomas. The data indicates that continual activation of PPAR α is necessary for the growth and maintenance of initiated cells in foci, adenomas and carcinomas in the liver of PP-treated rodents (Peters *et al.*, 1997; Kitamura *et al.*, 1999).

Some studies suggested that peroxisome proliferators act as tumour promoters rather than tumour initiators (Cattley *et al.*, 1989; Cattley and Popp, 1989) and these chemicals act upon spontaneously initiated lesions to produce tumours (Cattley *et al.*, 1991; Kraupp-Grasl *et al.*, 1991; Green, 1995). The carcinogenicity of DEHP and Wy-14,643 are related to sustained DNA replication, which induce tumours by influencing the growth of initiated lesion. DEHA and Wy-14,643 are more effective promoting agents in old rats compared with young rats. Since the number of preneoplastic hepatic foci is greater in the older rats, it is suggested that peroxisome

proliferators promote the growth of these 'spontaneously' initiated cells. Identifying any peroxisome proliferator regulated genes that are relevant to the growth of hepatocytes will provide support for this model.

It is reported that there are species differences in response to peroxisome proliferators. PP-induced pleiotropic responses (hepatic hypertrophy, peroxisome proliferation and hepatocellular carcinoma) occurred in rodents are not observed in human and primates. Gemfibrozil and fibrates, hypolipidemic drugs used for many years, however, no evidence of elevated peroxisomes and increased liver cancer have shown in the patients (Peters *et al.*, 1997; Everett *et al.*, 2000).

1.3 Mode of actions

Long term (11 months) administration of peroxisome proliferators will cause liver cancer. However, peroxisome proliferators are not directly mutagenic or genotoxic, the mechanism(s) of peroxisome proliferators induced liver is/are not yet confirmed. Many evidences suggest that hepatocarcinogenesis is a multifactorial process consisting of sustained oxidative stress, inhibition of apoptosis and increased cellular proliferation (alteration of cell cycle control).

1.3.1 Oxidative stress

The increase in peroxisomal fatty acid β -oxidation due to administration of peroxisome proliferators (both short-term and long-term) results in a greater production of hydrogen peroxide. The first enzyme in the peroxisomal β -oxidation, acyl-CoA oxidase, generates H_2O_2 during the first step of β -oxidation. However, peroxisomal catalase, which is responsible for the detoxification of hydrogen peroxide, is increased less than 2- to 3-fold (Nemali *et al.*, 1989). The increase in peroxisomal β -oxidation but no induction in catalase will result in an increase in H_2O_2 levels (oxidation stress). This effect is mediated by PPAR α as treatment with anti-oxidants can reduce the incidence of tumor formation in rats, which exposed to peroxisome proliferators chronically (Rao *et al.*, 1984).

Excess H_2O_2 can cause DNA damage through formation of adducts such as 8-hydroxyguanine or strand breaks and possibly tumour initiation. 8-Hydroxydeoxyguanosine (8-OH-dG) is a frequently used marker of DNA damage produced by oxygen radicals. It is observed that PPs increase 8-OH-dG levels in livers of treated rodents, but there is no clear link between the observed increase and carcinogenesis (Sausen *et al.*, 1995).

Hypolipidemic drugs such as fibrates have been used for many years, however, no evidence of elevated increased liver cancer have shown in the patients (Peters *et al.*,

1997; Everett *et al.*, 2000). This may be due to the activity of catalase in rodents is located primarily in the peroxisome, whereas it is mainly in the cytoplasm in humans, which make humans have greater protection against oxidative stress.

1.3.2 Inhibition of apoptosis

Apoptosis is one of the defense mechanism against neoplastic transformation. Inhibition of apoptosis is observed with the administration of peroxisome proliferators. Nafenopin and Wy-14,643 inhibit transforming growth factor- β 1-induced apoptosis in vitro (Bayly *et al.*, 1994). This interferes the eliminations of cells with damaged or mutated DNA. The inhibition of apoptosis is mediated by PPAR α since inhibition of apoptosis by the PPAR α ligand nafenopin can be blocked by a dominant negative form of the receptor (James *et al.*, 1998).

1.3.3 Cell proliferation

PP-induced increase in cell-proliferation is observed within 48 hours of PP treatment. With chronic Wy-14,643 treatment, cell proliferation is sustained whereas cell proliferation in the liver returns to control levels with weaker PPs e.g. nafenopin. The early increase in cell replication induced by PPs can increase the frequency of spontaneous mutations, which can be fixed by further rounds of cell division or clonal

expansion (Ashby *et al.*, 1994).

1.3.4 Alterations in cell cycle control

It is suggested that peroxisome proliferators will cause alterations in cell cycle control, which might contribute to underlying mechanism of peroxisome proliferator-induced carcinogenesis including inhibition in apoptosis, increase in DNA synthesis and cell replication and alterations in cell division in liver (Marsman *et al.*, 1988).

1.4 Objectives

In order to study the carcinogenic effect of peroxisome proliferator, Wy-14,643, a potent peroxisome proliferator and hyperlipidemic drug, was selected for the study. It is reported that the treatment of Wy-14,643 will lead to liver cancer in rodents after 1 year treatment, 11 months treatment was performed to identify the PPAR α dependent and peroxisome proliferator-responsive genes at the tumor stage. As the mechanism(s) of PP-induced hepatocarcinogenesis is/are still not clear, identification of the genes that are PPAR α and Wy-14,643 responsive can help to explain the mechanism(s). In order to identify the PPAR α -dependent and Wy-14,643-responsive genes that are at the tumor stage, Wy-14,643 was selected for 11 months treatment of the PPAR α (+/+) and PPAR α (-/-) mice. Temporal expressions of the

PPAR α -dependent and Wy-14,643 responsive genes were also studied.

Fluorescent differential display was used to identify the genes, which are regulated by PPAR α and affected by peroxisome proliferators, as its sensitive and ability of comparison of more than two treatment groups. Histology was performed to identify the liver damage caused by the chronic administration of Wy-14,643.

The objects of this project are as follows:

1. To examine the liver damage caused by chronic exposure of Wy-14,643.
2. To identify PPAR α -dependent and Wy-14,643-responsive genes at the tumor stage
3. To identify the temporal expression of PPAR α -dependent and Wy-14,643-responsive genes.

Chapter 2 Materials and Methods

2.1 Animal tail-genotyping

The genotypes of PPAR α (+/+) and PPAR α (-/-) mice were confirmed by PCR tail-genotyping before the animals were used for feeding treatment as there was no external phenotypic difference between PPAR α (+/+) and PPAR α (-/-) mice (Figure 2.1.1). PCR tail-genotyping was performed by using a pair of forward (F1, 5'-GCCTGGCCTTCTAAACAT-3') and reverse (R3, 5'-ACTCGGTCTTCTTGATGA-3') primers which located before the *Pst*I (1330-1347) and after the *Sph*I (1503-1520) sites of exon 8 of PPAR α gene, respectively (Figure 2.1.2). The expected size of PCR product amplified from genomic tail DNA of PPAR α (+/+) mice was 191 bp. Due to the replacement of a 83 bp genomic fragment by a 1.14 kb neo gene between *Pst*I and *Sph*I sites in exon 8 of PPAR α gene, the expected size of PCR product amplified from genomic tail DNA of PPAR α (-/-) mice was 1248 bp (Lee *et al.*, 2002).

2.1.1 Materials

Isopropanol was purchased from BDH (England). dNTP mix was purchased from Roche (Germany). EDTA was obtained from Riedel-de Haën (Germany). Proteinase K was purchased from Roche (Germany). DNA markers were from Invitrogen (USA). Ethidium bromide and SDS were obtained from Sigma (USA). Forward and reverse primers were synthesized and purchased from Invitrogen (USA). Agarose, boric acid, sodium chloride and trizma base were purchased from USB (USA). *Taq* polymerase and PCR buffer were from GenSys (UK).

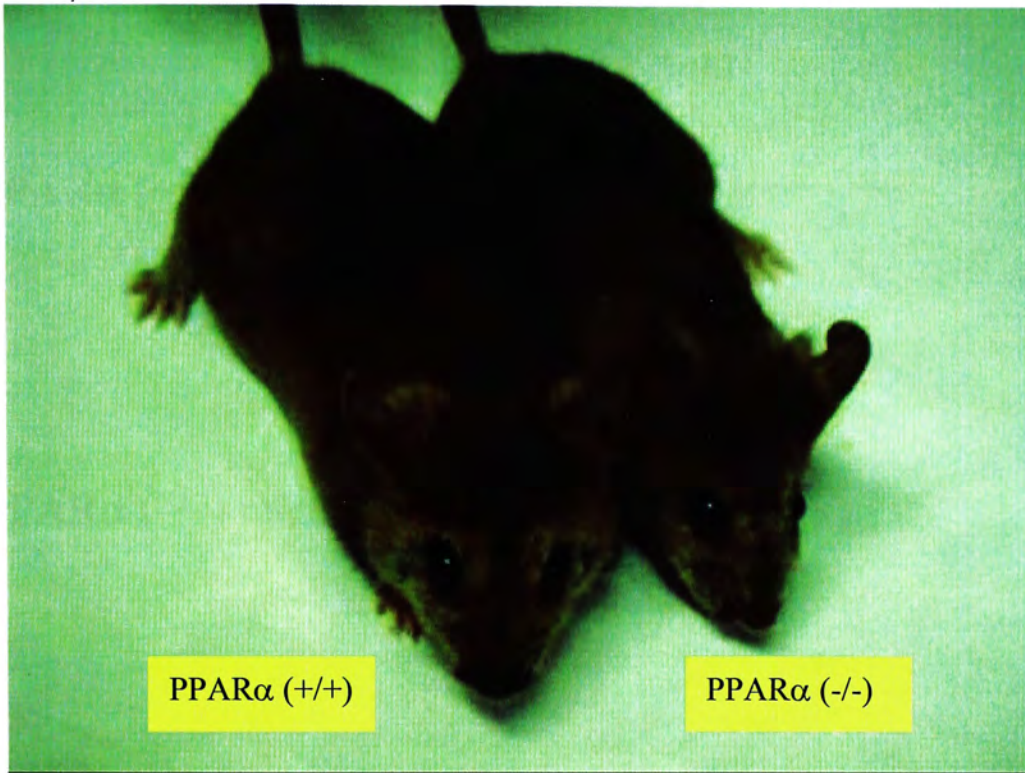


Figure 2.1.1. External morphology of 3 months old PPAR α (+/+) and PPAR α (-/-) male mice.

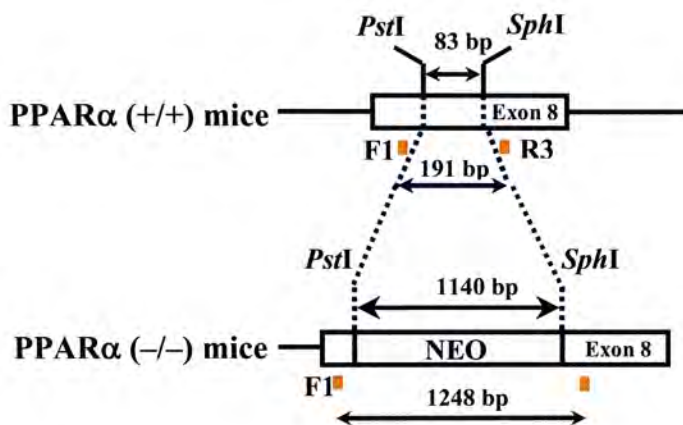


Figure 2.1.2. A schematic representation of *PPARα* (+/+) and *PPARα* (-/-) mouse genomic organization and the location of PCR primers designed for tail-genotyping. For *PPARα* (-/-) mice, a 83 bp genomic fragment between the *Pst*I and *Sph*I sites in exon 8 was replaced by a 1140 bp neo gene. A pair of primers, F1 and R3, which locate before the *Pst*I and after *Sph*I sites, respectively were designed for PCR. The expected sizes of PCR products for *PPARα* (+/+) mice was 191 bp, while that of *PPARα* (-/-) was 1248 bp (Lee *et al.*, 2002).

2.1.2 Methods

About 1 cm tail tip from PPAR α (+/+) and PPAR α (-/-) mice was excised and incubated in 0.5 ml of lysis buffer [100 mM Tris-HCl (pH 8.5), 5 mM EDTA (pH 8.0), 0.2% SDS, 200 mM NaCl and 100 μ g/ml proteinase K] in a 15 ml Falcon tube at 55°C with shaking for overnight digestion. After an overnight incubation, the Falcon tube was vortexed and incubated for an additional 2 hr. Then the Falcon tube was centrifuged at 3,000 rpm at room temperature for 10 min and the supernatant was collected into a new 1.5 ml eppendorf tube. The supernatant was centrifuged at 14,000 rpm at room temperature for 10 min and the resulting supernatant was transferred into a new 1.5 ml eppendorf tube which containing 0.5 ml isopropanol. The mixture was shaken laterally to precipitate the DNA and the DNA strand was transferred into a new 1.5 ml eppendorf tube using a P-100 pipette tip. The DNA strand was air-dried, dissolved in 100 μ l Tris-EDTA buffer [10 mM Tris-HCl (pH 7.5) and 0.1 mM EDTA (pH 7.5)] and incubated at 55°C water bath overnight. Next day the DNA pellet was resuspended by pipetting up and down and used for PCR reaction.

For each PCR reaction, 1 μ l of resuspended tail DNA was mixed with 1X PCR buffer, 0.05 mM dNTP mix, 0.35 μ M forward primer (F1), 0.35 μ M reverse primer (R3) and 0.1 U/ μ l *Taq* polymerase (Appendix A, Table A1). The PCR reaction was performed in a thermal cycler (GeneAmp[®] PCR system 9700) and the PCR cycle was as follows: 95°C for 2 min, followed by 34 cycles of 92°C for 15 sec and 72°C for 2 min and followed by 72°C for 7 min and hold at 4°C. The PCR products of PPAR α (+/+) and PPAR α (-/-) mice were resolved on 2% and 1% agarose gel, respectively and 0.5X TBE gels with ethidium bromide staining.

2.2 Animal treatment

PPAR α (+/+) and PPAR α (-/-) mice were used to study the molecular mechanism of PPAR α -mediated Wy-14,643 induced hepatocarcinogenesis.

2.2.1 Materials

For all the experiments, PPAR α (+/+) and PPAR α (-/-) mice on SV129 genetic background were used and they were the offspring of breeder mice obtained from the National Cancer Institute (USA). Wy-14,643 ([4-chloro-6-(2,3-xylidino)-2-pyrimidinylthio]-acetate) was purchased from Chemsyn Science Laboratories (USA) and methylcellulose was obtained from Sigma (USA). Formaldehyde was purchased from Riedel-de Haën (Germany). The mouse chow diet containing 0.0% (control diet) or 0.1% Wy-14,643 was custom-made by Bioserv Company (USA).

2.2.2 Methods

Three months old PPAR α (+/+) and PPAR α (-/-) male mice were kept in groups of 2-4 mice per cage and provided with ozonated water *ad libitum* on a 12 hr light/dark cycle. For 24 hr gavage treatment, PPAR α (+/+) and PPAR α (-/-) were given a single dose of 1% methylcellulose (control vehicle) or Wy-14,643 (50 mg/kg bw) in 1% methylcellulose by intragastric infusion. For feeding study, both PPAR α (+/+) and PPAR α (-/-) mice were either fed with a 0.0% (control) or a 0.1% Wy-14,643 rodent diet for 1 wk, 2 wk, 6 mo and 11 mo *ad libitum*. The body weight of mice was measured before and during (once per week) the feeding periods. At the end of experiment, mice were dissected and blood was collected for serum cholesterol and

triglyceride analyses. Other organs including liver, brown fat, white fat, spleen, kidney, heart, brain and testis were removed and weighed. About 1 cm³ of liver samples was fixed in 10% phosphate-buffered formalin (10-fold diluted 37% formaldehyde with 1X PBS) for histological analysis. The remaining organs were wrapped in aluminum foil and stored frozen in liquid nitrogen.

2.3 Serum cholesterol and triglyceride analyses

Previous studies have reported that the main effect of the hypolipidemic peroxisome proliferators is to lower the serum triglycerides and cholesterol levels (Havel and Kane, 1973).

Serum cholesterol was determined based on a modification of method described by Allain *et al.* (1974). Cholesterol ester in the serum is first hydrolyzed by cholesterol esterase to cholesterol and fatty acid. The cholesterol is then oxidized by cholesterol oxidase to cholesterolone and hydrogen peroxide. In the presence of peroxidase, hydrogen peroxide produced is then coupled with 4-aminoantipyrine and phenol to yield quinoneimine, a dye which can be measured at 500 nm. The intensity of the dye is directly proportional to the concentration of serum cholesterol.

Serum triglyceride was determined based on a modification of method described by Bucolo and David (1973). Serum triglyceride is first hydrolyzed by lipase to glycerol and fatty acids. The glycerol is then phosphorylated by adenosine triphosphate (ATP) to glycerol-3-phosphate and adenosine-5'-diphosphate (GDP) which catalyzed by glycerokinase. The glycerol-3-phosphate is then oxidized by glycerol-3-phosphate oxidase to dihydroxyacetone phosphate and hydrogen peroxide. In the presence of peroxidase, hydrogen peroxide produced is then coupled with 4-

aminoantipyrine and 4-chlorophenol to form quinoneimine which can be measured at 500 nm. The intensity of the colour is directly proportional to the serum triglyceride concentration in the sample.

2.3.1 Materials

Cholesterol and triglyceride determination enzyme kits were obtained from BioSystems (Spain). Plastic curvets were purchased from Nümbrecht (Germany).

2.3.2 Methods

2.3.2.1 Serum preparation

Blood samples were allowed to clot for 30 min at room temperature. The clotted blood samples were then centrifuged at 2,400 rpm at room temperature for 20 min. The supernatant which containing the serum was then transferred to a new 1.5 ml eppendorf tube and centrifuged at 2,400 rpm for 20 min. The clear serum was then transferred to a new 1.5 ml eppendorf tube and stored at -20°C.

2.3.2.2 Serum cholesterol analysis

Cholesterol reagent and cholesterol standard (200 mg/dl) were warmed to room temperature before use. Four microliters of cholesterol standard or serum samples from each mouse were added to curvets containing 400 μ l of cholesterol reagent. The contents were mixed and the samples were incubated for 15 min at room temperature. The absorbances (A) of standard and samples at 500 nm were measured using a spectrophotometer (Beckman DU[®] 640, USA) against the blank which

containing 400 μ l of cholesterol reagent. The concentration of serum cholesterol (mg/dl) was calculated using the following formula:

Conc. of serum cholesterol (mg/dl) = $A_{\text{sample}} / A_{\text{Standard}} \times \text{conc. of cholesterol standard}$

2.3.2.3 Serum triglyceride analysis

Triglyceride reagent and triglyceride standard (200 mg/dl) were warmed to room temperature. Four microliters of triglyceride standard or serum samples from each mouse were added to cuvettes containing 400 μ l of triglyceride reagent. The contents were mixed and the samples were incubated for 15 min at room temperature. The absorbances (A) of standard and samples at 500 nm were measured using a spectrophotometer (Beckman DU[®] 640, USA) against the blank which contained 400 μ l of triglyceride reagent. The concentration of serum triglyceride was calculated using the following equation:

Conc. of serum triglyceride (mg/dl) = $A_{\text{sample}} / A_{\text{Standard}} \times \text{conc. of triglyceride standard}$

2.4 Histological analysis

To assess the liver damage induced by Wy-14,643, hematoxylin and eosin staining was performed from each treatment group at 24 hr, 1 wk, 2 wk, 6 mo and 11 mo.

2.4.1 Materials

Mayer's hematoxylin was from Polysciences (USA). Concentrated HCl, ethanol and eosin were purchased from BDH (England). Paraffin was obtained from Merck (USA). Permount was purchased from Fisher (USA). Xylene was from Merck

(USA). Magnesium sulfate and sodium hydrogen carbonate were purchased from BDH (England).

2.4.2 Methods

The flow chart showing the steps for histological analysis is summarized in Figure. 2.4.1. The fixed liver samples were processed in an enclosed tissue processor (Shandon, England) with the following program: 70% ethanol at room temperature for 2 hr, 80% ethanol at room temperature for 2 hr, 95% ethanol at room temperature for 2 hr, 100% ethanol at room temperature for 2 hr three times, xylene at room temperature for 1 hr twice and paraffin at 60°C for 2 hr four times. The processed samples were then embedded in paraffin. Liver sections of 5 μ m thick were cut by microtome (Jung, Germany) and then dried at 40°C. For staining, the liver sections were first rinsed with xylene for 1 min three times and then in a serial graded ethanol (100%, 95%, 80% and 70%) for 1 min. The liver sections were stained with Mayer's hematoxylin for 5 min and washed with tap water. The sections were then rinsed with Scott tap water (0.04 M sodium hydrogen carbonate and 0.15 M magnesium sulfate) and washed with tap water. Excess staining was washed by dipping the section in acid alcohol (100-fold diluted concentrated HCl with 70% alcohol) for 1 sec and then washed with tap water. The sections were stained with eosin for 5 min. Excess staining was removed with tap water and the sections were rinsed with a serial graded ethanol (70%, 80% and 95%) for 1 min. The sections were then rinsed with absolute ethanol for 1 min and then followed by rinsing with xylene for 1 min three times. The sections were mounted with permount and photographs were taken with Integrated Biological Imaging System (Axiophot 2 universal microscope: Zeiss, Germany; spot

cooled colour digital camera and software-Spot 32: Diagnostic Instruments, USA; Software-MetaMorph 4.0: Universal Imaging Corporation, USA) (Figure 2.4.1).

2.5 Total RNA isolation

Total liver RNA of PPAR α (+/+) and PPAR α (-/-) mice treated with a 0.0% (control diet) or a 0.1% Wy-14,643 for 11 mo was isolated for non-fluoroDD, fluoroDD and Northern blot analyses. Liver RNA samples of 24 hr gavage feeding and 1 wk, 2 wk and 6 mo feeding treatments were used to study the temporal gene expression.

2.5.1 Materials

Chloroform was from Merck (USA). Ethanol and isopropanol were purchased from BDH (England). Trizol reagent was obtained from Invitrogen (USA).

2.5.2 Methods

The steps for isolation total RNA are summarized in Figure 2.5.2.1. Frozen liver samples were mixed with Trizol reagent (10 ml/g) and homogenized with a tissue tearor (Dremel[®], USA). The homogenate was allowed to stand for 5 min and then 1 ml of homogenate was added to a new 2 ml eppendrof tube which containing 0.2 ml chloroform. After vortexing, the mixture was allowed to stand for 2 min and then centrifuged at 14,000 rpm at 4°C for 15 min. The supernatant which containing the RNA was transferred into a new 1.5 ml eppendrof tube which containing 500 μ l of isopropanol. The sample was vortexed and then allowed to stand for 10 min at room

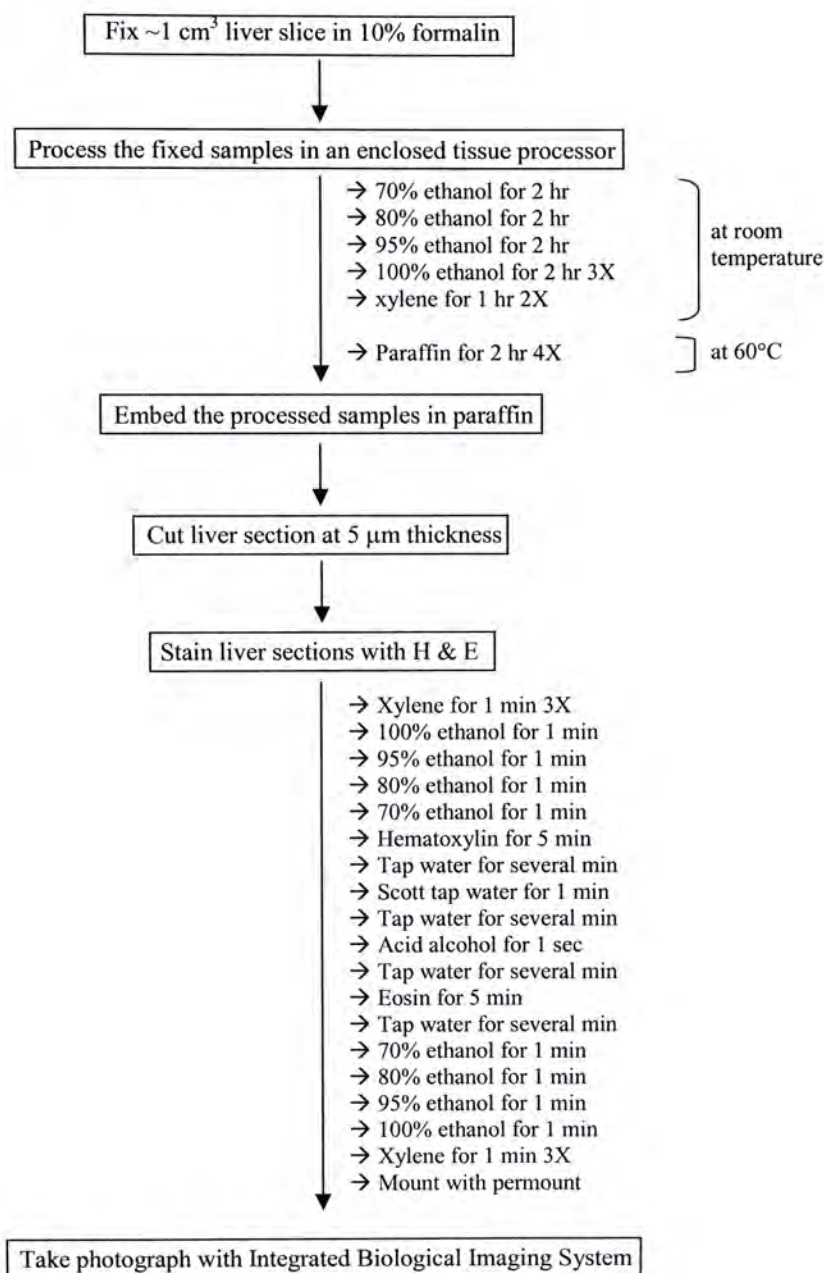


Figure 2.4.1. Flowchart showing the steps for histological analysis.

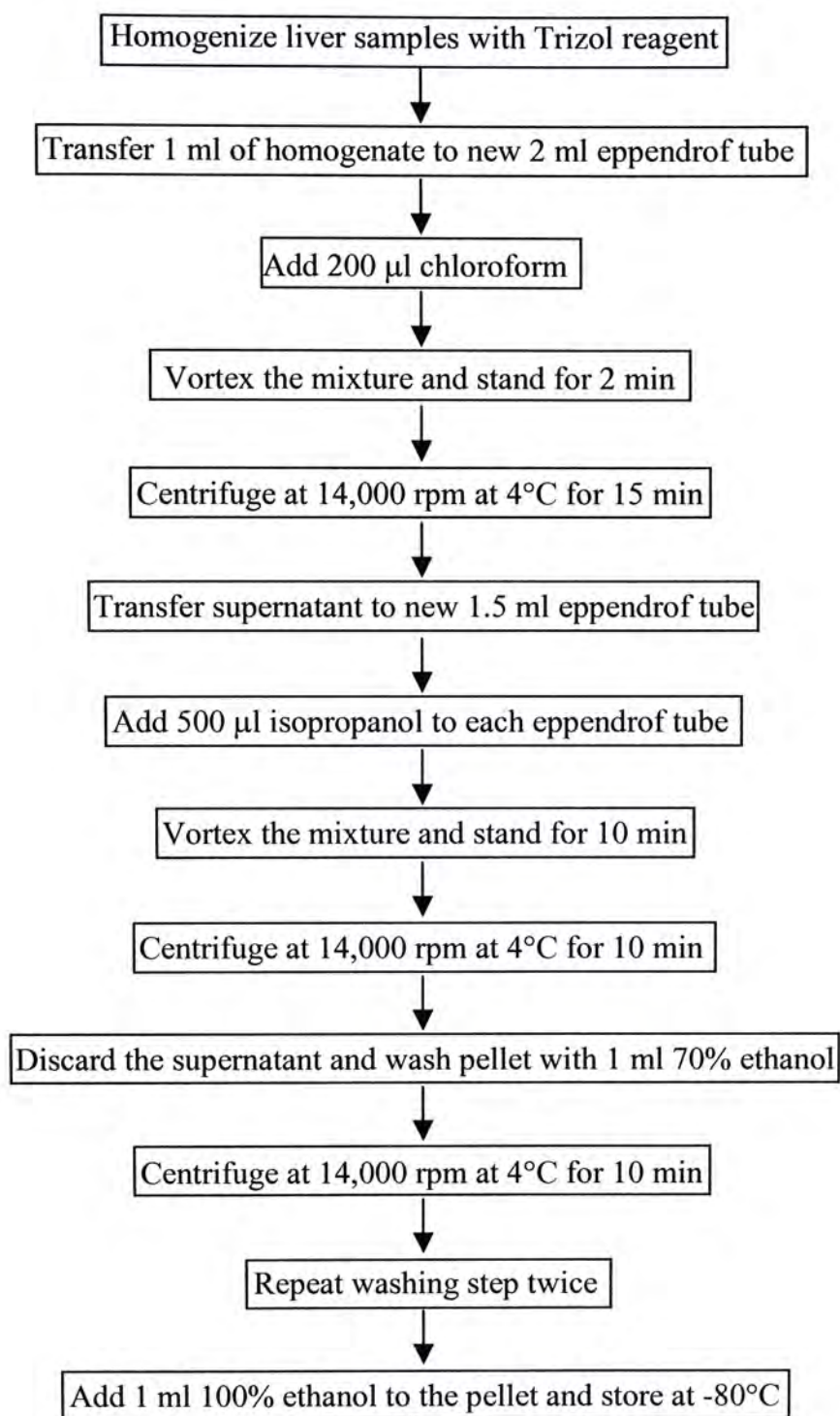


Figure 2.5.2.1 Flowchart showing the steps for isolation of total RNA.

temperature. The mixture was centrifuged at 14,000 rpm at 4°C for 10 min. After discarding the supernatant, the pellet was washed with 1 ml 70% ethanol. The sample was centrifuged at 14,000 rpm at 4°C for 10 min and the supernatant was discarded. The washing steps were repeated twice. For long-term storage, 1 ml of absolute ethanol was added to the pellet and the sample was stored at -80°C.

2.6 DNase I treatment of total liver RNA

DNase I treatment was used to remove any genomic DNA contamination in the RNA samples, as they will give false positive fluoroDD patterns during RT-PCR. Negative control was performed for checking any genomic DNA contamination after DNase I treatment.

2.6.1 Materials

Magnesium chloride and sodium acetate were obtained from Sigma (USA). Nuclease-free water was purchased from Promega (USA). Phenol: chloroform: isoamyl alcohol (25:24:1) was purchased from Invitrogen (USA). RNase-free DNase I, HPLC pure grade was from Amersham Biosciences (England). Trizma base was purchased from USB (USA).

2.6.2 Methods

Fifty micrograms of total liver RNA were mixed with 10 mM MgCl₂, 0.3 U/μl RNase-free DNase I and 50 mM Tris-HCl (pH 7.5) (Appendix A, Table A2). The mixture was then mixed by finger-tapping and incubated in 37°C water bath for 30 min. The sample was then diluted to 500 μl with nuclease-free water and 500 μl of

phenol/chloroform was added to each sample. After vortexing and centrifuged at 14,000 rpm at 4°C for 30 min, 400 μ l of supernatant was transferred to a new 1.5 ml eppendrof tube. Forty microliters of 3 M sodium acetate were added to each eppendrof tube and vortexed. Eight hundred microliters of absolute ethanol were added to each sample. The mixture was vortexed and allowed for overnight precipitation at -80°C. The precipitated RNA was centrifuged at 14,000 rpm at 4°C for 30 min. The supernatant was discarded and the pellet was washed with 70% ethanol and centrifuged at 14,000 rpm at 4°C for 30 mine. The washing steps were repeated twice and the pellet was air-dried. The RNA pellet was resuspended in 35 μ l nuclease-free water and stored at -80°C.

2.7 Reverse transcription (RT) of mRNA and non-fluorescent PCR (non-fluoroDD PCR)

The first-strand cDNA synthesis was carried out by using the HIEROGLYPHTM profile kit. This kit consists of 12 different 3'-oligo(dT) anchored primers (APs) (Figure 2.7.1) which are two-base different on the 3' end and it divides the mRNA pool into 12 first-strand cDNA pools. The double-strand DNA was performed by the fluoroDD adapter kit. It contains 20 ten-base different 5'-arbitrary primers (ARPs) (Figure 2.7.2) and 12 different 3'-tetramethylrhodamine-labeled oligo(dT) anchored primers (TMR-APs) (Figure 2.7.3) which have same sequence to their corresponding anchored primers (APs) in the HIEROGLYPHTM profile kit. There are total 240 different combinations of primers with 12 different APs and 20 different ARPs. However, not all the 240 primer combinations will give our desired differential display patterns, non-fluorescent PCR (non-fluoroDD PCR) (Figure 2.7.4)

	T7 promotor sequence	oligo(dT ₁₂)
AP1	5' ACGACTCACTATAGGGCTTTTTTTTTTTT	<u>GA</u> 3'
AP2	5' ACGACTCACTATAGGGCTTTTTTTTTTTT	<u>GC</u> 3'
AP3	5' ACGACTCACTATAGGGCTTTTTTTTTTTT	<u>GG</u> 3'
AP4	5' ACGACTCACTATAGGGCTTTTTTTTTTTT	<u>GT</u> 3'
AP5	5' ACGACTCACTATAGGGCTTTTTTTTTTTT	<u>CA</u> 3'
AP6	5' ACGACTCACTATAGGGCTTTTTTTTTTTT	<u>CC</u> 3'
AP7	5' ACGACTCACTATAGGGCTTTTTTTTTTTT	<u>CG</u> 3'
AP8	5' ACGACTCACTATAGGGCTTTTTTTTTTTT	<u>AA</u> 3'
AP9	5' ACGACTCACTATAGGGCTTTTTTTTTTTT	<u>AC</u> 3'
AP10	5' ACGACTCACTATAGGGCTTTTTTTTTTTT	<u>AG</u> 3'
AP11	5' ACGACTCACTATAGGGCTTTTTTTTTTTT	<u>AT</u> 3'
AP12	5' ACGACTCACTATAGGGCTTTTTTTTTTTT	<u>CT</u> 3'

Figure 2.7.1 Sequences of 12 different 3'-oligo(dT₁₂) anchored primers (APs). Each AP primer contains three domains and they are the same for the T7 (17-mer) promoter sequence for amplification and the oligo(dT₁₂) for annealing to polyA tail of mRNA. However, the 12 different APs are two-base different at the 3'end which divide mRNA pool into 12 subsets (adapted from fluoroDD manual, Beckman).

	M13 reverse primer sequence	Core annealing sequence
ARP1	5' ACAATTTCACACAGG	<u>ACGACTCCAAG</u> 3'
ARP2	5' ACAATTTCACACAGG	<u>AGCTAGCATGG</u> 3'
ARP3	5' ACAATTTCACACAGG	<u>AGACCATTGCA</u> 3'
ARP4	5' ACAATTTCACACAGG	<u>AGCTAGCAGAC</u> 3'
ARP5	5' ACAATTTCACACAGG	<u>AATGGTAGTCT</u> 3'
ARP6	5' ACAATTTCACACAGG	<u>ATACAACGAGG</u> 3'
ARP7	5' ACAATTTCACACAGG	<u>ATGGATTGGTC</u> 3'
ARP8	5' ACAATTTCACACAGG	<u>ATGGTAAAGGG</u> 3'
ARP9	5' ACAATTTCACACAGG	<u>ATAAGACTAGC</u> 3'
ARP10	5' ACAATTTCACACAGG	<u>AGATCTCAGAC</u> 3'
ARP11	5' ACAATTTCACACAGG	<u>AACGCTAGTGT</u> 3'
ARP12	5' ACAATTTCACACAGG	<u>AGGTACTAAGG</u> 3'
ARP13	5' ACAATTTCACACAGG	<u>AGTTGCACCAT</u> 3'
ARP14	5' ACAATTTCACACAGG	<u>ATCCATGACTC</u> 3'
ARP15	5' ACAATTTCACACAGG	<u>ACTTTCTACCC</u> 3'
ARP16	5' ACAATTTCACACAGG	<u>ATCGGTCATAG</u> 3'
ARP17	5' ACAATTTCACACAGG	<u>ACTGCTAGGTA</u> 3'
ARP18	5' ACAATTTCACACAGG	<u>ATGATGCTACC</u> 3'
ARP19	5' ACAATTTCACACAGG	<u>ATTTTGGCTCC</u> 3'
ARP20	5' ACAATTTCACACAGG	<u>ATCGATACAGG</u> 3'

Figure 2.7.2 Sequences of 20 different 5'-arbitrary primers (ARPs). Each ARP primer contains the same M13 (16-mer) reverse primer sequence for reamplification but they have ten-base different for the core annealing sequence for priming gene specific sequence in RT-PCR (adapted from fluoroDD manual, Beckman).

		T7 promotor sequence	oligo(dT ₁₂)
TMR-AP1	★5'	ACGACTCACTATAGGGC	TTTTTTTTTTTTTGA 3'
TMR-AP2	★5'	ACGACTCACTATAGGGC	TTTTTTTTTTTTTGC 3'
TMR-AP3	★5'	ACGACTCACTATAGGGC	TTTTTTTTTTTTTGG 3'
TMR-AP4	★5'	ACGACTCACTATAGGGC	TTTTTTTTTTTTTGT 3'
TMR-AP5	★5'	ACGACTCACTATAGGGC	TTTTTTTTTTTTTCA 3'
TMR-AP6	★5'	ACGACTCACTATAGGGC	TTTTTTTTTTTTTCC 3'
TMR-AP7	★5'	ACGACTCACTATAGGGC	TTTTTTTTTTTTTCG 3'
TMR-AP8	★5'	ACGACTCACTATAGGGC	TTTTTTTTTTTTTAA 3'
TMR-AP9	★5'	ACGACTCACTATAGGGC	TTTTTTTTTTTTTAC 3'
TMR-AP10	★5'	ACGACTCACTATAGGGC	TTTTTTTTTTTTTAG 3'
TMR-AP11	★5'	ACGACTCACTATAGGGC	TTTTTTTTTTTTTAT 3'
TMR-AP12	★5'	ACGACTCACTATAGGGC	TTTTTTTTTTTTTCT 3'

Figure 2.7.3 Sequences of 12 different 3'-tetramethylrhodamine-labeled oligo(dT₁₂) anchored primers (TMR-APs). Each TMR-AP primer has same sequence corresponding to the non-fluorescent-labeled anchored primer used for first-strand cDNA synthesis and the TMR fluorescent tag is indicated by the star (adapted from fluoroDD manual, Beckman).

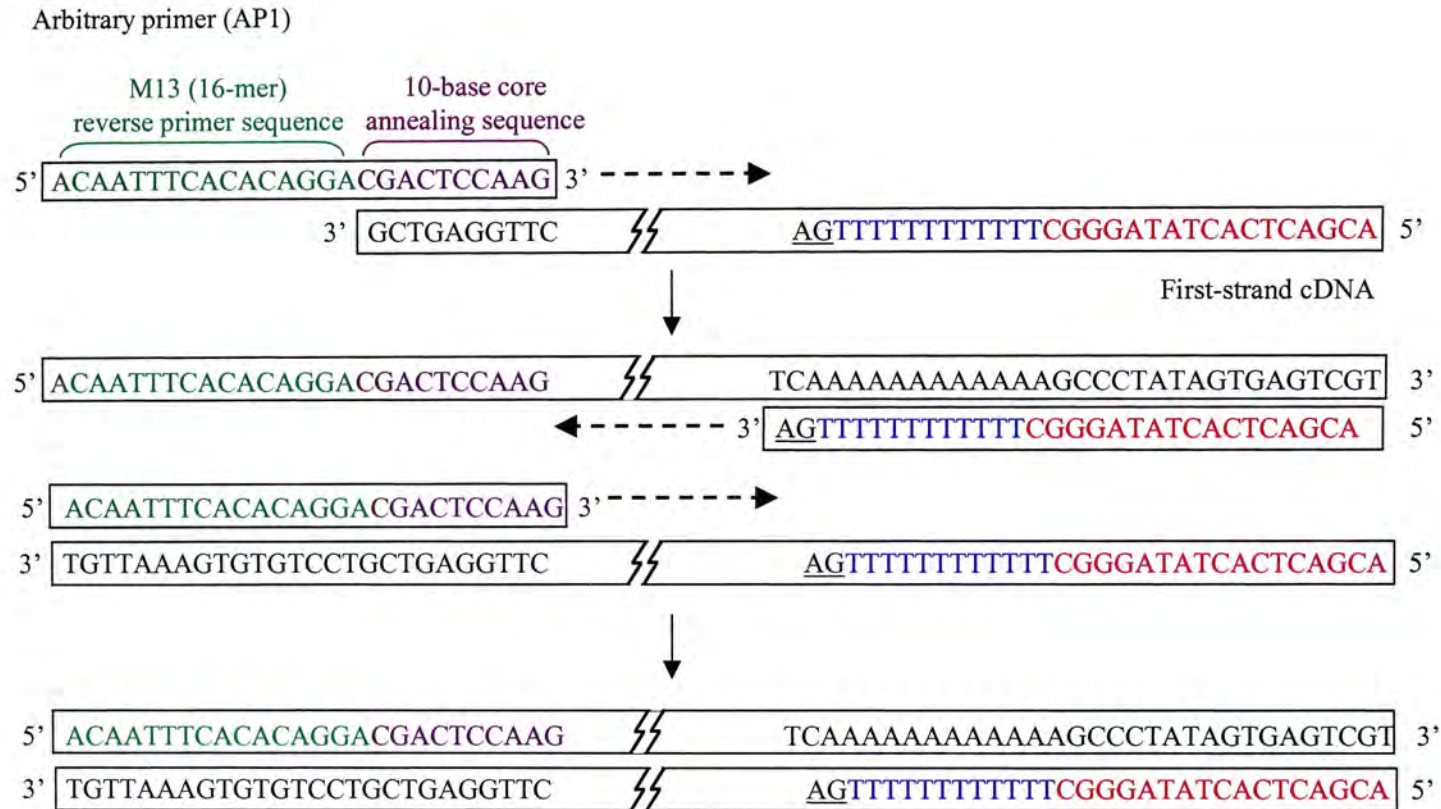


Figure 2.7.4. A schematic diagram showing the synthesis of non-fluoroDD PCR. Anchored primer (AP) and arbitrary primer (ARP) are used for the double-strand cDNA synthesis (adapted from fluoroDD manual, Genoymx).

was performed for initial screening of primer combinations which produced our desired differential display patterns. Non-fluorescent labeled APs were used in the non-fluoroDD RT-PCR which provides a cheaper and faster screening method.

2.7.1 Materials

DTT, SuperscriptTM II RT buffer and SuperscriptTM II RNase H⁻ reverse transcriptase, non-fluorescent labeled 3'-oligo(dT) anchored primers (APs), 5'-arbitrary primers (ARPs), dNTP mix (1:1:1:1), *Taq* polymerase and PCR buffer were obtained from Invitrogen (USA).

2.7.2 Methods

A schematic diagram showing the synthesis of non-fluoroDD PCR is shown in Figure 4.7.5. First-strand cDNA was synthesized from DNase I treated total RNA (0.2 μ g) by mixing with 0.2 μ M AP, 10 mM DTT, 25 μ M dNTP mix (1:1:1:1), 1X SuperscriptTM II RT buffer and 2 U/ μ l SuperscriptTM II RNase H⁻ reverse transcriptase (Appendix A, Table A3). For negative control, SuperscriptTM II RNase H⁻ reverse transcriptase was not added for the first-strand cDNA synthesis. The reverse transcription reaction was performed in a thermal cycler (GeneAmp[®] PCR system 9700) and the RT program was as follows: 42°C for 5 min, 50°C for 50 min, 70°C for 15 min and hold at 4°C. The synthesized first-strand cDNA was stored at -20°C.

After first-strand cDNA synthesis, 4 μ l RT mixture was used for the non-fluorescent RT-PCR (non-fluoroDD PCR). For each PCR reaction, the RT mixture was mixed with 0.35 μ M AP, 0.35 μ M ARP, 50 μ M dNTP mix (1:1:1:1), 1X PCR buffer and 0.05 U/ μ l of *Taq* polymerase (Appendix A, Table A4). The PCR was

performed in a thermal cycler (GeneAmp[®] PCR system 9700) and the PCR program was as follows: 95°C for 2 min, followed by 4 cycles of 92°C for 15 sec, 50°C for 30 sec, 72°C for 2 min and followed by 30 cycles of 92°C for 15 sec, 60°C for 30 sec, 72°C for 2 min and 72°C for 7 min and hold at 4°C. The double-strand cDNA synthesized was resolved on 1.5% agarose, 0.5X TBE gels with ethidium bromide staining.

2.8 Reverse transcription (RT) of mRNA and fluorescent PCR (fluoroDD PCR)

The AP-ARP primer combinations which showed differential display patterns in non-fluoro RT-PCR were chosen for fluorescent PCR (fluoroDD PCR).

2.8.1 Materials

HIEROGLYPH[™] mRNA profile and fluoroDD adapter kits were purchased from Beckman (USA).

2.8.2 Methods

FluoroDD RT-PCR was the same as non-fluoroDD RT-PCR described in sections 4.7.1 and 4.7.2 except that APs and dNTP mix (1:1:1:1) for first-strand cDNA synthesis were purchased from HIEROGLYPH[™] mRNA profile kit, while TMR-APs, ARPs and dNTP mix (1:1:1:1) for fluoroDD PCR were obtained from fluoroDD kit. The TMR-labeled cDNA fragments were stored at -20°C.

2.9 Fluorescent differential display (fluoroDD)

The TMR-labeled cDNA fragments were electrophoretically separated on high resolution polyacrylamide gel and detected by fluorescent scanning using GenomyxSCTM fluorescent imaging system.

2.9.1 Materials

FluoroDD loading dye, HR-1000TM 5.6% denaturing polyacrylamide gel, 0.5X TBE buffer, 1X TBE buffer and TMR-labeled molecular weight DNA marker were obtained from Beckman (USA). Ammonium persulfate and TEMED were purchased from Sigma (USA). GenomyxLRTM electrophoresis system and genomyxSCTM fluorescent imaging system were from Genomyx (USA).

2.9.2 Methods

2.9.2.1 FluoroDD gel preparation

High resolution polycarylamide gel was prepared by mixing 70 ml of 5.6% denaturing HR-1000 gel with 320 μ l of freshly prepared 10% ammonium persulfate and 32 μ l TEMED. The fluoroDD gel was allowed to polymerize for overnight at room temperature.

2.9.2.2 Sample preparation and electrophoresis

Four microliters of fluoroDD PCR products were mixed with 2 μ l fluoroDD loading dye, while 1.2 μ l TMR-molecular weight marker was mixed with 1.5 μ l fluoroDD loading dye. They were denatured at 95°C for 4 min in a thermal cycler (GeneAmp[®]PCR system 9700) before loading. The lower and upper buffer chambers

were filled with 250 ml 1X TBE buffer and 125 ml 0.5X TBE buffer, respectively. The TMR-molecular weight marker and fluoroDD PCR samples were loaded and run at 3000 V, 100 W at 50°C for 4 to 4.5 hr using a GenomylxLR™ DNA electrophoresis system (Genomylx, USA). The gel was then washed with double distilled water 3 times and dried at 55°C for 20 min. The image was scanned in GenomylxSC™ fluorescent imaging scanner (Genomylx, USA).

2.10 Excision of differentially expressed cDNA fragments

The cDNA fragments which showed differential expression patterns in the Wy-14,643 treated PPAR α (+/+) group but not in the Wy-14,643 treated PPAR α (-/-) group compared with their corresponding control groups were excised from the fluoroDD gels (Table 2.10.1).

2.10.1 Materials

A virtual grid was purchased from Genomylx (USA). Sterile blades were purchased from Swann-Morton® (England).

2.10.2 Methods

The computer-scanned image of the fluoroDD gel was aligned with a physical grid to accurately locate the positions of cDNA fragments which showed differential display patterns on the fluoroDD gel before gel excision. The fragments which showed differential display patterns were marked on the virtual grid. The cDNA fragments were excised by putting the fluoroDD gel on the virtual grid and excised

Table 2.10.1. The expected differential expression patterns of cDNA fragments displayed on non-fluoroDD and fluoroDD gels.

DD Patttens	PPARα (+/+)		PPARα (-/-)		Description
	Control	0.1% Wy- 14,643	Control	0.1% Wy- 14,643	
I	-	+	-	-	Up-regulated in 0.1% Wy-14,643 treatment and PPARα dependent
II	+	++	+	+	Up-regulated in 0.1% Wy-14,643 treatment and PPARα dependent
III	+	-	+	+	Down-regulated in 0.1% Wy-14,643 treatment and PPARα dependent
IV	++	+	++	++	Down-regulated in 0.1% Wy-14,643 treatment and PPARα dependent
A	-	+	-	+	Up-regulated in 0.1% Wy-14,643 treatment but PPARα-independent
B	+	-	+	-	Down-regulated in 0.1% Wy-14,643 treatment but PPARα-independent

‘+’represents the presence of a band (cDNA) on fluoroDD gel and the relative intensity of the gene expression among the four treatment groups is indicated by the number of ‘+’, while ‘-’ represents the corresponding band (cDNA) was not observed on the fluoroDD gel. Those AP and ARP combinations which shown the desired differential display pattern (I-IV) in the non-fluoroDD gels were selected for band excision. Differential display patterns A & B are 0.1% Wy-14,643 treatment responsive but they are not PPARα dependent, so they are not chosen for fluoroDD RT-PCR and gel band excision.

with sterile blades. The excised gel bands were incubated in 20 µl TE buffer [10 mM Tris-HCl (pH 7.5) and 0.1 mM EDTA (pH 7.5)] at 37°C for 1 hr for DNA elution and stored at -20°C. After gel excision, the gels were re-scanned to confirm the target bands were excised accurately.

2.11 Reamplification of differentially expressed cDNA fragments

The excised cDNA fragments were reamplified by PCR reaction with full length M13 reverse (-48) 24-mer (5'-AGCGGATAACAATTTACACAGGA-3') and T7 promoter 22-mer (5'-GTAATACGACTCACTATAGGGC-3') primers. The partial sequences of M13 reverse (16-mer) and T7 promoter (17-mer) were present in the 5'-ARP and 3'-AP primers of double-strand cDNA synthesis, respectively. As the M13 reverse primer was lengthened by 8 nucleotides and the T7 promoter primer was lengthened by 5 nucleotides, the expected size of reamplified PCR product is 13 nucleotides longer than the size of fluoroDD fragment size (Figure 2.11.1).

2.11.1 Materials

Agarose and trizma base were from USB (USA). dNTP mix (1:1:1:1), *Taq* polymerase and PCR buffer were obtained from Invitrogen (USA). Full-length T7 promoter 22-mer and M13 reverse (-48) 24-mer primers were purchased from Beckman (USA). EDTA and ethidium bromide were purchased from Sigma (USA).

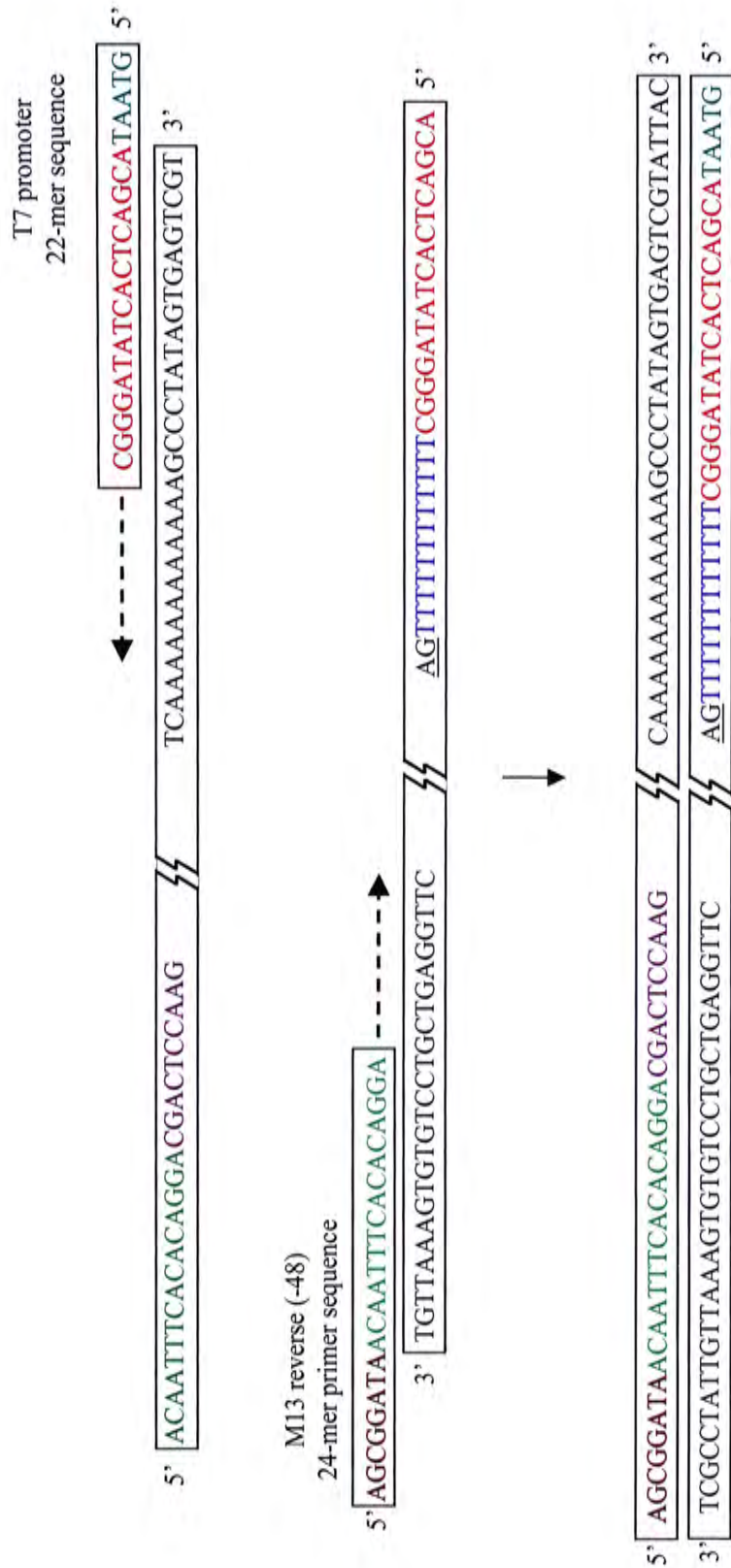


Figure 2.11.1 A schematic diagram showing the reamplification of excised cDNA fragments. Full-length M13 reverse (-48) 24-mer and T7 promoter primers were used for the reamplification of excised cDNA fragments (adapted from fluoroDD manual, Genovmx).

2.11.2 Methods

Four microliters of gel band elute were reamplified by mixing with 20 μ M dNTP mix (1:1:1:1), 0.2 μ M M13 reverse (-48) 24-mer primer, 0.2 μ M T7 promoter 22-mer primer, 1X PCR buffer and 0.05 U/ μ l of *Taq* polymerase (Appendix A, Table A5). The PCR reaction was performed in a thermal cycler (GeneAmp[®] PCR system 9700) and the program was as follows: 95°C for 2 min, followed by 4 cycles of 92°C for 30 sec, 50°C for 30 sec, 72°C for 2 min, followed by 25 cycles of 92°C for 30 sec, 60°C for 30 sec, 72°C for 2 min and 72°C for 7 min and hold at 4°C. Two microliters of reamplified PCR product were resolved on 1% or 2% agarose, 0.5X TBE with ethidium bromide staining.

2.12 Subcloning of reamplified cDNA fragments

Subcloning of reamplified cDNA fragments was performed by either AdvaTAge[™] PCR or TOPO TA cloning kits. The reamplified cDNA fragments with 3'-A overhang were subcloned by T/A cloning using either pT-Adv or pCR[®]II-TOPO[®] vector derived from AdvanTAge[™] PCR or TOPO TA cloning kit, respectively. The screening of recombinant subclones was performed by using phenol-chloroform extraction method (Ohyama, 1997) in which the recombinant plasmid DNA should be longer than the vector only [size of pT-Adv is 3.9 kb (Figure 2.12.1) and that of pCR[®]II-TOPO[®] is 4.0 kb (Figure 2.12.2)]. The size of the insert subcloned into the vector was further confirmed with *Eco*RI digestion.

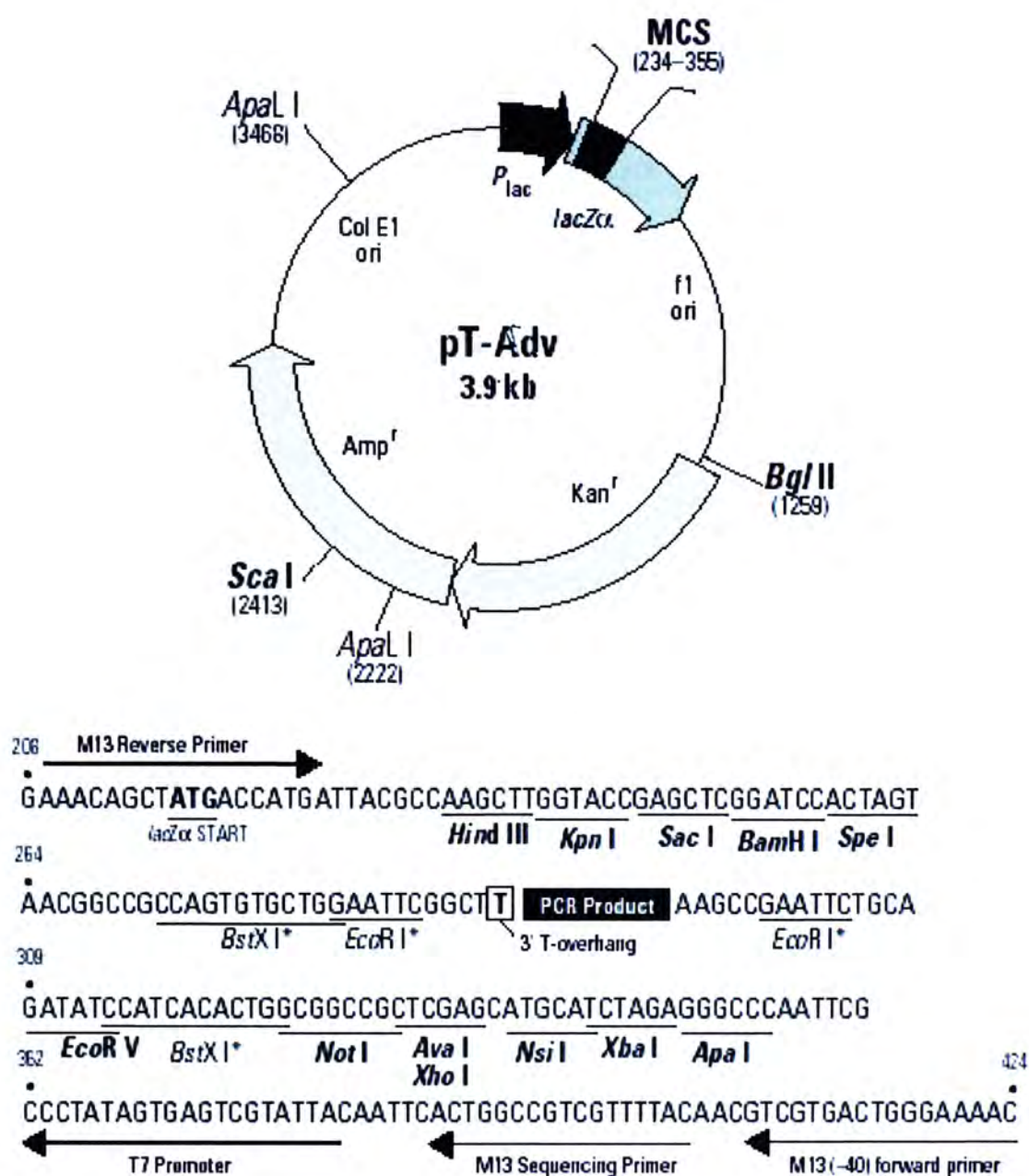
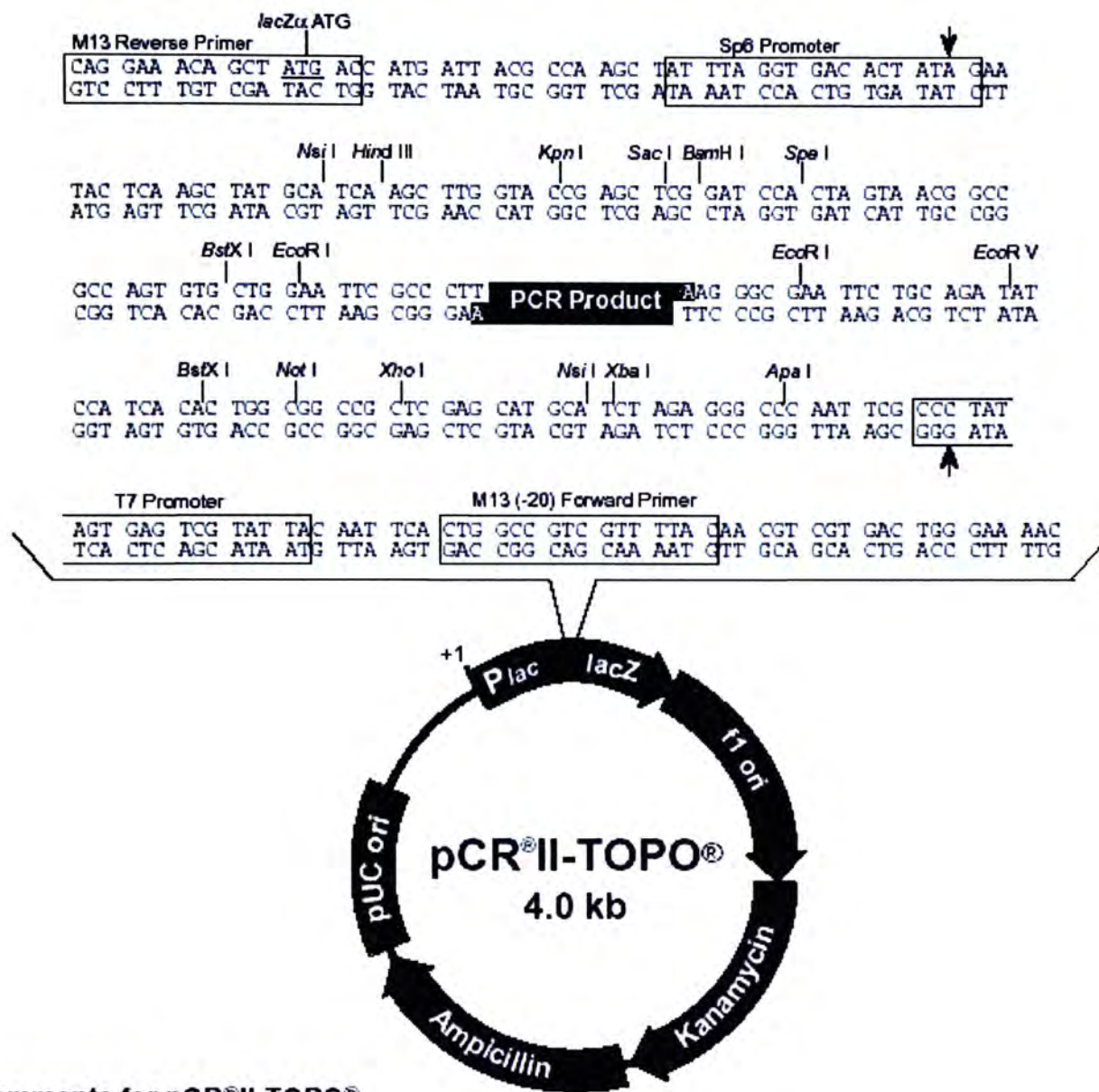


Figure 2.12.1 The restriction map and multiple cloning site (MCS) of pT-Adv vector used for subcloning of reamplified cDNA fragments (adapted from AdvanTage™ PCR cloning kit user manual).



Comments for pCR[®] II-TOPO[®]
3973 nucleotides

Figure 2.12.2 The restriction map and multiple cloning site (MCS) of PCR[®] II-TOPO[®] vector used for subcloning of reamplified cDNA fragments (adapted from TOPO cloning kit user manual).

2.12.1 Materials

Agarose, 5-bromo-4-chloro-3-indolyl-D-thiogalactoside (X-gal), Isopropyl- β -D-thiogalactoside (IPTG) and sodium chloride were obtained from USB (USA). AdvanTAgeTM PCR cloning kit was purchased from Clontech (USA). TOPO TA cloning kit was from Invitrogen (USA). Ethidium bromide and ampicillin were purchased from Sigma (USA). Restriction enzymes and buffers were obtained from New England Biolabs (UK). Trypton peptone, yeast extract and bacto agar were purchased from Becton Dickinson (USA). QIAGEN[®] spin miniprep kit was purchased from QIAGEN (Germany).

2.12.2 Methods

2.12.2.1 Ligation

Subcloning of reamplified cDNA fragments was performed either by AdvaTAgeTM PCR or TOPO TA cloning kits. For AdvaTAgeTM PCR subcloning kit, 1 μ l of reamplified PCR product was mixed with 1X ligation buffer, 5 ng/ μ l of pT-Adv vector and 4 U/ μ l of T4 DNA ligase for ligation. The mixture was then incubated at 14°C overnight. For TOPO TA cloning kits, 1 μ l of reamplified PCR product was mixed up with 0.2 M NaCl, 0.01 M MgCl₂ and 0.17 ng/ μ l pCR[®]II-TOPO[®] vector. The mixture was then incubated at room temperature for 5 min.

2.12.2.2 Transformation

Two microliters of ligation products were then mixed with TOP 10F' *E. coli* competent cells and chilled on ice for 30 min. The mixture was then incubated in 42°C water bath for 90 sec, chilled on ice immediately for 2 min. and then diluted to 1

ml by LB medium. Then the mixture was incubated at 37°C with shaking for 1 hr and centrifuged at 2,500 rpm at 4°C for 8 min. The supernatant was discarded and the cell pellet was resuspended with 300 µl LB medium. The transformed cells were spreaded on LB agar plates containing 100 µg/ml ampicillin, 40 µl of 100 mM IPTG and 40 µl of 40 mg/ml X-Gal. The plates were incubated at 37°C incubator for 16 hr.

2.12.2.3 Phenol-chloroform extraction

Single white colony was incubated in 3 ml LB medium containing 100 µg/ml of ampicillin at 37°C for 16 hours with shaking. Thirty microliters of bacterial culture were mixed with 30 µl of phenol: chloroform: isoamyl alcohol (25:24:1) for screening recombinant clones. The mixture was vortexed vigorously and then centrifuged at 14,000 rpm at room temperature for 2 min. Ten microliters of the supernatant were resolved on 0.6% agarose, 0.5X TBE gels with ethidium bromide staining.

2.12.2.4 Confirmation of insert size by *EcoRI* digestion

The recombinant clones which showed positive result in the phenol-cholorform extraction were selected for *EcoRI* digestion for further confirmation of the insert sizes. One milliliter of bacterial culture was centrifuged at 14,000 rpm at 4°C for 1 min. The supernatant was discarded and the cell pellet was resuspended with 17 µl autoclaved distilled water containing 250 µg/ml RNase A. The resuspended cells were boiled for 1 min and then centrifuged at 14,000 rpm at room temperature for 1 min. Seventeen microliters of supernatant were digested with 10 units of *EcoRI* in 1X *EcoRI* buffer at 37°C for 2 hr. The mixture was then resolved on 1% or 2% agarose, 0.5X TBE gels with ethidium bromide staining.

2.12.2.5 Mini-preparation of plasmid DNA from recombinant clones

Plasmid DNA of cDNA fragments was prepared for by QIAGEN[®] spin miniprep kit. Ten milliliters of bacterial culture were centrifuged at 2,500 rpm at 4°C for 10 min. The supernatant was discarded and cell pellet was resuspended in 250 µl of buffer P1 containing 100 µg/ml RNase A. The resuspended cells were then mixed with 250 µl of buffer P2 by inverting several times. The mixture was incubated at room temperature for about 5 min. Three hundred and fifty microliters of buffer P3 were added to the mixture and mixed by inverting several times. The mixture was centrifuged at 14,000 rpm at room temperature for 15 min. The supernatant was transferred to QIAprep spin columns in 2 ml collection tubes and centrifuged at 14,000 rpm for 1 min. The flow-through was discarded and the columns were washed with 750 µl buffer PE. The columns were transferred to new 1.5 ml eppendorf tube. The plasmid DNA was eluted by adding 50 µl of nuclease free water and centrifuged at 14,000 rpm at room temperature for 1 min twice. The samples were diluted to 6 µl with sterile water and stored at 4°C.

2.13 Sequencing of subcloned cDNA fragments

After confirming the sizes of the cDNA fragments, sequencing was performed by using CEQ dye terminator cycle sequencing kit, M13 forward (-20) (5'-GTAAAACGACGGCCAG-3') and M13 reverse sequencing primers (5'-CAGGAAACAGCTATGAC-3').

2.13.1 Materials

CEQ dye terminator cycle sequencing kit was purchased from Beckman (USA). EDTA, sterile water and sodium acetate were purchased from Sigma (USA). M13 forward (-20) and M13 reverse primers were obtained from Invitrogen (USA).

2.13.2 Methods

2.13.2.1 Sequencing of fluoroDD cDNA fragments

DNA sequencing reaction was prepared by mixing 100 fmol dsDNA in 6 μ l sterile water with 2 μ l of 10X sequencing reaction buffer, 1 μ l of dNTP mix, 2 μ l of ddUTP dye terminator, 2 μ l of ddGTP dye terminator, 2 μ l of ddCTP dye terminator, 2 μ l of ddATP dye terminator, 2 μ l of 1.6 μ M M13 forward (-20) or M13 reverse primer and 1 μ l of Taq polymerase in a 0.2 ml thin-wall PCR tube (Appendix A, Table A6). The mixture was mixed by finger-tapping and spinned down. PCR was performed in a thermal cycler (GeneAmp[®] PCR system 9700) and the PCR program was as follows: 30 cycles of 96°C for 20 sec, 50°C for 20 sec, 60°C for 4 min and hold at 4°C. Stop solution (final concentration of 1.5 M sodium acetate and 50 mM EDTA) was freshly prepared and 4 μ l stop solution was added to new 1.5 ml eppendorf tube. The mixture was transferred to a new 1.5 ml eppendorf tube and 1 μ l of 20 mg/ml of glycogen was added to each eppendorf tube. The mixture was vortexed vigorously and 60 μ l of cold 95% ethanol were added to the mixture and vortexed. The samples were then centrifuged at 14,000 rpm at 4°C for 20 min and the supernatant was discarded carefully to avoid disturbing the pellet. The pellet was washed with 200 μ l cold 70% ethanol and then centrifuged immediately at 14,000 rpm at 4°C for 25 min.

The supernatant was discarded carefully and the washing steps were repeated. The DNA pellet was vacuum dried for at least 45 min until all solvent was evaporated. Forty microliters of sample loading buffer (from the Beckman sequencing kit) were added to the DNA pellet. The DNA pellet was rehydrated for 30 min and then resuspended by pipetting up and down. The resuspended DNA samples were transferred to a 96-well polypropylene sample plate recommended for the CEQ automated DNA sequencer (Beckman). One drop of light mineral oil (provided by the sequencing kit) was added to each sample. The sample plate was loaded into the CEQ DNA sequencer and DTCS-2 method was used for dsDNA plasmid sequencing using long capillary column.

2.13.2.2 BLAST search against computer database

After DNA sequencing, sequence homology was performed by searching the computer database of Basic Local Alignment Search Tool of non-redundant, mouse and human ESTs (<http://www.ncbi.nlm.nih.gov/blast/Blast.cgi>).

2.14 Northern blot analysis of sequenced cDNA fragments

After sequencing and sequence homology searching, the differential display patterns of fluoroDD were further confirmed by Northern blot analysis. The plasmid DNA used for sequencing was used for the preparation of the probe for Northern blot analysis. DIG labeled RNA probe and PCR-DIG labeled cDNA probe were prepared.

2.14.1 Materials

DIG Easy Hyb, Tween 20, blocking reagent, anti-DIG-alkaline phosphatase antibody, DIG-labeled RNA molecular weight marker I (0.39-6.9 kb), DIG RNA labeling mix, T7 polymerase, PCR-DIG labeling mix, nitro blue tetrazolium chloride (NBT) and 5-bromo-4-chloro-3-indolyl-phosphate (BCIP) were obtained from Roche (Germany). Agarose, MOPS and sodium chloride were purchased from USB (USA). Magnesium chloride, PCR buffer and Taq polymerase were from GenSys (UK). Formaldehyde (37%) was obtained from Riedel-de Haën (Germany). Biodyne[®] membrane was purchased from Pall (USA). Gel blotting paper was obtained from Schleicher & Schuell (Germany). Three MM filter paper was purchased from Whatman[®] (UK). Kapak SealPAK pouches were from KAPAK[®] (USA). Ethidium bromide, maleic acid and sodium citrate were purchased from Sigma (USA).

2.14.2 Methods

2.14.2.1 Formaldehyde agarose gel electrophoresis of total RNA

Three mice from each treatment groups including PPAR α (+/+) control, PPAR α (+/+) 0.1% Wy-14,643, PPAR α (-/-) control and PPAR α (-/-) 0.1% Wy-14,643 were used for Northern blot analysis. For temporal study of gene expression, two mice from each treatment groups at 24 hr, 1 wk, 2 wk, 6 mo and 11 mo were used for Northern blot analysis. Total RNA (20 or 30 μ g in 10 μ l of formamide) samples and 10 μ l RNA molecular marker were mixed with 2 μ l of 10X MOPS, 3 μ l of 37% formaldehyde, 2 μ l of loading dye and 5 μ l of nuclease-free water. RNA samples were then denatured by heating at 68°C for 15 min and then chilled on ice immediately. RNA samples were then separated on a 1% formaldehyde-agarose gel at

30 V for about 15 hr. For temporal study of gene expression, the RNA samples of the 5 different treatment time points were resolved on two gels: PPAR α (+/+) control and PPAR α (+/+) 0.1% Wy-14,643 on one gel, while PPAR α (-/-) control and PPAR α (-/-) 0.1% Wy-14,643 on another gel. The RNA gel was post-stained with 0.5 $\mu\text{g}/\mu\text{l}$ ethidium bromide for 45 min and wash with distilled water for 20 min 3 times. After taking photos, RNA gel was washed in 10X SSC for 30 min and then transferred to a positively charged nylon membrane in 10X SSC buffer by capillary action for 24 hr. After washing with 5X SSC for 5 min, the membrane was baked for 2 hrs at 80°C for fixing the RNA onto the membrane.

2.14.2.2 Preparation of DIG-labeled RNA probes for hybridization

Two nanograms of plasmid DNA were mixed with 80 μM dNTP mix (1:1:1:1), 0.2 μM AP, 0.2 μM T7 ARP (same the primer pairs used for running the fluoroDD RT-PCR), 1X PCR buffer and 0.05 U/ μl of *Taq* polymerase (Appendix A, Table A7). PCR reaction was performed in a thermal cycler (GeneAmp[®] PCR system 9700) and the program was as follows: 95°C for 2 min, followed by 29 cycles of 92°C for 30 sec, 60°C for 30 sec, 72°C for 2 min and 72°C for 7 min and hold at 4°C. Two microliters of reamplified PCR product were resolved on 1% or 2 % agarose, 0.5X TBE with ethidium bromide staining. After confirming the size and specificity of the PCR product, 1 μg of PCR product was used for DIG RNA labeling. For each reaction, PCR product was mixed with 1 mM of DIG RNA labeling mix, 1X transcriptional buffer and 2 U/ μl of T7 polymerase. The mixture was mixed by finger-tapping and incubated at 37°C for 2 hr. The labeling was stopped by adding 2 μl of 0.2 M EDTA at pH 8.0. One microliter labeled probe was resolved on 1% or 2% agarose, 0.5X

TBE gel with ethidium bromide. The labeled probe was stored at -80°C or used immediately.

2.14.2.3 Preparation of PCR-DIG labeled cDNA probe for hybridization

Twenty nanograms of plasmid DNA were mixed with 200 µM PCR DIG labeling mix (1:1:1:1), 1 µM AP, 1 µM T7 ARP (same the primer pairs used for running the fluoroDD RT-PCR), 1X PCR buffer and 0.04 U/µl of *Taq* polymerase (Appendix A, Table A8). PCR reaction was performed in a thermal cycler (GeneAmp® PCR system 9700) and the program was as follows: 95°C for 7 min, followed by 30 cycles of 95°C for 45 sec, 60°C for 1 min, 72°C for 2 min and 72°C for 7 min and hold at 4°C. One microliter of PCR-DIG labeled cDNA probe was resolved on 1% or 2 % agarose, 0.5X TBE with ethidium bromide staining. After confirming the size and specificity of the PCR DIG-labeled cDNA probe, the labeled probe was stored at -80°C or used immediately.

2.14.2.4 Hybridization and colour development

The membrane was pre-hybridized with 20 ml DIG Easy Hyb buffer in a sealable bag at 42 °C for PCR DIG-labeled cDNA probe or 60°C for DIG-labeled RNA probe for 2 hr. For RNA probe, the labeled probe was added to the pre-hybridized buffer and mixed well in a 50 ml Falcon tube. For PCR DIG-labeled probe, the probe was first denatured by boiling for 10 min and then chilled on ice immediately. The denatured probe was added to the pre-hybridized buffer and mixed well in a 50 ml Falcon tube. The pre-hybridized buffer containing the labeled probe was added to the sealable bags and hybridized for overnight at 42 °C for PCR DIG-

labeled cDNA probe or 60°C for DIG-labeled RNA probe. For temporal study of gene expression, two membranes of PPAR α (+/+) and PPAR α (-/-) control and 0.1% Wy-14,643 groups were pre-hybridized and hybridized in 40 ml DIG-Easy Hyb buffer back to back in a sealable bag. The hybridized membrane was washed in 2X SSC (3 M sodium chloride and 0.3 M sodium citrate, pH 7.0) / 0.1% SDS at room temperature for 5 min twice and in either 0.1X SSC / 0.1% SDS at 68°C or 0.5X SSC / 0.1% SDS at 60°C for 5 min twice. The membrane was washed in washing buffer [0.3% Tween 20 in maleic acid buffer (pH 7.5)] for 5 min and then incubated with 1X blocking solution [1X blocking solution in maleic acid buffer (pH 7.5)] for 1 hr. After washing, the membrane was incubated with anti-DIG-alkaline phosphatase antibody in a final concentration of 0.075 U/ml of 1X blocking solution for 1 hr. The membrane was washed in washing buffer twice and then equilibrated in detection buffer [0.1 M Tris-HCl (pH 9.5), 0.1 M MgCl₂ 0.1 M NaCl] for 5 min. The membrane was allowed to develop colour in 25 ml of detection buffer containing 125 μ l and 93.8 μ l of NBT and BCIP, respectively.

Chapter 3 Results

3.1 Confirmation of genotypes by PCR

As there are no observable phenotypic differences between the PPAR α (+/+) and PPAR α (-/-) mice, the genotypes of these mice were confirmed before animal feeding. The sizes of the PCR products of PPAR α (+/+) and PPAR α (-/-) mice were 191 and 1248 bp, respectively (Figures 3.1.1-3.1.2), which was matched with the results from the previous study (Lee *et al.*, 2002).

3.2 Body weight changes

Body weight was significantly lower in the PPAR α (+/+) fed with 0.1% Wy-14,643 compared to the controls (6 and 11 months feeding experiments). In Figure 3.2.1, lower body weight was shown in 0.1% Wy-14,643 treated PPAR α (+/+) mice when compared to the control fed PPAR α (+/+) mice since 1 week feeding. After 6 months of feeding, there was a 9% decrease in body weight when compared with the original body weight. However, increase in body weight in the PPAR α (+/+) mice fed with control diet, PPAR α (-/-) mice fed with control and 0.1% Wy-14,643 were observed (21%, 17% and 21% of the original body weights, respectively). A significant decrease in body weight of 0.1% Wy-14,643 fed PPAR α (+/+) mice was also observed in the 11 months feeding on 0.1% Wy-14,643 diet (Figure 3.2.2). After 11 months feeding, there was a 14% decrease in body weight in the 0.1% Wy-14,643 fed PPAR α (+/+) mice. When compared with the body weight before starting the experiment, there were 23%, 22 % and 17% increase in body weight for the PPAR α

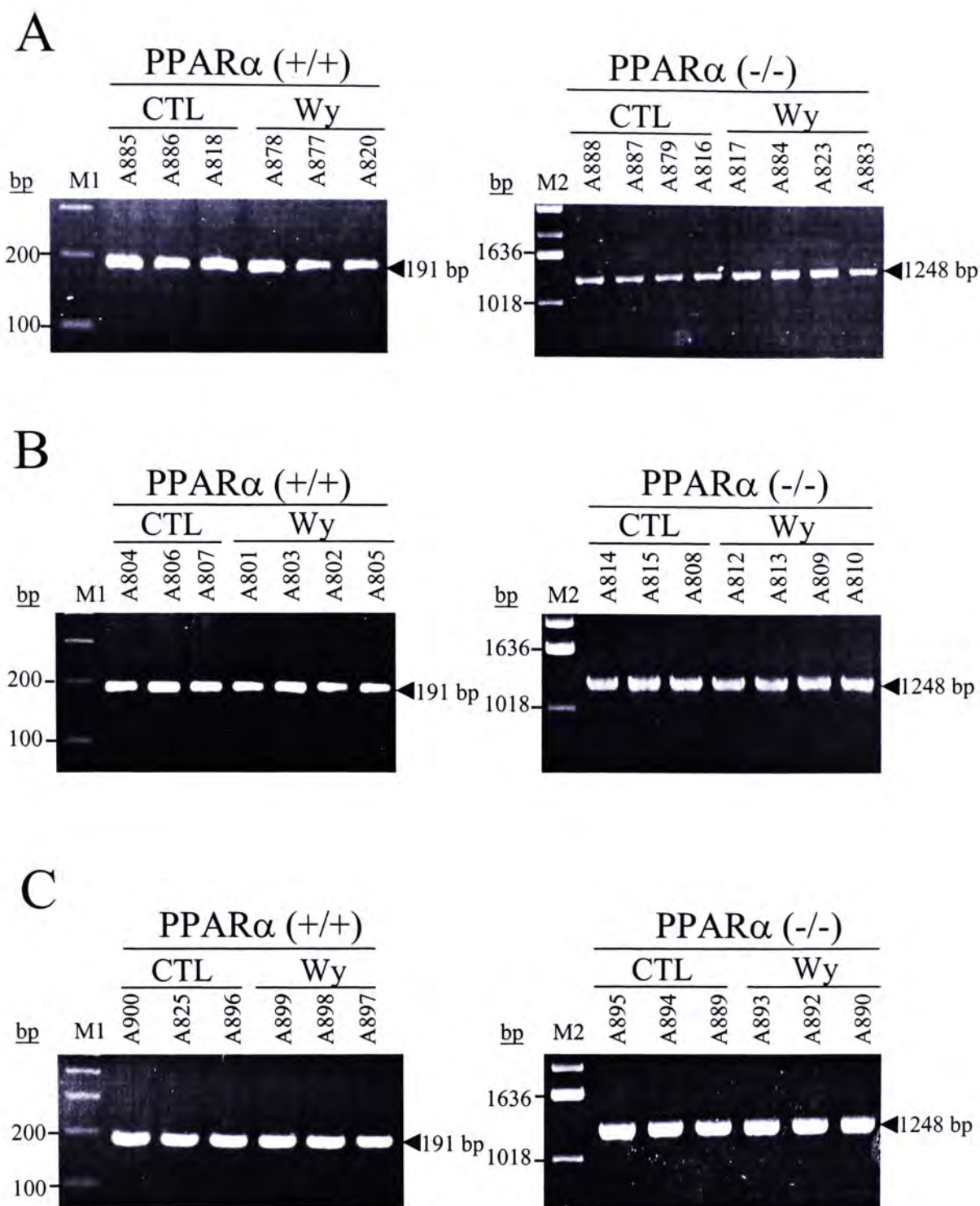


Figure 3.1.1. Confirmation of genotypes of PPAR α (+/+) and PPAR α (-/-) mice used for (A) 24 hours, (B) 1 week and (C) 2 weeks treatment. Tail genotypings of PPAR α (+/+) and PPAR α (-/-) mice fed with a control (CTL) or 0.1% (w/w) Wy-14,643 (Wy) diet for 24 hours, 1 week and 2 weeks were performed. The PCR products of PPAR α (+/+) and PPAR α (-/-) mice were resolved on 2% and 1% agarose, 0.5X TBE gels with ethidium bromide staining, respectively. The expected sizes of PCR products of PPAR α (+/+) and PPAR α (-/-) mice were 191 and 1248 bp, respectively. M1, 100 bp DNA marker; M2, 1 kb DNA marker.

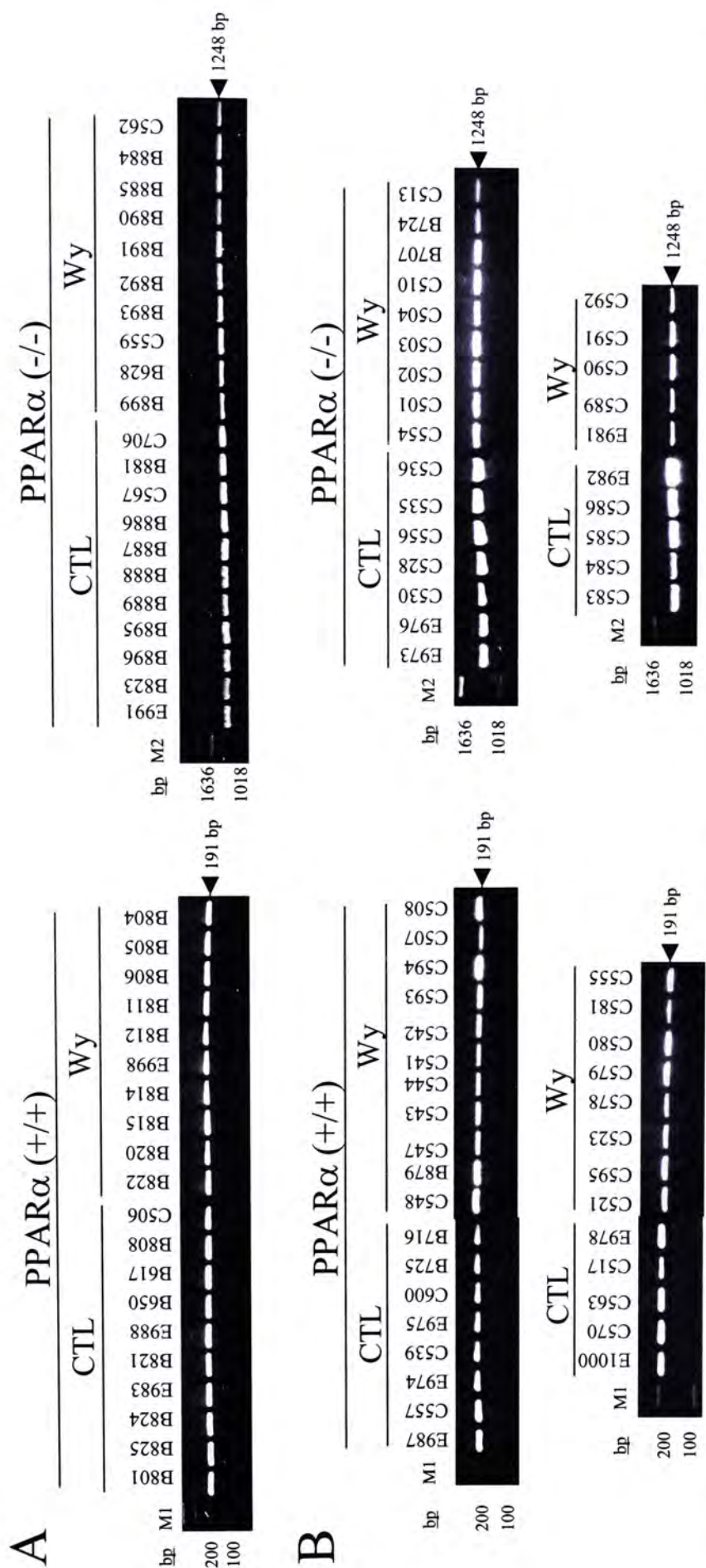
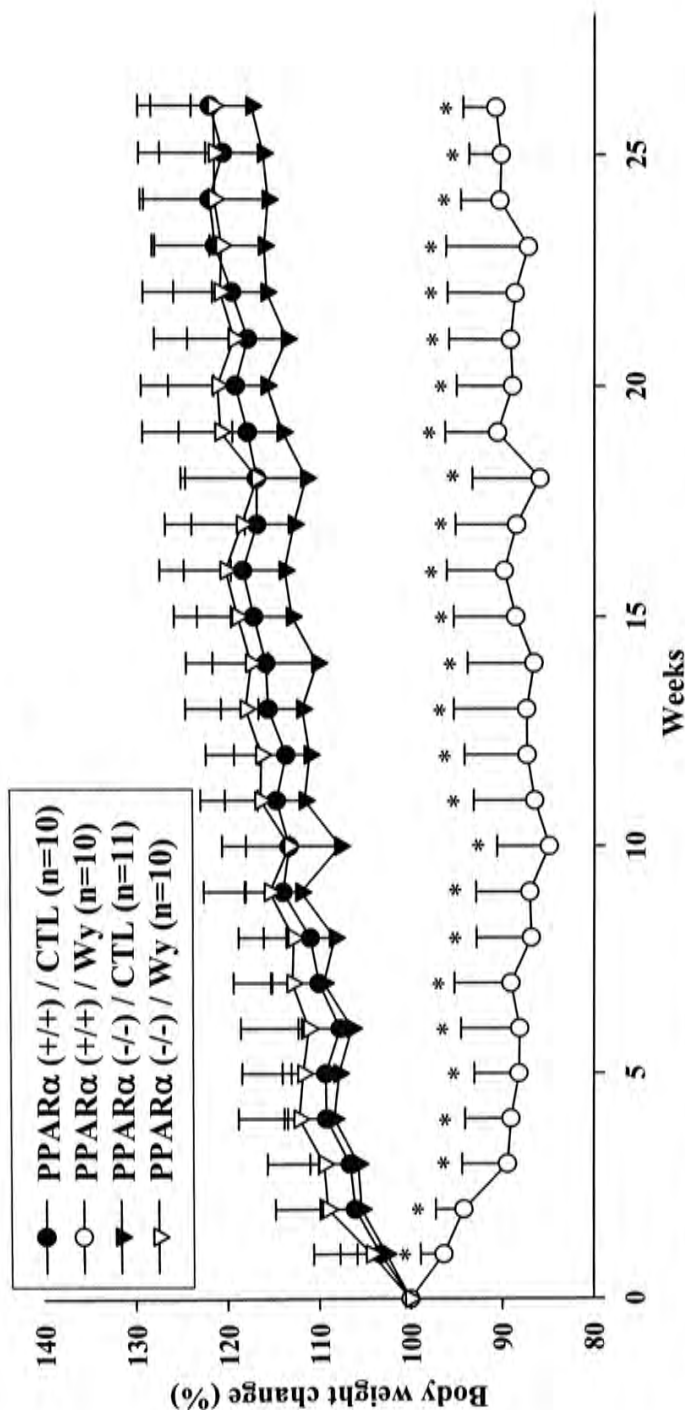


Figure 3.1.2. Confirmation of genotypes of PPAR α (+/+) and PPAR α (-/-) mice used for (A) 6 months and (B) 11 months treatment. Tail genotypings of PPAR α (+/+) and PPAR α (-/-) mice fed with a control (CTL) or 0.1% (w/w) Wy-14,643 (Wy) diet for 6 months and 11 months were performed. The PCR products of PPAR α (+/+) and PPAR α (-/-) mice were resolved on 2% and 1% agarose, 0.5X TBE gels with ethidium bromide staining, respectively. The expected sizes of PCR products of PPAR α (+/+) and PPAR α (-/-) mice were 191 and 1248 bp, respectively. M1, 100 bp DNA marker; M2, 1 kb DNA marker.



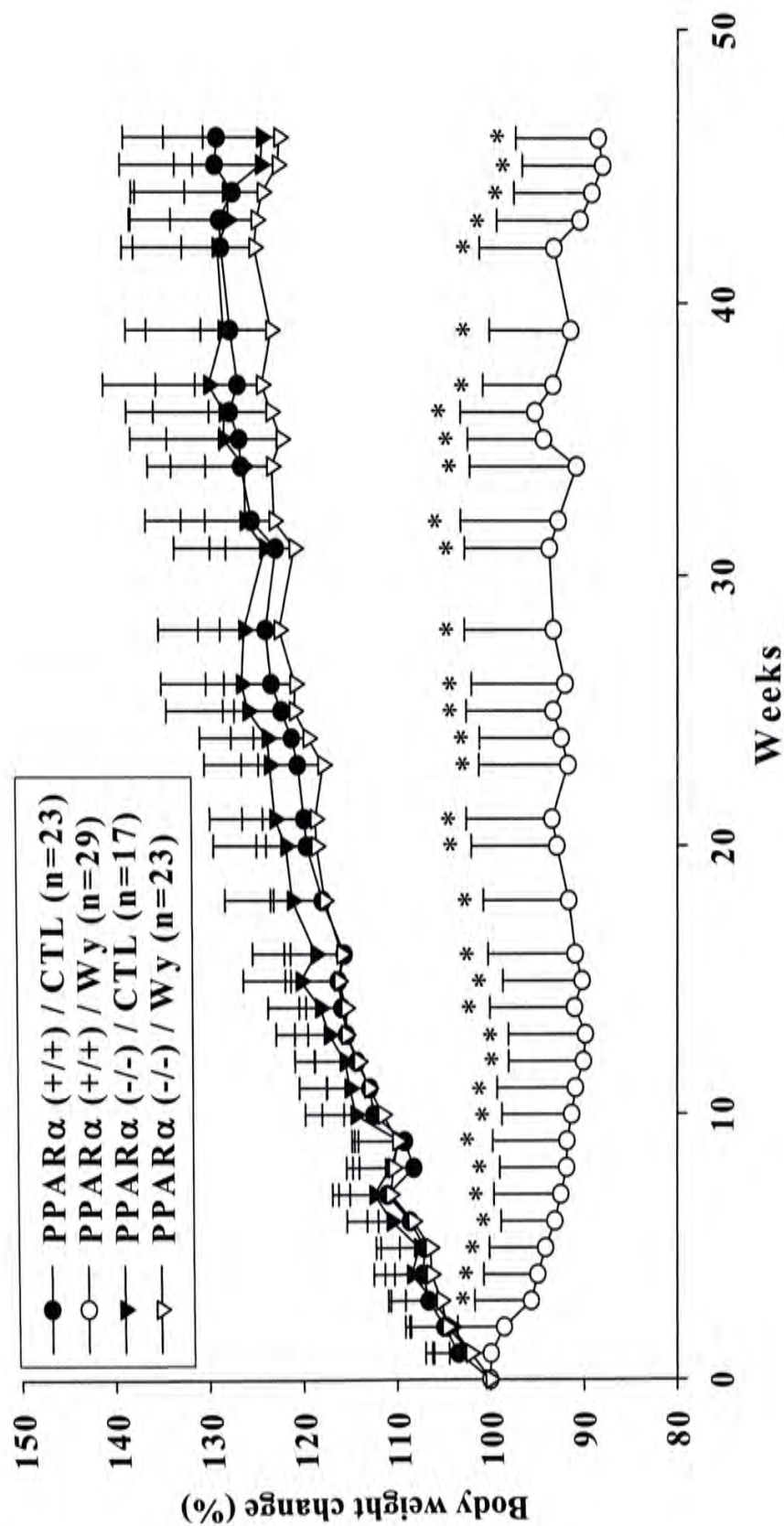


Figure 3.2.2. Effect of 11 months 0.1% Wy-14643 treatment on body weight change (%) in PPARα (+/+) and PPARα (-/-) mice. Data are expressed as mean \pm SD (n \geq 17). Two-way ANOVA was used to compare the differences in mean values within each time-point using SigmaStat Program. *Significant differences ($p \leq 0.001$) from control diet (CTL) group in PPARα (+/+), control diet (CTL) and 0.1% Wy-14,643 treated PPARα (-/-) mice were started from week 1 and till the end of 11 months treatment.

(+/+) mice fed with control diet, PPAR α (-/-) mice fed with control and 0.1% Wy-14,643, respectively. The lower body weight of 0.1% Wy-14,643 treatment of PPAR α (+/+) mice when compared with the other three treatment groups was matched with the previous study (Peters *et al.*, 1997).

Some of the PPAR α (+/+) mice treated with the 0.1% Wy-14,643 diet died before the end of the 6 and 11 months feeding experiment. The high mortality rate observed in PPAR α (+/+) mice fed with 0.1% Wy-14,643 treatment was also reported in the previous study (Peters *et al.*, 1997). Two out of ten mice died (after weeks 13 and 24) in the 6 months feeding experiment. The mortality rate was increased with prolonged treatment. Fifty-two percent of the PPAR α (+/+) mice fed with 0.1% Wy-14,643 started to die in the 11 months feeding experiment. The high mortality in PPAR α (+/+) mice fed with 0.1% Wy-14,643 might be due to the enlargement of liver and liver tumor formation.

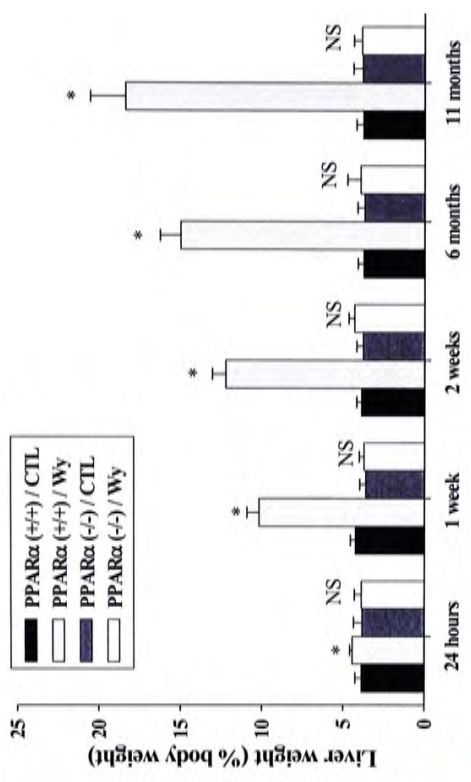
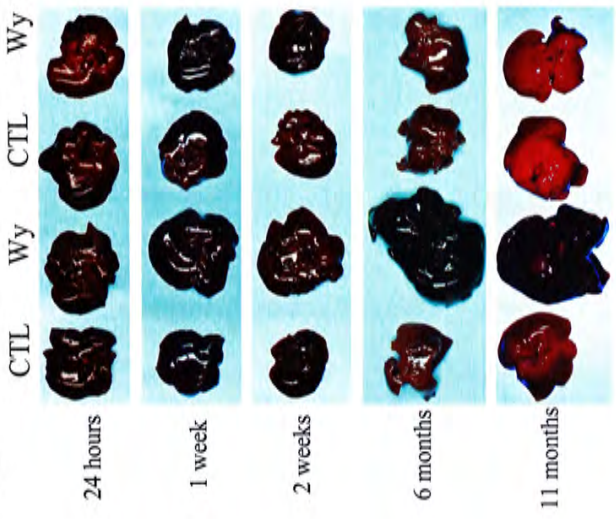
3.3 Organ weight changes

A time-dependent increase in liver weight was observed in PPAR α (+/+) mice fed with the 0.1% Wy-14,643 for 24 hours, 1 week, 2 weeks, 6 months and 11 months (Figure 3.3.1). The liver weights (% of body weight) of the PPAR α (+/+) mice fed with the 0.1% Wy-14,643 diet for 24 hours (1.14-fold), 1 week (1.56-fold), 2 weeks (2.23-fold), 6 months (3-fold) and 11 months (3.88-fold) higher than the PPAR α (+/+) mice fed with control diet. However, liver enlargement was not observed in the 0.1% Wy-14,643-treated PPAR α (-/-) mice at all time points investigated. This observation was agreed to the well-characterized phenomenon of peroxisome proliferators-induced hepatomegaly.

This is a blank page

Figure 3.3.1. Effect of 24 hours, 1 week, 2 weeks, 6 months and 11 months 0.1% Wy-14643 treatment on (A) liver morphology and (B) liver weights of PPAR α (+/+) and PPAR α (-/-) mice. Time-dependent increase in liver weights was observed in PPAR α (+/+) mice fed with a 0.1% Wy-14,643 diet for 24 hr, 1 wk, 2 wk, 6 mo and 11 mo. To account for change in body weights after fed with 0.1% Wy-14,643, liver weights were normalized as percentage of body weight. Data are expressed as mean \pm SD ($n \geq 8$). ANOVA on ranks was used to compare the differences in mean values within each time-point using SigmaStat Program. *Significant difference ($p \leq 0.05$) from control diet (CTL) group in PPAR α (+/+) mice. NS, no significant difference.

A $\text{PPAR}\alpha$ (+/+) $\text{PPAR}\alpha$ (-/-) **B**



In contrast to the liver weight, there was a time-dependent decrease in white fat weight PPAR α (+/+) mice fed with the 0.1% Wy-14,643 diet for 2 weeks (47%), 6 months (75%) and 11 months (86%) (Figure 3.3.2) compared with their corresponding controls. However, this time-dependent decrease in white fat weight was not observed in the 0.1% Wy-14,643-treated PPAR α (-/-) mice when compared to the controls. The decrease in white fat weight was due to the well-documented hypolipidemic effect of the Wy-14,643 compound.

Similar to the white fat weight, a significant time-dependent decrease in the relative brown fat weight was also found in the PPAR α (+/+) mice fed with the 0.1% Wy-14,643 diet for 2 weeks, 6 months and 11 months (Figure 3.3.3). The decrease in brown fat weight for 2 weeks, 6 months and 11 months was 29%, 53% and 62%, respectively and was due to the hypolipidemic action of Wy-14,643 compound.

There was a significant decrease in spleen weight in PPAR α (+/+) mice following 11 months Wy-14,643 treatment (48%) (Figure 3.3.4). The decrease in size of spleen was reported in a previous study (Yang *et al.*, 2000).

No significant change in the brain, heart, lung and testis weights observed in both PPAR α (+/+) and (-/-) mice fed the Wy-14,643 diet at all time points studied compared with their controls (Table 3.3.1).

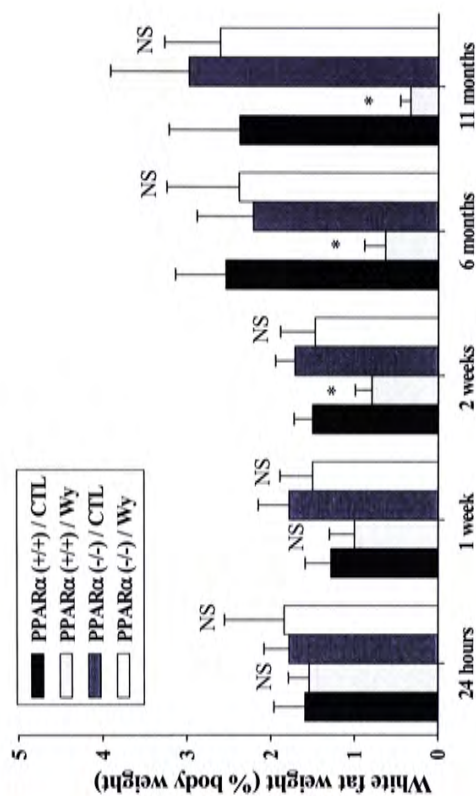
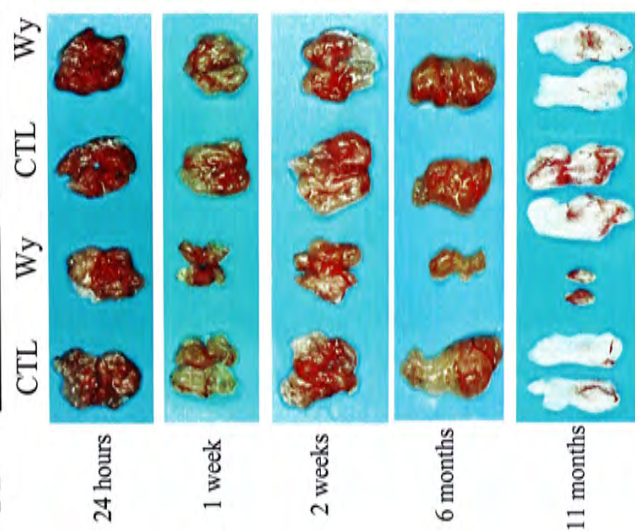
3.4 Serum cholesterol and triglyceride levels

Previous studies have shown that Wy-14,643 treatment decreased the serum cholesterol and triglyceride levels in PPAR α (+/+) mice (Isseman and Green, 1990). To determine the hypolipidemic effect of Wy-14,643, the serum cholesterol and triglyceride levels of all the treatment groups at different feeding treatments were

This is a blank page

Figure 3.3.2. Effect of 24 hours, 1 week, 2 weeks, 6 months and 11 months 0.1% Wy-14643 treatment on (A) white fat morphology and (B) white fat weights of PPAR α (+/+) and PPAR α (-/-) mice. Time-dependent decrease in white fat weights was observed in PPAR α (+/+) mice fed with 0.1% Wy-14,643 diet for 2 wk, 6 mo and 11 mo. To account for change in body weights after fed with a 0.1% Wy-14,643, white fat weights were normalized as percentage of body weight. Data are expressed as mean \pm SD (n \geq 8). ANOVA on ranks was used to compare the differences in mean values within each time-point using SigmaStat Program. *Significant difference ($p \leq 0.05$) from control diet (CTL) group in PPAR α (+/+) mice. NS, no significant difference.

A $\text{PPAR}\alpha$ (+/+) $\text{PPAR}\alpha$ (-/-)

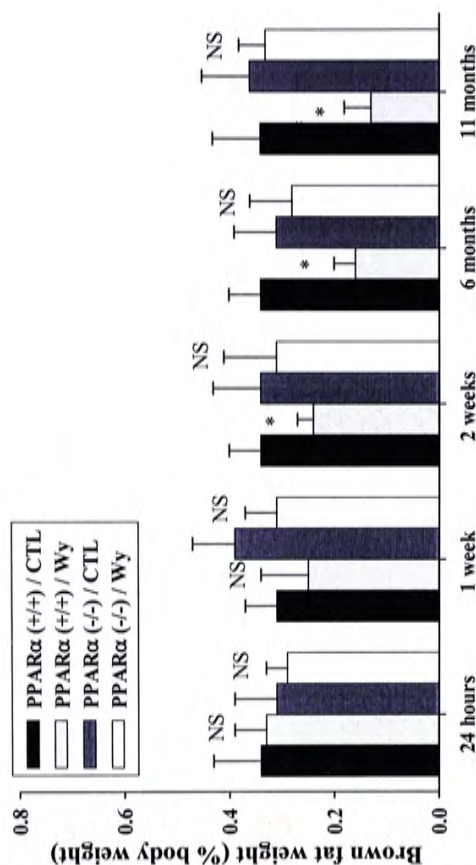
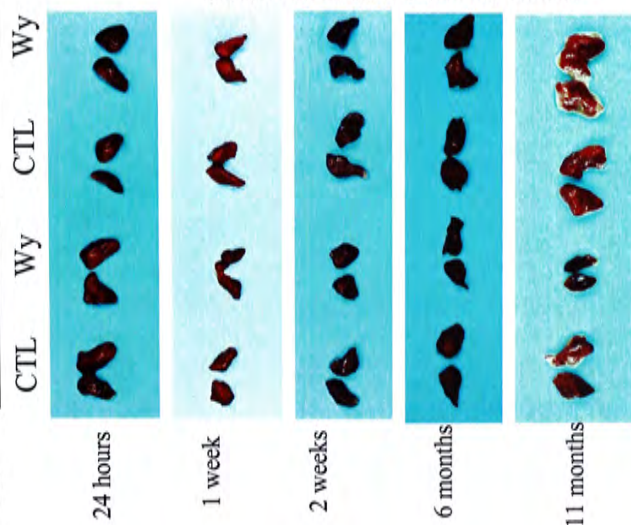


This is a blank page

Figure 3.3.3. Effect of 24 hours, 1 week, 2 weeks, 6 months and 11 months 0.1% Wy-14643 treatment on (A) brown fat morphology and (B) brown fat weights of PPAR α (+/+) and PPAR α (-/-) mice. Time-dependent decrease in brown fat weights was observed in PPAR α (+/+) mice fed with 0.1% Wy-14,643 diet for 2 wk, 6 mo and 11 mo. To account for change in body weights after fed with a 0.1% Wy-14,643, brown fat weights were normalized as percentage of body weight. Data are expressed as mean \pm SD ($n \geq 8$). ANOVA on ranks was used to compare the differences in mean values within each time-point using SigmaStat Program.

*Significant difference ($p \leq 0.05$) from control diet (CTL) group in PPAR α (+/+) mice. NS, no significant difference.

A $\text{PPAR}\alpha$ (+/+) $\text{PPAR}\alpha$ (-/-)



This is a blank page

Figure 3.3.4. Effect of 24 hours, 1 week, 2 weeks, 6 months and 11 months 0.1% Wy-14643 treatment on (A) spleen morphology and (B) spleen weights of PPAR α (+/+) and PPAR α (-/-) mice. Decrease in spleen weights was observed in PPAR α (+/+) mice fed with 0.1% Wy-14,643 diet for 11 mo. To account for change in body weights after fed with a 0.1% Wy-14,643, spleen weights were normalized as percentage of body weight. Data are expressed as mean \pm SD ($n \geq 8$). ANOVA on ranks was used to compare the differences in mean values within each time-point using SigmaStat Program. *Significant difference ($p \leq 0.05$) from control diet (CTL) group in PPAR α (+/+) mice. NS, no significant difference.

Table 3.3.1. Effect of Wy-14,643 feeding on kidney, heart, brain, lung and testis weight change of 24 hours, 1 week, 2 weeks, 6 months and 11 months feeding experiment.

	Group	Kidney (%)	Heart (%)	Brain (%)	Lung (%)	Testis (%)
24 hr	PPAR α (+/+)/CTL	1.48 \pm 0.13	0.54 \pm 0.04	1.63 \pm 0.19	0.65 \pm 0.11	0.94 \pm 0.14
	PPAR α (+/+)/Wy	1.49 \pm 0.15	0.54 \pm 0.07	1.73 \pm 0.19	0.71 \pm 0.11	0.74 \pm 0.09
	PPAR α (-/-)/CTL	1.45 \pm 0.16	0.58 \pm 0.07	1.66 \pm 0.15	0.62 \pm 0.09	0.79 \pm 0.04
	PPAR α (-/-)/Wy	1.55 \pm 0.38	0.59 \pm 0.07	1.51 \pm 0.15	0.67 \pm 0.23	0.79 \pm 0.06
1 wk	PPAR α (+/+)/CTL	1.55 \pm 0.13	0.56 \pm 0.08	1.76 \pm 0.31	0.72 \pm 0.23	0.86 \pm 0.04
	PPAR α (+/+)/Wy	1.60 \pm 0.16	0.59 \pm 0.12	2.04 \pm 0.13	0.78 \pm 0.24	0.94 \pm 0.06
	PPAR α (-/-)/CTL	1.51 \pm 0.21	0.55 \pm 0.11	1.53 \pm 0.07	0.74 \pm 0.23	1.08 \pm 0.36
	PPAR α (-/-)/Wy	1.54 \pm 0.23	0.56 \pm 0.10	1.64 \pm 0.14	0.91 \pm 0.25	0.74 \pm 0.06
2 wk	PPAR α (+/+)/CTL	1.51 \pm 0.09	0.53 \pm 0.03	1.74 \pm 0.06	0.81 \pm 0.16	0.87 \pm 0.23
	PPAR α (+/+)/Wy	1.60 \pm 0.09	0.55 \pm 0.05	1.92 \pm 0.12	0.71 \pm 0.15	0.79 \pm 0.12
	PPAR α (-/-)/CTL	1.43 \pm 0.12	0.51 \pm 0.07	1.65 \pm 0.17	0.69 \pm 0.10	0.90 \pm 0.38
	PPAR α (-/-)/Wy	1.51 \pm 0.18	0.53 \pm 0.04	1.48 \pm 0.14	0.65 \pm 0.16	0.73 \pm 0.05
6 mo	PPAR α (+/+)/CTL	1.51 \pm 0.10	0.50 \pm 0.06	1.44 \pm 0.14	0.67 \pm 0.13	0.66 \pm 0.10
	PPAR α (+/+)/Wy	1.47 \pm 0.11	0.71 \pm 0.06	1.90 \pm 0.16	0.95 \pm 0.21	0.73 \pm 0.05
	PPAR α (-/-)/CTL	1.58 \pm 0.19	0.56 \pm 0.06	1.47 \pm 0.18	0.77 \pm 0.17	0.68 \pm 0.13
	PPAR α (-/-)/Wy	1.57 \pm 0.21	0.52 \pm 0.06	1.43 \pm 0.16	0.71 \pm 0.14	0.67 \pm 0.16
11 mo	PPAR α (+/+)/CTL	1.62 \pm 0.13	0.54 \pm 0.07	1.43 \pm 0.15	0.63 \pm 0.11	0.68 \pm 0.07
	PPAR α (+/+)/Wy	1.50 \pm 0.17	0.75 \pm 0.10	1.90 \pm 0.22	0.93 \pm 0.16	0.64 \pm 0.08
	PPAR α (-/-)/CTL	1.57 \pm 0.18	0.54 \pm 0.05	1.35 \pm 0.18	0.61 \pm 0.10	0.60 \pm 0.14
	PPAR α (-/-)/Wy	1.54 \pm 0.11	0.53 \pm 0.05	1.42 \pm 0.12	0.61 \pm 0.09	0.64 \pm 0.14

Relative body weight was expressed as organ weight (g)/ body weight (g) X 100%.

measured in this study. There were no significant differences in serum cholesterol level among the four treatment groups at 24 hours gavage, 1 week, 2 weeks and 6 months feeding (Figure 3.4.1). There was a 29% increase in serum cholesterol level in PPAR α (+/+) mice fed the Wy-14,643 diet for 11 months when compared with the PPAR α (+/+) mice fed the control diet. This increase was not observed in the PPAR α (-/-) mice fed with 0.1% Wy-14,643. In contrast, a time-dependent decrease in serum triglyceride level was observed in the PPAR α (+/+) mice fed with the 0.1% Wy-14,643 diet for 24 hours (44%), 1 week (38%), 2 weeks (35%), 6 months (66%) and 11 months (77%) (Figure 3.4.2) feeding studies were observed. However, no significant changes were found in the PPAR α (-/-) mice fed with the 0.1% Wy-14,643 diet when compared with the controls.

3.5 Liver histology

To examine the liver damage resulting from Wy-14,643 treatment, liver sections from 24 hour, 1 week, 2 weeks, 6 months and 11 months Wy-14,643 treatment were used for histological studies. Figures 3.5.1 and 3.5.2 showed the central vein region of the four treatment groups after 24 hours gavage treatment with Wy-14,643 compound. Normal hepatocytes were arranged in a series of anastomosing plates with one cell thick. Between the anastomosing plates were sinusoidal spaces. These plates extended from the periphery of a lobule to the central vein at its center. Normal liver histology was found in the central vein (Figure 3.5.1A, 3.5.1B, 3.5.2A, 3.5.2B), middle zone (Figures 3.5.3A, 3.5.3B, 3.5.4A, 3.5.4B) and portal vein region (Figures 3.5.5A, 3.5.5B, 3.5.6A, 3.5.6B) of the PPAR α (+/+) mice fed with a control or 0.1% Wy-14,643 diet. However, severe accumulation of lipid droplets was

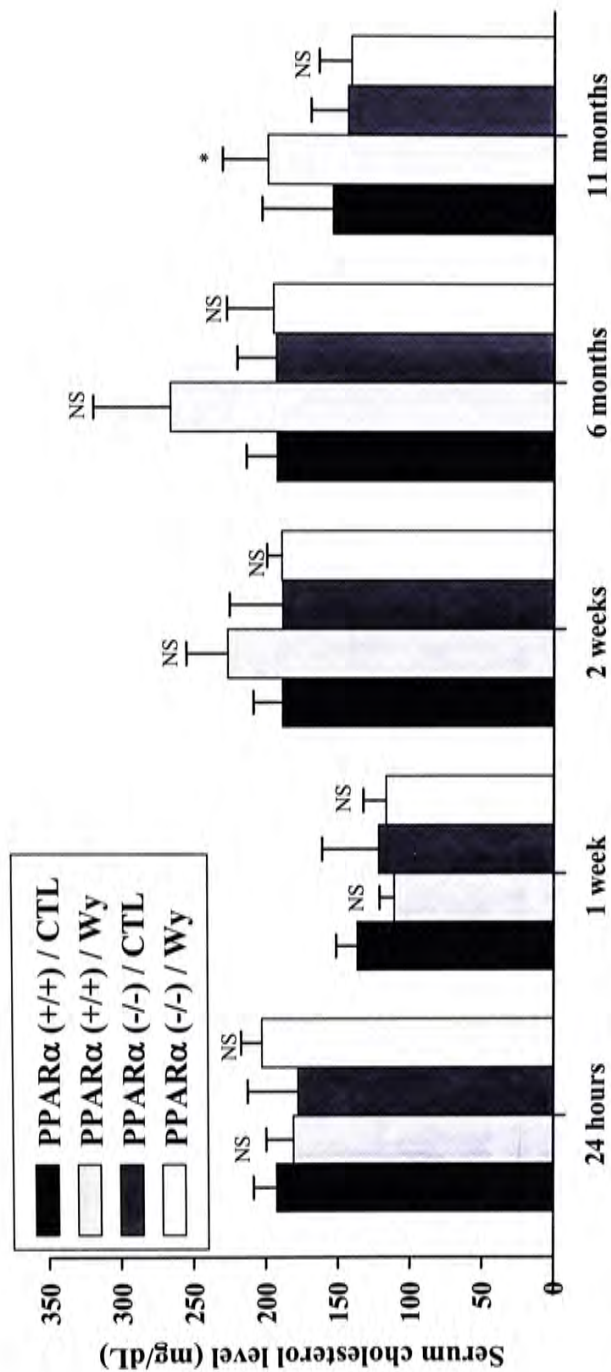


Figure 3.4.1. Effect of 24 hours, 1 week, 2 weeks, 6 months and 11 months 0.1% Wy-14643 treatment on serum cholesterol level of PPARα (+/+) and PPARα (-/-) mice. Data are expressed as mean \pm SD ($n \geq 8$). ANOVA on ranks was used to compare the differences in mean values within each time-point using SigmaStat Program. *Significant difference ($p \leq 0.05$) from control (CTL) fed PPARα (+/+) mice. NS, no significant difference.

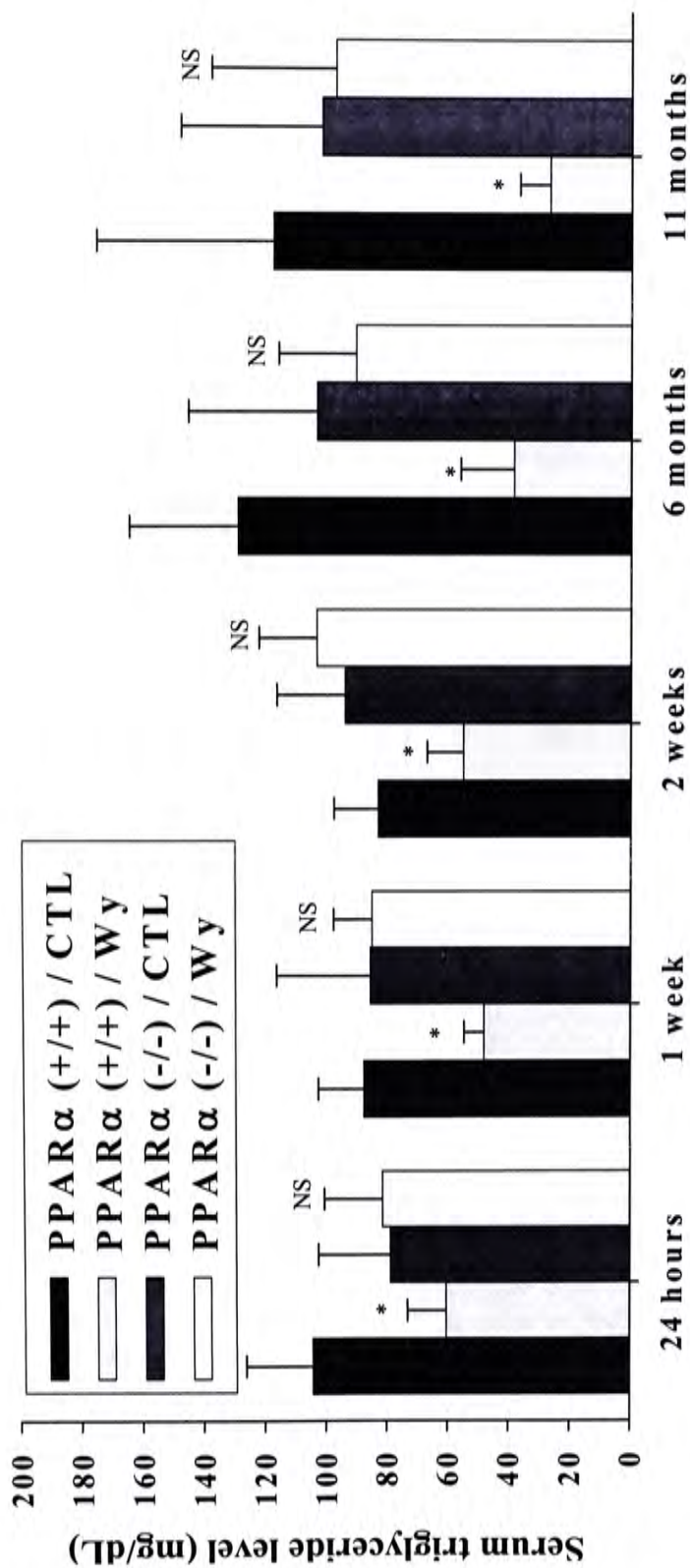


Figure 3.4.2. Effect of 24 hours, 1 week, 2 weeks, 6 months and 11 months 0.1% Wy-14643 treatment on serum triglyceride level of PPARα (+/+) and PPARα (-/-) mice. Data are expressed as mean \pm SD ($n \geq 8$). ANOVA on ranks was used to compare the differences in mean values within each time-point using SigmaStat Program. *Significant difference ($p \leq 0.05$) from control (CTL) fed PPARα (+/+).

24 hours
Central vein region (20X)

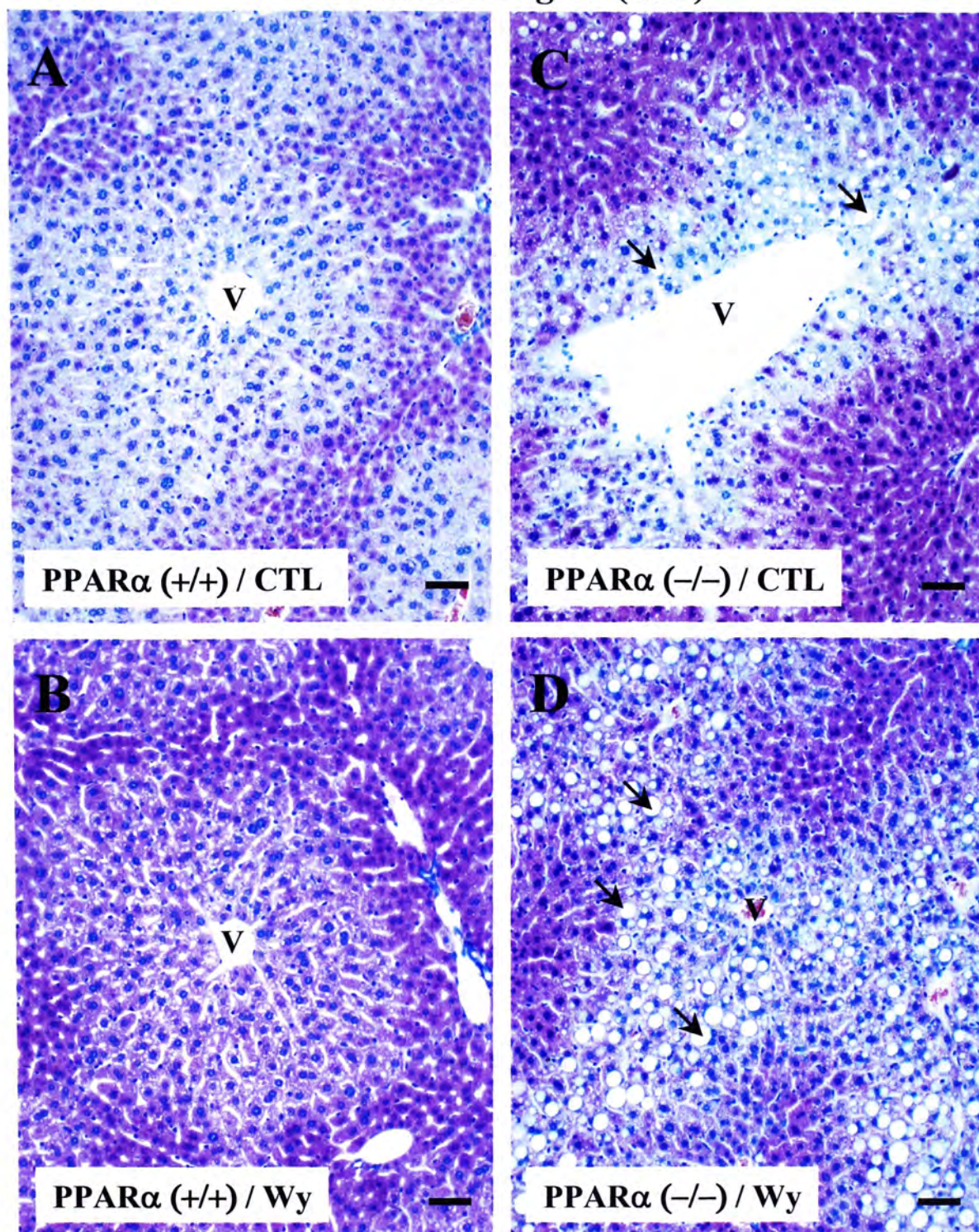


Figure 3.5.1. Hematoxylin and eosin staining of the central vein region (20X) of liver sections (5 μ m) taken from PPAR α (+/+) and PPAR α (-/-) mice after 24 hours gavage feeding with 1% methylcellulose (control vehicle) (panels A, B) or Wy-14,643 (50 mg/kg bw) (panels C, D) (n=3). Hepatocytes were arranged radially from the central vein. Normal liver histology was found in the central vein region of both control vehicle and Wy-14,643 fed PPAR α (+/+) mice. Severe lipid accumulation (arrows) was found around the central vein region in both control vehicle and Wy-14,643 fed PPAR α (-/-) mice. V, central vein. Bars, 50 μ m.

24 hours
Central vein region (40X)

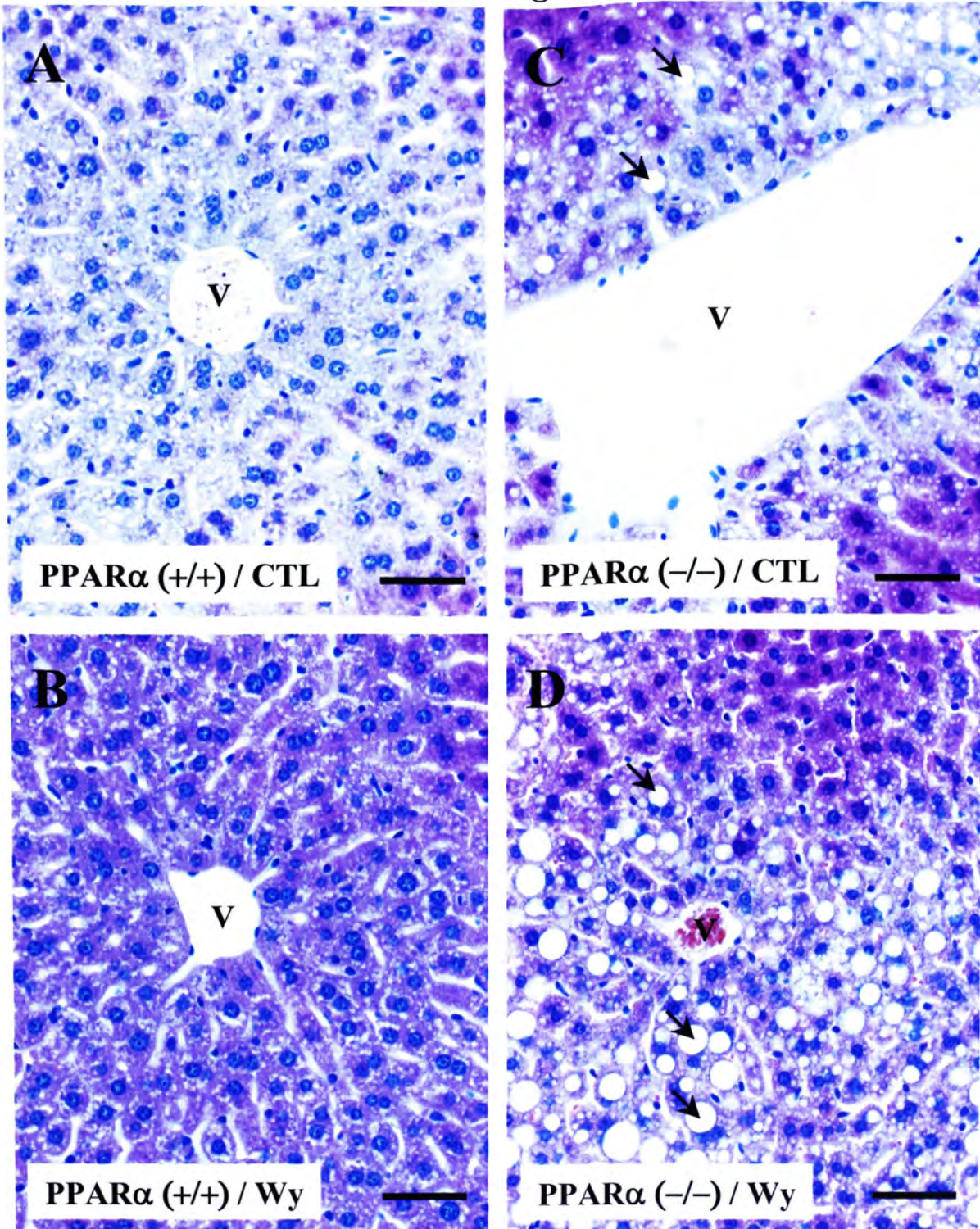


Figure 3.5.2. Hematoxylin and eosin staining of the central vein region (40X) of liver sections (5 μ m) taken from PPAR α (+/+) and PPAR α (-/-) mice after 24 hours gavage feeding with 1% methylcellulose (control vehicle) (panels A, B) or Wy-14,643 (50 mg/kg bw) (panels C, D) (n=3). Normal liver histology was found in the central vein region of both control vehicle and Wy-14,643 fed PPAR α (+/+) mice. Severe lipid accumulation (arrows) was found around the central vein region in both control vehicle and Wy-14,643 fed PPAR α (-/-) mice. Macrovesicular droplets were formed inside the hepatocytes which displaced the nuclei to the periphery of the hepatocytes. V, central vein. Bars, 50 μ m.

24 hours
Middle zone (20X)

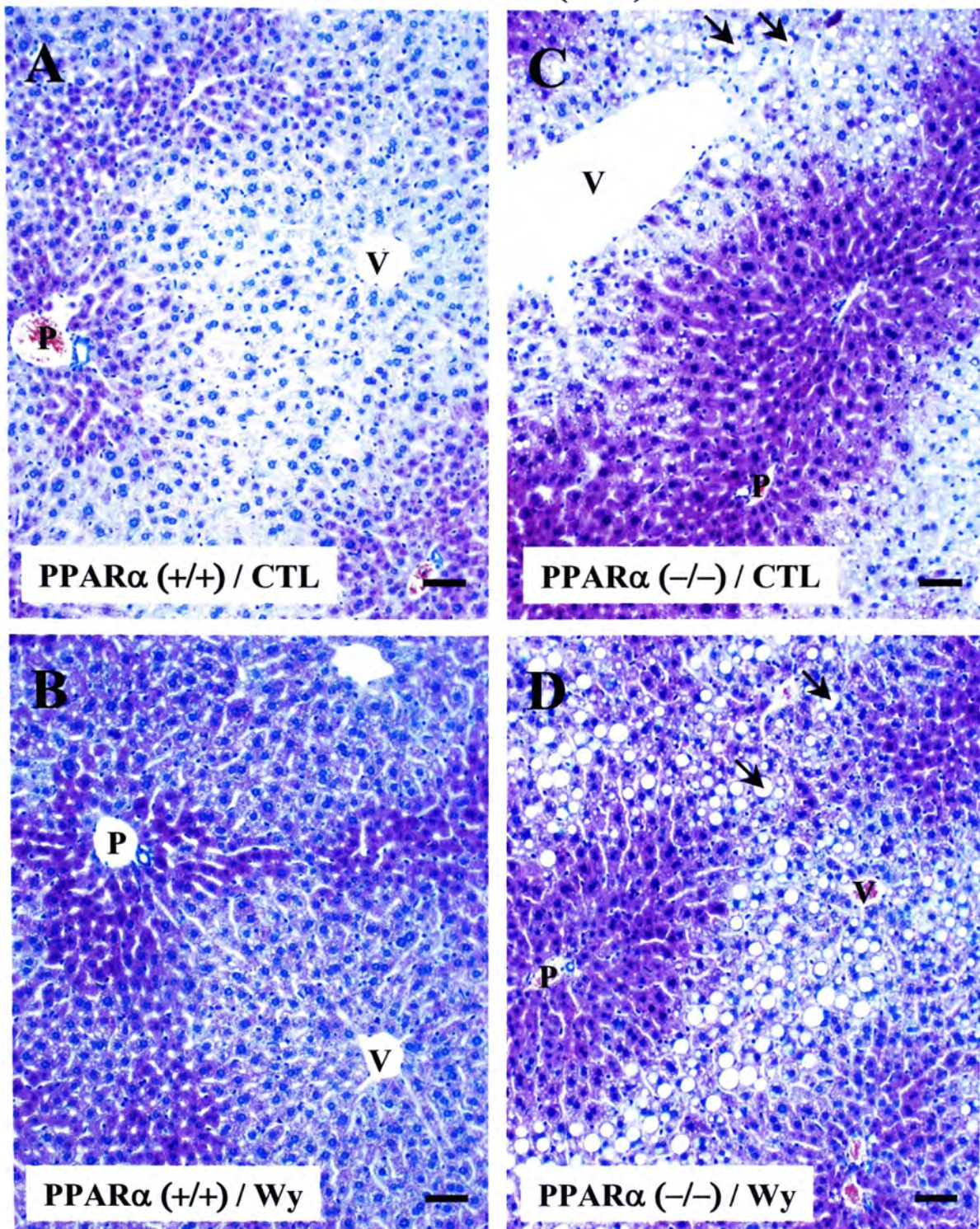


Figure 3.5.3. Hematoxylin and eosin staining of the middle zone (20X) of liver sections (5 μ m) taken from PPAR α (+/+) and PPAR α (-/-) mice after 24 hours gavage feeding with 1% methylcellulose (control vehicle) (panels A, B) or Wy-14,643 (50 mg/kg bw) (panels C, D) (n=3). Normal liver histology was found in the middle zone of both control vehicle and Wy-14,643 fed PPAR α (+/+) mice. Severe lipid accumulation (arrows) were found around the central vein region in both control vehicle and Wy-14,643 fed PPAR α (-/-) mice. P, portal vein. V, central vein. Bars, 50 μ m.

24 hours
Middle zone (40X)

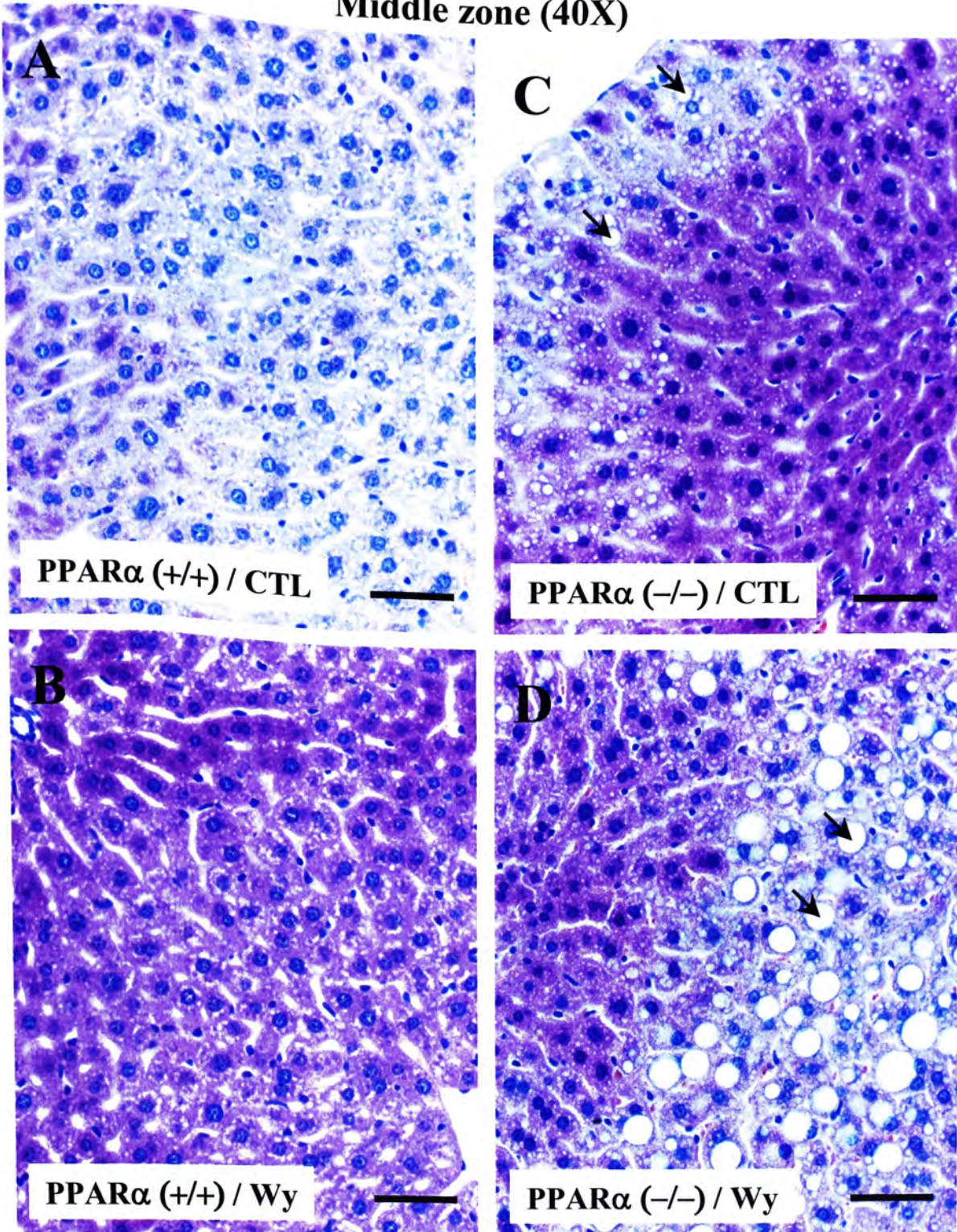


Figure 3.5.4. Hematoxylin and eosin staining of the middle zone (40X) of liver sections (5 μ m) taken from PPAR α (+/+) and PPAR α (-/-) mice after 24 hours gavage feeding with 1% methylcellulose (control vehicle) (panels A, B) or Wy-14,643 (50 mg/kg bw) (panels C, D) (n=3). Normal liver histology was found in the middle zone of both control vehicle and Wy-14,643 fed PPAR α (+/+) mice. P, portal triad. Bars, 50 μ m.

24 hours
Portal vein region (20X)

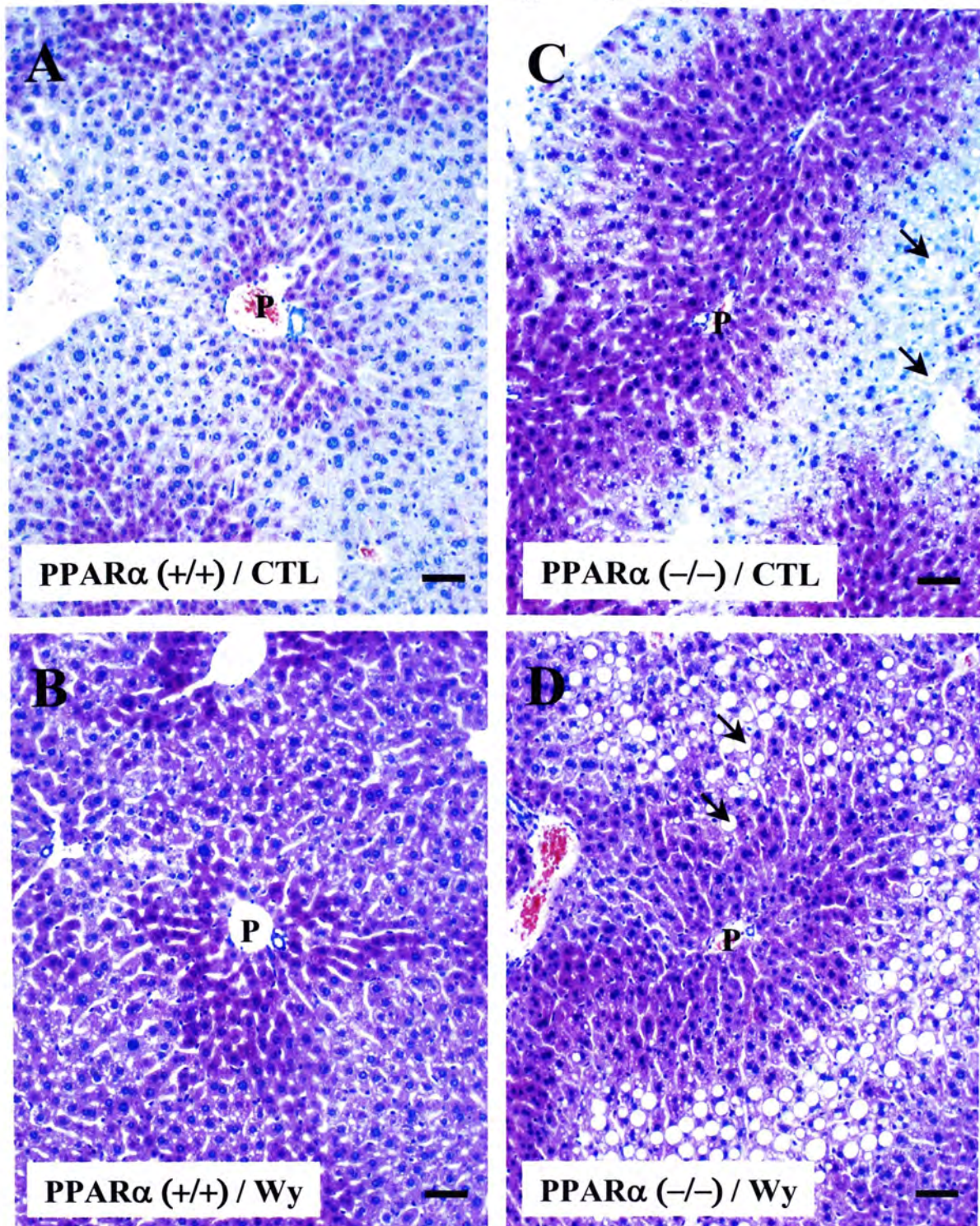


Figure 3.5.5. Hematoxylin and eosin staining of the portal vein region (20X) of liver sections (5 μ m) taken from PPAR α (+/+) and PPAR α (-/-) mice after 24 hours gavage feeding with 1% methylcellulose (control vehicle) (panels A, B) or Wy-14,643 (50 mg/kg bw) (panels C, D) (n=3). Normal liver histology was found in the portal vein region of both control vehicle and Wy-14,643 fed PPAR α (+/+) mice fed. P, portal triad. Bars, 50 μ m.

24 hours
Portal vein region (40X)

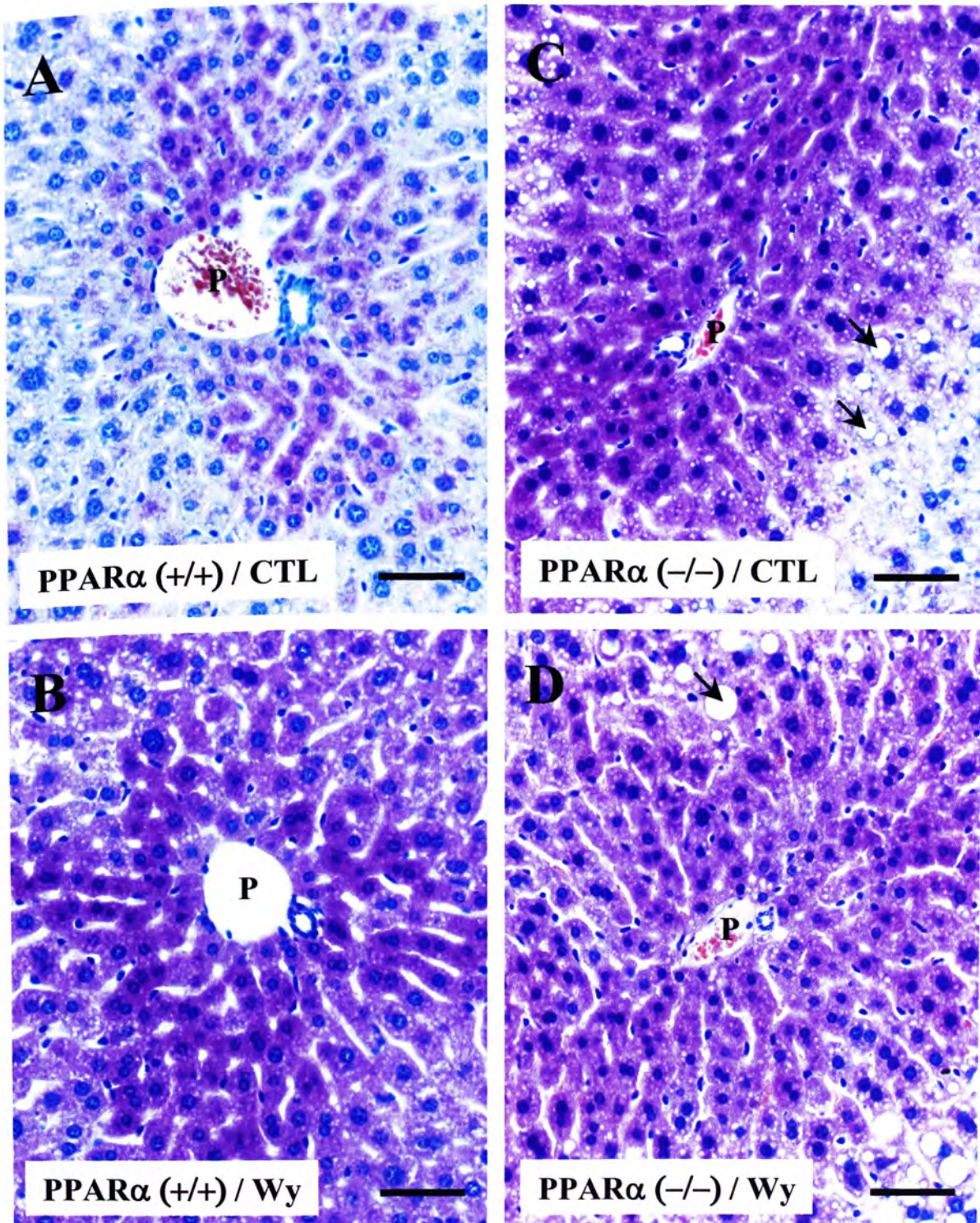


Figure 3.5.6. Hematoxylin and eosin staining of the portal vein region (40X) of liver sections (5 μm) taken from PPARα (+/+) and PPARα (-/-) mice after 24 hours gavage feeding with 1% methylcellulose (control vehicle) (panels A, B) or Wy-14,643 (50 mg/kg bw) (panels C, D) (n=3). Normal liver histology was found in the portal vein region of both control vehicle and Wy-14,543 fed PPARα (+/+) mice. P, portal triad. Bars, 50 μm.

observed near the central vein for both the control (Figure 3.5.1C) and 0.1% Wy-14,643 fed PPAR α (-/-) mice (Figure 5.5.1D). Macrovesicular droplets were formed inside the hepatocytes which displaced the nuclei to the periphery of the hepatocytes (Figures 3.5.2C, 3.5.2D). The accumulation of the lipid droplets in both the control and treatment groups of the PPAR α (-/-) mice suggesting that the disruption of PPAR α gene is involved in the lipid metabolism.

Similar to the 24 hour gavage feeding, normal liver histology was found in the central vein (Figures 3.5.7A, 3.5.8A), middle zone (Figures 3.5.9A, 3.5.10A) and portal vein region (Figures 3.5.11A, 3.5.12A) in PPAR α (+/+) mice fed with control diet. However, the normal arrangement of the hepatocytes was not found in the PPAR α (+/+) mice fed with 0.1% Wy-14,643 (Figures 3.5.7B, 3.5.8B). The sinusoids between hepatocytes become larger in the 0.1% Wy-14,643-treated PPAR α (+/+) mice. Accumulation of the lipid droplets were found around the central veins in both the control and treated groups of the PPAR α (-/-) mice (Figures 3.5.7C, 3.5.7D, 3.5.8C, 3.5.8D).

Large sinusoidal spaces were observed in the PPAR α (+/+) mice treated with 0.1% Wy-14,643 at 2 week feeding study in the central vein region (Figures 3.5.13B, 3.5.14B), middle zone (Figures 3.5.15B, 3.5.16B) and portal vein region (Figures 3.5.17B, 3.5.18B). In addition, abnormal and irregular hepatocytes arrangement was also found in the Wy-14,643-treated group in PPAR α (+/+) mice in the central vein region (Figures 3.5.13B, 3.5.14B), middle zone (Figures 3.5.15B, 3.5.16B) and portal vein region (Figures 3.5.17B, 3.5.18B). Lipid accumulation was found in central vein region of both the control and treatment groups of the PPAR α (-/-) mice (Figures 3.5.13C, 3.5.14D, 3.5.13C, 3.5.14D).

1 week
Central vein region (20X)

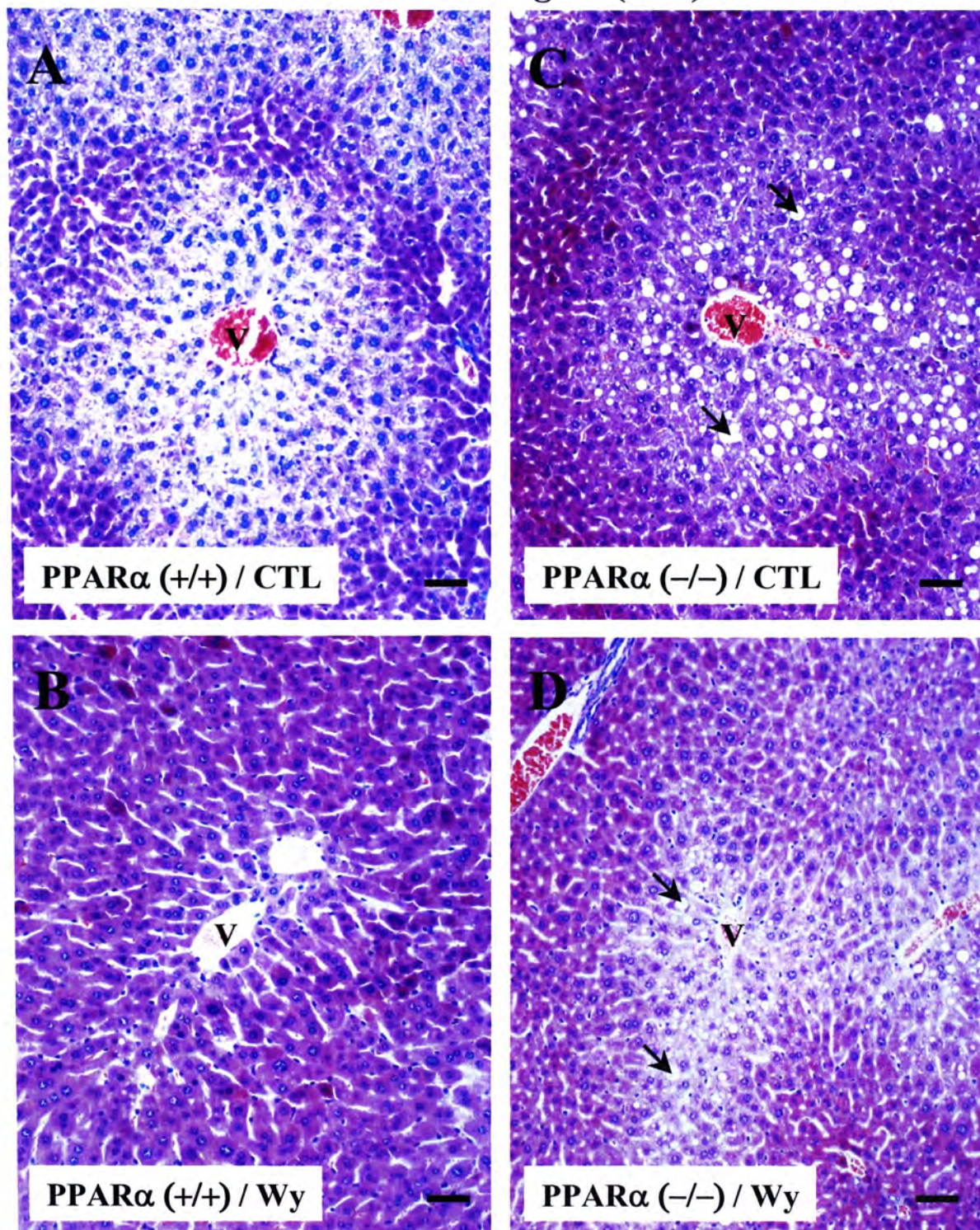


Figure 3.5.7. Hematoxylin and eosin staining of the central vein region (20X) of liver sections (5 μ m) taken from PPAR α (+/+) and PPAR α (-/-) mice after 1 week treatment with a 0.0% Wy-14,643 (control diet) (panels A, B) or a 0.1% Wy-14,643 diet (panels C, D) (n=3). Normal liver histology was found in central vein region of PPAR α (+/+) mice fed with control diet. Increased sinusoid spaces was found in the 0.1% Wy-14,643 fed PPAR α (+/+) mice. Severe lipid accumulation (arrows) was found around the central vein region in both control and Wy-14,643 fed PPAR α (-/-) mice. V, central vein. Bars, 50 μ m.

1 week
Central vein region (40X)

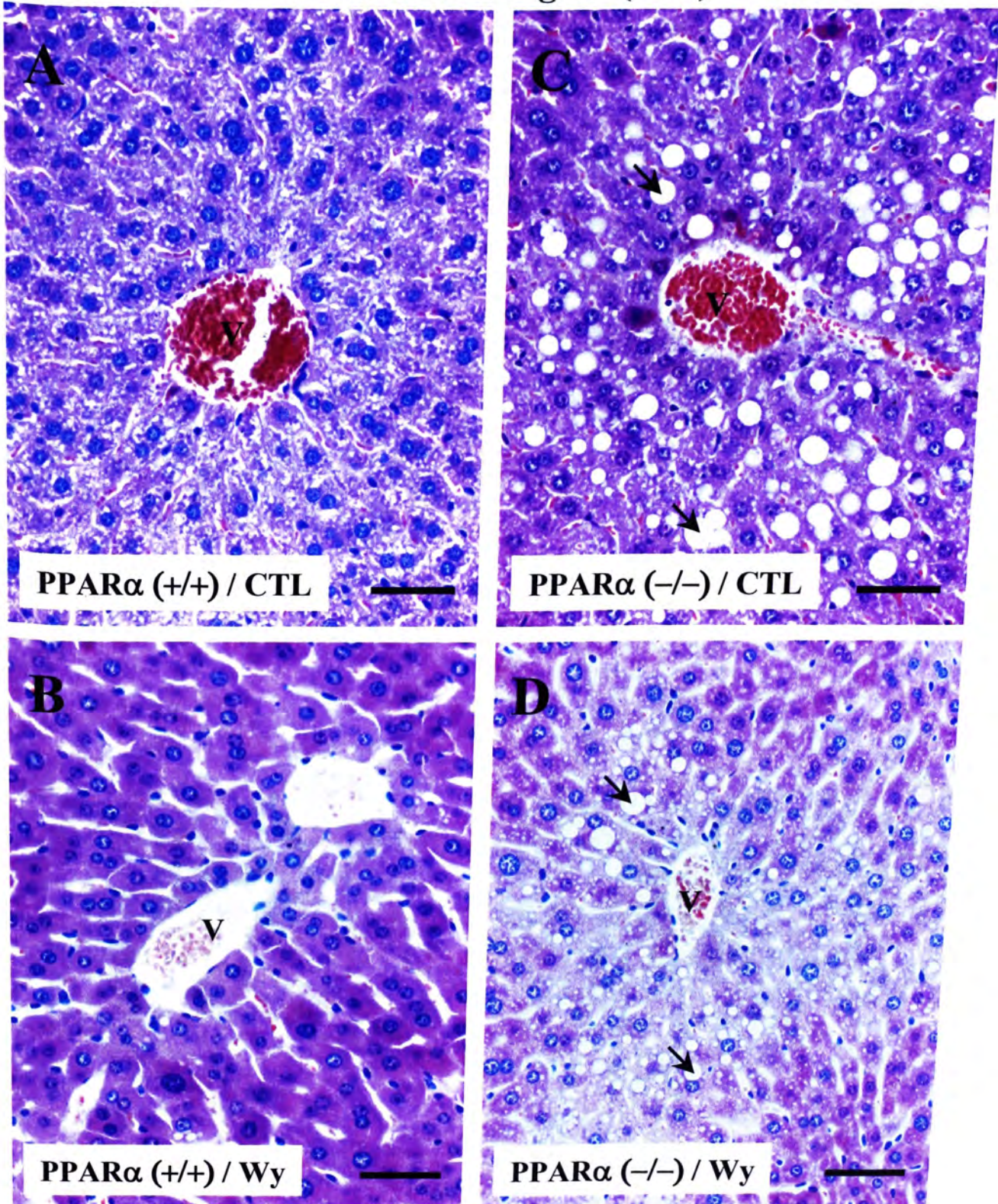


Figure 3.5.8. Hematoxylin and eosin staining of the central vein region (40X) of liver sections (5 μ m) taken from PPAR α (+/+) and PPAR α (-/-) mice after 1 week treatment with a 0.0% Wy-14,643 (control diet) (panels A, B) or a 0.1% Wy-14,643 diet (panels C, D) (n=3). Sinusoidal spaces between hepatocytes of PPAR α (+/+) 0.1% Wy-14,643 treated mice were more obvious. Severe lipid accumulation (arrows) was found around the central vein region in both control and Wy-14,643 diet fed PPAR α (-/-) mice. Macrovesicular droplets were formed inside the hepatocytes and displace the nuclei to the periphery of the hepatocytes. V, central vein. Bars, 50 μ m.

1 week
Middle zone (20X)

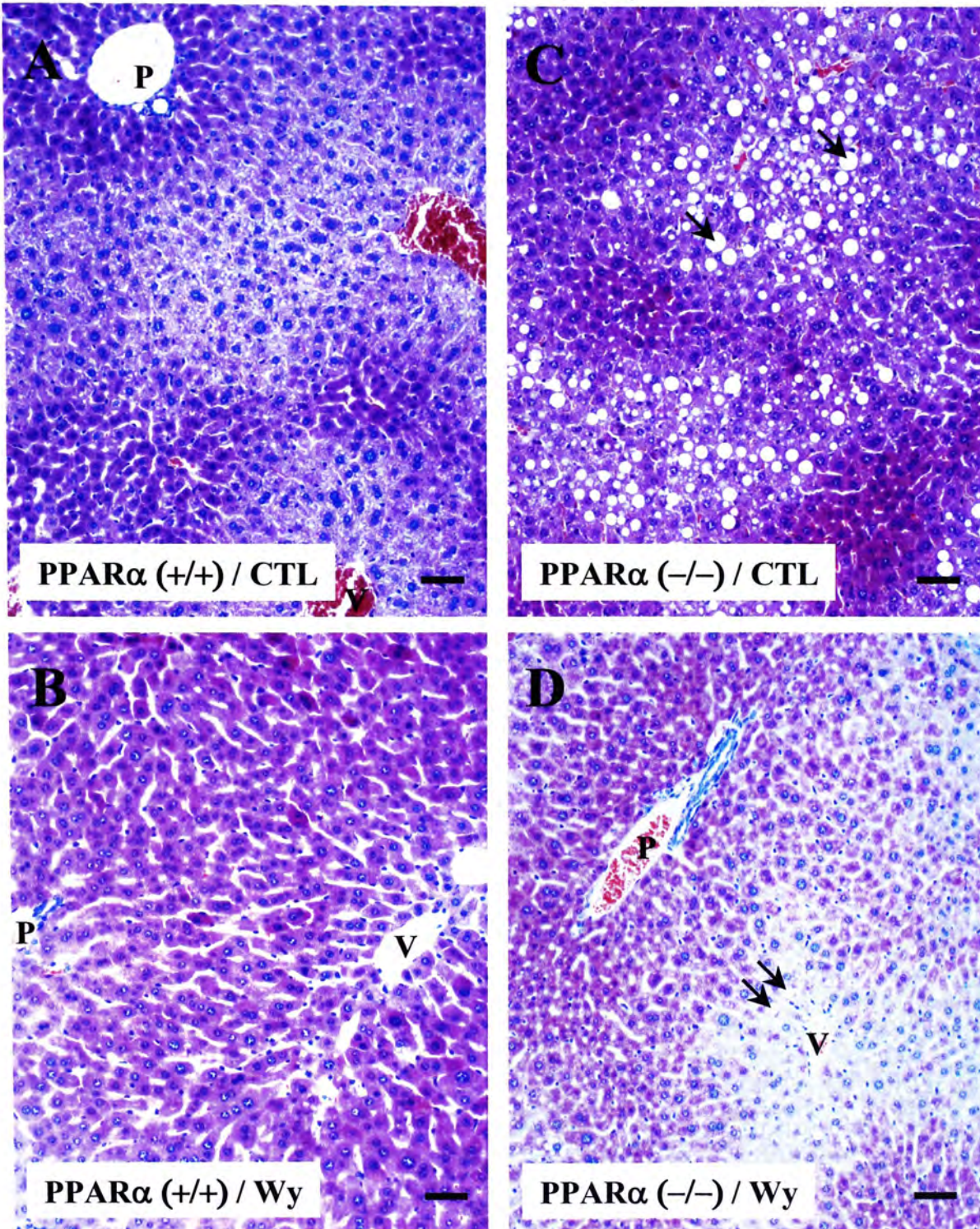


Figure 3.5.9. Hematoxylin and eosin staining of the middle zone (20X) of liver sections (5 μm) taken from PPARα (+/+) and PPARα (-/-) mice after 1 week treatment with a 0.0% Wy-14,643 (control diet) (panels A, B) or a 0.1% Wy-14,643 diet (panels C, D) (n=3). Severe lipid accumulation (arrows) was found around the central vein region in both control and Wy-14,643 fed PPARα (-/-) mice. P, portal triad. V, central vein. Bars, 50 μm.

1 week
Middle zone (40X)

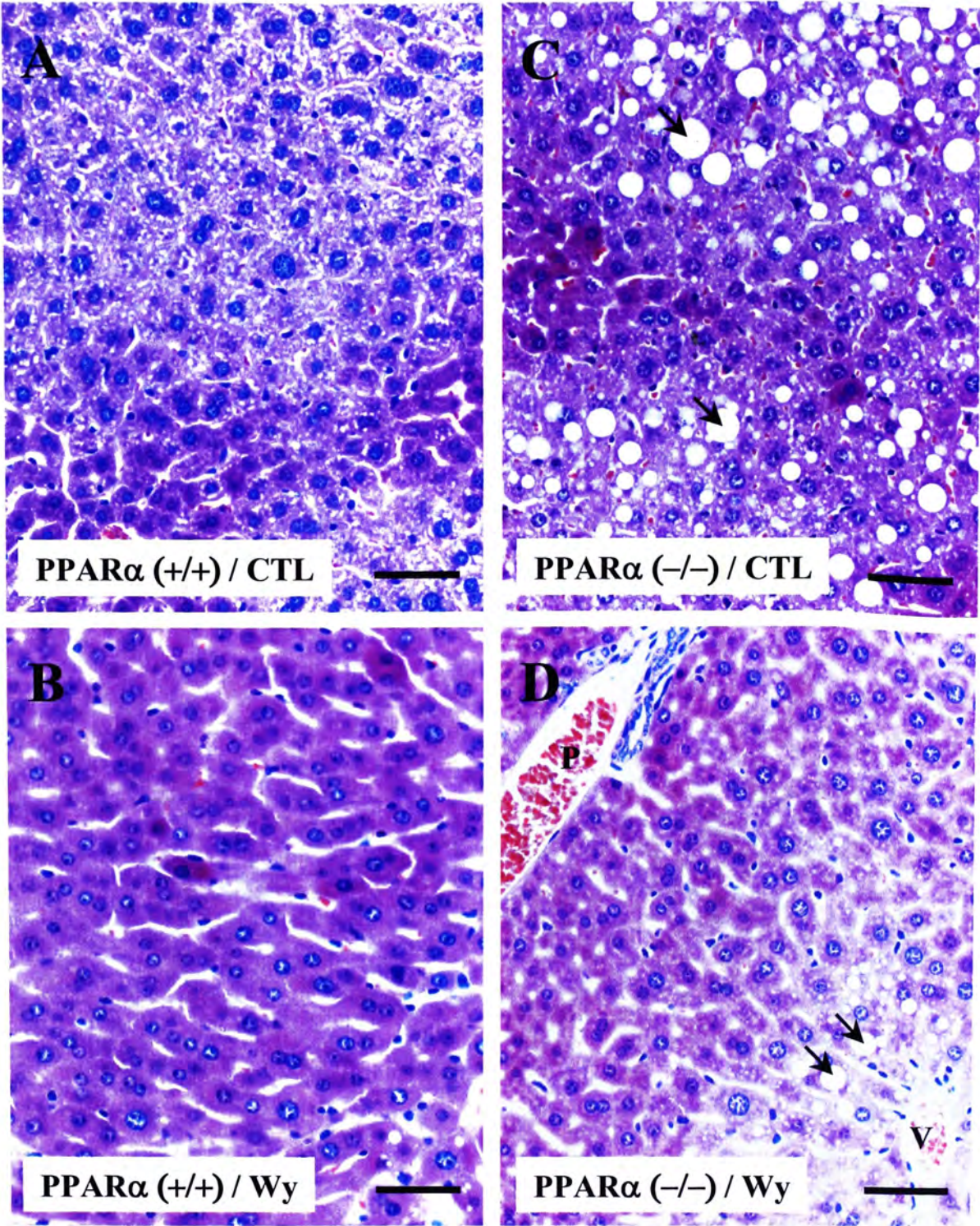


Figure 3.5.10. Hematoxylin and eosin staining of the middle zone (40X) of liver sections (5 μ m) taken from PPAR α (+/+) and PPAR α (-/-) mice after 1 week treatment with a 0.0% Wy-14,643 (control diet) (panels A, B) or a 0.1% Wy-14,643 diet (panels C, D) (n=3). Lipid accumulation (arrows) was found around the central vein region in both control and Wy-14,643 fed PPAR α (-/-) mice. P, portal triad. V, central vein. Bars, 50 μ m.

1 week
Portal vein region (20X)

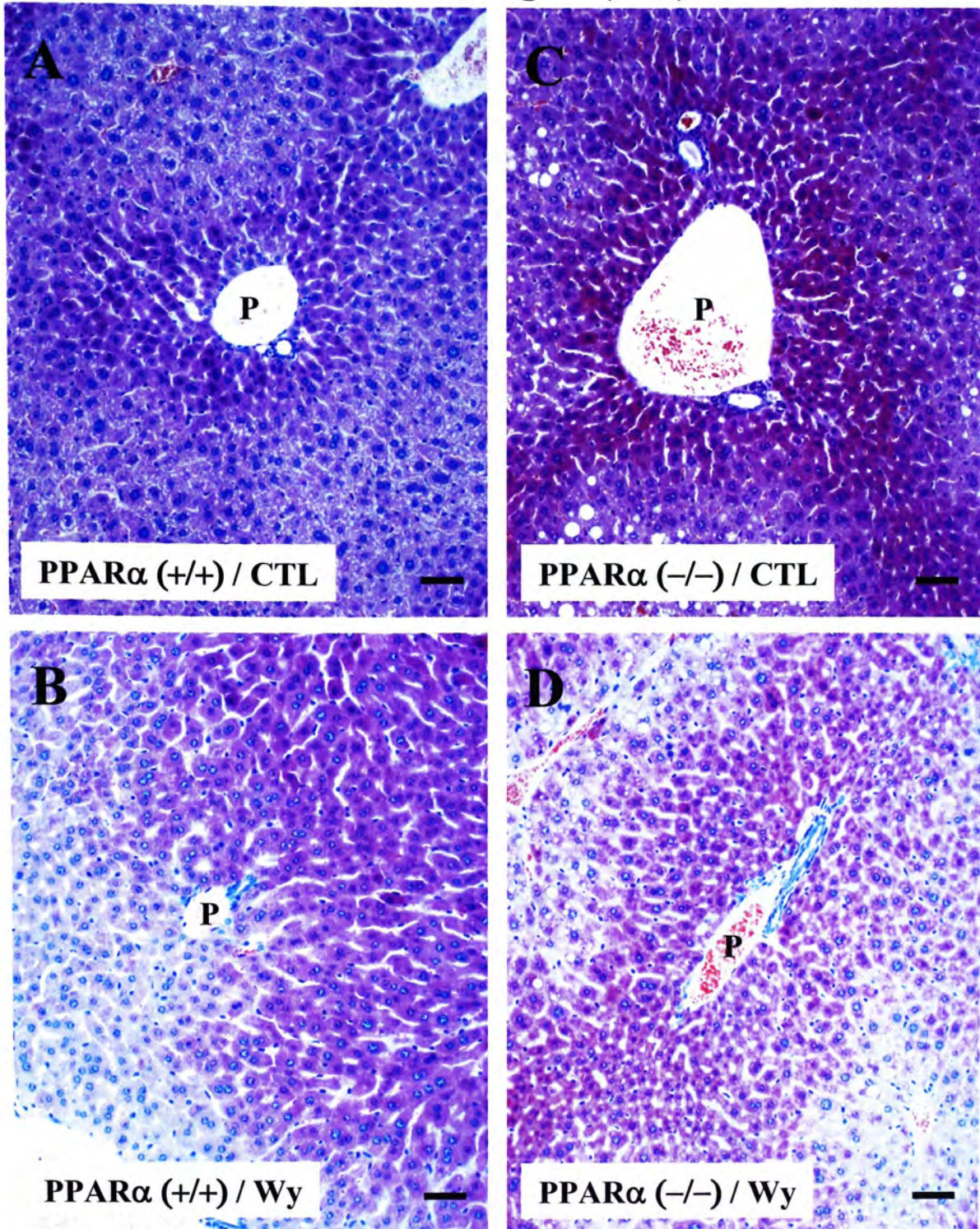


Figure 3.5.11. Hematoxylin and eosin staining of the portal vein region (20X) of liver sections (5 μm) taken from PPARα (+/+) and PPARα (-/-) mice after 1 week treatment with a 0.0% Wy-14,643 (control diet) (panels A, B) or a 0.1% Wy-14,643 diet (panels C, D) (n=3). Normal liver histology was found in the portal vein region of control fed PPARα (+/+) mice. Sinusoidal spaces between hepatocytes of PPARα (+/+) 0.1% Wy-14,643 treated mice were more obvious. P, portal triad. Bars, 50 μm.

1 week
Portal vein region (40X)

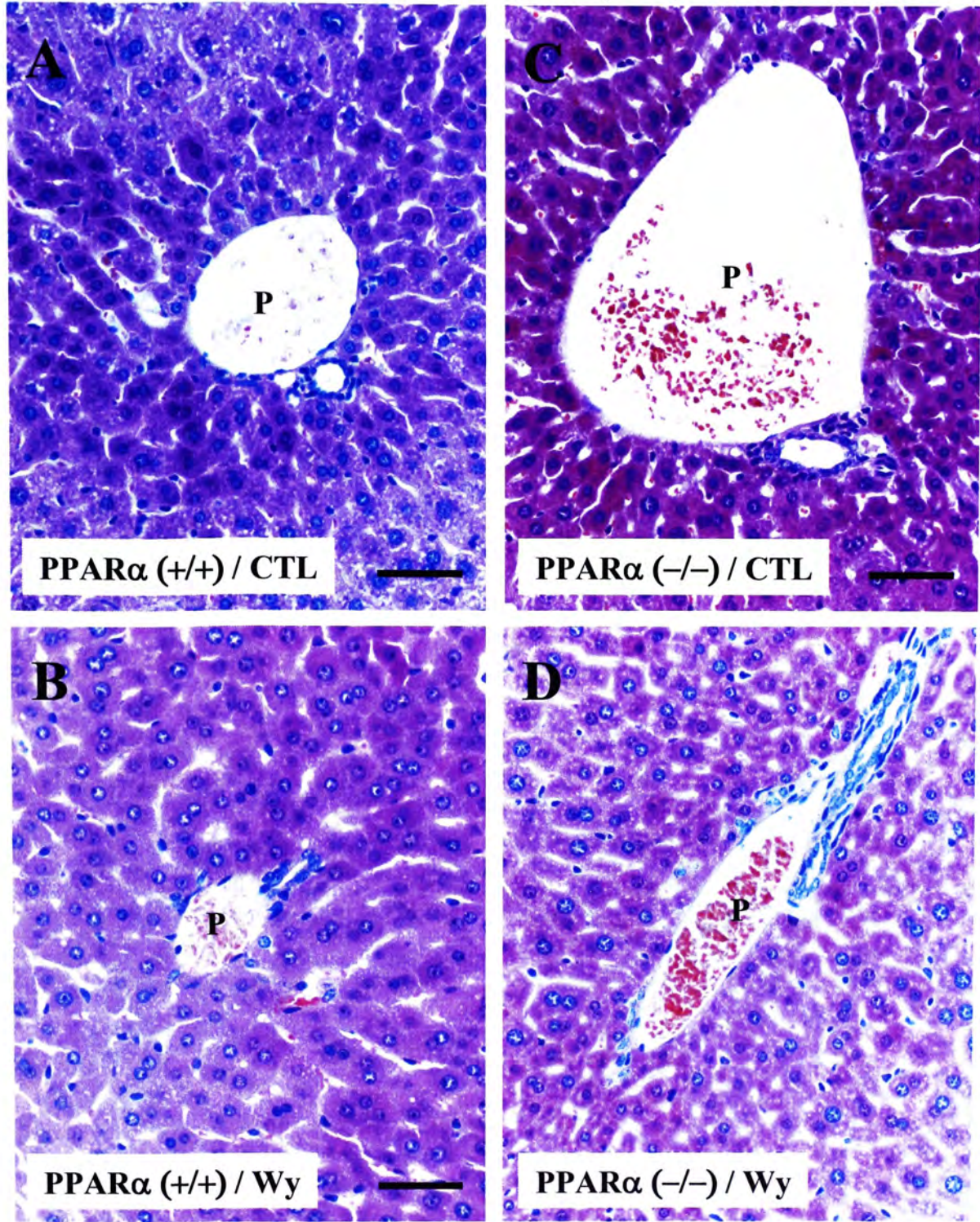


Figure 3.5.12. Hematoxylin and eosin staining of the portal vein region (40X) of liver sections (5 μm) taken from PPARα (+/+) and PPARα (-/-) mice after 1 week treatment with a 0.0% Wy-14,643 (control diet) (panels A, B) or a 0.1% Wy-14,643 diet (panels C, D) (n=3). Normal liver histology was found in the portal vein region of control fed PPARα (+/+) mice. Sinusoidal spaces between hepatocytes of PPARα (+/+) 0.1% Wy-14,643 treated mice were more obvious. P, portal triad. Bars, 50 μm.

2 weeks
Central vein region (20X)

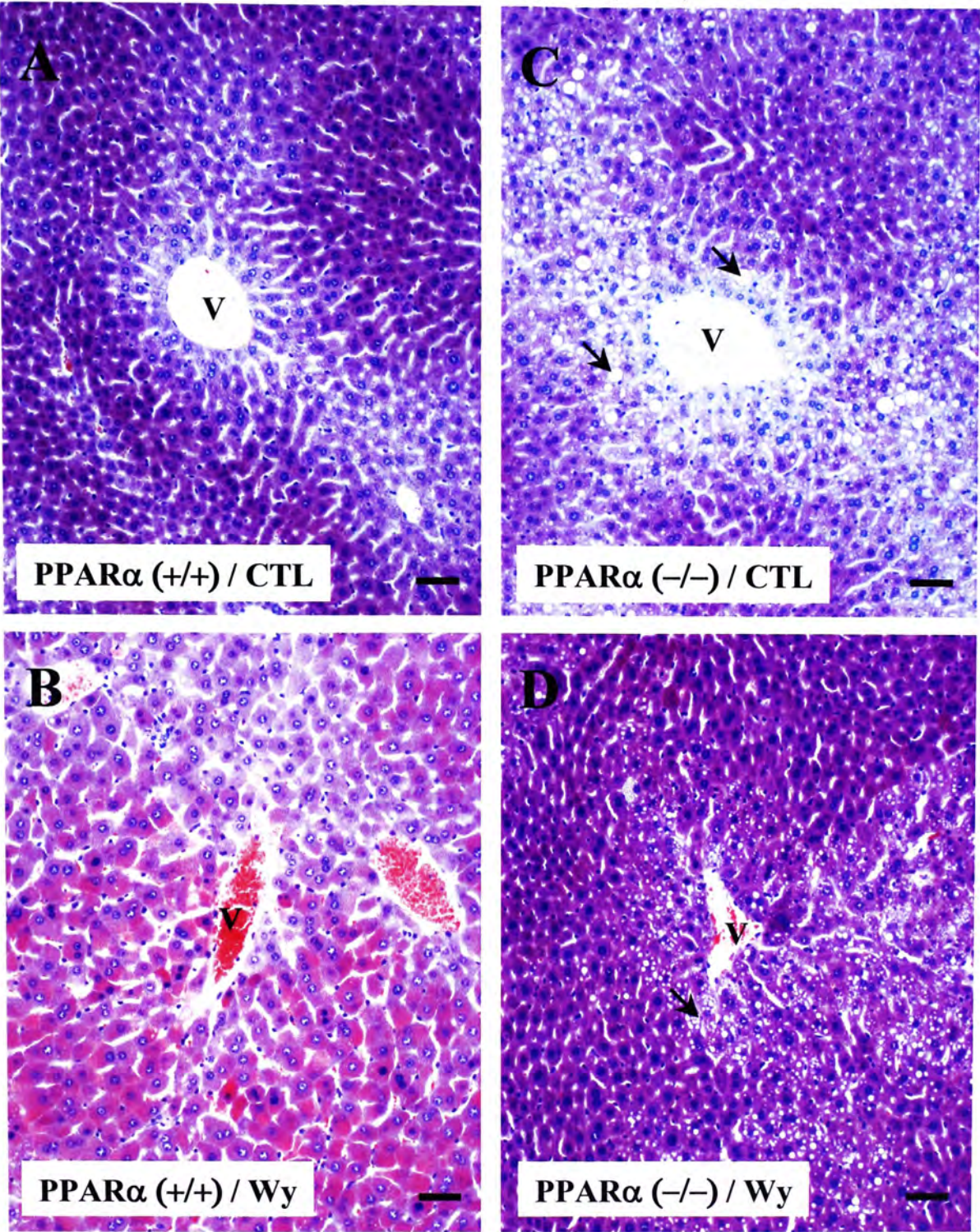


Figure 3.5.13. Hematoxylin and eosin staining of the central vein region (20X) of liver sections (5 μ m) taken from PPAR α (+/+) and PPAR α (-/-) mice after 2 weeks treatment with a 0.0% Wy-14,643 (control diet) (panels A, B) or a 0.1% Wy-14,643 diet (panels C, D) (n=3). Normal liver histology was found in the central vein region of PPAR α (+/+) mice fed with control diet. Larger sinusoidal spaces were observed in the 0.1% Wy-14,643 fed PPAR α (+/+) mice. Severe lipid accumulation (arrows) was found around the central vein region in both control and Wy-14,643 fed PPAR α (-/-) mice. V, central vein. Bars, 50 μ m.

2 week
Central vein region (40X)

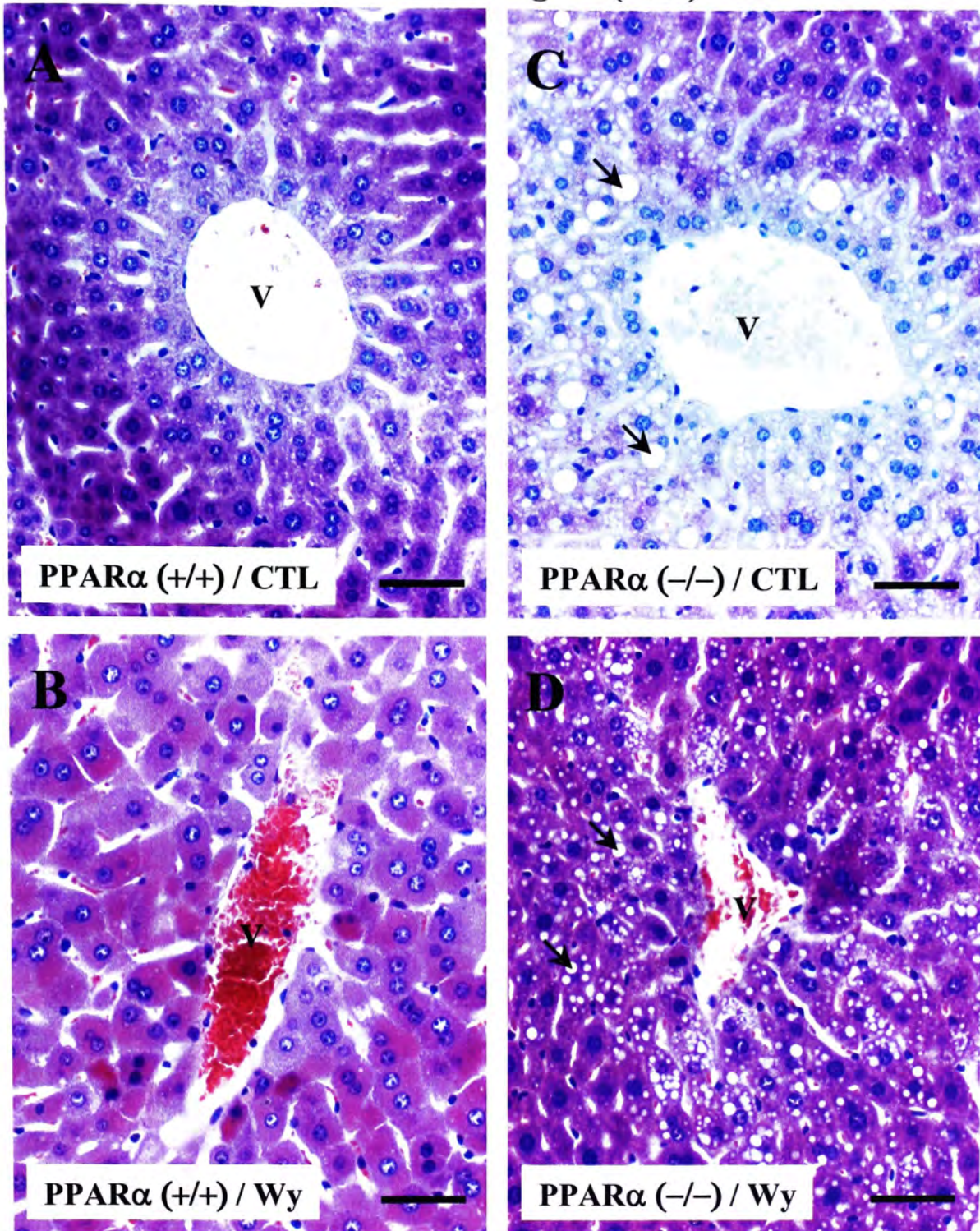


Figure 3.5.14. Hematoxylin and eosin staining of the central vein region (40X) of liver sections (5 μ m) taken from PPAR α (+/+) and PPAR α (-/-) mice after 2 weeks treatment with a 0.0% Wy-14,643 (control diet) (panels A, B) or a 0.1% Wy-14,643 diet (panels C, D) (n=3). Severe lipid accumulation (arrows) was found around the central vein region in both control and Wy-14,643 fed PPAR α (-/-) mice. Macrovesicular droplets were formed inside the hepatocytes. The nuclei were displaced to the periphery of the hepatocytes. V, central vein. Bars, 50 μ m.

2 weeks
Middle zone (20X)

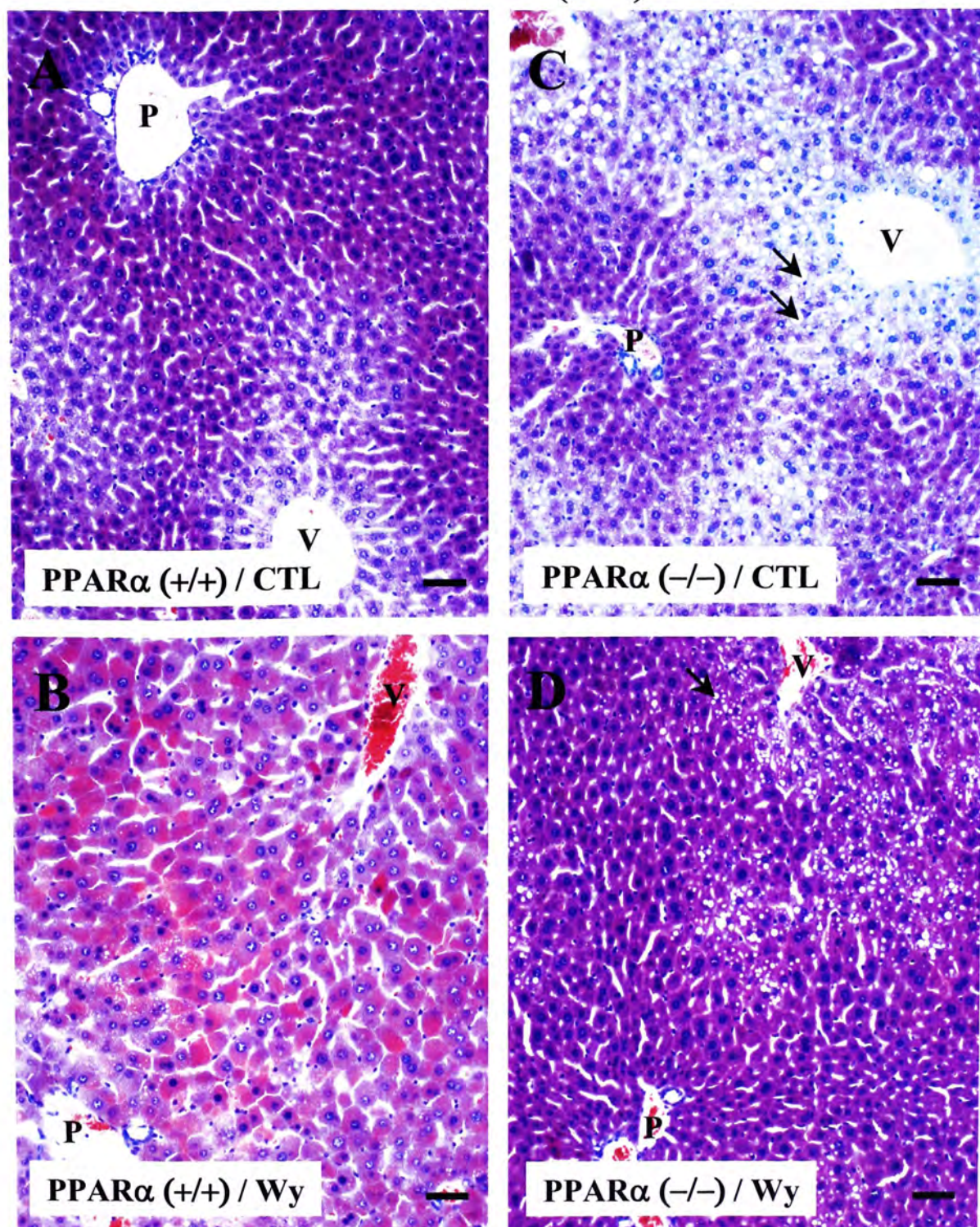


Figure 3.5.15. Hematoxylin and eosin staining of the middle zone (20X) of liver sections (5 μ m) taken from PPAR α (+/+) and PPAR α (-/-) mice after 2 weeks treatment with a 0.0% Wy-14,643 (control diet) (panels A, B) or a 0.1% Wy-14,643 diet (panels C, D) (n=3). Normal liver histology was found in the middle zone region of PPAR α (+/+) mice fed with control diet. Larger sinusoidal spaces were observed in the 0.1% Wy-14,643 fed PPAR α (+/+) mice. Severe lipid accumulation (arrows) was found around the central vein region in both control and Wy-14,643 fed PPAR α (-/-) mice. P, portal triad. V, central vein. Bars, 50 μ m.

2 weeks
Middle zone (40X)

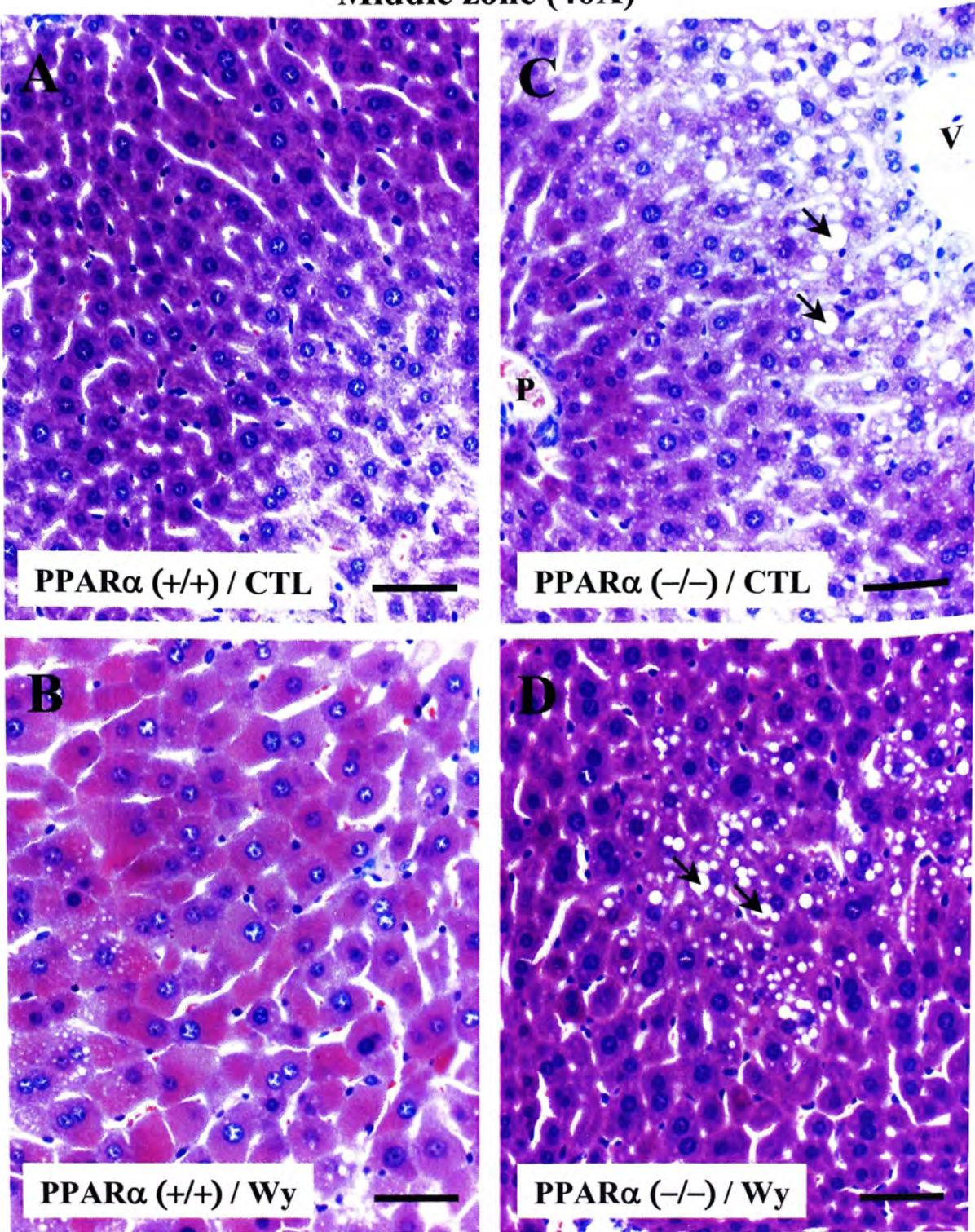


Figure 3.5.16. Hematoxylin and eosin staining of the middle zone (40X) of liver sections (5 μ m) taken from PPAR α (+/+) and PPAR α (-/-) mice after 2 weeks treatment with a 0.0% Wy-14,643 (control diet) (panels A, B) or a 0.1% Wy-14,643 diet (panels C, D) (n=3). Lipid accumulation (arrows) was found in both control and Wy-14,643 fed PPAR α (-/-) mice. P, portal triad. V, central vein. Bars, 50 μ m.

2 weeks
Portal vein region (20X)

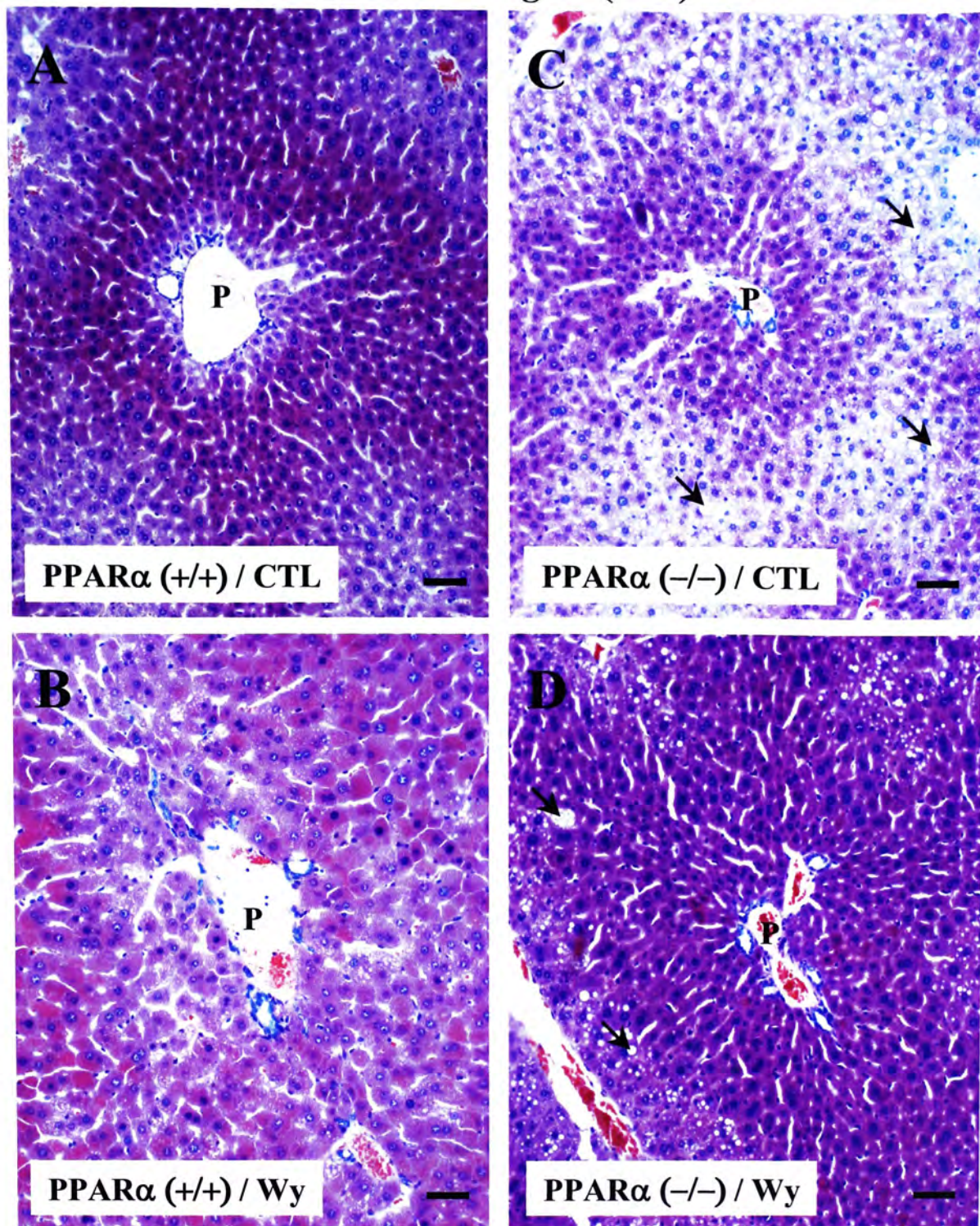


Figure 3.5.17. Hematoxylin and eosin staining of the portal vein region (20X) of liver sections (5 μ m) taken from PPAR α (+/+) and PPAR α (-/-) mice after 2 weeks treatment with a 0.0% Wy-14,643 (control diet) (panels A, B) or a 0.1% Wy-14,643 diet (panels C, D) (n=3). Normal liver histology was found in the portal vein region of control fed PPAR α (+/+) mice. Abnormal arrangement of hepatocytes in the 0.1% Wy-14,643 treated PPAR α (+/+) was observed. P, portal triad. Bars, 50 μ m.

2 weeks
Portal vein region (40X)

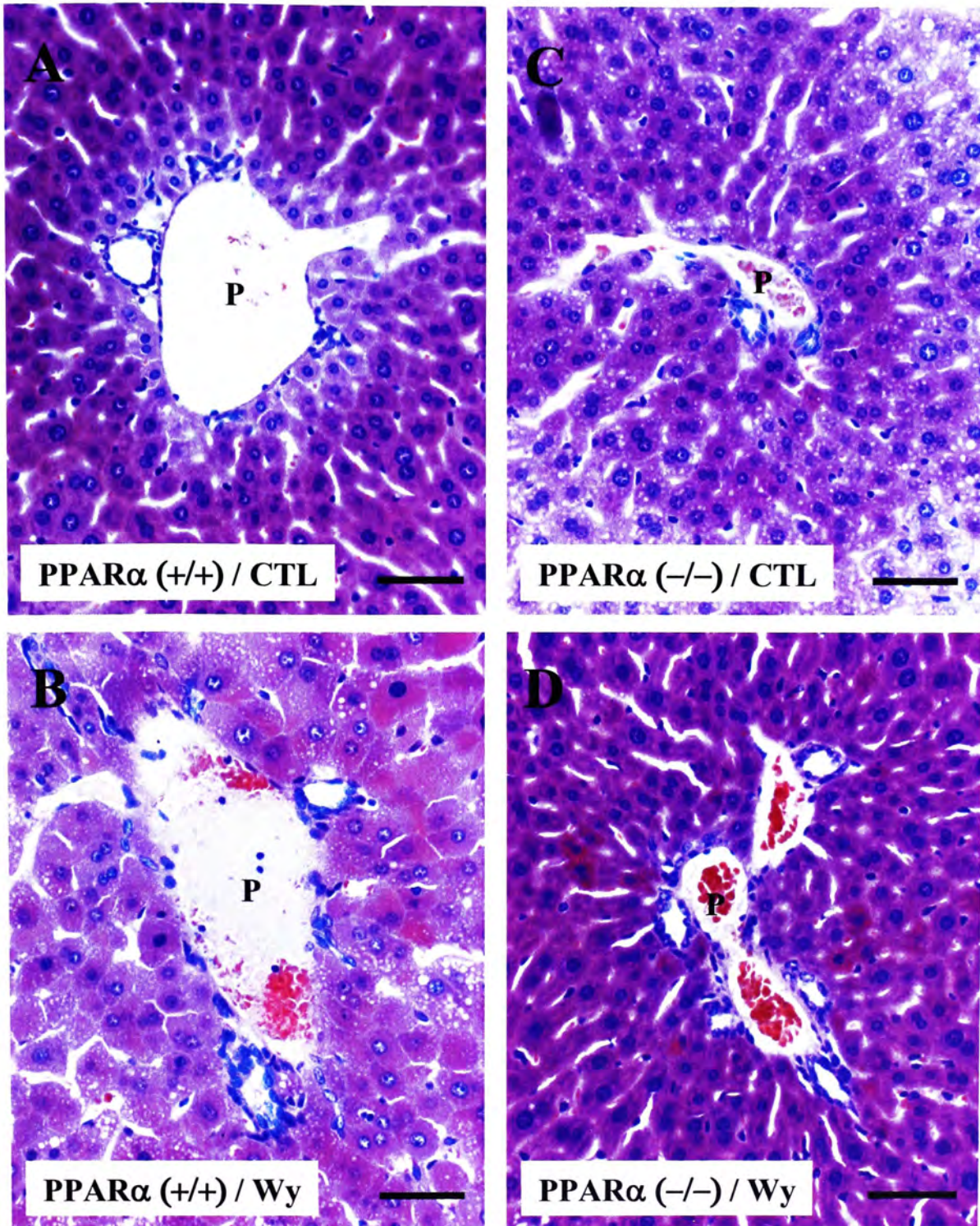


Figure 3.5.18. Hematoxylin and eosin staining of the portal vein region (40X) of liver sections (5 μ m) taken from PPAR α (+/+) and PPAR α (-/-) mice after 2 weeks treatment with a 0.0% Wy-14,643 (control diet) (panels A, B) or a 0.1% Wy-14,643 diet (panels C, D) (n=3). Normal liver histology was found in the portal vein region of control fed PPAR α (+/+) mice. Abnormal arrangement of hepatocytes in the 0.1% Wy-14,643 treated PPAR α (+/+) was observed. P, portal triad. Bars, 50 μ m.

Abnormal hepatocytes arrangement and large sinusoids were more obvious in the 6 months feeding study. Trabecular cell clusters were observed in PPAR α (+/+) mice fed with the 0.1% Wy-14,643 diet in the central vein region (Figures 3.5.19B, 3.5.20B), middle zone (Figure 3.5.21B, 3.5.22B) and portal vein region (Figures 3.5.23B, 3.5.24B). In addition, lipid droplets were accumulated near the portal vein region of the PPAR α (+/+) mice fed with the 0.1% Wy-14,643 diet (Figure 3.5.22B, 3.5.24B). For PPAR α (-/-) mice, both control and Wy-14,643-treated groups showed accumulation of the lipid droplets around the central vein (Figures 3.5.19C, 3.5.19D, 3.5.20C, 3.5.20D).

After 11 months Wy-14,643 treatment, abnormal hepatocytes arrangement, large sinusoids in the central vein region (Figures 3.5.25B, 3.5.26B), middle zone (Figures 3.5.27B, 3.5.28B) and portal vein region (Figure 3.5.29B, 3.5.30B) and lipid accumulation (Figures 3.5.29B, 3.5.30B) around the portal vein region were more obvious in the Wy-14,643 treated group of PPAR α (+/+) mice. The accumulation of lipid droplets around the central vein for the PPAR α (-/-) mice (Figures 3.5.25C, 3.5.25D) was very severe as the lipid metabolism was affected with the removal of peroxisome proliferators-activated receptor alpha. Irregular and trabecular cell clusters were found in the 0.1% Wy-14,643 fed PPAR α (+/+) mice (Figures 3.5.25B, 3.5.27B, 3.5.29B).

Hepatocytes without nuclei (Figures 3.5.31A, 3.5.31D), trabecular cell clusters (Figure 3.5.31B, 3.5.31E) and invasion of blood, dark nucleus (Figures 3.5.31C, 3.5.31F) were observed in Wy-14,643-treated PPAR α (+/+) after 11 months treatment. Trabecular cell clusters observed in 0.1% Wy-14,643 fed PPAR α (+/+) mice was reported in previous study (Peters *et al.*, 1997).

6 months
Central vein region (20X)

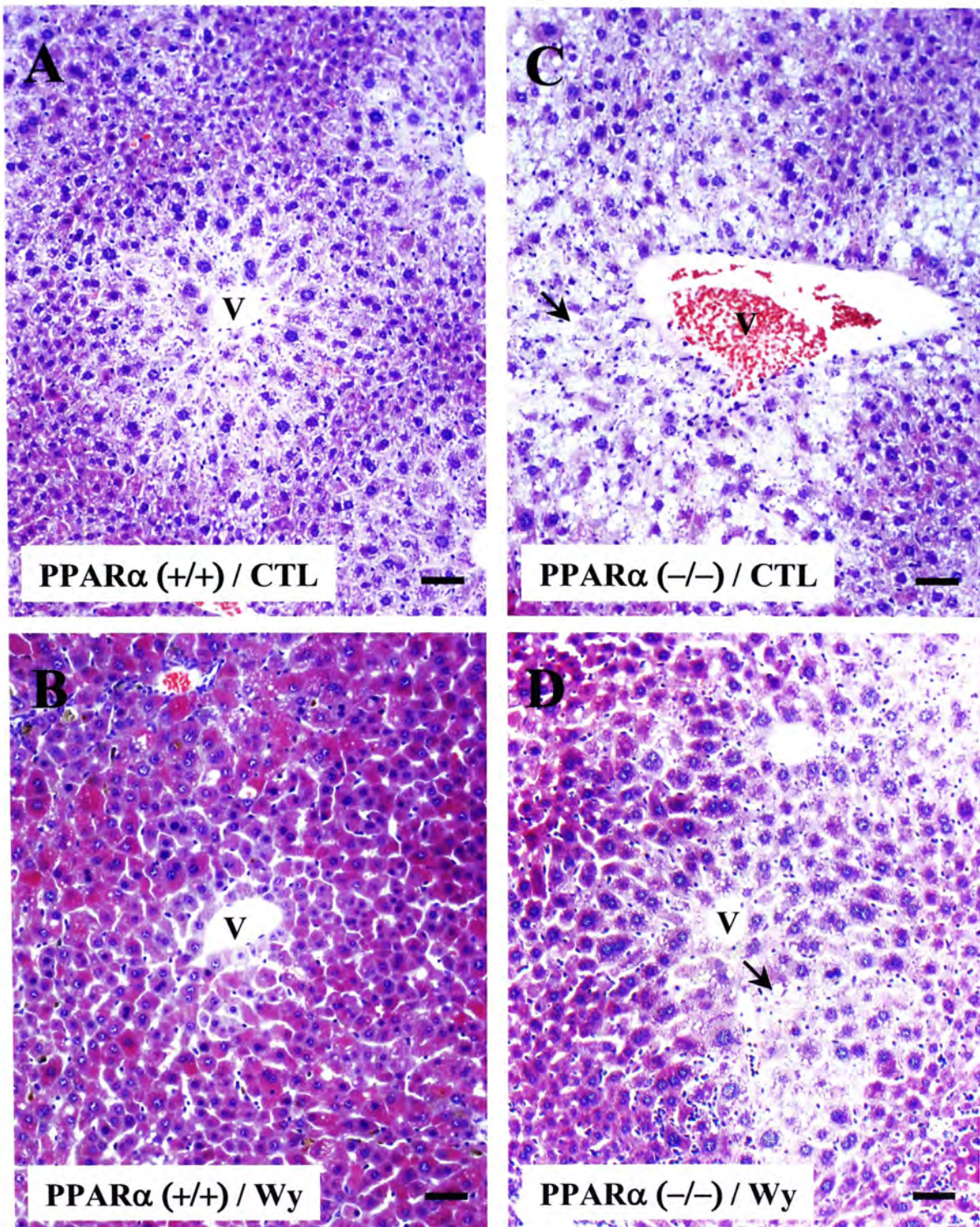


Figure 3.5.19. Hematoxylin and eosin staining of the central vein region (20X) of liver sections (5 μ m) taken from PPAR α (+/+) and PPAR α (-/-) mice after 6 months treatment with a 0.0% Wy-14,643 (control diet) (panels A, B) or a 0.1% Wy-14,643 diet (panels C, D) (n=3). Normal liver histology was found in the central vein region of PPAR α (+/+) mice fed with control diet. Severe lipid accumulation (arrows) was found around the central vein region in both control and Wy-14,643 fed PPAR α (-/-) mice. Irregular and trabecular cell clusters were observed in Wy-14,643 treated PPAR α (+/+) mice. V, central vein. Bars, 50 μ m.

6 months
Central vein region (40X)

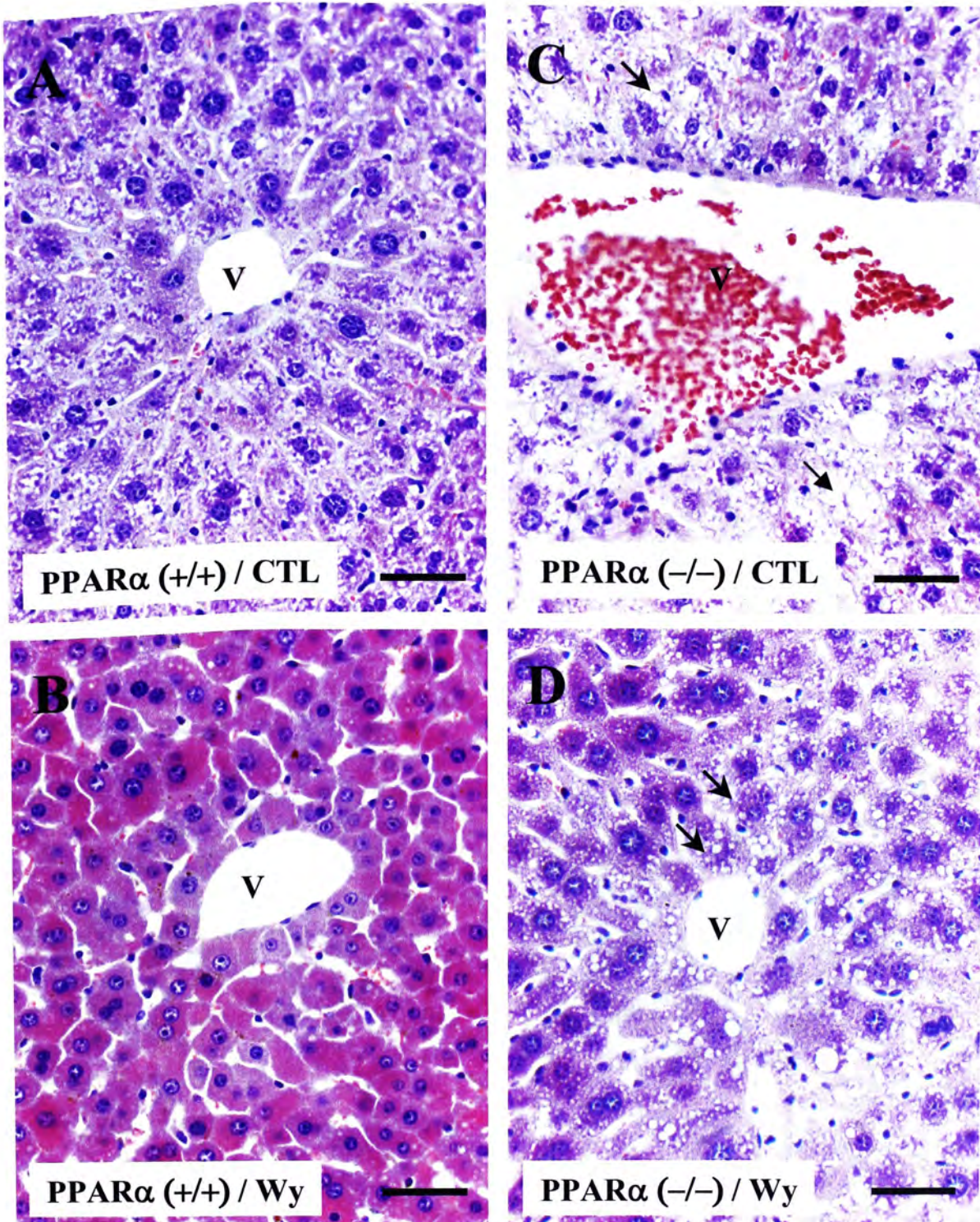


Figure 3.5.20. Hematoxylin and eosin staining of the central vein region (40X) of liver sections (5 μ m) taken from PPAR α (+/+) and PPAR α (-/-) mice after 6 months treatment with a 0.0% Wy-14,643 (control diet) (panels A, B) or a 0.1% Wy-14,643 diet (panels C, D) (n=3). Normal liver histology was found in the central vein region of PPAR α (+/+) mice fed with control diet. Severe lipid accumulation (arrows) was found around the central vein region in both control and Wy-14,643 fed PPAR α (-/-) mice. Macrovesicular droplets were formed inside the hepatocytes and the nuclei were displaced to the periphery of the hepatocytes. V, central vein. Bars, 50 μ m.

6 months
Middle zone (20X)

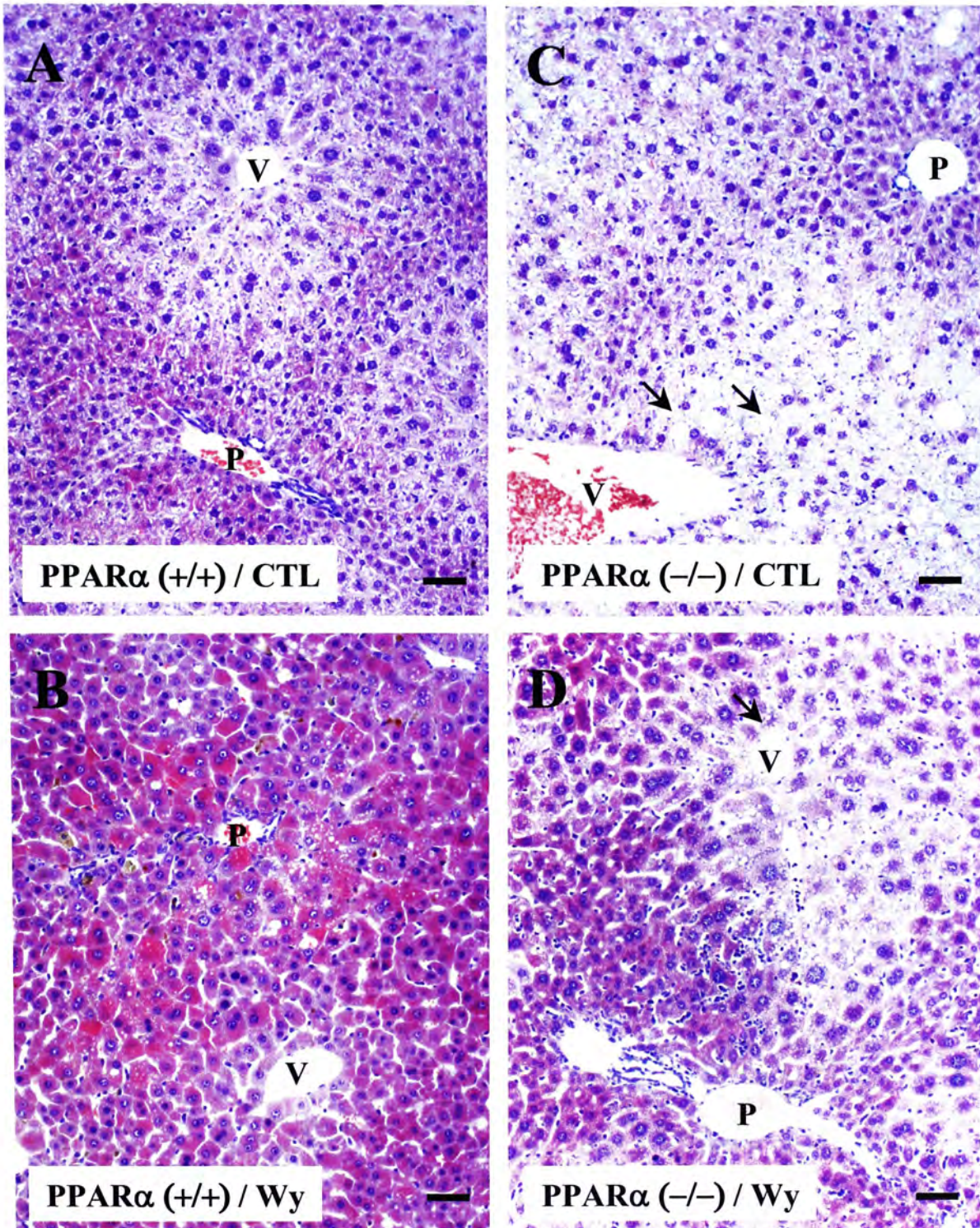


Figure 3.5.21. Hematoxylin and eosin staining of the middle zone (20X) of liver sections (5 μ m) taken from PPAR α (+/+) and PPAR α (-/-) mice after 6 months treatment with a 0.0% Wy-14,643 (control diet) (panels A, B) or a 0.1% Wy-14,643 diet (panels C, D) (n=3). Severe lipid accumulation (arrows) was found around the central vein region in both control and Wy-14,643 fed PPAR α (-/-) mice. Irregular and trabecular cell clusters were observed in Wy-14,643 treated PPAR α (+/+) mice. P, portal triad. V, central vein. Bars, 50 μ m.

6 months
Middle zone (40X)

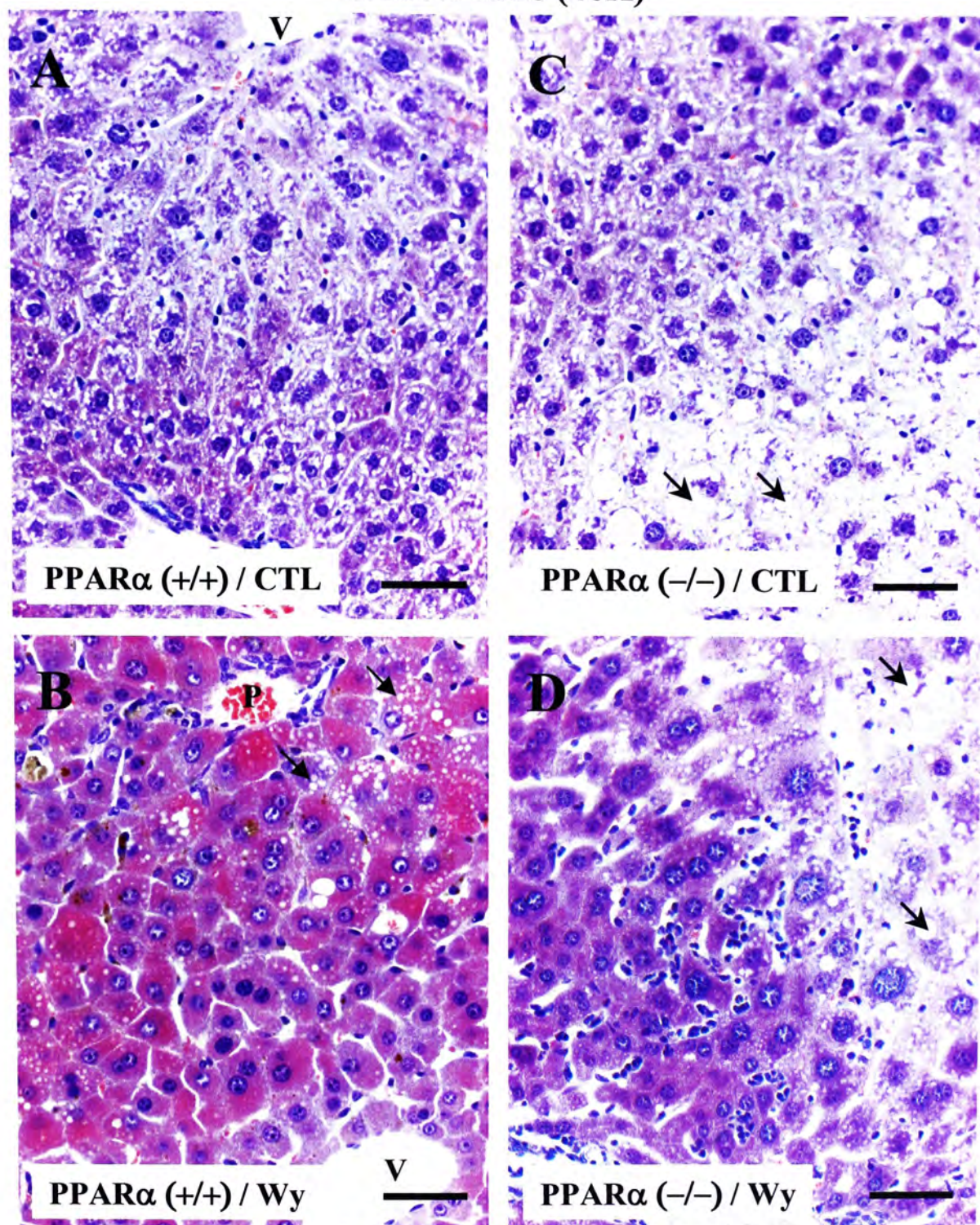


Figure 3.5.22. Hematoxylin and eosin staining of the middle zone (40X) of liver sections (5 μm) taken from PPARα (+/+) and PPARα (-/-) mice after 6 months treatment with a 0.0% Wy-14,643 (control diet) (panels A, B) or a 0.1% Wy-14,643 diet (panels C, D) (n=3). Normal liver histology was found in PPARα (+/+) mice fed with control diet. Severe lipid accumulation (arrows) were found in both control and Wy-14,643 fed PPARα (-/-) mice. Lipid accumulation was also observed in PPARα (+/+) fed with control diet. P, portal triad. V, central vein. Bars, 50 μm.

6 months
Portal vein region (20X)

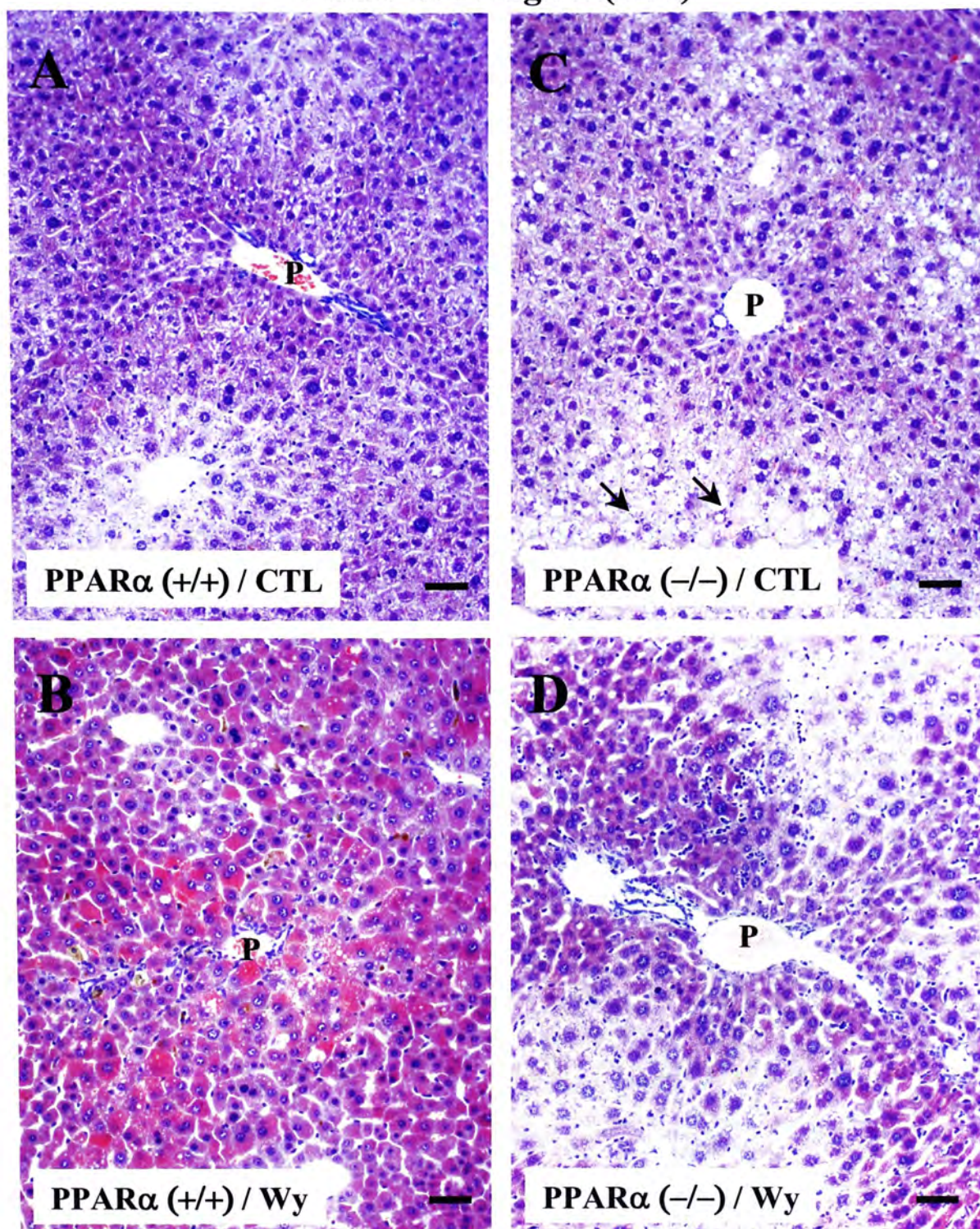


Figure 3.5.23. Hematoxylin and eosin staining of the portal vein region (20X) of liver sections (5 μ m) taken from PPAR α (+/+) and PPAR α (-/-) mice after 6 months treatment with a 0.0% Wy-14,643 (control diet) (panels A, B) or a 0.1% Wy-14,643 diet (panels C, D) (n=3). Normal liver histology was found in the portal vein region of both PPAR α (+/+) and PPAR α (-/-) mice fed with control diet. P, portal triad. Bars, 50 μ m.

6 months
Portal vein region (40X)

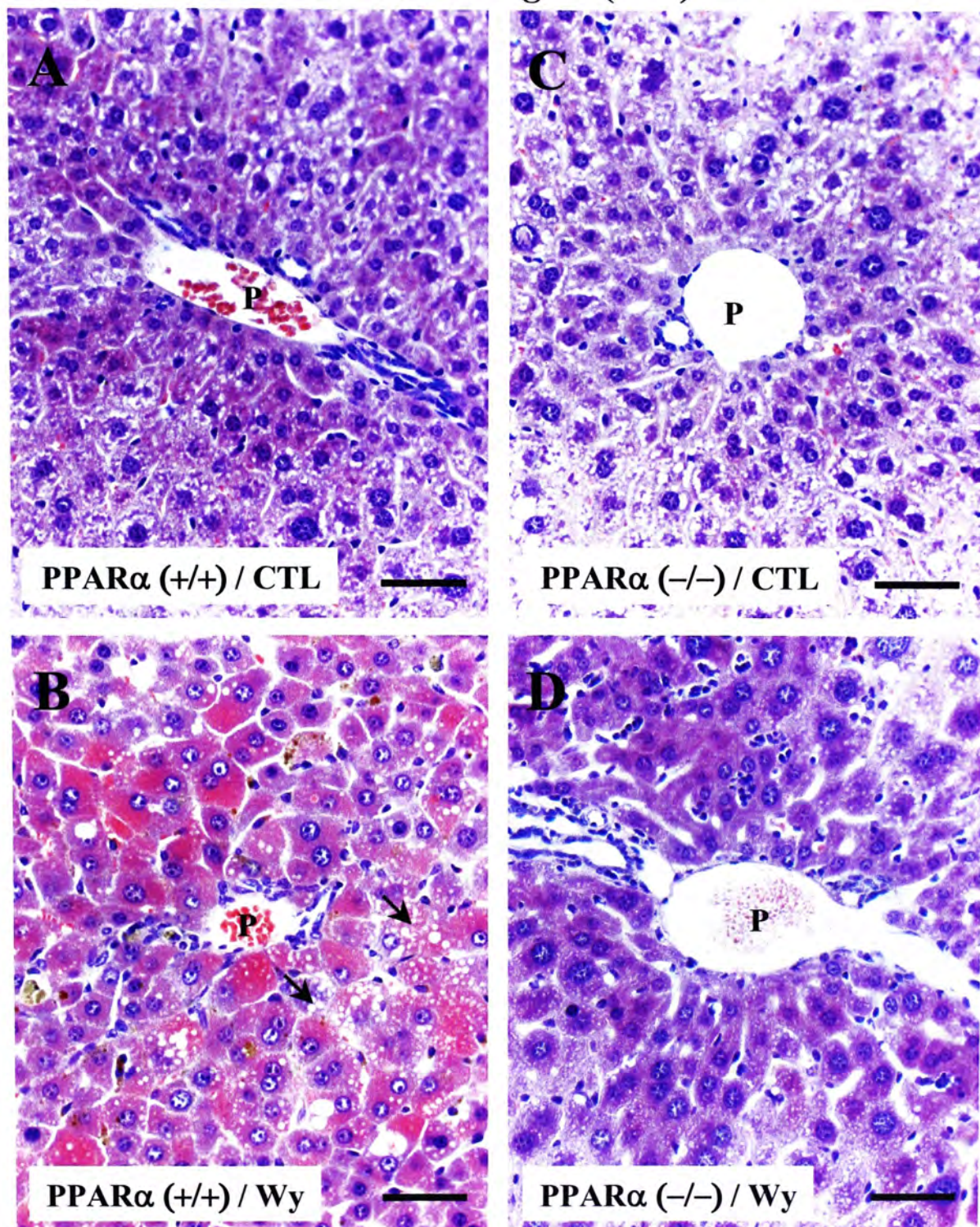


Figure 3.5.24. Hematoxylin and eosin staining of the portal vein region (40X) of liver sections (5 μm) taken from PPARα (+/+) and PPARα (-/-) mice after 6 months treatment with a 0.0% Wy-14,643 (control diet) (panels A, B) or a 0.1% Wy-14,643 diet (panels C, D) (n=3). Normal liver histology was found in portal vein region both PPARα (+/+) and PPARα (-/-) mice fed with control diet. Lipid accumulation (arrows) was found in PPARα (+/+) mice fed with 0.1% Wy-14,643 diet. P, portal triad. Bars, 50 μm.

11 months
Central vein region (20X)

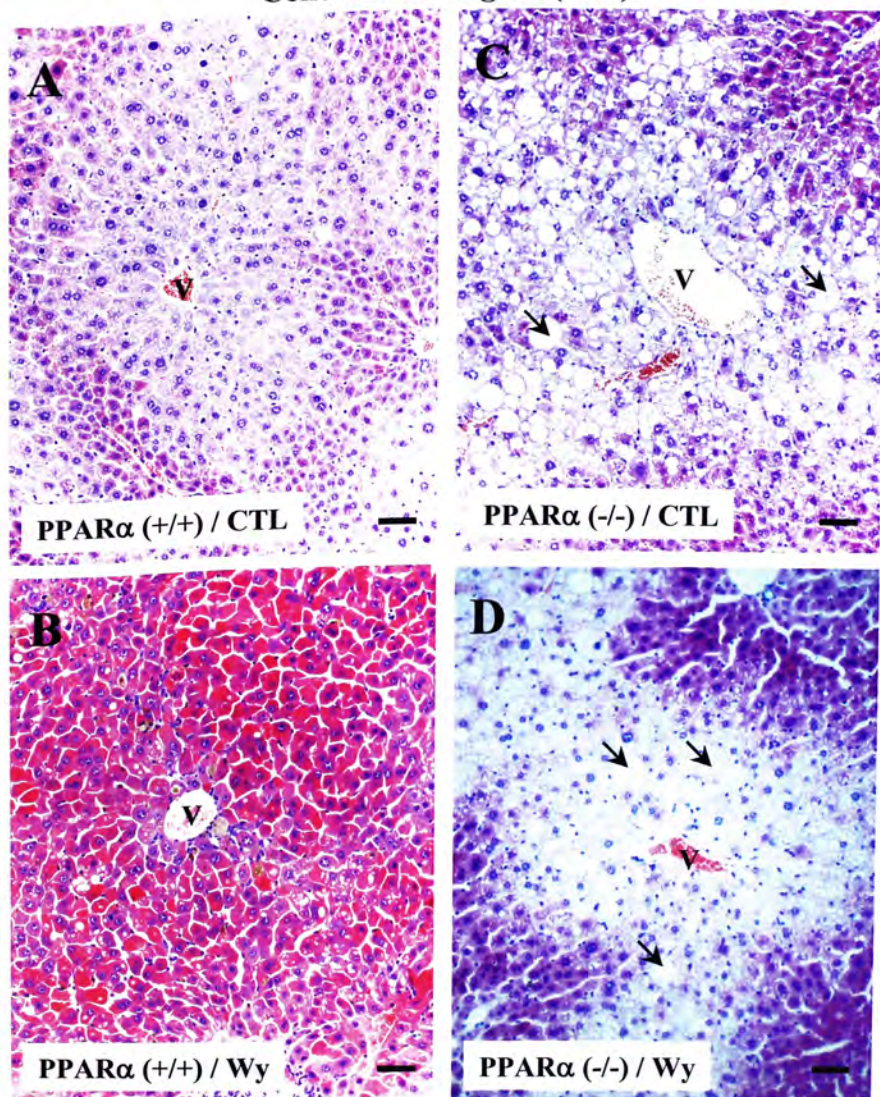


Figure 3.5.25. Hematoxylin and eosin staining of the central vein region (20X) of liver sections (5 μ m) taken from PPAR α (+/+) and PPAR α (-/-) mice after 11 months treatment with a 0.0% Wy-14,643 (control diet) (panels A, B) or a 0.1% Wy-14,643 diet (panels C, D) (n=3). Normal liver histology was found in PPAR α (+/+) mice fed with control diet. Severe lipid accumulation (arrows) were found around the central vein region in both control and Wy-14,643 fed PPAR α (-/-) mice. Irregular and trabecular cell clusters were observed in PPAR α (+/+) fed with Wy-14643. V, central vein. Bars, 50 μ m.

11 months
Central vein region (40X)

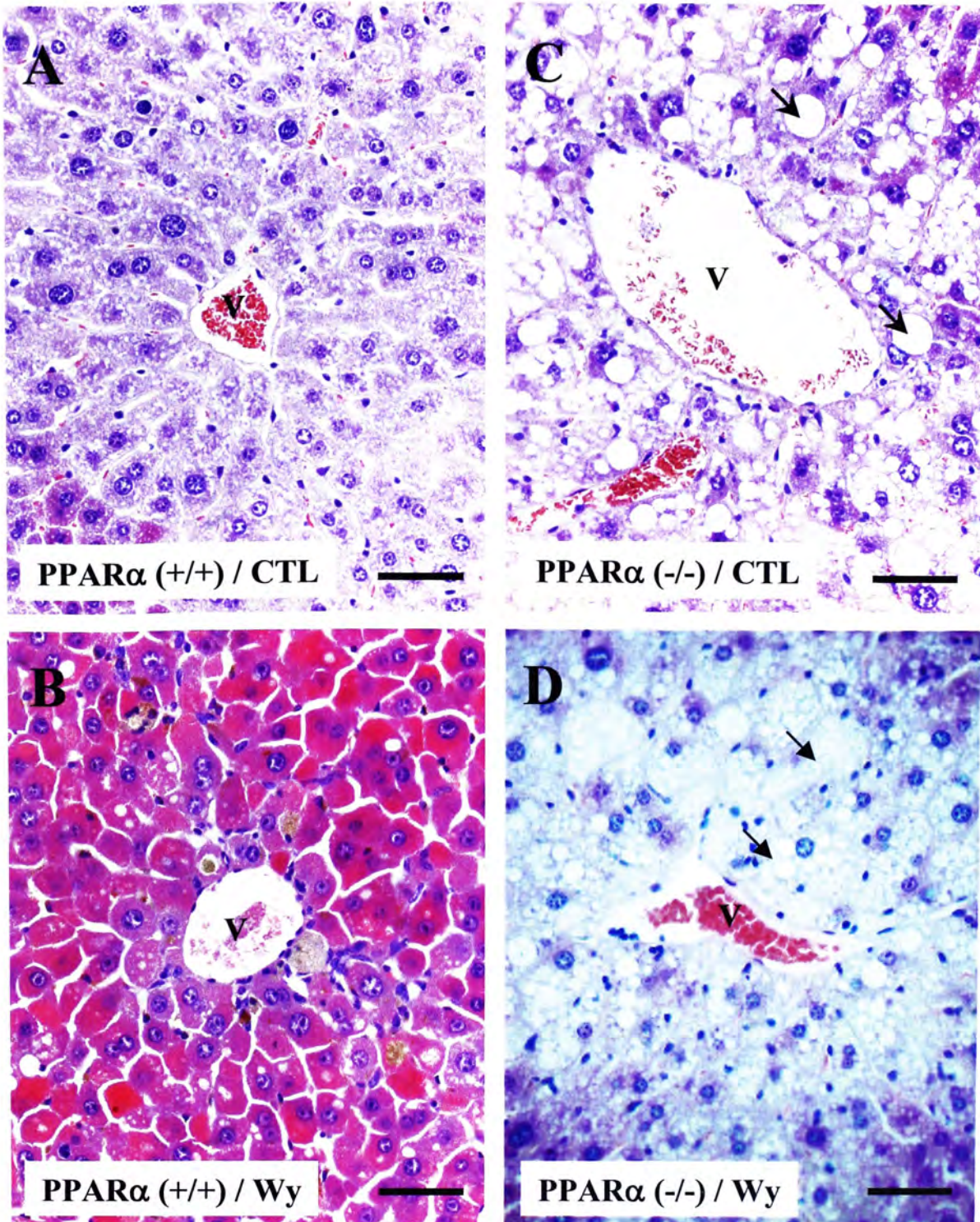


Figure 3.5.26. Hematoxylin and eosin staining of the central vein region (40X) of liver sections (5 μ m) taken from PPAR α (+/+) and PPAR α (-/-) mice after 11 treatment with a 0.0% Wy-14,643 (control diet) (panels A, B) or a 0.1% Wy-14,643 diet (panels C, D) (n=3). Normal liver histology was found in the central vein region of PPAR α (+/+) mice fed with control diet. Severe lipid accumulation (arrows) was found around the central vein region in both control and Wy-14,643 fed PPAR α (-/-) mice. Macrovesicular droplets were formed inside the hepatocytes and the nuclei were displaced to the periphery of the hepatocytes. V, central vein. Bars, 50 μ m.

11 months
Middle zone (20X)

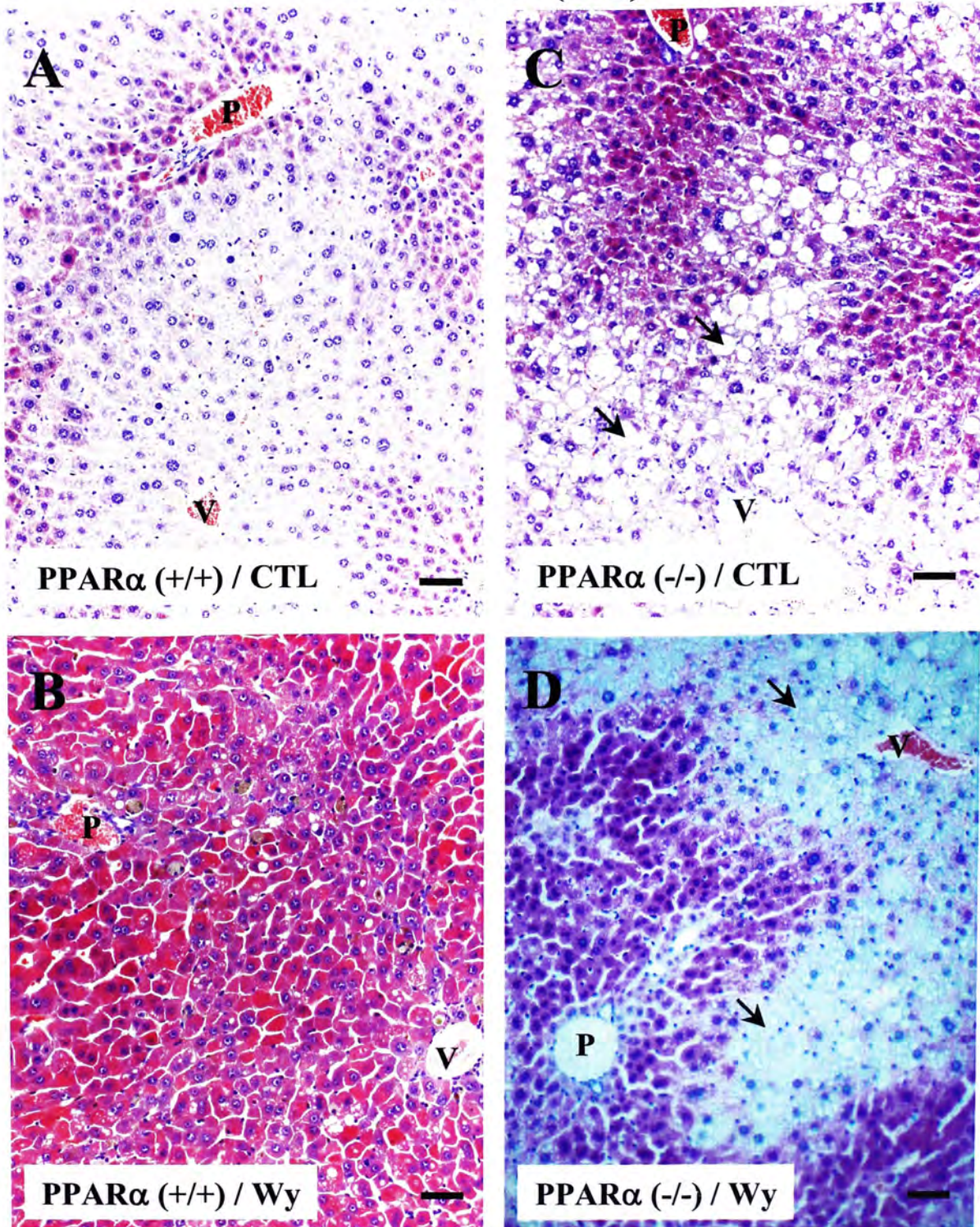


Figure 3.5.27. Hematoxylin and eosin staining of the middle zone (20X) of liver sections (5 μ m) taken from PPAR α (+/+) and PPAR α (-/-) mice after 11 months treatment with a 0.0% Wy-14,643 (panels A, B) or a 0.1% Wy-14,643 diet (panels C, D) (n=3). Normal liver histology was found in the central vein region of PPAR α (+/+) fed with control diet while irregular and trabecular cell clusters were observed in Wy-14,643 fed PPAR α (+/+) mice. Lipid accumulation (arrows) was found around the central vein region in both control and Wy-14,643 fed PPAR α (-/-) mice. P, portal triad. V, central vein. Bars, 50 μ m.

11 months
Middle zone (40X)

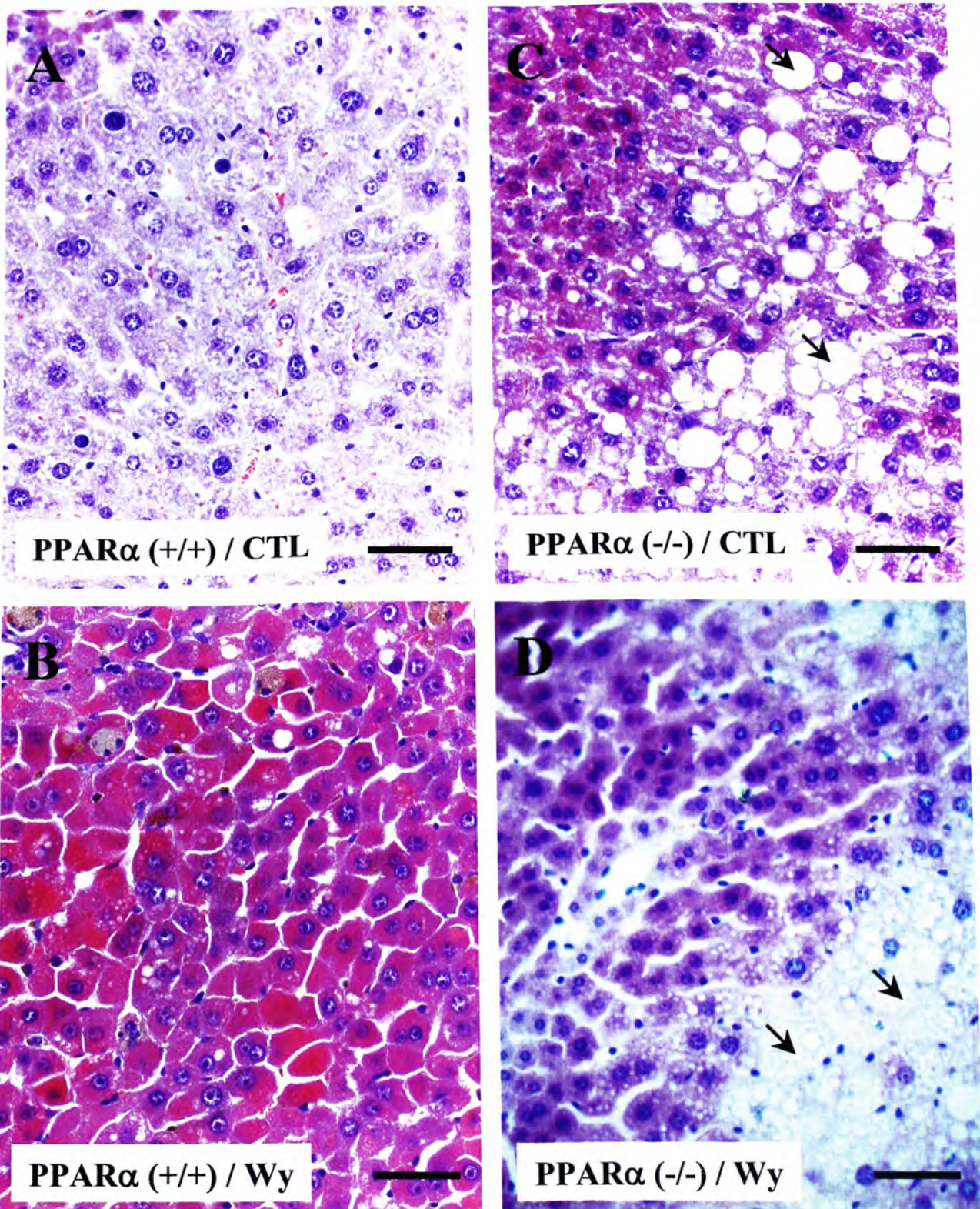


Figure 3.5.28. Hematoxylin and eosin staining of the middle zone (40X) of liver sections (5 μ m) taken from PPAR α (+/+) and PPAR α (-/-) mice after 11 months treatment with a 0.0% Wy-14,643 (panels A, B) or a 0.1% Wy-14,643 diet (panels C, D) (n=3). Severe lipid accumulation (arrows) were found around in both control and Wy-14,643 fed PPAR α (-/-) mice. Macrovesicular droplets were formed inside the hepatocytes and the nuclei were displaced to the periphery of the hepatocytes. Bars, 50 μ m.

11 months
Portal vein region (20X)

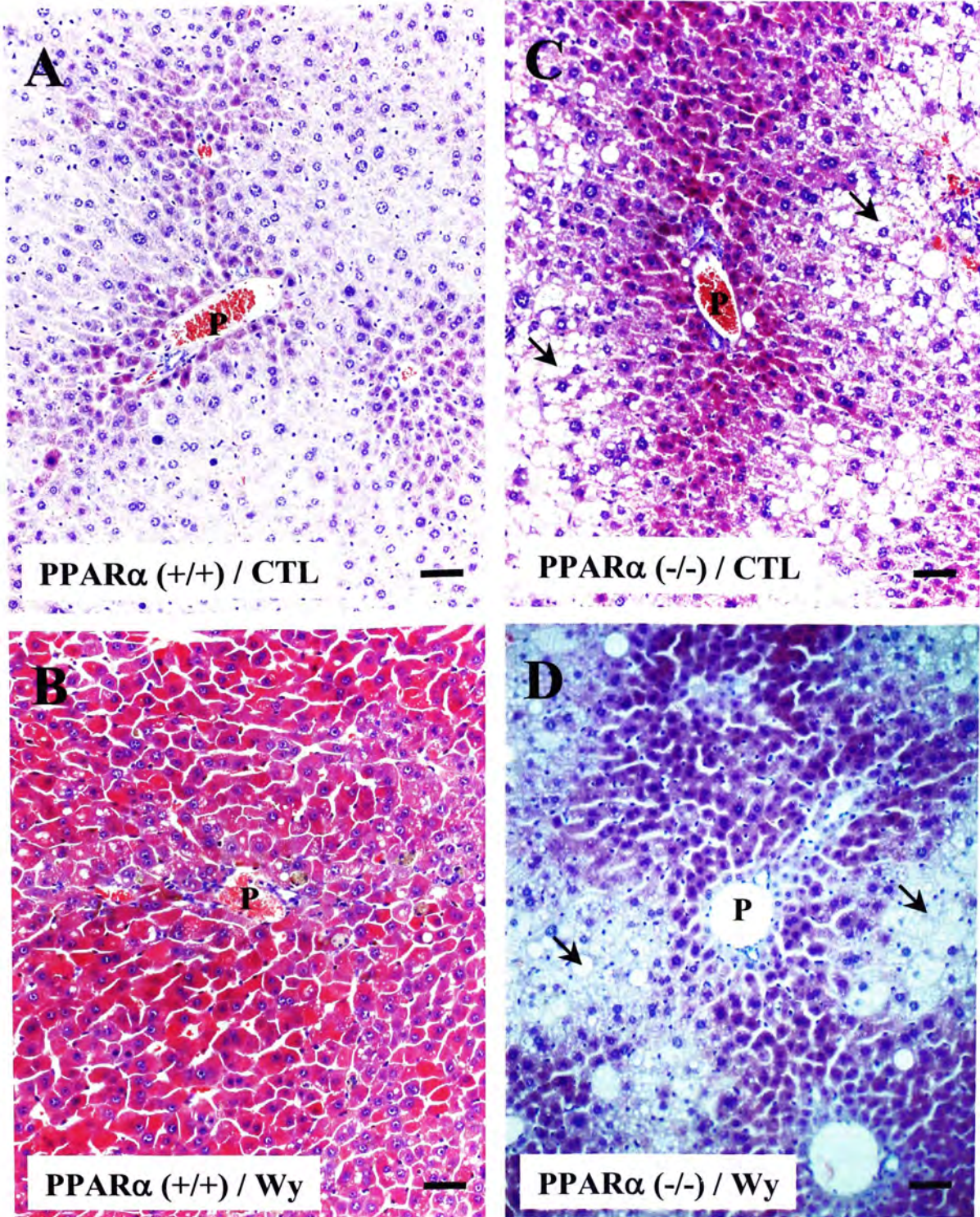


Figure 3.5.29. Hematoxylin and eosin staining of the portal vein region (20X) of liver sections (5 μ m) taken from PPAR α (+/+) and PPAR α (-/-) mice after 11 months treatment with a 0.0% Wy-14,643 (control diet) (panels A, B) or a 0.1% Wy-14,643 diet (panels C, D) (n=3). Severe lipid accumulation (arrows) was found around the central vein region in both control and Wy-14,643 fed PPAR α (-/-) mice. P, portal triad. Bars, 50 μ m.

11 months
Portal vein region (40X)

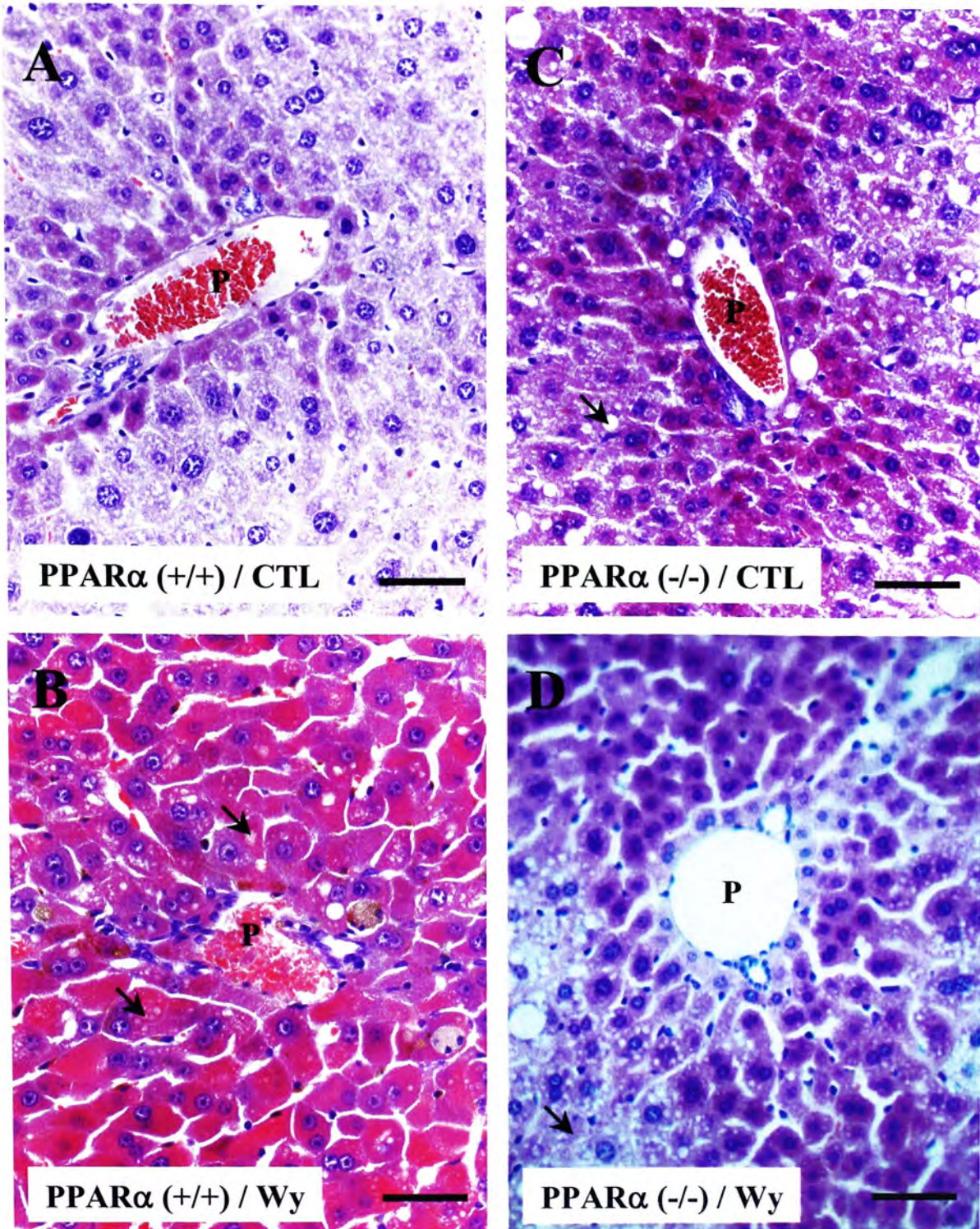


Figure 3.5.30. Hematoxylin and eosin staining of the portal vein region (40X) of liver sections (5 μ m) taken from PPAR α (+/+) and PPAR α (-/-) mice after 11 months treatment with a 0.0% Wy-14,643 (control diet) (panels A, B) or a 0.1% Wy-14,643 diet (panels C, D) (n=3). Lipid accumulation (arrows) was found in both PPAR α (+/+) and PPAR α (-/-) mice fed with 0.1% Wy-14,643 diet and PPAR α (-/-) mice fed with control diet. P, portal triad. Bars, 50 μ m.

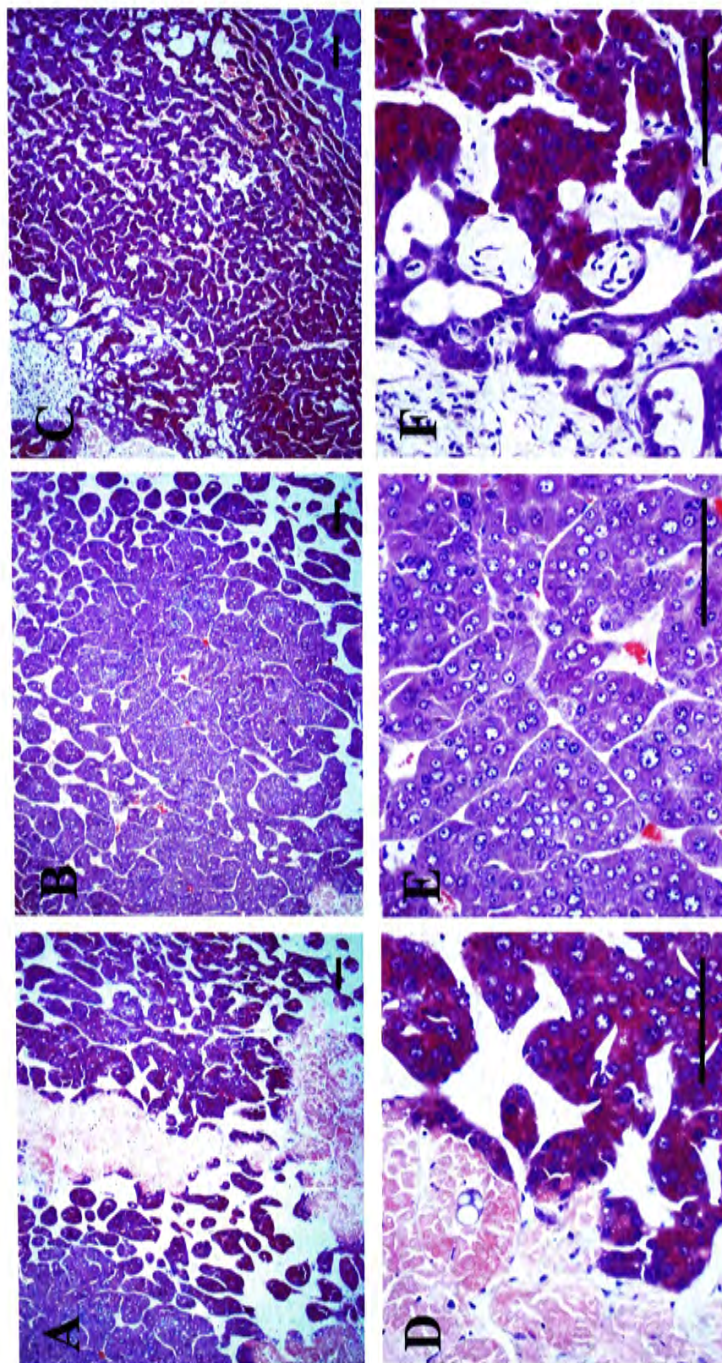


Figure 3.5.31. Hematoxylin and eosin staining of liver sections (5 μ m) taken from PPAR α (+/+) after 11 months treatment with a 0.1% Wy-14,643 diet (10X: panels A, B, C; 40X: panels D, E, F). Hepatocytes without nuclei (panels A, D) and trabecular cell clusters were observed (panels B, E). Dark nucleus and invasion of blood in sinusoidal spaces were also shown (panels C, F). Bars, 100 μ m.

3.6 Reverse transcription (RT) of mRNA and non-fluorescent PCR (non-fluoroDD PCR)

Since there are twelve different anchored primers (AP) and twenty different arbitrary primers (ARP), a total of 240 different combinations of AP and ARP can be used for the RT-PCR. However, not all the combinations will generate our desired differential display patterns (fluoroDD patterns) (Figure 2.10.1). In order to screen out the primer pairs which will show our desired fluoroDD patterns, reverse transcription (RT) of mRNA with non-fluorescent PCR (non-fluoroDD PCR), a faster and more economic way, were performed in this study.

Forty-three different primer combinations (AP1 & ARP2, ARP3, ARP6, ARP10, ARP16 and ARP20; AP2+ARP1, ARP3, ARP10, ARP12, ARP16, ARP18 and ARP19; AP3 & ARP3; AP5 & ARP1, ARP2, ARP3, ARP10, ARP12 and ARP18; AP6 & ARP1, ARP4, ARP5, ARP8, ARP12 and ARP14; AP7 & ARP10 and ARP15; AP10 & ARP1, ARP6, ARP10, ARP12, ARP13 and ARP16; AP11 & ARP1, ARP3, ARP5, ARP8, ARP12, ARP17, ARP19 and ARP20; and AP12 & ARP2) were used to perform non-fluoroDD RT-PCR. Twenty-six primer pairs including AP1 & ARP2, ARP3 and ARP20 (Figure 3.6.1); AP2 & ARP1, ARP10, ARP12, ARP18 and ARP19 (Figure 3.6.2); AP3 & ARP3 (Figure 3.6.3); AP5 & ARP1, ARP2, ARP3, ARP10 and ARP12 (Figure 3.6.4); AP6 & ARP1, ARP4 and ARP14 (Figure 3.6.5); AP7 & ARP15 (Figure 3.6.6); AP10 & ARP1, ARP12 and ARP13 (Figure 3.6.7); AP11 & ARP1, ARP3, ARP12 and ARP19 (Figure 3.6.8); and AP12 & ARP2 (Figure 3.6.9) showed differential display patterns, while the others did not show obvious differential display patterns or gave inconsistent patterns (Table 3.6.1). Eleven primer pairs, including AP1 & ARP2 (Figure 3.6.1); AP2 & ARP18 and ARP19 (Figure 3.6.2);

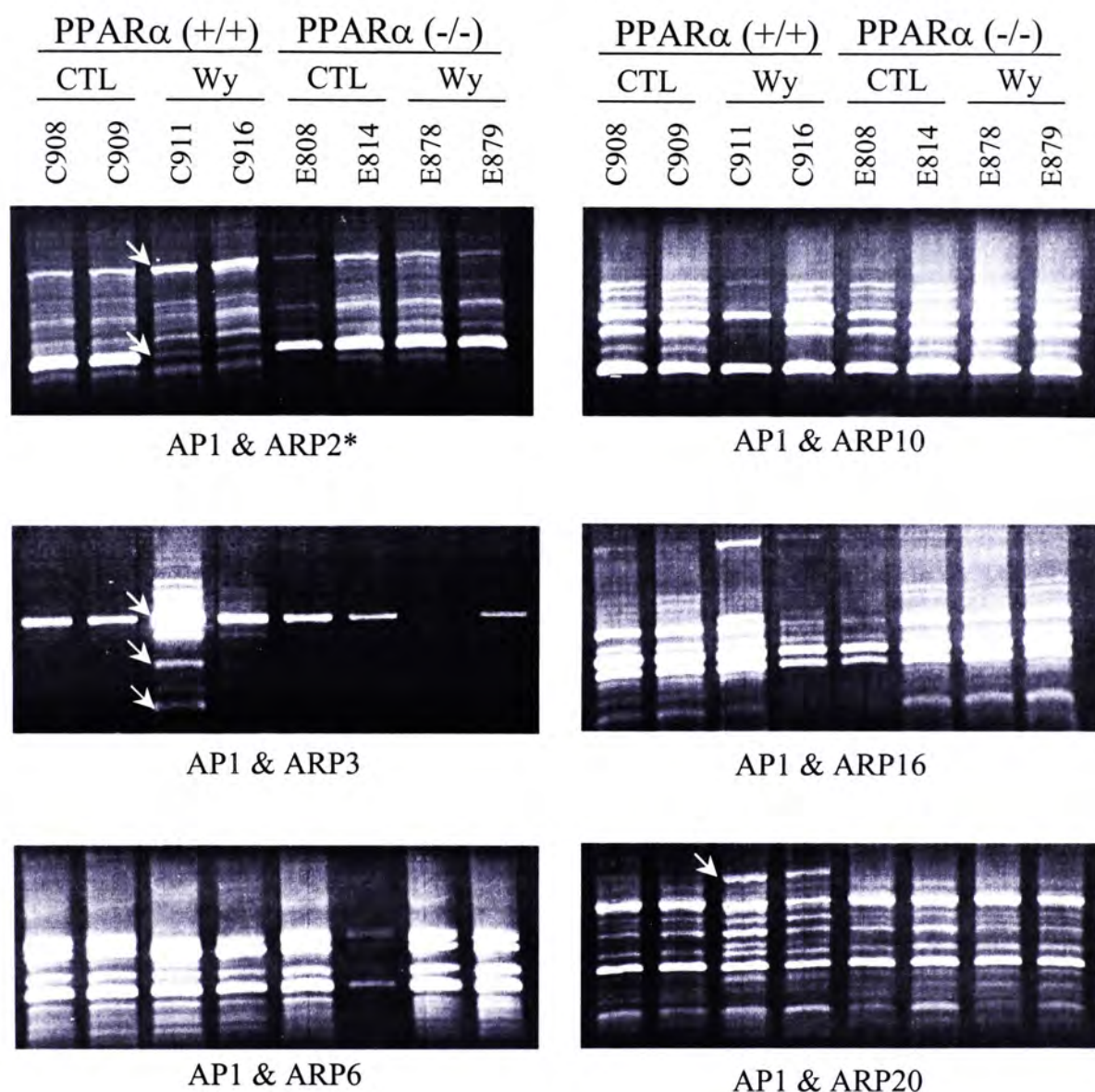


Figure 3.6.1. Preliminary screening for differential display patterns using non-fluorescent AP1 in combinations with ARP2, ARP3, ARP6, ARP10, ARP16 and ARP20. Total RNA from PPAR α (+/+) and PPAR α (-/-) mouse livers treated with a 0.0% control (CTL) or 0.1% (w/w) Wy-14,643 (Wy) diet for 11 months was reverse transcribed with AP1 primer and amplified by PCR using 3'-AP1 and 5'-ARPs (ARP2, ARP3, ARP6, ARP10, ARP16 and ARP20). Each treatment group consists of two mice and the PCR products were resolved on 1% agarose, 0.5X TBE gels with ethidium bromide staining. Arrow heads indicate the Wy-14,643 responsive and PPAR α -dependent cDNA fragments. *Primer pair used for subsequent fluorescent differential display analysis.

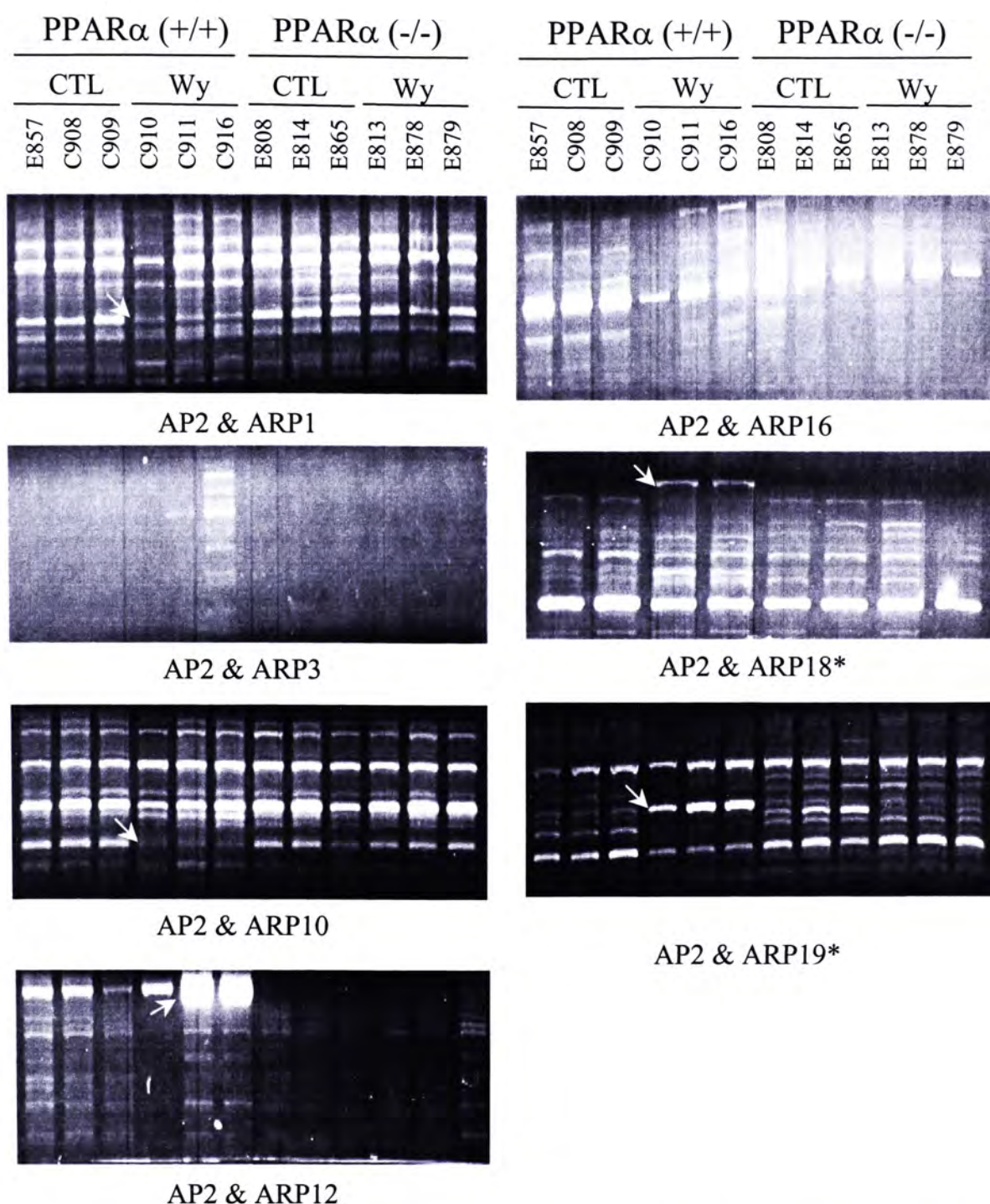


Figure 3.6.2. Preliminary screening for differential display patterns using non-fluorescent AP2 in combinations with ARP1, ARP3, ARP10, ARP12, ARP16, ARP18 and ARP19. Total RNA from PPAR α (+/+) and PPAR α (-/-) mouse livers treated with a 0.0% control (CTL) or 0.1% (w/w) Wy-14,643 (Wy) diet for 11 months was reverse transcribed with AP2 primer and amplified by PCR using 3'-AP2 and 5'-ARPs (ARP1, ARP3, ARP10, ARP12, ARP16, ARP18 and ARP19). Each treatment group consists of two or three mice and the PCR products were resolved on 1% agarose, 0.5X TBE gels with ethidium bromide staining. Arrow heads indicate the Wy-14,643 responsive and PPAR α -dependent cDNA fragments. *Primer pairs used for subsequent fluorescent differential display analysis.

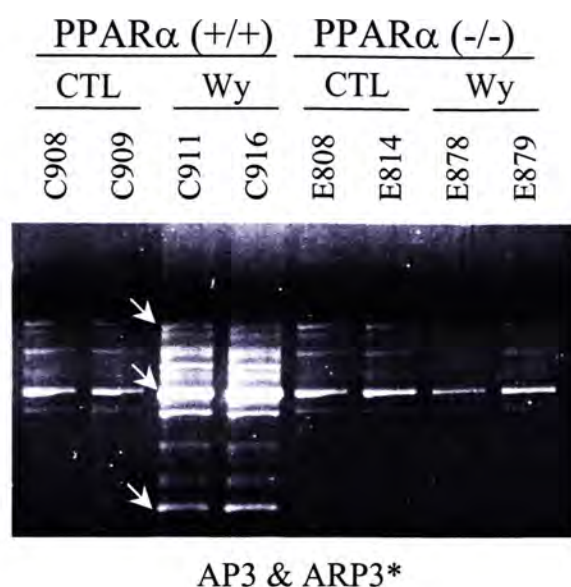


Figure 3.6.3. Preliminary screening for differential display patterns using non-fluorescent AP3 in combination with ARP3. Total RNA from PPAR α (+/+) and PPAR α (-/-) mouse livers treated with a 0.0% control (CTL) or 0.1% (w/w) Wy-14,643 (Wy) diet for 11 months was reverse transcribed with AP3 primer and amplified by PCR using 3'-AP3 and 5'-ARP3. Each treatment group consists of two mice and the PCR products were resolved on 1% agarose, 0.5X TBE gels with ethidium bromide staining. Arrow heads indicate the Wy-14,643 responsive and PPAR α -dependent cDNA fragments. *Primer pair used for subsequent fluorescent differential display analysis.

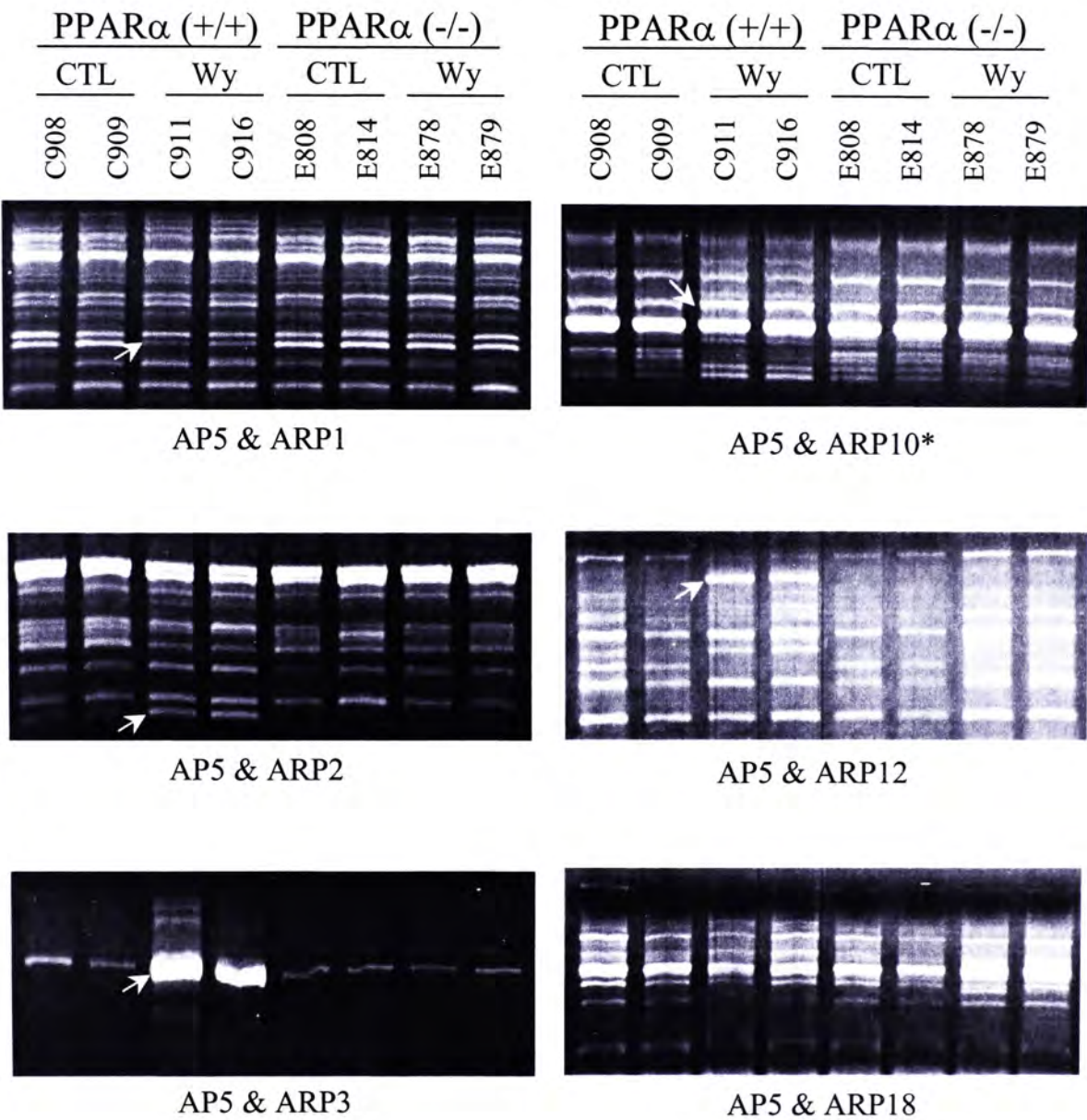


Figure 3.6.4. Preliminary screening for differential display patterns using non-fluorescent AP5 in combinations with ARP1, ARP2, ARP3, ARP10, ARP12 and ARP18. Total RNA from PPAR α (+/+) and PPAR α (-/-) mouse livers treated with a 0.0% control (CTL) or 0.1% (w/w) Wy-14,643 (Wy) diet for 11 months was reverse transcribed with AP5 primer and amplified by PCR using 3'-AP5 and 5'-ARPs (ARP1, ARP2, ARP3, ARP10, ARP12 and ARP18). Each treatment group consists of two mice and the PCR products were resolved on 1% agarose, 0.5X TBE gels with ethidium bromide staining. Arrow heads indicate the Wy-14,643 responsive and PPAR α -dependent cDNA fragments. *Primer pair used for subsequent fluorescent differential display analysis.

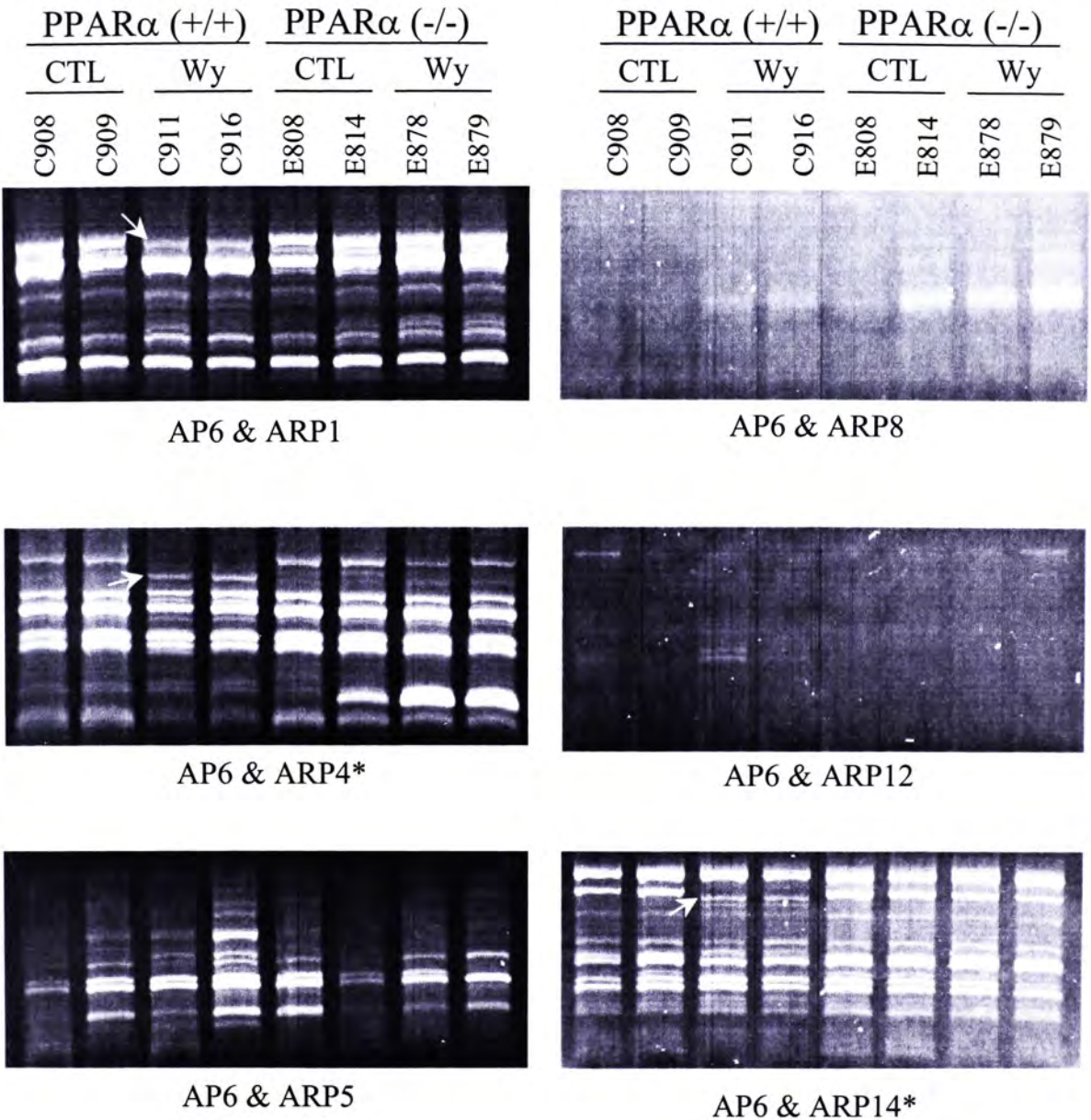


Figure 3.6.5. Preliminary screening for differential display patterns using non-fluorescent AP6 in combinations with ARP1, ARP4, ARP5, ARP8, ARP12 and ARP14. Total RNA from PPAR α (+/+) and PPAR α (-/-) mouse livers treated with a 0.0% control (CTL) or 0.1% (w/w) Wy-14,643 (Wy) diet for 11 months was reverse transcribed with AP6 primer and amplified by PCR using 3'-AP6 and 5'-ARPs (ARP1, ARP4, ARP5, ARP8, ARP12 and ARP14). Each treatment group consists of two mice and the PCR products were resolved on 1% agarose, 0.5X TBE gels with ethidium bromide staining. Arrow heads indicate the Wy-14,643 responsive and PPAR α -dependent cDNA fragments. *Primer pairs used for subsequent fluorescent differential display analysis.

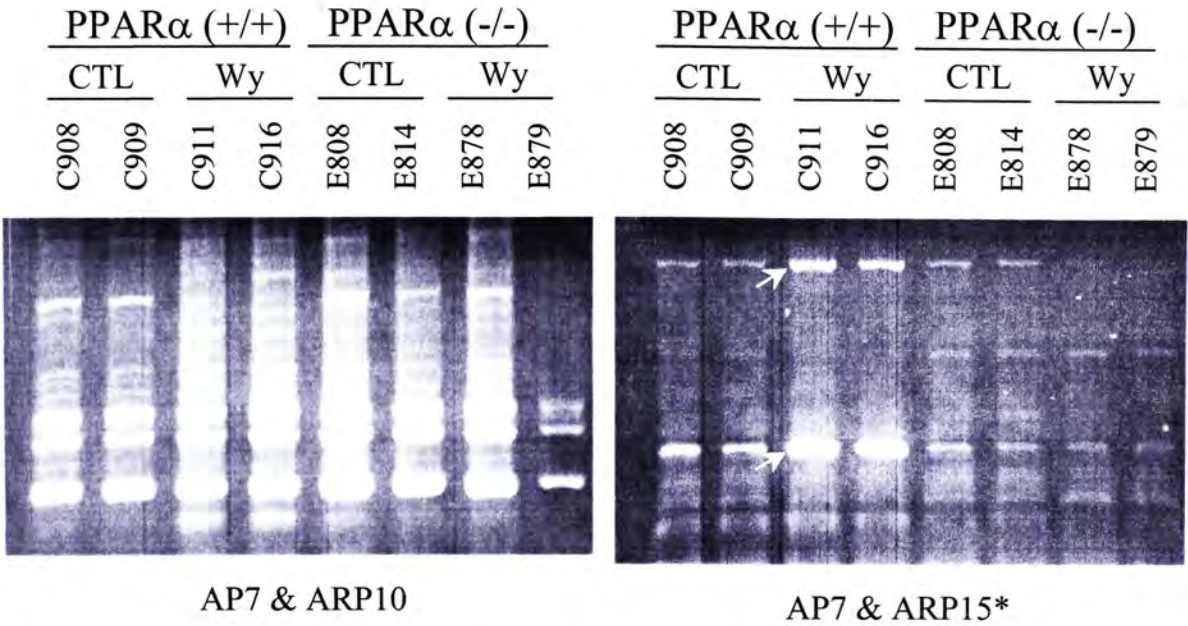


Figure 3.6.6. Preliminary screening for differential display patterns using non-fluorescent AP7 in combinations with ARP10 and ARP15. Total RNA from PPAR α (+/+) and PPAR α (-/-) mouse livers treated with a 0.0% control (CTL) or 0.1% (w/w) Wy-14,643 (Wy) diet for 11 months was reverse transcribed with AP7 primer and amplified by PCR using 3'-AP7 and 5'-ARPs (ARP10 and ARP15). Each treatment group consists of two mice and the PCR products were resolved on 1% agarose, 0.5X TBE gels with ethidium bromide staining. Arrow heads indicate the Wy-14,643 responsive and PPAR α -dependent cDNA fragments. *Primer pair used for subsequent fluorescent differential display analysis.

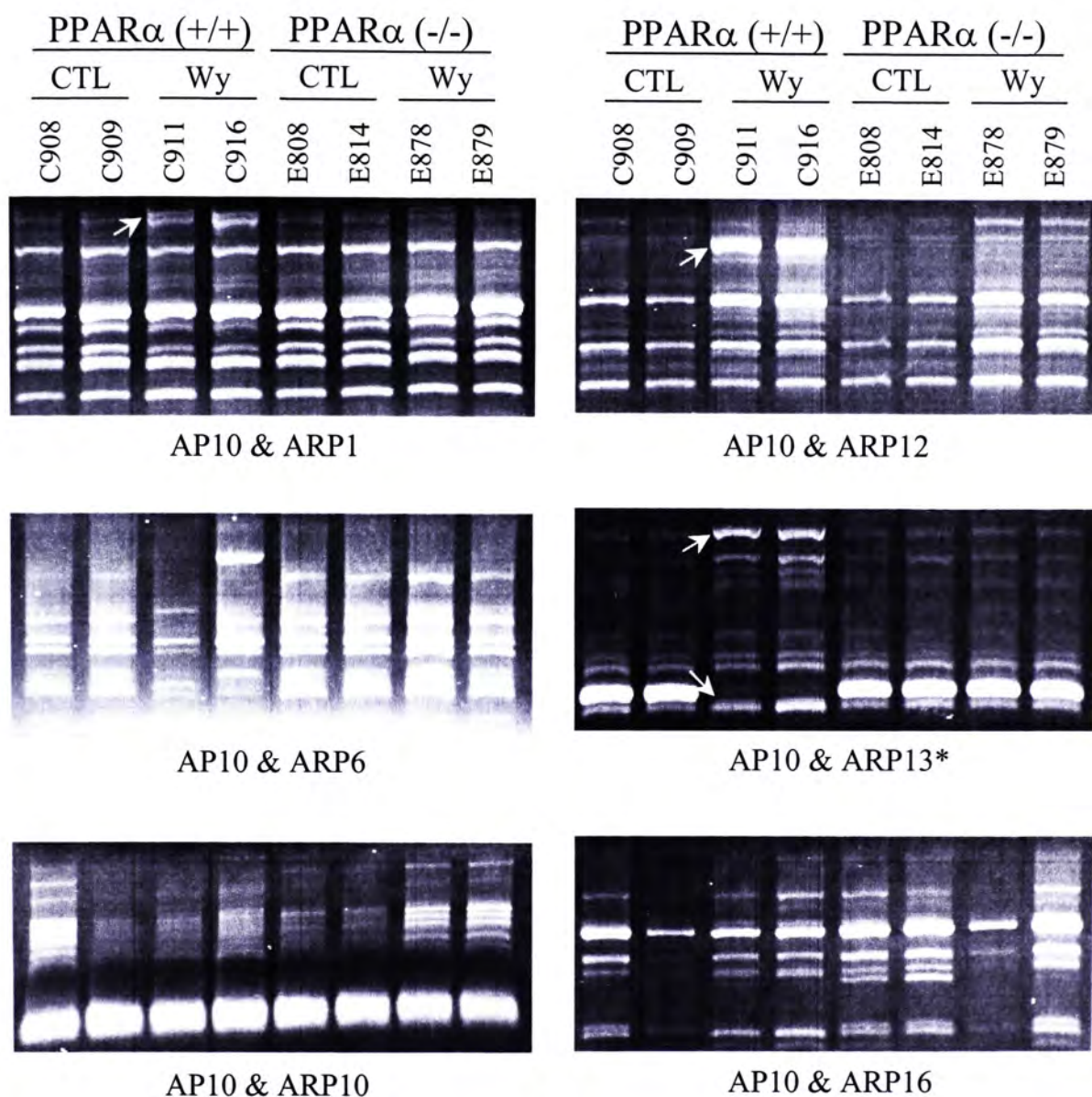


Figure 3.6.7. Preliminary screening for differential display patterns using non-fluorescent AP10 in combinations with ARP1, ARP6, ARP10, ARP12, ARP13 and ARP16. Total RNA from PPAR α (+/+) and PPAR α (-/-) mouse livers treated with a 0.0% control (CTL) or 0.1% (w/w) Wy-14,643 (Wy) diet for 11 months was reverse transcribed with AP10 primer and amplified by PCR using 3'-AP10 and 5'-ARPs (ARP1, ARP6, ARP10, ARP12, ARP13 and ARP16). Each treatment group consists of two mice and the PCR products were resolved on 1% agarose, 0.5X TBE gels with ethidium bromide staining. Arrow heads indicate the Wy-14,643 responsive and PPAR α -dependent cDNA fragments. *Primer pair used for subsequent fluorescent differential display analysis.

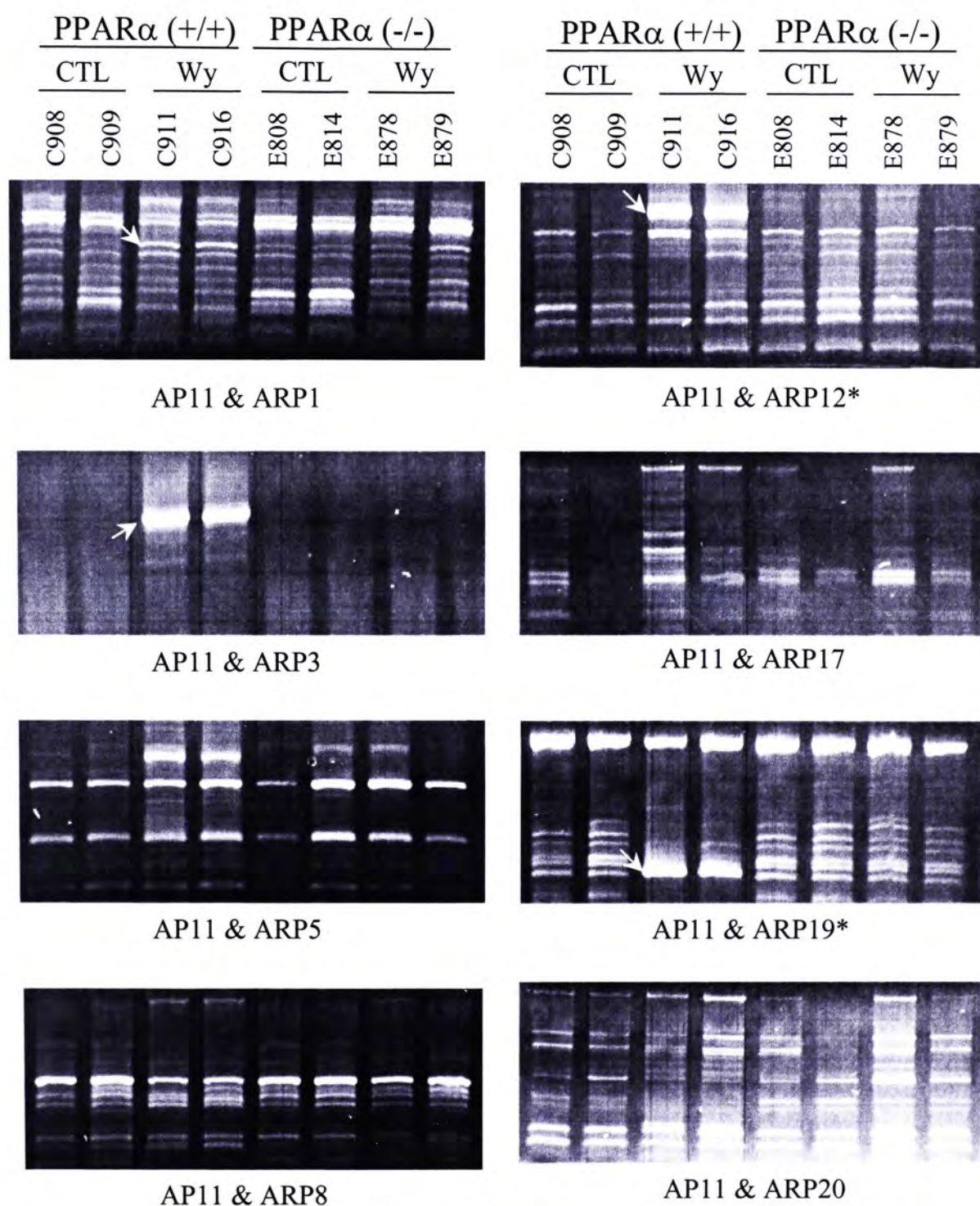


Figure 3.6.8. Preliminary screening for differential display patterns using non-fluorescent AP11 in combinations with ARP1, ARP3, ARP5, ARP8, ARP12, ARP17, ARP19 and ARP20. Total RNA from PPAR α (+/+) and PPAR α (-/-) mouse livers treated with a 0.0% control (CTL) or 0.1% (w/w) Wy-14,643 (Wy) diet for 11 months was reverse transcribed with AP11 primer and amplified by PCR using 3'-AP11 and 5'-ARPs (ARP1, ARP3, ARP5, ARP8, ARP12, ARP17, ARP19 and ARP20). Each treatment group consists of two mice and the PCR products were resolved on 1% agarose, 0.5X TBE gels with ethidium bromide staining. Arrow heads indicate the Wy-14,643 responsive and PPAR α -dependent cDNA fragments. *Primer pairs used for subsequent fluorescent differential display analysis.

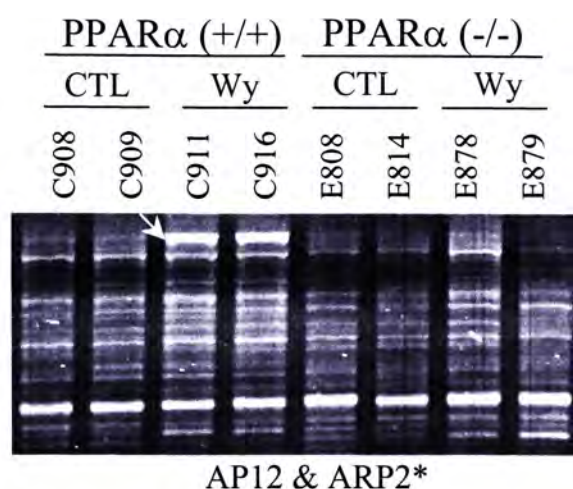


Figure 3.6.9. Preliminary screening for differential display patterns using non-fluorescent AP12 in combinations with ARP2. Total RNA from PPAR α (+/+) and PPAR α (-/-) mouse livers treated with a 0.0% control (CTL) or 0.1% (w/w) Wy-14,643 (Wy) diet for 11 months was reverse transcribed with AP12 primer and amplified by PCR using 3'-AP12 and 5'-ARP2. Each treatment group consists of two mice and the PCR products were resolved on 1% agarose, 0.5X TBE gels with ethidium bromide staining. Arrow head indicates the Wy-14,643 responsive and PPAR α -dependent cDNA fragments. *Primer pair used for subsequent fluorescent differential display analysis.

Table 3.6.1. Combinations of anchored primers (APs) and arbitrary primers (ARPs) used for non-fluoroDD RT-PCR

	ARP1	ARP2	ARP3	ARP4	ARP5	ARP6	ARP7	ARP8	ARP9	ARP10	ARP11	ARP12	ARP13	ARP14	ARP15	ARP16	ARP17	ARP18	ARP19	ARP20
AP1		1-2* [†]	1-3*			1-6				1-10						1-16				1-20*
AP2	2-1*		2-3							2-10*		2-12*				2-16		2-18* [†]	2-19* [†]	
AP3			3-3* [†]																	
AP4																				
AP5	5-1*	5-2*	5-3*							5-10* [†]		5-12*						5-18		
AP6	6-1*			6-4* [†]	6-5			6-8				6-12		6-14* [†]						
AP7										7-10					7-15* [†]					
AP8																				
AP9																				
AP10	10-1*					10-6				10-10		10-12*	10-13* [†]			10-16				
AP11	11-1*		11-3*		11-5			11-8				11-12* [†]					11-17		11-19* [†]	11-20
AP12		12-2* [†]																		

Forty-three AP-ARP pairs which are highlighted in gray were chosen randomly for preliminary non-fluoroDD RT-PCR. *The AP-ARP pairs displayed differential expression patterns and [†]the AP-ARP pairs selected for subsequent fluoroDD RT-PCR.

南京中医药大学图书馆藏

AP3 & ARP3 (Figure 3.6.3); AP5 & ARP10 (Figure 3.6.4); AP6 & ARP4 and ARP14 (Figure 3.6.5); AP7 & ARP15 (Figure 3.6.6); AP10 & ARP13 (Figure 3.6.7); AP11 & ARP19 (Figure 3.6.8); and AP12 & ARP2 (Figure 3.6.9), which showed differential display patterns in the fast screening of non-fluoro PCR were used for fluorescent RT-PCR (fluoroDD RT-PCR).

3.7 Reverse transcription (RT) of mRNA and fluorescent PCR (fluoroDD PCR)

Eleven fluoroDD gels were performed with eleven AP-ARP primer pairs which yield desired differential display patterns. They included gels AA (AP1 & ARP2) (Figure 3.7.1), AB (AP3 & ARP3) (Figure 3.7.2), AC (AP2 & ARP19) (Figure 3.7.3), AD (AP2 & ARP18) (Figure 3.7.4), AF (AP10 & ARP13) (Figure 3.7.5), AH (AP11 & ARP19) (Figure 3.7.6), AI (AP6 & ARP4) (Figure 3.7.7), AJ (AP6 & ARP14) (Figure 3.7.8), AL (AP7 & ARP15) (Figure 3.7.9), AO (AP5 & ARP10) (Figure 3.7.10) and AP (AP12 & ARP2) (Figure 3.7.11).

One hundred fifty-seven fluoroDD fragments which showed our desired differential display patterns were excised from the eleven fluoroDD gels (Tables 3.7.1-3.7.10). All together, forty-one fluoroDD fragments were down-regulated by 0.1% Wy-14,643 in PPAR α (+/+) group, whereas the other one hundred and sixteen fluoroDD fragments were up-regulated by 0.1% Wy-14,643 in PPAR α (+/+) mice. For gel AA, sixteen bands were excised (AA1, AA2, AA3, AA4, AA5, AA6, AA7, AA8, AA9, AA10, AA11, AA12, AA14, AA15, AA16 and AA17) (Figure 3.7.1) (Table 3.7.1). For gel AB, thirty-four bands were excised (AB1, AB2, AB3, AB4, AB5, AB6, AB7, AB8, AB9, AB10, AB11, AB12, AB13, AB14, AB15, AB16,

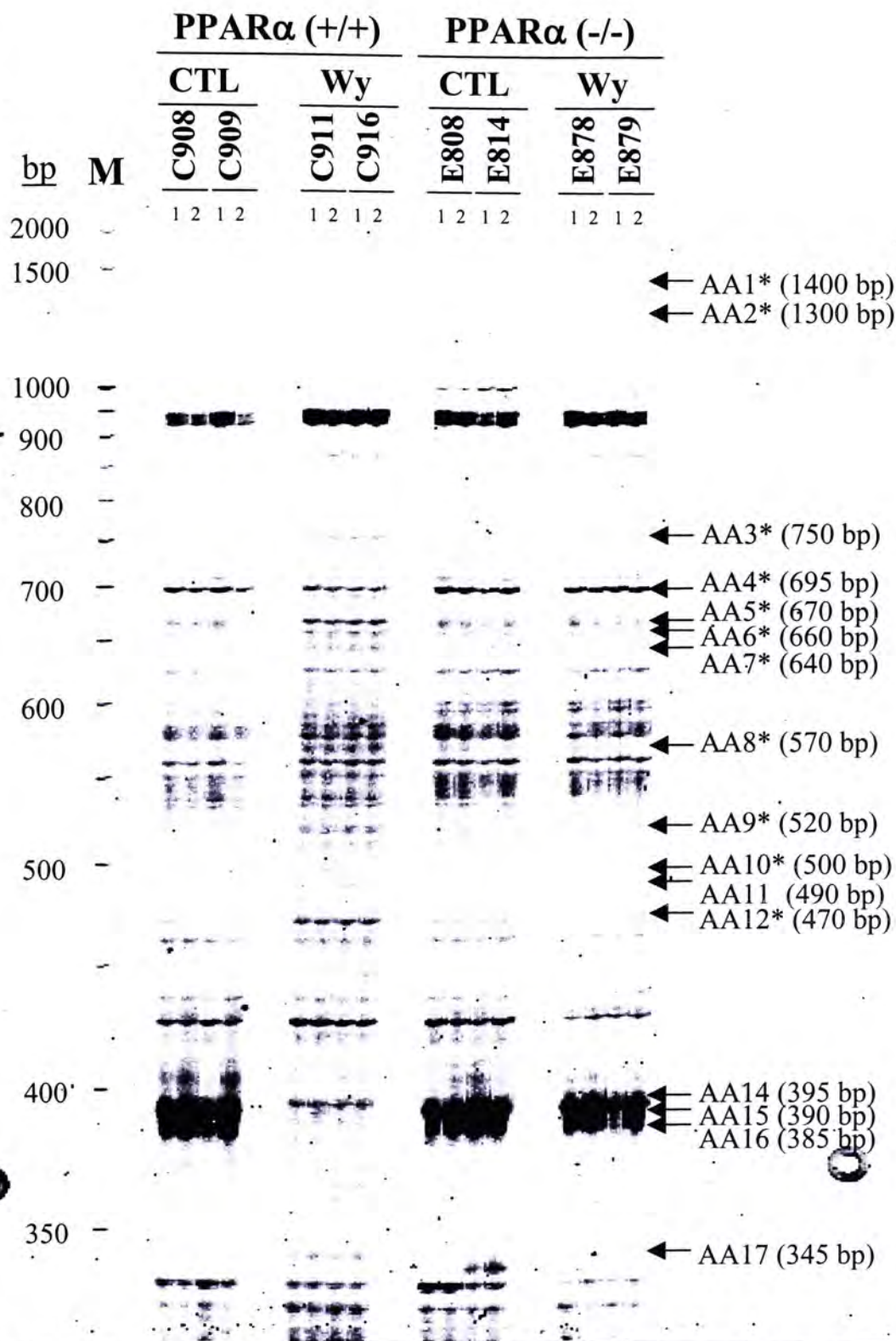


Figure 3.7.1. Fluorescent differential display of gel AA performed with AP1 and ARP2. Total RNA from PPARα (+/+) and PPARα (-/-) mouse livers treated with a 0.0% control (CTL) or 0.1% (w/w) Wy-14,643 (Wy) diet for 11 months was reverse transcribed with AP1 and duplicate PCR reactions were performed for each mouse with 3'-TMR-labeled AP1 (ACGACTCACTATAGGGCTTTTTTTTTTTTGA) and 5'-ARP2 (ACAATTTACACAGGAGCTAGCATGG). The TMR-labeled fluorescent PCR products were run on a 5.6% denaturing polyacrylamide gel. In gel AA, sixteen cDNA fragments showing differential display patterns were excised. *Fragments selected for reamplification. M, TMR-labeled molecular weight DNA marker.

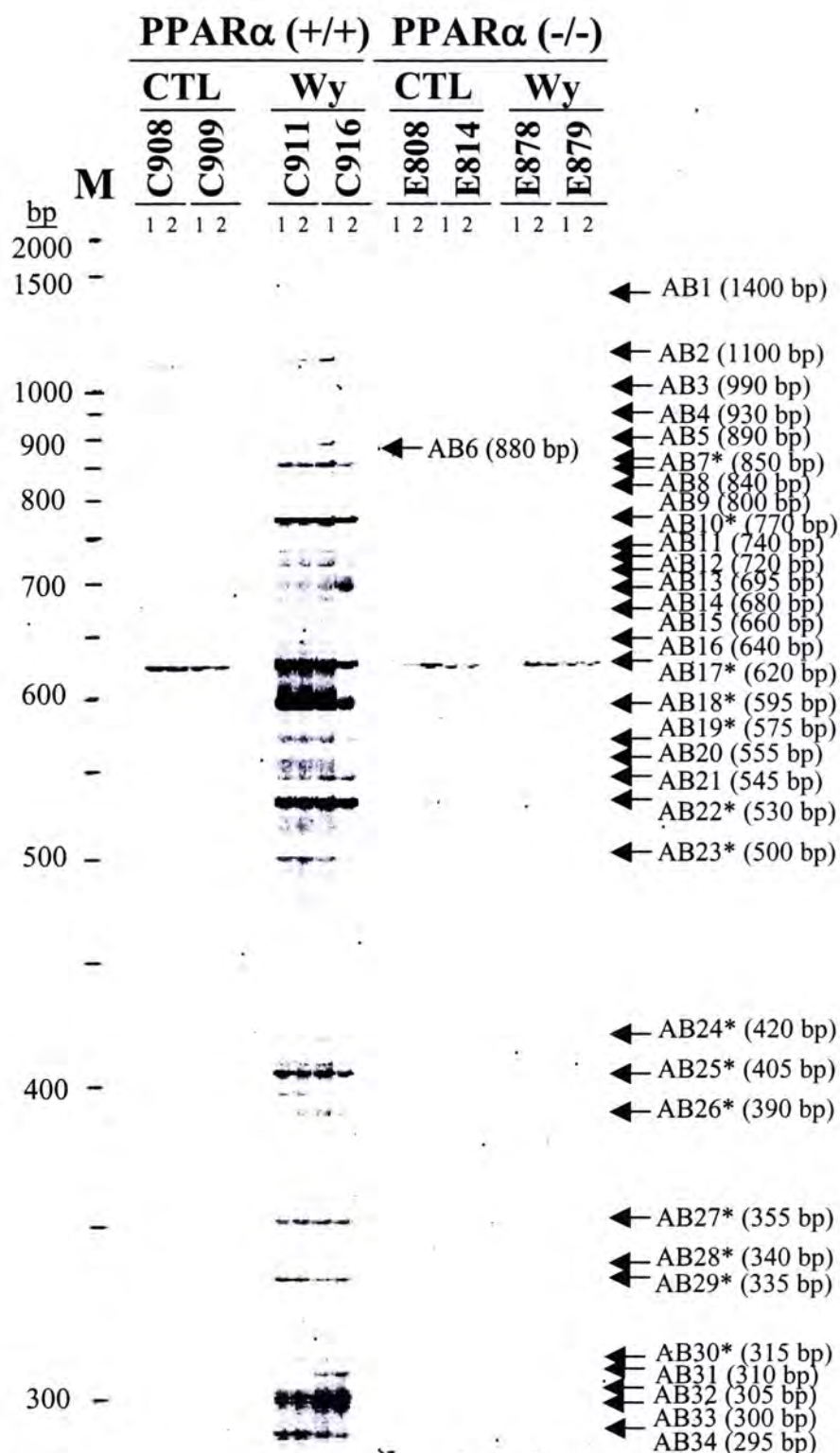


Figure 3.7.2. Fluorescent differential display of gel AB performed with AP3 and ARP3. Total RNA from PPAR α (+/+) and PPAR α (-/-) mouse livers treated with a 0.0% control (CTL) or 0.1% (w/w) Wy-14,643 (Wy) diet for 11 months was reverse transcribed with AP3 and duplicate PCR reactions were performed for each mouse with 3'-TMR-labeled AP3 (ACGACTCACTATAGGGCTTTTTTTTTTTTGG) and 5'-ARP3 (ACAATTTACACAGGAGACCATTGCA). The TMR-labeled fluorescent PCR products were run on a 5.6% denaturing polyacrylamide gel. In gel AB, thirty-four cDNA fragments showing differential display patterns were excised. *Fragments selected for reamplification. M, TMR-labeled molecular weight DNA marker.

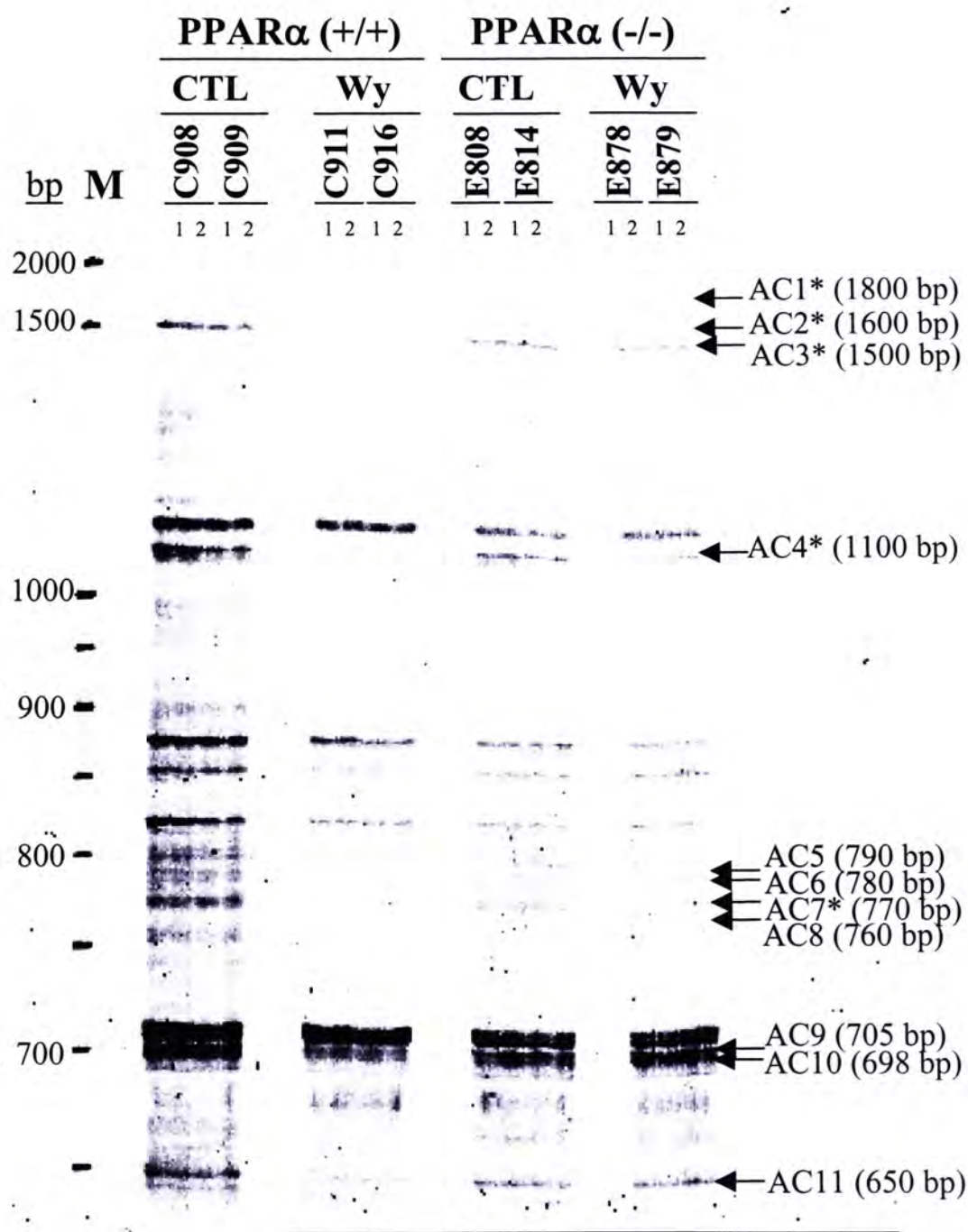


Figure 3.7.3. Fluorescent differential display of gel AC performed with AP2 and ARP19. Total RNA from PPAR α (+/+) and PPAR α (-/-) mouse livers treated with a 0.0% control (CTL) or 0.1% (w/w) Wy-14,643 (Wy) diet for 11 months was reverse transcribed with AP2 and duplicate PCR reactions were performed for each mouse with 3'-TMR-labeled AP2 (ACGACTCACTATAGGGCTTTTTTTTTTTTGC) and 5'-ARP19 (ACAATTTTCACACAGGATTTTGGCTCC). The TMR-labeled fluorescent PCR products were run on a 5.6% denaturing polyacrylamide gel. In gel AC, eleven cDNA fragments showing differential display patterns were excised. *Fragments selected for reamplification. M, TMR-labeled molecular weight DNA marker.

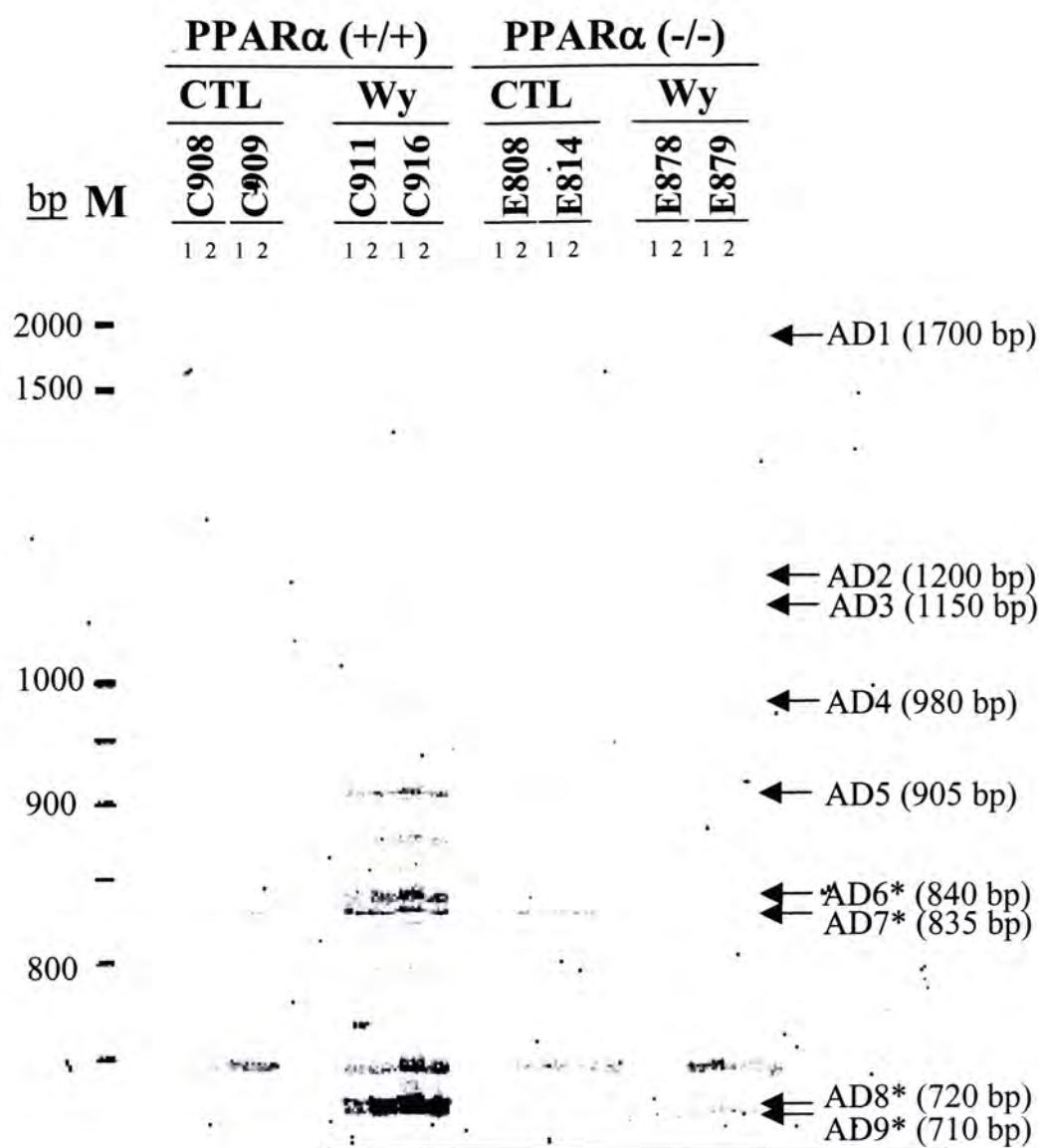


Figure 3.7.4. Fluorescent differential display of gel AD performed with AP2 and ARP18. Total RNA from PPAR α (+/+) and PPAR α (-/-) mouse livers treated with a 0.0% control (CTL) or 0.1% (w/w) Wy-14,643 (Wy) diet for 11 months was reverse transcribed with AP2 and duplicate PCR reactions were performed for each mouse with 3'-TMR-labeled AP2 (ACGACTCACTATAGGGCTTTTTTTTTTTTGC) and 5'-ARP18 (ACAATTTTCACACAGGATGATGCTACC). The TMR-labeled fluorescent PCR products were run on a 5.6% denaturing polyacrylamide gel. In gel AD, nine cDNA fragments showing differential display patterns were excised. *Fragments selected for reamplification. M, TMR-labeled molecular weight DNA marker.

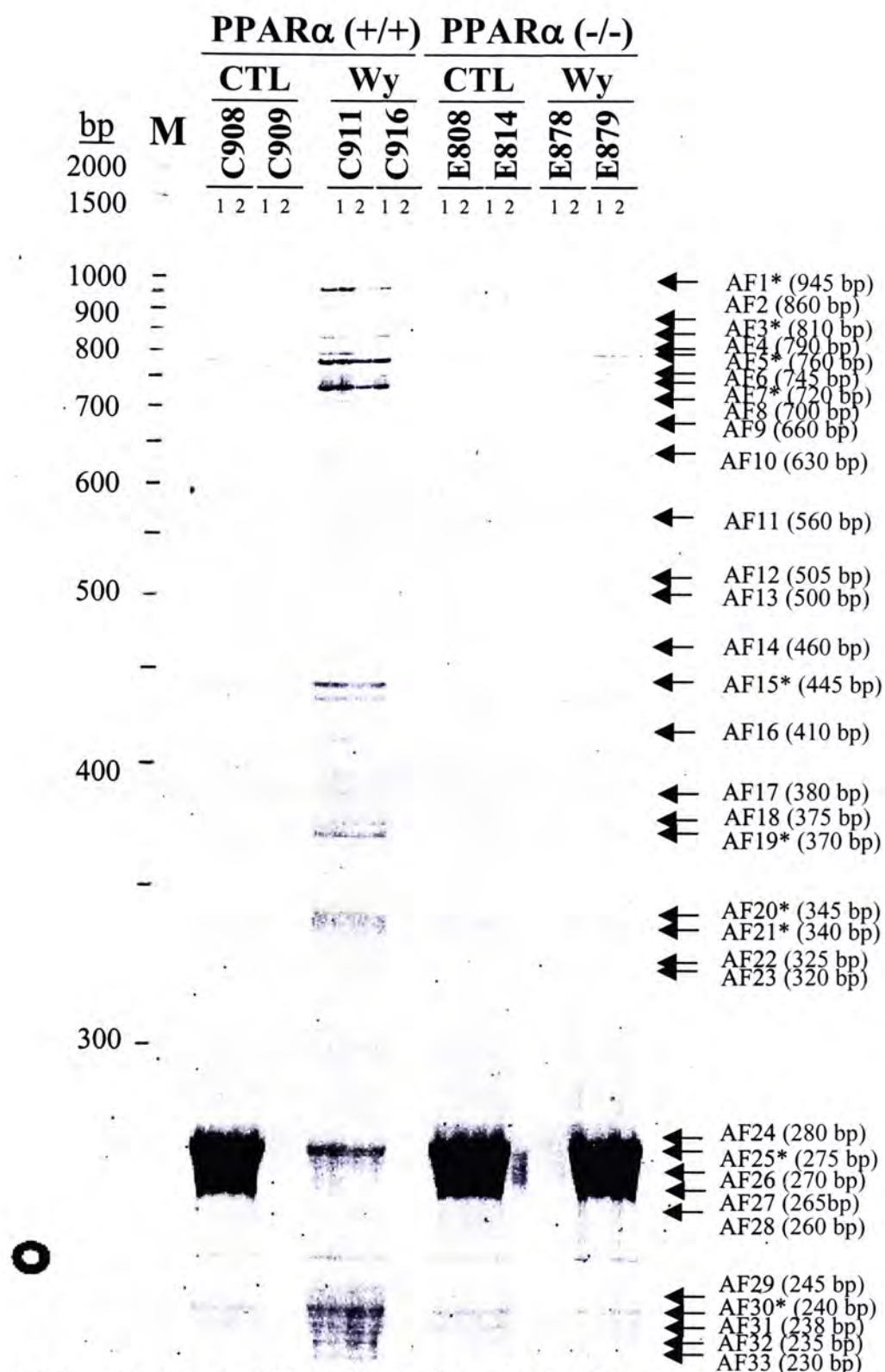


Figure 3.7.5. Fluorescent differential display of gel AF performed with AP10 and ARP13. Total RNA from PPAR α (+/+) and PPAR α (-/-) mouse livers treated with a 0.0% control (CTL) or 0.1% (w/w) Wy-14,643 (Wy) diet for 11 months was reverse transcribed with AP10 and duplicate PCR reactions were performed for each mouse with 3'-TMR-labeled AP10 (ACGACTCACTATAGGGCTTTTTTTTTTTT) and 5'-ARP13 (ACAATTTACACAGGAGTTGCACCAT). The TMR-labeled fluorescent PCR products were run on a 5.6% denaturing polyacrylamide gel. In gel AF, thirty-three cDNA fragments showing differential display patterns were excised. *Fragments selected for reamplification. M, TMR-labeled molecular weight DNA marker.

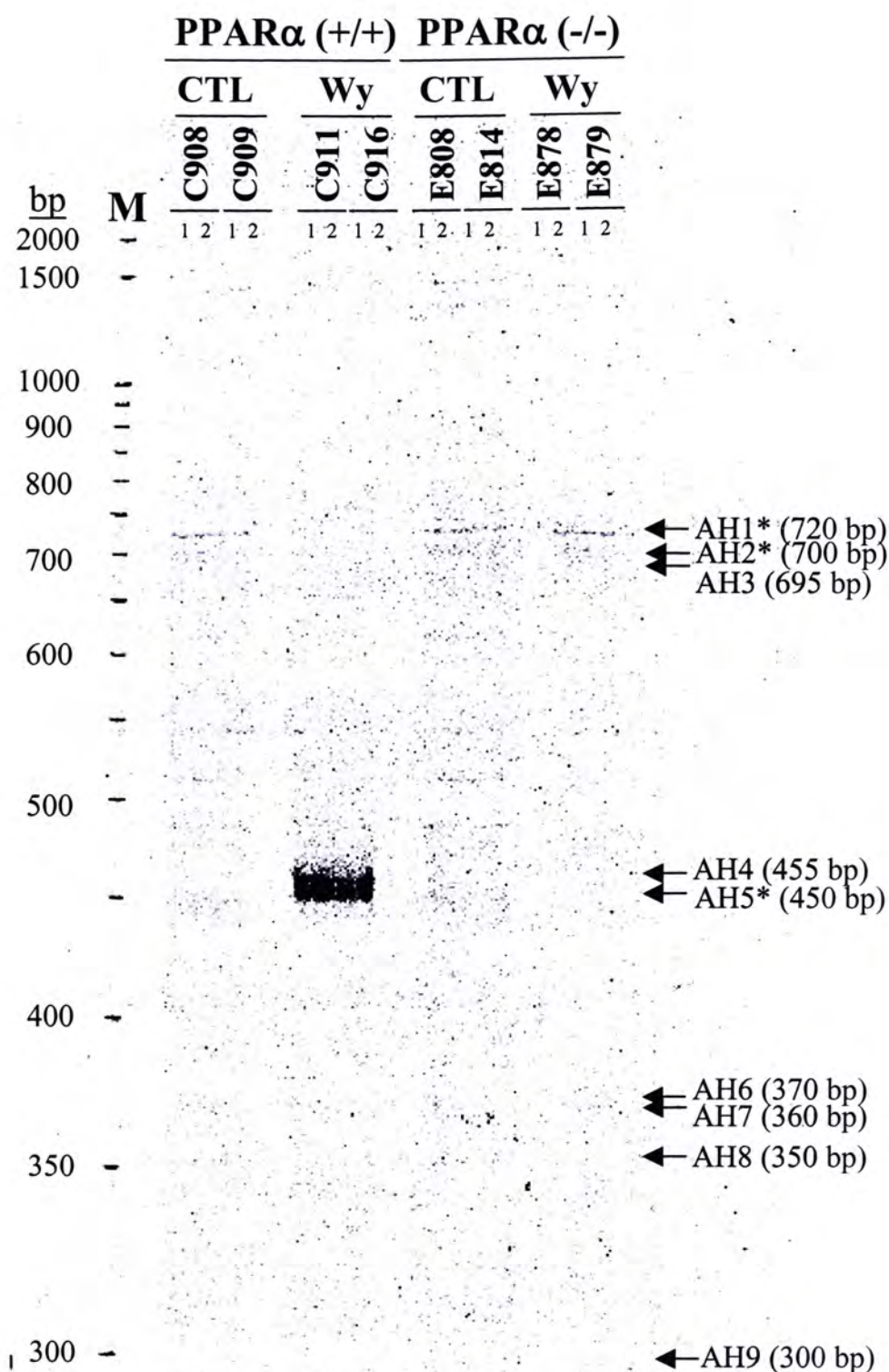


Figure 3.7.6. Fluorescent differential display of gel AH performed with AP11 and ARP19. Total RNA from PPAR α (+/+) and PPAR α (-/-) mouse livers treated with a 0.0% control (CTL) or 0.1% (w/w) Wy-14,643 (Wy) diet for 11 months was reverse transcribed with AP11 and duplicate PCR reactions were performed for each mouse with 3'-TMR-labeled AP11 (ACGACTCACTATAGGGCTTTTTTTTTTTTAT) and 5'-ARP19 (ACAATTTCACACAGGATTTTGGCTCC). The TMR-labeled fluorescent PCR products were run on a 5.6% denaturing polyacrylamide gel. In gel AH, nine cDNA fragments showing differential display patterns were excised. *Fragments selected for reamplification. M, TMR-labeled molecular weight DNA marker.

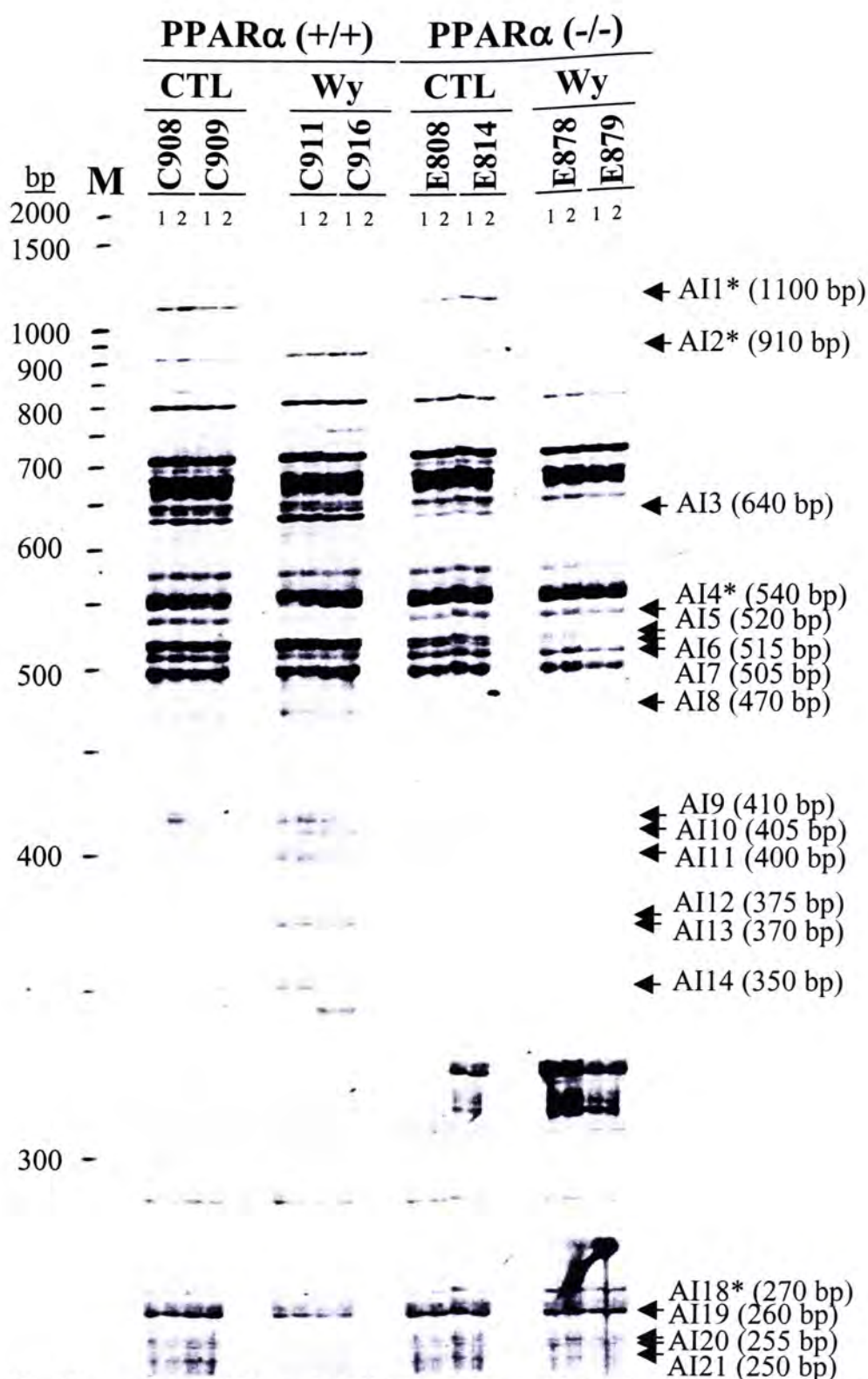


Figure 3.7.7. Fluorescent differential display of gel AI performed with AP6 and ARP4. Total RNA from PPAR α (+/+) and PPAR α (-/-) mouse livers treated with a 0.0% control (CTL) or 0.1% (w/w) Wy-14,643 (Wy) diet for 11 months was reverse transcribed with AP6 and duplicate PCR reactions were performed for each mouse with 3'-TMR-labeled AP6 (ACGACTCACTATAGGGCTTTTTTTTTTTTCC) and 5'-ARP4 (ACAATTTTCACACAGGAGCTAGCAGAC). The TMR-labeled fluorescent PCR products were run on a 5.6% denaturing polyacrylamide gel. In gel AI, eighteen cDNA fragments showing differential display patterns were excised. *Fragments selected for reamplification. M, TMR-labeled molecular weight DNA marker.

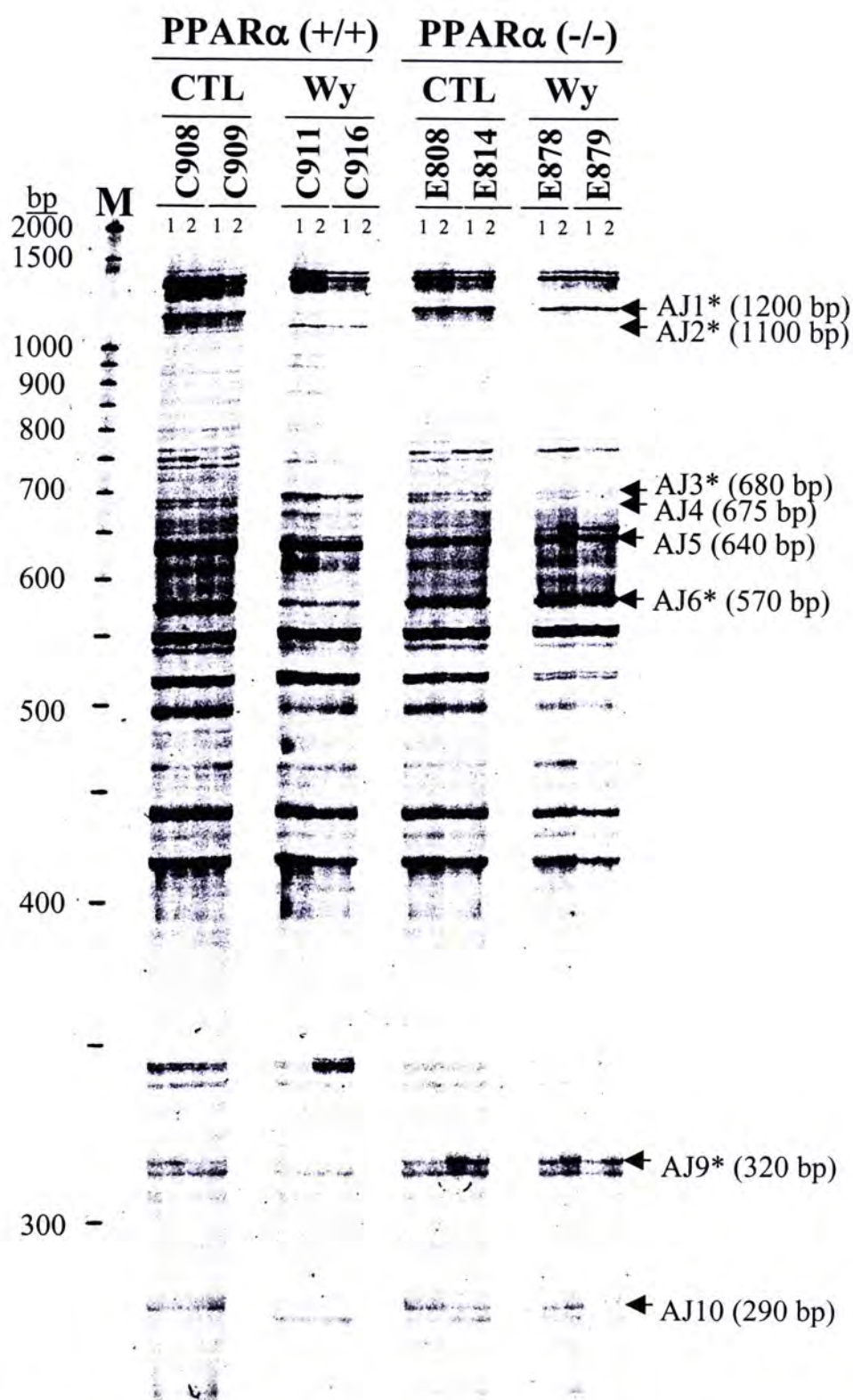


Figure 3.7.8. Fluorescent differential display of gel AJ performed with AP6 and ARP14. Total RNA from PPAR α (+/+) and PPAR α (-/-) mouse livers treated with a 0.0% control (CTL) or 0.1% (w/w) Wy-14,643 (Wy) diet for 11 months was reverse transcribed with AP6 and duplicate PCR reactions were performed for each mouse with 3'-TMR-labeled AP6 (ACGACTCACTATAGGGCTTTTTTTTTTTTCC) and 5'-ARP14 (ACAATTTCACACAGGATCCATGACTC). The TMR-labeled fluorescent PCR products were run on a 5.6% denaturing polyacrylamide gel. In gel AJ, eight cDNA fragments showing differential display patterns were excised. *Fragments selected for reamplification. M, TMR-labeled molecular weight DNA marker.

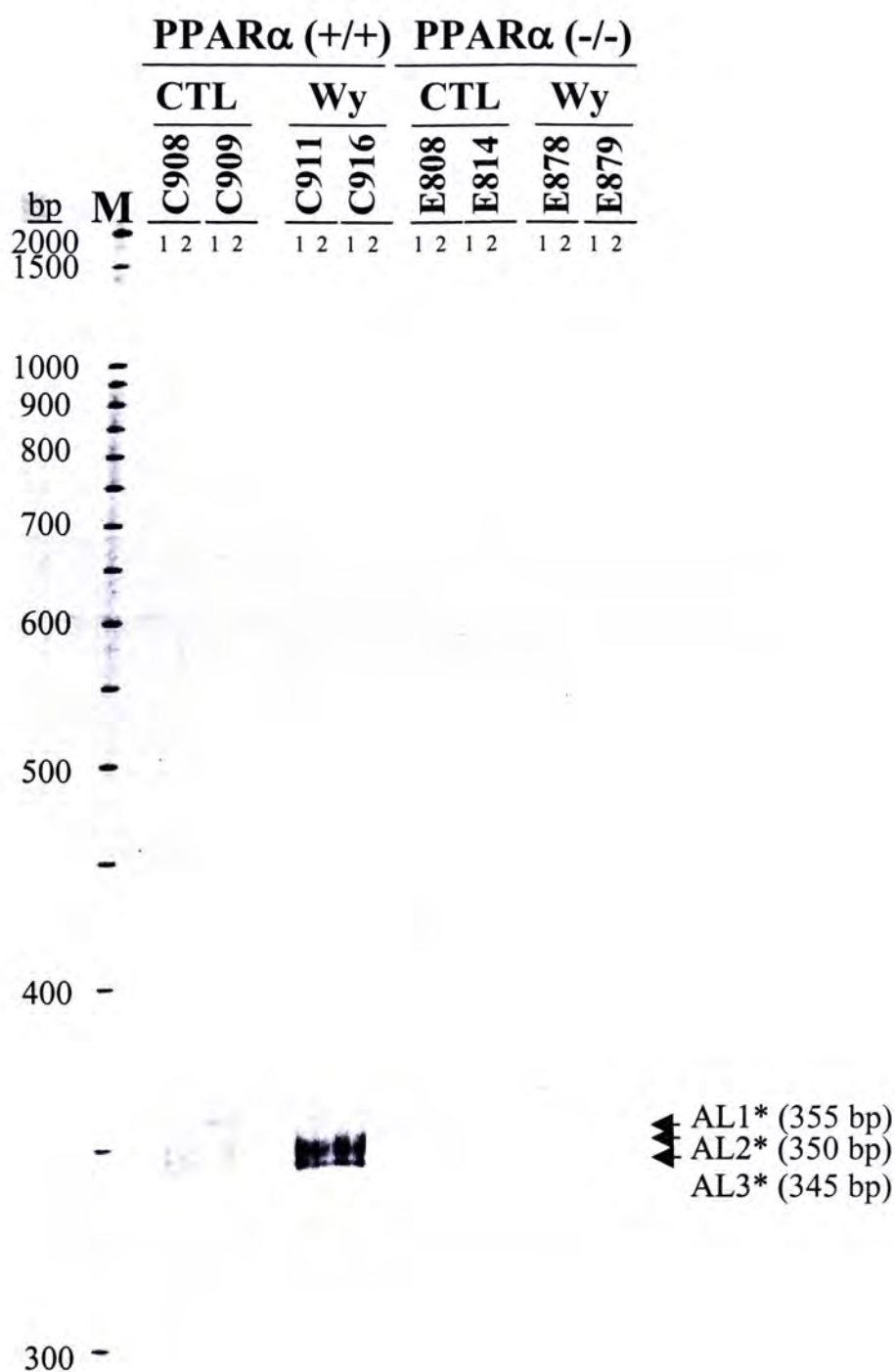


Figure 3.7.9. Fluorescent differential display of gel AL performed with AP7 and ARP15. Total RNA from PPAR α (+/+) and PPAR α (-/-) mouse livers treated with a 0.0% control (CTL) or 0.1% (w/w) Wy-14,643 (Wy) diet for 11 months was reverse transcribed with AP7 and duplicate PCR reactions were performed for each mouse with 3'-TMR-labeled AP7 (ACGACTCACTATAGGGCTTTTTTTTTTTTCG) and 5'-ARP15 (ACAATTTTCACACAGGACTTTCTACCC). The TMR-labeled fluorescent PCR products were run on a 5.6% denaturing polyacrylamide gel. In gel AL, three cDNA fragments showing differential display patterns were excised. *Fragments selected for reamplification. M, TMR-labeled molecular weight DNA marker.

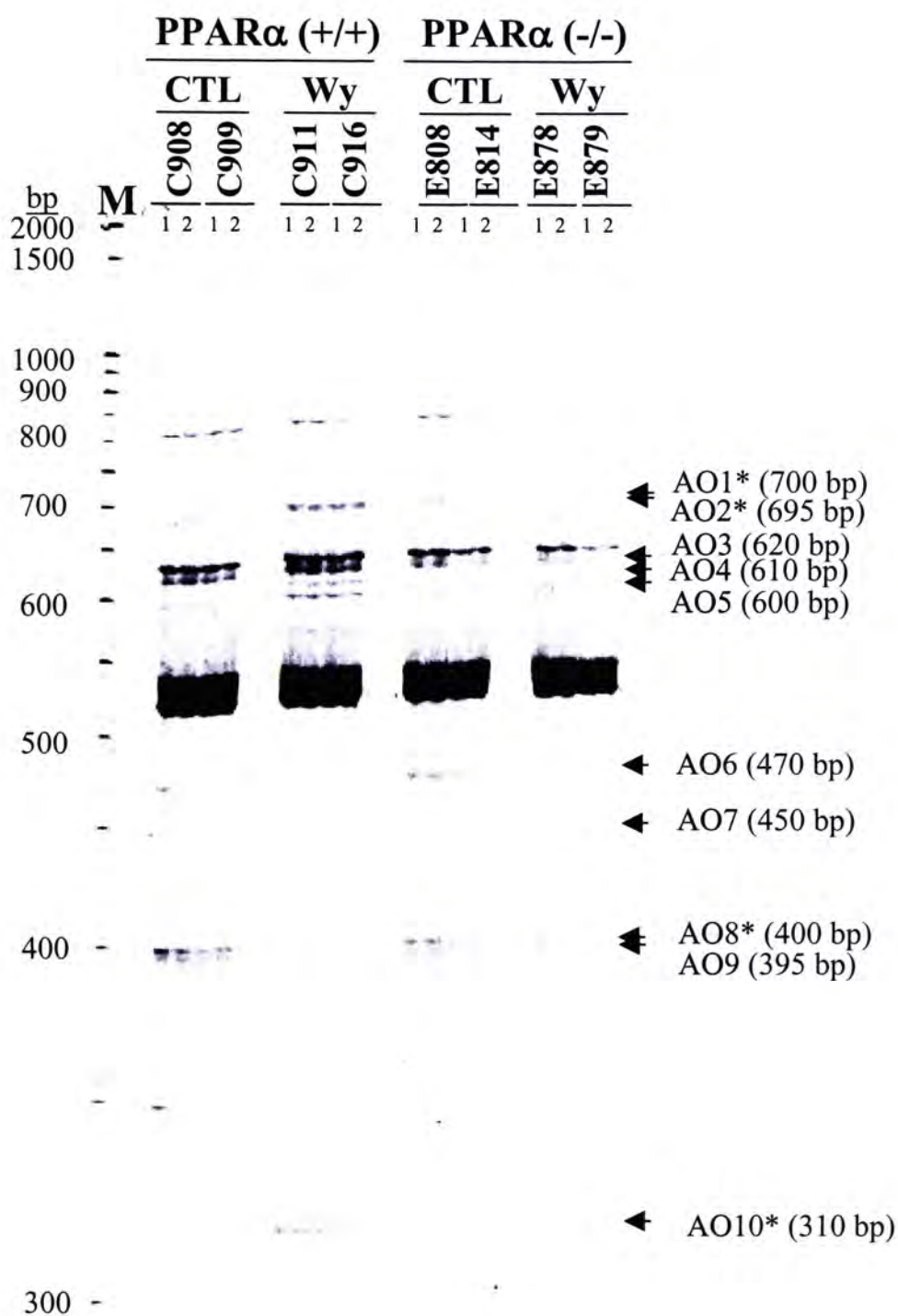


Figure 3.7.10. Fluorescent differential display of gel AO performed with AP5 and ARP10. Total RNA from PPAR α (+/+) and PPAR α (-/-) mouse livers treated with a 0.0% control (CTL) or 0.1% (w/w) Wy-14,643 (Wy) diet for 11 months was reverse transcribed with AP5 and duplicate PCR reactions were performed for each mouse with 3'-TMR-labeled AP5 (ACGACTCACTATAGGGCTTTTTTTTTTTTCA) and 5'-ARP10 (ACAATTTCACACAGGAGATCTCAGAC). The TMR-labeled fluorescent PCR products were run on a 5.6% denaturing polyacrylamide gel. In gel AO, ten cDNA fragments showing differential display patterns were excised. *Fragments selected for reamplification. M, TMR-labeled molecular weight DNA marker.

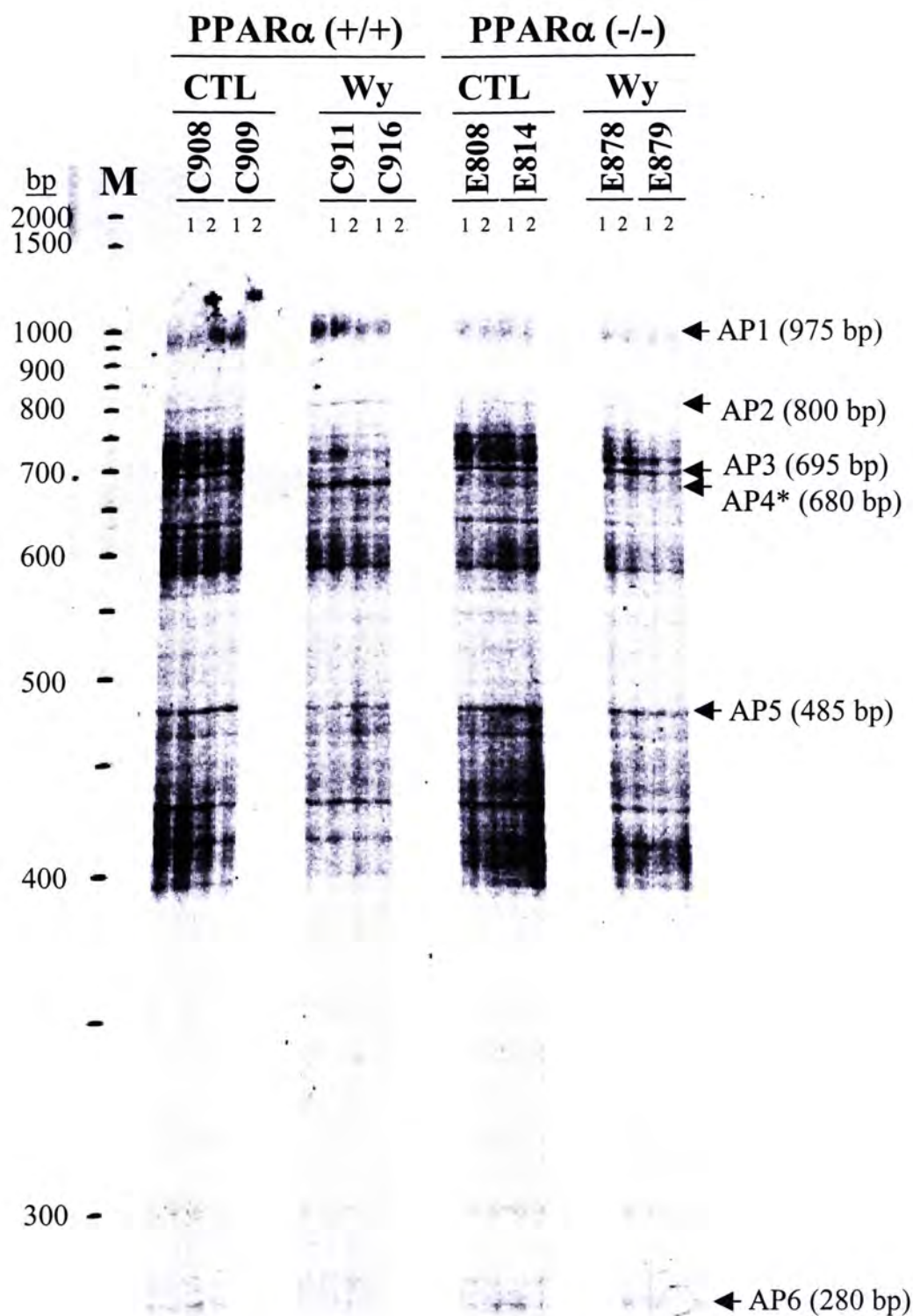


Figure 3.7.11. Fluorescent differential display of gel AP performed with AP12 and ARP2. Total RNA from PPAR α (+/+) and PPAR α (-/-) mouse livers treated with a 0.0% control (CTL) or 0.1% (w/w) Wy-14,643 (Wy) diet for 11 months was reverse transcribed with AP12 and duplicate PCR reactions were performed for each mouse with 3'-TMR-labeled AP12 (ACGACTCACTATAGGGCTTTTTTTTTTTTCT) and 5'-ARP2 (ACAATTTTCACACAGGAGCTAGCATGG). The TMR-labeled fluorescent PCR products were run on a 5.6% denaturing polyacrylamide gel. In gel AP, six cDNA fragments showing differential display patterns were excised. *Fragments selected for reamplification. M, TMR-labeled molecular weight DNA marker.

Table 3.7.1.1. Summary of cDNA fragments excised from gel AA (AP1 and ARP2)

Gel	FluoroDD fragment I.D.	FluoroDD fragment size (bp)	Differential display pattern						PPAR α -dependent genes that were either up- or down-regulated in PPAR α (+/+) mice treated with 0.1% Wy-14,643 compared to their corresponding controls
			PPAR α (+/+)		PPAR α (-/-)		FluoroDD pattern [§]		
			CTL	Wy	CTL	Wy			
AA (AP1 & ARP2)	AA1*	1400	-	+	-	-	I	Up-regulated in 0.1% Wy-14,643 treatment and PPAR α dependent	
	AA2*	1300	+	++	+	+	II	Up-regulated in 0.1% Wy-14,643 treatment and PPAR α dependent	
	AA3*	750	+	++	+	+	II	Up-regulated in 0.1% Wy-14,643 treatment and PPAR α dependent	
	AA4*	695	++	+	++	++	IV	Down-regulated in 0.1% Wy-14,643 treatment and PPAR α dependent	
	AA5*	670	+	++	+	+	II	Up-regulated in 0.1% Wy-14,643 treatment and PPAR α dependent	
	AA6*	660	+	++	+	+	II	Up-regulated in 0.1% Wy-14,643 treatment and PPAR α dependent	
	AA7*	640	+	++	+	+	II	Up-regulated in 0.1% Wy-14,643 treatment and PPAR α dependent	
	AA8*	570	+	++	+	+	II	Up-regulated in 0.1% Wy-14,643 treatment and PPAR α dependent	
	AA9*	520	+	++	+	+	II	Up-regulated in 0.1% Wy-14,643 treatment and PPAR α dependent	
	AA10*	500	+	++	+	+	II	Up-regulated in 0.1% Wy-14,643 treatment and PPAR α dependent	
	AA11	490	+	++	+	+	II	Up-regulated in 0.1% Wy-14,643 treatment and PPAR α dependent	
	AA12*	470	+	++	+	+	II	Up-regulated in 0.1% Wy-14,643 treatment and PPAR α dependent	
	AA14	395	++	+	++	++	IV	Down-regulated in 0.1% Wy-14,643 treatment and PPAR α dependent	
	AA15	390	+	-	+	+	III	Down-regulated in 0.1% Wy-14,643 treatment and PPAR α dependent	
	AA16	385	+	-	+	+	III	Down-regulated in 0.1% Wy-14,643 treatment and PPAR α dependent	
	AA17	345	+	++	+	+	II	Up-regulated in 0.1% Wy-14,643 treatment and PPAR α dependent	

'+' represents the presence of a band (cDNA) on fluoroDD gel, while '-' represents the corresponding band (cDNA) that was not observed on the fluoroDD gel. The relative intensity of the gene expression among the four treatment groups is indicated by the number of '+'. *Fragments selected for reamplification. [§]Differential expression patterns as shown in Table 4.1.

AB17, AB18, AB19, AB20, AB21, AB22, AB23, AB24, AB25, AB26, AB27, AB28, AB29, AB30, AB31, AB32, AB33 and AB34) (Figure 3.7.2) (Tables 3.7.2-3.7.3). For gel AC, eleven bands were excised (AC1, AC2, AC3, AC4, AC5, AC6, AC7, AC8, AC9, AC10 and AC11) (Figure 3.7.3) (Table 3.7.4). For gel AD, nine bands were excised (AD1, AD2, AD3, AD4, AD5, AD6, AD7, AD8 and AD9) (Figure 3.7.4) (Table 3.7.5). For gel AF, thirty-three bands were excised (AF1, AF2, AF3, AF4, AF5, AF6, AF7, AF8, AF9, AF10, AF11, AF12, AF13, AF14, AF15, AF16, AF17, AF18, AF19, AF20, AF21, AF22, AF23, AF24, AF25, AF26, AF27, AF28, AF29, AF30, AF31, AF32 and AF33) (Figure 3.7.5) (Tables 3.7.6-3.7.7). Nine fragments were excised from gel AH (AH1, AH2, AH3, AH4, AH5, AH6, AH7, AH8 and AH9) (Figure 3.7.6) (Table 3.7.8). For gel AI, eighteen fragments were selected for excision (AI1, AI2, AI3, AI4, AI5, AI6, AI7, AI8, AI9, AI10, AI11, AI12, AI13, AI14, AI18, AI19, AI20 and AI21) (Figure 3.7.7) (Table 3.7.9). For gel AJ, eight fragments were selected for excision (AJ1, AJ2, AJ3, AJ4, AJ5, AJ6, AJ9 and AJ10) (Figure 3.7.8) (Table 3.7.10). For gel AL, three fragments were excised (AL1, AL2 and AL3) (Figure 3.7.9) (Table 3.7.10). Ten fragments were excised from gel AO (AO1, AO2, AO3, AO4, AO5, AO6, AO7, AO8, AO9 and AO10) (Figure 3.7.10) (Table 3.7.11). For gel AP, six fragments were excised (AP1, AP2, AP3, AP4, AP5 and AP6) (Figure 3.7.11) (Table 3.7.11).

3.8 Reamplification of fluorescent differential display (fluoroDD) fragments

The cDNA fragments were reamplified with full-length M13 reverse (-48) 24-mer (5'-AGCGGATAACAATTTTCACACAGGA-3') and T7 promoter 22-mer (5'-

Table 3.7.2. Summary of cDNA fragments excised from gel AB (AP3 and ARP3) Part I

Gel	FluoroDD fragment I.D.	FluoroDD fragment size (bp)	Differential display pattern						PPAR α -dependent genes that were either up- or down-regulated in PPAR α (+/+) mice treated with 0.1% Wy-14,643 compared to their corresponding controls
			PPAR α (+/+)		PPAR α (-/-)		FluoroDD pattern ^s		
			CTL	Wy	CTL	Wy			
AB (AP3 & ARP3)	AB1	1400	-	+	-	-	I	Up-regulated in 0.1% Wy-14,643 treatment and PPAR α dependent	
	AB2	1100	+	++	+	+	II	Up-regulated in 0.1% Wy-14,643 treatment and PPAR α dependent	
	AB3	990	-	+	-	-	I	Up-regulated in 0.1% Wy-14,643 treatment and PPAR α dependent	
	AB4	930	-	+	-	-	I	Up-regulated in 0.1% Wy-14,643 treatment and PPAR α dependent	
	AB5	890	-	+	-	-	I	Up-regulated in 0.1% Wy-14,643 treatment and PPAR α dependent	
	AB6	880	-	+	-	-	I	Up-regulated in 0.1% Wy-14,643 treatment and PPAR α dependent	
	AB7*	850	+	++	+	+	II	Up-regulated in 0.1% Wy-14,643 treatment and PPAR α dependent	
	AB8	840	-	+	-	-	I	Up-regulated in 0.1% Wy-14,643 treatment and PPAR α dependent	
	AB9	800	-	+	-	-	I	Up-regulated in 0.1% Wy-14,643 treatment and PPAR α dependent	
	AB10*	770	+	++	+	+	II	Up-regulated in 0.1% Wy-14,643 treatment and PPAR α dependent	
	AB11	740	-	+	-	-	I	Up-regulated in 0.1% Wy-14,643 treatment and PPAR α dependent	
	AB12	720	-	+	-	-	I	Up-regulated in 0.1% Wy-14,643 treatment and PPAR α dependent	
	AB13	695	-	+	-	-	I	Up-regulated in 0.1% Wy-14,643 treatment and PPAR α dependent	
	AB14	680	-	+	-	-	I	Up-regulated in 0.1% Wy-14,643 treatment and PPAR α dependent	
	AB15	660	-	+	-	-	I	Up-regulated in 0.1% Wy-14,643 treatment and PPAR α dependent	
	AB16	640	-	+	-	-	I	Up-regulated in 0.1% Wy-14,643 treatment and PPAR α dependent	
	AB17*	620	+	++	+	+	II	Up-regulated in 0.1% Wy-14,643 treatment and PPAR α dependent	

'+' represents the presence of a band (cDNA) on fluoroDD gel, while '-' represents the corresponding band (cDNA) that was not observed on the fluoroDD gel. The relative intensity of the gene expression among the four treatment groups is indicated by the number of '+'. *Fragments selected for reamplification. ^sDifferential expression patterns as shown in Table 4.1.

Table 3.7.3. Summary of cDNA fragments excised from gel AB (AP3 and ARP3) Part II

Gel	FluoroDD fragment I.D.	FluoroDD fragment size (bp)	Differential display pattern						PPAR α -dependent genes that were either up- or down-regulated in PPAR α (+/+) mice treated with 0.1% Wy-14,643 compared to their corresponding controls
			PPAR α (+/+)		PPAR α (-/-)		FluoroDD pattern [§]		
			CTL	Wy	CTL	Wy			
AB (AP3 & ARP3)	AB18*	595	+	++	+	+	+	II	Up-regulated in 0.1% Wy-14,643 treatment and PPAR α dependent
	AB19*	575	-	+	-	-	-	I	Up-regulated in 0.1% Wy-14,643 treatment and PPAR α dependent
	AB20	555	-	+	-	-	-	I	Up-regulated in 0.1% Wy-14,643 treatment and PPAR α dependent
	AB21	545	-	+	-	-	-	I	Up-regulated in 0.1% Wy-14,643 treatment and PPAR α dependent
	AB22*	530	+	++	+	+	+	II	Up-regulated in 0.1% Wy-14,643 treatment and PPAR α dependent
	AB23*	500	-	+	-	-	-	I	Up-regulated in 0.1% Wy-14,643 treatment and PPAR α dependent
	AB24*	420	-	+	-	-	-	I	Up-regulated in 0.1% Wy-14,643 treatment and PPAR α dependent
	AB25*	405	-	+	-	-	-	I	Up-regulated in 0.1% Wy-14,643 treatment and PPAR α dependent
	AB26*	390	-	+	-	-	-	I	Up-regulated in 0.1% Wy-14,643 treatment and PPAR α dependent
	AB27*	355	-	+	-	-	-	I	Up-regulated in 0.1% Wy-14,643 treatment and PPAR α dependent
	AB28*	340	-	+	-	-	-	I	Up-regulated in 0.1% Wy-14,643 treatment and PPAR α dependent
	AB29*	335	-	+	-	-	-	I	Up-regulated in 0.1% Wy-14,643 treatment and PPAR α dependent
	AB30*	315	-	+	-	-	-	I	Up-regulated in 0.1% Wy-14,643 treatment and PPAR α dependent
	AB31	310	-	+	-	-	-	I	Up-regulated in 0.1% Wy-14,643 treatment and PPAR α dependent
	AB32	305	-	+	-	-	-	I	Up-regulated in 0.1% Wy-14,643 treatment and PPAR α dependent
	AB33	300	-	+	-	-	-	I	Up-regulated in 0.1% Wy-14,643 treatment and PPAR α dependent
	AB34	295	-	+	-	-	-	I	Up-regulated in 0.1% Wy-14,643 treatment and PPAR α dependent

*+ represents the presence of a band (cDNA) on fluoroDD gel, while '-' represents the corresponding band (cDNA) that was not observed on the fluoroDD gel. The relative intensity of the gene expression among the four treatment groups is indicated by the number of '+'. *Fragments selected for reamplification. [§]Differential expression patterns as shown in Table 4.1.

Table 3.7.4. Summary of cDNA fragments excised from gel AC (AP2 and ARP19)

Gel	FluoroDD fragment I.D.	FluoroDD fragment size (bp)	Differential display pattern					
			PPAR α (+/+)		PPAR α (-/-)		FluoroDD pattern ^s	PPAR α -dependent genes that were either up- or down-regulated in PPAR α (+/+) mice treated with 0.1% Wy-14,643 compared to their corresponding controls
			CTL	Wy	CTL	Wy		
AC (AP2 & ARP19)	AC1*	1800	+	-	+	+	III	Down-regulated in 0.1% Wy-14,643 treatment and PPAR α dependent
	AC2*	1600	-	+	-	-	I	Up-regulated in 0.1% Wy-14,643 treatment and PPAR α dependent
	AC3*	1500	++	+	++	++	IV	Down-regulated in 0.1% Wy-14,643 treatment and PPAR α dependent
	AC4*	1100	++	+	++	++	IV	Down-regulated in 0.1% Wy-14,643 treatment and PPAR α dependent
	AC5	790	+	-	+	+	III	Down-regulated in 0.1% Wy-14,643 treatment and PPAR α dependent
	AC6	780	+	-	+	+	III	Down-regulated in 0.1% Wy-14,643 treatment and PPAR α dependent
	AC7*	770	+	-	+	+	III	Down-regulated in 0.1% Wy-14,643 treatment and PPAR α dependent
	AC8	760	+	++	+	+	II	Up-regulated in 0.1% Wy-14,643 treatment and PPAR α dependent
	AC9	705	++	+	++	++	IV	Down-regulated in 0.1% Wy-14,643 treatment and PPAR α dependent
	AC10	698	++	+	++	++	IV	Down-regulated in 0.1% Wy-14,643 treatment and PPAR α dependent
	AC11	650	++	+	++	++	IV	Down-regulated in 0.1% Wy-14,643 treatment and PPAR α dependent

'+' represents the presence of a band (cDNA) on fluoroDD gel, while '-' represents the corresponding band (cDNA) that was not observed on the fluoroDD gel. The relative intensity of the gene expression among the four treatment groups is indicated by the number of '+'. *Fragments selected for reamplification. §Differential expression patterns as shown in Table 4.1.

Table 3.7.5. Summary of cDNA fragments excised from gel AD (AP2 and ARP18)

Gel	FluoroDD fragment I.D.	FluoroDD fragment size (bp)	Differential display pattern						PPAR α -dependent genes that were either up- or down-regulated in PPAR α (+/+) mice treated with 0.1% Wy-14,643 compared to their corresponding controls
			PPAR α (+/+)		PPAR α (-/-)		FluoroDD pattern [§]		
			CTL	Wy	CTL	Wy			
AD (AP2 & ARP18)	AD1	1700	-	+	-	-	I	Up-regulated in 0.1% Wy-14,643 treatment and PPAR α dependent	
	AD2	1200	-	+	-	-	I	Up-regulated in 0.1% Wy-14,643 treatment and PPAR α dependent	
	AD3	1150	-	+	-	-	I	Up-regulated in 0.1% Wy-14,643 treatment and PPAR α dependent	
	AD4	980	-	+	-	-	I	Up-regulated in 0.1% Wy-14,643 treatment and PPAR α dependent	
	AD5	905	+	++	+	+	II	Up-regulated in 0.1% Wy-14,643 treatment and PPAR α dependent	
	AD6*	840	+	++	+	+	II	Up-regulated in 0.1% Wy-14,643 treatment and PPAR α dependent	
	AD7*	835	+	++	+	+	II	Up-regulated in 0.1% Wy-14,643 treatment and PPAR α dependent	
	AD8*	720	+	++	+	+	II	Up-regulated in 0.1% Wy-14,643 treatment and PPAR α dependent	
	AD9*	710	+	++	+	+	II	Up-regulated in 0.1% Wy-14,643 treatment and PPAR α dependent	

‘+’ represents the presence of a band (cDNA) on fluoroDD gel, while ‘-’ represents the corresponding band (cDNA) that was not observed on the fluoroDD gel. The relative intensity of the gene expression among the four treatment groups is indicated by the number of ‘+’. *Fragments selected for reamplification. [§]Differential expression patterns as shown in Table 4.1.

Table 3.7.6. Summary of cDNA fragments excised from gel AF (AP10 and ARP13) Part I

Gel	FluoroDD fragment I.D.	FluoroDD fragment size (bp)	Differential display pattern					PPAR α -dependent genes that were either up- or down-regulated in PPAR α (+/+) mice treated with 0.1% Wy-14,643 compared to their corresponding controls
			PPAR α (+/+)		PPAR α (-/-)		FluoroDD pattern ^s	
			CTL	Wy	CTL	Wy		
AF (AP10 & ARP13)	AF1*	945	+	++	+	+	II	Up-regulated in 0.1% Wy-14,643 treatment and PPAR α dependent
	AF2	860	-	+	-	-	I	Up-regulated in 0.1% Wy-14,643 treatment and PPAR α dependent
	AF3*	810	+	++	+	+	II	Up-regulated in 0.1% Wy-14,643 treatment and PPAR α dependent
	AF4	790	+	++	+	+	II	Up-regulated in 0.1% Wy-14,643 treatment and PPAR α dependent
	AF5*	760	+	++	+	+	II	Up-regulated in 0.1% Wy-14,643 treatment and PPAR α dependent
	AF6	745	+	++	+	+	II	Up-regulated in 0.1% Wy-14,643 treatment and PPAR α dependent
	AF7*	720	+	++	+	+	II	Up-regulated in 0.1% Wy-14,643 treatment and PPAR α dependent
	AF8	700	-	+	-	-	I	Up-regulated in 0.1% Wy-14,643 treatment and PPAR α dependent
	AF9	660	+	++	+	+	II	Up-regulated in 0.1% Wy-14,643 treatment and PPAR α dependent
	AF10	630	-	+	-	-	I	Up-regulated in 0.1% Wy-14,643 treatment and PPAR α dependent
	AF11	560	-	+	-	-	I	Up-regulated in 0.1% Wy-14,643 treatment and PPAR α dependent
	AF12	505	+	++	+	+	II	Up-regulated in 0.1% Wy-14,643 treatment and PPAR α dependent
	AF13	500	+	++	+	+	II	Up-regulated in 0.1% Wy-14,643 treatment and PPAR α dependent
	AF14	460	-	+	-	-	I	Up-regulated in 0.1% Wy-14,643 treatment and PPAR α dependent
	AF15*	445	+	++	+	+	II	Up-regulated in 0.1% Wy-14,643 treatment and PPAR α dependent
	AF16	410	-	+	-	-	I	Up-regulated in 0.1% Wy-14,643 treatment and PPAR α dependent
	AF17	380	-	+	-	-	I	Up-regulated in 0.1% Wy-14,643 treatment and PPAR α dependent

'+' represents the presence of a band (cDNA) on fluoroDD gel, while '-' represents the corresponding band (cDNA) that was not observed on the fluoroDD gel. The relative intensity of the gene expression among the four treatment groups is indicated by the number of '+'. *Fragments selected for reamplification. [§]Differential expression patterns as shown in Table 4.1.

Table 3.7.7. Summary of cDNA fragments excised from gel AF (AP10 and ARP13) Part II

Gel	FluoroDD fragment I.D.	FluoroDD fragment size (bp)	Differential display pattern					
			PPAR α (+/+)		PPAR α (-/-)		FluoroDD pattern [§]	PPAR α -dependent genes that were either up- or down-regulated in PPAR α (+/+) mice treated with 0.1% Wy-14,643 compared to their corresponding controls
			CTL	Wy	CTL	Wy		
AF (AP10 & ARP13)	AF18	375	-	+	-	-	I	Up-regulated in 0.1% Wy-14,643 treatment and PPAR α dependent
	AF19*	370	+	++	+	+	II	Up-regulated in 0.1% Wy-14,643 treatment and PPAR α dependent
	AF20*	345	+	++	+	+	II	Up-regulated in 0.1% Wy-14,643 treatment and PPAR α dependent
	AF21*	340	+	++	+	+	II	Up-regulated in 0.1% Wy-14,643 treatment and PPAR α dependent
	AF22	325	-	+	-	-	I	Up-regulated in 0.1% Wy-14,643 treatment and PPAR α dependent
	AF23	320	-	+	-	-	I	Up-regulated in 0.1% Wy-14,643 treatment and PPAR α dependent
	AF24	280	+	-	+	+	III	Down-regulated in 0.1% Wy-14,643 treatment and PPAR α dependent
	AF25*	275	++	+	++	++	IV	Down-regulated in 0.1% Wy-14,643 treatment and PPAR α dependent
	AF26	270	+	-	+	+	III	Down-regulated in 0.1% Wy-14,643 treatment and PPAR α dependent
	AF27	265	+	-	+	+	III	Down-regulated in 0.1% Wy-14,643 treatment and PPAR α dependent
	AF28	260	-	+	-	-	I	Up-regulated in 0.1% Wy-14,643 treatment and PPAR α dependent
	AF29	245	+	++	+	+	II	Up-regulated in 0.1% Wy-14,643 treatment and PPAR α dependent
	AF30*	240	+	++	+	+	II	Up-regulated in 0.1% Wy-14,643 treatment and PPAR α dependent
	AF31	238	+	++	+	+	II	Up-regulated in 0.1% Wy-14,643 treatment and PPAR α dependent
	AF32	235	+	++	+	+	II	Up-regulated in 0.1% Wy-14,643 treatment and PPAR α dependent
	AF33	230	+	++	+	+	II	Up-regulated in 0.1% Wy-14,643 treatment and PPAR α dependent

'+' represents the presence of a band (cDNA) on fluoroDD gel, while '-' represents the corresponding band (cDNA) that was not observed on the fluoroDD gel. The relative intensity of the gene expression among the four treatment groups is indicated by the number of '+'. *Fragments selected for reamplification. [§]Differential expression patterns as shown in Table 4.1.

Table 3.7.8. Summary of cDNA fragments excised from gel AH (AP11 and ARP19)

Gel	FluoroDD fragment I.D.	FluoroDD fragment size (bp)	Differential display pattern					
			PPAR α (+/+)		PPAR α (-/-)		FluoroDD pattern [§]	PPAR α -dependent genes that were either up- or down-regulated in PPAR α (+/+) mice treated with 0.1% Wy-14,643 compared to their corresponding controls
			CTL	Wy	CTL	Wy		
AH (AP11 & ARP19)	AH1*	720	+	-	+	+	III	Down-regulated in 0.1% Wy-14,643 treatment and PPAR α dependent
	AH2*	700	+	-	+	+	III	Down-regulated in 0.1% Wy-14,643 treatment and PPAR α dependent
	AH3	695	+	-	+	+	III	Down-regulated in 0.1% Wy-14,643 treatment and PPAR α dependent
	AH4	455	-	+	-	-	I	Up-regulated in 0.1% Wy-14,643 treatment and PPAR α dependent
	AH5*	450	+	++	+	+	II	Up-regulated in 0.1% Wy-14,643 treatment and PPAR α dependent
	AH6	370	+	-	+	+	III	Down-regulated in 0.1% Wy-14,643 treatment and PPAR α dependent
	AH7	360	+	-	+	+	III	Down-regulated in 0.1% Wy-14,643 treatment and PPAR α dependent
	AH8	350	+	-	+	+	III	Down-regulated in 0.1% Wy-14,643 treatment and PPAR α dependent
	AH9	300	+	-	+	+	III	Down-regulated in 0.1% Wy-14,643 treatment and PPAR α dependent

'+' represents the presence of a band (cDNA) on fluoroDD gel, while '-' represents the corresponding band (cDNA) that was not observed on the fluoroDD gel. The relative intensity of the gene expression among the four treatment groups is indicated by the number of '+'. *Fragments selected for reamplification. [§]Differential expression patterns as shown in Table 4.1.

Table 3.7.9. Summary of cDNA fragments excised from gel AI (AP6 and ARP4)

Gel	FluoroDD fragment I.D.	FluoroDD fragment size (bp)	Differential display pattern						PPAR α -dependent genes that were either up- or down-regulated in PPAR α (+/+) mice treated with 0.1% Wy-14,643 compared to their corresponding controls
			PPAR α (+/+)		PPAR α (-/-)		FluoroDD pattern ^s		
			CTL	Wy	CTL	Wy			
AI (AP6 & ARP4)	AI1*	1100	+	-	+	+	III	Down-regulated in 0.1% Wy-14,643 treatment and PPAR α dependent	
	AI2*	910	+	++	+	+	II	Up-regulated in 0.1% Wy-14,643 treatment and PPAR α dependent	
	AI3	640	+	++	+	+	II	Up-regulated in 0.1% Wy-14,643 treatment and PPAR α dependent	
	AI4*	540	++	+	++	++	IV	Down-regulated in 0.1% Wy-14,643 treatment and PPAR α dependent	
	AI5	520	+	++	+	+	II	Up-regulated in 0.1% Wy-14,643 treatment and PPAR α dependent	
	AI6	515	+	++	+	+	II	Up-regulated in 0.1% Wy-14,643 treatment and PPAR α dependent	
	AI7	505	++	+	++	++	IV	Down-regulated in 0.1% Wy-14,643 treatment and PPAR α dependent	
	AI8	470	+	++	+	+	II	Up-regulated in 0.1% Wy-14,643 treatment and PPAR α dependent	
	AI9	410	+	++	+	+	II	Up-regulated in 0.1% Wy-14,643 treatment and PPAR α dependent	
	AI10	405	+	++	+	+	II	Up-regulated in 0.1% Wy-14,643 treatment and PPAR α dependent	
	AI11	400	+	++	+	+	II	Up-regulated in 0.1% Wy-14,643 treatment and PPAR α dependent	
	AI12	375	+	++	+	+	II	Up-regulated in 0.1% Wy-14,643 treatment and PPAR α dependent	
	AI13	370	+	++	+	+	II	Up-regulated in 0.1% Wy-14,643 treatment and PPAR α dependent	
	AI14	350	+	++	+	+	II	Up-regulated in 0.1% Wy-14,643 treatment and PPAR α dependent	
	AI18*	270	++	+	++	++	IV	Down-regulated in 0.1% Wy-14,643 treatment and PPAR α dependent	
	AI19	260	+	-	+	+	III	Down-regulated in 0.1% Wy-14,643 treatment and PPAR α dependent	
	AI20	255	+	-	+	+	III	Down-regulated in 0.1% Wy-14,643 treatment and PPAR α dependent	
	AI21	250	+	-	+	+	III	Down-regulated in 0.1% Wy-14,643 treatment and PPAR α dependent	

'+' represents the presence of a band (cDNA) on fluoroDD gel, while '-' represents the corresponding band (cDNA) that was not observed on the fluoroDD gel. The relative intensity of the gene expression among the four treatment groups is indicated by the number of '+'. *Fragments selected for reamplification. ^sDifferential expression patterns as shown in Table 4.1.

Table 3.7.10. Summary of cDNA fragments excised from gels AJ (AP6 and ARP14) and AL (AP7 and ARP15)

Gel	FluoroDD fragment I.D.	FluoroDD fragment size (bp)	Differential display pattern						PPAR α -dependent genes that were either up- or down-regulated in PPAR α (+/+) mice treated with 0.1% Wy-14,643 compared to their corresponding controls
			PPAR α (+/+)		PPAR α (-/-)		FluoroDD pattern ^s		
			CTL	Wy	CTL	Wy			
AJ (AP6 & ARP14)	AJ1*	1200	++	+	++	++	IV	Down-regulated in 0.1% Wy-14,643 treatment and PPAR α dependent	
	AJ2*	1100	+	++	+	+	II	Up-regulated in 0.1% Wy-14,643 treatment and PPAR α dependent	
	AJ3*	680	+	++	+	+	II	Up-regulated in 0.1% Wy-14,643 treatment and PPAR α dependent	
	AJ4	675	+	++	+	+	II	Up-regulated in 0.1% Wy-14,643 treatment and PPAR α dependent	
	AJ5	640	+	++	+	+	II	Up-regulated in 0.1% Wy-14,643 treatment and PPAR α dependent	
	AJ6*	570	++	+	++	++	IV	Down-regulated in 0.1% Wy-14,643 treatment and PPAR α dependent	
AL (AP7 & ARP15)	AJ9*	320	+	-	+	+	III	Down-regulated in 0.1% Wy-14,643 treatment and PPAR α dependent	
	AJ10	290	+	-	+	+	III	Down-regulated in 0.1% Wy-14,643 treatment and PPAR α dependent	
	AL1*	355	+	++	+	+	II	Up-regulated in 0.1% Wy-14,643 treatment and PPAR α dependent	
	AL2*	350	+	++	+	+	II	Up-regulated in 0.1% Wy-14,643 treatment and PPAR α dependent	
	AL3*	345	+	++	+	+	II	Up-regulated in 0.1% Wy-14,643 treatment and PPAR α dependent	

'+' represents the presence of a band (cDNA) on fluoroDD gel, while '-' represents the corresponding band (cDNA) that was not observed on the fluoroDD gel. The relative intensity of the gene expression among the four treatment groups is indicated by the number of '+'. *Fragments selected for reamplification. [§]Differential expression patterns as shown in Table 4.1.

Table 3.7.11. Summary of cDNA fragments excised from gels AO (AP5 and ARP10) and AP (AP12 and ARP2)

Gel	FluoroDD fragment I.D.	FluoroDD fragment size (bp)	Differential display pattern				PPAR α -dependent genes that were either up- or down-regulated in PPAR α (++) mice treated with 0.1% Wy-14,643 compared to their corresponding controls	
			PPAR α (++)		PPAR α (-/-)			FluoroDD pattern ^s
			CTL	Wy	CTL	Wy		
AO (AP5 & ARP10)	AO1*	700	+	++	+	+	II	Up-regulated in 0.1% Wy-14,643 treatment and PPAR α dependent
	AO2*	695	+	++	+	+	II	Up-regulated in 0.1% Wy-14,643 treatment and PPAR α dependent
	AO3	620	+	++	+	+	II	Up-regulated in 0.1% Wy-14,643 treatment and PPAR α dependent
	AO4	610	-	+	-	-	I	Up-regulated in 0.1% Wy-14,643 treatment and PPAR α dependent
	AO5	600	+	++	+	+	II	Up-regulated in 0.1% Wy-14,643 treatment and PPAR α dependent
	AO6	470	+	-	+	+	III	Down-regulated in 0.1% Wy-14,643 treatment and PPAR α dependent
	AO7	450	+	++	+	+	II	Up-regulated in 0.1% Wy-14,643 treatment and PPAR α dependent
AP (AP12 & ARP2)	AO8*	400	+	-	+	+	III	Down-regulated in 0.1% Wy-14,643 treatment and PPAR α dependent
	AO9	395	+	-	+	+	III	Down-regulated in 0.1% Wy-14,643 treatment and PPAR α dependent
	AO10*	310	+	++	+	+	II	Up-regulated in 0.1% Wy-14,643 treatment and PPAR α dependent
	AP1	975	+	++	+	+	II	Up-regulated in 0.1% Wy-14,643 treatment and PPAR α dependent
	AP2	800	+	++	+	+	II	Up-regulated in 0.1% Wy-14,643 treatment and PPAR α dependent
	AP3	695	++	+	++	++	IV	Down-regulated in 0.1% Wy-14,643 treatment and PPAR α dependent
	AP4*	680	+	++	+	+	II	Up-regulated in 0.1% Wy-14,643 treatment and PPAR α dependent
	AP5	485	++	+	++	++	IV	Down-regulated in 0.1% Wy-14,643 treatment and PPAR α dependent
	AP6	280	+	-	+	+	III	Down-regulated in 0.1% Wy-14,643 treatment and PPAR α dependent

*+ represents the presence of a band (cDNA) on fluoroDD gel, while '-' represents the corresponding band (cDNA) that was not observed on the fluoroDD gel. The relative intensity of the gene expression among the four treatment groups is indicated by the number of '+'. *Fragments selected for reamplification. [§]Differential expression patterns as shown in Table 4.1.

GTAATACGACTCACTATAGGGC-3') primers. As partial sequences of M13 reverse (16-mer) and T7 promoter (17-mer) were present in the 5'-ARP and 3'-AP primers of double-strand cDNA synthesis, respectively, the reamplified PCR products were lengthened by 8 nucleotides from the M13 reverse primer and 5 nucleotides from the T7 promoter primer. The expected size of reamplified PCR product was 13 nucleotides longer than the size of fluoroDD fragments. A total of sixty-four (41%) cDNA fragments were chosen for reamplification [AA1, AA2, AA3, AA4, AA5, AA6, AA7, AA8, AA9, AA10 and AA12 (Figure 3.8.1) (Table 3.8.1); AB7, AB10, AB17, AB18, AB19, AB22, AB23, AB24, AB25, AB26, AB27, AB28, AB29 and AB30 (Figures 3.8.2-3.8.3) (Table 3.8.2); AC1, AC2, AC3, AC4, AC7, AD6, AD7, AD8, AD9, AF1, AF3, AF5, AF7, AF15, AF19, AF20, AF21, AF25 and AF30 (Figures 3.8.4-3.8.5) (Table 3.8.3); AH1, AH2, AH5, AI1, AI2, AI4, AI18, AJ1, AJ2, AJ3, AJ6, AJ9, AL1, AL2, AL3, AO1, AO2, AO8, AO10 and AP4 (Figures 3.8.6-3.8.7) (Tables 3.8.4-3.8.5)]. The sizes of fragments AB19 and AB26 (Table 3.8.2); AD6 and AF30 (Table 3.8.3); AH2 (Table 3.8.4); and AL3 (Table 3.8.5) were bigger than the expected sizes, while the fragment sizes of AA2 (Table 3.8.1); AB10 (Table 3.8.2); AC7 (Table 3.8.3); and AO1 (Table 3.8.5) were smaller than the expected sizes. These might be due to the contamination during band excision. cDNA fragments AA1 and AA5 (Table 3.8.1); AB23 (Table 3.8.2); AC2 and AF7 (Table 3.8.3); and AJ6 (Table 3.8.4) contained extra PCR products, which might be due to contamination of co-migration and/or nearby cDNA fragments during bands excision. All the reamplified fragments with expected sizes were selected for subcloning.

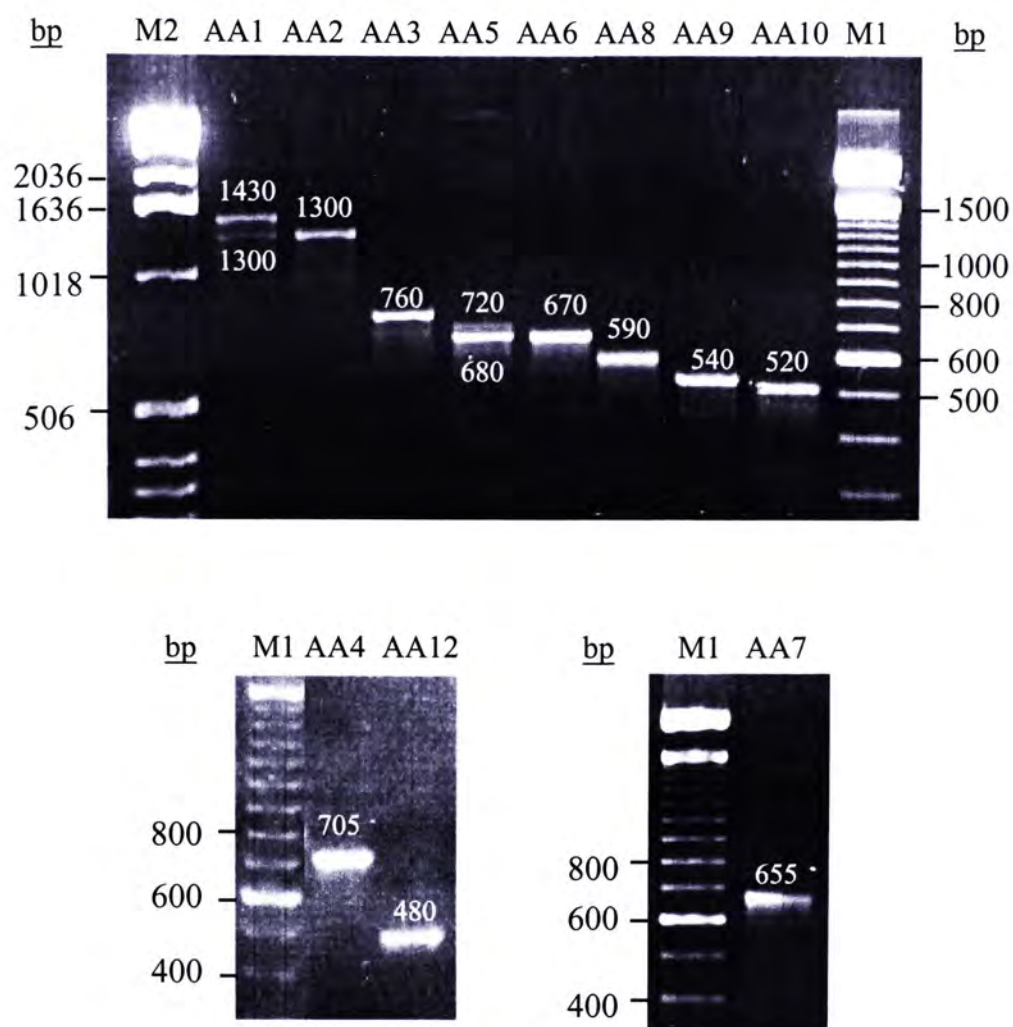


Figure 3.8.1. Reamplification of cDNA fragments excised from fluoroDD gel AA (AP1 and ARP2). The cDNA fragments excised from the gel were amplified by PCR using full-length M13 reverse (-48) 24-mer (5'-AGCGGATAACAATTTTCACACAGGA-3') and T7 promoter 22-mer (5'-GTAATACGACTCACTATAGGGC-3') primers. The PCR products were resolved on 1% agarose, 0.5X TBE gels with ethidium bromide staining. M1, 100 bp DNA marker; M2, 1 kb DNA marker.

Table 3.8.1. Summary of reamplified cDNA fragments excised from gel AA (AP1 and ARP2)

Gel	FluoroDD fragment I.D.	FluoroDD fragment size (bp)	Differential display pattern						Reamplified fragment size (bp)
			PPARα (+/+)		PPARα (-/-)				
			CTL	Wy	CTL	Wy	CTL	Wy	
AA (AP1 & ARP2)	AA1	1400	-	+	-	-	-	1430+1300	
	AA2	1300	+	++	+	+	+	1300	
	AA3	750	+	++	+	+	+	760	
	AA4	695	++	+	++	++	++	705	
	AA5	670	+	++	+	+	+	720+680	
	AA6	660	+	++	+	+	+	670	
	AA7	640	+	++	+	+	+	655	
	AA8	570	+	++	+	+	+	590	
	AA9	520	+	++	+	+	+	540	
	AA10	500	+	++	+	+	+	520	
	AA12	470	+	++	+	+	+	480	

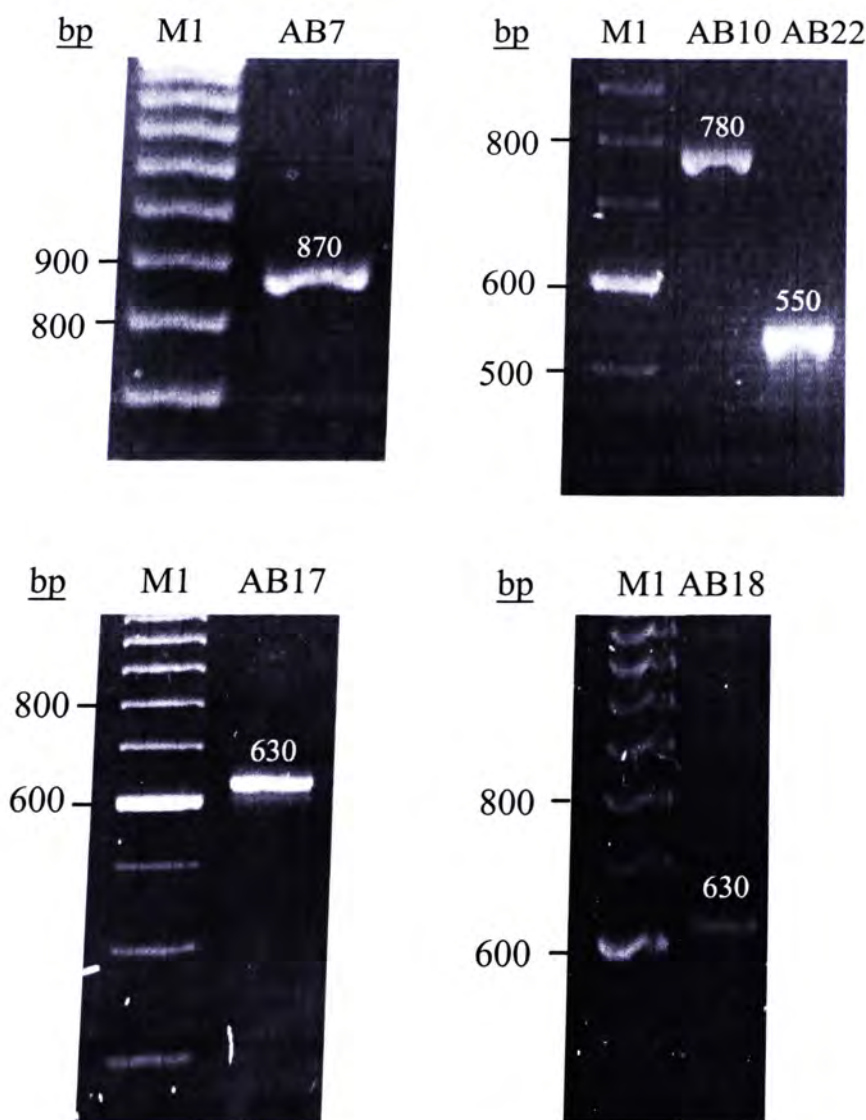


Figure 3.8.2. Reamplification of cDNA fragments excised from fluoroDD gel AB (AP3 and ARP3) Part I. The cDNA fragments excised from the gel were amplified by PCR using full-length M13 reverse (-48) 24-mer (5'-AGCGGATAACAATTTTCACACAGGA-3') and T7 promoter 22-mer (5'-GTAATACGACTCACTATAGGGC-3') primers. The PCR products were resolved on 1% agarose, 0.5X TBE gels with ethidium bromide staining. M1, 100 bp DNA marker.

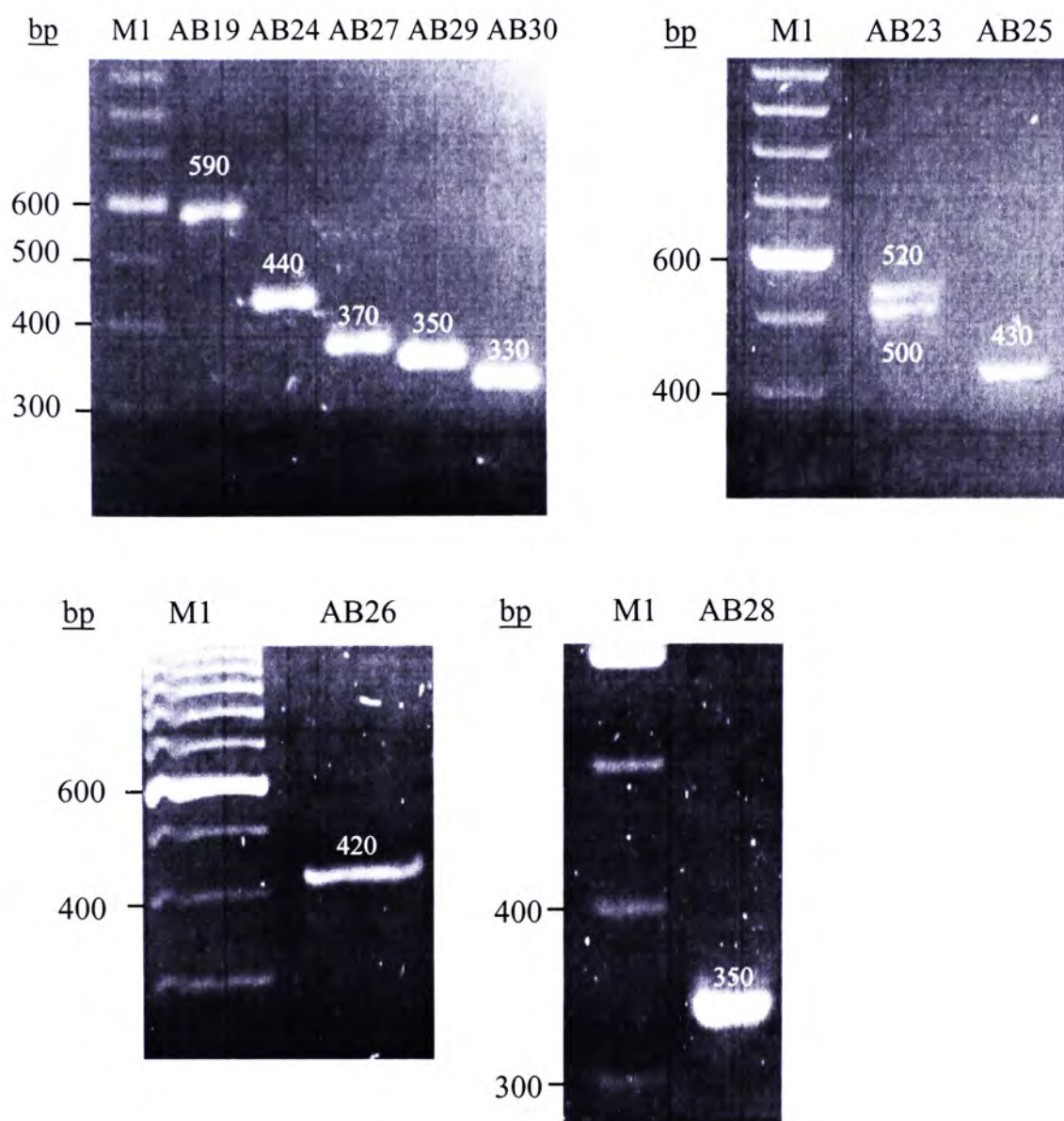


Figure 3.8.3. Reamplification of cDNA fragments excised from fluoroDD gel AB (AP3 and ARP3) Part II. The cDNA fragments excised from the gel were amplified by PCR using full-length M13 reverse (-48) 24-mer (5'-AGCGGATAACAATTTACACAGGA-3') and T7 promoter 22-mer (5'-GTAATACGACTCACTATAGGGC-3') primers. The PCR products were resolved on 1% agarose, 0.5X TBE gels with ethidium bromide staining. M1, 100 bp DNA marker.

Table 3.8.2. Summary of reamplified cDNA fragments excised from gel AB (AP3 and ARP3)

Gel	FluoroDD fragment I.D.	FluoroDD fragment size (bp)	Differential display pattern				Reamplified fragment size (bp)
			PPARα (+/+)		PPARα (-/-)		
			CTL	Wy	CTL	Wy	
AB (AP3 & ARP3)	AB7	850	+	++	+	+	870
	AB10	770	+	++	+	+	780
	AB17	620	+	++	+	+	630
	AB18	595	+	++	+	+	630
	AB19	575	-	+	-	-	590
	AB22	530	+	++	+	+	550
	AB23	500	-	+	-	-	500+520
	AB24	420	-	+	-	-	440
	AB25	405	-	+	-	-	430
	AB26	390	-	+	-	-	420
	AB27	355	-	+	-	-	370
	AB28	340	-	+	-	-	350
	AB29	335	-	+	-	-	350
	AB30	315	-	+	-	-	330

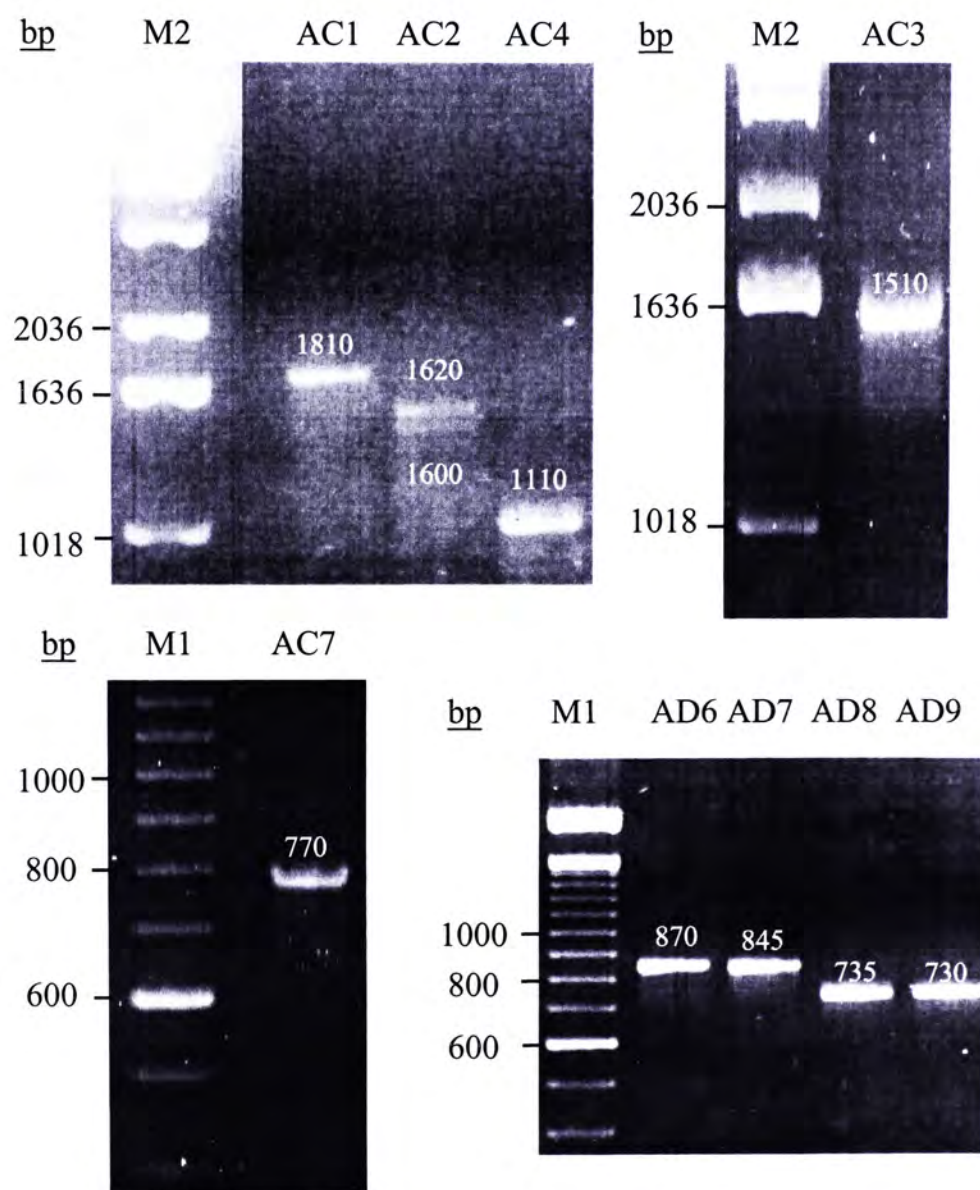


Figure 3.8.4. Reamplification of cDNA fragments excised from fluoroDD gels AC (AP2 and ARP19) and AD (AP2 and ARP18). The cDNA fragments excised from the gel were amplified by PCR using full-length M13 reverse (-48) 24-mer (5'-AGCGGATAACAATTTACACAGGA-3') and T7 promoter 22-mer (5'-GTAATACGACTCACTATAGGGC-3') primers. The PCR products were resolved on 1% agarose, 0.5X TBE gels with ethidium bromide staining. M1, 100 bp DNA marker; M2, 1 kb DNA marker.

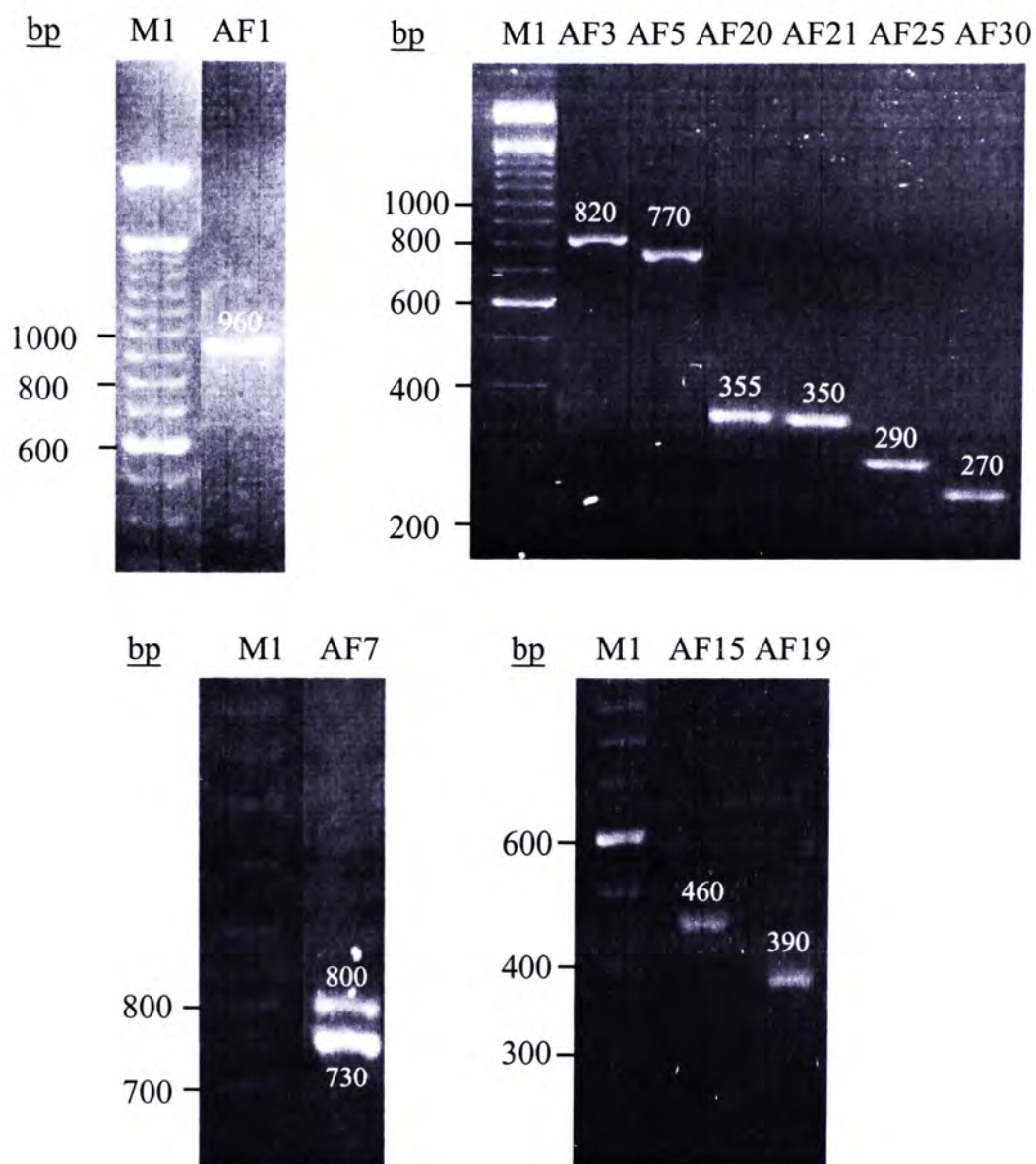


Figure 3.8.5. Reamplification of cDNA fragments excised from fluoroDD gel AF (AP10 and ARP13). The cDNA fragments excised from the gel were amplified by PCR using full-length M13 reverse (-48) 24-mer (5'-AGCGGATAACAATTTTCACACAGGA-3') and T7 promoter 22-mer (5'-GTAATACGACTCACTATAGGGC-3') primers. The PCR products were resolved on 1% agarose, 0.5X TBE gels with ethidium bromide staining. M1, 100 bp DNA marker.

Table 3.8.3. Summary of reamplified cDNA fragments excised from gels AC (AP2 and ARP19), AD (AP2 and ARP18) and AF (AP10 and ARP13)

Gel	FluoroDD fragment I.D.	FluoroDD fragment size (bp)	Differential display pattern				Reamplified fragment size (bp)
			PPAR α (+/+)		PPAR α (-/-)		
			CTL	Wy	CTL	Wy	
AC (AP2 & ARP19)	AC1	1800	+	-	+	+	1810
	AC2	1600	-	+	-	-	1620 + 1600
	AC3	1500	++	+	++	++	1510
	AC4	1100	++	+	++	++	1110
	AC7	770	+	-	+	+	770
AD (AP2 & ARP18)	AD6	840	+	++	+	+	870
	AD7	835	+	++	+	+	845
	AD8	720	+	++	+	+	735
	AD9	710	+	++	+	+	730
	AF1	945	+	++	+	+	960
AF (AP10 & ARP13)	AF3	810	+	++	+	+	820
	AF5	760	+	++	+	+	770
	AF7	720	+	++	+	+	730+800
	AF15	445	+	++	+	+	460
	AF19	370	+	++	+	+	390
	AF20	345	+	++	+	+	355
	AF21	340	+	++	+	+	350
	AF25	275	++	+	++	++	290
	AF30	240	+	++	+	+	270

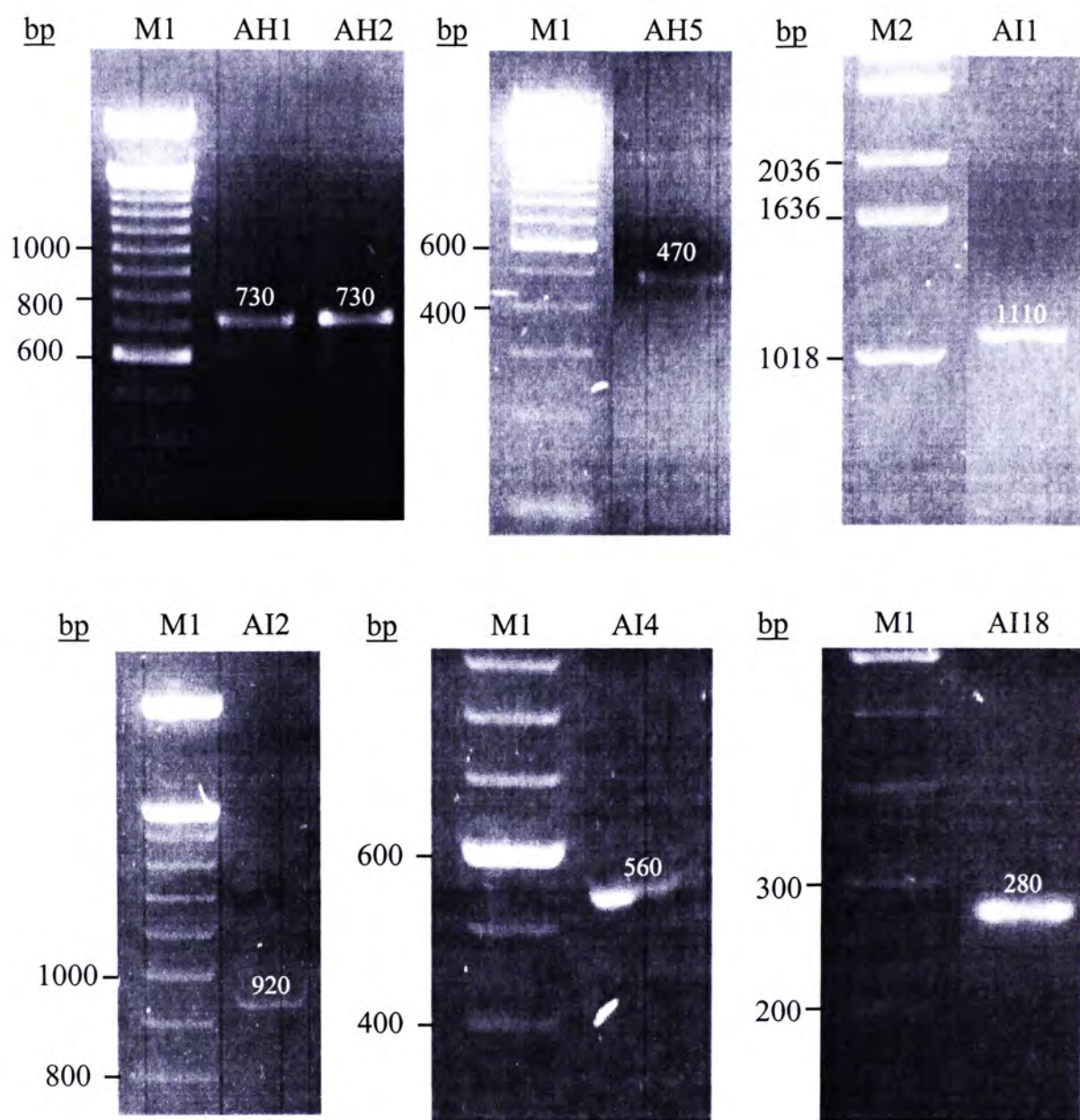


Figure 3.8.6. Reamplification of cDNA fragments excised from fluoroDD gels AH (AP11 and ARP19) and AI (AP6 and ARP4). The cDNA fragments excised from the gel were amplified by PCR using full-length M13 reverse (-48) 24-mer (5'-AGCGGATAACAATTTTCACACAGGA-3') and T7 promoter 22-mer (5'-GTAATACGACTCACTATAGGGC-3') primers. The PCR products were resolved on 1% agarose, 0.5X TBE gels with ethidium bromide staining. M1, 100 bp DNA marker; M2, 1 kb DNA marker.

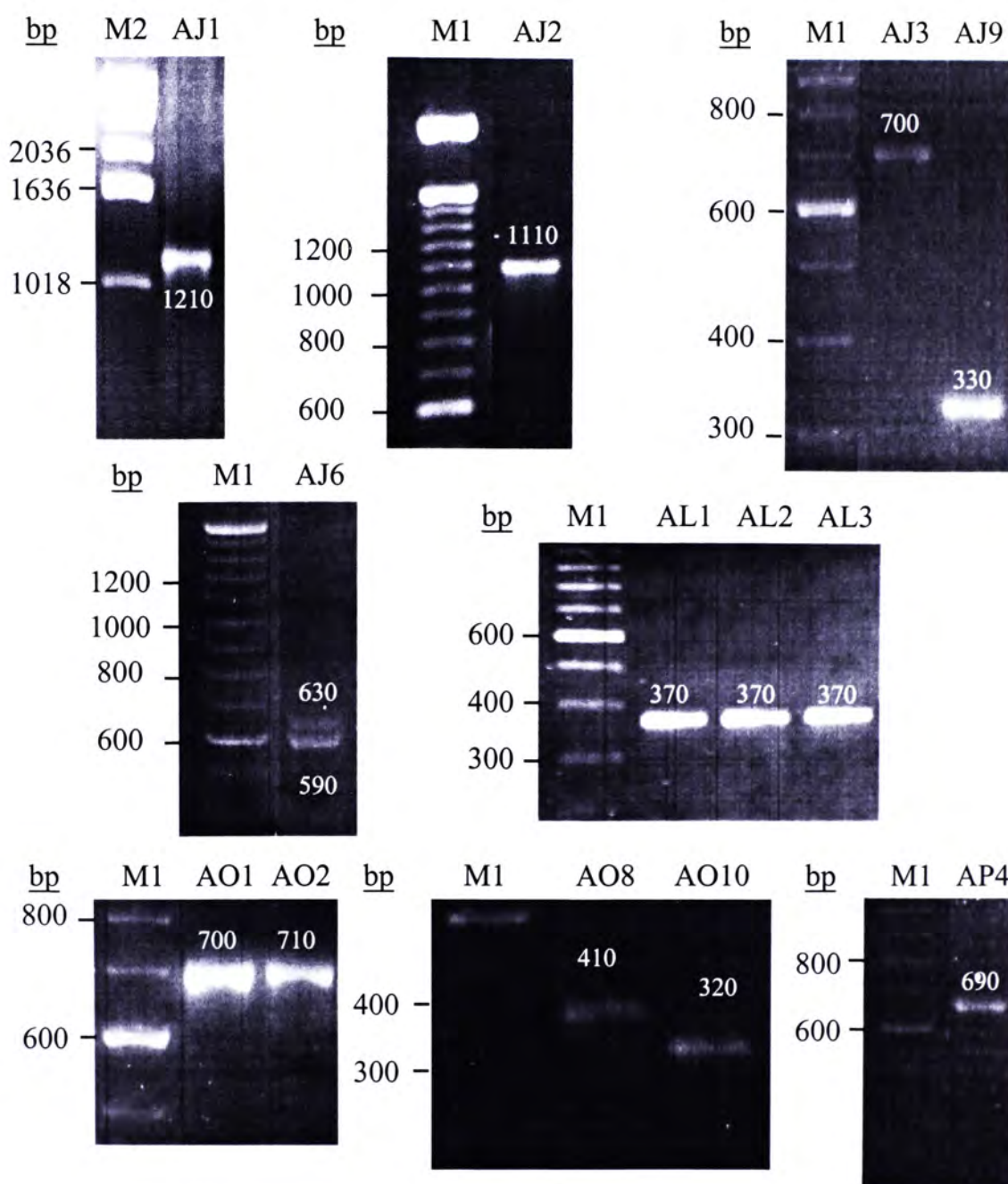


Figure 3.8.7. Reamplification of cDNA fragments excised from fluororDD gels AJ (AP6 and ARP14), AL (AP7 and ARP15), AO (AP5 and ARP10) and AP (AP12 and ARP2). The cDNA fragments excised from the gel were amplified by PCR using full-length M13 reverse (-48) 24-mer (5'-AGCGGATAACAATTTTCACACAGGA-3') and T7 promoter 22-mer (5'-GTAATACGACTCACTATAGGGC-3') primers. The PCR products were resolved on 1% agarose, 0.5X TBE gels with ethidium bromide staining. M1, 100 bp DNA marker; M2, 1 kb DNA marker.

Table 3.8.4. Summary of reamplified cDNA fragments excised from gels AH (AP11 and ARP19), AI (AP6 and ARP4) and AJ (AP6 and ARP14)

Gel	FluoroDD fragment I.D.	FluoroDD fragment size (bp)	Differential display pattern				Reamplified fragment size (bp)
			PPAR α (++)		PPAR α (-/-)		
			CTL	Wy	CTL	Wy	
AH (AP11 & ARP19)	AH1	720	+	-	+	+	730
	AH2	700	+	-	+	+	730
	AH5	450	+	++	+	+	470
	AI1	1100	+	-	+	+	1110
	AI2	910	+	++	+	+	920
AI4 & ARP4)	AI4	540	++	+	++	++	560
	AI18	270	++	+	++	++	280
	AJ1	1200	++	+	++	++	1210
	AJ2	1100	+	++	+	+	1110
AJ (AP6 & ARP14)	AJ3	680	+	++	+	+	700
	AJ6	570	++	+	++	++	590+630
	AJ9	320	+	-	+	+	330

2025-08-28 14:14:14

Table 3.8.5. Summary of reamplified cDNA fragments excised from gels AL (AP7 and ARP15), AO (AP5 and ARP10) and AP (AP12 and ARP2)

Gel	FluoroDD fragment I.D.	FluoroDD fragment size (bp)	Differential display pattern				Reamplified fragment size (bp)
			PPAR α (+/+)		PPAR α (-/-)		
			CTL	Wy	CTL	Wy	
AL (AP7 & ARP15)	AL1	355	+	++	+	+	370
	AL2	350	+	++	+	+	370
	AL3	345	+	++	+	+	370
	AO1	700	+	++	+	+	700
AP5 & ARP10)	AO2	695	+	++	+	+	710
	AO8	400	+	-	+	+	410
	AO10	310	+	++	+	+	320
AP (AP12 & ARP2)	AP4	680	+	++	+	+	690

3.9 Subcloning of reamplified fluoroDD fragments

A total of forty-two reamplified cDNA fragments were chosen for subcloning. For the cDNA fragments which subcloned into pT-Adv vector, the sizes of the inserts released by *EcoRI* digestion were 18 bp longer than the reamplified PCR products as extra 8 nucleotides were added before and after T/A cloning site and 10 nucleotides were added after *EcoRI* digestion. They included AA1, AA5, AA6, AA7, AA10 and AA12 (Figure 3.9.1) (Table 3.9.1); AB18 and AB26 (Figure 3.9.2) (Table 3.9.2); AC3 and AC7 (Figure 3.9.4) (Table 3.9.3); and AD8 and AD9 (Figure 3.9.5) (Table 3.9.3). For the cDNA fragments that subcloned into PCR[®] II-TOPO[®], including AA4 (Figure 3.9.1) (Table 3.9.1); AB7, AB17, AB19, AB22, AB24, AB27 and AB29 (Figures 3.9.2-3.9.3) (Table 3.9.2); AC1, AC2 and AC4 (Figure 3.9.4) (Table 3.9.3); AD6 (Figure 3.9.5) (Table 3.9.3); AF1, AF21, AF25 and AF30 (Figure 3.9.5) (Table 3.9.4); AH1, AH2, AI1 and AI18 (Figure 3.9.6) (Table 3.9.4); AJ1, AJ2 and AJ9 (Figure 3.9.7) (Table 3.9.4); AL2, AL3, AO1, AO2, AO8 and AP4 (Figure 3.9.8) (Table 3.9.5), the sizes of the inserts released by *EcoRI* digestion were 20 bp longer than the reamplified PCR products as extra 10 nucleotides were added before and after T/A cloning sites, and 10 nucleotides were added after *EcoRI* digestion.

Some of the subcloned cDNA fragments showed did not release the expected insert sizes after *EcoRI* digestion. cDNA fragments AA1 (Figure 3.9.1) (Table 3.9.1); AB17 and AB19 (Figure 3.9.2) (Table 3.9.2); AC1 and AC2 (Figure 3.9.4) (Table 3.9.3); AD6 (Figure 3.9.5) (Table 3.9.3) and AO2 (Figure 3.9.8) (Table 3.9.5) contained different subclones that showed different *EcoRI* restriction patterns while cDNA fragments AA1, AA6 and AA7 (Figure 3.9.1) (Table 3.9.1); AC2 (Figure 3.9.4) (Table 3.9.3); AD8 (Figure 3.9.5) (Table 3.9.3); and AO2 (Figure 3.9.8) (Table 3.9.5) showed larger insert sizes after *EcoRI* digestion. The different *EcoRI* restriction

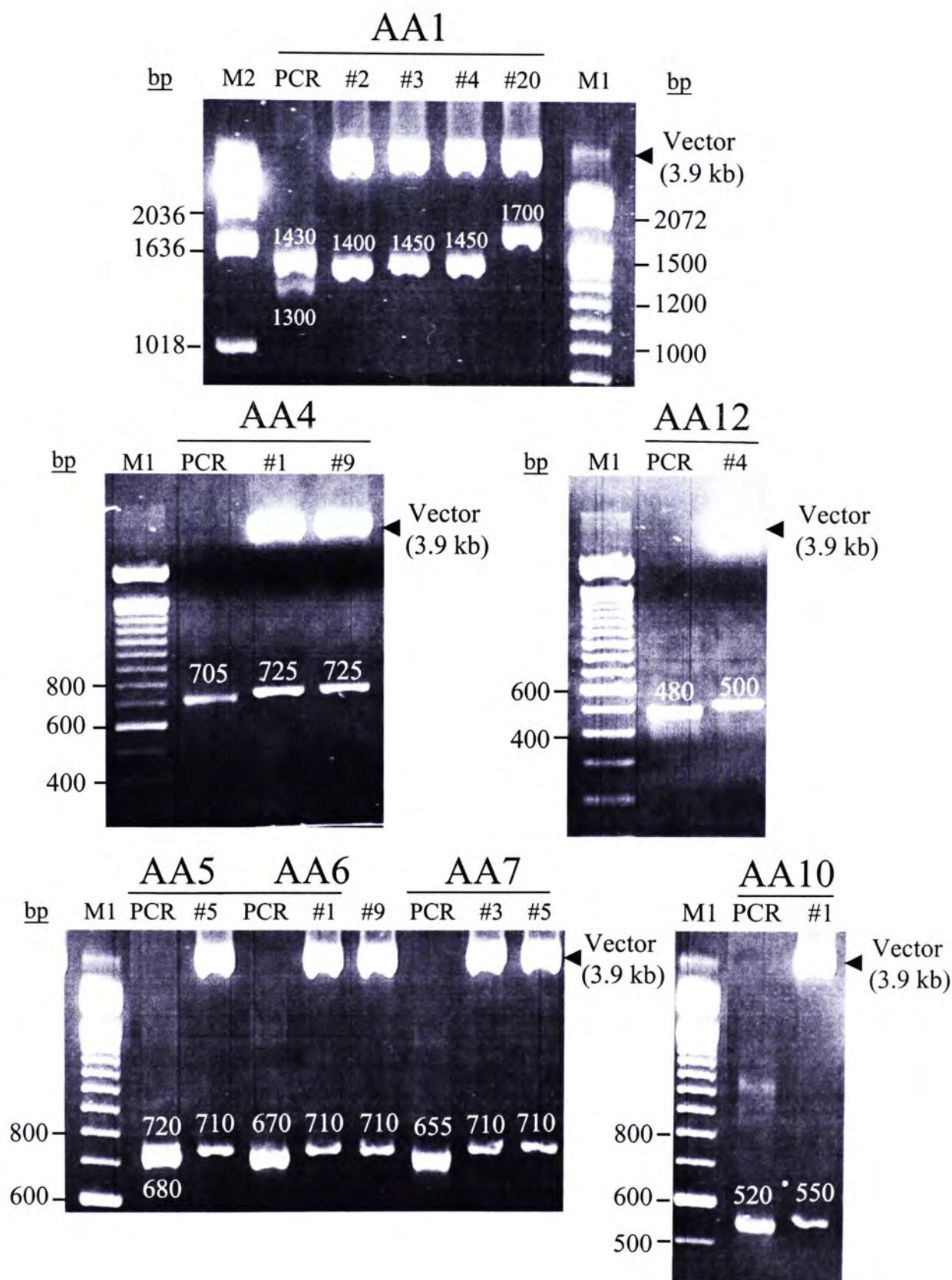


Figure 3.9.1. *EcoRI* digested cDNA fragments excised from gel AA (AP1 and ARP2). The *EcoRI* digested cDNA fragments were resolved on 1% agarose, 0.5X TBE gels with ethidium bromide staining. M1, 100 bp DNA marker; M2, 1 kb DNA marker. PCR, reamplified PCR product of the corresponding cDNA fragment.

Table 3.9.1. Summary of cDNA fragments subcloned from gel AA (AP1 and ARP2)

Gel	FluoroDD fragment I.D.	FluoroDD fragment size (bp)	Reamplified fragment size (bp)	Subclone I.D.	Size of vector (kb)	Size of insert after <i>EcoRI</i> cut (bp)
AA (AP1 & ARP2)	AA1	1400	1430 + 1300	AA1#2	3.9 (pT-Adv)	1400
				AA1#3	3.9 (pT-Adv)	1450
				AA1#4	3.9 (pT-Adv)	1450
				AA1#20	3.9 (pT-Adv)	1700
	AA4	695	705	AA4#1	4.0 (pCR [®] IL-TOPO [®])	725
	AA5	670	720+680	AA4#9	4.0 (pCR [®] IL-TOPO [®])	725
	AA6	660	670	AA5#5	3.9 (pT-Adv)	710
				AA6#1	3.9 (pT-Adv)	710
	AA7	640	655	AA6#9	3.9 (pT-Adv)	710
				AA7#3	3.9 (pT-Adv)	710
	AA10	500	520	AA7#5	3.9 (pT-Adv)	710
	AA12	470	480	AA10#1	3.9 (pT-Adv)	550
				AA12#4	3.9 (pT-Adv)	500

Phenol:chloroform extraction was performed for screening the subclones which contained inserts. Those subclones containing plasmid DNA larger than the vector only (3.9 or 4.0 kb) were selected for performing *EcoRI* cut to confirm correct insert sizes and further used for sequencing and Northern blot analysis.

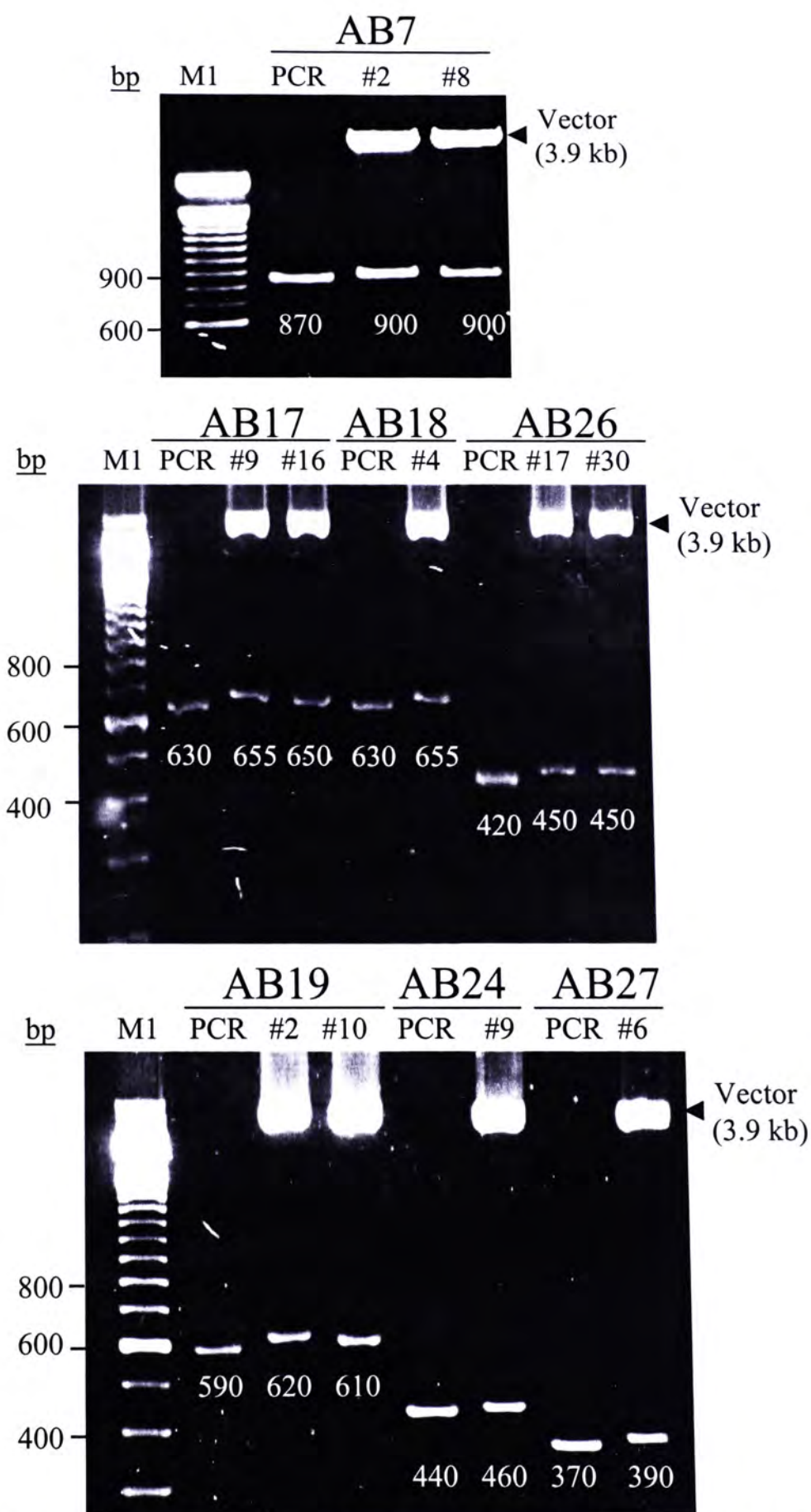


Figure 3.9.2. *Eco*RI digested cDNA fragments excised from gel AB (AP3 and ARP3) Part I. The *Eco*RI digested cDNA fragments were resolved on 1% agarose, 0.5X TBE gels with ethidium bromide staining. M1, 100 bp DNA marker. PCR, reamplified PCR product of the corresponding cDNA fragment.

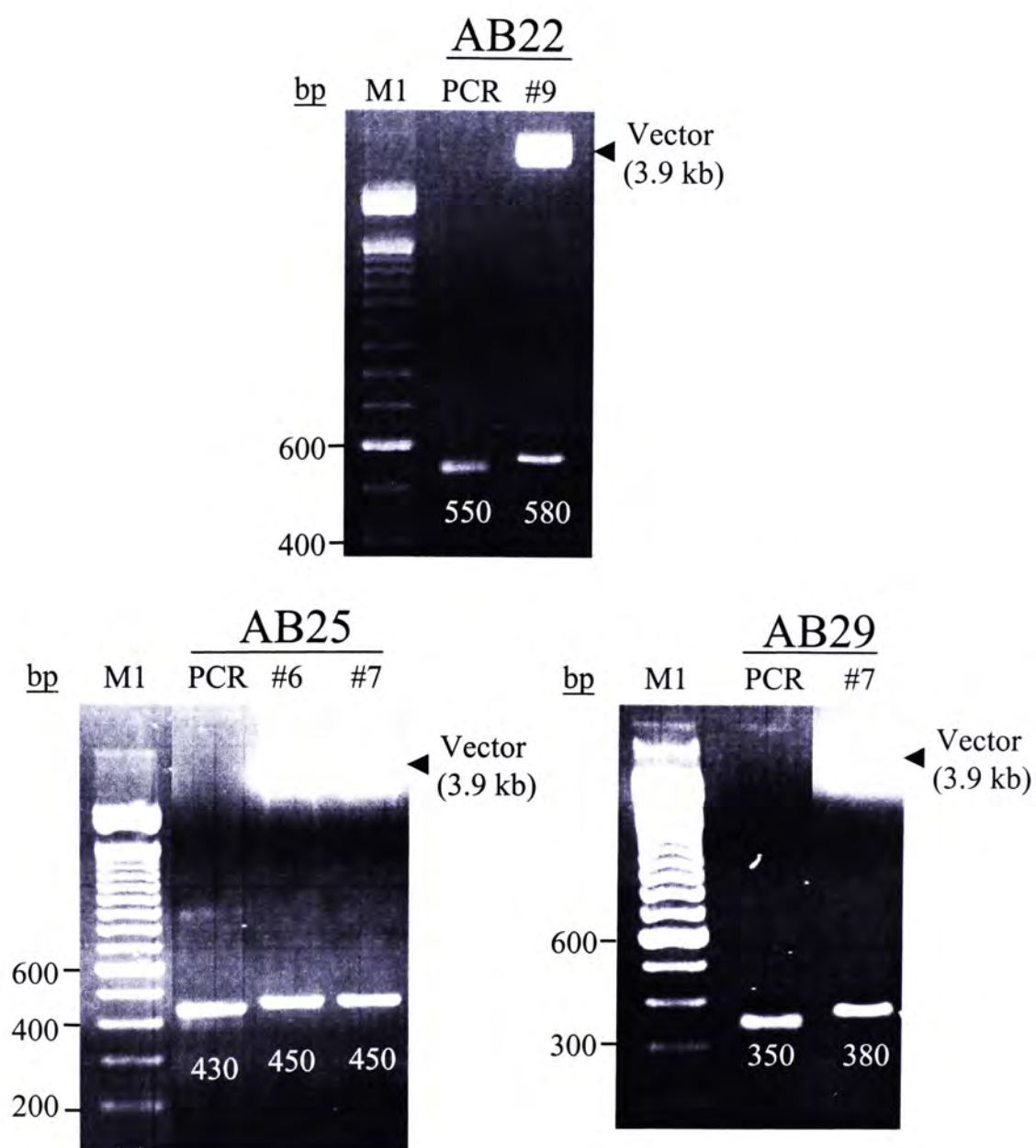


Figure 3.9.3. *Eco*RI digested cDNA fragments excised from gel AB (AP3 and ARP3) Part II. The *Eco*RI digested cDNA fragments were resolved on 1% agarose, 0.5X TBE gels with ethidium bromide staining. M1, 100 bp DNA marker. PCR, reamplified PCR product of the corresponding cDNA fragment.

Table 3.9.2. Summary of cDNA fragments subcloned from gel AB (AP3 and ARP3)

Gel	FluoroDD fragment I.D.	FluoroDD fragment size (bp)	Reamplified fragment size (bp)	Subclone I.D.	Size of vector (kb)	Size of insert after <i>EcoRI</i> cut (bp)
AB (AP3 & ARP3)	AB7	850	870	AB7#2	4.0 (pCR [®] II-TOPO [®])	900
				AB7#8	4.0 (pCR [®] II-TOPO [®])	900
	AB17	620	630	AB17#9	4.0 (pCR [®] II-TOPO [®])	655
				AB17#16	4.0 (pCR [®] II-TOPO [®])	650
	AB18	595	630	AB18#4	3.9 (pT-Adv)	655
	AB19	575	590	AB19#2	4.0 (pCR [®] II-TOPO [®])	620
				AB19#10	4.0 (pCR [®] II-TOPO [®])	610
	AB22	530	550	AB22#9	4.0 (pCR [®] II-TOPO [®])	580
	AB24	420	440	AB24#9	4.0 (pCR [®] II-TOPO [®])	460
	AB25	405	430	AB25#6	4.0 (pCR [®] II-TOPO [®])	450
				AB25#7	4.0 (pCR [®] II-TOPO [®])	450
	AB26	390	420	AB26#17	3.9 (pT-Adv)	450
				AB26#30	3.9 (pT-Adv)	450
	AB27	355	370	AB27#6	4.0 (pCR [®] II-TOPO [®])	390
	AB29	335	350	AB29#7	4.0 (pCR [®] II-TOPO [®])	380

Phenol:chloroform extraction was performed for screening the subclones which contained inserts. Those subclones containing plasmid DNA larger than the vector only (3.9 or 4.0 kb) were selected for performing *EcoRI* cut to confirm correct insert sizes and further used for sequencing and Northern blot analysis.

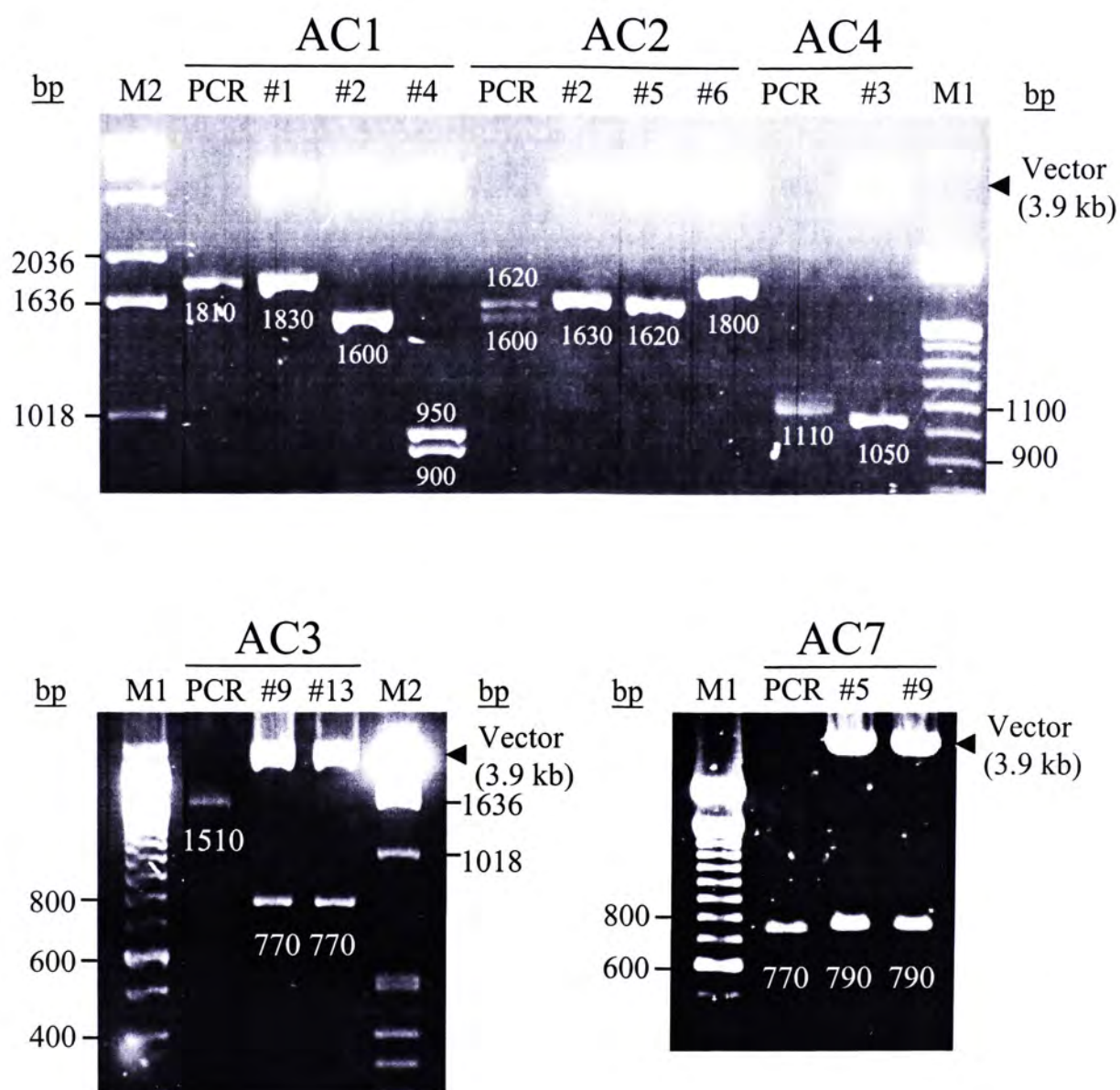


Figure 3.9.4. *EcoRI* digested cDNA fragments excised from gel AC (AP2 and ARP19). The *EcoRI* digested cDNA fragments were resolved on 1% agarose, 0.5X TBE gels with ethidium bromide staining. M1, 100 bp DNA marker; M2, 1 kb DNA marker. PCR, reamplified PCR product of the corresponding cDNA fragment.

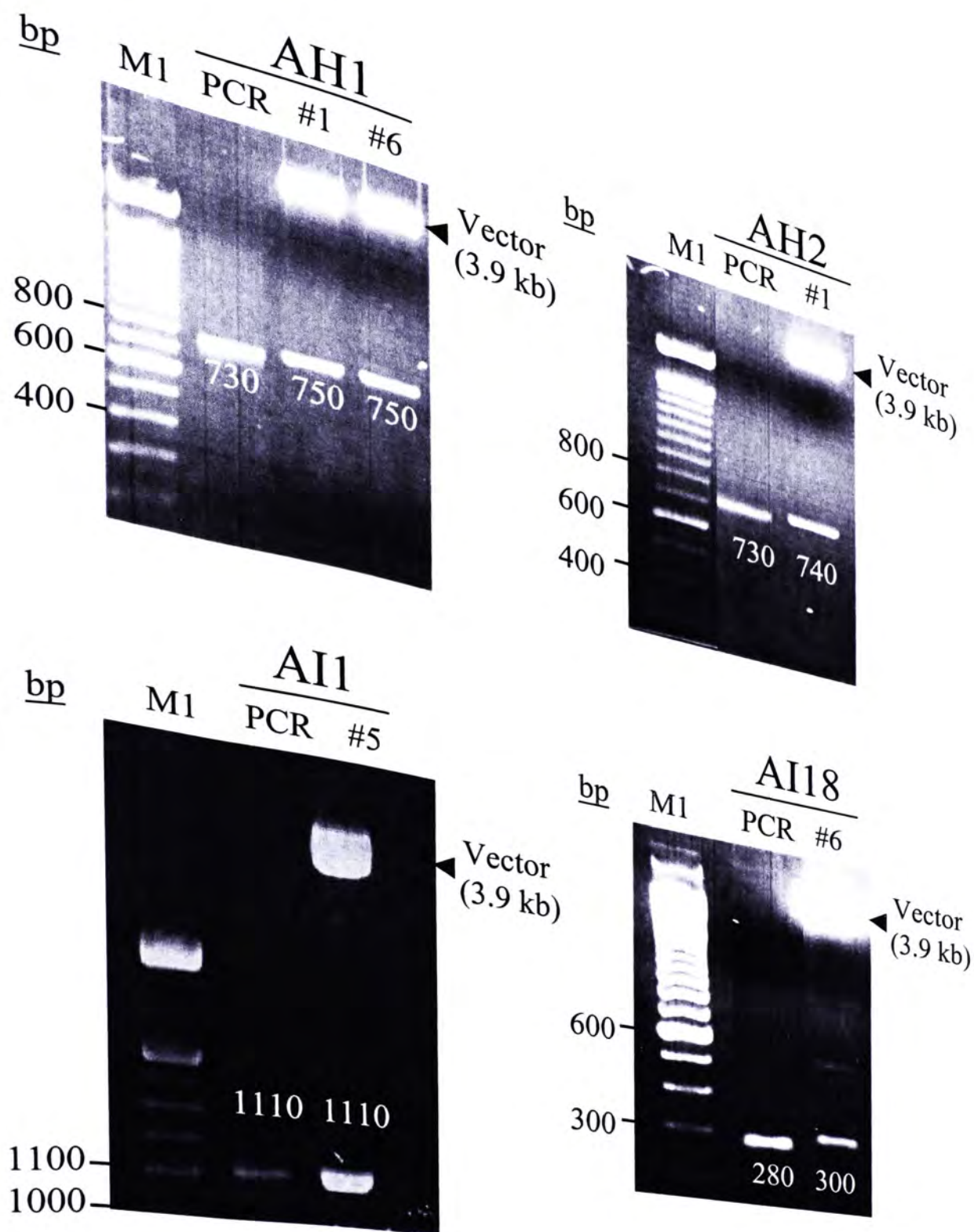


Figure 3.9.6. *Eco*RI digested cDNA fragments excised from gels AH (AP11 and ARP19) and AI (AP6 and ARP4). The *Eco*RI digested cDNA fragments were resolved on 1% agarose, 0.5X TBE gels with ethidium bromide staining. M1, 100 bp DNA marker. PCR, reamplified PCR product of the corresponding cDNA fragment.



Table 3.9.3. Summary of cDNA fragments subcloned from gels AC (AP2 and ARP19) and AD (AP2 and ARP18)

Gel	FluoroDD fragment I.D.	FluoroDD fragment size (bp)	Reamplified fragment size (bp)	Subclone I.D.	Size of vector (kb)	Size of insert after <i>EcoRI</i> cut (bp)
AC (AP2 & ARP19)	AC1	1800	1810	AC1#1	4.0 (pCR [®] II-TOPO [®])	1830
				AC1#2	4.0 (pCR [®] II-TOPO [®])	1600
				AC1#4	4.0 (pCR [®] II-TOPO [®])	900+950
	AC2	1600	1620 +1600	AC2#2	4.0 (pCR [®] II-TOPO [®])	1630
				AC2#5	4.0 (pCR [®] II-TOPO [®])	1620
				AC2#6	4.0 (pCR [®] II-TOPO [®])	1800
				AC3#9	3.9 (pT-Adv)	770+770
	AC3	1500	1510	AC3#13	3.9 (pT-Adv)	770+770
	AC4	1100	1110	AC4#3	4.0 (pCR [®] II-TOPO [®])	1050
	AC7	770	770	AC7#5	3.9 (pT-Adv)	790
				AC7#9	3.9 (pT-Adv)	790
AD (AP2 & ARP18)	AD6	840	870	AD6#4	4.0 (pCR [®] II-TOPO [®])	860
				AD6#10	4.0 (pCR [®] II-TOPO [®])	850
	AD8	720	735	AD8#2	3.9 (pT-Adv)	780
				AD8#7	3.9 (pT-Adv)	780
	AD9	710	730	AD9#2	3.9 (pT-Adv)	765
				AD9#3	3.9 (pT-Adv)	765

Phenol:chloroform extraction was performed for screening the subclones which contained inserts. Those subclones containing plasmid DNA larger than the vector only (3.9 or 4.0 kb) were selected for performing *EcoRI* cut to confirm correct insert sizes and further used for sequencing and Northern blot analysis.

Table 3.9.4. Summary of cDNA fragments subcloned from gels AF (AP10 and ARP13), AH (AP11 and ARP19), AI (AP6 and ARP4) and AJ (AP6 and ARP14)

Gel	FluoroDD fragment I.D.	FluoroDD fragment size (bp)	Reamplified fragment size (bp)	Subclone I.D.	Size of vector (kb)	Size of insert after <i>Eco</i> RI cut (bp)
AF (AP10 & ARP13)	AF1	945	960	AF1#8	4.0 (pCR [®] II-TOPO [®])	990
	AF21	340	350	AF21#5	4.0 (pCR [®] II-TOPO [®])	370
	AF25	275	290	AF25#6	4.0 (pCR [®] II-TOPO [®])	310
				AF25#7	4.0 (pCR [®] II-TOPO [®])	310
	AF30	240	270	AF30#4	4.0 (pCR [®] II-TOPO [®])	290
AH (AP11 & ARP19)	AH1	720	730	AF30#5	4.0 (pCR [®] II-TOPO [®])	290
				AH1#1	4.0 (pCR [®] II-TOPO [®])	750
	AH2	700	730	AH1#6	4.0 (pCR [®] II-TOPO [®])	750
				AH2#1	4.0 (pCR [®] II-TOPO [®])	740
	AI1	1100	1110	AI1#5	4.0 (pCR [®] II-TOPO [®])	1110
AI (AP6 & ARP4)	AI18	270	280	AI18#6	4.0 (pCR [®] II-TOPO [®])	300
AJ (AP6 & ARP14)	AJ1	1200	1210	AJ1#4	4.0 (pCR [®] II-TOPO [®])	990+220
	AJ2	1100	1110	AJ1#5	4.0 (pCR [®] II-TOPO [®])	990+220
				AJ2#8	4.0 (pCR [®] II-TOPO [®])	1130
				AJ2#10	4.0 (pCR [®] II-TOPO [®])	1130
	AJ9	320	330	AJ9#1	4.0 (pCR [®] II-TOPO [®])	360

Phenol:chloroform extraction was performed for screening the subclones which contained inserts. Those subclones containing plasmid DNA larger than the vector only (3.9 or 4.0 kb) were selected for performing *Eco*RI cut to confirm correct insert sizes and further used for sequencing and Northern blot analysis.

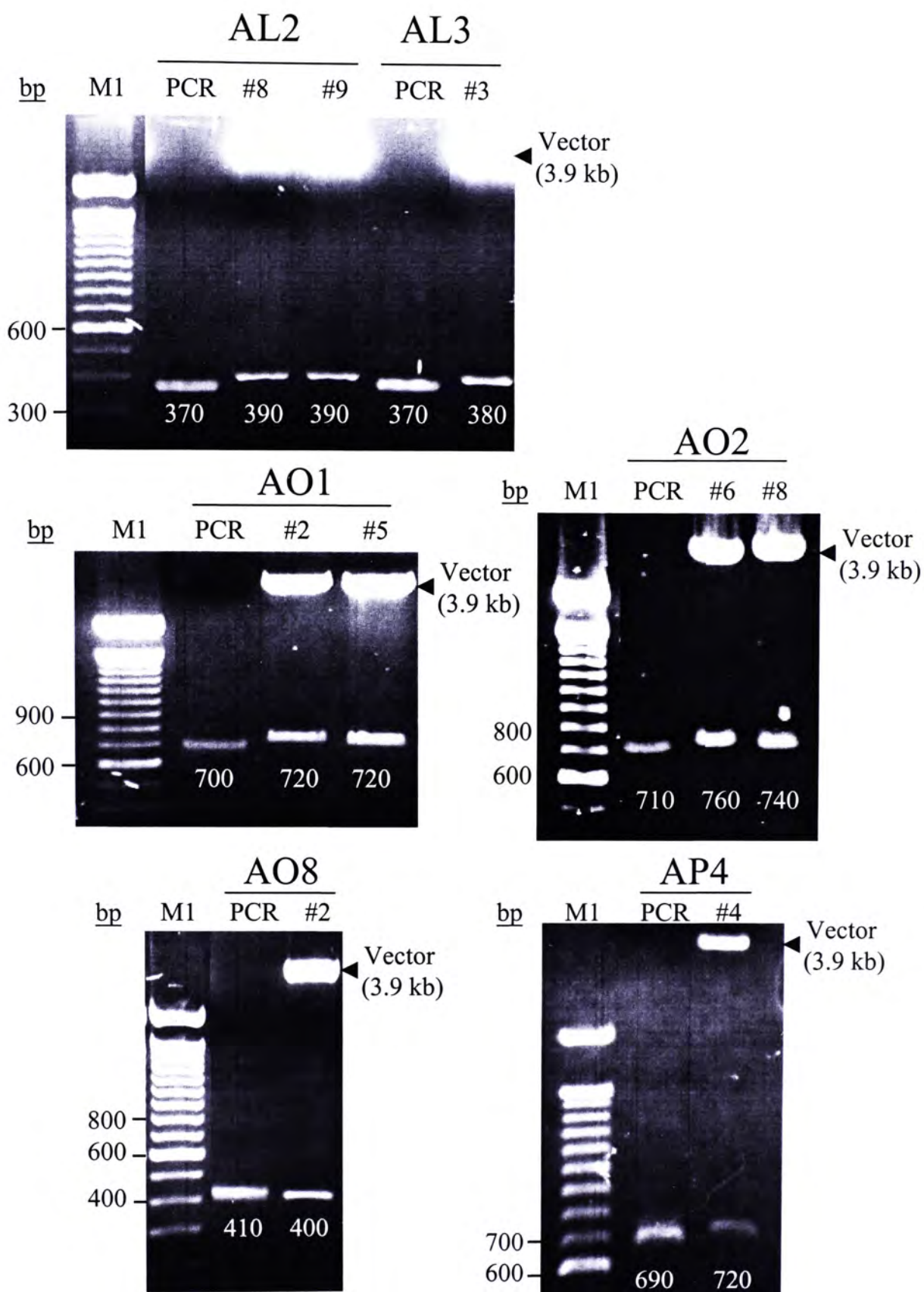


Figure 3.9.8. *Eco*RI digested cDNA fragments excised from gels AL (AP7 and ARP15), AO (AP5 and ARP10) and AP (AP12 and ARP2). The *Eco*RI digested cDNA fragments were resolved on 1% agarose, 0.5X TBE gels with ethidium bromide staining. M1, 100 bp DNA marker. PCR, reamplified PCR product of the corresponding cDNA fragment.

Table 3.9.5. Summary of cDNA fragments subcloned from gels AL (AP7 and ARP15), AO (AP5 and ARP10) and AP (AP12 and ARP2)

Gel	FluoroDD fragment I.D.	FluoroDD fragment size (bp)	Reamplified fragment size (bp)	Subclone I.D.	Size of vector (kb)	Size of insert after <i>EcoRI</i> cut (bp)
AL (AP7 & ARP15)	AL2	350	370	AL2#8	4.0 (pCR [®] II-TOPO [®])	390
				AL2#9	4.0 (pCR [®] II-TOPO [®])	390
	AL3	345	370	AL3#3	4.0 (pCR [®] II-TOPO [®])	380
AO (AP5 & ARP10)	AO1	700	700	AO1#2	4.0 (pCR [®] II-TOPO [®])	720
				AO1#5	4.0 (pCR [®] II-TOPO [®])	720
	AO2	695	710	AO2#6	4.0 (pCR [®] II-TOPO [®])	760
				AO2#8	4.0 (pCR [®] II-TOPO [®])	740
	AO8	400	410	AO8#2	4.0 (pCR [®] II-TOPO [®])	400
AP (AP12 & ARP2)	AP4	680	690	AP4#4	4.0 (pCR [®] II-TOPO [®])	720

Phenol:chloroform extraction was performed for screening the subclones which contained inserts. Those subclones containing plasmid DNA larger than the vector only (3.9 or 4.0 kb) were selected for performing *EcoRI* cut to confirm correct insert sizes and further used for sequencing and Northern blot analysis.

patterns and larger insert sizes might be due to contamination and/or nearby co-migrated cDNA fragments. In contrast, cDNA fragments AA1 (Figure 3.9.1) (Table 3.9.1); AC1, AC3 and AC4 (Figure 3.9.4) (Table 3.9.3); AD6 (Figure 3.9.5) (Table 3.9.3); AI1 (Figure 3.9.6) (Table 3.9.4); AJ1 (Figure 3.9.7) (Table 3.9.4) and AO8 (Figure 3.9.8) (Table 3.9.5) showed smaller insert sizes and these might be due to the presence of *Eco*RI site in those inserts. In addition, contamination of nearby co-migrated cDNA fragments or other cDNA fragments during bands excision would also give small sizes of inserts after *Eco*RI digestion.

3.10 Sequencing of subcloned cDNA fragments

A total of forty-two subcloned cDNA fragments (seventy subclones) were sequenced and twenty-six different known genes and one expressed sequence tag (EST) were obtained. They included mouse peroxisomal delta3, delta2-enoyl-Coenzyme A isomerase (Peci) [subclones AA1#2, AA1#3, AA1#4 and #20 (Table 3.10.1)]; mouse apolipoprotein A-V (Apoa5) [subclones AA4#1 and AA4#9 (Table 3.10.1)]; mouse complete mitochondrial genome (mitochondria) [subclones AA5#5, AA6#1 and AA6#9 (Table 3.10.1); AA7#3 and AA7#5 (Table 3.10.2); AB17#16 and AB18#4 (Table 3.10.3); AB19#2 and AB19#10 (Table 3.10.4); AF30#5 (Table 3.10.11) and AP4#4 (Table 3.10.16)]; mouse cysteine sulfinic acid decarboxylase (Csd) [subclone AA10#1 (Table 3.10.2)]; mouse acetyl-Coenzyme A dehydrogenase, medium chain (MCAD) [subclone AA12#4 (Table 3.10.2)]; mouse UDP-glucuronosyltransferase (UGT2b5) [subclones AB7#2 and AB7#8 (Table 3.10.3)]; mouse peroxisome biogenesis factor 16 (Pex 16) [subclone AB22#9 (Table 3.10.4)]; mouse cytochrome P450 (Cyp4a14) [subclones AB24#9 and AB25#6 (Table 3.10.4); AB26#17 and AB26#30 (Table 3.10.5)]; mouse catalase [subclones AB29#7 (Table 3.10.5); AC2#5

(Table 3.10.7) and AJ9#1 (Table 3.10.13)]; mouse serine (or cysteine) proteinase inhibitor, clade F, member 2 (Serpinf2) [subclones AC1#1 (Table 3.10.6) and AC2#6 (Table 3.10.7)]; serine (or cysteine) proteinase inhibitor, clade A, member 1a (SPI) [subclone AC1#2 (Table 3.10.6); AC4#3 and AC7#5 (Table 3.10.8)]; serine (or cysteine) proteinase inhibitor, clade A, member 3K (Spi2) [subclone AI1#5 (Table 3.10.12)]; mouse peroxisomal bifunctional enzyme (PBFE) [subclone AC2#2 (Table 3.10.7)]; mouse cytochrome P450 2a5 (Cyp2a5) [subclone AC4#3 (Table 3.10.8)]; mouse N-terminal Asn amidase [subclone AD6#4 (Table 3.10.9)]; mouse cytochrome P450 4a10 (Cyp4a10) [subclones AD6#10, AD8#2, AD8#7, AD9#2 and AD9#3 (Table 3.10.9)]; mouse very-long-chain acyl-CoA synthetase (VLACS) [subclone AF1#8 (Table 3.10.10)]; mouse cell death-inducing DNA fragmentation factor, alpha subunit-like effector B (Cidef) [subclone AF21#5 (Table 3.10.10)]; mouse major urinary protein II (MUP II) [subclones AF25#6 and AF25#7 (Table 3.10.10)]; mouse suppressor of actin mutations (SAC1 gene) [subclone AF30#4 (Table 3.10.11) and AJ9#1 (Table 3.10.13)]; mouse expressed sequence tags (EST) [subclone AH1#1 (Table 3.10.11)]; mouse argininosuccinate lyase (Asl) [subclone AI18#6 (Table 3.10.12)]; mouse carboxyesterase [subclones AJ1#4 and AJ1#5 (Table 3.10.13)]; mouse peroxisomal acyl-CoA oxidase (AOX) [subclone AJ2#10 (Table 3.10.13)]; mouse hydroxysteroid (17-beta) dehydrogenase 11 (Hsd17 β 11) [subclones AL2#8 and AL3#3 (Table 3.10.14)]; mouse adipose differentiation related protein (ADRP) [subclone AO1#2 (Table 3.10.15)]; mouse carnitine O-octanoyltransferase (Crot) [subclones AO1#5 and AO2#8 (Table 3.10.15)]; mouse ribonuclease, RNase A family 4 (RNase4) [subclones AO2#6 and AO8#2 (Table 3.10.15)] (Appendix B, B1.1-16.1).

The abundance of genes were shown in Figure 3.10.1, including mitochondrial (19.1%) > SPI (7.1%), Catalase (7.1%), Cyp4a10 (7.1%) and Cyp4a14 (7.1%) > Crot

Table 3.10.1. DNA sequences of cDNA fragments subcloned from gel AA (AP1 and ARP2) part I

Gel	FluoroDD fragment I.D.	FluoroDD fragment size (bp)	Reamplified fragment size (bp)	Subclone I.D.	Size of insert (bp)	Sequencing		
						Sequencing primer	Gene homology (Transcript size)	E value
AA (AP1 & ARP2)	AA1	1400	1430 + 1300	AA1#2*	1400	M13 forward (-20)	<i>Mus musculus</i> peroxisomal delta 3, delta 2-enoyl-coenzyme A isomerase, Peci (1581 bp)	447/474 (94%)
				AA1#3	1450	M13 forward (-20)		187/191 (97%)
				AA1#4	1450	M13 reverse		199/209 (95%)
				AA1#20	1700	M13 forward (-20)		541/569 (95%)
	AA4	695	705	AA4#1	725	M13 forward (-20)	<i>Mus musculus</i> apolipoprotein A-V, ApoA5 (1819 bp)	112/121 (92%)
				AA4#9*	725	M13 reverse		231/245 (94%)
	AA5	670	720+680	AA5#5	710	M13 forward (-20)	<i>Mus musculus</i> clone LA9 mitochondrion, complete genome (16300 bp)	496/524 (94%)
				AA6#1	710	M13 forward (-20)		495/517 (95%)
	AA6	660	670	AA6#9	710	M13 reverse	<i>Mus musculus</i> clone LA9 mitochondrion, complete genome (16300 bp)	563/579 (97%)
								0

M13 (-20) forward (5'-GTAAACGACGGCCAG-3') and M13 reverse (5'-CAGGAACAGCTATGAC-3') primers were used for sequencing. After sequencing, sequence homology of the identified genes was searched against the known genes and ESTs in GenBank using BLAST. The identities indicate the percentage of the cDNA fragment match with the BLAST search sequence, while the expect value (E) is the parameter to describe the probability of the cDNA fragment that occurred in the database by chance. *Subclones selected for subsequent Northern blot analysis.

Table 3.10.2. DNA sequences of cDNA fragments subcloned from gel AA (AP1 and ARP2) part II

Gel	FluoroDD fragment I.D.	FluoroDD fragment size (bp)	Reamplified fragment size (bp)	Subclone I.D.	Size of insert (bp)	Sequencing			E value
						Sequencing primer	Gene homology (Transcript size)	Identities	
AA (AP1 & ARP2)	AA7	640	655	AA7#3	710	M13 forward (-20)	<i>Mus musculus</i> clone LA9 mitochondrion, complete genome (16300 bp)	495/522 (94%)	0
				AA7#5	710	M13 reverse		440/454 (96%)	0
	AA10	500	520	AA10#1*	550	M13 forward (-20)	<i>Mus musculus</i> cysteine sulfinic acid decarboxylase, Csad (2265 bp)	304/311 (97%)	e-143
						M13 reverse		163/182 (89%)	3e-32
	AA12	470	480	AA12#4*	500	M13 forward (-20)	<i>Mus musculus</i> acetyl-coenzyme A dehydrogenase, medium chain, MCAD (1857 bp)	419/419 (100%)	0
						M13 reverse		100/103 (97%)	5e-38

M13 (-20) forward (5'-GTAAACGACGGCCAG-3') and M13 reverse (5'-CAGGAACAGCTATGAC-3') primers were used for sequencing. After sequencing, sequence homology of the identified genes was searched against the known genes and ESTs in GenBank using BLAST. The identities indicate the percentage of the cDNA fragment match with the BLAST search sequence, while the expect value (E) is the parameter to describe the probability of the cDNA fragment that occurred in the database by chance. *Subclones selected for subsequent Northern blot analysis.

Table 3.10.3. DNA sequences of cDNA fragments subcloned from gel AB (AP3 and ARP3) part I

Gel	FluoroDD fragment I.D.	FluoroDD fragment size (bp)	Reamplified fragment size (bp)	Subclone I.D.	Size of insert (bp)	Sequencing			
						Sequencing primer	Gene homology (Transcript size)	Identities	E value
AB (AP3 & ARP3)	AB7	850	870	AB7#2*	900	M13 forward (-20)	Mouse UDP-glucuronosyltransferase 2 family, member 5, UGT2b5 (1648 bp)	584/642 (90%)	0
				AB7#8	900	M13 reverse		482/534 (90%)	0
	AB17	620	630	AB17#9	655	M13 forward (-20)	Failed in sequencing		
				AB17#16	650	M13 reverse		<i>Mus musculus</i> clone LA9 mitochondrion, complete genome (16300 bp)	478/496 (96%)
	AB18	595	630	AB18#4	655	M13 forward (-20)	<i>Mus musculus</i> clone LA9 mitochondrion, complete genome (16300 bp)	477/490 (97%)	0
						M13 reverse		524/538 (97%)	0

M13 (-20) forward (5'-GTAAACGACGGCCAG-3') and M13 reverse (5'-CAGGAACAGCTATGAC-3') primers were used for sequencing. After sequencing, sequence homology of the identified genes was searched against the known genes and ESTs in GenBank using BLAST. The identities indicate the percentage of the cDNA fragment match with the BLAST search sequence, while the expect value (E) is the parameter to describe the probability of the cDNA fragment that occurred in the database by chance. *Subclones selected for subsequent Northern blot analysis.

Table 3.10.4. DNA sequences of cDNA fragments subcloned from gel AB (AP3 and ARP3) part II

Gel	FluoroDD fragment I.D.	FluoroDD fragment size (bp)	Reamplified fragment size (bp)	Subclone I.D.	Sequencing				Identities	E value
					Size of insert (bp)	Sequencing primer	Gene homology (Transcript size)			
AB (AP3 & ARP3)	AB19	575	590	AB19#2	620	M13 forward (-20)	<i>Mus musculus</i> clone LA9 mitochondrion, complete genome (16300 bp)	523/530 (98%)	0	
				AB19#10	610	M13 reverse		513/516 (99%)		0
	AB22	530	550	AB22#9*	580	M13 forward (-20)	<i>Mus musculus</i> peroxisome biogenesis factor 16, Pex16 (1221 bp)	405/430 (94%)	e-178	
						M13 reverse		482/486 (99%)		0
	AB24	420	440	AB24#9	460	M13 forward (-20)	<i>Mus musculus</i> cytochrome P450, family 4, subfamily a, polypeptide 14, Cyp4a14 (2547 bp)	354/355 (99%)	0	
						M13 reverse		331/339 (97%)		e-165
	AB25	405	430	AB25#6*	450	M13 forward (-20)	<i>Mus musculus</i> cytochrome P450, family 4, subfamily a, polypeptide 14, Cyp4a14 (2547 bp)	150/162 (92%)	7e-47	
						M13 reverse				
				AB25#7	450	M13 reverse	Failed in sequencing			

M13 (-20) forward (5'-GTAAACGACGGCCAG-3') and M13 reverse (5'-CAGGAACAGCTATGAC-3') primers were used for sequencing. After sequencing, sequence homology of the identified genes was searched against the known genes and ESTs in GenBank using BLAST. The identities indicate the percentage of the cDNA fragment match with the BLAST search sequence, while the expect value (E) is the parameter to describe the probability of the cDNA fragment that occurred in the database by chance. *Subclones selected for subsequent Northern blot analysis.

Table 3.10.5. DNA sequences of cDNA fragments subcloned from gel AB (AP3 and ARP3) part III

Gel	FluoroDD fragment I.D.	FluoroDD fragment size (bp)	Reamplified fragment size (bp)	Subclone I.D.	Sequencing			
					Size of insert (bp)	Sequencing primer	Gene homology (Transcript size)	E value
AB (AP3 & ARP3)	AB26	390	420	AB26#17	450	M13 forward (-20)	<i>Mus musculus</i> cytochrome P450, family 4, subfamily a, polypeptide 14, Cyp4a14 (2547 bp)	0
				AB26#30	450	M13 reverse		0
	AB27	355	370	AB27#6	390	M13 forward (-20)	Failed in sequencing	
						M13 reverse	Failed in sequencing	
	AB29	335	350	AB29#7	380	M13 forward (-20)	i84a04.x1 Kaestner ngn3 -- subtracted <i>Mus musculus</i> cDNA 3'similar to SW-CATA_CAMJE Q59296 CATALASE (283 bp)	e-114
						M13 reverse	Failed in sequencing	

M13 (-20) forward (5'-GTAAACGACGGCCAG-3') and M13 reverse (5'-CAGGAACAGCTATGAC-3') primers were used for sequencing. After sequencing, sequence homology of the identified genes was searched against the known genes and ESTs in GenBank using BLAST. The identities indicate the percentage of the cDNA fragment match with the BLAST search sequence, while the expect value (E) is the parameter to describe the probability of the cDNA fragment that occurred in the database by chance. *Subclones selected for subsequent Northern blot analysis.

Table 3.10.6. DNA sequences of cDNA fragments subcloned from gel AC (AP2 and ARP19) part I

Gel	FluoroDD fragment I.D.	FluoroDD fragment size (bp)	Reamplified fragment size (bp)	Subclone I.D.	Sequencing				
					Size of insert (bp)	Sequencing primer	Gene homology (Transcript size)	Identities	E value
AC (AP2 & ARP19)	AC1	1800	1810	AC1#1	1830	M13 forward (-20)	<i>Mus musculus</i> serine (or cysteine) proteinase inhibitor, clade F, member 2, Serpinf2 (2187 bp)	495/503 (98%)	0
						M13 reverse		119/123 (96%)	7e-52
				AC1#2*	1600	M13 forward (-20)	<i>Mus musculus</i> serine (or cysteine) proteinase inhibitor, clade A, member 1a, SPI (1393bp)	406/422 (96%)	0
						M13 reverse		237/241 (98%)	e-116
								900 + 950	M13 reverse

M13 (-20) forward (5'-GTAAACGACGGCCAG-3') and M13 reverse (5'-CAGGAACAGCTATGAC-3') primers were used for sequencing. After sequencing, sequence homology of the identified genes was searched against the known genes and ESTs in GenBank using BLAST. The identities indicate the percentage of the cDNA fragment match with the BLAST search sequence, while the expect value (E) is the parameter to describe the probability of the cDNA fragment that occurred in the database by chance. *Subclones selected for subsequent Northern blot analysis.

Table 3.10.7. DNA sequences of cDNA fragments subcloned from gel AC (AP2 and ARP 19) part II

Gel	FluoroDD fragment I.D.	FluoroDD fragment size (bp)	Reamplified fragment size (bp)	Subclone I.D.	Sequencing			Identities	E value
					Size of insert (bp)	Sequencing primer	Gene homology (Transcript size)		
AC (AP2 & ARP19)	AC2	1600	1620+1600	AC2#2*	1630	M13 reverse	<i>Mus musculus</i> peroxisomal bifunctional enzyme (PBE) (PBFE) [includes: enoyl-CoA hydratase (EC 4.2.1.17); 3,2-trans_ enoyl-CoA isomerase (EC 5.3.3.8); 3-hydroxyacyl-CoA dehydrogenase (EC 1.1.1.35)], PBFE (2979 bp)	525/545 (96%)	0
				AC2#5	1620	M13 reverse	if84h05.x1 Kaestner ngn3 - - subtracted <i>Mus musculus</i> cDNA 3' similar to SW: CATA_CAMJE Q59296 CATALASE (280 bp)	93/99 (93%)	4e-19
				AC2#6	1800	M13 forward (-20)	<i>Mus musculus</i> serine (or cysteine) proteinase inhibitor, clade F, member 2, Serpin2 (2187 bp)	633/641 (98%)	0

M13 (-20) forward (5'-GTAAACGACGGCCAG-3') and M13 reverse (5'-CAGGAACAGCTATGAC-3') primers were used for sequencing. After sequencing, sequence homology of the identified genes was searched against the known genes and ESTs in GenBank using BLAST. The identities indicate the percentage of the cDNA fragment match with the BLAST search sequence, while the expect value (E) is the parameter to describe the probability of the cDNA fragment that occurred in the database by chance. *Subclones selected for subsequent Northern blot analysis.

Table 3.10.8. DNA sequences of cDNA fragments subcloned from gel AC (AP2 and ARP19) part III

Gel	FluoroDD fragment I.D.	FluoroDD fragment size (bp)	Reamplified fragment size (bp)	Subclone I.D.	Sequencing				E value
					Size of insert (bp)	Sequencing primer	Gene homology (Transcript size)	Identities	
AC (AP2 & ARP19)	AC3	1500	1510	AC3#9	770 + 770	M13 forward (-20)	Failed in sequencing		
				AC3#13	770 + 770	M13 reverse			
	AC4	1100	1110	AC4#3	1050	M13 forward (-20)	<i>Mus musculus</i> cytochrome P450, family 2, subfamily a, polypeptide 5, Cyp2a5 (1720 bp)	302/329 (91%)	e-121
						M13 reverse	<i>Mus musculus</i> serine (or cysteine) proteinase inhibitor, clade A, member 1a, SPI (1393 bp)	219/229 (95%)	4e-85
	AC7	770	770	AC7#5	790	M13 forward (-20)	<i>Mus musculus</i> serine (or cysteine) proteinase inhibitor, clade A, member 1a, SPI (1393 bp)	394/406 (97%)	0
				AC7#9	790	M13 reverse	Failed in sequencing		

M13 (-20) forward (5'-GTAAACGACGGCCAG-3') and M13 reverse (5'-CAGGAACAGCTATGAC-3') primers were used for sequencing. After sequencing, sequence homology of the identified genes was searched against the known genes and ESTs in GenBank using BLAST. The identities indicate the percentage of the cDNA fragment match with the BLAST search sequence, while the expect value (E) is the parameter to describe the probability of the cDNA fragment that occurred in the database by chance. *Subclones selected for subsequent Northern blot analysis.

Table 3.10.9. DNA sequences of cDNA fragments subcloned from gel AD (AP2 and ARP18)

Gel	FluoroDD fragment I.D.	FluoroDD fragment size (bp)	Reamplified fragment size (bp)	Subclone I.D.	Size of insert (bp)	Sequencing			E value
						Sequencing primer	Gene homology (Transcript size)	Identities	
AD (AP2 & ARP18)	AD6	840	870	AD6#4	860	M13 forward (-20)	Failed in sequencing	476/494 (96%)	0
						M13 reverse			
	AD6	840	870	AD6#10	850	M13 forward (-20)	<i>Mus musculus</i> cytochrome P450, family 4, subfamily a, polypeptide 10, Cyp4a10 (2085 bp)	460/507 (90%)	e-159
						M13 reverse			
	AD8	720	735	AD8#2*	780	M13 forward (-20)	<i>Mus musculus</i> cytochrome P450, family 4, subfamily a, polypeptide 10, Cyp4a10 (2085 bp)	474/515 (92%)	0
						M13 reverse			
	AD9	710	730	AD9#2	765	M13 forward (-20)	<i>Mus musculus</i> cytochrome P450, family 4, subfamily a, polypeptide 10, Cyp4a10 (2085 bp)	353/396 (89%)	e-105
						M13 reverse			
				AD9#3	765	M13 reverse		398/439 (90%)	e-153

M13 (-20) forward (5'-GTAAAACGACGGCCAG-3') and M13 reverse (5'-CAGGAAACAGCTATGAC-3') primers were used for sequencing. After sequencing, sequence homology of the identified genes was searched against the known genes and ESTs in GeneBank using BLAST. The identities indicate the percentage of the cDNA fragment match with the BLAST search sequence, while the expect value (E) is the parameter to describe the probability of the cDNA fragment that occurred in the database by chance. *Subclones selected for subsequent Northern blot analysis.

Table 3.10.10. DNA sequences of cDNA fragments subcloned from gel AF (AP10 and ARP13)

Gel	FluoroDD fragment I.D.	FluoroDD fragment size (bp)	Reamplified fragment size (bp)	Subclone I.D.	Size of insert (bp)	Sequencing			
						Sequencing primer	Gene homology (Transcript size)	Identities	E value
AF (AP10 & ARP13)	AF1	945	960	AF1#8*	990	M13 forward (-20) M13 reverse	<i>Mus musculus</i> very-long-chain acyl-CoA synthetase, VLACS (2209 bp)	606/623 (97%) 119/230 (86%)	0 1e-56
						M13 forward (-20)	Failed in sequencing		
	AF21	340	350	AF21#5	370	M13 reverse		285/292 (97%)	e-140
						M13 forward (-20) M13 reverse	<i>Mus musculus</i> cell death-inducing DNA fragmentation factor, alpha subunit-like effector B, Cideb (1182 bp)		
	AF25	275	290	AF25#6 AF25#7*	310 310	M13 forward (-20) M13 reverse	<i>Mus musculus</i> major urinary protein 2, MUP II (891 bp)	218/223 (97%) 217/219 (99%)	e-103 e-114

M13 (-20) forward (5'-GTAAACGACGGCCAG-3') and M13 reverse (5'-CAGGAACAGCTATGAC-3') primers were used for sequencing. After sequencing, sequence homology of the identified genes was searched against the known genes and ESTs in GenBank using BLAST. The identities indicate the percentage of the cDNA fragment match with the BLAST search sequence, while the expect value (E) is the parameter to describe the probability of the cDNA fragment that occurred in the database by chance. *Subclones selected for subsequent Northern blot analysis.

Table 3.10.11. DNA sequences of cDNA fragments subcloned from gels AF (AP10 and ARP13) and AH (AP11 and ARP19)

Gel	FluoroDD fragment I.D.	FluoroDD fragment size (bp)	Reamplified fragment size (bp)	Subclone I.D.	Sequencing				E value
					Size of insert (bp)	Sequencing primer	Gene homology (Transcript size)	Identities	
AF (AP10 & ARP13)	AF30	240	270	AF30#4	290	M13 forward (-20)	<i>Mus musculus</i> suppressor of actin mutations, SAC1 gene (2029 bp)	82/85 (96%)	1e-29
				AF30#5	290	M13 reverse	<i>Mus musculus</i> clone LA9 mitochondrion, complete genome (16300 bp)	170/173 (98%)	1e-72
AH (AP11 & ARP19)	AH1	720	730	AH1#1	750	M13 forward (-20)	vm09c03.r1 Knowles Solter mouse blastocyst B1 <i>Mus musculus</i> cDNA clone IMAGE:989668 5' similar to gb:U15647_cds1 <i>Mus musculus</i> (624 bp)	377/447 (84%)	2e-82
				AH1#6	750	M13 reverse	Failed in sequencing		
				AH2#1	740	M13 forward (-20)	Failed in sequencing		
	AH2	700	730			M13 reverse	Failed in sequencing		

M13 (-20) forward (5'-GTAAACGACGGCCAG-3') and M13 reverse (5'-CAGGAACAGCTATGAC-3') primers were used for sequencing. After sequencing, sequence homology of the identified genes was searched against the known genes and ESTs in GenBank using BLAST. The identities indicate the percentage of the cDNA fragment match with the BLAST search sequence, while the expect value (E) is the parameter to describe the probability of the cDNA fragment that occurred in the database by chance. *Subclones selected for subsequent Northern blot analysis.

Table 3.10.12. DNA sequences of cDNA fragments subcloned from gel AI (AP6 and ARP4)

Gel	FluoroDD fragment I.D.	FluoroDD fragment size (bp)	Reamplified fragment size (bp)	Subclone I.D.	Size of insert (bp)	Sequencing			E value
						Sequencing primer	Gene homology (Transcript size)	Identities	
AI (AP6 & ARP4)	AI1	1100	1110	AI1#5	1110	M13 forward (-20)	<i>Mus musculus</i> serine (or cysteine) proteinase inhibitor, clade A, member 3K, Spi2 (1645 bp)	343/356 (96%)	0
						M13 reverse		262/269 (97%)	
	AI18	270	280	AI18#6	300	M13 forward (-20)	<i>Mus musculus</i> argininosuccinate lyase, Asl (1589 bp)	184/188 (97%)	6e-84
						M13 reverse		215/217 (99%)	
									e-110

M13 (-20) forward (5'-GTAAACGACGCCAG-3') and M13 reverse (5'-CAGGAAACAGCTATGAC-3') primers were used for sequencing. After sequencing, sequence homology of the identified genes was searched against the known genes and ESTs in GenBank using BLAST. The identities indicate the percentage of the cDNA fragment match with the BLAST search sequence, while the expect value (E) is the parameter to describe the probability of the cDNA fragment that occurred in the database by chance. *Subclones selected for subsequent Northern blot analysis.

Table 3.10.13. DNA sequences of cDNA fragments subcloned from gel AJ (AP6 and ARP14)

Gel	FluoroDD fragment I.D.	FluoroDD fragment size (bp)	Reamplified fragment size (bp)	Subclone I.D.	Size of insert (bp)	Sequencing			
						Sequencing primer	Gene homology (Transcript size)	Identities	E value
AJ (AP6 & ARP14)	AJ1	1200	1210	AJ1#4	990+220	M13 forward (-20)	Mouse carboxylesterase, carboxylesterase (2006 bp)	354/393 (90%)	e-123
				AJ1#5*	990+220	M13 reverse		353/379 (93%)	e-127
	AJ2	1100	1110	AJ2#8	1130	M13 forward (-20)	Failed in sequencing		
				AJ2#10*	1130	M13 forward (-20)			
						M13 reverse	<i>Mus musculus</i> peroxisomal acyl-coA oxidase, AOX (3778 bp)	481/509 (94%)	0
	AJ9	320	330	AJ9#1	360	M13 forward (-20)	if84h05.x1 Kaestner ngn3 -- subtracted <i>Mus musculus</i> cDNA 3' similar to SW:CATA_CAMJE Q59296 CATALASE (280 bp)	206/212 (97%)	1e-93
						M13 reverse	<i>Mus musculus</i> suppressor of actin mutations, SAC1 gene (2029 bp)	77/84 (91%)	2e-24

M13 (-20) forward (5'-GTAAAAACGACGGCCAG-3') and M13 reverse (5'-CAGGAAACAGCTATGAC-3') primers were used for sequencing. After sequencing, sequence homology of the identified genes was searched against the known genes and ESTs in GenBank using BLAST. The identities indicate the percentage of the cDNA fragment match with the BLAST search sequence, while the expect value (E) is the parameter to describe the probability of the cDNA fragment that occurred in the database by chance. *Subclones selected for subsequent Northern blot analysis.

Table 3.10.14. DNA sequences of cDNA fragments subcloned from AL (AP7 and ARP15)

Gel	FluoroDD fragment I.D.	FluoroDD fragment size (bp)	Reamplified fragment size (bp)	Subclone I.D.	Size of insert (bp)	Sequencing		
						Sequencing primer	Gene homology (Transcript size)	Identities
AL (AP7 & ARP15)	AL2	350	370	AL2#8	390	M13 forward (-20)	<i>Mus musculus</i> hydroxysteroid (17-beta) dehydrogenase 11, HSD17b11 (1713 bp)	308/308 (100%)
				AL2#9	390	M13 reverse	Failed in sequencing	
	AL3	345	370	AL3#3*	380	M13 forward (-20)	<i>Mus musculus</i> hydroxysteroid (17-beta) dehydrogenase 11, HSD17b11 (1713 bp)	306/307 (99%)
						M13 reverse		304/308 (98%)
								e-171
								e-166
								e-155

M13 (-20) forward (5'-GTAAACGACGGCCAG-3') and M13 reverse (5'-CAGGAACAGCTATGAC-3') primers were used for sequencing. After sequencing, sequence homology of the identified genes was searched against the known genes and ESTs in GenBank using BLAST. The identities indicate the percentage of the cDNA fragment match with the BLAST search sequence, while the expect value (E) is the parameter to describe the probability of the cDNA fragment that occurred in the database by chance. *Subclones selected for subsequent Northern blot analysis.

Table 3.10.15. DNA sequences of cDNA fragments subcloned from gel AO (AP5 and ARP10)

Gel	FluoroDD fragment I.D.	FluoroDD fragment size (bp)	Reamplified fragment size (bp)	Subclone I.D.	Sequencing				
					Size of insert (bp)	Sequencing primer	Gene homology (Transcript size)	Identities	E value
AO (AP5 & ARP10)	AO1	700	700	AO1#2*	720	M13 forward (-20)	Mouse adipose differentiation related protein, ADRP (1680 bp)	530/564 (93%)	0
				AO1#5	720	M13 reverse	<i>Mus musculus</i> carnitine O-octanoyltransferase, Crot (2844 bp)	461/498 (92%)	e-152
	AO2	695	710	AO2#6	760	M13 forward (-20)	<i>Mus musculus</i> ribonuclease, RNase A family 4, Rnase4 (1412 bp)	458/471 (97%)	0
						M13 reverse		435/454 (95%)	0
				AO2#8*	740	M13 forward (-20)	Failed in sequencing		
	AO8	400	410	AO8#2	400	M13 reverse	<i>Mus musculus</i> carnitine O-octanoyltransferase, Crot (2844 bp)	319/330 (96%)	e-160
						M13 forward (-20)	<i>Mus musculus</i> ribonuclease, RNase A family 4, Rnase4 (1412 bp)	294/315 (93%)	e-121

M13 (-20) forward (5'-GTAAACGACGGCCAG-3') and M13 reverse (5'-CAGGAACAGCTATGAC-3') primers were used for sequencing. After sequencing, sequence homology of the identified genes was searched against the known genes and ESTs in GenBank using BLAST. The identities indicate the percentage of the cDNA fragment match with the BLAST search sequence, while the expect value (E) is the parameter to describe the probability of the cDNA fragment that occurred in the database by chance. *Subclones selected for subsequent Northern blot analysis.

Table 3.10.16. DNA sequences of cDNA fragments subcloned from gel AP (AP12 and ARP2)

Gel	FluoroDD fragment I.D.	FluoroDD fragment size (bp)	Reamplified fragment size (bp)	Subclone I.D.	Size of insert (bp)	Sequencing		
						Sequencing primer	Gene homology (Transcript size)	E value
AP (AP12 & ARP2)	AP4	680	690	AP4#4	720	M13 forward (-20)	<i>Mus musculus</i> clone LA9 mitochondrion, complete genome (16300 bp)	113/123 (91%)
						M13 reverse		221/232 (95%)

M13 (-20) forward (5'-GTAAACGACGGCCAG-3') and M13 reverse (5'-CAGGAACAGCTATGAC-3') primers were used for sequencing. After sequencing, sequence homology of the identified genes was searched against the known genes and ESTs in GenBank using BLAST. The identities indicate the percentage of the cDNA fragment match with the BLAST search sequence, while the expect value (E) is the parameter to describe the probability of the cDNA fragment that occurred in the database by chance. *Subclones selected for subsequent Northern blot analysis.

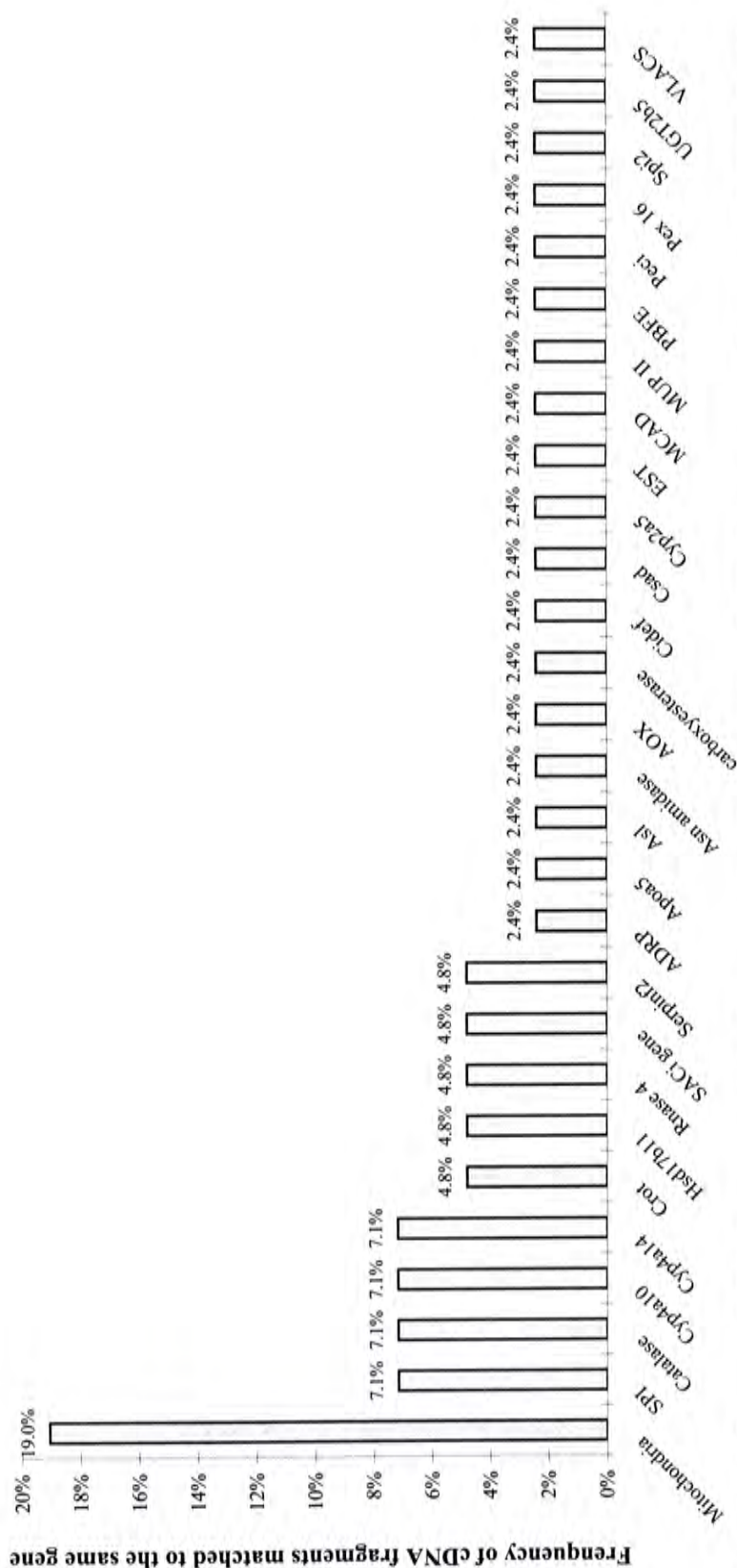


Figure 3.10.1. Frequency of cDNA fragments matched to the same gene (no. of cDNA / total no. of cDNA fragments successfully sequenced X 100%). Total 26 different genes sequenced, which are PPAR α -dependent and Wy-14, 643 responsive, were obtained. ADRP, adipose differentiation related protein; ApoA5, apolipoprotein A-V; Asl, argininosuccinate lyase; Asn amidase, N-terminal Asn amidase; AOX, peroxisomal acyl-CoA oxidase; Carboxyesterase, carboxyesterase; Catalase, catalase; Crot, carnitine O-octanoyltransferase; Cidef, cell death-inducing DNA fragmentation factor, alpha subunit-like effector B; Csad, cysteine sulfinic acid decarboxylase; Cyp2a5, cytochrome P450 2a5; Cyp4a10, cytochrome P450 4a10; Cyp4a14, cytochrome P450 4a14; Peci, peroxisomal delta3, delta2-enoyl-Coenzyme A isomerase; EST, mouse EST; Hsd17b11, hydroxysteroid (17-beta) dehydrogenase 11; MCAD, medium chain acetyl-Coenzyme A dehydrogenase; Mitochondria, mouse complete mitochondrial genome; MUP II, major urinary protein II; PBFE, peroxisomal bifunctional enzyme; Pex 16, peroxisome biogenesis factor 16; RNase 4, ribonuclease, RNase A family 4; SPI, serine (or cysteine) proteinase inhibitor; SAC1 gene, suppressor of actin mutations; UGT2b5, UDP-glucuronosyltransferase; and VLACS, very-long-chain acyl-CoA synthetase.

(4.8%), Hsd17 β 11 (4.8%), Rnase 4 (4.8%), SAC1 gene (4.8%) and Serpinf2 (4.8%) > ADRP (2.4%), Apoa5 (2.4%), Asl (2.4%), Asn amidase (2.4%), AOX (2.4%), Carboxyesterase (2.4%), Cidef (2.4%), Csad (2.4%), Cyp2a5 (2.4%), EST (2.4%), MCAD (2.4%), MUP II (2.4%), PBFE (2.4%), Peci (2.4%), Pex16 (2.4%), Spi2 (2.4%), UGT2b5 (2.4%) and VLACS (2.4%).

3.11 Northern blot analysis of sequenced cDNA fragments

A total of seventeen subcloned cDNA fragments were confirmed. They included AA1#2 [mouse peroxisomal delta3, delta2-enoyl-Coenzyme A isomerase (Peci) (Figure 3.11.1)]; AA4#9 [mouse apolipoprotein A-V (Apoa5) (Figure 3.11.2)]; AA10#1 [cysteine sulfinic acid decarboxylase (Csad) (Figure 3.11.3)]; AA12#4 [mouse acetyl-Coenzyme A dehydrogenase, medium chain (MCAD) (Figure 3.11.4)]; AB7#2 [mouse UDP-glucuronosyltransferase 2 family member 5, (UDP2b5) (Figure 3.11.5)]; AB22#9 [peroxisome biogenesis factor 16 (Pex 16) (Figure 3.11.6)]; AB25#6 [mouse cytochrome P450 4a14 (Cyp4a14) (Figure 3.11.7)]; AC1#2 [mouse serine protease inhibitor, clade A, member 1a (SPI) (Figure 3.11.8)]; AC2#2 [mouse peroxisomal bifunctional enzyme (PBFE) (Figure 3.11.9)]; AD8#2 [mouse cytochrome P450 4a10 (Cyp4a10) (Figure 3.11.10)]; AF1#8 [very-long-chain acyl-CoA synthetase (VLACS) (Figure 3.11.11)]; AF25#7 [mouse major urinary protein II (MUP II) (Figure 3.11.12)]; AJ1#5 [mouse carboxyesterase (carboxyesterase) (Figure 3.11.13)]; AJ2#10 [mouse peroxisomal acyl-CoA oxidase (AOX) (Figure 3.11.14)]; AL3#3 [mouse hydroxysteroid (17-beta) dehydrogenase 11, (Hsd17 β 11) (Figure 3.11.15)]; AO1#2 [mouse adipose differentiation related protein (ADRP) (Figure 3.11.16)] and AO2#8 [mouse carnitine O-octanoyltransferase (Crot) (Figure 3.11.17)]. The results of the Northern blot analysis were then quantified by MultiAnalyst and the

fold changes of Wy-14,643 / Control of PPAR α (+/+) and PPAR α (-/-) mice were calculated.

For loading normalization, the RNA gel photo for each Northern blot analysis was showed. Housekeeping gene glyceraldehyde-3-phosphate dehydrogenase (GAPDH) was not used for normalization of northern blot analysis as its expression was up-regulated in the Wy-14,643 treated PPAR α (+/+) mice after 11 months treatment (Figure 3.11.18) and this observation was also mentioned in previous studie (Anderson *et al.*, 1999).

Some of the subcloned cDNA fragments could not be confirmed by Northern blot analysis as no differential display pattern was observed. They included AA7#3, AB19#10 and AP4#4 [mouse complete mitochondrial genome (mitochondria) (Figure 3.11.19)]; AC1#1 [mouse serine (or cysteine) proteinase inhibitor, clade F, member 2 (Serpinf2)]; AF21#5 [mouse cell death-inducing DNA fragmentation factor, alpha subunit-like effector B (Cidef)]; AJ9#1 [mouse suppressor of actin mutations (SAC1 gene)] and AI18#6 [mouse argininosuccinate lyase (Asl)]. In addition, some of the subcloned cDNA fragments did not give any signal in the Northern blot analysis, including AB29#7 [mouse catalase]; AD6#4 [mouse N-terminal Asn amidase]; AH1#1 [mouse expressed sequence tags (EST) (Figure 3.11.20)] and AO2#6 [mouse ribonuclease, RNase A family 4 (RNase4)].

Up-regulation in PPAR α (+/+) mice fed with the 0.1% Wy-14,643 diet was observed in subcloned cDNA fragments AA1#2 [mouse peroxisomal delta3, delta2-enoyl-Coenzyme A isomerase (Peci) (3-fold) (Figure 3.11.1) (Table3.11.1)]; AA10#1 [cysteine sulfinic acid decarboxylase (Csad) (20-fold) (Figure 3.11.3) (Table 3.11.1)]; AA12#4 [mouse acetyl-Coenzyme A dehydrogenase, medium chain (MCAD) (3.35-fold) (Figure 3.11.4) (Table 3.11.1)]; AB22#9 [peroxisome biogenesis factor 16 (Pex

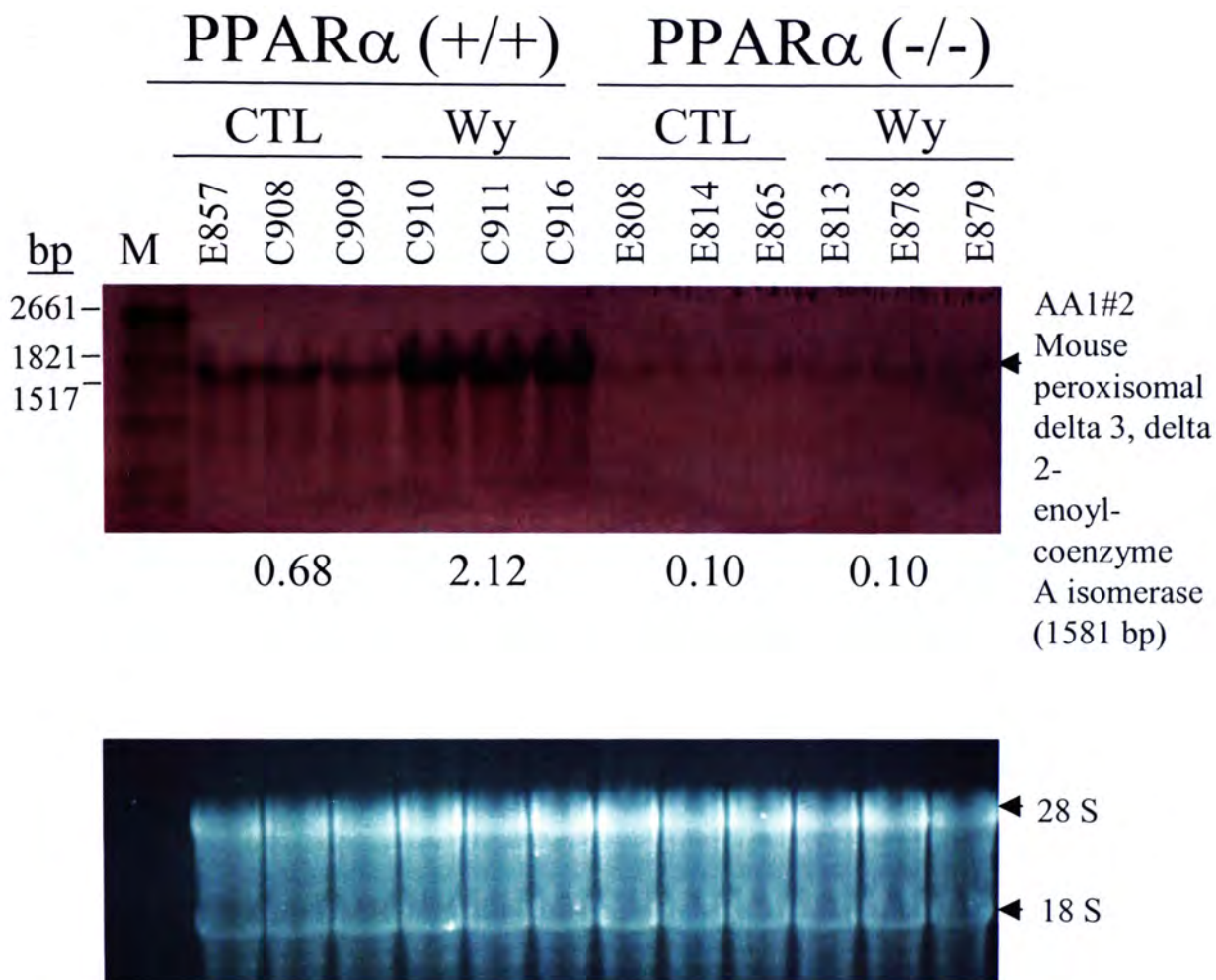


Figure 3.11.1. Confirmation of fluoroDD expression pattern of subclone AA1#2 (peroxisomal delta 3, delta 2-enoyl-coenzyme A isomerase) by Northern blot analysis. Total liver RNA (30 μ g) of three mice each of PPAR α (+/+) and PPAR α (-/-) fed with a 0.0% control (CTL) or 0.1% (w/w) Wy-14,643 (Wy) diet for 11 months was separated on a 1% agarose-formaldehyde gel and transferred to a nylon membrane. The membrane was then hybridized with a PCR DIG-labeled cDNA probe and signals were detected by colorimetric method with NBT and BCIP reagents. For normalization, ethidium bromide staining of RNA gel was used. M, RNA molecular weight marker I, DIG-labeled.



198

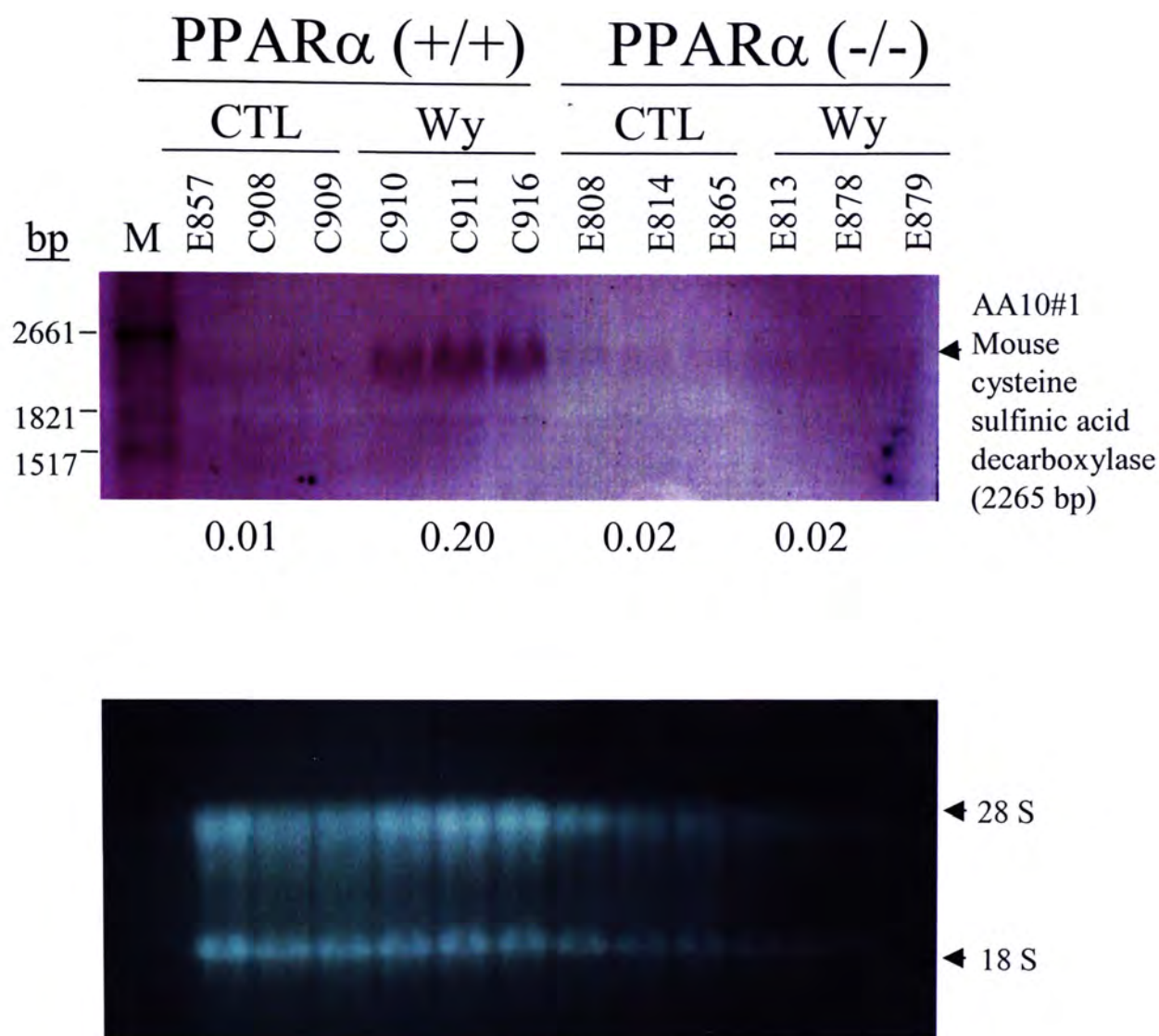


Figure 3.11.3. Confirmation of fluoroDD expression pattern of subclone AA10#1 (cysteine sulfinic acid decarboxylase) by Northern blot analysis. Total liver RNA (30 μ g) of three mice each of PPAR α (+/+) and PPAR α (-/-) fed with a 0.0% control (CTL) or 0.1% (w/w) Wy-14,643 (Wy) diet for 11 months was separated on a 1% agarose-formaldehyde gel and transferred to a nylon membrane. The membrane was then hybridized with a DIG-labeled RNA probe and signals were detected by colorimetric method with NBT and BCIP reagents. For normalization, ethidium bromide staining of RNA gel was used. M, RNA molecular weight marker I, DIG-labeled.

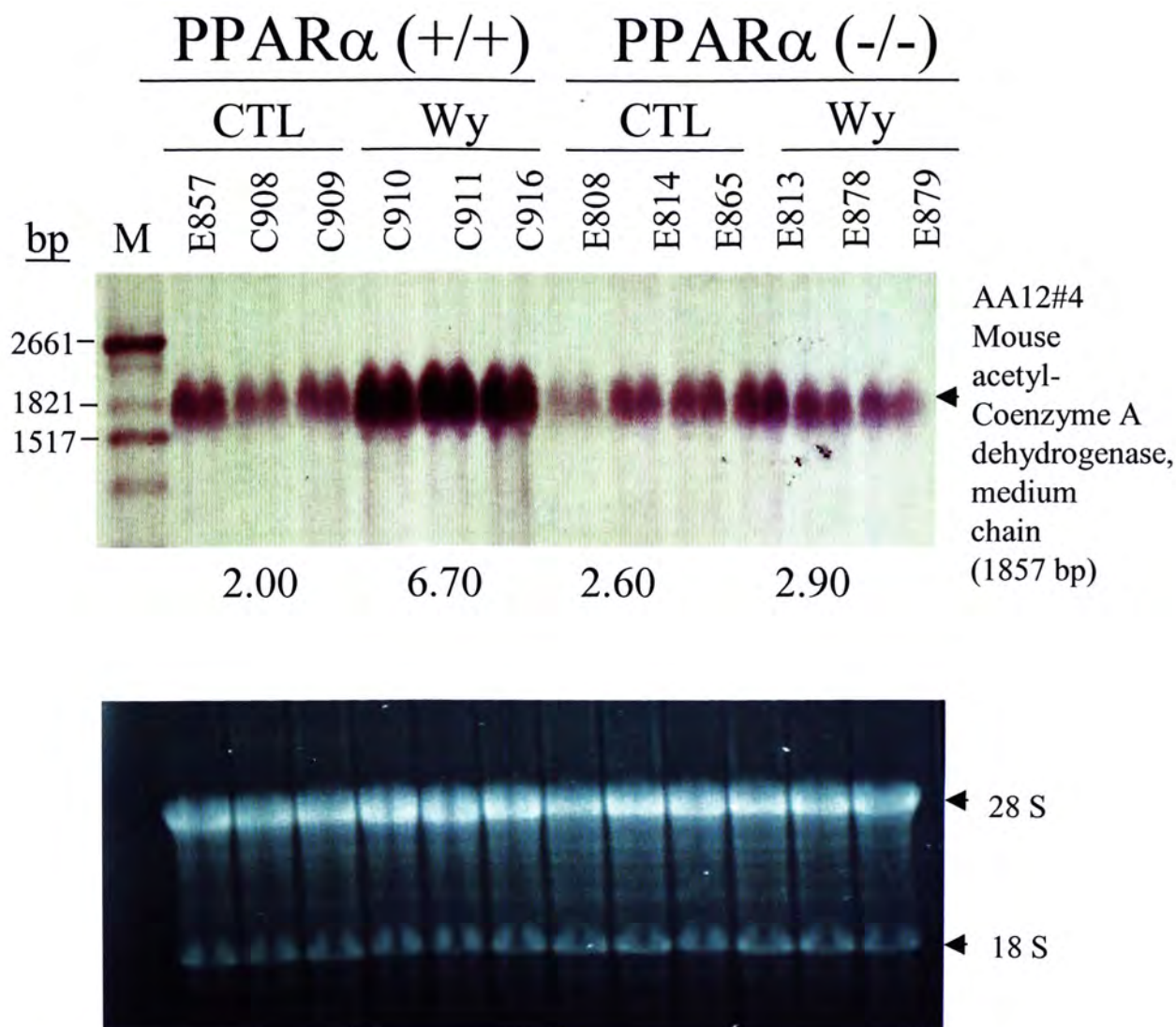


Figure 3.11.4. Confirmation of fluoroDD expression pattern of subclone AA12#4 (acetyl-Coenzyme A dehydrogenase, medium chain) by Northern blot analysis. Total liver RNA (30 μ g) of three mice each of PPAR α (+/+) and PPAR α (-/-) fed with a 0.0% control (CTL) or 0.1% (w/w) Wy-14,643 (Wy) diet for 11 months was separated on a 1% agarose-formaldehyde gel and transferred to a nylon membrane. The membrane was then hybridized with a DIG-labeled RNA probe and signals were detected by colorimetric method with NBT and BCIP reagents. For normalization, ethidium bromide staining of RNA gel was used. M, RNA molecular weight marker I, DIG-labeled.

Table 3.11.1. Summary of Northern blot analysis of cDNA fragments subcloned from gel AA (AP1 and ARP2)

Gel	Subclone I.D.	Differential display pattern				Gene homology (Transcript size)	Northern blot analysis densitometry reading (arbitrary unit)						
		PPAR α (+/+)		PPAR α (-/-)			PPAR α (+/+)		PPAR α (-/-)				
		CTL	Wy	CTL	Wy		CTL	Wy	CTL	Wy			
AA (AP1 & ARP2)	AA1#2	-	+	-	-	<i>Mus musculus</i> peroxisomal delta 3, delta 2-enoyl-coenzyme A isomerase, Peci (1581 bp)	0.68 ± 0.13	2.12 ± 0.17	0.10 ± 0.01	0.10 ± 0.01	3.12	0.10	1.00
							++	+++	-	-			
	AA4#9	++	+	++	++	<i>Mus musculus</i> apolipoprotein A-V, Apoa5 (1819 bp)	0.91 ± 0.17	0.47 ± 0.02	1.08 ± 0.11	1.07 ± 0.41	0.52	++	0.99
							++	+	++	++			
	AA10#1	+	++	+	+	<i>Mus musculus</i> cysteine sulfinic acid decarboxylase, Csad (2265 bp)	0.01 ± 0.01	0.20 ± 0.03	0.02 ± 0.01	0.02 ± 0.01	20.00	-	1.00
							-	+	-	-			
	AA12#4	+	++	+	+	<i>Mus musculus</i> acetyl-coenzyme A dehydrogenase, medium chain, MCAD (1857 bp)	2.00 ± 0.89	6.70 ± 1.68	2.60 ± 0.59	2.90 ± 0.44	3.35	+	1.12
							+	++	+	+			

Values represent mean \pm S.D. '+' represents the presence of a band (cDNA) on fluoroDD gel or Northern blot, while '-' represents the corresponding band (cDNA) was not observed on the fluoroDD gel or Northern blot. The relative intensity of the gene expression among the four treatment groups is indicated by the number of '+'. The signal intensity of a band on Northern blot was quantified by MultiAnalyst.

16) (4-fold) (Figure 3.11.6) (Table 3.11.2)]; AB25#6 [mouse cytochrome P450 4a14 (Cyp4a14) (105-fold) (Figure 3.11.7) (Table 3.11.2)]; AC2#2 [mouse peroxisomal bifunctional enzyme (PBFE) (20-fold) (Figure 3.11.9) (Table 3.11.3)]; AD8#2 [mouse cytochrome P450 4a10 (Cyp4a10) (115-fold) (Figure 3.11.10) (Table 3.11.3)]; AF1#8 [very-long-chain acyl-CoA synthetase (VLACS) (2-fold) (Figure 3.11.20) (Table 3.11.4)]; AJ2#10 [mouse peroxisomal acyl-CoA oxidase (AOX) (10-fold) (Figure 3.11.14) (Table 3.11.4)]; AL3#3 [mouse hydroxysteroid (17-beta) dehydrogenase 11, (Hsd17 β 11) (10-fold) (Figure 3.11.15) (Table 3.11.5)]; AO1#2 [mouse adipose differentiation related protein (ADRP) (16-fold) (Figure 3.11.16) (Table 3.11.5)] and AO2#8 [mouse carnitine O-octanoyltransferase (Crot) (4-fold) (Figure 3.11.17) (Table 3.11.5)] were confirmed.

Subcloned cDNA fragments AA4#9 [mouse apolipoprotein A-V (Apoa5) (0.5-fold) (Figure 3.11.2) (Table 3.11.1)]; AB7#2 [mouse UDP-glucuronosyltransferase 2 family member 5, (UDP2b5) (0.5-fold) (Figure 3.11.5) (Table 3.11.2)]; AC1#2 [mouse serine protease inhibitor, clade A, member 1a (SPI) (0.24-fold) (Figure 3.11.8) (Table 3.11.3)]; AF25#7 [mouse major urinary protein II (MUP II) (0.08-fold) (Figure 3.11.12) (Table 3.11.4)] and AJ1#5 [mouse carboxyesterase (carboxyesterase) (0.08-fold) (Figure 3.11.13) (Table 3.11.4)] were confirmed to be down-regulated by 0.1% Wy-14,643 and PPAR α -dependent.

Subcloned cDNA fragments AB7#2 [mouse UDP-glucuronosyltransferase 2 family member 5, (UDP2b5)], AC1#2 [mouse serine protease inhibitor, clade A, member 1a (SPI)], AD8#2 [mouse cytochrome P450 4a10 (Cyp4a10)] and AF25#7 [mouse major urinary protein II (MUP II)] showed several bands in the Northern blot analysis. The different bands might be different isoforms of the genes. Subcloned cDNA fragments AB7#2 [mouse UDP-glucuronosyltransferase 2 family member 5,

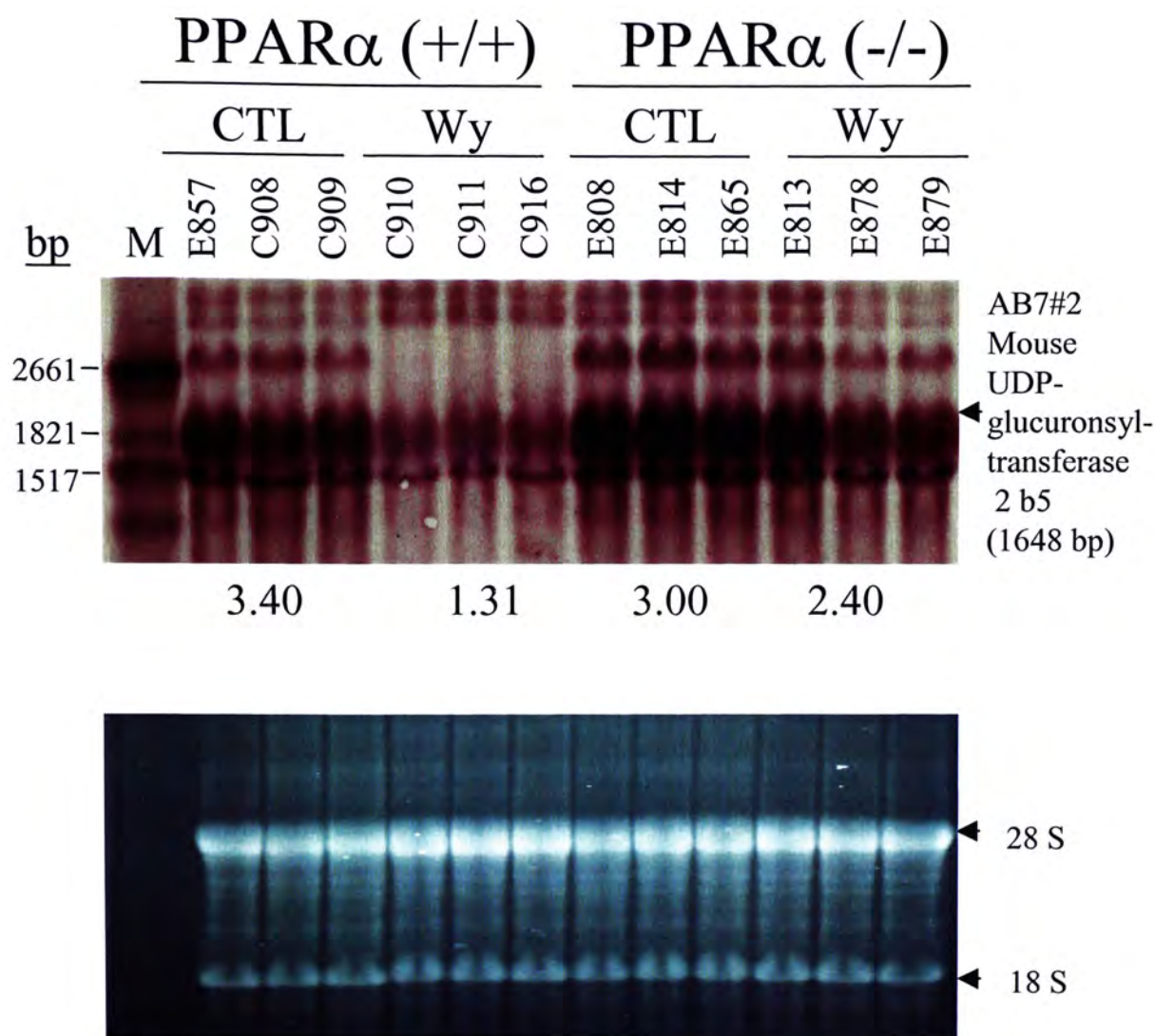


Figure 3.11.5. Confirmation of fluoroDD expression pattern of subclone AB7#2 (UDP-glucuronosyltransferase 2b5) by Northern blot analysis. Total liver RNA (30 μ g) of three mice each of PPAR α (+/+) and PPAR α (-/-) fed with a 0.0% control (CTL) or 0.1% (w/w) Wy-14,643 (Wy) diet for 11 months was separated on a 1% agarose-formaldehyde gel and transferred to a nylon membrane. The membrane was then hybridized with a PCR DIG-labeled cDNA probe and signals were detected by colorimetric method with NBT and BCIP reagents. For normalization, ethidium bromide staining of RNA gel was used. M, RNA molecular weight marker I, DIG-labeled.



205

Table 3.11.2. Summary of Northern blot analysis of cDNA fragments subcloned from gel AB (AP3 and ARP3)

Gel	Subclone I.D.	Differential display pattern				Gene homology (Transcript size)	Northern blot analysis densitometry reading (arbitrary unit)				
		PPAR α (+/+)		PPAR α (-/-)			PPAR α (+/+)		PPAR α (-/-)		
		CTL	Wy	CTL	Wy		CTL	Wy	Fold change (W _y /CTL)	CTL	Wy
AB (AP3 & ARP3)	AB7#2	+	++	+	+	Mouse UDP- glucuronosyltransferase 2 family, member 5, UGT2b5 (1648 bp)	3.40 ± 0.53	1.31 ± 0.08	3.00 ± 0.61	2.40 ± 0.21	0.80
							++	+	++	++	
							0.39				
	AB22#9	+	++	+	+	<i>Mus musculus</i> peroxisome biogenesis factor 16, Pex16 (1221 bp)	0.21 ± 0.05	0.83 ± 0.06	0.10 ± 0.01	0.09 ± 0.05	0.90
							+	++	+	+	
							3.95				
	AB25#6	-	+	-	-	<i>Mus musculus</i> cytochrome P450, family 4, subfamily a, polypeptide 14, Cyp4a14 (2547 bp)	0.03 ± 0.02	3.15 ± 0.64	0.01 ± 0.01	0.01 ± 0.01	1.00
							-	++	-	-	
							105.00				

Values represent mean \pm S.D. '+' represents the presence of a band (cDNA) on fluoroDD gel or Northern blot, while '-' represents the corresponding band (cDNA) was not observed on the fluoroDD gel or Northern blot. The relative intensity of the gene expression among the four treatment groups is indicated by the number of '+'. The signal intensity of a band on Northern blot was quantified by MultiAnalyst.

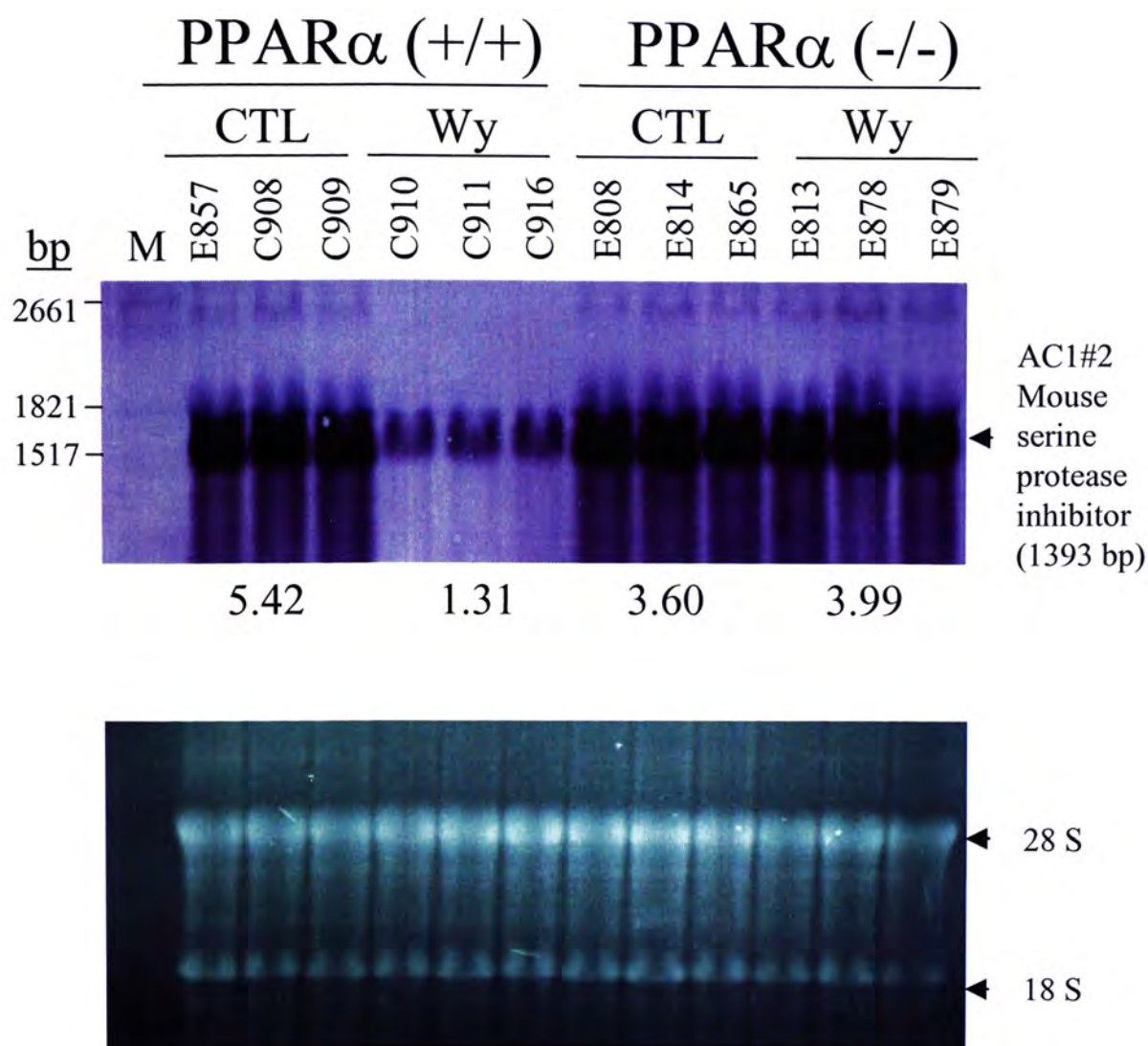


Figure 3.11.8. Confirmation of fluoroDD expression pattern of subclone AC1#2 (serine protease inhibitor) by Northern blot analysis. Total liver RNA (30 μ g) of three mice each of PPAR α (+/+) and PPAR α (-/-) fed with a 0.0% control (CTL) or 0.1% (w/w) Wy-14,643 (Wy) diet for 11 months was separated on a 1% agarose-formaldehyde gel and transferred to a nylon membrane. The membrane was then hybridized with a DIG-labeled RNA probe and signals were detected by colorimetric method with NBT and BCIP reagents. For normalization, ethidium bromide staining of RNA gel was used. M, RNA molecular weight marker I, DIG-labeled.

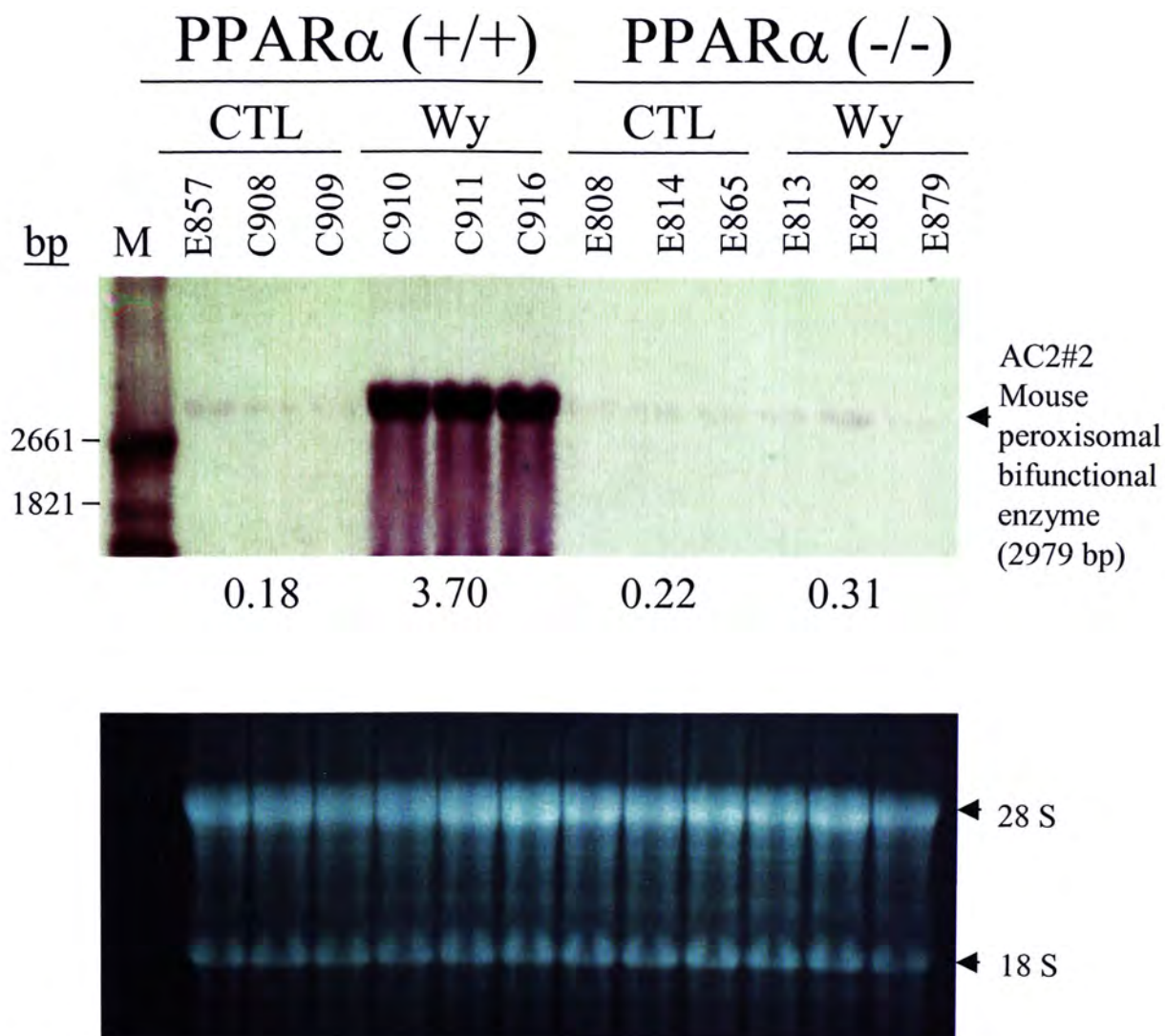


Figure 3.11.9. Confirmation of fluoroDD expression pattern of subclone AC2#2 (peroxisomal bifunctional enzyme) by Northern blot analysis. Total liver RNA (30 μ g) of three mice each of PPAR α (+/+) and PPAR α (-/-) fed with a 0.0% control (CTL) or 0.1% (w/w) Wy-14,643 (Wy) diet for 11 months was separated on a 1% agarose-formaldehyde gel and transferred to a nylon membrane. The membrane was then hybridized with a DIG-labeled RNA probe and signals were detected by colorimetric method with NBT and BCIP reagents. For normalization, ethidium bromide staining of RNA gel was used. M, RNA molecular weight marker I, DIG-labeled.

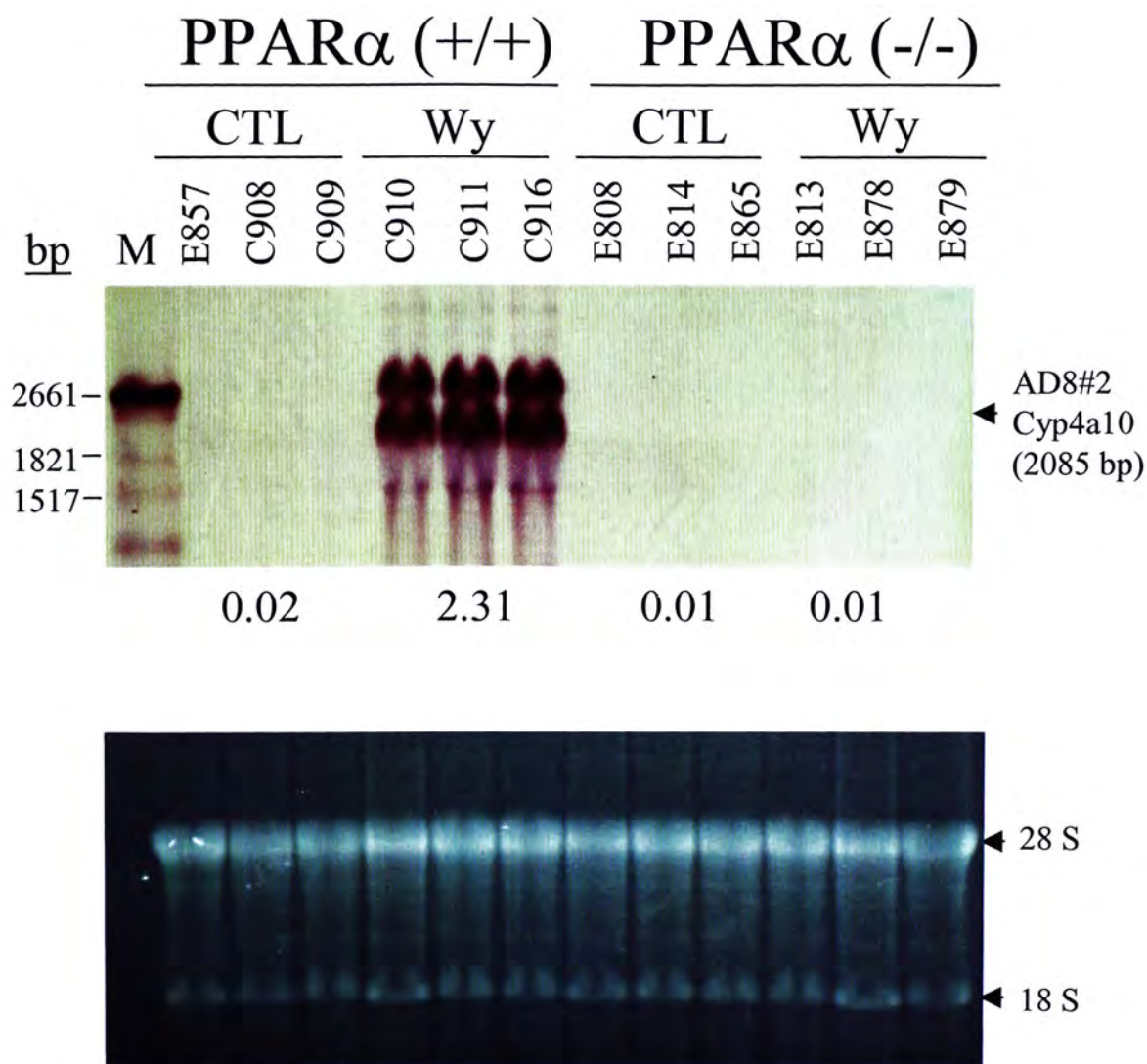


Figure 3.11.10. Confirmation of fluoroDD expression pattern of subclone AD8#2 (cytochrome P450, family 4, subfamily a, polypeptide 10) by Northern blot analysis. Total liver RNA (30 μ g) of three mice each of PPAR α (+/+) and PPAR α (-/-) fed with a 0.0% control (CTL) or 0.1% (w/w) Wy-14,643 (Wy) diet for 11 months was separated on a 1% agarose-formaldehyde gel and transferred to a nylon membrane. The membrane was then hybridized with a DIG-labeled RNA probe and signals were detected by colorimetric method with NBT and BCIP reagents. For normalization, ethidium bromide staining of RNA gel was used. M, RNA molecular weight marker I, DIG-labeled.

Table 3.11.3. Summary of Northern blot analysis of cDNA fragments subcloned from gels AC (AP2 and ARP19) and AD (AP2 and ARP18)

Gel	Subclone I.D.	Differential display pattern				Gene homology (Transcript size)	Northern blot analysis densitometry reading (arbitrary unit)							
		PPAR α (+/+)		PPAR α (-/-)			PPAR α (+/+)		PPAR α (-/-)					
		CTL	Wy	CTL	Wy		CTL	Wy	CTL	Wy	Fold change (Wy/CTL)			
AC (AP2 & ARP19)	AC1#2	+	-	+	+	<i>Mus musculus</i> serine (or cysteine) proteinase inhibitor, SPI (1393 bp)	5.42	1.31	3.60	3.99	0.24	0.22	0.31	1.11
							± 0.68	± 0.15	± 0.72	± 0.68				
							+++	+	+++	+++				
	AC2#2	-	+	-	-	<i>Mus musculus</i> peroxisomal bifunctional enzyme (PBE) (PBFE) [includes: enoyl-CoA hydratase (EC 4.2.1.17); 3,2-trans enoyl-CoA isomerase (EC 5.3.3.8); 3-hydroxyacyl-CoA dehydrogenase (EC 1.1.1.35)], PBFE (2979 bp)	0.18	3.70	0.22	0.31	20.56	+	+	1.41
	AD (AP2 & ARP18)	AD8#2	+	++	+	<i>Mus musculus</i> cytochrome P450, family 4, subfamily a, polypeptide 10, Cyp4a10 (2085 bp)	0.02	2.31	0.01	0.01	115.50	0.01	0.01	1.00
							± 0.02	± 0.18	± 0.01	± 0.00				
							-	+++	-	-				

Values represent mean \pm S.D. '+' represents the presence of a band (cDNA) on fluoroDD gel or Northern blot, while '-' represents the corresponding band (cDNA) was not observed on the fluoroDD gel or Northern blot. The relative intensity of the gene expression among the four treatment groups is indicated by the number of '+'. The signal intensity of a band on Northern blot was quantified by MultiAnalyst.

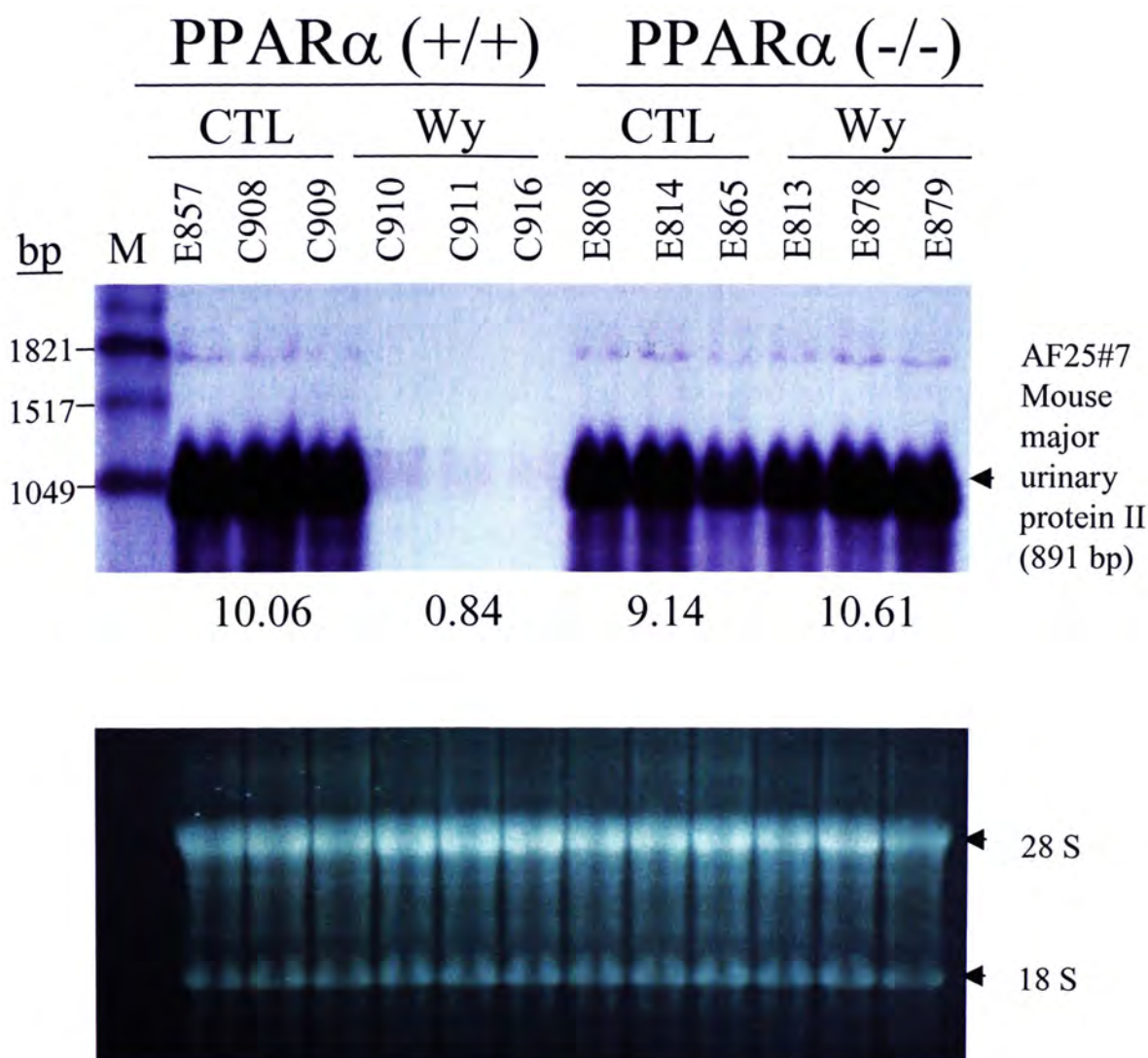


Figure 3.11.12. Confirmation of fluoroDD expression pattern of subclone AF25#7 (mouse major urinary protein II) by Northern blot analysis. Total liver RNA (30 μ g) of three mice each of PPAR α (+/+) and PPAR α (-/-) fed with a 0.0% control (CTL) or 0.1% (w/w) Wy-14,643 (Wy) diet for 11 months was separated on a 1% agarose-formaldehyde gel and transferred to a nylon membrane. The membrane was then hybridized with a DIG-labeled RNA probe and signals were detected by colorimetric method with NBT and BCIP reagents. For normalization, ethidium bromide staining of RNA gel was used. M, RNA molecular weight marker I, DIG-labeled.

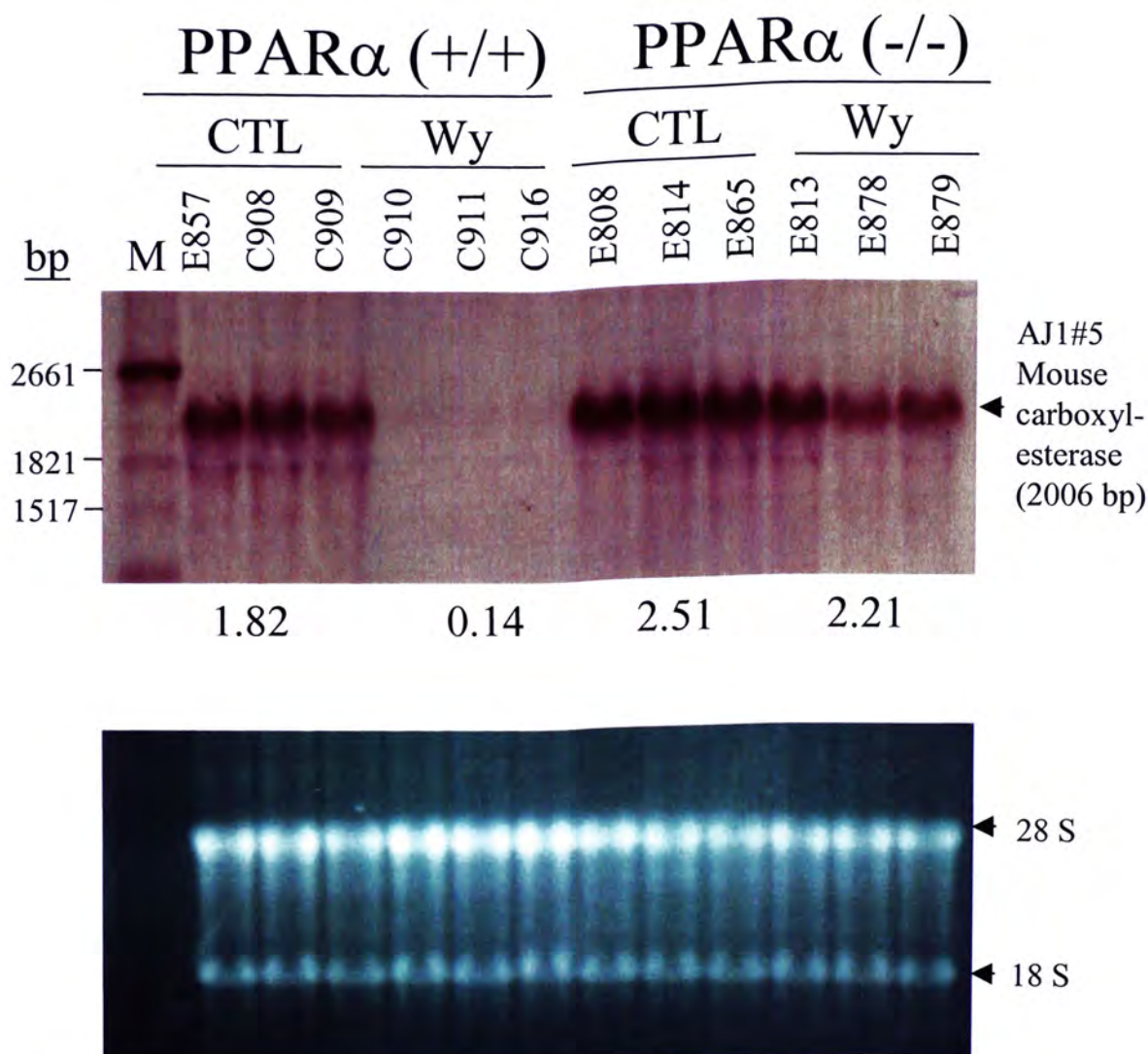


Figure 3.11.13. Confirmation of fluoroDD expression pattern of subclone AJ1#5 (carboxylesterase) by Northern blot analysis. Total liver RNA (30 μ g) of three mice each of PPAR α (+/+) and PPAR α (-/-) fed with a 0.0% control (CTL) or 0.1% (w/w) Wy-14,643 (Wy) diet for 11 months was separated on a 1% agarose-formaldehyde gel and transferred to a nylon membrane. The membrane was then hybridized with a DIG-labeled RNA probe and signals were detected by colorimetric method with NBT and BCIP reagents. For normalization, ethidium bromide staining of RNA gel was used. M, RNA molecular weight marker I, DIG-labeled.

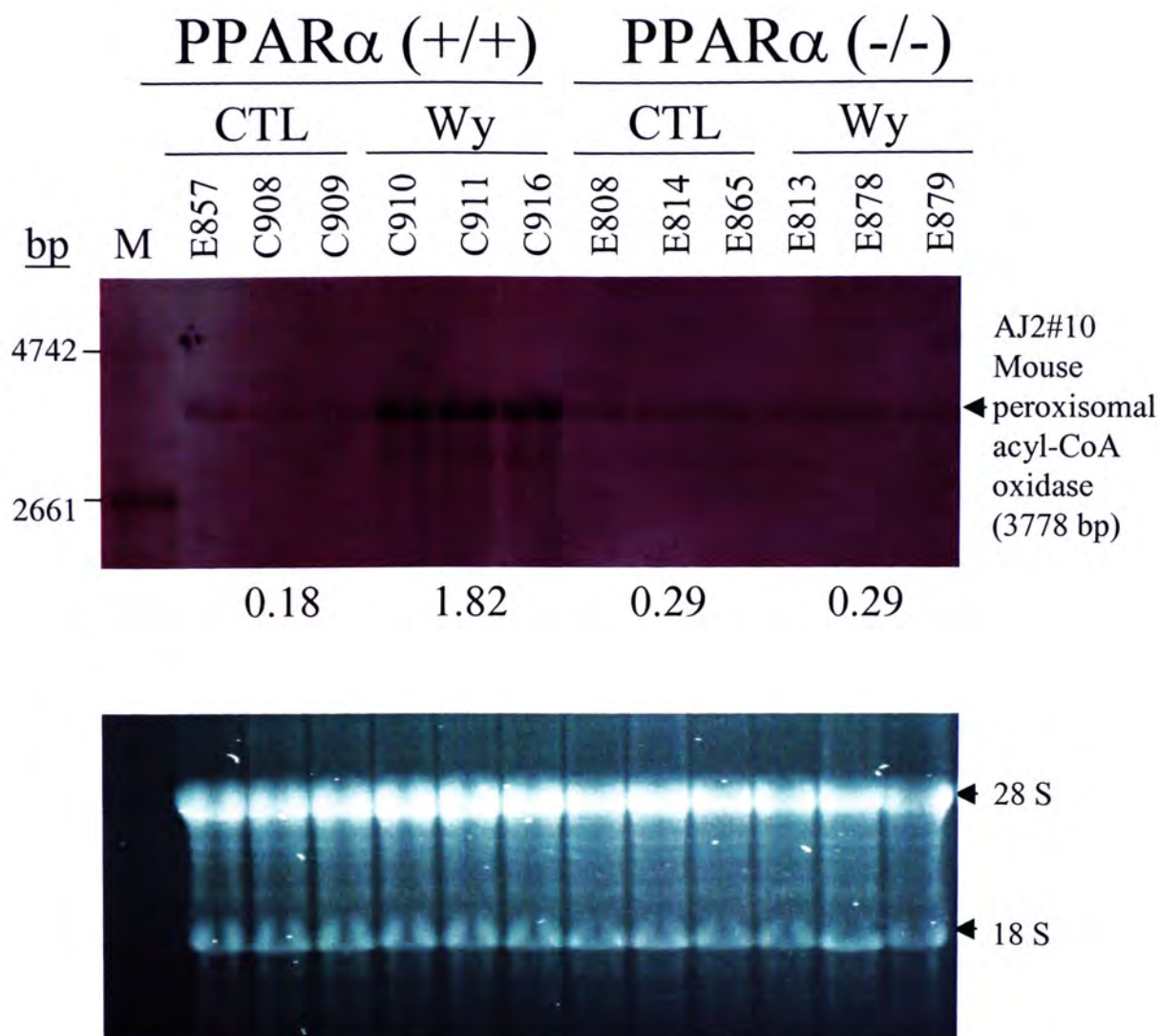
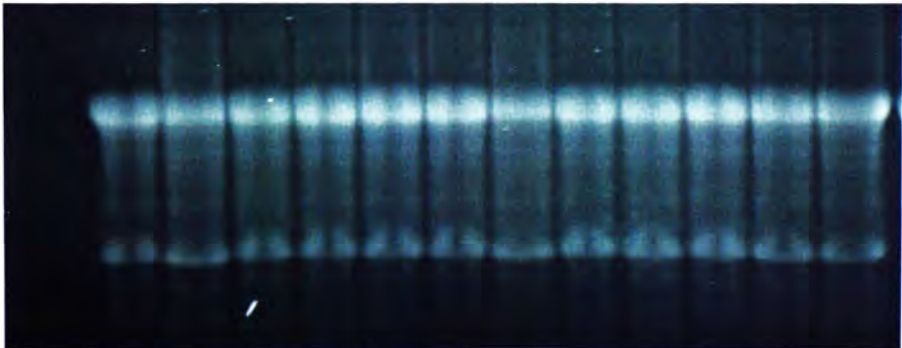


Figure 3.11.14. Confirmation of fluoroDD expression pattern of subclone AJ2#10 (peroxisomal acyl-CoA oxidase) by Northern blot analysis. Total liver RNA (30 μ g) of three mice each of PPAR α (+/+) and PPAR α (-/-) fed with a 0.0% control (CTL) or 0.1% (w/w) Wy-14,643 (Wy) diet for 11 months was separated on a 1% agarose-formaldehyde gel and transferred to a nylon membrane. The membrane was then hybridized with a DIG-labeled RNA probe and signals were detected by colorimetric method with NBT and BCIP reagents. For normalization, ethidium bromide staining of RNA gel was used. M, RNA molecular weight marker I, DIG-labeled.

Table 3.11.4. Summary of Northern blot analysis of cDNA fragments subcloned from gels AF (AP10 and ARP13) and AJ (AP6 and ARP14)

Gel	Subclone I.D.	Differential display pattern				Gene homology (Transcript size)	Northern blot analysis densitometry reading (arbitrary unit)						
		PPAR α (+/+)		PPAR α (-/-)			PPAR α (+/+)			PPAR α (-/-)			
		CTL	Wy	CTL	Wy		Fold change (Wy/CTL)	CTL	Wy	Fold change (Wy/CTL)	CTL	Wy	Fold change (Wy/CTL)
AF (AP10 & ARP13)	AF1#8	+	++	+	+	<i>Mus musculus</i> very-long-chain acyl-CoA synthetase, VLACS (2209 bp)	1.30 \pm 0.21	2.70 \pm 0.32	2.08	0.80 \pm 0.17	1.10 \pm 0.44	1.38	
		++	+++	++	+	+							
		AF25#7	++	+	++	++	<i>Mus musculus</i> major urinary protein 2, MUP II (891 bp)	10.06 \pm 1.04	0.84 \pm 0.32	0.08	9.14 \pm 1.57	10.61 \pm 1.21	1.16
			+++	+	+++	+++	+++	+++					
AJ (AP6 & ARP14)	AJ1#5		++	+	++	++	Mouse carboxylesterase, Carboxylesterase (2006 bp)	1.82 \pm 0.20	0.14 \pm 0.03	0.08	2.51 \pm 0.26	2.21 \pm 0.97	0.88
			+++	-	+++	+++	+++	+++					
		AJ2#10	+	++	+	+	<i>Mus musculus</i> peroxisomal acyl-CoA oxidase, AOX (3778 bp)	0.18 \pm 0.07	1.82 \pm 0.10	10.11	0.29 \pm 0.04	0.29 \pm 0.02	1.00
			+	++	+	+	+	++	+		+		

Values represent mean \pm S.D. '+' represents the presence of a band (cDNA) on fluoroDD gel or Northern blot, while '-' represents the corresponding band (cDNA) was not observed on the fluoroDD gel or Northern blot. The relative intensity of the gene expression among the four treatment groups is indicated by the number of '+'. The signal intensity of a band on Northern blot was quantified by MultiAnalyst.



216

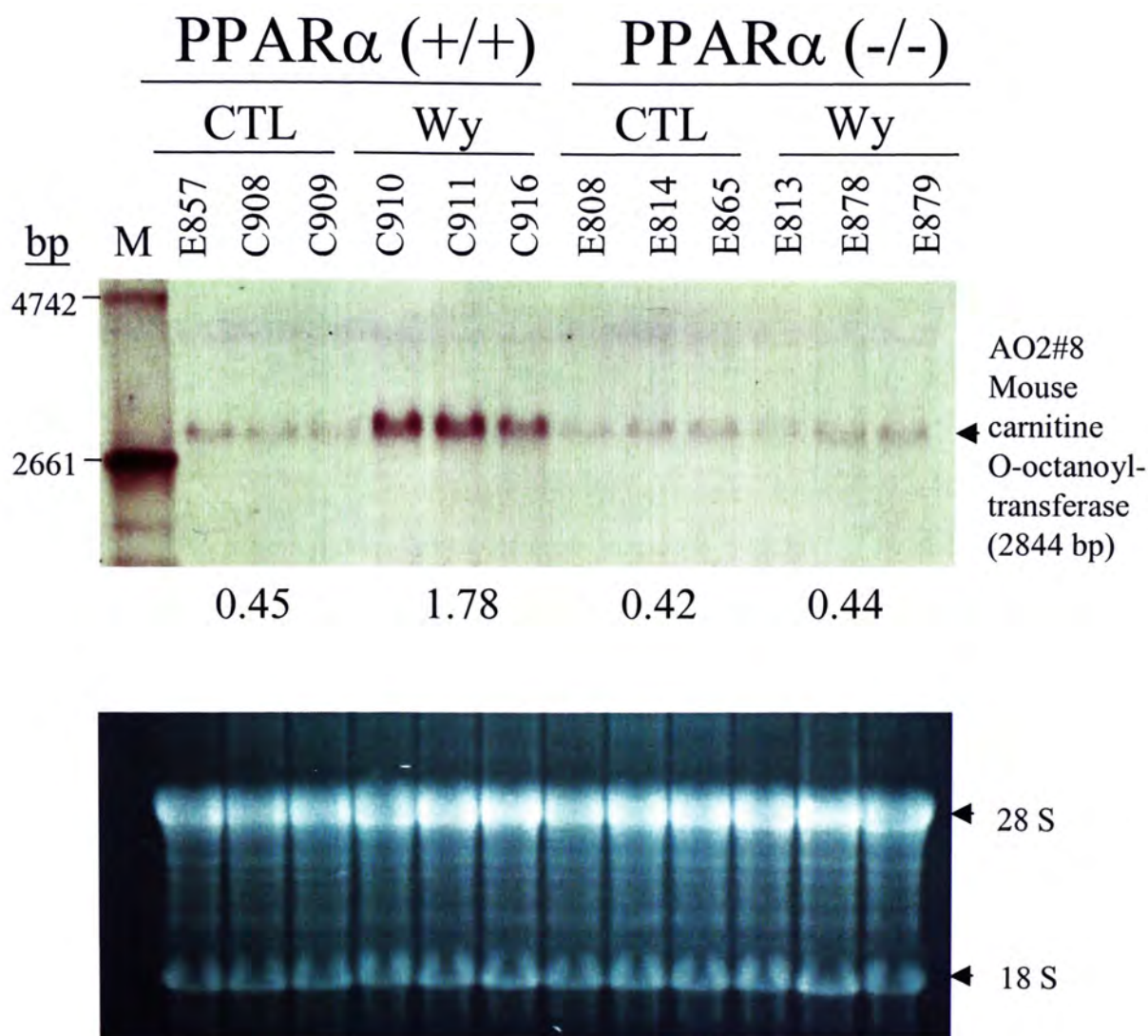


Figure 3.11.17. Confirmation of fluoroDD expression pattern of subclone AO2#8 (carnitine O-octanoyltransferase) by Northern blot analysis. Total liver RNA (30 μ g) of three mice each of PPAR α (+/+) and PPAR α (-/-) fed with a 0.0% control (CTL) or 0.1% (w/w) Wy-14,643 (Wy) diet for 11 months was separated on a 1% agarose-formaldehyde gel and transferred to a nylon membrane. The membrane was then hybridized with a DIG-labeled RNA probe and signals were detected by colorimetric method with NBT and BCIP reagents. For normalization, ethidium bromide staining of RNA gel was used. M, RNA molecular weight marker I, DIG-labeled.

Table 3.11.5. Summary of Northern blot analysis of cDNA fragments subcloned from gels AL (AP7 and ARP15) and AO (AP5 and ARP10)

Gel	Subclone I.D.	Differential display pattern				Gene homology (Transcript size)	Northern blot analysis densitometry reading (arbitrary unit)					
		PPAR α (+/+)		PPAR α (-/-)			PPAR α (+/+)			PPAR α (-/-)		
		CTL	Wy	CTL	Wy		CTL	Wy	Fold change (W _y /CTL)	CTL	Wy	Fold change (W _y /CTL)
AL (AP7 & ARP15)	AL3#3	+	++	+	+	<i>Mus musculus</i> hydroxysteroid (17-beta) dehydrogenase 11, HSD17 β 11 (1713 bp)	0.30 \pm 0.07	3.15 \pm 0.85	10.50	0.27 \pm 0.09	0.31 \pm 0.07	1.15
							+	++		+	+	
AO (AP5 & ARP10)	AO1#2	+	++	+	+	Mouse adipose differentiation related protein, ADRP (1680 bp)	0.13 \pm 0.06	2.08 \pm 0.12	16.00	0.07 \pm 0.05	0.07 \pm 0.04	1.00
							-	+		-	-	
	AO2#8	+	++	+	+	<i>Mus musculus</i> carnitine O-octanoyltransferase, Crot (2844 bp)	0.45 \pm 0.06	1.78 \pm 0.32	3.96	0.42 \pm 0.12	0.44 \pm 0.12	1.05
							+	++		+	+	

Values represent mean \pm S.D. '+' represents the presence of a band (cDNA) on fluoroDD gel or Northern blot, while '-' represents the corresponding band (cDNA) was not observed on the fluoroDD gel or Northern blot. The relative intensity of the gene expression among the four treatment groups is indicated by the number of '+'. The signal intensity of a band on Northern blot was quantified by MultiAnalyst.

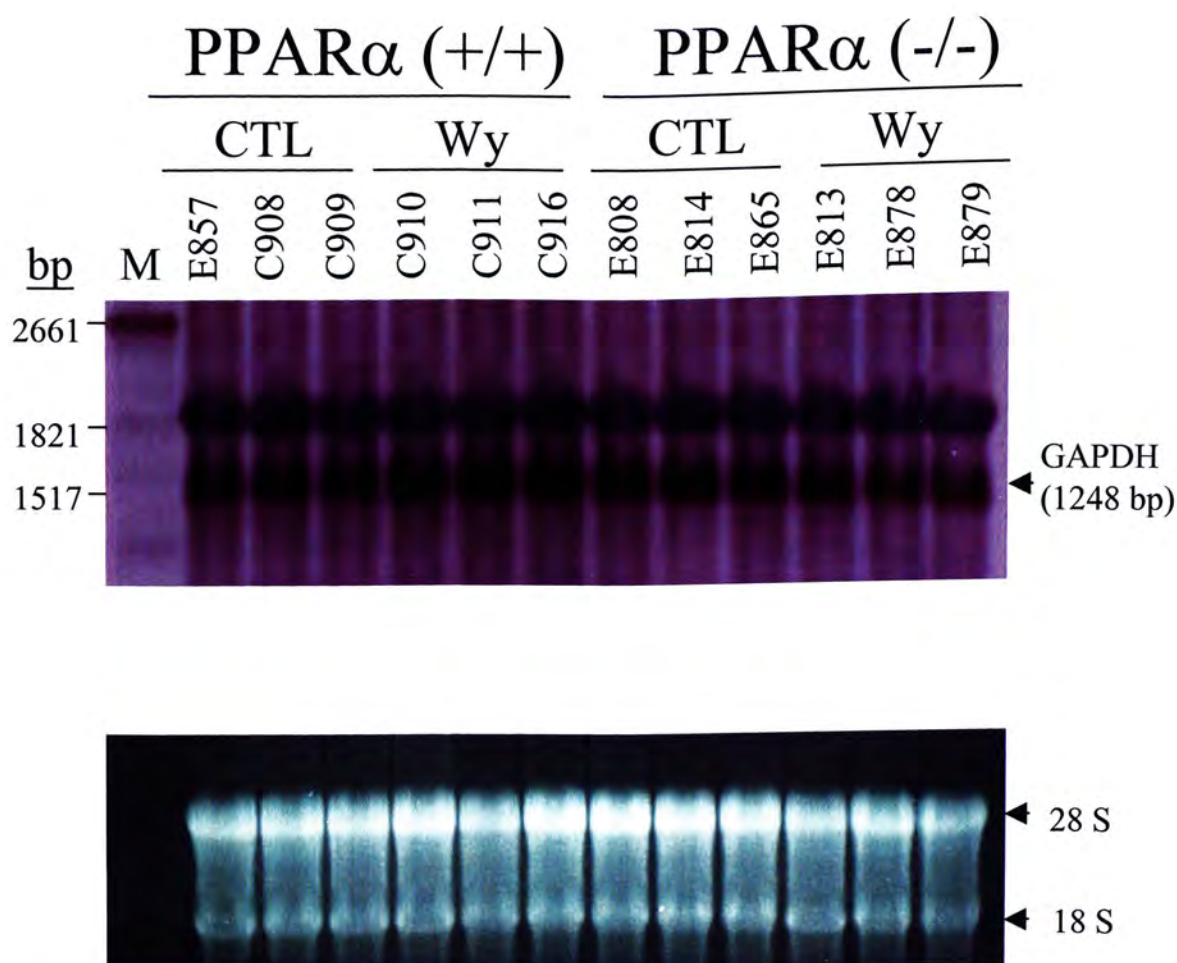


Figure 3.11.18. Up-regulation of GAPDH was observed in PPAR α (+/+) mice fed with a 0.1% (w/w) Wy-14,643 diet for 11 months. Total liver RNA (30 μ g) of three mice each of PPAR α (+/+) and PPAR α (-/-) fed with a 0.0% control (CTL) or 0.1% (w/w) Wy-14,643 (Wy) diet for 11 months was separated on a 1% agarose-formaldehyde gel and transferred to a nylon membrane. The membrane was then hybridized with a DIG-labeled RNA probe and signals were detected by colorimetric method with NBT and BCIP reagents. For normalization, ethidium bromide staining of RNA gel was used. M, RNA molecular weight marker I, DIG-labeled.

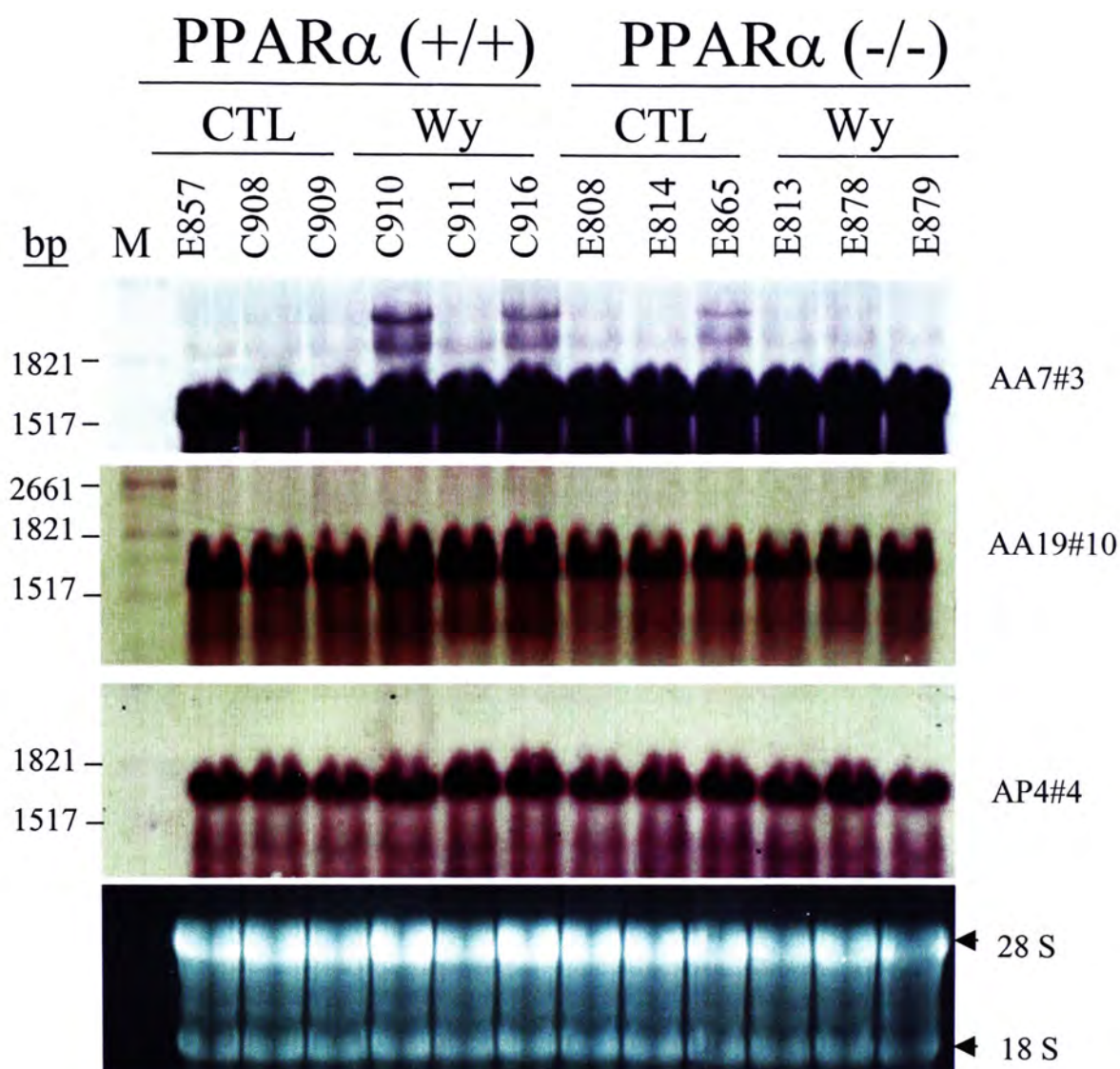


Figure 3.11.19. Confirmation of fluoroDD expression pattern of mitochondria by Northern blot analysis. Total liver RNA (30 μ g) of three mice each of PPAR α (+/+) and PPAR α (-/-) fed with a 0.0% control (CTL) or 0.1% (w/w) Wy-14,643 (Wy) diet for 11 months was separated on a 1% agarose-formaldehyde gel and transferred to a nylon membrane. The membrane was then hybridized with a DIG-labeled RNA probe and signals were detected by colorimetric method with NBT and BCIP reagents. For normalization, ethidium bromide staining of RNA gel was used. M, RNA molecular weight marker I, DIG-labeled.

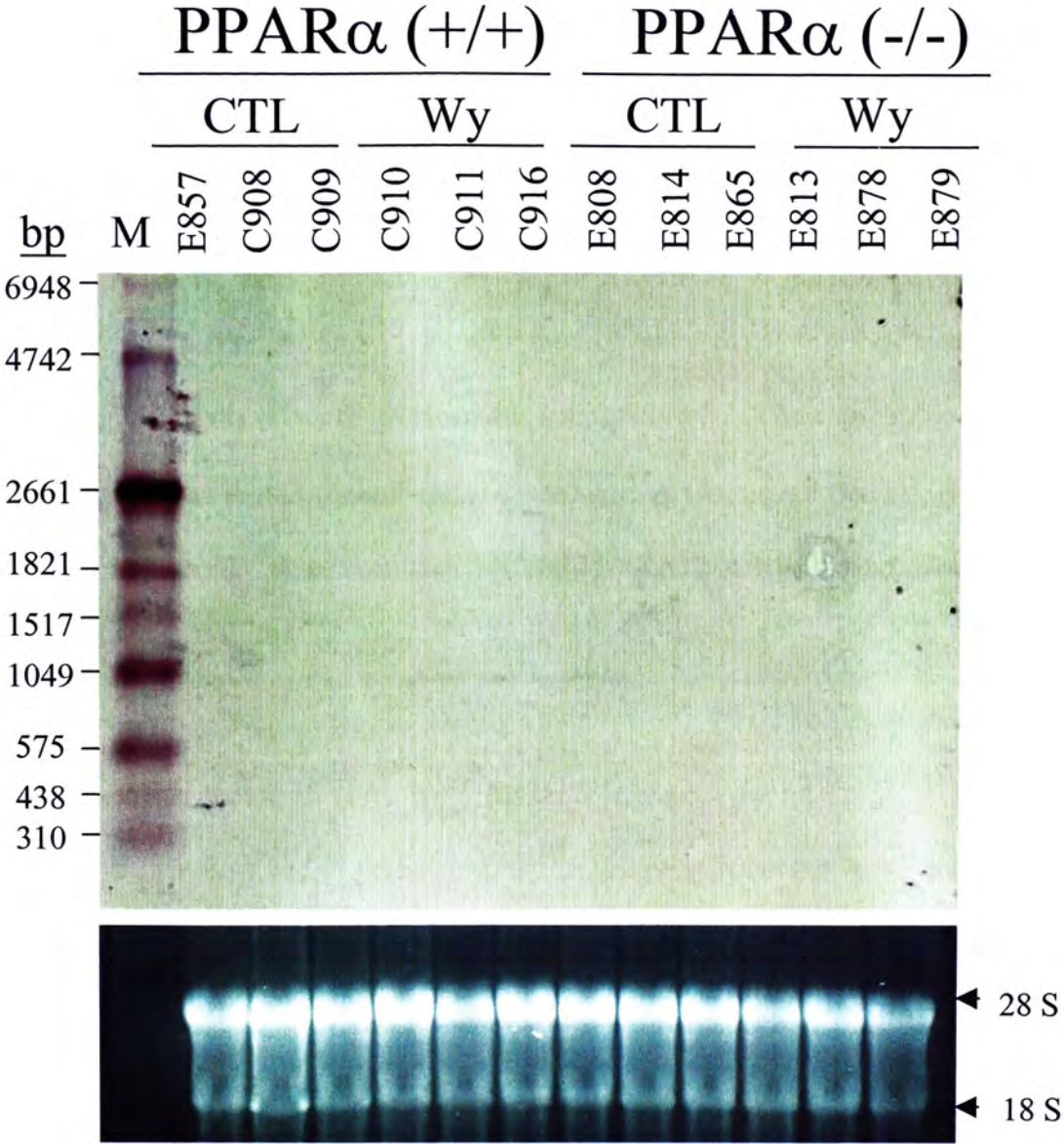


Figure 3.11.20. Confirmation of fluoroDD expression pattern of EST by Northern blot analysis. Total liver RNA (30 μg) of three mice each of PPARα (+/+) and PPARα (-/-) fed with a 0.0% control (CTL) or 0.1% (w/w) Wy-14,643 (Wy) diet for 11 months was separated on a 1% agarose-formaldehyde gel and transferred to a nylon membrane. The membrane was then hybridized with a DIG-labeled RNA probe and signals were detected by colorimetric method with NBT and BCIP reagents. For normalization, ethidium bromide staining of RNA gel was used. M, RNA molecular weight marker I, DIG-labeled.

(UDP2b5)] gave different patterns from fluoroDD patterns in Northern blot analysis. It might be due to the co-migrated cDNA fragments in fluoroDD gel which have other fluoroDD pattern.

In order to study the time effect of the Wy-14,643 on the PPAR α regulated gene, Northern blot analysis was performed with RNA samples from 24 hour, 1 week, 2 weeks, 6 months and 11 months feeding mice of all the four treatment groups. A total of sixteen were performed successfully. They included AA1#2 [mouse peroxisomal delta3, delta2-enoyl-Coenzyme A isomerase (Peci)]; AA10#1 [cysteine sulfinic acid decarboxylase (Csad)]; AA12#4 [mouse acetyl-Coenzyme A dehydrogenase, medium chain (MCAD)]; AB7#2 [mouse UDP-glucuronosyltransferase 2 family member 5, (UDP2b5)]; AB22#9 [peroxisome biogenesis factor 16 (Pex 16)]; AB25#6 [mouse cytochrome P450 4a14 (Cyp4a14)]; AC1#2 [mouse serine protease inhibitor, clade A, member 1a (SPI)]; AC2#2 [mouse peroxisomal bifunctional enzyme (PBFE)]; AD8#2 [mouse cytochrome P450 4a10 (Cyp4a10)]; AF1#8 [very-long-chain acyl-CoA synthetase (VLACS)]; AF25#7 [mouse major urinary protein II (MUP II)]; AJ1#5 [mouse carboxyesterase (carboxyesterase)]; AJ2#10 [mouse peroxisomal acyl-CoA oxidase (AOX)]; AL3#3 [mouse hydroxysteroid (17-beta) dehydrogenase 11, (Hsd17 β 11)]; AO1#2 [mouse adipose differentiation related protein (ADRP)] and AO2#8 [mouse carnitine O-octanoyltransferase (Crot)]. The signals were quantified by MultiAnalyst and fold change was calculated.

Up-regulation of AA1#2 [mouse peroxisomal delta3, delta2-enoyl-Coenzyme A isomerase (Peci) (Figure 3.11.21) (Table 3.11.6)] in PPAR α (+/+) mice fed with the 0.1% Wy-14,643 diet was started at 24 hours gavage feeding and continued to 11 months feeding. Maximum induction was observed at 24 hours gavage feeding (6.6-

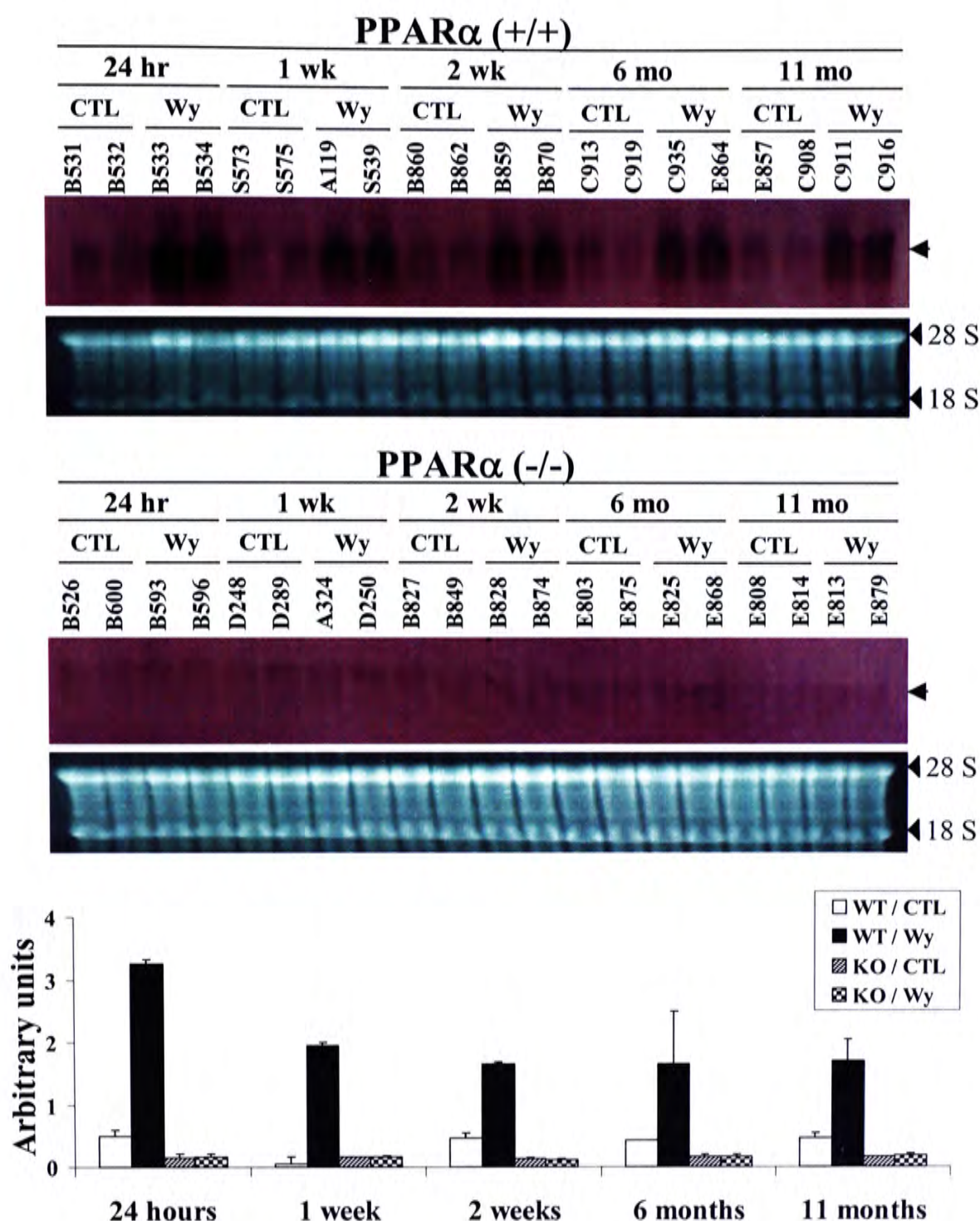


Figure 3.11.21. Temporal expression of AA1#2 (peroxisomal delta 3, delta 2-enoyl-coenzyme A isomerase). Total liver RNA (30 μ g) of two mice of PPAR α (+/+) and PPAR α (-/-) fed with a 0.0% control (CTL) or 0.1% (w/w) Wy-14,643 (Wy) diet for 24 hours, 1 week, 2 weeks, 6 months and 11 months treatment was separated on 1% agarose-formaldehyde gels and transferred to nylon membranes. The membranes were then hybridized with a PCR DIG-labeled cDNA probe and signals were detected by colorimetric method with NBT and BCIP reagents.

Table 3.11.6. Summary of Northern blot analysis on temporal expression patterns of cDNA fragments subcloned from gel AA (API and ARP2)

Gel	Subclone I.D.	Gene homology (Transcript size)	Northern blot densitometry reading (arbitrary units)											
			PPAR α (+/+)						PPAR α (-/-)					
			24 hr		1 wk		2 wk		6 mo		11 mo		24 hr	
			CTL	Wy	CTL	Wy	CTL	Wy	CTL	Wy	CTL	Wy	CTL	Wy
AA (API & ARP2)	AA 1#2	<i>Mus musculus</i> peroxisomal delta 3, delta 2-enoyl-coenzyme A isomerase, Peci (1581 bp)	0.49 \pm 0.11	3.25 \pm 0.08	0.53 \pm 0.11	1.95 \pm 0.05	0.46 \pm 0.09	1.69 \pm 0.02	0.43 \pm 0.00	1.66 \pm 0.84	0.46 \pm 0.08	1.70 \pm 0.35	0.15 \pm 0.06	0.17 \pm 0.04
													0.16 \pm 0.03	0.16 \pm 0.04
	Fold change (Wy/CTL)		6.63	3.67	3.67	3.67	3.67	3.67	3.86	3.70	1.13	2.00	0.92	0.94
														1.13
	AA 10#1	<i>Mus musculus</i> cysteine sulfinic acid decarboxylase, Csad (2265 bp)	0.01 \pm 0.02	0.02 \pm 0.02	0.06 \pm 0.00	0.12 \pm 0.00	0.03 \pm 0.00	0.10 \pm 0.03	0.02 \pm 0.01	0.09 \pm 0.02	0.04 \pm 0.02	0.11 \pm 0.01	0.01 \pm 0.00	0.01 \pm 0.00
													0.02 \pm 0.01	0.04 \pm 0.00
	Fold change (Wy/CTL)		2.00	2.00	2.00	3.33	3.33	4.5	2.75	1.00	1.00	1.00	1.00	1.00
														1.00
	AA 12#4	<i>Mus musculus</i> acetyl-coenzyme A dehydrogenase, medium chain, MCAD (1857 bp)	0.12 \pm 0.07	0.46 \pm 0.13	0.14 \pm 0.03	0.57 \pm 0.24	0.10 \pm 0.08	0.32 \pm 0.08	0.10 \pm 0.03	0.27 \pm 0.07	0.13 \pm 0.01	0.41 \pm 0.04	0.03 \pm 0.00	0.03 \pm 0.00
													0.01 \pm 0.00	0.01 \pm 0.00
	Fold change (Wy/CTL)		3.83	4.07	3.20	2.70	3.15	1.00	1.00	1.00	1.00	1.00	1.00	1.00
														1.00

Values represent mean \pm S.D. ‘+’ represents the presence of a band (cDNA) on fluoroDD gel or Northern blot, while ‘-’ represents the corresponding band (cDNA) was not observed on the fluoroDD gel or Northern blot. The relative intensity of the gene expression among the four treatment groups is indicated by the number of ‘+’. The signal intensity of a band on Northern blot was quantified by MultiAnalyst.

fold). However, no induction was observed in PPAR α (-/-) mice fed with 0.1% Wy-14,643 when compared with the controls.

Very weak signal was obtained for the Northern blot analysis of time-dependent expression of fragment AA4#9 [mouse apolipoprotein A-V (Apoa5)].

Although weak signals were observed in the temporal expression of fragment AA10#1 [mouse cysteine sulfinic acid decarboxylase (Csd) (Figure 3.11.22) (Table 3.11.6)] consistent induction (2 to 5-fold) in 0.1% Wy-14,643 fed PPAR α (+/+) was started at 1 week and continued to 11 months treatment. The PPAR α (-/-) mice fed with the 0.1% Wy-14,643 diet did not show any induction when compared with the controls.

Similar to AA10#1, weak signals were found in the temporal expression of AA12#4 [mouse acetyl-Coenzyme A dehydrogenase, medium chain, MCAD (Figure 3.11.23) (Table 3.11.6)]. Consistent up-regulation (2 to 4-fold) started at 24 hours and continued to 11 months treatment of AA12#4 was observed. The up-regulation was not shown in 0.1% Wy-14,643-treated PPAR α (-/-) after short-term and long-term treatment.

cDNA fragment AB7#2 [mouse UDP-glucuronosyltransferase 2 family member 5, UGT2b5 (Figure 3.11.24) (Table 3.11.7)] showed down-regulation which started at 2 weeks and continued to 11 months treatment. Maximum down-regulation (0.39-fold) was observed at 11 months treatment. However, down-regulation was not observed in the PPAR α (-/-) mice fed with the 0.1% Wy-14,643 diet. Down-regulation bands were observed at about 2661 bp transcript in Wy-treated PPAR α (+/+) mice. This might be the other member of the UDP-glucuronosyltransferase 2 family that has similar homology to UGT2b5, e.g. UGT2b4 which transcriptional size is 2093 bp and show high homology to UGT2b5.

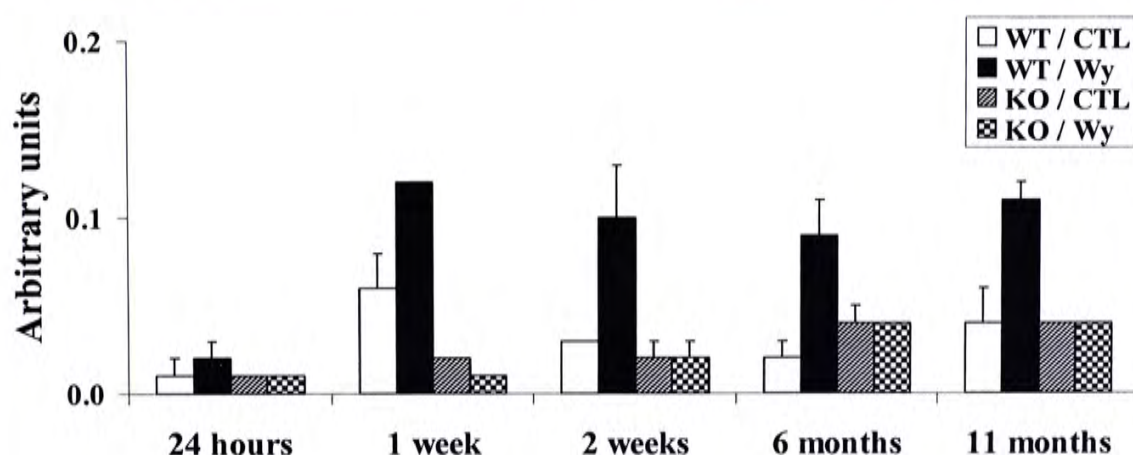
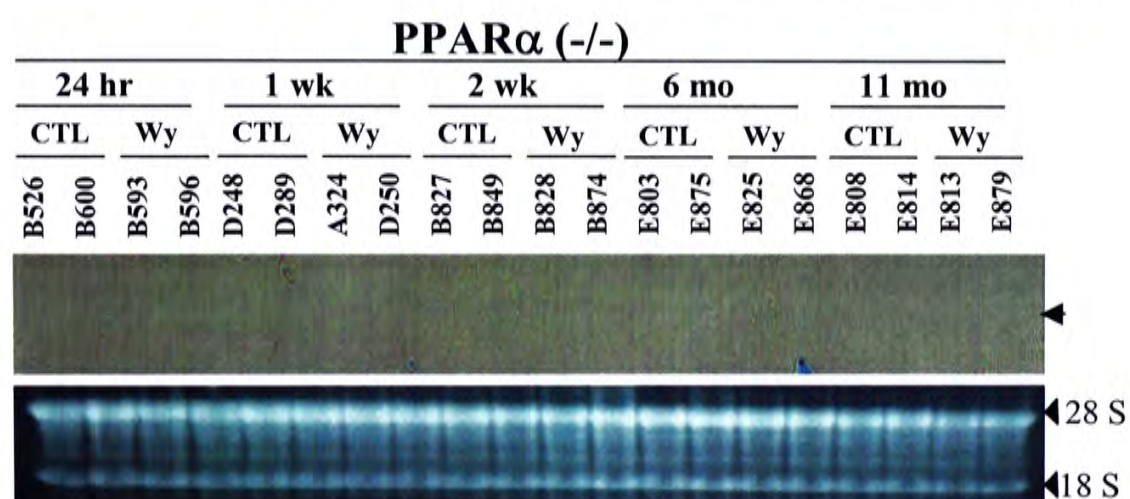
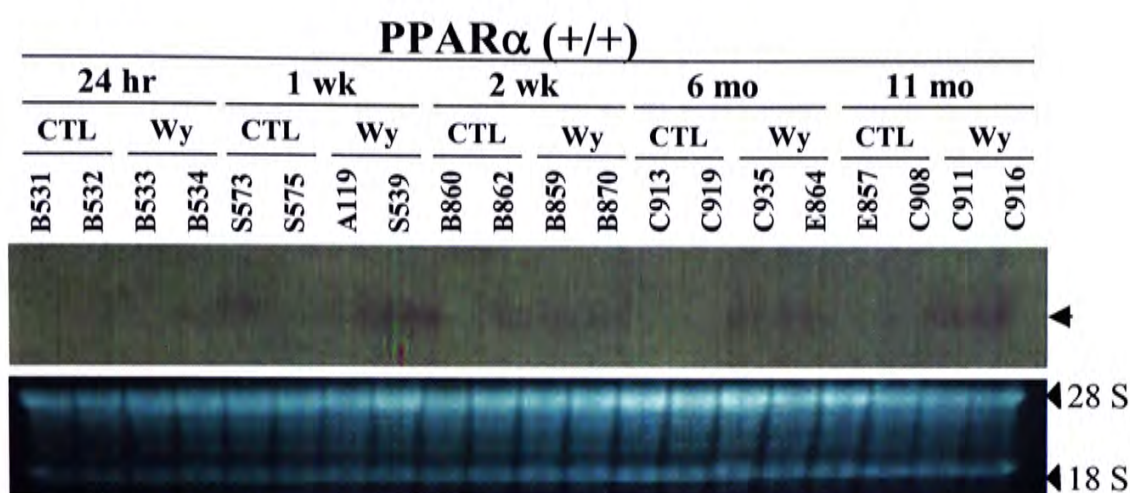


Figure 3.11.22. Temporal expression of AA10#1 (cysteine sulfinic acid decarboxylase). Total liver RNA (30 μ g) of two mice of PPAR α (+/+) and PPAR α (-/-) fed with a 0.0% control (CTL) or 0.1% (w/w) Wy-14,643 (Wy) diet for 24 hours, 1 week, 2 weeks, 6 months and 11 months treatment were separated on 1% agarose-formaldehyde gels and transferred to nylon membranes. The membranes were then hybridized with a PCR DIG cDNA probe and signals were detected by colorimetric method with NBT and BCIP reagents.

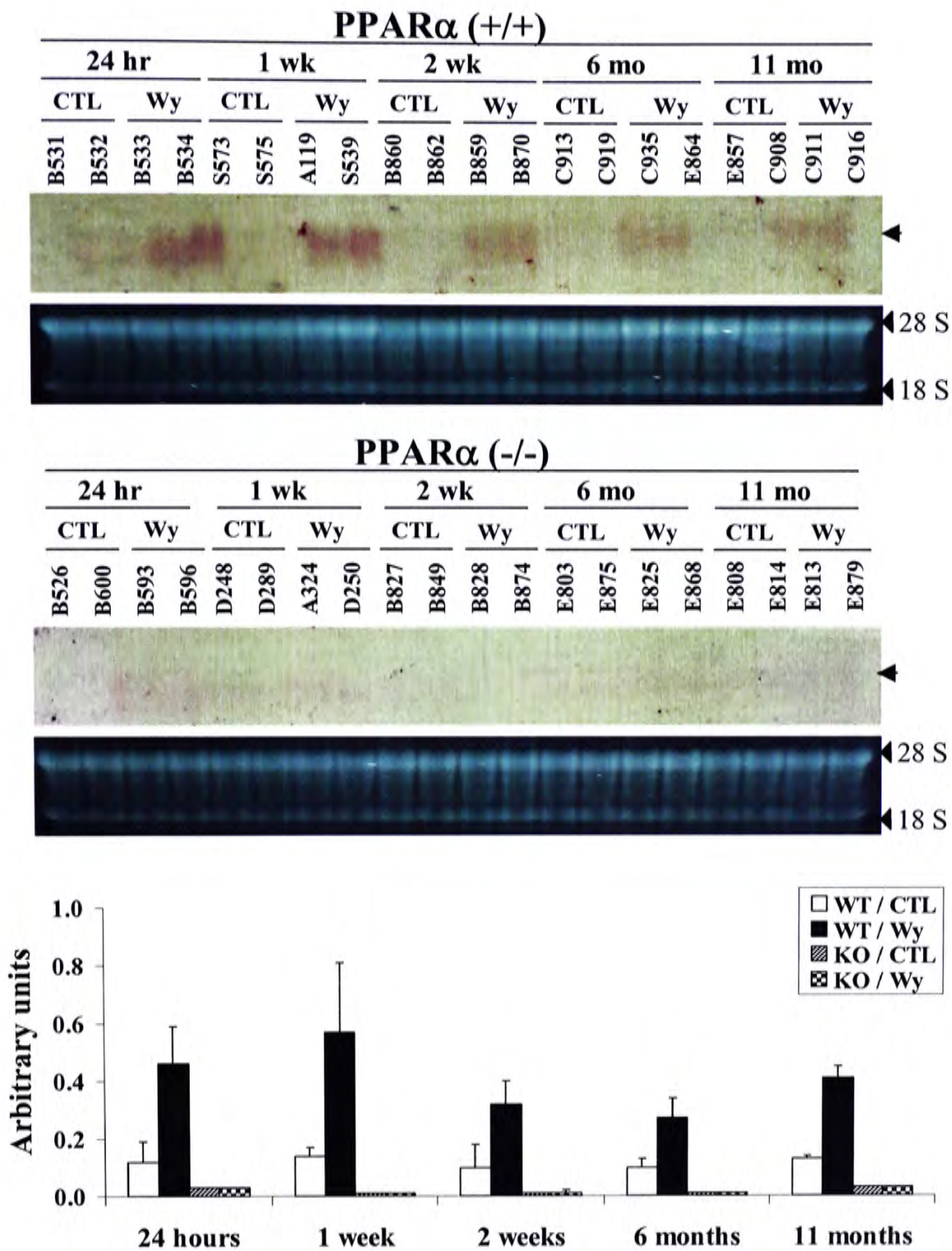


Figure 3.11.23. Temporal expression of AA12#4 (acetyl-Coenzyme A dehydrogenase, medium chain). Total liver RNA (30 μ g) of two mice of PPAR α (+/+) and PPAR α (-/-) fed with a 0.0% control (CTL) or 0.1% (w/w) Wy-14,643 (Wy) diet for 24 hours, 1 week, 2 weeks, 6 months and 11 months treatment were separated on 1% agarose-formaldehyde gels and transferred to nylon membranes. The membranes were then hybridized with a DIG-RNA labeled probe and signals were detected by colorimetric method with NBT and BCIP reagents.

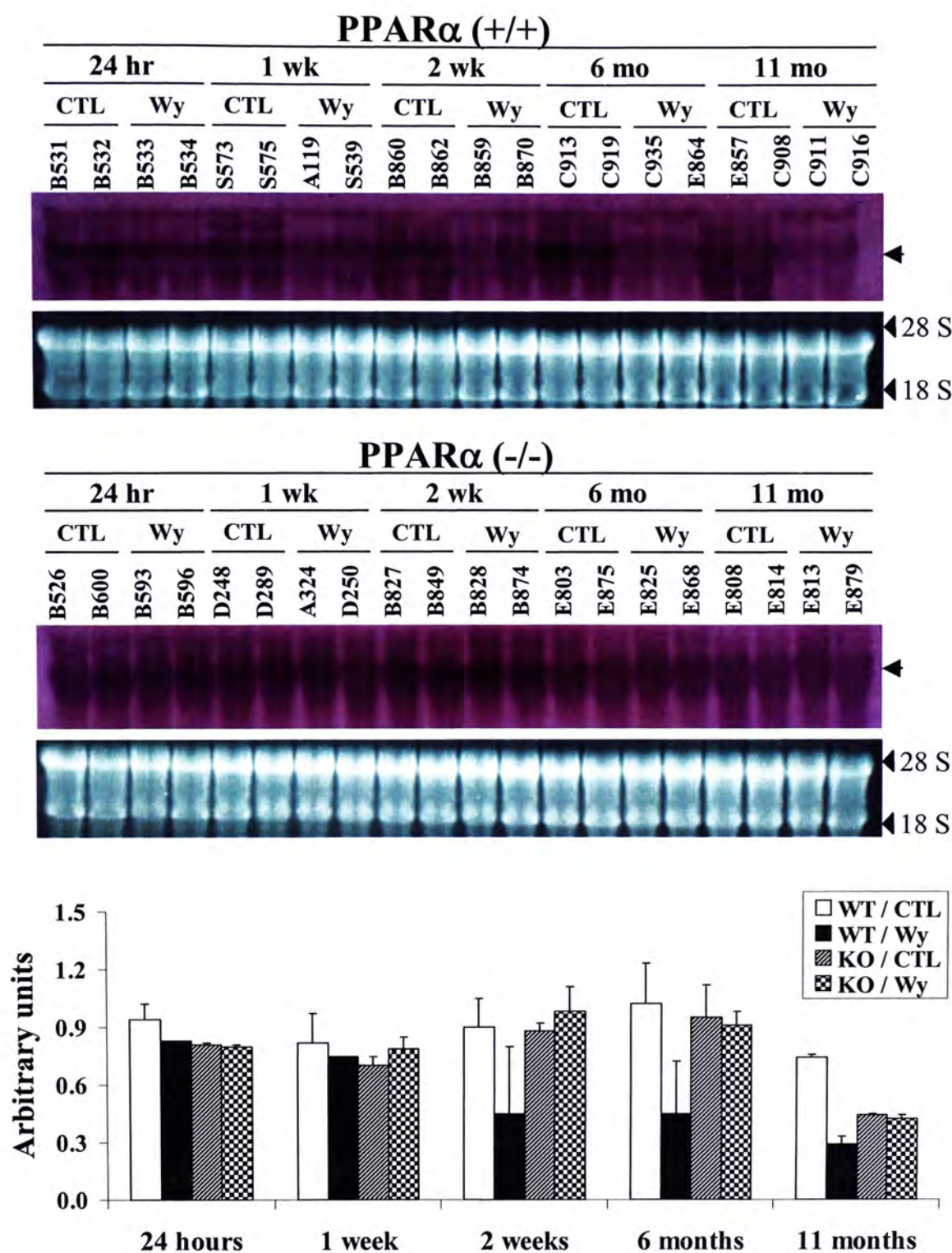


Figure 3.11.24. Temporal expression of AB7#2 (UDP-glucuronosyltransferase 2b5). Total liver RNA (30 μ g) of two mice of PPAR α (+/+) and PPAR α (-/-) fed with a 0.0% control (CTL) or 0.1% (w/w) Wy-14,643 (Wy) diet for 24 hours, 1 week, 2 weeks, 6 months and 11 months treatment were separated on 1% agarose-formaldehyde gels and transferred to nylon membranes. The membranes were then hybridized with a PCR DIG-labeled cDNA probe and signals were detected by colorimetric method with NBT and BCIP reagents.

Table 3.11.7. Summary of Northern blot analysis on temporal expression patterns of cDNA fragments subcloned from gel AB (AP3 and ARP3)

Gel	Subclone I.D.	Gene homology (Transcript size)	Northern blot densitometry reading (arbitrary units)																			
			PPAR α (+/+)							PPAR α (-/-)												
			24 hr		1 wk		2 wk		6 mo		11 mo		24 hr		1 wk		2 wk		6 mo		11 mo	
			CTL	Wy	CTL	Wy	CTL	Wy	CTL	Wy	CTL	Wy	CTL	Wy	CTL	Wy	CTL	Wy	CTL	Wy	CTL	Wy
AB (AP3 & ARP3)	AB7#2	Mouse UDP-glucuronosyl-transferase 2 family, member 5, UGT2b5 (1648 bp)	0.94 \pm 0.08	0.83 \pm 0.00	0.82 \pm 0.15	0.75 \pm 0.00	0.90 \pm 0.15	0.45 \pm 0.35	1.02 \pm 0.21	0.45 \pm 0.27	0.74 \pm 0.02	0.29 \pm 0.04	0.81 \pm 0.01	0.80 \pm 0.01	0.70 \pm 0.05	0.79 \pm 0.06	0.88 \pm 0.04	0.98 \pm 0.13	0.95 \pm 0.17	0.91 \pm 0.07	0.44 \pm 0.01	0.42 \pm 0.02
	Fold change (Wy/CTL)		0.88		0.91		0.50		0.44		0.39		0.99		1.13		1.11		0.96		0.95	
	AB22#9	<i>Mus musculus</i> peroxisome biogenesis factor 16, Pex16 (1221 bp)	0.10 \pm 0.02	0.33 \pm 0.19	0.16 \pm 0.01	0.49 \pm 0.04	0.15 \pm 0.03	0.42 \pm 0.04	0.15 \pm 0.03	0.45 \pm 0.16	0.11 \pm 0.01	0.37 \pm 0.04	0.02 \pm 0.01	0.02 \pm 0.00	0.02 \pm 0.00	0.02 \pm 0.00	0.05 \pm 0.1	0.05 \pm 0.00	0.05 \pm 0.00	0.05 \pm 0.01	0.04 \pm 0.01	0.04 \pm 0.01
Fold change (Wy/CTL)		3.30		3.06		2.80		3.00		3.36		1.00		1.00		1.00		1.00		1.00		
AB25#6	<i>Mus musculus</i> Cyp4a14 (2547 bp)	0.02 \pm 0.00	1.03 \pm 0.08	0.03 \pm 0.03	2.03 \pm 0.56	0.02 \pm 0.01	1.23 \pm 0.26	0.03 \pm 0.01	1.27 \pm 0.09	0.03 \pm 0.01	0.91 \pm 0.14	0.02 \pm 0.01	0.03 \pm 0.01	0.04 \pm 0.01	0.04 \pm 0.01	0.02 \pm 0.03	0.02 \pm 0.01	0.04 \pm 0.01	0.04 \pm 0.01	0.05 \pm 0.00	0.05 \pm 0.01	
Fold change (Wy/CTL)		51.50		67.67		61.50		42.33		30.33		1.50		1.00		1.00		1.00		1.00		

Values represent mean \pm S.D. ‘+’ represents the presence of a band (cDNA) on fluoroDD gel or Northern blot, while ‘-’ represents the corresponding band (cDNA) was not observed on the fluoroDD gel or Northern blot. The relative intensity of the gene expression among the four treatment groups is indicated by the number of ‘+’. The signal intensity of a band on Northern blot was quantified by MultiAnalyst.

Subcloned cDNA fragment AB22#9 [mouse peroxisome biogenesis factor 16 (Pex 16) (Figure 3.11.25) (Table 3.11.7)] showed consistent (2 to 3-fold) induction which started at 24 hours and continued to 11 months treatment. In PPAR α (-/-) mice fed with the 0.1% Wy-14,643 diet, no induction was observed after both short-term and long-term treatment.

Very obvious up-regulation of AB25#6 [mouse cytochrome P450 4a14 (Cyp4a14) (Figure 3.11.26) (Table 3.11.7)] started at 24 hours and induced consistently until 11 months treatment was observed. The induction was not observed in PPAR α (-/-) mice fed with the 0.1% Wy-14,643.

cDNA fragment AC1#2 [mouse serine protease inhibitor, clade A, member 1a, (SPI) (Figure 3.11.27) (Table 3.11.8)] showed down-regulation in the PPAR α (+/+) mice fed with the 0.1% Wy-14,643 diet. The down-regulation was started at 1 week and persisted to 11 months treatment. Maximum down-regulation was observed at 11 months treatment (0.17-fold). Down-regulation was not observed in the PPAR α (-/-) mice fed with the 0.1% Wy-14,643 diet.

Subcloned cDNA fragment AC2#2 [mouse peroxisomal bifunctional enzyme (PBFE) (Figure 3.11.28) (Table 3.11.8)] was consistently up-regulated at 24 hours, 1 week, 2 weeks, 6 months and 11 months in the 0.1% Wy-14,643 fed PPAR α (+/+) mice. In PPAR α (-/-) mice fed with the 0.1% Wy-14,643 diet, no induction was observed after both short-term and long-term treatment.

cDNA fragment AD8#2 [mouse cytochrome P450 4a10 (Cyp4a10) (Figure 3.11.29) (Table 3.11.8)] was induced in 0.1% Wy-14,643 fed PPAR α (+/+) mice. The induction was observed since 24 hours. Maximum induction was observed at 1 week (33-fold) and up-regulation was continued to 11 months (13-fold). No induction was observed in the PPAR α (-/-) mice fed with the 0.1% Wy-14,643 diet.

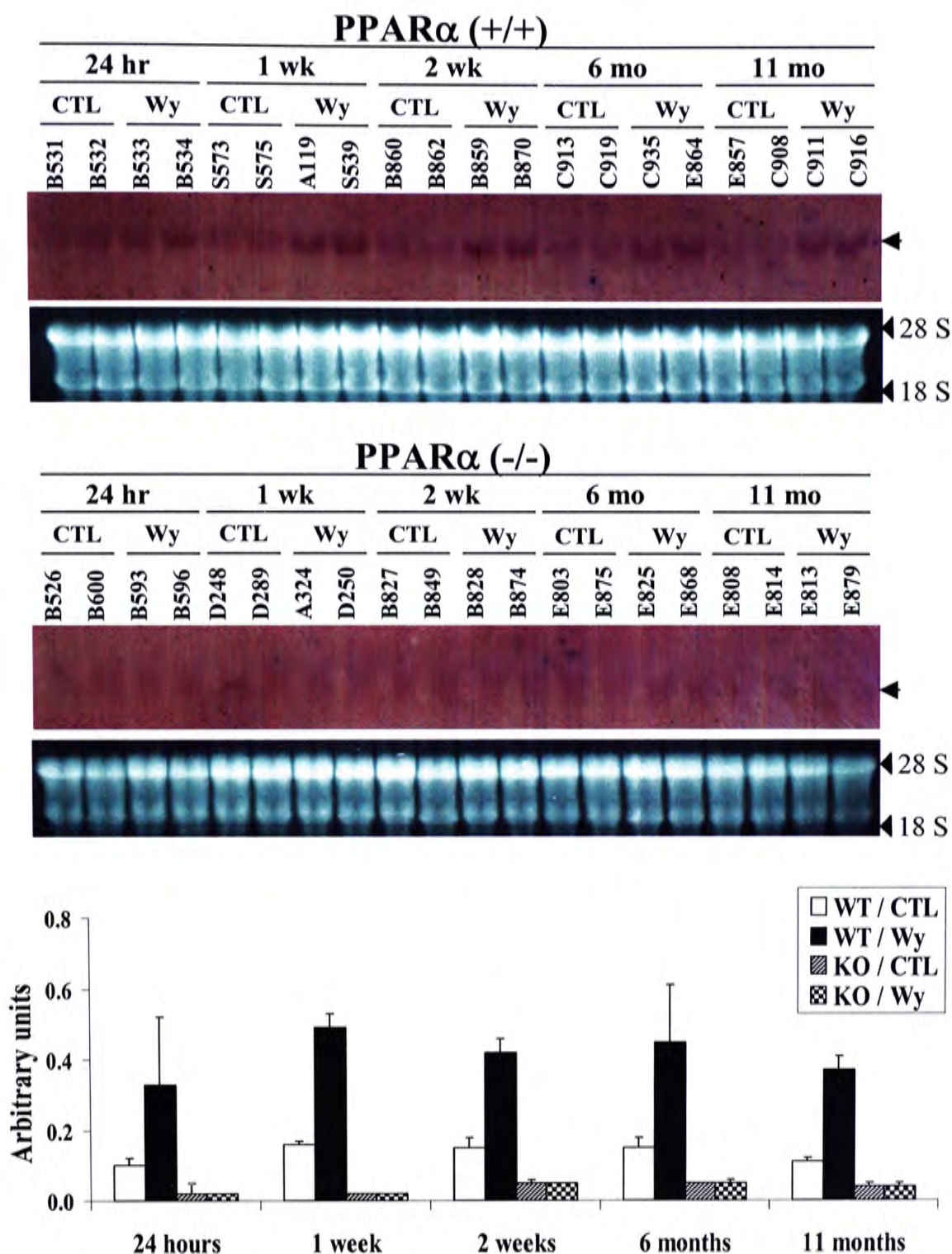


Figure 3.11.25. Temporal expression of AB22#9 (peroxisome biogenesis factor 16). Total liver RNA (30 μ g) of two mice of PPAR α (+/+) and PPAR α (-/-) fed with a 0.0% control (CTL) or 0.1% (w/w) Wy-14,643 (Wy) diet for 24 hours, 1 week, 2 weeks, 6 months and 11 months treatment were separated on 1% agarose-formaldehyde gels and transferred to nylon membranes. The membranes were then hybridized with a PCR DIG-labeled cDNA probe and signals were detected by colorimetric method with NBT and BCIP reagents.

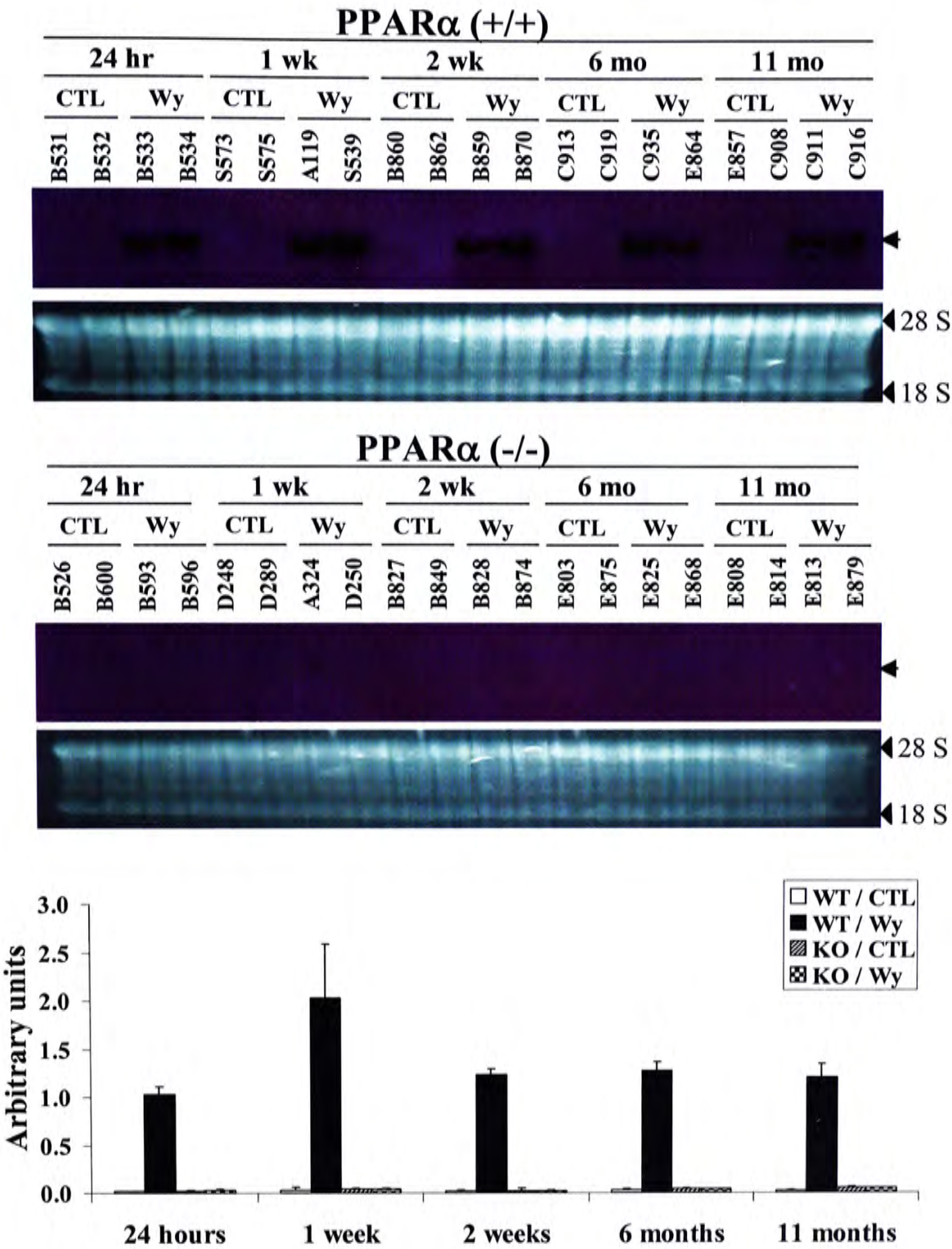


Figure 3.11.26. Temporal expression of AB25#6 (cytochrome P450, family 4, subfamily a, polypeptide 14). Total liver RNA (30 μ g) of two mice of PPAR α (+/+) and PPAR α (-/-) fed with a 0.0% control (CTL) or 0.1% (w/w) Wy-14,643 (Wy) diet for 24 hours, 1 week, 2 weeks, 6 months and 11 months treatment were separated on 1% agarose-formaldehyde gels and transferred to nylon membranes. The membranes were then hybridized with a DIG-labeled RNA probe and signals were detected by colorimetric method with NBT and BCIP reagents.

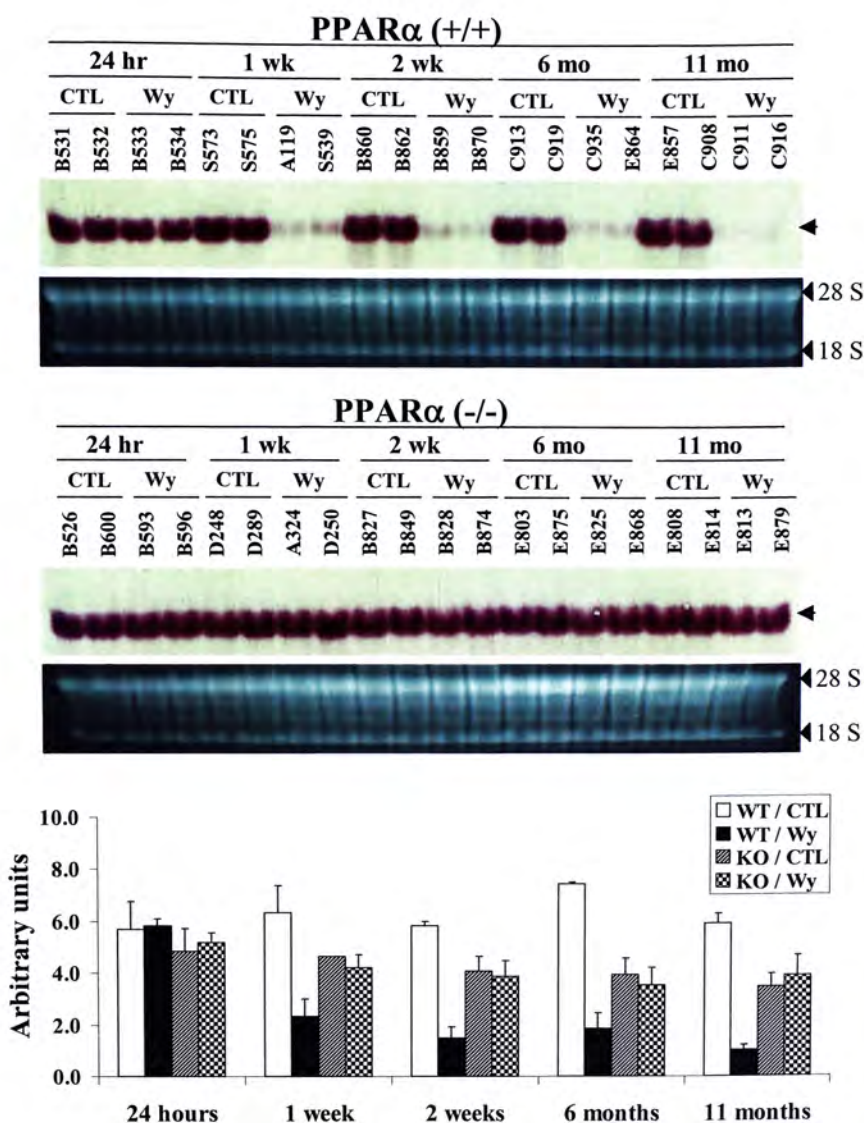


Figure 3.11.27. Temporal expression of AC1#2 (serine protease inhibitor). Total liver RNA (30 μ g) of two mice of PPAR α (+/+) and PPAR α (-/-) fed with a 0.0% control (CTL) or 0.1% (w/w) Wy-14,643 (Wy) diet for 24 hours, 1 week, 2 weeks, 6 months and 11 months treatment were separated on 1% agarose-formaldehyde gels and transferred to nylon membranes. The membranes were then hybridized with a DIG-labeled RNA probe and signals were detected by colorimetric method with NBT and BCIP reagents.

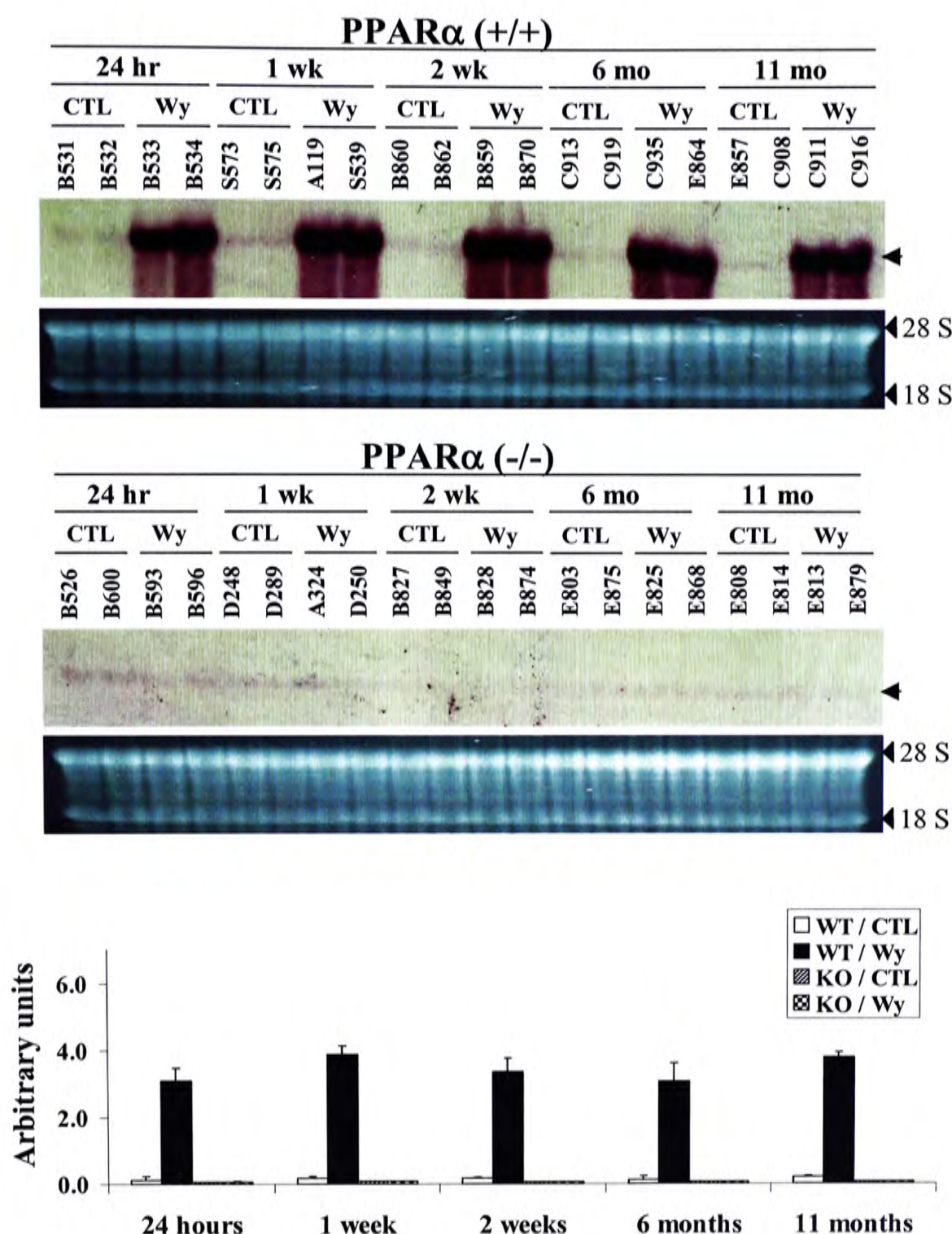


Figure 3.11.28. Temporal expression of AC2#2 (peroxisomal bifunctional enzyme). Total liver RNA (30 μ g) of two mice of PPAR α (+/+) and PPAR α (-/-) fed with a 0.0% control (CTL) or 0.1% (w/w) Wy-14,643 (Wy) diet for 24 hours, 1 week, 2 weeks, 6 months and 11 months treatment were separated on 1% agarose-formaldehyde gels and transferred to nylon membranes. The membranes were then hybridized with a DIG-labeled RNA probe and signals were detected by colorimetric method with NBT and BCIP reagents.

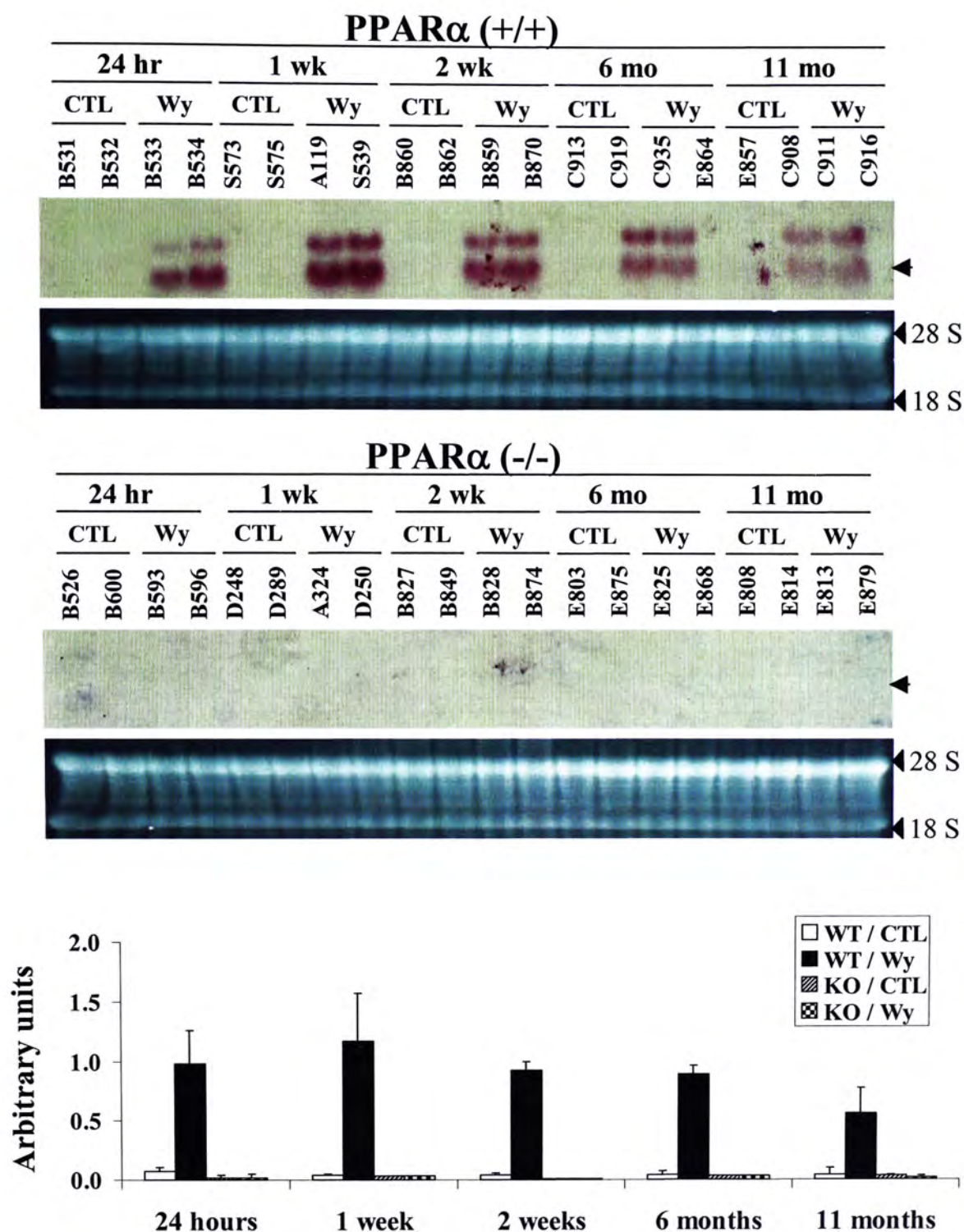


Figure 3.11.29. Temporal expression of AD8#2 (cytochrome P450, family 4, subfamily a, polypeptide 10). Total liver RNA (30 μ g) of two mice of PPAR α (+/+) and PPAR α (-/-) fed with a 0.0% control (CTL) or 0.1% (w/w) Wy-14,643 (Wy) diet for 24 hours, 1 week, 2 weeks, 6 months and 11 months treatment were separated on 1% agarose-formaldehyde gels and transferred to nylon membranes. The membranes were then hybridized with a DIG-labeled RNA probe and signals were detected by colorimetric method with NBT and BCIP reagents.

Table 3.11.8. Summary of Northern blot analysis on temporal expression patterns of cDNA fragments subcloned from gels AC (AP2 and ARP19) and AD (AP2 and ARP18)

Gel	Subclone I.D.	Gene homology (Transcript size)	Northern blot densitometry reading (arbitrary units)																				
			PPAR α (+/+)								PPAR α (-/-)												
			24 hr		1 wk		2 wk		6 mo		11 mo		24 hr		1 wk		2 wk		6 mo		11 mo		
CTL	Wy	CTL	Wy	CTL	Wy	CTL	Wy	CTL	Wy	CTL	Wy	CTL	Wy	CTL	Wy	CTL	Wy	CTL	Wy	CTL	Wy		
AC (AP2 & ARP19)	AC1#2	<i>Mus musculus</i> serine (or cysteine) proteinase inhibitor, SPI (1393 bp)																					
			5.68 \pm 1.08	5.80 \pm 0.29	6.32 \pm 1.05	2.33 \pm 0.66	5.83 \pm 0.16	1.47 \pm 0.45	7.43 \pm 0.09	1.84 \pm 0.61	5.91 \pm 0.40	1.01 \pm 0.20	4.86 \pm 0.86	5.19 \pm 0.37	4.63 \pm 0.01	4.22 \pm 0.49	4.07 \pm 0.59	3.88 \pm 0.59	3.95 \pm 0.64	3.53 \pm 0.68	3.46 \pm 0.50	3.90 \pm 0.79	
	Fold change (Wy/CTL)		1.02		0.37		0.25		0.25		0.17		1.07		0.91		0.95		0.89		1.13		
	AC2#2	<i>Mus musculus</i> peroxisomal bifunctional enzyme (PBFEE) (2979 bp)		0.11 \pm 0.11	3.09 \pm 0.39	0.18 \pm 0.25	3.89 \pm 0.25	0.18 \pm 0.02	3.36 \pm 0.40	0.13 \pm 0.09	3.06 \pm 0.57	0.21 \pm 0.03	3.80 \pm 0.12	0.06 \pm 0.01	0.06 \pm 0.02	0.08 \pm 0.01	0.08 \pm 0.00	0.05 \pm 0.01	0.05 \pm 0.01	0.06 \pm 0.01	0.06 \pm 0.01	0.05 \pm 0.02	0.05 \pm 0.01
Fold change (Wy/CTL)			30.90		21.61		18.67		23.54		18.10		1.00		1.00		1.00		1.00		1.00		
AD8#2			<i>Mus musculus</i> Cyp4a10 (2085 bp)		0.07 \pm 0.04	0.98 \pm 0.28	0.04 \pm 0.01	1.17 \pm 0.40	0.04 \pm 0.02	0.92 \pm 0.08	0.04 \pm 0.03	0.89 \pm 0.07	0.04 \pm 0.06	0.56 \pm 0.21	0.02 \pm 0.02	0.02 \pm 0.03	0.03 \pm 0.00	0.03 \pm 0.00	0.01 \pm 0.00	0.01 \pm 0.00	0.03 \pm 0.00	0.03 \pm 0.00	0.03 \pm 0.01
	Fold change (Wy/CTL)			14.00		20.25		23.00		22.25		14.00		1.00		1.00		1.00		1.00		0.67	

Values represent mean \pm S.D. '+' represents the presence of a band (cDNA) on fluoroDD gel or Northern blot, while '-' represents the corresponding band (cDNA) was not observed on the fluoroDD gel or Northern blot. The relative intensity of the gene expression among the four treatment groups is indicated by the number of '+'. The signal intensity of a band on Northern blot was quantified by MultiAnalyst.

cDNA fragment AF1#8 [mouse very-long-chain acyl-CoA synthetase (VLACS) (Figure 3.11.30) (Table 3.11.9)] was up-regulated consistently (about 2-fold which was started at 24 hours and continued to 11 months. The up-regulation was not shown in PPAR α (-/-) mice fed with the 0.1% Wy-14,643 diet.

cDNA fragment AF25#7 [mouse major urinary protein II (MUP II) (Figure 3.11.31) (Table 3.11.9)] was down-regulated in PPAR α (+/+) mice fed with the 0.1% Wy-14,643 diet. This down-regulation was started at 2 weeks and maximum down-regulation was found at 11 months treatment (0.01-fold). No down-regulation was observed in the PPAR α (-/-) mice fed with the 0.1% Wy-14,643 diet after short-term and long-term treatment.

Down-regulation of AJ1#5 [mouse carboxyesterase (carboxyestersae) (Figure 3.11.32) (Table 3.11.10)] started at 1 week and maximum down-regulation (0.05-fold) was found at 11 months 0.1% Wy-14,643 treatment. No down-regulation was observed in the PPAR α (-/-) mice fed with the 0.1% Wy-14,643 diet after short-term and long-term treatment.

cDNA fragment AJ2#10 [mouse peroxisomal acyl-CoA oxidase (AOX) (Figure 3.11.33) (Table 3.11.10)] was up-regulated in 0.1% Wy-14,643 treated PPAR α (+/+) mice when compared with the controls. Maximum induction was observed at 24 hours and 1 week 0.1% Wy-14,643 treatment of PPAR α (+/+) mice. The induction was persisted to 11 months and not found in PPAR α (-/-) mice fed with the 0.1% Wy-14,643 diet.

Up-regulation of AL3#3 [mouse hydroxysteroid (17-beta) dehydrogenase 11 (HSD17 β 11) (Figure 3.11.34) (Table 3.11.10)] was found in 0.1% Wy-14,643 treated PPAR α (+/+) mice. Induction of AL3#3 was started at 24 hours and continued to 11

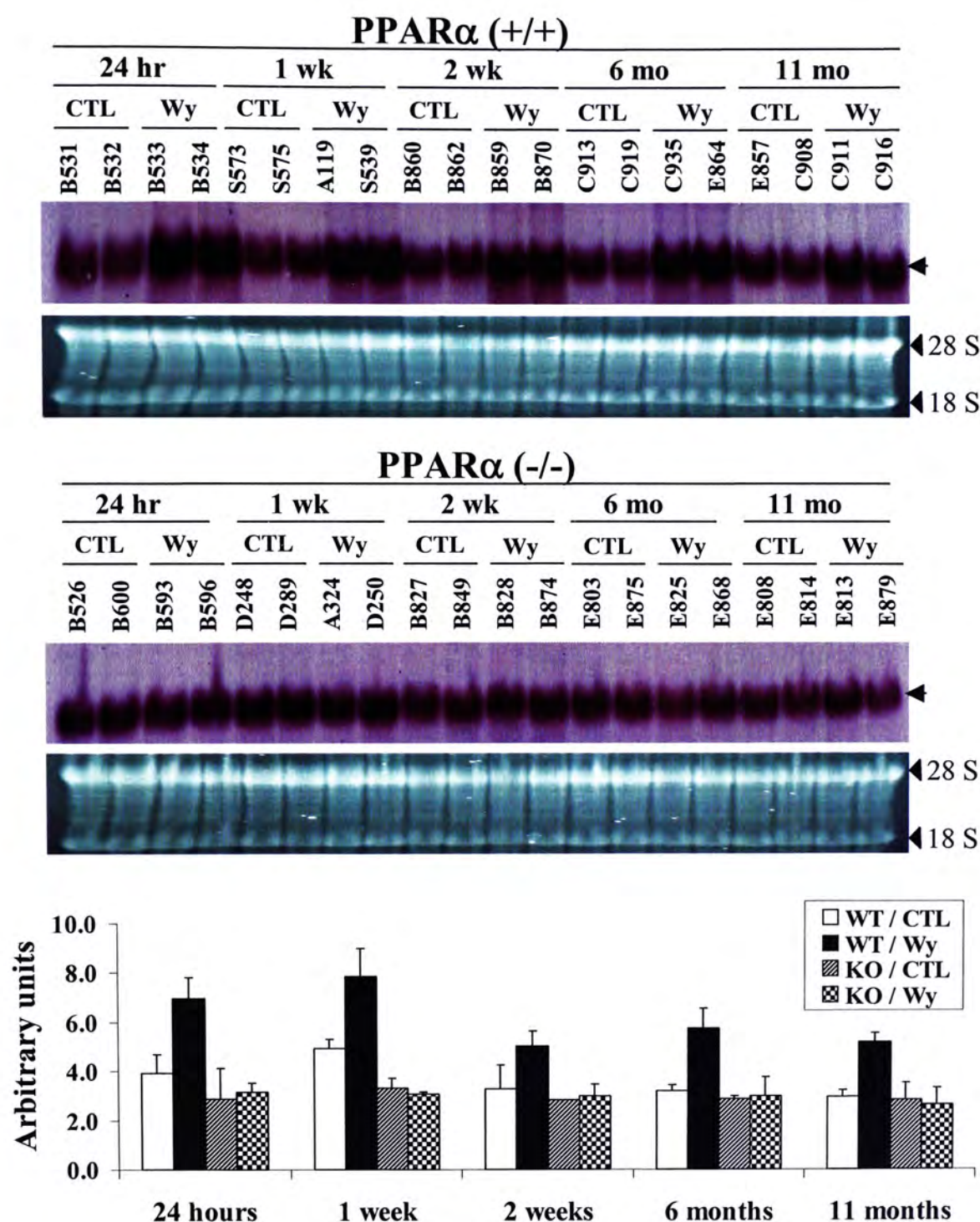


Figure 3.11.30. Temporal expression of AF1#8 (very long chain acyl-CoA synthetase). Total liver RNA (30 μ g) of two mice of PPAR α (+/+) and PPAR α (-/-) fed with a 0.0% control (CTL) or 0.1% (w/w) Wy-14,643 (Wy) diet for 24 hours, 1 week, 2 weeks, 6 months and 11 months treatment were separated on 1% agarose-formaldehyde gels and transferred to nylon membranes. The membranes were then hybridized with a DIG-labeled RNA probe and signals were detected by colorimetric method with NBT and BCIP reagents.

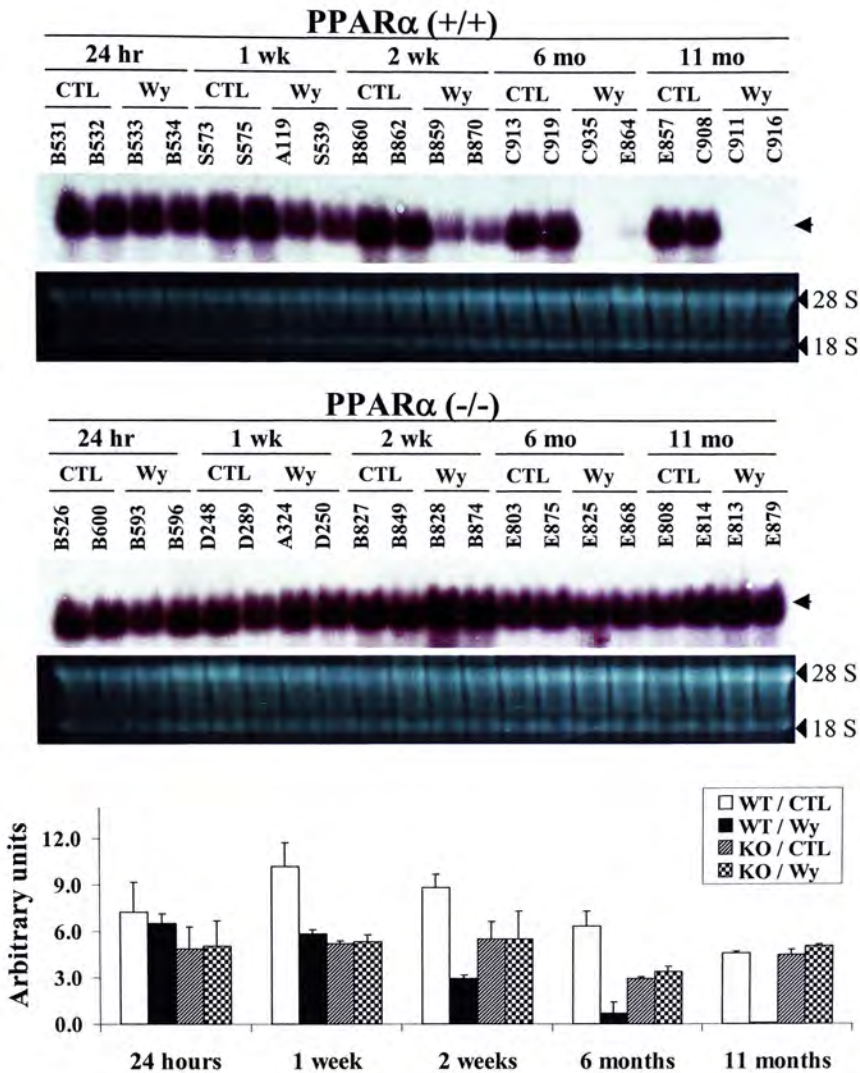


Figure 3.11.31. Temporal expression of AF25#7 (mouse major urinary protein II). Total liver RNA (30 μ g) of two mice of PPAR α (+/+) and PPAR α (-/-) fed with a 0.0% control (CTL) or 0.1% (w/w) Wy-14,643 (Wy) diet for 24 hours, 1 week, 2 weeks, 6 months and 11 months treatment were separated on 1% agarose-formaldehyde gels and transferred to nylon membranes. The membranes were then hybridized with a DIG-labeled RNA probe and signals were detected by colorimetric method with NBT and BCIP reagents.

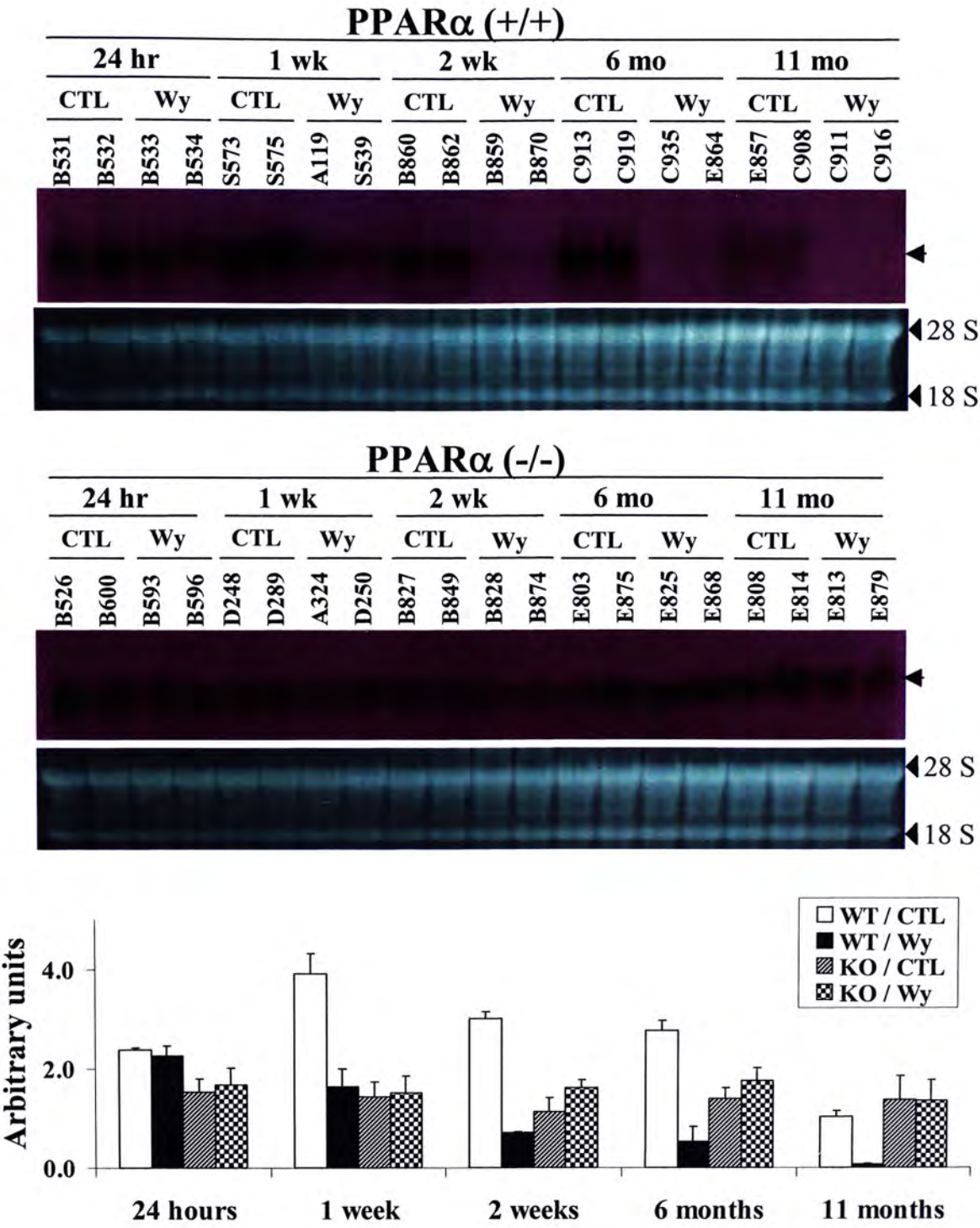


Figure 3.11.32. Temporal expression of AJ1#5 (carboxylesterase). Total liver RNA (30 μ g) of two mice of PPAR α (+/+) and PPAR α (-/-) fed with a 0.0% control (CTL) or 0.1% (w/w) Wy-14,643 (Wy) diet for 24 hours, 1 week, 2 weeks, 6 months and 11 months treatment were separated on 1% agarose-formaldehyde gels and transferred to nylon membranes. The membranes were then hybridized with a DIG-labeled RNA probe and signals were detected by colorimetric method with NBT and BCIP reagents.

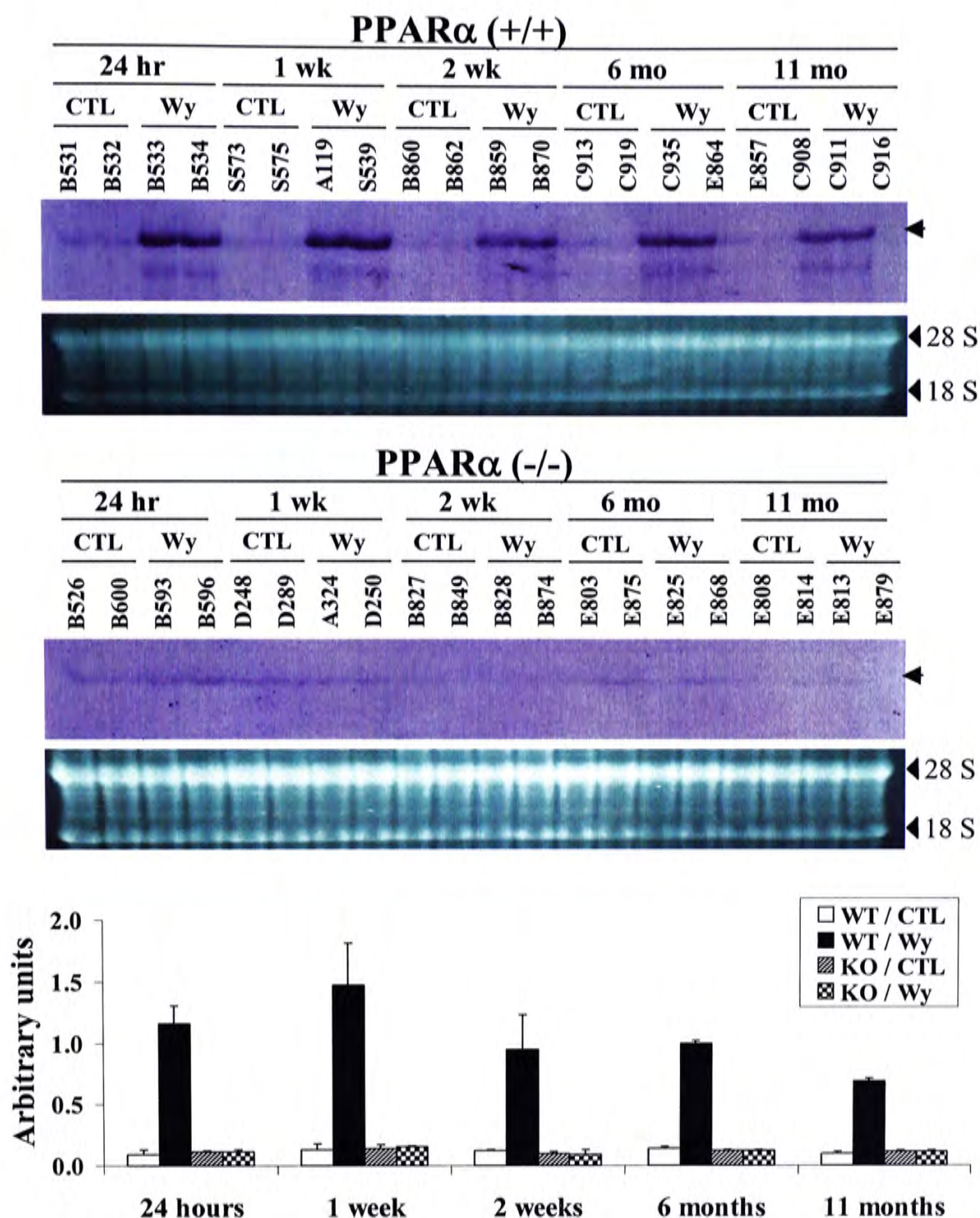


Figure 3.11.33. Temporal expression of AJ2#10 (peroxisomal acyl-CoA oxidase). Total liver RNA (30 μ g) of two mice of PPAR α (+/+) and PPAR α (-/-) fed with a 0.0% control (CTL) or 0.1% (w/w) Wy-14,643 (Wy) diet for 24 hours, 1 week, 2 weeks, 6 months and 11 months treatment were separated on 1% agarose-formaldehyde gels and transferred to nylon membranes. The membranes were then hybridized with a DIG-labeled RNA probe and signals were detected by colorimetric method with NBT and BCIP reagents.

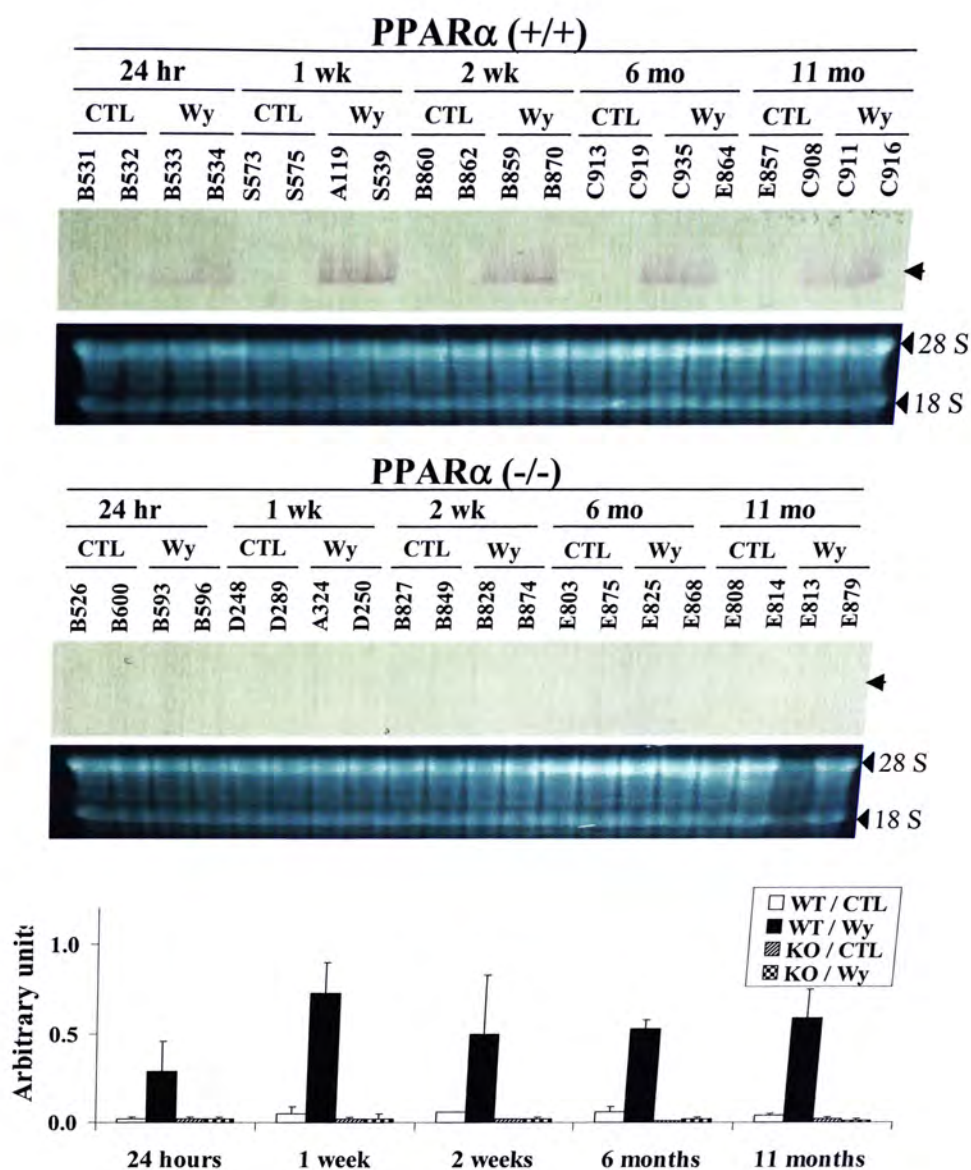


Figure 3.11.34. Temporal expression of AL3#3 (hydroxysteroid (17-beta) dehydrogenase 11). Total liver RNA (30 μ g) of two mice of PPAR α (+/+) and PPAR α (-/-) fed with a 0.0% control (CTL) or 0.1% (w/w) Wy-14,643 (Wy) diet for 24 hours, 1 week, 2 weeks, 6 months and 11 months treatment were separated on 1% agarose-formaldehyde gels and transferred to nylon membranes. The membranes were then hybridized with a DIG-labeled RNA probe and signals were detected by colorimetric method with NBT and BCIP reagents.

Table 3.11.10. Summary of Northern blot analysis on temporal expression patterns of cDNA fragments subcloned from gels AJ (AP6 and ARP14) and AL (AP7 and ARP15)

Gel	Subclone I.D.	Gene homology (Transcript size)	Northern blot densitometry reading (arbitrary units)																			
			PPAR α (+/+)						PPAR α (-/-)													
			24 hr		1 wk		2 wk		6 mo		11 mo		24 hr		1 wk		2 wk		6 mo		11 mo	
AJ (AP6 & ARP14)	AJ1#5	Mouse carboxylesterase, Carboxylesterase (2006 bp)	CTL	Wy	CTL	Wy	CTL	Wy	CTL	Wy	CTL	Wy	CTL	Wy	CTL	Wy	CTL	Wy	CTL	Wy	CTL	Wy
			2.39 \pm 0.04	2.27 \pm 0.19	3.92 \pm 0.42	1.64 \pm 0.37	3.02 \pm 0.13	0.71 \pm 0.01	2.77 \pm 0.21	0.53 \pm 0.31	1.03 \pm 0.06	0.06 \pm 0.02	1.52 \pm 0.28	1.69 \pm 0.34	1.43 \pm 0.32	1.51 \pm 0.35	1.13 \pm 0.28	1.61 \pm 0.17	1.39 \pm 0.22	1.77 \pm 0.25	1.37 \pm 0.49	1.35 \pm 0.43
			0.95		0.42		0.23		0.19		0.06		1.11		1.06		1.42		1.28		0.98	
	AJ2#10	<i>Mus musculus</i> peroxisomal acyl-coA oxidase, AOX (3778 bp)	CTL	Wy	CTL	Wy	CTL	Wy	CTL	Wy	CTL	Wy	CTL	Wy	CTL	Wy	CTL	Wy	CTL	Wy	CTL	Wy
			0.09 \pm 0.04	1.16 \pm 0.14	0.13 \pm 0.05	1.47 \pm 0.34	0.12 \pm 0.01	0.95 \pm 0.28	0.14 \pm 0.01	1.00 \pm 0.02	0.10 \pm 0.01	0.69 \pm 0.02	0.11 \pm 0.01	0.11 \pm 0.02	0.14 \pm 0.03	0.15 \pm 0.01	0.10 \pm 0.01	0.09 \pm 0.04	0.12 \pm 0.01	0.12 \pm 0.01	0.11 \pm 0.01	0.11 \pm 0.01
			12.89		11.31		7.92		7.14		6.90		1.00		1.07		0.90		1.00		1.00	
AL (AP7 & ARP15)	AL3#3	<i>Mus musculus</i> hydroxysteroid (17-beta) dehydrogenase 11, HSD17 β 11 (1713 bp)	CTL	Wy	CTL	Wy	CTL	Wy	CTL	Wy	CTL	Wy	CTL	Wy	CTL	Wy	CTL	Wy	CTL	Wy	CTL	Wy
			0.02 \pm 0.00	0.34 \pm 0.24	0.05 \pm 0.04	0.73 \pm 0.17	0.06 \pm 0.00	0.77 \pm 0.23	0.06 \pm 0.03	0.64 \pm 0.11	0.04 \pm 0.01	0.60 \pm 0.12	0.02 \pm 0.01	0.02 \pm 0.01	0.02 \pm 0.01	0.02 \pm 0.03	0.02 \pm 0.00	0.02 \pm 0.00	0.01 \pm 0.00	0.01 \pm 0.00	0.02 \pm 0.01	0.02 \pm 0.01
			17.00		14.6		12.83		10.67		15.00		1.00		1.00		1.00		1.00		1.00	

Values represent mean \pm S.D. '+' represents the presence of a band (cDNA) on fluoroDD gel or Northern blot, while '-' represents the corresponding band (cDNA) was not observed on the fluoroDD gel or Northern blot. The relative intensity of the gene expression among the four treatment groups is indicated by the number of '+'. The signal intensity of a band on Northern blot was quantified by MultiAnalyst.

months. Maximum induction was found at 1 week 0.1% Wy-14,643 treatment. In PPAR α (-/-) mice fed with the 0.1% Wy-14,643 diet, no induction was found after short-term and long-term exposure.

Fragment AO1#2 [mouse adipose differentiation related protein (ADRP) (Figure 3.11.35) (Table 3.11.11)] was up-regulated in 0.1% Wy-14,643 treated PPAR α (+/+) mice. The up-regulation was started at 24 hours and consistently induced to 11 months. No induction was observed in the PPAR α (-/-) mice fed with the 0.1% Wy-14,643 diet after short-term and long-term treatment.

Up-regulation of AO2#8 [mouse carnitine O-octanoyltransferase (Crot) (Figure 3.11.36) (Table 3.11.11)] was found in 0.1% Wy-14,643 treated PPAR α (+/+) mice. The up-regulation of AO2#8 was started at 24 hours and continued to 11 months treatment. In PPAR α (-/-) mice fed with the 0.1% Wy-14,643 diet, no induction was found after short-term and long-term exposure.

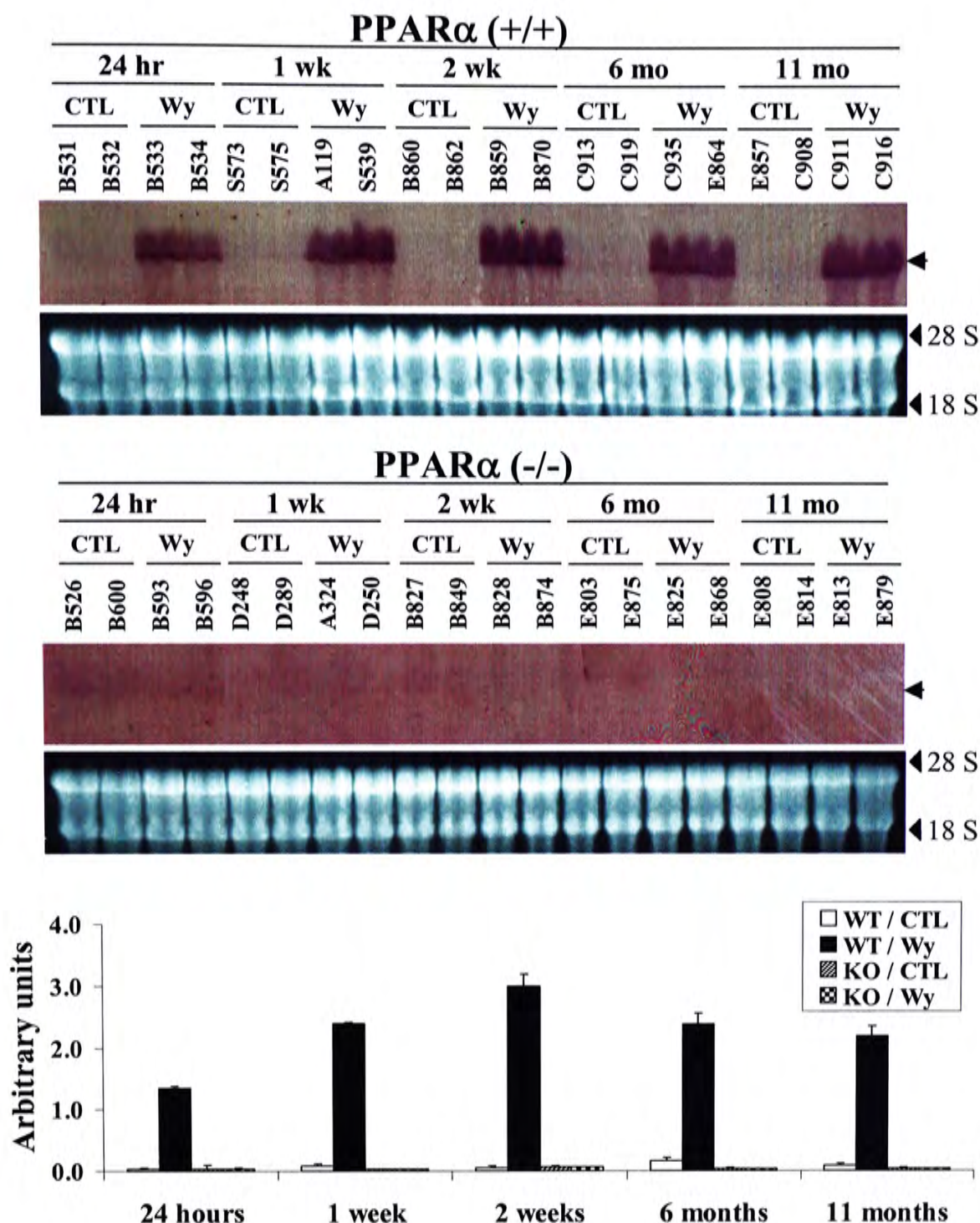


Figure 3.11.35. Temporal expression of AO1#2 (adipose differentiation related protein). Total liver RNA (30 μ g) of two mice of PPAR α (+/+) and PPAR α (-/-) fed with a 0.0% control (CTL) or 0.1% (w/w) Wy-14,643 (Wy) diet for 24 hours, 1 week, 2 weeks, 6 months and 11 months treatment were separated on 1% agarose-formaldehyde gels and transferred to nylon membranes. The membranes were then hybridized with a PCR DIG-labeled cDNA probe and signals were detected by colorimetric method with NBT and BCIP reagents.

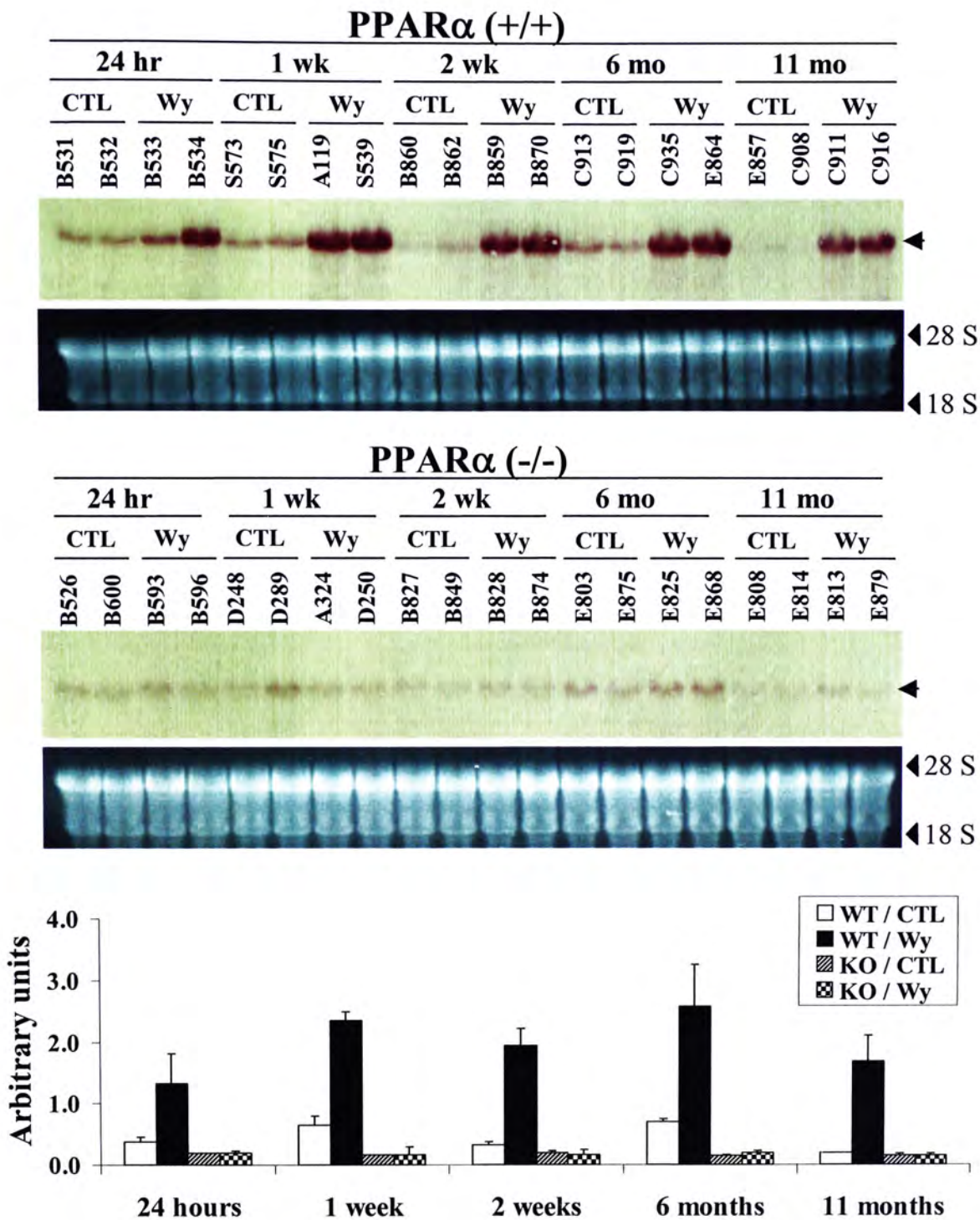


Figure 3.11.36. Temporal expression of AO2#8 (carnitine O-octanoyltransferase). Total liver RNA (30 μ g) of two mice of PPAR α (+/+) and PPAR α (-/-) fed with a 0.0% control (CTL) or 0.1% (w/w) Wy-14,643 (Wy) diet for 24 hours, 1 week, 2 weeks, 6 months and 11 months treatment were separated on 1% agarose-formaldehyde gels and transferred to nylon membranes. The membranes were then hybridized with a PCR DIG-labeled cDNA probe and signals were detected by colorimetric method with NBT and BCIP reagents.

Table 3.11.11. Summary of Northern blot analysis on temporal expression patterns of cDNA fragments subcloned from gel AO (AP5 and ARP10)

Gel	Subclone I.D.	Gene homology (Transcript size)	Northern blot densitometry reading (arbitrary units)																			
			PPARα (+/+)							PPARα (-/-)												
			24 hr		1 wk		2 wk		6 mo		11 mo		24 hr		1 wk		2 wk		6 mo		11 mo	
AO (AP5 & ARP10)	AO1#2	Mouse adipose differentiation related protein, ADRP (1680 bp)	CTL	Wy	CTL	Wy	CTL	Wy	CTL	Wy	CTL	Wy	CTL	Wy	CTL	Wy	CTL	Wy	CTL	Wy	CTL	Wy
			0.03 ± 0.02	1.34 ± 0.09	0.08 ± 0.03	2.40 ± 0.01	0.05 ± 0.03	2.99 ± 0.20	0.17 ± 0.04	2.38 ± 0.18	0.08 ± 0.04	2.19 ± 0.16	0.04 ± 0.05	0.04 ± 0.01	0.03 ± 0.01	0.06 ± 0.02	0.03 ± 0.01	0.06 ± 0.02	0.03 ± 0.00	0.04 ± 0.01	0.04 ± 0.01	0.04 ± 0.01
			44.67		30.00		59.80		14.00		27.38		1.00		1.00		1.00		1.00		1.00	
	AO2#8	<i>Mus musculus</i> carnitine O-octanoyl-transferase, Crot (2844 bp)		0.38 ± 0.08	1.32 ± 0.49	0.64 ± 0.15	2.35 ± 0.14	0.32 ± 0.06	1.95 ± 0.27	0.70 ± 0.04	2.57 ± 0.69	0.19 ± 0.01	1.69 ± 0.42	0.19 ± 0.01	0.20 ± 0.03	0.16 ± 0.01	0.16 ± 0.01	0.19 ± 0.04	0.16 ± 0.08	0.14 ± 0.02	0.19 ± 0.04	0.15 ± 0.03
			3.47		3.67		6.09		3.67		8.89		1.05		1.00		0.84		1.36		1.00	

Values represent mean \pm S.D. ‘+’ represents the presence of a band (cDNA) on fluoroDD gel or Northern blot, while ‘-’ represents the corresponding band (cDNA) was not observed on the fluoroDD gel or Northern blot. The relative intensity of the gene expression among the four treatment groups is indicated by the number of ‘+’. The signal intensity of a band on Northern blot was quantified by MultiAnalyst.

Chapter 4 Discussion

4.1 Body weight changes

There was significant decrease in body weights of the PPAR α (+/+) mice after chronic exposure (6 and 11 months) of the Wy-14,643 diet. Decrease in body weights of rodents after Wy-14,643 treatment were reported in previous studies (Biegel *et al.*, 1992; Peters *et al.*, 1997; Biegel *et al.*, 2001). These decrease in body weights were due to the hypolipidemic effect of the Wy-14,643 compound but not due to starvation of mice. Enough food was provided and food consumption of different treatment groups was more or less the same for both short-term and long-term treatment. In this project, we mentioned that the expression of genes that involved in lipid metabolism was enhanced after Wy-14,643 treatment. The up-regulation of genes that involved in lipid metabolism lead to the decrease of the body weight. Besides, the serum triglyceride level was decreased due to the hypolipidemic effect of Wy-14,643 compound. The combined effect of enhancement of lipid metabolism and triglyceride catabolism result in the loss of body weight in PPAR α (+/+) mice. The decrease in body weights were not observed in PPAR α (-/-) mice that fed with Wy-14,643 as the hypolipidemic effect is mediated by PPAR α (Peters *et al.*, 1997).

High mortality rate that found in the 0.1% Wy-14,643 treated PPAR α (+/+) mice was mentioned in the previous study (Peters *et al.*, 1997; Biegel *et al.*, 2001) and might be due to the liver enlargement and probably liver cancer. Besides, no mice died in the other treatment groups during the 6 and 11 months treatment suggested that the high mortality rate was Wy-14,643-induced and mediated by PPAR α .

4.2 Organ weight changes

Hepatomegaly was observed in PPAR α (+/+) mice after short term (1 week) exposure with the 0.1% Wy-14,643 diet and the level of hepatomegaly was increased during the chronic administration of Wy-14,643. Liver enlargement of rodent induced after acute and chronic exposure of Wy-14,643 was reported in previous studies (Marsman *et al.*, 1988; Crunkhorn *et al.*, 2004). As hepatomegaly was not observed in PPAR α (-/-) mice fed with the 0.1% Wy-14,643 diet for both short-term and long-term treatment, it indicated that the enlargement of liver was mediated by PPAR α (Lee *et al.*, 1995; Peters *et al.*, 1997). Liver enlargement in Wy-14,643-treated PPAR α (+/+) is due to the increase in cell replication and size of the hepatocytes (Carthew *et al.*, 1998; Corton *et al.*, 2000).

Relative white fat and brown fat weights were decreased in the 0.1% Wy-14,643 treated PPAR α (+/+) mice started at 2 weeks treatment. However, these

were not observed in the PPAR α (-/-) mice for short-term and long-term Wy-14,643 treatment. The decrease in the white fat and brown fat support the hypolipidemic effect of Wy-14,643 compound. Genes that involved in the lipid metabolism were up-regulated after Wy-14,643 treatment. With the enhancement of lipid catabolism, fat that stored in white fat and brown fat will be burnt that lead to the decrease in sizes of white fat and brown fat.

Relative spleen weight was also decreased after 11 months treatment in PPAR α (+/+) mice fed with the 0.1% Wy-14,643 diet. Significant atrophy of spleen after treatment with potent peroxisome proliferators such as perfluorooctanoic acid (PFOA), di(2-ethylhexyl)phthalate (DEHP), Wy-14643 and nafenopin was reported in the previous study (Yang *et al.*, 2000). Decrease in the number of splenocytes (about 50%) was greater than the decrease in spleen weight after treatment with PFOA. This suggested that the loss of splenocytes rather than the organ matrix. The decrease in no. of splenocytes might be due to enhancement of apoptotsis and/or decrease in cell proliferation. The decrease in size of spleen might be also due to the decrease in size of the splenocytes.

The relative organ weights of brain, heart and lung were higher in 0.1% Wy-14,643 fed PPAR α (+/+) mice compared to controls. The body weights were decrease with the hypolipidemic effect of Wy-14,643, however, the sizes and absolute

weights of brain, heart and lung were not change. Hence, the relative organ weights of brain, heart and lung were higher when compared with the controls (David *et al.*, 2000).

4.3 Serum cholesterol and triglyceride levels

The level of serum cholesterol is significantly increased at 11 months 0.1% Wy-14,643-treated PPAR α (+/+). However, this result was not matched to previous reported that serum cholesterol level was lowered with the administration of Wy-14,643 (Isseman and Green, 1990). Increase in serum cholesterol level induced by perfluorooctanoic acid (PFOA) was mentioned in a previous study (Xie *et al.*, 2003). The serum cholesterol level was first decreased by PFOA but increase after seventh day of treatment. Xie *et al.* suggested that the increase in serum cholesterol level might be due to other changes caused by peroxisome proliferators.

Serum triglyceride level of PPAR α (+/+) mice treated with 0.1% Wy-14,643 was decreased in all the different time points (24 hours, 1 week, 2 weeks, 6 months and 11 months). The decrease in serum triglyceride level is due to the hypolipidemic effect of Wy-14,643 (Isseman and Green, 1990). The hypolipidemic drugs enhance the triglyceride catabolism by suppressing the ApoCIII and induced the activities of lipoprotein lipase which lead to the induction of lipoprotein lysis (Staels *et al.*, 1997).

4.4 Liver histology

Abnormal hepatocytes arrangement and enlarged sinusoidal spaces were observed only in the 0.1% Wy-14,643-treated PPAR α (+/+) mice and started at 1 week treatment. Trabecular cell clusters, hepatocytes without nucleus or dark nucleus and invasion of blood was found in 0.1% Wy-14,643-treated PPAR α (+/+) mice after 11 months treatment and all of these are the characteristics of tumor cells. These features and severe liver damages were not observed in other treatment groups. Hepatocarcinoma caused by chronic exposure of Clofibrate and Wy-15,643 to mice were reported in previous studies (Reddy and Qureshi, 1979; Peters *et al.*, 1997).

Lipid accumulation was observed in both the control and treatment groups of PPAR α (-/-) mice and Wy-14,643 treated PPAR α (+/+) mice. The hepatic lipid accumulation in the PPAR α (-/-) mice may be due to inhibition mitochondrial fatty acid import (Gervois *et al.*, 2000). The lipid accumulation of Wy-14,643 treated PPAR α (+/+) mice at 2 weeks, 6 months and 11 months may be due to the enhanced catabolism of lipid that induced by Wy-14,643. In my study, several PPAR α -dependent and Wy-14,643-responsive genes that involved in lipid metabolism were confirmed. The obvious and early inductions of these genes support the PP-induced catabolism of lipid. The accumulation of lipid droplets in the

report (Lalwani *et al.*, 1981; Gorgas and Krisans, 1989).

4.5 Functions and roles of identified PPAR α -dependent and Wy-14,643-responsive genes

Total 17 different genes (12 up-regulated and 5 down-regulated) were identified to be PPAR α -dependent (Table 4.5.1). Most of the genes identified are related to lipid metabolism, whereas the others are involved in peroxisome biogenesis, plasma triglyceride metabolism, xenobiotics metabolism, adipocyte differentiation or sterol carrier protein, and some are cancer marker genes.

Mouse peroxisomal delta3, delta2-enoyl-Coenzyme A isomerase (Peci) is involved in the β -oxidation of unsaturated fatty acids. Delta3, delta2-enoyl-Coenzyme A is found in both peroxisome and mitochondria. The breakdown of unsaturated fatty acid requires the enzymes that catalyze the isomerization and reduction of double bonds (Kunau *et al.*, 1995). The peroxisomal delta3, delta2-enoyl-Coenzyme A is involved in the 3-cis \rightarrow 2-trans and 3-trans \rightarrow 2-trans activity (Zhang *et al.*, 2002). In this study, it showed that maximum induction of Peci was observed at 24 hours treatment. Induction of Peci was started at 24 hours and continued to 11 months in PPAR α (+/+) mice fed with the 0.1% Wy-14,643 diet. However, this time-dependent induction was not observed in the

Table 4.5.1. List of PPAR α regulated genes in liver (with the genes identified in this project)

Function of gene	Genes	
Adipose differentiation	Adipose differentiation related protein	
Amino acid metabolism	Alanine aminotransferase	Cysteine sulfinic acid decarboxylase function
	Alanine glyoxylate transaminase	Cytosolic aspartate aminotransferase
	Arginase	Glutaminase
	Arginino-succinate lyase	Hydroxypyruvate/ gloxylate reductase
	Arginino-succinate synthase	Mitochondrial aspartate aminotransferase
	Carbamoyl-phosphate synthase-I	Ornithine transcarbamoylase
Acute phase response	Alpha-1 acid glycoprotein/serine protease inhibitor	Fibrinogen
Bile acid metabolism	Cytochrome P450 7A1	
Bile salt transport	Na+ taurocholate cotransporting polypeptide	
Biotransformation	Aldehyde dehydrogenase type 3	Glutathione-S-transferase alpha
	Carboxyesterase	Cytochrome P450 3A11
	Cytochrome P450 2A5	UDP-glycuronosyltransferase 1A9
	Cytochrome P450 2C29	UDP-glucuronosyltransferase 2b5
	Cytosolic epoxide hydrolase	
Cell cycle	c-myc	Cyclin D1
Cell cycle regulation	G0/G1 switch gene 2	
Cellular proliferation	glucose-regulated protein-94	
Cholesterol metabolism	Cytochrome P450 12A1	Liver X receptor α
	Cytochrome P450 27A1	
Cholesterol transport	ABCA-a (via LXR α)	ABCG-8 (via LXR α)
	ABCG-5 (via LXR α)	
Desaturation of fatty acid	Delta-6-Desaturase	Stearoyl-CoA desaturase
	Delta-5-desaturase	
Fatty acid activation	Long-chain acyl-CoA synthetase	
Fatty acid binding/transport	Cytosolic fatty acid binding protein	
Fatty acid transport	Fatty acid transport protein-1	Fatty acid translocase
Fatty acid β -oxidation	Acyl-CoA oxidase	Medium-chain acyl-CoA dehydrogenase
		Long-chain acyl-CoA dehydrogenase
	ATP-binding cassette half-transporter type 2	Short-chain-specific
	ATP-binding cassette half-transporter type 3	3-ketoacyl-CoA thiolase
	Bifunctional enzyme	Short-chain acyl-CoA
	Carnitine palmitoyl-transferase I	Sterol carrier protein-X
	Carnitine palmitoyl-transferase II	Thiolase B
	Carnitine O-octanoyltransferase	Very long chain acyl-CoA dehydrogenase
		Very-long-chain acyl-CoA synthetase
Fatty acid ω -hydroxylation	Cytochrome P450 4A1	Cytochrome P450 4A10
	Cytochrome P450 4A3	Cytochrome P450 4A14
	Cytochrome P450 4A6-Z	
Fatty acid synthesis	Malic enzyme	

Table 4.5.1. List of PPAR α regulated genes in liver (with the genes identified in this project) (con't)

Function of gene	Genes	
Fatty acyl-CoA ester transport	Acyl-CoA binding protein	
Gluconeogenesis	Lactate dehydrogenase A4	
Glucose oxidation	Pyruvate dehydrogenase kinase isoform 4	
Heme biosynthesis	Coproporphyrinogen oxidase	
Hepatic sterol	Farnesoid X receptor/Bile acid receptor	
Hepatobiliary lipid transport	Multidrug resistance 2	
Hydrolysis of Acyl-CoA	Cytosolic acyl-CoA thioesterase-I	Peroxisomal acyl-CoA thioesterase 1A
	Cytosolic acyl-CoA thioesterase-II	Peroxisomal acyl-CoA thioesterase 1B
	Mitochondrial acyl-CoA thioesterase-I	Peroxisomal acyl-CoA thioesterase 2
Iron-binding protein	Lactoferrin	
Inflammation/ apoptosis	I κ B α	
Iron transport	Transferrin	
Ketogenesis	Mitochondrial HMG-CoA synthase	Mitochondrial HMG CoA synthase
Oxygen-free radical metabolism	Superoxide dimutase	
Peroxisome biogenesis	Peroxisome biogenesis factor 16	
Plasma HDL metabolism	Apolipoprotein-AI	Apolipoprotein-AV
	Apolipoprotein-A I (via rev-erb α)	Apolipoprotein-CIII
	Apolipoprotein-AII	Phospholipid transfer protein
	Apolipoprotein-A IV	Scavenger receptor B-type I
Pheromone carrier	Alpha-2 urinary globulin/MUP-I	
Repressor of gene transcription	Rev-erb α	
ROS production	Uncoupling protein-2	
Triglyceride clearance	Lipoprotein lipase	
Steroid metabolism	11-beta-Hydroxysteroid dehydrogenase I	17-beta-hydroxysteroid dehydrogenase XI
	17-beta-hydroxysteroid dehydrogenase IV	
Steroid hydroxylase	Cytochrome P450 2C11	Cytochrome P450 2C12
Vascular inflammation	Interleukin-6	Interleukin-6 receptor
	Interleukin-1 receptor-type 1	

Genes that highlighted were confirmed in this study.

controls. This suggested that the induction of Peci was mediated by PPAR α and Wy-14,643-responsive. Up-regulation of Peci was reported in 2 weeks Wy-14,643 treatment (Cherkaoui-Malki *et al.*, 2001). Up-regulation of the genes involved in peroxisomal β -oxidation was the effect of peroxisome proliferators. The induction of Peci increase peroxisomal β -oxidation which will increase the production of H₂O₂. Imbalance between production and catabolism of H₂O₂ will lead to oxidative stress, which is one of the proposed mechanisms of PP-induced hepatocarcinogenesis.

Mouse apolipoprotein A-V (ApoA5) is suggested to be involved in regulations of plasma triglyceride levels. Human ApoA5 is induced with the administration of Wy-14,643 and this induction is associated with suppression of plasma triglyceride (Vu-Dac *et al.*, 2003). However, mouse ApoA5 that identified in this project is down-regulated with the chronic exposure of Wy-14,643. This species difference in gene regulation between human and rodents in response to peroxisome proliferators treatment is also observed for ApoA1 and ApoA2 (Desvergne and Wahli, 1999). ApoA1 and ApoA2, which are major HDL apolipoproteins and PPAR α mediated, are down-regulated in rodents but up-regulated in humans. The reason for difference in species gene regulation of ApoA1, ApoA2 and ApoA5 is still not known. PPARE is identified in the human ApoA5 genes and human ApoA5 is believed as a positive and a direct target gene of PPAR α activators (Desvergne and Wahli, 1999; Vu-Dac *et al.*,

2003). Identification of PPRE in ApoA5 will help to explain its role in plasma triglyceride regulation in rodent and also the difference in species gene regulation between human and rodent.

Mouse medium-chain acyl-CoA dehydrogenase (MCAD; C₄-C₁₂) catalyses the formation of 2-enoyl-CoA from the fatty acyl-CoA (Eaton *et al.*, 1996). PPAR α regulates the mitochondrial β -oxidation by modulating the expression of medium-chain acyl-CoA dehydrogenase (MCAD) gene (Gulick *et al.*, 1994). The substrates for MCAD included medium-chain length acyl-CoA thioesters derived from medium-chain fatty acids that enter mitochondria by diffusion, products of mitochondrial β -oxidation of saturated and unsaturated long-chain fatty acids and products of peroxisomal β -oxidation of long-chain and very long-chain fatty acids. The mRNA expression of MCAD is predominantly in the tissue that use fatty acids as energy substrates, such as liver and heart (Kelly *et al.*, 1989). Induction of MCAD was observed started at 24 hours and persisted to 11 months in Wy-14,643-treated PPAR α (+/+) mice. The induction of MCAD was PPAR α -mediated as such induction was not observed in Wy-14,643-treated PPAR α (-/-) mice. The induction of MCAD leads to the increase in mitochondrial β -oxidation.

Mouse Cyp4a10 and Cyp4a14 belong to the Cyp4a family (Cyp4a). Both Cyp4a10 and Cyp4a14 were up-regulated in PPAR α (+/+) mice after 24 hours 0.1%

Wy-14,643 treatment and the inductions were persisted to 11 months. Such inductions were not found in PPAR α (-/-) mice suggested that the mRNA expressions of Cyp4a10 and Cyp4a14 were PPAR α -dependent (Lee *et al.*, 1995). The cytochrome monooxygenase system plays a central role in the oxidation of a wide variety of endogenous as well as exogenous compounds. The Cyp4a enzymes participate in this system as a distinct group of the cytochrome P450 superfamily. They catalyze the ω -hydroxylation of fatty acids and eicosanoids and are induced by fibrates and other peroxisome proliferators in liver and kidney. The first step of ω -hydroxylation generates ω -hydroxy fatty acid which is then dehydrogenated to a dicarboxylic acid in the cytosol (Johnson *et al.*, 1996; Reddy and Hashimoto, 2001). The dicarboxylic acid is then converted to its CoA derivative which can further be metabolized via peroxisomal β -oxidation. The increase in substrates for peroxisomal β -oxidation will lead to oxidative stress. ω -hydroxylation of fatty acids can also generate superoxide and/or H₂O₂ as the rate of NADPH consumption increases. PPAR α can provide a negative feedback on the intracellular levels of an endogenous ligand and PPAR α may have an important role in the detoxification of some xenobiotics (Desvergne and Wahli, 1999).

Mouse peroxisomal bifunctional enzyme (PBFE) is also named enoyl-CoA hydratase/L-3-hydroxyacyl-CoA dehydrogenase. It is induced by Wy-14,643 in

PPAR α (+/+) mice. Consistent induction of PBFE was observed at 24 hours and until 11 months treatment. No induction of PBFE in PPAR α (-/-) mice for both short-term and long-term Wy-14,643 treatment (Lee *et al.*, 1995). PBFE is involved in the L-hydroxy-specific peroxisome proliferator-inducible β -oxidation system while the D-PBE is involved in the D-hydroxy-specific β -oxidation system (Qi *et al.*, 1999). PBFE acts on long- and very long-straight chain acyl-CoAs, long-chain dicarboxylyl-CoAs and the CoA esters of prostaglandins whereas the non-inducible D-3-hydroxy-specific peroxisomal β -oxidation system is for branch chain acyl-CoA (Figure 4.5.1.1). The induction of PBFE expression and functional PPRE in PBFE are reported in previous studies (Zhang *et al.*, 1992; Bardot *et al.*, 1993).

Mouse very-long-chain acyl-CoA synthetase (VLCAS) is involved very long-chain fatty acid metabolism. Induction of VLCAS was observed in PPAR α (+/+) mice fed with 0.1% Wy-14,643 and started at 24 hours. The induction was persisted to 11 months treatment and maximum induction was observed at 1 week treatment. VLCAS was up-regulated by Wy-14,643 and PPAR α -dependent (Fischer *et al.*, 2003). Very long-chain fatty acid (VLCFA; \geq C22:0) can be β -oxidized predominantly in peroxisome. VLCFA is first activated to VLCFA-CoA in the β -oxidation. This reaction is catalyzed by very long-chain acyl-CoA synthetase (VLCAS) which is found in peroxisomes and microsomes but not in mitochondria

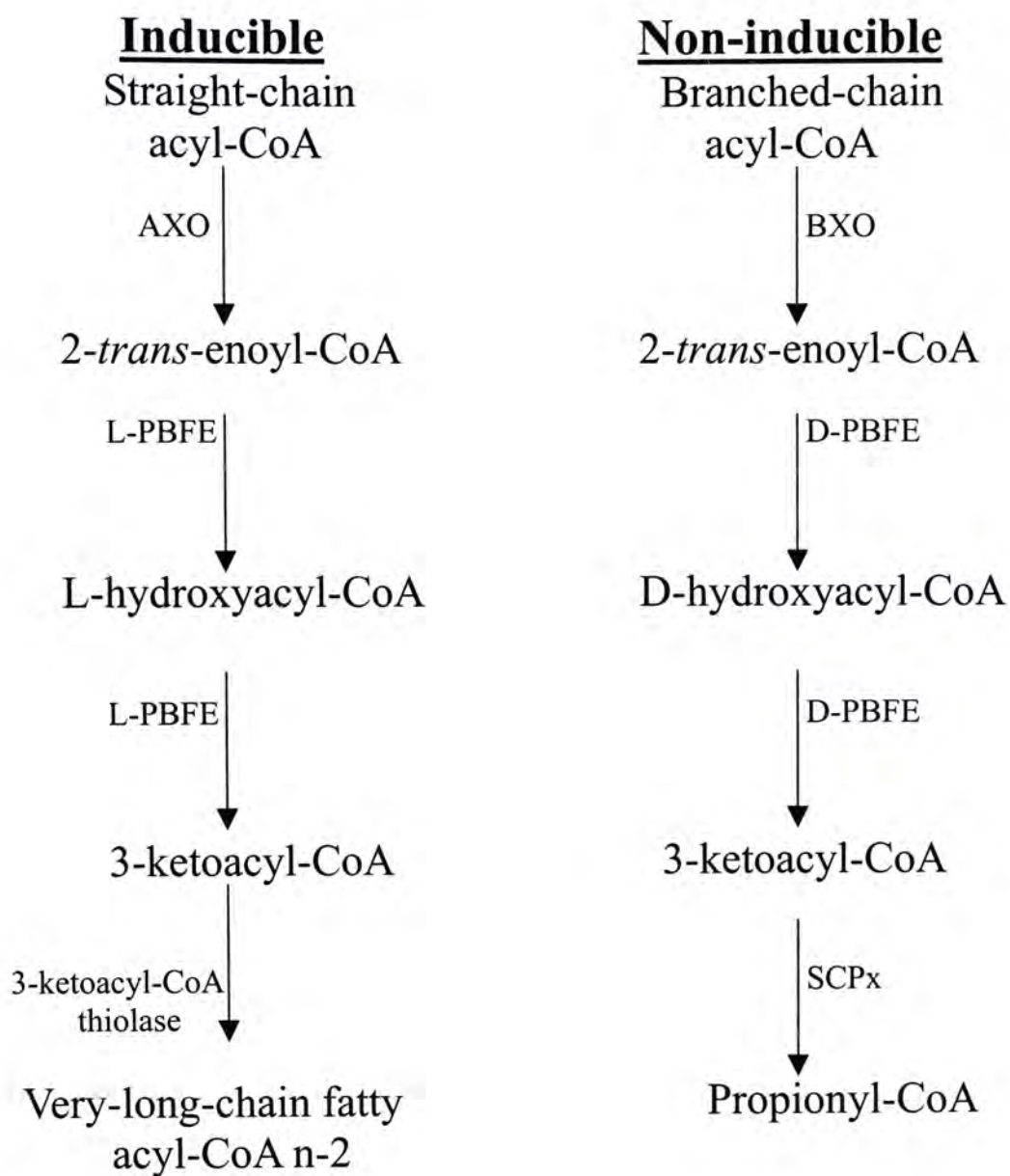


Figure 4.5.1.1. Peroxisome β -oxidation systems, inducible and non-inducible.

(Kalish *et al.*, 1995). However, rat liver mitochondria can β -oxidize hexacosanoyl CoA but not hexacosanoic acid (C26:0), whereas peroxisome can β -oxidize both substrates. It suggests that mitochondria can also β -oxidize VLFAs, provided that it is first converted to their CoAs by VLCAS (Singh *et al.*, 1987).

Mouse peroxisomal acyl-CoA oxidase (AOX) is the rate-limiting step of the pathway that show 10- to 30- fold induction with the administration of the peroxisome proliferators. The induction of peroxisomal fatty acid oxidation is important in protecting the liver against FFA toxicity as steatohepatitis is found in acyl-CoA oxidase knock-out mice (Everett *et al.*, 2000). Early and obvious up-regulation of AOX was found in PPAR α (+/+) mice fed with the 0.1% Wy-14,643 diet. Maximum induction was observed at 1 week and continued to 11 months treatment. Induction of AOX causes the increase production of H₂O₂ and oxidative stress when there is no sufficient catalase, which is involved in the detoxification of H₂O₂ (Reddy and Rao, 1989).

Up-regulation of mouse carnitine O-octanoyltransferase (Crot) was found in PPAR α (+/+) mice for both short-term and long-term treatment with 0.1% Wy-14,643. Crot is one of the carnitine acyltransferases in rat liver (CAT, carnitine acetyltransferase; Crot, carnitine O-octanoyltransferase; CPT, carnitine palmitoyltransferase), which is markedly increased by administration of peroxisome proliferators such as DEHP

(Ozasa *et al.*, 1983). Crot is suggested to be a peroxisomal enzyme whereas CAT and CPT are mitochondrial enzymes. Recent studies suggested that Crot plays a role in the transport of peroxisomal β -oxidation products to mitochondria. CAT, Crot and CPT showed different substrate specificities as CAT reacts with short-chain acyl derivatives, and CPT reacts with medium-chain and long-chain acyl derivatives. Crot is believed to be most active with hexanoyl derivatives although it also catalyze the reaction with medium-chain length substrates and to be most active toward octanoyl derivatives (Miyazama *et al.*, 1983). Crot can also reactive with the substrates with C₂-C₂₀. Crot is suggested to play a role in pumping out the peroxisomal β -oxidation products (short- and medium-chain acyl-CoA's) to the cytosolic compartment by their conversion to carnitine derivatives.

Mouse cysteine sulfinic acid decarboxylase (CSAD) is suggested to be markers genes of hepatocarcinogenesis. CSAD synthesizes a precursor of taurine, which becomes a major component of bile, and a neurotransmitter in brain. CSAD is suggested to be important in both maintenance and growth of hepatocytes as it is found in normal liver and its expression was induced during liver regeneration (Kishimoto *et al.*, 1996). CSAD expression is induced during hepatocarcinogenesis in the precancerous liver and maintained its high expression afterward. However, the relationship between over-expression of CSAD and hepatocarcinogenesis is still not

known. Over-expression of CSAD may cause hepatocarcinogenesis as the action of CSAD may result in some actual carcinogenic substrates *in vivo* in addition to taurine. In contrast, the over-expression of CSAD may be due to hepatocarcinogenesis. Intrinsic oncogene may transcriptionally activated CSAD. Over-expression of CSAD may be also due to the increase in demand for the removal of carcinogenic substances from the liver that require more bile (Kishimoto *et al.*, 1996). In this study, CSAD was weakly induced in PPAR α (+/+) fed with the 0.1% Wy-14,643 diet after 24 hours and persisted to 11 months treatment. PPAR α (-/-) mice treated with the 0.1% Wy-14,643 diet did not show any induction when compared the controls. This suggested the regulation CSAD was mediated by PPAR α . The over-expression of CSAD may be due to the demand for the removal of Wy-14,643 compound.

Mouse major urinary protein II (MUP II) that also called α 2- urinary globulin (α 2U) in rat is induced by the male-specific pulsatile release of growth hormone but repressed by inflammation. Obvious down-regulation of MUP II was observed started at 1 week Wy-14,643 treatment in PPAR α (+/+). The down-regulation of MUP with chronic exposure to Wy-14,643 has been mentioned and MUP might serve as an early tumor marker during hepatocarcinogenesis of mouse (Anderson *et al.*, 1999).

Mouse UDP-glucuronosyltransferase 2 family member 5 (UGT2b5) belongs to

the superfamily UDP-glucuronosyltransferases (UGTs). Down-regulation of UGT2b5 was observed in PPAR α (+/+) mice fed with the 0.1% Wy-14,643 diet after 2 weeks treatment and this down-regulation was not observed in the controls. UGTs are located in the endoplasmic reticulum and perform a key process in endobiotic and xenobiotic metabolism. UGTs enhance the eliminations of their substrates via bile, faeces and urine through catalyse the conversion of lipophilic molecules into more polar, and thus hydrophilic, glucuronides. UGTs substrates include phenolics, steroid hormones, carcinogens such as benzo(α)pyrene metabolites and drugs. Thus, UGTs is important in the detoxification of endogenous, dietary and clinically administered agents as well as environmentally present chemical, which have been reported to be carcinogenic (Strassburg *et al.*, 1999). Down-regulation of UGT in pre-malignant adenomatous hyperomatous hyperplasia of the liver and malignant hepatocellular carcinoma is reported. It is suggested that UGT may be involved in genoprotection, however, further studies should be carried out before used it as an early marker in cancer development (Tukey and Strassburg, 2000).

Peroxisome biogenesis factor 16 (Pex16) is involved in the membrane-assembly step of peroxisome biogenesis (Honsho *et al.*, 2002). Pex16 was up-regulated at 24 hours Wy-14,643 treatment in PPAR α (+/+) mice. The up-regulation was persisted to 11 months treatment and was not found in the PPAR α (-/-) mice fed with the 0.1%

Wy-14,643 diet after short-term or long-term treatment. The up-regulation of Pex16 may play a role in peroxisome proliferation. Pex16 is required for the import of certain matrix proteins. Over-expression of Pex 16 caused accumulation of enlarged peroxisomes (Subramani, 1998). Peroxisome proliferation, which means increase in both numbers and size of peroxisomes, is observed with the administration of peroxisome proliferators after short-term treatment, so the induction of Pex16 is responsible for the PP-induced peroxisome proliferation.

Mouse serine protease inhibitor, clade A, member 1a (SPI) is also named α -1 antitrypsin (ATT). SPI is an acute phase protein which is synthesized primarily in the liver. SPI is an important factor in controlling tissue damage by protease in inflammatory diseases for example atherosclerosis. The maintenance of balance between protease and antiprotease is important in preventing tissue damage induced by proteinases in the microenvironment of injury and inflammation where inflammatory cells tend to accumulate (Dichtl *et al.*, 2000). Down-regulation of SPI was found in PPAR α (+/+) mice fed with the 0.1% Wy-14,643 diet after 1 week treatment. The down-regulation was not found in PPAR α (-/-) mice fed with 0.1% Wy-14,643 suggested the regulation of SPI was mediated by PPAR α . Down-regulation of SPI after chronic (13 weeks) exposure with Wy-14,643 is reported in previous study. The suppression of the gene may be due to the anti-inflammatory

effect in mice that elicit by Wy-14,643 which possibly through increased leukotrine B₄ catabolism or inhibition of IL-1-induced production of IL-6, prostaglandin and cyclooxygenase-2 (Anderson *et al.*, 1999)

Mouse hydroxysteroid (17-beta) dehydrogenase 11 (Hsd17 β 11) is a member of the 17 β -hydroxysteroid dehydrogenase. The function of human Hsd17b11 is involved in estrogen and androgen inactivation (Mindnich *et al.*, 2004). The substrates for Hsd17 β including glucocorticoids, sex steroids, bile acids, fatty acids and branched chain amino acids (Shafqat *et al.*, 2003; Mindnich *et al.*, 2004). The Hsd17 β 11 may be important for the metabolization of toxic compounds (Chai *et al.*, 2003; Motojima, 2004). Up-regulation of Hsd17 β 11 was started at 1 week treatment and only found in PPAR α (+/+) mice fed with the 0.1% Wy-14,643 diet. Another member of the 17 β -hydroxysteroid dehydrogenase, Hsd17 β 4 that has the same functions as Hsd17b11 in human and rodents is induced by peroxisome proliferators (Corton *et al.*, 1996).

Mouse carboxyesterase plays a role in the metabolism of xenobiotics and endogenous lipids. Carboxyesterases are distributed in different tissues and present in several subcellular organelles, whereas the highest abundant of carboxyesterase is observed in liver microsomes, where they are loosely bound to the luminal surface of the endoplasmic reticulum. They hydrolyze lipid substrates and thus may have

different lipid-metabolizing functions. Carboxyesterase was down-regulated after 1 week 0.1% Wy-14,643 treatment in PPAR α (+/+) mice. Carboxyesterase is down-regulated with chronic exposure of Wy-14,643 and this suppression is observed between 1 and 5 weeks of exposure. The delayed response of carboxyesterase to Wy-14,643 treatment suggested that carboxyesterase regulation is not a direct effect of PP-regulated activity of PPAR α . The down-regulation of carboxyesterase may be the secondary event after long-term exposure to high doses of peroxisome proliferators (Poole *et al.*, 2001).

Mouse adipose differentiation related protein (ADRP) was up-regulated by 0.1% Wy-14,643 through PPAR α . The up-regulation of ADRP was observed started at 24 hours and maximum up-regulation was found at 2 weeks Wy-14,643 treatment. Expression of ADRP is induced by PPAR α ligands (Liu *et al.*, 2003). ADRP is a lipid droplets-associated protein that stimulates lipid accumulation and lipid droplets formation in murine fibroblasts and is expressed early during adipose differentiation (Imamura *et al.*, 2002). ADRP expression is induced by long-chain fatty acids but such induction is stimulated by short-chain fatty acids. ADRP, which bound to the surface of lipid droplets, may serve as concentrate unesterified fatty acids. They are then converted to fatty acyl-CoA thioesters for subsequent cellular utilization (Serrero *et al.*, 2000).

However, not all PPAR α -dependent and Wy-14,643 responsive fragments could be confirmed by Northern blot analysis. No differential display patterns (e.g. mitochondria) and detectable signals (e.g. EST) were observed. The up-regulation of the genes might be not so obvious that could be observed and confirmed by Northern blot analysis.

4.6 Mechanism of PP-induced hepatocarcinogenesis

Oxidative stress, inhibition of apoptosis and increase cellular proliferation are the mechanism suggested so far for the PP-induced hepatocarcinogenesis. However, the mechanism(s) of PP-induced hepatocarcinogenesis is/are still not confirmed. Identification of PPAR α -dependent and Wy-14,643-responsive genes can help us to explain the mechanism of PP-induced hepatocarcinogenesis. The genes that confirmed in this project are mainly involved in the fatty acid β -oxidation which is suggested to increase the oxidative stress (Figure 4.6.1). Increase in oxidative stress will lead to DNA damage that is one the proposed PP-induced hepatocarcinogenesis.

The PPAR α dependent and Wy-14,643 responsive genes that confirmed in this project and related to oxidative stress was summarized in Figure 4.6.1. Peroxisomal delta3, delta2-enoyl-Coenzyme A isomerase, peroxisomal bifunctional enzyme, very-long-chain acyl-CoA synthetase and peroxisomal acyl CoA oxidase are the genes

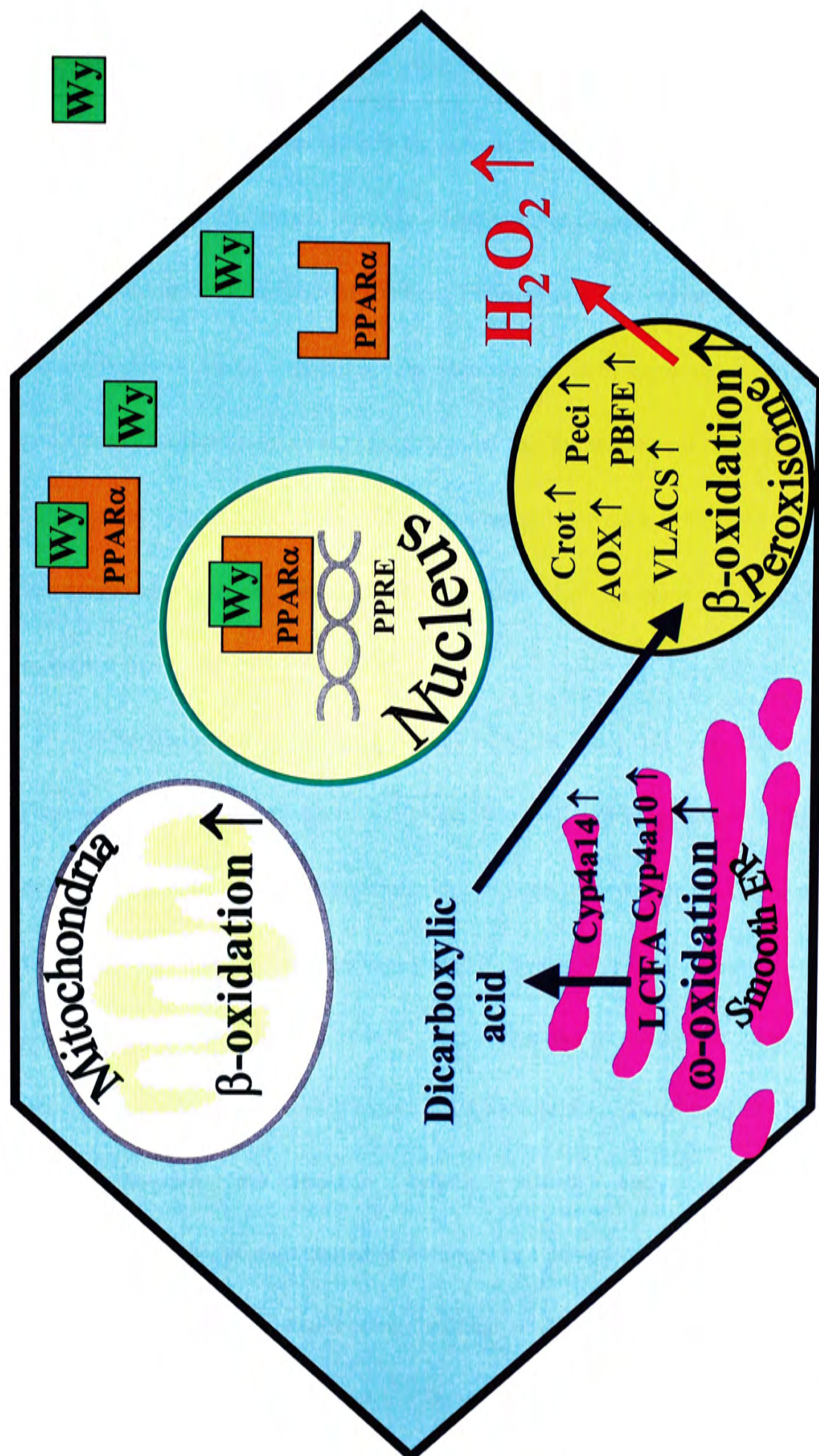


Figure 4.6.1. Summary of PPARα dependent and Wy-14,643 responsive genes caused oxidation stress.

that involved in peroxisomal β -oxidation. The over-expression of these genes especially acyl CoA oxidase leads to the induction of peroxisomal β -oxidation that in turns, increase the production of H_2O_2 . However, as catalase that act on the H_2O_2 is only induced to 2- to 3-fold (Nemali *et al.*, 1989), excess H_2O_2 cannot be removed and cause oxidative stress. Besides, the increase in ω -hydroxylation increases the generation dicarboxylic acids. Dicarboxylic acids are one of the substrates for peroxisomal β -oxidation. The H_2O_2 generates by ω -hydroxylation and in turns of increasing substrates for peroxisomal β -oxidation also contribute to the increase in oxidative stress.

The alterations of gene expressions of all of the genes were observed after short-term Wy-14,643 treatment. Up-regulation of mouse peroxisomal delta 3, delta 2-enoyl-Coenzyme A isomerase, mouse acetyl-Coenzyme A dehydrogenase, medium chain, peroxisome biogenesis factor 16, mouse Cyp4a14, mouse peroxisomal bifunctional enzyme, mouse Cyp4a10, very-long-chain acyl-CoA synthetase, mouse peroxisomal acyl-CoA oxidase, mouse hydroxysteroid (17-beta) dehydrogenase 11, mouse adipose differentiation related protein and mouse carnitine O-octanoyltransferase were started at 24 hours and persisted to 11 months treatment while up-regulation of mouse cysteine sulfinic acid decarboxylase was started at 1 week and persisted to 11 months. Down-regulation of mouse serine protease

inhibitor 1-1, mouse major urinary protein II and mouse carboxyesterase was started at 1 week and continued to 11 months. Mouse UDP-glucuronosyltransferase 2 family member 5 was down-regulated at 2 weeks and persisted to 11 months. As the alteration of the genes observed after short-term treatment and persisted to cancer stage, these enable these genes to be cancer marker genes. Chemicals which induce these genes after short-term exposure to rodents may cause hepatocarcinogenesis after long-term exposure.

Chapter 5 Conclusion

Hepatomegaly, loss of body weight and hepatocarcinoma with trabecular patterns were observed in the 0.1% Wy-14,643 treated PPAR α (+/+) mice after chronic exposure. Besides, relative organ weight of white fat, brown fat and spleen was lower in the 0.1% Wy-14,643 treated PPAR α (+/+) mice compared with the controls.

Alterations of gene expression were also observed after 11 months treatment of Wy-14,643. Total 17 PPAR α dependent and Wy-14,643 responsive genes were identified in this project. Peroxisomal delta3, delta2-enoyl-Coenzyme A isomerase, mouse cysteine sulfinic acid decarboxylase, mouse acetyl-Coenzyme A dehydrogenase, medium chain, peroxisome biogenesis factor 16, mouse Cyp4a14, mouse peroxisomal bifunctional enzyme, mouse Cyp4a10, very-long-chain acyl-CoA synthetase, mouse peroxisomal acyl-CoA oxidase, mouse hydroxysteroid (17-beta) dehydrogenase 11, mouse adipose differentiation related protein and mouse carnitine O-octanoyltransferase were confirmed to be up-regulated by 0.1% Wy-14,643 and PPAR α dependent. Mouse apolipoprotein A-V, mouse UDP-glucuronosyltransferase 2 family member 5, mouse serine protease inhibitor 1-1, mouse major urinary protein II and mouse carboxyesterase were confirmed to be down-regulated by 0.1%

Wy-14,643 and PPAR α dependent. Temporal expression of all the identified genes except apolipoprotein A-V were also performed.

Based on the genes identified, oxidative stress is suggested to be the mechanism of PP-induced hepatocarcinogenesis. However, whether the PP-induced hepatocarcinogenesis is induced by other mechanisms are not still clear. It is suggested that PP-induced hepatocarcinogenesis is due to the oxidative stress and also the effect of inhibition of apoptosis and increase in cell replication. Further studies are necessary to find out the relationship of different mechanisms and the chronic effect of peroxisome proliferators on humans.

- Aldridge, T. C., Tugwood, J. D., and Green, S. (1995). Identification and characterization of DNA elements implicated in the regulation of CYP4A1 transcription. *Biochem J* **306** (Pt 2), 473-479.
- Allain, C. A., Poon, L. S., Ghan, C. S. G., Richmond, W., and Fu, P. C. (1974). Enzymatic determination of total serum cholesterol. *Clin Chem* **1**, 12-16.
- Anderson, S. P., Cattley, R. C., and Corton, J. C. (1999). Hepatic expression of acute-phase protein genes during carcinogenesis induced by peroxisome proliferators. *Molecular carcinogenesis* **26**, 226-238.
- Ashby, J., Brady, A., Elcombe, C. R., Elliott, B. M., Ishmael, J., Odum, J., Tugwood, J. D., Kettle, S., and Purchase, I. F. (1994). Mechanistically-based human hazard assessment of peroxisome proliferator-induced hepatocarcinogenesis. *Hum Exp Toxicol* **13 Suppl 2**, S1-117.
- Bardot, O., Aldridge, T. C., Latruffe, N., and Green, S. (1993). PPAR-RXR heterodimer activates a peroxisome proliferator response element upstream of the bifunctional enzyme gene. *Biochem Biophys Res Commun* **192**, 37-45.
- Bayly, A. C., Roberts, R. A., and Dive, C. (1994). Suppression of liver cell apoptosis in vitro by the non-genotoxic hepatocarcinogen and peroxisome proliferator nafenopin. *J Cell Biol* **125**, 197-203.
- Beck, F., Plummer, S., Senior, P. V., Byrne, S., Green, S., and Brammar, W. J. (1992). The ontogeny of peroxisome-proliferator-activated receptor gene expression in the mouse and rat. *Proc Biol Sci* **247**, 83-87.
- Bell, F. P. (1983). Effect of the plasticizer di(2-ethylhexyl) adipate (dioctyladipate, DOA) on lipid metabolism in the rat: I. Inhibition of cholesterolgenesis and modification of phospholipid synthesis. *Lipids* **18**, 211-215.
- Berger, J., and Moller, D. E. (2002). The mechanisms of action of PPARs. *Annu Rev Med* **53**, 409-435.
- Biegel, L. B., Hurtt, M. E., Frame, S. R., Applegate, M., O'Connor, J. C., and Cook, J. C. (1992). Comparison of the effects of Wyeth-14,643 in Crl:CD BR and Fisher-344 rats. *Fundam Appl Toxicol* **19**, 590-597.
- Biegel, L. B., Hurtt, M. E., Frame, S. R., O'Connor, J. C., and Cook, J. C. (2001). Mechanisms of extrahepatic tumor induction by peroxisome proliferators in male CD rats. *Toxicol Sci* **60**, 44-55.
- Braissant, O., Fougelle, F., Scotto, C., Dauca, M., and Wahli, W. (1996). Differential expression of peroxisome proliferator-activated receptors (PPARs): tissue distribution of PPAR-alpha, -beta, and -gamma in the adult rat. *Endocrinology* **137**, 354-366.
- Braissant, O., and Wahli, W. (1998). Differential expression of peroxisome proliferator-activated receptor-alpha, -beta, and -gamma during rat embryonic development. *Endocrinology* **139**, 2748-2754.
- Bucolo, G., and David, H. (1973). Quantitative determination of serum triglycerides by the use of enzymes. *Clin Chem* **19**, 476-483.
- Butler, E. G., Tanaka, T., Ichida, T., Maruyama, H., Leber, A. P., and Williams, G. M. (1988). Induction of hepatic peroxisome proliferation in mice by lactofen, a diphenyl ether herbicide. *Toxicol Appl Pharmacol* **93**, 72-80.
- Cajaraville, M. P., Cancio, I., Ibabe, A., and Orbea, A. (2003). Peroxisome proliferation as a biomarker in environmental pollution assessment. *Microsc Res Tech* **61**, 191-202.

- Carthew, P., Edwards, R. E., and Nolan, B. M. (1998). New approaches to the quantitation of hypertrophy and hyperplasia in hepatomegaly. *Toxicol Lett* **102-103**, 411-415.
- Cattley, R. C., Marsman, D. S., and Popp, J. A. (1989). Failure of the peroxisome proliferator WY-14,643 to initiate growth-selectable foci in rat liver. *Toxicology* **56**, 1-7.
- Cattley, R. C., Marsman, D. S., and Popp, J. A. (1991). Age-related susceptibility to the carcinogenic effect of the peroxisome proliferator WY-14,643 in rat liver. *Carcinogenesis* **12**, 469-473.
- Cattley, R. C., and Popp, J. A. (1989). Differences between the promoting activities of the peroxisome proliferator WY-14,643 and phenobarbital in rat liver. *Cancer Res* **49**, 3246-3251.
- Chai, Z., Brereton, P., Suzuki, T., Sasano, H., Obeyesekere, V., Escher, G., Saffery, R., Fuller, P., Enriquez, C., and Krozowski, Z. (2003). 17 beta-hydroxysteroid dehydrogenase type XI localizes to human steroidogenic cells. *Endocrinology* **144**, 2084-2091.
- Cherkaoui-Malki, M., Meyer, K., Cao, W. Q., Latruffe, N., Yeldandi, A. V., Rao, M. S., Bradfield, C. A., and Reddy, J. K. (2001). Identification of novel peroxisome proliferator-activated receptor alpha (PPARalpha) target genes in mouse liver using cDNA microarray analysis. *Gene Expr* **9**, 291-304.
- Cheung, C., Akiyama, T. E., Ward, J. M., Nicol, C. J., Feigenbaum, L., Vinson, C., and Gonzalez, F. J. (2004). Diminished hepatocellular proliferation in mice humanized for the nuclear receptor peroxisome proliferator-activated receptor alpha. *Cancer Res* **64**, 3849-3854.
- Corton, J. C., Anderson, S. P., and Stauber, A. (2000). Central role of peroxisome proliferator-activated receptors in the actions of peroxisome proliferators. *Annu Rev Pharmacol Toxicol* **40**, 491-518.
- Corton, J. C., Bocos, C., Moreno, E. S., Merritt, A., Marsman, D. S., Sausen, P. J., Cattley, R. C., and Gustafsson, J. A. (1996). Rat 17 beta-hydroxysteroid dehydrogenase type IV is a novel peroxisome proliferator-inducible gene. *Mol Pharmacol* **50**, 1157-1166.
- Crunkhorn, S. E., Plant, K. E., Gibson, G. G., Kramer, K., Lyon, J., Lord, P. G., and Plant, N. J. (2004). Gene expression changes in rat liver following exposure to liver growth agents: role of Kupffer cells in xenobiotic-mediated liver growth. *Biochem Pharmacol* **67**, 107-118.
- David, R. M., Moore, M. R., Finney, D. C., and Guest, D. (2000). Chronic toxicity of di(2-ethylhexyl)phthalate in rats. *Toxicol Sci* **55**, 433-443.
- Desvergne, B., and Wahli, W. (1999). Peroxisome proliferator-activated receptors: nuclear control of metabolism. *Endocr Rev* **20**, 649-688.
- Devchand, P. R., Keller, H., Peters, J. M., Vazquez, M., Gonzalez, F. J., and Wahli, W. (1996). The PPARalpha-leukotriene B4 pathway to inflammation control. *Nature* **384**, 39-43.
- Dichtl, W., Moraga, F., Ares, M. P. S., Crisby, M., Nilsson, J., Lingren, S., and Janciauskiene, S. (2000). The carboxyl-terminal fragment of alpha1-antitrypsin is present in atherosclerotic plaques and regulates inflammatory transcription factors in primary human monocytes. *molecular cell biology research communications* **4**, 50-61.

- Dreyer, C., Keller, H., Mahfoudi, A., Laudet, V., Krey, G., and Wahli, W. (1993). Positive regulation of the peroxisomal beta-oxidation pathway by fatty acids through activation of peroxisome proliferator-activated receptors (PPAR). *Biol Cell* **77**, 67-76.
- Dzhekova-Stojkova, S., Bogdanska, J., and Stojkova, Z. (2001). Peroxisome proliferators: their biological and toxicological effects. *Clin Chem Lab Med* **39**, 468-474.
- Eaton, S., Bartlett, K., and Pourfarzam, M. (1996). Mammalian mitochondrial beta-oxidation. *Biochem J* **320** (Pt 2), 345-357.
- Everett, L., Galli, A., and Crabb, D. (2000). The role of hepatic peroxisome proliferator-activated receptors (PPARs) in health and disease. *Liver* **20**, 191-199.
- Fischer, M., You, M., Matsumoto, M., and Crabb, D. W. (2003). Peroxisome proliferator-activated receptor alpha (PPARalpha) agonist treatment reverses PPARalpha dysfunction and abnormalities in hepatic lipid metabolism in ethanol-fed mice. *J Biol Chem* **278**, 27997-28004.
- Forman, B. M., Chen, J., and Evans, R. M. (1997). Hypolipidemic drugs, polyunsaturated fatty acids, and eicosanoids are ligands for peroxisome proliferator-activated receptors alpha and delta. *Proc Natl Acad Sci U S A* **94**, 4312-4317.
- Frenkel, R. A., Slaughter, C. A., Orth, K., Moomaw, C. R., Hicks, S. H., Snyder, J. M., Bennett, M., Prough, R. A., Putnam, R. S., and Milewich, L. (1990). Peroxisome proliferation and induction of peroxisomal enzymes in mouse and rat liver by dehydroepiandrosterone feeding. *J Steroid Biochem* **35**, 333-342.
- Gearing, K. L., Gottlicher, M., Teboul, M., Widmark, E., and Gustafsson, J. A. (1993). Interaction of the peroxisome-proliferator-activated receptor and retinoid X receptor. *Proc Natl Acad Sci U S A* **90**, 1440-1444.
- Gervois, P., Torra, I. P., Fruchart, J. C., and Staels, B. (2000). Regulation of lipid and lipoprotein metabolism by PPAR activators. *Clin Chem Lab Med* **38**, 3-11.
- Gonzalez, F. J. (1997). Recent update on the PPAR alpha-null mouse. *Biochimie* **79**, 139-144.
- Gorgas, K., and Krisans, S. K. (1989). Zonal heterogeneity of peroxisome proliferation and morphology in rat liver after gemfibrozil treatment. *J Lipid Res* **30**, 1859-1875.
- Gottlicher, M., Widmark, E., Li, Q., and Gustafsson, J. A. (1992). Fatty acids activate a chimera of the clofibric acid-activated receptor and the glucocorticoid receptor. *Proc Natl Acad Sci U S A* **89**, 4653-4657.
- Grant, D. F., Storms, D. H., and Hammock, B. D. (1993). Molecular cloning and expression of murine liver soluble epoxide hydrolase. *J Biol Chem* **268**, 17628-17633.
- Green, S. (1995). PPAR: a mediator of peroxisome proliferator action. *Mutat Res* **333**, 101-109.
- Gulick, T., Cresci, S., Caira, T., Moore, D. D., and Kelly, D. P. (1994). The peroxisome proliferator-activated receptor regulates mitochondrial fatty acid oxidative enzyme gene expression. *Proc Natl Acad Sci U S A* **91**, 11012-11016.
- Havel, R. J., and Kane, J. P. (1973). Drugs and lipid metabolism. *Annu Rev Pharmacol* **13**, 287-308.
- Hertz, R., Bishara-Shieban, J., and Bar-Tana, J. (1995). Mode of action of peroxisome proliferators as hypolipidemic drugs. Suppression of apolipoprotein C-III. *J Biol Chem* **270**, 13470-13475.

- Honsho, M., Hiroshige, T., and Fujiki, Y. (2002). The membrane biogenesis peroxin Pex16p. Topogenesis and functional roles in peroxisomal membrane assembly. *J Biol Chem* **277**, 44513-44524.
- IARC (1982). Di(2-ethylhexyl) phthalate. *IARC Monogr Eval Carcinog Risk Chem Hum* **29**, 269-294.
- Imamura, M., Inoguchi, T., Ikuyama, S., Taniguchi, S., Kobayashi, K., Nakashima, N., and Nawata, H. (2002). ADRP stimulates lipid accumulation and lipid droplet formation in murine fibroblasts. *Am J Physiol Endocrinol Metab* **283**, E775-783.
- Issemann, I., and Green, S. (1990). Activation of a member of the steroid hormone receptor superfamily by peroxisome proliferators. *Nature* **347**, 645-650.
- James, N. H., Gill, J. H., Brindle, R., Woodyatt, N. J., Macdonald, N., Rolfe, M., Hasmall, S. C., Tugwood, J. D., Holden, P. R., and Roberts, R. A. (1998). Peroxisome proliferator-activated receptor (PPAR) alpha-regulated growth responses and their importance to hepatocarcinogenesis. *Toxicol Lett* **102-103**, 91-96.
- Johnson, E. F., Palmer, C. N., Griffin, K. J., and Hsu, M. H. (1996). Role of the peroxisome proliferator-activated receptor in cytochrome P450 4A gene regulation. *Faseb J* **10**, 1241-1248.
- Kalish, J. E., Chen, C. I., Gould, S. J., and Watkins, P. A. (1995). Peroxisomal activation of long- and very long-chain fatty acids in the yeast *Pichia Pastoris*. *Biochemical and biophysical research communications* **206**, 335-340.
- Keller, H., Dreyer, C., Medin, J., Mahfoudi, A., Ozato, K., and Wahli, W. (1993). Fatty acids and retinoids control lipid metabolism through activation of peroxisome proliferator-activated receptor-retinoid X receptor heterodimers. *Proc Natl Acad Sci U S A* **90**, 2160-2164.
- Kelly, D. P., Gordon, J. I., Alpers, R., and Strauss, A. W. (1989). The tissue-specific expression and developmental regulation of two nuclear genes encoding rat mitochondrial proteins. Medium chain acyl-CoA dehydrogenase and mitochondrial malate dehydrogenase. *J Biol Chem* **264**, 18921-18925.
- Kishimoto, T., Kokura, K., Nakadai, T., Miyazawa, Y., Wakamatsu, T., Makino, Y., Nakamura, T., Hara, E., Oda, K., Muramatsu, M., and Tamura, T. (1996). Overexpression of cysteine sulfinic acid decarboxylase stimulated by hepatocarcinogenesis results in autoantibody production in rats. *Cancer Res* **56**, 5230-5237.
- Kitamura, S., Miyazaki, Y., Shinomura, Y., Kondo, S., Kanayama, S., and Matsuzawa, Y. (1999). Peroxisome proliferator-activated receptor gamma induces growth arrest and differentiation markers of human colon cancer cells. *Jpn J Cancer Res* **90**, 75-80.
- Kliwer, S. A., Forman, B. M., Blumberg, B., Ong, E. S., Borgmeyer, U., Mangelsdorf, D. J., Umesono, K., and Evans, R. M. (1994). Differential expression and activation of a family of murine peroxisome proliferator-activated receptors. *Proc Natl Acad Sci U S A* **91**, 7355-7359.
- Kliwer, S. A., Sundseth, S. S., Jones, S. A., Brown, P. J., Wisely, G. B., Koble, C. S., Devchand, P., Wahli, W., Willson, T. M., Lenhard, J. M., and Lehmann, J. M. (1997). Fatty acids and eicosanoids regulate gene expression through direct interactions with peroxisome proliferator-activated receptors alpha and gamma. *Proc Natl Acad Sci U S A* **94**, 4318-4323.

- Kliewer, S. A., Umesono, K., Noonan, D. J., Heyman, R. A., and Evans, R. M. (1992). Convergence of 9-cis retinoic acid and peroxisome proliferator signalling pathways through heterodimer formation of their receptors. *Nature* **358**, 771-774.
- Kota, B. P., Huang, T. H., and Roufogalis, B. D. (2005). An overview on biological mechanisms of PPARs. *Pharmacol Res* **51**, 85-94.
- Kraupp-Grasl, B., Huber, W., Taper, H., and Schulte-Hermann, R. (1991). Increased susceptibility of aged rats to hepatocarcinogenesis by the peroxisome proliferator nafenopin and the possible involvement of altered liver foci occurring spontaneously. *Cancer Res* **51**, 666-671.
- Krey, G., Braissant, O., L'Horsset, F., Kalkhoven, E., Perroud, M., Parker, M. G., and Wahli, W. (1997). Fatty acids, eicosanoids, and hypolipidemic agents identified as ligands of peroxisome proliferator-activated receptors by coactivator-dependent receptor ligand assay. *Mol Endocrinol* **11**, 779-791.
- Kunau, W. H., Dommes, V., and Schulz, H. (1995). beta-oxidation of fatty acids in mitochondria, peroxisomes, and bacteria: a century of continued progress. *Prog Lipid Res* **34**, 267-342.
- Lalwani, N. D., Reddy, M. K., Qureshi, S. A., and Reddy, J. K. (1981). Development of hepatocellular carcinomas and increased peroxisomal fatty acid beta-oxidation in rats fed [4-chloro-6-(2,3-xylidino)-2-pyrimidinylthio] acetic acid (Wy-14,643) in the semipurified diet. *Carcinogenesis* **2**, 645-650.
- Laughter, A. R., Dunn, C. S., Swanson, C. L., Howroyd, P., Cattley, R. C., and Corton, J. C. (2004). Role of the peroxisome proliferator-activated receptor alpha (PPARalpha) in responses to trichloroethylene and metabolites, trichloroacetate and dichloroacetate in mouse liver. *Toxicology* **203**, 83-98.
- Lee, S. S., Pineau, T., Drago, J., Lee, E. J., Owens, J. W., Kroetz, D. L., Fernandez-Salguero, P. M., Westphal, H., and Gonzalez, F. J. (1995). Targeted disruption of the alpha isoform of the peroxisome proliferator-activated receptor gene in mice results in abolishment of the pleiotropic effects of peroxisome proliferators. *Mol Cell Biol* **15**, 3012-3022.
- Lee, S. S., Tian, L., Lee, W. S., and Cheung, W. T. (2002). Application of fluorescent differential display and peroxisome proliferator-activated receptor (PPAR) alpha-null mice to analyze PPAR target genes. *Methods Enzymol* **357**, 214-240.
- Lim, H., Gupta, R. A., Ma, W. G., Paria, B. C., Moller, D. E., Morrow, J. D., DuBois, R. N., Trzaskos, J. M., and Dey, S. K. (1999). Cyclo-oxygenase-2-derived prostacyclin mediates embryo implantation in the mouse via PPARdelta. *Genes Dev* **13**, 1561-1574.
- Liu, P. C. C., Huber, R., Stow, M. D., Schlingmann, K. L., Collier, P., Liao, B., John Link, T. C. B., Hollis, G., Young, P. R., and Mukherjee, R. (2003). Induction of endogenous genes by peroxisome proliferator activated receptor alpha ligands in a human kidney cell line and in vivo. *The journal of steroid biochemistry and molecular biology* **85**, 71-79.
- MacDougald, O. A., and Lane, M. D. (1995). Transcriptional regulation of gene expression during adipocyte differentiation. *Annu Rev Biochem* **64**, 345-373.
- Mandard, S., Muller, M., and Kersten, S. (2004). Peroxisome proliferator-activated receptor alpha target genes. *Cell Mol Life Sci* **61**, 393-416.
- Mangelsdorf, D. J., Thummel, C., Beato, M., Herrlich, P., Schutz, G., Umesono, K., Blumberg, B., Kastner, P., Mark, M., Chambon, P., and Evans, R. M. (1995). The nuclear receptor superfamily: the second decade. *Cell* **83**, 835-839.

- Marsman, D. S., Cattley, R. C., Conway, J. G., and Popp, J. A. (1988). Relationship of hepatic peroxisome proliferation and replicative DNA synthesis to the hepatocarcinogenicity of the peroxisome proliferators di(2-ethylhexyl)phthalate and [4-chloro-6-(2,3-xylidino)-2-pyrimidinylthio]acetic acid (Wy-14,643) in rats. *Cancer Res* **48**, 6739-6744.
- Marsman, D. S., and Popp, J. A. (1994). Biological potential of basophilic hepatocellular foci and hepatic adenoma induced by the peroxisome proliferator, Wy-14,643. *Carcinogenesis* **15**, 111-117.
- Melnick, R. L. (2001). Is peroxisome proliferation an obligatory precursor step in the carcinogenicity of di(2-ethylhexyl)phthalate (DEHP)? *Environ Health Perspect* **109**, 437-442.
- Mindnich, R., Moller, G., and Adamski, J. (2004). The role of 17 beta-hydroxysteroid dehydrogenases. *Mol Cell Endocrinol* **218**, 7-20.
- Miyazama, S., Ozasa, H., Osumi, T., and Hashimoto, T. (1983). Purification and properties of carnitine Octanoyltransferase. *J. Biochem* **94**, 529-542.
- Moody, D. E., and Reddy, J. K. (1978). The hepatic effects of hypolipidemic drugs (clofibrate, nafenopin, tibric acid, and Wy-14,643) on hepatic peroxisomes and peroxisome-associated enzymes. *Am J Pathol* **90**, 435-450.
- Motojima, K. (1993). Peroxisome proliferator-activated receptor (PPAR): structure, mechanisms of activation and diverse functions. *Cell Struct Funct* **18**, 267-277.
- Motojima, K. (2004). 17beta-hydroxysteroid dehydrogenase type 11 is a major peroxisome proliferator-activated receptor alpha-regulated gene in mouse intestine. *Eur J Biochem* **271**, 4141-4146.
- Mukherjee, R., Jow, L., Croston, G. E., and Paterniti, J. R., Jr. (1997). Identification, characterization, and tissue distribution of human peroxisome proliferator-activated receptor (PPAR) isoforms PPARgamma2 versus PPARgamma1 and activation with retinoid X receptor agonists and antagonists. *J Biol Chem* **272**, 8071-8076.
- Nemali, M. R., Reddy, M. K., Usuda, N., Reddy, P. G., Comeau, L. D., Rao, M. S., and Reddy, J. K. (1989). Differential induction and regulation of peroxisomal enzymes: predictive value of peroxisome proliferation in identifying certain nonmutagenic carcinogens. *Toxicol Appl Pharmacol* **97**, 72-87.
- Nemali, M. R., Usuda, N., Reddy, M. K., Oyasu, K., Hashimoto, T., Osumi, T., Rao, M. S., and Reddy, J. K. (1988). Comparison of constitutive and inducible levels of expression of peroxisomal beta-oxidation and catalase genes in liver and extrahepatic tissues of rat. *Cancer Res* **48**, 5316-5324.
- Okita, R., and Chance, C. (1984). Induction of laurate omega-hydroxylase by di (2-ethylhexyl)phthalate in rat liver microsomes. *Biochem Biophys Res Commun* **121**, 304-309.
- Ozasa, H., Miyazawa, S., and Osumi, T. (1983). Biosynthesis of carnitine octanoyltransferase and carnitine palmitoyltransferase. *J. Biochem* **94**, 543-549.
- Palmer, C. N., Hsu, M. H., Griffin, K. J., Raucy, J. L., and Johnson, E. F. (1998). Peroxisome proliferator activated receptor-alpha expression in human liver. *Mol Pharmacol* **53**, 14-22.
- Peters, J. M., Cattley, R. C., and Gonzalez, F. J. (1997a). Role of PPAR alpha in the mechanism of action of the nongenotoxic carcinogen and peroxisome proliferator Wy-14,643. *Carcinogenesis* **18**, 2029-2033.

- Peters, J. M., Hennuyer, N., Staels, B., Fruchart, J. C., Fievet, C., Gonzalez, F. J., and Auwerx, J. (1997b). Alterations in lipoprotein metabolism in peroxisome proliferator-activated receptor alpha-deficient mice. *J Biol Chem* **272**, 27307-27312.
- Qi, C., Zhu, Y., Pan, J., Usuda, N., Maeda, N., Yeldandi, A. V., Rao, M. S., Hashimoto, T., and Reddy, J. K. (1999). Absence of spontaneous peroxisome proliferation in enoyl-CoA Hydratase/L-3-hydroxyacyl-CoA dehydrogenase-deficient mouse liver. Further support for the role of fatty acyl CoA oxidase in PPARalpha ligand metabolism. *J Biol Chem* **274**, 15775-15780.
- Rao, M. S., Lalwani, N. D., Watanabe, T. K., and Reddy, J. K. (1984). Inhibitory effect of antioxidants ethoxyquin and 2(3)-tert-butyl-4-hydroxyanisole on hepatic tumorigenesis in rats fed ciprofibrate, a peroxisome proliferator. *Cancer Res* **44**, 1072-1076.
- Reddy, J. K., Goel, S. K., Nemali, M. R., Carrino, J. J., Laffler, T. G., Reddy, M. K., Sperbeck, S. J., Osumi, T., Hashimoto, T., Lalwani, N. D., and et al. (1986). Transcription regulation of peroxisomal fatty acyl-CoA oxidase and enoyl-CoA hydratase/3-hydroxyacyl-CoA dehydrogenase in rat liver by peroxisome proliferators. *Proc Natl Acad Sci U S A* **83**, 1747-1751.
- Reddy, J. K., and Hashimoto, T. (2001). Peroxisomal beta-oxidation and peroxisome proliferator-activated receptor alpha: an adaptive metabolic system. *Annu Rev Nutr* **21**, 193-230.
- Reddy, J. K., and Krishnakantha, T. P. (1975). Hepatic peroxisome proliferation: induction by two novel compounds structurally unrelated to clofibrate. *Science* **190**, 787-789.
- Reddy, J. K., and Mannaerts, G. P. (1994). Peroxisomal lipid metabolism. *Annu Rev Nutr* **14**, 343-370.
- Reddy, J. K., and Qureshi, S. A. (1979). Tumorigenicity of the hypolipidaemic peroxisome proliferator ethyl-alpha-p-chlorophenoxyisobutyrate (clofibrate) in rats. *Br J Cancer* **40**, 476-482.
- Reddy, J. K., and Rao, M. S. (1989). Oxidative DNA damage caused by persistent peroxisome proliferation: its role in hepatocarcinogenesis. *Mutat Res* **214**, 63-68.
- Reddy, J. K., Rao, S., and Moody, D. E. (1976). Hepatocellular carcinomas in acatalasemic mice treated with nafenopin, a hypolipidemic peroxisome proliferator. *Cancer Res* **36**, 1211-1217.
- Sausen, P. J., Lee, D. C., Rose, M. L., and Cattley, R. C. (1995). Elevated 8-hydroxydeoxyguanosine in hepatic DNA of rats following exposure to peroxisome proliferators: relationship to mitochondrial alterations. *Carcinogenesis* **16**, 1795-1801.
- Serrero, G., Frolov, A., Schroeder, F., Tanaka, K., and Gelhaar, L. (2000). Adipose differentiation related protein: expression, purification of recombinant protein in Escherichia coli and characterization of its fatty acid binding properties. *Biochim Biophys Acta* **1488**, 245-254.
- Shafqat, N., Marschall, H. U., Filling, C., Nordling, E., Wu, X. Q., Bjork, L., Thyberg, J., Martensson, E., Salim, S., Jornvall, H., and Oppermann, U. (2003). Expanded substrate screenings of human and Drosophila type 10 17beta-hydroxysteroid dehydrogenases (HSDs) reveal multiple specificities in bile acid and steroid hormone metabolism: characterization of multifunctional 3alpha/7alpha/7beta/17beta/20beta/21-HSD. *Biochem J* **376**, 49-60.

- Singh, H., Derwas, N., and Poulos, A. (1987). Very long chain fatty acid beta-oxidation by rat liver mitochondria and peroxisomes. *Archives of biochemistry and biophysics* **259**, 382-390.
- Smith, L. L., and Elcombe, C. R. (1989). Mechanistic studies: their role in the toxicological evaluation of pesticides. *Food Addit Contam* **6 Suppl 1**, S57-65.
- Staels, B., Koenig, W., Habib, A., Merval, R., Lebre, M., Torra, I. P., Delerive, P., Fadel, A., Chinetti, G., Fruchart, J. C., Najib, J., Macclouf, J., and Tedgui, A. (1998). Activation of human aortic smooth-muscle cells is inhibited by PPARalpha but not by PPARgamma activators. *Nature* **393**, 790-793.
- Staels, B., Schoonjans, K., Fruchart, J. C., and Auwerx, J. (1997). The effects of fibrates and thiazolidinediones on plasma triglyceride metabolism are mediated by distinct peroxisome proliferator activated receptors (PPARs). *Biochimie* **79**, 95-99.
- Stott, W. T., Yano, B. L., Williams, D. M., Barnard, S. D., Hannah, M. A., Cieslak, F. S., and Herman, J. R. (1995). Species-dependent induction of peroxisome proliferation by haloxyfop, an aryloxyphenoxy herbicide. *Fundam Appl Toxicol* **28**, 71-79.
- Strassburg, C. P., Strassburg, A., Nguyen, N., Li, Q., Manns, M. P., and Tukey, R. H. (1999). Regulation and function of family 1 and family 2 UDP-glucuronosyltransferase genes (UGT1A, UGT2B) in human oesophagus. *Biochem J* **338**, 489-498.
- Subramani, S. (1998). Components involved in peroxisome import, biogenesis, proliferation, turnover, and movement. *Physiological Reviews* **78**, 171-188.
- Takagi, A., Sai, K., Umemura, T., Hasegawa, R., and Kurokawa, Y. (1992). Hepatomegaly is an early biomarker for hepatocarcinogenesis induced by peroxisome proliferators. *J Environ Pathol Toxicol Oncol* **11**, 145-149.
- Tontonoz, P., Hu, E., Graves, R. A., Budavari, A. I., and Spiegelman, B. M. (1994). mPPAR gamma 2: tissue-specific regulator of an adipocyte enhancer. *Genes Dev* **8**, 1224-1234.
- Tugwood, J. D., Aldridge, T. C., Lambe, K. G., Macdonald, N., and Woodyatt, N. J. (1996). Peroxisome proliferator-activated receptors: structures and function. *Ann N Y Acad Sci* **804**, 252-265.
- Tukey, R. H., and Strassburg, C. P. (2000). Human UDP-glucuronosyltransferases: metabolism, expression, and disease. *Annu Rev Pharmacol Toxicol* **40**, 581-616.
- von Daniken, A., Lutz, W. K., and Schlatter, C. (1981). Lack of covalent binding to rat liver DNA of the hypolipidemic drugs clofibrate and fenofibrate. *Toxicol Lett* **7**, 305-310.
- Vu-Dac, N., Gervois, P., Jakel, H., Nowak, M., Bauge, E., Dehondt, H., Staels, B., Pennacchio, L. A., Rubin, E. M., Fruchart-Najib, J., and Fruchart, J. C. (2003). Apolipoprotein A5, a crucial determinant of plasma triglyceride levels, is highly responsive to peroxisome proliferator-activated receptor alpha activators. *J Biol Chem* **278**, 17982-17985.
- Wang, C., Youssef, J., Cunningham, M., and Badr, M. (2004). Correlation between thyroid hormone status and hepatic hyperplasia and hypertrophy caused by the peroxisome proliferator-activated receptor alpha agonist Wy-14,643. *J Carcinog* **3**, 9.

- Werman, A., Hollenberg, A., Solanes, G., Bjorbaek, C., Vidal-Puig, A. J., and Flier, J. S. (1997). Ligand-independent activation domain in the N terminus of peroxisome proliferator-activated receptor gamma (PPARgamma). Differential activity of PPARgamma1 and -2 isoforms and influence of insulin. *J Biol Chem* **272**, 20230-20235.
- Xie, Y., Yang, Q., Nelson, B. D., and DePierre, J. W. (2003). The relationship between liver peroxisome proliferation and adipose tissue atrophy induced by peroxisome proliferator exposure and withdrawal in mice. *Biochem Pharmacol* **66**, 749-756.
- Yamazaki, K., Kuromitsu, J., and Tanaka, I. (2002). Microarray analysis of gene expression changes in mouse liver induced by peroxisome proliferator-activated receptor alpha agonists. *Biochem Biophys Res Commun* **290**, 1114-1122.
- Yang, Q., Xie, Y., and Depierre, J. W. (2000). Effects of peroxisome proliferators on the thymus and spleen of mice. *Clin Exp Immunol* **122**, 219-226.
- Yu, S., Cao, W. Q., Kashireddy, P., Meyer, K., Jia, Y., Hughes, D. E., Tan, Y., Feng, J., Yeldandi, A. V., Rao, M. S., Costa, R. H., Gonzalez, F. J., and Reddy, J. K. (2001). Human peroxisome proliferator-activated receptor alpha (PPARalpha) supports the induction of peroxisome proliferation in PPARalpha-deficient mouse liver. *J Biol Chem* **276**, 42485-42491.
- Zhang, B., Marcus, S. L., Sajjadi, F. G., Alvares, K., Reddy, J. K., Subramani, S., Rachubinski, R. A., and Capone, J. P. (1992). Identification of a peroxisome proliferator-responsive element upstream of the gene encoding rat peroxisomal enoyl-CoA hydratase/3-hydroxyacyl-CoA dehydrogenase. *Proc Natl Acad Sci U S A* **89**, 7541-7545.
- Zhang, D., Yu, W., Geisbrecht, B. V., Gould, S. J., Sprecher, H., and Schulz, H. (2002). Functional characterization of Delta3,Delta2-enoyl-CoA isomerases from rat liver. *J Biol Chem* **277**, 9127-9132.
- Zhou, Y. C., and Waxman, D. J. (1998). Activation of peroxisome proliferator-activated receptors by chlorinated hydrocarbons and endogenous steroids. *Environ Health Perspect* **106 Suppl 4**, 983-988.

Appendix A. Tables of preparation of reaction mix

Table A1. Preparation of animal tail genotyping PCR reaction

Reagent	Stock conc.	Vol. per reaction (μl)	Final conc.
Nuclease-free water	-	19.125	-
10X PCR buffer	10X	2.5	1X
dNTP mix	10 mM	0.125	0.05 mM
Forward primer (F1)	10 μM	0.875	0.35 μM
Reverse primer (R3)	10 μM	0.875	0.35 μM
Taq polymerase	5 U/μl	0.5	0.1 U/μl
10-fold diluted DNA	-	1.0	-
Total	-	25	-

Table A2. Preparation of DNase I treatment

Reagent	Stock conc.	Vol. per reaction (μl)	Final conc.
MgCl ₂	25 mM	40	10 mM
Tris-HCl (pH 7.5)	1 M	5	50 mM
RNase-free Dnase I	7.5 U/μl	4.2	0.3 U/μl
Total liver RNA	-	50.8	50 μg
Total	-	100	-

Table A3. Preparation of reverse transcription of non-fluoroDD and fluoroDD

Reagent	Stock conc.	Vol. per reaction (μl)	Final conc.
Nuclease-free water	-	7.8	-
Anchored primer (AP)	2 μM	2.0	0.2 μM
DTT	100 mM	2.0	10 mM
dNTP mix	250 μM	2.0	25 μM
Superscript™ II RT buffer	5X	4.0	1X
Superscript™ II RNase H ⁻ reverse transcriptase	200 U/μl	0.2	2 U/μl
DNase I treated RNA	0.1 μg/μl	2.0	10 ng/μl
Total	--	20	-

Appendix A: Tables of preparation of reaction mix (Con't)

Table A4. Preparation of non-fluoroDD and fluoroDD RT-PCR

Reagent	Stock conc.	Vol. per reaction (μl)	Final conc.
Nuclease-free water	-	0.45	-
Anchored primer (AP)	5 μM	0.7	0.35 μM
Arbitrary primer (ARP)	2 μM	1.75	0.35 μM
dNTP mix	250 μM	2.0	50 μM
10X PCR buffer	10X	1.0	1X
<i>Taq</i> polymerase	5 U/μl	0.1	0.05 U/μl
RT mixture	-	4.0	-
Total	-	10	-

Table A5. Preparation of reamplification of differentially expressed cDNA fragments

Reagent	Stock conc.	Vol. per reaction (μl)	Final conc.
Nuclease-free water	-	8.2	-
10X PCR buffer	10X	2.0	1X
dNTP mix	250 μM	1.6	20 μM
M13 reverse primer	2 μM	2.0	0.2 μM
T7 promoter primer	2 μM	2.0	0.2 μM
<i>Taq</i> polymerase	5 U/μl	0.2	0.05 U/μl
Gel band elute	-	4.0	-
Total	-	20	-

Table A6. Preparation of PCR reaction for DNA sequencing

Reagent	Stock conc.	Vol. per reaction (μl)	Final conc.
10X Sequencing reaction buffer	10X	2	1X
dNTP mix	-	1	-
DdUTP Dye terminator	-	2	-
DdGTP Dye terminator	-	2	-
DdCTP Dye terminator	-	2	-
DdATP Dye terminator	-	2	-
M13 forward (-20) primer/ M13 reverse primer	1.6 μM	2	0.16 μM
Polymerase enzyme	-	1	-
DNA template	100 fmol	6	30 fmol
Total	-	20	-

Appendix A: Tables of preparation of reaction mix (Con't)

Table A7. Preparation of PCR reaction for RNA probe

Reagent	Stock conc.	Vol. per reaction (μl)	Final conc.
Nuclease-free water	-	5.4	-
10X PCR buffer	10X	2.0	1X
dNTP mix	250 μM	6.4	80 μM
Anchored primer (AP)	2 μM	2.0	0.2 μM
Arbitrary primer (ARP)	2 μM	2.0	0.2 μM
Taq polymerase	5 U/μl	0.2	0.05 U/μl
Plasmid DNA	1 ng/μl	2.0	2 ng/μl
Total	-	20	-

Table A8. Preparation of PCR reaction for cDNA probe

Reagent	Stock conc.	Vol. per reaction (μl)	Final conc.
Nuclease-free water	-	24.6	-
10X PCR buffer	10X	5.0	1X
PCR-DIG labeling mix	2 mM	5.0	200 μM
MgCl ₂	25 mM	3.0	1.5 mM
Anchored primer (AP)	10 μM	5.0	1 μM
Arbitrary primer (ARP)	10 μM	5.0	1 μM
Taq polymerase	5 U/μl	0.4	0.04 U/μl
Plasmid DNA	20 ng/μl	2.0	0.8 ng/μl
Total	-	50	-

B 1.1: DNA sequence of cDNA subclone AA1#2 (AP1 & ARP2) using M13 forward (-20) primer

1	GAATGTTACG	ACTCACTATA	GGGCGAATTG	GGCCCTCTAG	ATGCATGCTC	GAGCGGCCGC	
61	CAGTGTGATG	GATATCTGCA	GAATTCGGCT	TAGCGGATAA	CAATTTTACA	CAAGGAGCTA	ARP2*
121	GCATGG CGGC	AGTGACCTGG	AGTCGGGCTC	GATGCTGGTG	TCCGAGGTCT	TCAGATTACA	
181	AGTGGCTAAA	CTGCACTTGG	GCAGACCAAC	AATGAGAGCC	AGTCAGCAGG	ACTTTGAAAA	
241	TGCATTGAAC	CAGGTGAAAC	TCTTGAAGAA	GGACCCGGGA	AACGAAGTGA	AGCTAAGACT	
301	CTATGCACTG	TACAAGCAGG	CCACAGAAGG	ACCCTGTAAT	ATGCCTAAGC	CTGGTATGCT	
361	TGACTTTGTC	AACAAAGCCA	AGTGGGATGC	ATGGAGTGCC	CTGGGCAGCC	TACCCAAGGA	
421	AACTGCCAGG	CAGAACTATG	TGGATCTCGT	ATCCAAAAAG	AGTNCCTCAT	CTGAAGCCNC	
481	GAGCCAGGGA	NAGCGTGGAG	CTGATGAGAA	AGCCGGGGAG	TCCAAAGACA	TNCTGNTAAC	
541	TTCTGANGAT	GGTATCACGA	AGATCACGTT	CANNCCGNCC	NCCCAAAAGA	NTGCCATATN	
601	CTNNCAGATG	TATCNNGATA	TNATACTCGC	CCTTAAATG	NCAGCNNNGA	TACACTNTNA	
661	TGCTGTTNNA	CANGANCTNN	GACACTACTG	CNNNGGANGA	CNGACTACNT	NCTANTGCAG	
721	G						

B 1.2: Sequencing alignment of cDNA subclone **AA1#2** with **mouse peroxisomal delta 3, delta 2-enoyl-Coenzyme A isomerase (Peci)** by BLAST searching against the National Center for Biotechnology Information database

AA1#2	:	165	aggtcttccagattacaagtggctaaactgcacttgggcagaccaacaatgagagccagtc	224
Mouse Peci:	:	296	aggtcttccagattacaagtggctaaactgcacttgggcagaccaacaatgagagccagtc	355
AA1#2	:	225	agcaggactttgaaaatgcattgaaccaggtgaaactcttgaagaaggacccgggaaacg	284
Mouse Peci:	:	356	agcaggactttgaaaatgcattgaaccaggtgaaactcttgaagaaggacccgggaaacg	415
AA1#2	:	285	aagtgaagctaagactctatgcactgtacaagcaggccacagaaggaccctgtaatatgc	344
Mouse Peci:	:	416	aagtgaagctaagactctatgcactgtacaagcaggccacagaaggaaacctgtaatatgc	475
AA1#2	:	345	ctaagcctgggatgcttgactttgtcaacaaagccaagtgggatgcatggagtgccttg	404
Mouse Peci:	:	476	ctaagcctgggatgcttgactttgtcaacaaagccaagtgggatgcatggaatgccttg	535
AA1#2	:	405	gcagcctacccaaggaaactgccaggcagaactatgtggatctcgtatccaaaaagagtn	464
Mouse Peci:	:	536	gcagcctacccaaggaaactgccaggcagaactatgtggatctcgtatccagtttagtt	595
AA1#2	:	465	cctcatctgaagccnccgagccaggganagcgtggagctgatgagaaagccggggagtcca	524
Mouse Peci:	:	596	cctcatctgaagcccccagccagggaaagcgtggagctgatgagaaagccggggagtcca	655
AA1#2	:	525	aagacatnctgntaacttctgangatggatatcacgaagatcacggtcannccgncnccc	584
Mouse Peci:	:	656	aagacatcctggtaacttctgaagatggatatcacgaagatcacggtcaatcggcccacca	715
AA1#2	:	585	aaaagantgccatatnctnnccagatgtatcnnngatatnatactcgcccttaaaa	638
Mouse Peci:	:	716	aaaagaatgccatatccttccagatgtatcgggatattatactcgccacttaaaa	769

B 1.3: Summary of sequence alignment of cDNA subclone **AA1#2** with mouse **Peci**

FluoroDD gel AA (AP1 + ARP2)						Subcloning		Sequencing		
Fragment no.	PPAR α (+/+)		PPAR α (-/-)		FluoroDD fragment size (bp)	Subclone I.D.	Size of insert after <i>EcoRI</i> cut (bp)	Primer	Gene homology to Blast search (Transcript size)	E-value (% Identity)
	CTL	Wy	CTL	Wy						
AA1	-	+	-	-	1400	AA1#2	1400	M13 forward (-20)	<i>Mus musculus</i> peroxisomal delta 3, delta 2-enoyl-coenzyme A isomerase (Peci) (1581 bp)	0 447/474 (94%)

* Sequence of primer was not completely matched with the expected sequence.

Appendix B. DNA sequences and sequencing alignments of FluoroDD fragments

B 2.1: DNA sequence of cDNA subclone AA1#3 (AP1 & ARP2) using M13 forward (-20) primer

1 TTACGACTCA CTATAGGGCG AATTGGGCCC TCTANNTGCA TGCTCGAGCG GCCGCCAGTG
61 TGATGGATAT CTGCAGAATT CGGCTTAGCG GATA**ACAATT TCACACAAGG AGCTAGCATG** ARP2*
121 **G**CGGCAGTGA CCTGGAGTCG GGCTCGATGC TGGTGTCCGA GTGTCCTGCA GGTCTTCAGA
181 TTACAAGTGG CTAAACTGCA CTTGGGCAGA CCAACAATGA GAGCCAGTCA GCAGGACTTT
241 GAAAATGCAT TGAACCAGGT GAAACTCTTG AAGAAGGACC CGGGAAACGA ACGTGAAGCT
301 AAAGACTCTA TGCATGTAC AAGCAGGCCA CAGNAAGGAC CCTGTAATAT GACACATNNA
361 NCNAAAAAAA AAACAAAANA ANNNNTACAC CNNAAGCCCA AGGTNGGGAT TGCATNGGGA
421 ATGCCCTGGG NAGCCTACCC AAAGGAAACT GCCAGGCAGA ACTNTGTGGA TCTCGTATCC
481 NGTTTGTAGTT CCTCATCTGA AGCCCCGAGC CAGGGAAAGC GTGGAGCTGA TGAGAAAGCC
541 CNGGAGTCCN AAGACNTNCT GGTAACCTTCT GAAGATGGTA TCCCGAAGAT CNNGTNCATT
601 CNGCCCCCCA AAAGANTGCC TATCCTTCCG ATGTTTTCGGA TNTNTCTCGC CNTANNTNCN
661 GCCTGNNNCC TGTNTGNTGT NNNNGGACTG TGACT

B 2.2: Sequencing alignment of cDNA subclone AA1#3 with **mouse peroxisomal delta 3, delta 2-enoyl-Coenzyme A isomerase (Peci)** by BLAST searching against the National Center for Biotechnology Information database

AA1#3 : 161 gtgtcctgcaggtcttcagattacaagtggctaaactgcacttgggcagaccaacaatga 220
Mouse Peci: 287 gtgtcctgcaggtcttcagattacaagtggctaaactgcacttgggcagaccaacaatga 346
AA1#3 : 221 gagccagtcagcaggactttgaaaatgcattgaaccaggtgaaactcttgaagaaggacc 280
Mouse Peci: 347 gagccagtcagcaggactttgaaaatgcattgaaccaggtgaaactcttgaagaaggacc 406
AA1#3 : 281 cgggaaacgaacgtgaagctaaagactctatgcactgtacaagcaggccacagnaaggac 340
Mouse Peci: 407 cgggaaacgaa-gtgaagct-aagactctatgcactgtacaagcaggccacag-aaggaa 463
AA1#3 : 341 cctgtaatatg 351
Mouse Peci: 464 cctgtaatatg 474

B 2.3: Summary of sequence alignment of cDNA subclone AA1#3 with mouse Peci

FluoroDD gel AA (AP1 + ARP2)					Subclone I.D.	Sequencing				
Fragment no.	PPARα (+/+)		PPARα (-/-)			FluoroDD fragment size (bp)	Size of insert after <i>Eco</i> RI cut (bp)	Primer	Gene homology to Blast search (Transcript size)	E-value (% Identity)
	CTL	Wy	CTL	Wy						
AA1	-	+	-	-	1400	AA1#3	1450	M13 forward (-20)	<i>Mus musculus</i> peroxisomal delta 3, delta 2-enoyl-coenzyme A isomerase (Peci) (1581 bp)	3e-85 187/191 (97%)

* Sequence of primer was not completely matched with the expected sequence.

Appendix B. DNA sequences and sequencing alignments of FluoroDD fragments

B 3.1: DNA sequence of cDNA subclone AA1#4 (AP1 & ARP2) using M13 reverse primer

1 TNNCCAAGCT TGNGTACCGA GACTACNNGA TACCCTATT AAACGGACCG ACACGNGTGA
61 CTGGAATTNC GGACTTGNTA ATA**ACGACTC** **ACTATAGGGC** **TTTTTTTTTT** **GATTTATGAA** **AP1***
121 AAGTTTATT TATCAGTACT GTGAAGAATT CTCATCATAA TTGCTACGTT AATCAAGGAA
181 AAGGCACAGA GAANCATGTG TCGTTTGAGT CCTCAGNAAA CTGGACCTCC CNAGCCCNAT
241 GCTCCCTATG AGGAGTCTAG CNTGCTGTGG TGGTCTTCAN AGCTTTGGTT TTCTGGAGAC
301 GAAGCTCNAT GATTGNGTTN CATGCAACTC CNTCTGNACN AGCCACCNTT GCCTTGCCAG
361 AAGTTAGTNC NACNTCCTTC NAGCAGTNGG ANNTGCNGTN AGCAGCATTT TTCTTCCCTC
421 CATTTTTTTC NTNGATTNAA CTCTTNTGG NNNATTCTCC ATGGCGTTTG GGCNNGGAGC
481 TCCGCANNTG TTTTCCGGCC NGGTCCNNNN NNTCCTGTCT CAAAAAGTGC TCCTCCAGGG
541 GAAAAACNNN NCAGTTNGAA CNAANGGCC CT'NGNNANN CNCCCAANG CCCNTCCTTN
601 CNNTNNGNCN NTNGNTTCCA AGCCTTTTCN NTNNCCCCCN NAAAAANGNN AGNNANGCNC
661 ATCNTNCNAA NCNTGGNCCC TTTTGCNTN GNAGCNCNA TNNNATCTTT CCNGGNACNN
721 ANTTNNTTAA GNAAGGANCN NTNGCTTTC CCGNGCCNCN TGGGCCCGNA GNTNN

B 3.2: Sequencing alignment of cDNA subclone **AA1#4** with **mouse peroxisomal delta 3, delta 2-enoyl-Coenzyme A isomerase (Peci)** by BLAST searching against the National Center for Biotechnology Information database

AA1#4 : 111 gatztatgaaaagttttatztatcagtactgtgaagaattctcatcataattgctacgtt 170
Mouse Peci: 1580 gatztatgaaaagttttatztatcagtactgtgaagaattctcatcataattgctacgtt 1521
AA1#4 : 171 aatcaaggaaaaggcacagagaancatgtgtcggttgagtcctcagnaaactggacctcc 230
Mouse Peci: 1520 aatcaaggaaaaggcacagagaagcatgtgtcggttgagtcctc--gaaactggacctcc 1463
AA1#4 : 231 cnagcccnatgctccctatgaggagtctagcntgctgtggtggtcttcacagctttggtt 290
Mouse Peci: 1462 c-agccc-atgctccctatgaggagtctagc-tgctgtggtggtcttcacagctttggtt 1406
AA1#4 : 291 ttctggagacgaagctcnaatgattgngtt 319
Mouse Peci: 1405 ttctggagacgaagctc-atgattgctgtt 1378

B 3.3: Summary of sequence alignment of cDNA subclone AA1#4 with mouse Peci

FluoroDD gel AA (AP1 + ARP2)					Subclone I.D.	Sequencing				
Fragment no.	PPARα (+/+)		PPARα (-/-)			FluoroDD fragment size (bp)	Size of insert after <i>Eco</i> RI cut (bp)	Primer	Gene homology to Blast search (Transcript size)	E-value (% Identity)
	CTL	Wy	CTL	Wy						
AA1	-	+	-	-	1400	AA1#4	1450	M13 reverse	<i>Mus musculus</i> peroxisomal delta 3, delta 2-enoyl-coenzyme A isomerase (Peci) (1581 bp)	8e-80 199/209 (95%)

* Sequence of primer was not completely matched with the expected sequence.

Appendix B. DNA sequences and sequencing alignments of FluoroDD fragments

B 4.1: DNA sequence of cDNA subclone AA1#20 (AP1 & ARP2) using M13 forward (-20) primer

1 TNTACGACTC ACTATAGGGC GAATTGGGCC CTCTAGAATG CATGCNTNNA CAANCGGCCG

61 CCANTGTGAT GGATATCTGC AGAATTCGGC TTGTAATACG **ACTCACTATA** **GGGCTTTTTT** **AP1***

121 **TTTTTG**ATTT ATGAAAAGTT TTATTTATCA GTACTGTGAA GAATTCTCAT CATAATTGCT

181 ACGTTAATCA AGGAAAAGGC ACAGAGAAGC ATGTGTCGTT TGAGTCCTCN NAACTGGACC

241 TCCCAGCCCA TGCTCCCTAT GACGANATAC TAGCTGCTGT GGTGGTCTTC ACAGCTTTGG

301 TTTTCTGGAG ACGAAGCTCA TGATTGCGTT CATGCACTCC TCTGACAGCC ACCTTGCTTG

361 CAGAGTAGTG CACTCTTCAG CGTTGACTGC GTAGAGCTTT TCTTTCTCAT TTTTCTGAT

421 TAACTCTTTG GNAAATTCCT CATGGCGTTT GCGGGGAGCT TCGCATATAT TTTCAGCCTG

481 GTCCCGACTT CTGTCTCAAA AGTGCTCTCA GGGAAACTT CAGTGACAAG GCCTTGAGCN

541 CAGGCCTCTC TTGCTGTCAG CTTCTTCCCA AAGAGAAGCA TCTCAGCTGC CTTTGCTGAG

601 CCCATCATCT TCNGAACGCT GTACGAAGAG CATGCNTCCN NGGCTCTGGC CGAGNTGGGC

661 TGAATGNAGT ATGAAACGTN GNCCNGTNTG ATGCCNAGAC NNNC

B 4.2: Sequencing alignment of cDNA subclone AA1#20 with **mouse peroxisomal delta 3, delta 2-enoyl-Coenzyme A isomerase (Peci)** by BLAST searching against the National Center for Biotechnology Information database

AA1#20 : 126 gatttatgaaaagttttatattatcagtactgtgaagaattctcatcataattgctacgtt 185

Mouse Peci: 1580 gatttatgaaaagttttatattatcagtactgtgaagaattctcatcataattgctacgtt 1521

AA1#20 : 186 aatcaaggaaaaggcacagagaagcatgtgtcgtttgagtcctcnaactggacctccca 245

Mouse Peci: 1520 aatcaaggaaaaggcacagagaagcatgtgtcgtttgagtcctcgaaactggacctccca 1461

AA1#20 : 246 gcccatgctccctatgacganatactagctgctgtggtggtcttcacagctttggttttc 305

Mouse Peci: 1460 gcccatgctccctatgaggagt--ctagctgctgtggtggtcttcacagctttggttttc 1403

AA1#20 : 306 tggagacgaagctcatgattgcgttcctgacagccaccttgcttgagag 365

Mouse Peci: 1402 tggagacgaagctcatgattgcgttcctgacagccaccttgcttgagag 1343

AA1#20 : 366 tagtgcaactcttcagcgttgactgcgtagagcttttcttctcatttttctgattaact 425

Mouse Peci: 1342 tagtgcaactcttcagcgttgactgcgtagagcttttcttctcattttgctgattaact 1283

AA1#20 : 426 ctttggnaaatcctcatggcgtttggcgggagcttcgcatatattttcagcctggtccc 485

Mouse Peci: 1282 ctttgg-aaattc-tcatggcgtttggcgggagcttcgcatatgttttcagcctggtcca 1225

AA1#20 : 486 gacttctgtctcaaaagtgtctcagggaaaacttcagtgacaaggccttgagcncaggc 545

Mouse Peci: 1224 gacttctgtctcaaaagtgtctcagggaaaacttcagtgacaaggccttgagcccaggc 1165

AA1#20 : 546 ctctcttgctgtcagcttcttcccaaagagaagcatctcagctgcctttgctgagcccat 605

Mouse Peci: 1164 ctctcttgctgtcagcttcttcccaaagagaagcatctcagctgcctttgctgagcccat 1105

AA1#20 : 606 catcttcngaaacgtgtacgaagagcatgcntccnnggctctggccgagntgggctgaat 665

Mouse Peci: 1104 catcttcggaaacgtgtaaaggagcatgcttcc-gggctctggccgagtt-ggctgaat 1047

AA1#20 : 666 gnagtatgaaacgtngnccngtntgatgc 694

Mouse Peci: 1046 ggagtatgaaacgttgccctgtctgatgc 1018

B 4.3: Summary of sequence alignment of cDNA subclone AA1#20 with mouse Peci

FluoroDD gel AA (AP1 + ARP2)					Subclone I.D.	Sequencing				
Fragment no.	PPARα (+/+)		PPARα (-/-)			FluoroDD fragment size (bp)	Size of insert after <i>Eco</i> RI cut (bp)	Primer	Gene homology to Blast search (Transcript size)	E-value (% Identity)
	CTL	Wy	CTL	Wy						
AA1	-	+	-	-	1400	AA1#20	1700	M13 forward (-20)	<i>Mus musculus</i> peroxisomal delta 3, delta 2-enoyl-coenzyme A isomerase (Peci) (1581 bp) 0 541/569 (95%)	

Sequence of primer was not completely matched with the expected sequence.

Appendix B. DNA sequences and sequencing alignments of FluoroDD fragments

B 5.1: DNA sequence of cDNA subclone AA4#1 (AP1 & ARP2) using M13 forward (-20) primer

1 ANGNCCCCC TNATACNNCC CGNNCANNTC CCGNGGNNCN NCTNANNATC GCATCGCNNC
61 NNNAGCGGCC GCCAGCTGNT GATGGATATC CTGCNANCNA ATNCNCNCCN TGCCTAATAC
121 NNN**ACTCACC TATAGGGCTT TTTTTTCTGA** CCNNTNCCCA TCCACNNANC NATCTATNNT **AP1***
181 NCCATCCCNA ACCAAAANGT CAGNNCNCCA CCCCTGCAGC AGCTCCACGN AGGGTACCGG
241 CACCTGNTAT TGNAATGNAG GNAAGCGCCA CACCAGTCCC NGNTCNNGN TACCANCGNA
301 TCCTCCCCTA ACAAAGCCCC TCCCTTCCAT CGTNGGTGGN ATGGCTCAGT CCCCTTNATC
361 TGGNATCCCA CACTCTCTAA GNGAAATAAG GGCTCTGCCC GGTCCCATCA CTGGGACCCA
421 CCACCAGGAC ACTGGCAGGA ACGTACACAC TCCATCACAT GTTCNNTGCA TTATGCTCTC
481 CTCCTGCTCC CTTTNCAACA AANAGCTCCT CAATGAANNA CCCCTGNNGG NANNACANGG
541 ANNTCCCCTC CTCCCATNGG ACCCAAACCTG GTNAAACANG CCCAGCNAAC CCAGGCCTNG
601 CCGANANTNN ANCAAGAAGC CCCAACTCCA NGGTTGTAGT GGGATGGGT TTTAGCAGGG
661 NNAAGCACTG GCTTGCGGTT AGTTACCCCC AAANNNATTN TCCCAATCTT GTTANCTCAC
721 TTCTTGCTA NNTTANNAN TTGCCCCAAT GAGTTNCCAN AANNCTTGGG TTNTGCAAAA
781 GCCTAANTGG ANNTGTTAAT GCCCCCTGAA GTAGNGGGNA TTNGAGGAA GGNNTGGGTA
841 NNGTTGGGGA AANGCAATCC CTNTNGGGTG GTGTNNNGG NANNCTNNAA CATNNGGCCT
901 TATTTAAANN NTGNTCGCCT TGNGTGTTAA NNTTNTTNTC CNTTANNGGN NANTNNGGN
961 GNNNTTNNGT GG

B 5.2: Sequencing alignment of cDNA subclone AA4#1 with **mouse apolipoprotein A-V (Apoa5)** by BLAST searching against the National Center for Biotechnology Information database

AA4#1 : 374 tctctaagngaataagggctctgcccgggtcccatcactgggacccaccaccaggac-ac 432
Mouse Apoa5: 1645 tctctaag-gaaataggggctctgcccgggtcccatcactgg-acccaccagcaggaccac 1588
AA4#1 : 433 tggcaggaacgtacacactccatcacatgttcnntgcattatgctctcctcctgctccct 492
Mouse Apoa5: 1587 tggcagggacgtacacactccatcacatgttctctgcatcatgctctcctcctgctccct 1528
AA4#1 : 493 t 494
Mouse Apoa5: 1527 t 1527

B 5.3: Summary of sequence alignment of cDNA subclone AA4#1 with mouse Apoa5

FluoroDD gel AA (AP1 + ARP2)					Subclone I.D.	Sequencing				
Fragment no.	PPARα (+/+)		PPARα (-/-)			FluoroDD fragment size (bp)	Size of insert after <i>Eco</i> RI cut (bp)	Primer	Gene homology to Blast search (Transcript size)	E-value (% Identity)
	CTL	Wy	CTL	Wy						
AA4	++	+	++	++	695	AA4#1	725	M13 forward (-20)	<i>Mus musculus</i> apolipoprotein A-V (Apoa5) (1819 bp)	1e-32 112/121 (92%)

* Sequence of primer was not completely matched with the expected sequence.

Appendix B. DNA sequences and sequencing alignments of FluoroDD fragments

B 6.1: DNA sequence of cDNA subclone AA4#9 (AP1 & ARP2) using M13 reverse primer

1 NCNCTATTTA GGTGACCTAT AGAATACTCA AGCTATGCAT CAAGCTTGGT ACCGAGCTCG
61 GATNCACTAG TANC GCCCGC CAGTGTGCTG GAATCGCCCT TAGCGGATAA **CAATTTCACA** ARP2
121 **CAGGAGCTAG CATGGT**CTAT TAGGCAGAGG GTGGAGGGTC CTGCACACCA CCAAAGGTGC
181 TGCCTGTCCC AACCTACCCA GCCTCCTCAA CNTCCCCTAC TCAGGGGCAT NACANCNTCA
241 GTAGGCTTTG CAAACCCAGC TTCTGGTACT CATTGGCAA TCCTAAGTAN CCAGAGTGAG
301 GTGACAGNG TGGNNGATGG TGTGTGGGGT GACTGACCGC AACCAGTGC TTGACCCGTG
361 CCGGAAACCC CATGCCACN NACAAACCTG NNAAGTTGGG GCCTCCCCTG GTTAAAAATTN
421 CTTCCCCAAG CCCCTNGGGG NNGCTTGGGC CTNGGTTAAC ACAGGTTGNG GGTNCCNATG
481 GGGAAGAAAN GGNANCCTCC CCTGGTTTTT CCCNCCNNNN GGTTNGTTNN ATTGAANAAN
541 CNNTNNTGGT TTGGGGAANN GGGGAANNCA NGGAAAGGAA AAAAACCCAT GGAATGNNNN
601 NNNAANAAAA CNNTNNGNTG GAATGTGGAA AGTTGGTGTN TTNNCCGTTN NCCCCTTGGG
661 NNCAAGNTTN GGGTTTTNTCN TTGGNCNNNN GGGTGNNNGN NNTNNCNAAG NTTGGAATNT
721 TNNNGGGGNA CNNCNNGGGG GNAAAAAANA GNCCCCNNT TANNNNNNNC NTNTNNAAAA
781 AAANNNNNNT GNNNANTNNN NNNANATNNN NANNGANAAN NNNNAACNCN TTTNNNNNNN
841 TTNAANGNGN GNNGGGGGCT NTNNNTTANN NNAANAAATA TTTNNNNNNN NTNTNNAAAA
901 ANANAANNNN NGGTTGT

B 6.2: Sequencing alignment of cDNA subclone AA4#9 with **mouse apolipoprotein A-V (Apoa5)** by BLAST searching against the National Center for Biotechnology Information database

AA4#9 : 126 gctagcatggtctattagcagaggggtggagggctcctgcacaccaccaaagggtgctgcct 185
Mouse Apoa5: 1167 gctagcatggtctattagcagaggggtggagggctcctgcacaccaccaaagggtgctgc-t 1225
AA4#9 : 186 gtcccaacctaccagcctcctcaacntcccctactcaggggcatnacancntcagtagg 245
Mouse Apoa5: 1226 gtcccaacctaccagcctcctcaac-tcccctactcaggggcattacac--tcagtagg 1282
AA4#9 : 246 ctttgcaaacccagcttctggtactcatttggcaatcctaagtanccagagtggagtgac 305
Mouse Apoa5: 1283 ctttgcaaacccagcttctggtactcatttggcaatcctaagtagcaagagtggagtgac 1342
AA4#9 : 306 aggngtggnngatggtgtgtgggggtgactgaccgcaaccagtgcttgaccggtgccgga 365
Mouse Apoa5: 1343 aggagtgggagatggtgtgtgggggtgactgaccgcaagccagtgcttga-ccgtgctgga 1401
AA4#9 : 366 aaccc 370
Mouse Apoa5: 1402 aaccc 1406

B 6.3: Summary of sequence alignment of cDNA subclone AA4#9 with mouse Apoa5

FluoroDD gel AA (AP1 + ARP2)						Sequencing				
Fragment no.	PPARα (+/+)		PPARα (-/-)		FluoroDD fragment size (bp)	Subclone I.D.	Size of insert after <i>Eco</i> RI cut (bp)	Primer	Gene homology to Blast search (Transcript size)	E-value (% Identity)
	CTL	Wy	CTL	Wy						
AA4	++	+	++	++	695	AA4#9	725	M13 reverse	<i>Mus musculus</i> apolipoprotein A-V (Apoa5) (1819 bp)	3e-95 231/245 (94%)

Appendix B. DNA sequences and sequencing alignments of FluoroDD fragments

B 7.1: DNA sequence of cDNA subclone AA5#5 (AP1 & ARP2) using M13 forward (-20) primer

1 TNNACGACTC ACTATAGGGC GAATTGGGGC CTCTAGATGC ATGCTCGAGC GGCCGCCAGT
61 GTGATGGATA TCTGCAGAAT TCGGCTTAGC GGATA**ACAAT** **TTCACACAAG** **GAGCTAGCAT** ARP2*
121 **GGACGGCTAA** ACGAGGGTCC AACTGTCTCT TATCTTTAAT CAGCGAAATT GACCTTTNCA
181 GTGAAGAGGC TGAAATATAA TAATAAGACG AGAAGACCCT ATGGAGCTTA AATTATATAA
241 CTTATCTATT TAATTTATTA AACCTAATGG CCCAAAAACT ATAGTATAAG TTTGAAATTT
301 CGGTTGGGGT GACCTCGGAG AATAAAAAAT CCTCCGAATG ATTATAACCT AGACTTACAA
361 GTCAAAGTAA AATCAACATA TCTTATTGAC CCAGATATAT TTTGATCAAC GGACCAAGTT
421 ACCCTAGGGA TAACAGCGCA ATCCATANNTA AGGGTTCATA TCGACAATNA NGGTTNACGA
481 CCTCGATGTT GGATCANGAC ATCCCAATGG TGTANANGCT ATTAATGGGT TCGTNTTGTT
541 CANNGATTAA AGTCCTACGT GATCTGAGTT CAGACCCGAG CANTCAGGTN NGTNNCTATC
601 TATTNACGAT TTTCTCCAGT ACGAAAGGAC ANGAGANNTN NAGNCCNCCT NACNANTAAG
661 NGCNNTCANC NTANNTTANT GANNTAAATT NTAAATTNAA TATATTCGTT ANCNCCCCTA
721 NNCNGAAANN

B 7.2: Sequencing alignment of cDNA subclone AA5#5 with mouse mitochondrion by BLAST searching against the National Center for Biotechnology Information database

AA5#5 : 114 ctagcatggacggctaaacgaggggtccaactgtctcttattctttaatcagcgaaattgac 173
Mouse mitochondrion: 2061 ctagcatgaacggctaaacgaggggtccaactgtctcttattctttaatcagtgaattgac 2120
AA5#5 : 174 ctttncagtgaaagaggtgaaatataataataagacgagaagaccctatggagcttaaat 233
Mouse mitochondrion: 2121 cttt-cagtgaaagaggtgaaatataataataagacgagaagaccctatggagcttaaat 2179
AA5#5 : 234 tatataacttatctatttaattttattaaacctaattggcccaaaaactatagtataagttt 293
Mouse mitochondrion: 2180 tatataacttatctatttaattttattaaacctaattggcccaaaaactatagtataagttt 2239
AA5#5 : 294 gaaatttcggttggggtgacctcggagaataaaaaatcctccgaatgattataacctaga 353
Mouse mitochondrion: 2240 gaaatttcggttggggtgacctcggagaataaaaaatcctccgaatgattataacctaga 2299
AA5#5 : 354 cttacaagtcaaagtaaaatcaacatatcttattgacccagatatattttgatcaacgga 413
Mouse mitochondrion: 2300 cttacaagtcaaagtaaaatcaacatatcttattgacccagatatattttgatcaacgga 2359
AA5#5 : 414 ccaagttaccctagggataaacagcgcaatcctanntaagggttcatatcgacaatnangg 473
Mouse mitochondrion: 2360 ccaagttaccctagggataaacagcgcaatcctatttaagagttcatatcgacaattaggg 2419
AA5#5 : 474 ttnacgacctcgatgttgatcangacatcccaatggtgtanangctattaatgggttcg 533
Mouse mitochondrion: 2420 tttacgacctcgatgttgatcaggacatcccaatggtgtagaagctattaat-ggttcg 2478
AA5#5 : 534 tnttgttcanngattaaagtcctacgtgatctgagttcagacccgagcant-caggttng 592
Mouse mitochondrion: 2479 t-ttgttcaacgattaaagtcctacgtgatctgagttcagacccgagcaatccaggtcgg 2537
AA5#5 : 593 tnnctatctattnacgattttctccagtacgaaaggacangaga 636
Mouse mitochondrion: 2538 tttctatctatttacgattttctccagtacgaaaggacaagaga 2581

B 7.3: Summary of sequence alignment of cDNA subclone AA5#5 with mouse mitochondrion

FluoroDD gel AA (AP1 + ARP2)					Subclone I.D.	Sequencing				
Fragment no.	PPARα (+/+)		PPARα (-/-)			FluoroDD fragment size (bp)	Size of insert after <i>Eco</i> RI cut (bp)	Primer	Gene homology to Blast search (Transcript size)	E-value (% Identity)
	CTL	Wy	CTL	Wy						
AA5	+	++	+	+	670	AA5#5	710	M13 forward (-20)	<i>Mus musculus</i> clone LA9 mitochondrion, complete genome (16300 bp)	0 496/524 (94%)

* Sequence of primer was not completely matched with the expected sequence.

Appendix B. DNA sequences and sequencing alignments of FluoroDD fragments

B 8.1: DNA sequence of cDNA subclone AA6#1 (AP1 & ARP2) using M13 forward (-20) primer

1 TTACGACTCA CTATAGGGCG AATTGGGCCC TCTAGATGCA TGCTCGNAGC GGCCGCCAGT

61 GTGATGGATA TCTGCAGAAT TCGGCTTAGC GGATA**ACAAT** **TTCACACAAG** **GAGCTAGCAT** ARP2*

121 **GG**ACGGCTAA ACGAGGGTCC AACTGTCTCT TATCTTTAAT CAGTGAAATT GACCTTTCAG

181 TGAAGAGGCT GAAATATAAT AATAAGACGA GAAGACCCTA TGGAGCTTAA ATTATATAAC

241 TTATCTATTT AATTTATTAA ACCTAATGGC CCAAAAACTA TAGTATAAGT TTGAAATTTT

301 GGTTGGGGTG ACCTCGGAGA ATAAAAAATC CCCCGAATGA TTATAACCTA GACTTACAAG

361 TCAAAGTAAA ATCAACATAT CTTATTGACC CAGATATATT TTGATCAACG GACCAAGTTA

421 CCCTAGGGAT AACAGCGCAA TCCATTATTAN GAGTTCATAT CGACAATNAG GCTTTACGAC

481 CTCGATGTTG GATCAGGACA TNCCAATGGT GTAGAAGCTA TTANTGGTTC GTTTGTNCAA

541 CGATTAAAGT CCTACGTGAT TTGAGTNCAG ANCCGAGCAN TCCAGGNTCN GTTTNTATCT

601 ATTNACGATN NCTNNCAGTA CGANNGGACA NGANANNTAN ANCCNNCINN CAANTNNN

B 8.2: Sequencing alignment of cDNA subclone **AA6#1** with **mouse mitochondrion** by BLAST searching against the National Center for Biotechnology Information database

AA6#1 : 114 ctagcatggacgggctaaacgaggggtccaactgtctcttattctttaatcagtgaaattgac 173

Mouse mitochondrion: 2061 ctagcatgaacgggctaaacgaggggtccaactgtctcttattctttaatcagtgaaattgac 2120

AA6#1 : 174 ctttcagtgaagagggtgaaatataataataagacgagaagaccctatggagcttaaatt 233

Mouse mitochondrion: 2121 ctttcagtgaagagggtgaaatataataataagacgagaagaccctatggagcttaaatt 2180

AA6#1 : 234 atataacttatctattttaattttattaaacctaattggcccaaaaaactatagtataagtttg 293

Mouse mitochondrion: 2181 atataacttatctattttaattttattaaacctaattggcccaaaaaactatagtataagtttg 2240

AA6#1 : 294 aaatttcggttggttgacctcggagaataaaaaatccccgaatgattataacctagac 353

Mouse mitochondrion: 2241 aaatttcggttggttgacctcggagaataaaaaatcctccgaatgattataacctagac 2300

AA6#1 : 354 ttacaagtcaaagtaaaatcaacatatcttattgaccagatatattttgatcaacggac 413

Mouse mitochondrion: 2301 ttacaagtcaaagtaaaatcaacatatcttattgaccagatatattttgatcaacggac 2360

AA6#1 : 414 caagttaccctagggataacagcgcaatcctatttangagttcatatcgacaatnagggg 473

Mouse mitochondrion: 2361 caagttaccctagggataacagcgcaatcctatttaagagttcatatcgacaattagggg 2420

AA6#1 : 474 ttacgacctcgatgttggatcaggacatnccaatggtgtagaagctattantggttcggt 533

Mouse mitochondrion: 2421 ttacgacctcgatgttggatcaggacatcccaatggtgtagaagctattaatggttcggt 2480

AA6#1 : 534 tgtncaacgattaaagtccctacgtgatattgagtncagancggagcantccaggntcngtt 593

Mouse mitochondrion: 2481 tgttcaacgattaaagtccctacgtgatctgagttcagaccggagcaatccagg-tcgggt 2539

AA6#1 : 594 tntatctattnacgatnctnncagtaggannggaca 630

Mouse mitochondrion: 2540 tctatctatttacgatttctcccagtaggaaaggaca 2576

B 8.3: Summary of sequence alignment of cDNA subclone AA6#1 with mouse mitochondion

FluoroDD gel AA (AP1 + ARP2)					Subclone I.D.	Sequencing				
Fragment no.	PPARα (+/+)		PPARα (-/-)			FluoroDD fragment size (bp)	Size of insert after <i>Eco</i> RI cut (bp)	Primer	Gene homology to Blast search (Transcript size)	E-value (% Identity)
	CTL	Wy	CTL	Wy						
AA6	+	++	+	+	660	AA6#1	710	M13 forward (-20)	<i>Mus musculus</i> clone LA9 mitochondrion, complete genome (16300 bp)	0 495/517 (95%)

* Sequence of primer was not completely matched with the expected sequence.

Appendix B. DNA sequences and sequencing alignments of FluoroDD fragments

B 9.1: DNA sequence of cDNA subclone AA6#9 (AP1 & ARP2) using M13 reverse primer

1 GCCAGCTTGN GTACCGAGCT CGGATCCACT AGTTAACGGC CGCCAGTGTG CTGGAATTCG
61 GCTTAGCGGA **TAACAATTC ACACAAGGAG TAGCATGGAC** GGCTAAACGA GGGTCCAAC**ARP2***
121 GTCTCTTATC TTTAATCAGT GAAATTGACC TTTCAGTGAA GAGGCTGAAA TATAATAATA
181 AGACGAGAAG ACCCTATGGA GCTTAAATTA TATAACTTAT CTATTTAATT TATTAAACCT
241 AATGGCCCCA AAACATAGT ATAAGTTTGA AATTTCGGTT GGGTGACCTC GGAGAATAAA
301 AAATCCTCCG AATGATTATA ACCTAGACTT ACAAGTCAAA GTAAATCAA CATATCTTAT
361 TGACCCAGAT ATATTTTGAT CAACGGACCA AGTTACCCTA GGGATAACAG CGCAATCCTA
421 TTTAAGAGTT CATATCGACA ATNANGTTT ACGACCTCGA TGTGGATCA GGACATCCCA
481 ATGGTGTAGA AGCTATTAAT GGTTCGTTT TTCAACGATT AAAGTCCTAC GTGATCTGAG
541 TTCAGACCGG AGCANTCCAG GTCGGTTTCT ATCTATTNAC GATTCTCCC AGTACGAAAG
601 GACNAGAGAA NTAGAGCCNN CNTACNAATA NGCGCTCTCA ACTNATTAN GAATAAAATC
661 TAAATAANNN NNTNNGTNCN CCCTCTACCN AGAGANNGTC NAAAAAAA AGCCNNN

B 9.2: Sequencing alignment of cDNA subclone AA6#9 with **mouse mitochondrion** by BLAST searching against the National Center for Biotechnology Information database

AA6#9 : 91 tagcatggacggctaacgaggggtccaactgtctcttatctttaatcagtgaaattgacc 150
Mouse mitochondrion: 2062 tagcatgaacggctaacgaggggtccaactgtctcttatctttaatcagtgaaattgacc 2121
AA6#9 : 151 tttcagtgaagaggctgaaatataataataagacgagaagaccctatggagcttaaatta 210
Mouse mitochondrion: 2122 tttcagtgaagaggctgaaatataataataagacgagaagaccctatggagcttaaatta 2181
AA6#9 : 211 tataacttatctatttaattattaaacctaattggcccaaaaactatagtataagtttga 270
Mouse mitochondrion: 2182 tataacttatctatttaattattaaacctaattggcccaaaaactatagtataagtttga 2241
AA6#9 : 271 aatttcggttgagg-tgacctcgagagaataaaaaatcctccgaatgattataacctagact 329
Mouse mitochondrion: 2242 aatttcggttgagggtgacctcgagagaataaaaaatcctccgaatgattataacctagact 2301
AA6#9 : 330 tacaagtcaaagtaaaatcaacatatcttattgacctagatataattttgatcaacggacc 389
Mouse mitochondrion: 2302 tacaagtcaaagtaaaatcaacatatcttattgacctagatataattttgatcaacggacc 2361
AA6#9 : 390 aagttaccctagggataacagcgcaatcctatttaagagttcatatcgacaatnanggtt 449
Mouse mitochondrion: 2362 aagttaccctagggataacagcgcaatcctatttaagagttcatatcgacaattagggtt 2421
AA6#9 : 450 tacgacctcgatggttgatcaggacatcccaatggtgtagaagctattaatggttcgttt 509
Mouse mitochondrion: 2422 tacgacctcgatggttgatcaggacatcccaatggtgtagaagctattaatggttcgttt 2481
AA6#9 : 510 gttcaacgattaaagtcctacgtgatctgagttcagaccggagcantccaggtcggtttc 569
Mouse mitochondrion: 2482 gttcaacgattaaagtcctacgtgatctgagttcagaccggagcaatccaggtcggtttc 2541
AA6#9 : 570 tatctattnacgatttctcccagtagcgaaggaacnagagaantagagccnnctacnaat 629
Mouse mitochondrion: 2542 tatctattnacgatttctcccagtagcgaaggaacnagagaantagagccacctacaaat 2601
AA6#9 : 630 angcgctctcaac-tnatttangaataaaaatctaaataa 667
Mouse mitochondrion: 2602 aagcgctctcaacttaatttatgaataaaaatctaaataa 2640

B 9.3: Summary of sequence alignment of cDNA subclone AA6#9 with mouse mitochondrion

FluoroDD gel AA (AP1 + ARP2)						Sequencing				
Fragment no.	PPARα (+/+)		PPARα (-/-)		FluoroDD fragment size (bp)	Subclone I.D.	Size of insert after <i>EcoRI</i> cut (bp)	Primer	Gene homology to Blast search (Transcript size)	E-value (% Identity)
	CTL	Wy	CTL	Wy						
AA6	+	++	+	+	660	AA6#9	710	M13 reverse	<i>Mus musculus</i> clone LA9 mitochondrion, complete genome (16300 bp)	0 563/579 (97%)

* Sequence of primer was not completely matched with the expected sequence.

Appendix B. DNA sequences and sequencing alignments of FluoroDD fragments

B 10.1: DNA sequence of cDNA subclone AA7#3 (AP1 & ARP2) using M13 forward (-20) primer

1

AATGTTACGA

CTCACTATAG

GGCGAATTGG

GCCCTCTAGA

TGCATGCTCG

AGCGGCCGCC

61

AGTGTGATGG

ATATCTGCAG

AATTCGGCTT

AGCGGATAAC

AATTTACAC

AAGGAGCTAG

121

CATGGACGGC

TAAACGAGGG

TCCAACGTGTC

TCTTATCTTT

AATCAGTGAA

ATTGACCTTT

181

CAGTGAAGAG

GCTGAAATAT

AATAATAAGA

CGAGAAGACC

CTATGGAGCT

TAAATTATAT

241

AACTTATCTA

TTTAATTTAT

TAAACCTAAT

GGCCCCAAAA

CTATAGTATA

AGTTTGAAAT

301

TTCGGTTGGG

GTGACCTCGG

AGAATAAAAA

ATCCTCCGAA

TGATTATAAC

CTAGACTTAC

361

AAGTCAAAGT

AAAATCAACA

TATCTTATCG

ACCCAGATAT

ATCTTGATCA

ACGGACCAAG

421

TTACCCTAGG

GATAACAGCG

CAATCCTATT

TAAGAGNNCA

TATCGACAAT

NAGGGTANAC

481

GANNTCGATG

TTGGATCANG

ACATCCCCAA

TGGTGTAGAA

GCTATTAATG

GTTCGTTTGT

541

TCAACGATAA

ANGTNTACG

TGATCTGAGT

TCAGANCCGA

GCNATNCAGG

TCGGTTTCTA

601

TCTATTNACG

ATNNCTNNCA

GTACGANANG

ACANGAGANN

NNAGCNCCNT

NACNANTNNC

661

NCTNNNACNT

ANTTATGAAT

AAATCTAATN

AANNNNTCGT

NNCCNCTANC

NAANGAGTNN

721

ANAAAAA

ARP2 *

B 10.2: Sequencing alignment of cDNA subclone AA7#3 with **mouse mitochondrion** by BLAST searching against the National Center for Biotechnology Information database

AA7#3

:

117

ctagcatggacgggcta

aaacgaggggtcca

actgtctctt

tatctttaatcagt

gaaattgac

176

Mouse mitochondrion:

2061

ctagcatgaacgggcta

aaacgaggggtcca

actgtctctt

tatctttaatcagt

gaaattgac

2120

AA7#3

:

177

ctttcagtgaagaggct

gaaatataataa

taagacgagaag

accctatggagct

ttaaatt

236

Mouse mitochondrion:

2121

ctttcagtgaagaggct

gaaatataataa

taagacgagaag

accctatggagct

ttaaatt

2180

AA7#3

:

237

atataacttatctat

ttaatttatt

aaacctaata

ggcccaaaa

actatagtata

aagtttg

296

Mouse mitochondrion:

2181

atataacttatctat

ttaatttatt

aaacctaata

ggcccaaaa

actatagtata

aagtttg

2240

AA7#3

:

297

aaatttcggttggggt

gacctcggaga

ataaaaaat

cctccgaat

gattataac

cctagac

356

Mouse mitochondrion:

2241

aaatttcggttggggt

gacctcggaga

ataaaaaat

cctccgaat

gattataac

cctagac

2300

AA7#3

:

357

ttacaagtcaaagta

aaatcaacata

tcttatcgacc

catatata

tcttgatca

acggac

416

Mouse mitochondrion:

2301

ttacaagtcaaagta

aaatcaacata

tcttatcgacc

catatata

tcttgatca

acggac

2360

AA7#3

:

417

caagttaccctaggg

ataacagcgca

atcctat

ttaagagn

catatcgaca

atnaggg

476

Mouse mitochondrion:

2361

caagttaccctaggg

ataacagcgca

atcctat

ttaagagn

catatcgaca

atnaggg

2420

AA7#3

:

477

anacganntcgatgt

tggatcangac

atccccaat

gggtgtaga

agctatta

aatggttcgt

536

Mouse mitochondrion:

2421

ttacgacctcgatgt

tggatcaggac

atccccaat

gggtgtaga

agctatta

aatggttcgt

2479

AA7#3

:

537

ttgttcaacgataaa

ngtntacgtga

ctctgagtt

caganccgag

cnatncaggt

cgggt

596

Mouse mitochondrion:

2480

ttgttcaacgattaa

agtcctacgtg

atctgagtt

cagaccggag

caatccaggt

cgggt

2539

AA7#3

:

597

tctatctattnacga

tnnctnn

cagtacgan

angacangaga

638

Mouse mitochondrion:

2540

tctatctattnacga

tnnctnn

cagtacgaa

aggacaagaga

2581

B 10.3: Summary of sequence alignment of cDNA subclone AA7#3 with mouse mitochondrion

FluoroDD gel AA (AP1 + ARP2)					Subclone I.D.	Sequencing				
Fragment no.	PPARα (+/+)		PPARα (-/-)			FluoroDD fragment size (bp)	Size of insert after <i>Eco</i> RI cut (bp)	Primer	Gene homology to Blast search (Transcript size)	E-value (% Identity)
	CTL	Wy	CTL	Wy						
AA7	+	++	+	+	640	AA7#3	710	M13 forward (-20)	<i>Mus musculus</i> clone LA9 mitochondrion, complete genome (16300 bp)	0 495/522 (94%)

* Sequence of primer was not completely matched with the expected sequence.

Appendix B. DNA sequences and sequencing alignments of FluoroDD fragments

B 11.1: DNA sequence of cDNA subclone AA7#5 (AP1 & ARP2) using M13 reverse primer

1 GCCAAGCTTG NGTACCGAGC TCGGATCCAC TAGTAACGGC CGCCAGTGTG CTGGAATTCG
61 GCTNGTAATA **CGACTCACTA TAGGGCTTTT TTTTTTTGAC** CTTCTCTAGG TTAGAGGGTG **AP1**
121 TACGTATATA TTTTATTTAG ATTTTATTCA TAAATTAAGT TGAGAGCGCT TATTTGTAAG
181 GTGGCTCTAT TTCTCTTGTC CTTTCGTACT GGGAGAAATC GTAAATAGAT AGAAACCGAC
241 CTGGATTGCT CCGGTCTGAA CTCAGATCAC GTAGGACTTT AATCGTTGAA CAAACGAACC
301 ATTAATAGCT TCTACACCAT TGGGATGTCC TGATCCAACA TCGAGGTCGT AAACCCTAAT
361 TGTCGATATG AACTCTTAAA TAGGATTGCG CTGTTATCCC TAGGGTAACT TGGTCCGTTG
421 ATCAAAATAT ATCTGGGTCA ATAAGATATG TNGATTTTAC TTTGACTNGT AAGTCTAGGT
481 NATAATCATT CGGANGATNT TTATTCCTNCG AGGTCNNCCN ANNGAAATTT CAACTTATAC
541 TATAGTTTTN GGNCATANGT TTATAATAAA TAGATAGTAT ATANTTANCN CATAGGTCTC
601 TGTCTATATA ATTCGCTCTC CTGAAGTCAT CACTATNANA TGAACGTGAN NGTTAGCGTA
661 GN

B 11.2: Sequencing alignment of cDNA subclone AA7#5 with **mouse mitochondrion** by BLAST searching against the National Center for Biotechnology Information database

AA7#5 : 99 accttctctaggttagaggggtgtacgtatataatctttagattttattcataaattaa 158
Mouse mitochondrion: 2674 accttctctaggttagaggggtgtacgtatataatctttagattttattcataaattaa 2615
AA7#5 : 159 gttgagagcgcttatttgaaggtggctctatttctcttgctctttcgtactgggagaaa 218
Mouse mitochondrion: 2614 gttgagagcgcttatttgaaggtggctctatttctcttgctctttcgtactgggagaaa 2555
AA7#5 : 219 tcgtaaatagatagaaaccgacctggattgctccggtctgaactcagatcacgtaggact 278
Mouse mitochondrion: 2554 tcgtaaatagatagaaaccgacctggattgctccggtctgaactcagatcacgtaggact 2495
AA7#5 : 279 ttaatcgttgaacaaacgaaccattaatagcttctacaccattgggatgtcctgatccaa 338
Mouse mitochondrion: 2494 ttaatcgttgaacaaacgaaccattaatagcttctacaccattgggatgtcctgatccaa 2435
AA7#5 : 339 catcgaggtcgtaaaccctaattgtcgatatgaactcctaaataggattgcgctgttatc 398
Mouse mitochondrion: 2434 catcgaggtcgtaaaccctaattgtcgatatgaactcctaaataggattgcgctgttatc 2375
AA7#5 : 399 cctagggtaacttgggtccgttgatcaaaatataatctgggtcaataagatatgtngatttt 458
Mouse mitochondrion: 2374 cctagggtaacttgggtccgttgatcaaaatataatctgggtcaataagatatgttgatttt 2315
AA7#5 : 459 actttgactngtaagtctaggttataatcattcgganga-tntttattctnccgaggtc-n 516
Mouse mitochondrion: 2314 actttgactngtaagtctaggttataatcattcggaggattttttattctccgaggtcac 2255
AA7#5 : 517 nccnanngaaatttc-aacttatactatagtttt 549
Mouse mitochondrion: 2254 cccaaccgaaatttc aaacttatactatagtttt 2221

B 11.3: Summary of sequence alignment of cDNA subclone AA7#5 with **mouse mitochondrion**

FluoroDD gel AA (AP1 + ARP2)					Subclone I.D.	Sequencing				
Fragment no.	PPARα (+/+)		PPARα (-/-)			FluoroDD fragment size (bp)	Size of insert after <i>Eco</i> RI cut (bp)	Primer	Gene homology to Blast search (Transcript size)	E-value (% Identity)
	CTL	Wy	CTL	Wy						
AA7	+	++	+	+	640	AA7#5	710	M13 reverse	<i>Mus musculus</i> clone LA9 mitochondrion, complete genome (16300 bp) 0 440/454 (96%)	

Appendix B. DNA sequences and sequencing alignments of FluoroDD fragments

B 12.1: DNA sequence of cDNA subclone AA10#1 (AP1 & ARP2) using M13 forward (-20) primer

1 TATACGACTC ACTATAGGGC GAATTGGGCC CTCTAGAATG CATGCTCGAG CGGCCGCCAG
61 TGTGATGGAT ATCTGCAGAA TTCGGCTTAG CGGATAACAA TTTCACACAA GGAGCTAGCA ARP2*
121 TGGTGGAAGAA GGGGACCATG ATGATTGGCT ACCAGCCCCA TGGGACCCGG GCCAACTTCT
181 TCCGAATGGT GGTGGCCAAC CCCATACTGG CCCAGGCCGA TATANGATT CTTTCTNNGG
241 CGAGCTGGAG CTCCTGGGCC AGGAACCTGT GAGCTGCTTC TGCTCTCTGC CCCACCCAAA
301 GCTCTGCGTA GTCTCCTGGG TTCTCAAAAT CGACCTTTCT AGGAAACAGT GGCCTTGNAC
361 TGTGTGTGCT CCCACACACT CACTCTCCCA GCTAAGTATT GGCTGTCAGG AAGGTGTGCT
421 AAACACACAC ACCTACTGTA TGTTCCTTAA CGAAAATATG CTTANATNAA AAGTNGGGCA
481 ACAANGGNGC ACACACCCNT TTANCTACCC AGCATTGGGG NGGGACNNAA AGCAGCCCAG
541 TNNTGAANGC CAGCCTGAAC TACAGAGCTN GGCTACACAG AAAAAGTGTG TCNNANANN
601 AAAGCCCNNN TNNTNNATTN NNNTNCCGC CNGATTNCCN GCCCNCNNGG CNNGGCNGNT
661 NCNTANGTNG GATNCNGAGC CCTCGGNTAN NCCAAGCCNT NNGGCNGTTA NNTCTTTGGN
721 NTNNTNNNCG N

B 12.2: Sequencing alignment of cDNA subclone AA10#1 with **mouse cysteine sulfinic acid decarboxylase (Csad)** by BLAST searching against the National Center for Biotechnology Information database

AA10#1 : 118 gcatggtgaagaaggggaccatgatgattggctaccagcccatgggacccgggccaact 177
Mouse Csad: 1500 gcatggtgaagaaggggaccatgatgattggctaccagcccatgggacccgggccaact 1559
AA10#1 : 178 tcttccgaatggtggtggccaacccatactggcccaggccgatatangatttccttctn 237
Mouse Csad: 1560 tcttccgaatggtggtggccaacccatactggcccaggccgatata-gatttccttct- 1617
AA10#1 : 238 nggcgagctggagctcctgggccaagaaacctgtgagctgcttctgctctctgccccaccc 297
Mouse Csad: 1618 ggcgagctggagctcctgggccaag-acctgtgagctgcttctgctctctgccccaccc 1676
AA10#1 : 298 aaagctctgcgtagtctcctgggttctcaaaatcgacctttctaggaacagtggccttg 357
Mouse Csad: 1677 -aagctctgcgtagtctcctgggttctcaaaatcgacctttctaggaacagtggccttg 1735
AA10#1 : 358 nactgtgtgtgctccacacactcactctcccagctaagtattggctgtcaggaaggtgt 417
Mouse Csad: 1736 -actgtgtgtgctccacacactcactctcccagctaagtattggctgtcaggaaggtgt 1794
AA10#1 : 418 gctaaacacac 428
Mouse Csad: 1795 -ctaaacacac 1804

B 12.3: Summary of sequence alignment of cDNA subclone AA10#1 with mouse Csad

FluoroDD gel AA (AP1 + ARP2)					Subclone I.D.	Sequencing				
Fragment no.	PPARα (+/+)		PPARα (-/-)			FluoroDD fragment size (bp)	Size of insert after <i>Eco</i> RI cut (bp)	Primer	Gene homology to Blast search (Transcript size)	E-value (% Identity)
	CTL	Wy	CTL	Wy						
AA10	+	++	+	+	500	AA10#1	550	M13 forward (-20)	<i>Mus musculus</i> cysteine sulfinic acid decarboxylase (Csad) (2265 bp)	e-143 304/311 (97%)

* Sequence of primer was not completely matched with the expected sequence.

Appendix B. DNA sequences and sequencing alignments of FluoroDD fragments

B 13.1: DNA sequence of cDNA subclone AA10#1 (AP1 & ARP2) using M13 reverse primer

1 TCAGCCAGCT TGNGTACCGA GACTCGGATN CACTATTAAC GGCCGCCAGT GTGCTGGAAT
61 TCGGCTGTAA **TACGACTCAC TATAGGGACT TTTTTTTTTT TGAGANCAGT TTCNNTGTGT** **AP1**
121 AGACCCAGAC NNTGTAGTCC AGGACTGGNC CTCAAACCTGG ACTGCTTCTG TNACCCCCAA
181 TGCTGGTAGT AAAGGTGTGT GCCCCTGTGN CCCANNTTAA TAAAAGACAT ATTTTCGTAAG
241 ANNATAACTG TAGTGTGTTT AAGAACACCC TTCCTGNNAG CCAATACTTA GACTGGGAGA
301 GTGAGTGTGT GGGANNNNA NCAACAGTCA AGGCCNACTG TTTCCCTANG AAAAGGTCCG
361 ATTTTGANGA NACCCAGGAG AACTANCGNC AGAGCTTGGG TGGGGNCAGA NGANGCAGAA
421 AGCCGCNCCA CAGGTCCCTG GNCCAGGAG NCTCCNGNCT CGCCCCAGAA ANNAAAATCT
481 ATANTCGGCC CCGCCGCCAC GTAATGGGNG NTCGGCCCCC CCCCCCTNC CCGAANNAAC
541 GTNNGGNCCC GGGGGTCCCC ANTNNGGGCC TNGGTANGCC CANTTTATTN CNTNGGGTNN
601 CCCCCTNTCT TTCCNCNNT GGCTAGCCTC CCNTNNGNTN GNTGANNTT TNGNTTANTT
661 CCCGNTNAN NGNCCGAAA TTNTTTGGGC NNNNTNNTN NNCTTTCCCN CCNNNGGGNG
721 GGGGGAGGGT TTTNGNNGNC NNT

B 13.2: Sequencing alignment of cDNA subclone AA10#1 with **mouse cysteine sulfinic acid decarboxylase (Csad)** by BLAST searching against the National Center for Biotechnology Information database

AA10#1 : 133 tgtagtccaggactggnccctcaaactggactgcttctgtgnaccccccaatgctggtagtaa 192
Mouse Csad: 1917 tgtagtccagg-ctgg-cctcaaactgg-ctgcttctgtc-cccccaatgctggtagtaa 1862
AA10#1 : 193 aggtgtgtgcccctgtgnccannttaataaaagacatatattcgtgaagannataactgta 252
Mouse Csad: 1861 aggtgtgtgcccctgtg-cccaacttaataaaag-catatttcgtgaagaacat-actgta 1805
AA10#1 : 253 gtgtgtttaagaacacccttcctggnagccaatacttagactgggagagtgagtgtgtgg 312
Mouse Csad: 1804 gtgtgttta--gaca-ccttcctgacagccaatacttag-ctgggagagtgagtgtgtgg 1749
AA10#1 : 313 ga 314
Mouse Csad: 1748 ga 1747

B 13.3: Summary of sequence alignment of cDNA subclone AA10#1 with mouse Csad

FluoroDD gel AA (AP1 + ARP2)						Subclone I.D.	Sequencing			
Fragment no.	PPARα (+/+)		PPARα (-/-)		FluoroDD fragment size (bp)		Size of insert after <i>Eco</i> RI cut (bp)	Primer	Gene homology to Blast search (Transcript size)	E-value (% Identity)
	CTL	Wy	CTL	Wy						
AA10	+	++	+	+	500	AA10#1	550	M13 reverse	<i>Mus musculus</i> cysteine sulfinic acid decarboxylase (Csad) (2265 bp)	3e-32 163/182 (89%)

Appendix B. DNA sequences and sequencing alignments of FluoroDD fragments

B 14.1: DNA sequence of cDNA subclone AA12#4 (AP1 & ARP2) using M13 forward (-20) primer

1 CCCACCNCAC TTNAGGGCGA ATTGGGCCCT CTAGATGCAT GCTCGAGCGG CCGCCAGTGT
61 GATGGATATC TGCAGAATTC GCCCTTAGCG GATA**ACAATT TCACACAGGA GCTAGCATGG** ARP2
121 CAGCGGCGTT CCGCAGAGGC TGCAGGGTCC TGAGAAAGTGT TTCTCATTTT GAGTGTGCGAA
181 CACAACACTC GAAAGCGGCT CACAAGCAGG AGCCCGGATT AGGGTTTAGT TTTGAGTTGA
241 CGGAACAGCA GAAAGAGTTT CAAGCAACTG CCCGCAAGTT TGCCAGAGAG GAGATTATCC
301 CCGTCGCCCC GGAATATGAC AAAAGCGGGG AGTACCCGTT CCCTCTCATC AAAAGAGCCT
361 GGGAACTCGG CTTGATCAAC GCGCACATTC CGGAAAGTTG CGGTGGTCTT GGCCTGGGAA
421 CGTTCGATGC TTGTTTAATT ACCGAAGAGT TGGCGTATGG GTGTACAGGG GTGCAAACTG
481 CTATTGAAGC AAATTCTTTG GGGCAAATGC CTGTGATTCT TGCTGGAAAT GATCAAAAAA
541 AAGCCCTATA GTGAGTCGTA TTACAAGGGC GAATTCCAGC ACACTGGCGG CCCGTTACTA
601 GTGGATNCGA GCTCGGTACC AAGCTTGATG CATAGCTTGA GTATTCTATA GTGTCACCTA
661 AATAGCTNGG CGTAATCATG GTCATAGCTG TNMCCTGTGT GAAATGGTTA TCCGCTCACN
721 NTTNCACACA AATACNAGCN GGNANCATAA GTGTAAGNCN GGGNTGCTAA TGAGTGAGCT
781 AA

B 14.2: Sequencing alignment of cDNA subclone AA12#4 with **mouse acetyl-coenzyme A dehydrogenase, medium chain (MCAD)** by BLAST searching against the National Center for Biotechnology Information database

AA12#4 : 116 catggcagcggcggttccgcagaggtgcagggtcctgagaagtgtttctcattttgagtg 175
Mouse MCAD: 3 catggcagcggcggttccgcagaggtgcagggtcctgagaagtgtttctcattttgagtg 62
AA12#4 : 176 tcgaacacaaactcgaaagcggctcacaagcaggagcccgattagggtttagttttga 235
Mouse MCAD: 63 tcgaacacaaactcgaaagcggctcacaagcaggagcccgattagggtttagttttga 122
AA12#4 : 236 gttgacggaacagcagaaagagtttcaagcaactgcccgcaagtttgccagagaggagat 295
Mouse MCAD: 123 gttgacggaacagcagaaagagtttcaagcaactgcccgcaagtttgccagagaggagat 182
AA12#4 : 296 tatccccgtcgccccggaatatgacaaaagcggggagtaccggttccctctcatcaaaag 355
Mouse MCAD: 183 tatccccgtcgccccggaatatgacaaaagcggggagtaccggttccctctcatcaaaag 242
AA12#4 : 356 agcctgggaactcggttgatcaacgcgcacattccggaaagtgtcggtggtcttggcct 415
Mouse MCAD: 243 agcctgggaactcggttgatcaacgcgcacattccggaaagtgtcggtggtcttggcct 302
AA12#4 : 416 gggaacggttcgatgcttggttaattaccgaagagttggcgtatgggtgtacaggggtgca 475
Mouse MCAD: 303 gggaacggttcgatgcttggttaattaccgaagagttggcgtatgggtgtacaggggtgca 362
AA12#4 : 476 aactgctattgaagcaaattctttggggcaaatgcctgtgattcttgctggaaatgatc 534
Mouse MCAD: 363 aactgctattgaagcaaattctttggggcaaatgcctgtgattcttgctggaaatgatc 421

B 14.3: Summary of sequence alignment of cDNA subclone AA12#4 with mouse MCAD

FluoroDD gel AA (AP1 + ARP2)					Subclone I.D.	Sequencing				
Fragment no.	PPARα (+/+)		PPARα (-/-)			FluoroDD fragment size (bp)	Size of insert after <i>Eco</i> RI cut (bp)	Primer	Gene homology to Blast search (Transcript size)	E-value (% Identity)
	CTL	Wy	CTL	Wy						
AA12	+	++	+	+	470	AA12#4	500	M13 forward (-20)	<i>Mus musculus</i> acetyl-coenzyme A dehydrogenase, medium chain (MCAD) (1857 bp) 0 419/419 (100%)	

Appendix B. DNA sequences and sequencing alignments of FluoroDD fragments

B 15.1: DNA sequence of cDNA subclone AA12#4 (AP1 & ARP2) using M13 reverse primer

1 AGACTATTAG GTGACNCTAT AGAATACTCA AGNCTATGCA TCAAGCTTGG TACCGAGCTC
61 GGATCCACTA GTAACGGCCG CCAGTGTGCT GGAATTCGCC CTTGTAATAC GACTCACTAT AP1*
121 AGGGCTTTTT TTTGATCATT TCCAGCAAGA ATCACAGGCA TTTGCCCCAA AGAATTTGCT
181 TCAATAGNCA GTTTGCNCCC CTGTACACCC ATACGACCAA CTCTTCGGTA ATTAAANCAA
241 GNCATCNGAA ACGTNNCCCA GGGNCCAAGA ANCCANCCGC CAAACTTTTN CCGGGAAATG
301 GTGNCGNCGN TTGNNNNAAG NCCGANGTNC CCCAGGGCTC TTTTGATGAA GANGGAAACN
361 GGGTACTCCC CNCTTTTNNAT ATATNNCGGG GCGACNNGGN TAATNCTCCT CNCTGNNAAA
421 CTNNCGGGNN CNNTGCTTGG AAACCTCTTC CTGGCTGTTC CCGGTAAANC CNNAAAAACCT
481 AAAAACCCCTN AAATNCCGGG GGCTNCCTGC CTTTGGNNNA GNCCGCTTTT CCGAGGTGGT
541 TGNTGGTTNC GACACCNNA AAAATGANNA AAACNCTTTC NNAGGGAACC CTGNAGGNCT
601 CCTGGGCGAA NCGNCCGNCN GNNCANTGCC AACCNNCCCT GGTGNNNAAA AATTGNTTAA
661 TTNCCGCTAA NGGGGGCGAA TTNTNGNNN NANTNATTNC ACTNCNNACN NNGGNCNNCC
721 GCGNTTCNNA CNTTNNNNNN NANGANNNC CCCNNTTTNN CCCTANTNNN TGGANNTNGT
781 AANTTAAANN AAATTTAACN NNNGNNNCGG

B 15.2: Sequencing alignment of cDNA subclone AA12#4 with mouse acetyl-coenzyme A dehydrogenase, medium chain (MCAD) by BLAST searching against the National Center for Biotechnology Information database

AA12#4 : 134 gatcattttccagcaagaatcacaggcatttgccccaaagaatttgcttcaatagncagtt 193
Mouse MCAD: 421 gatcattttccagcaagaatcacaggcatttgccccaaagaatttgcttcaatag-cagtt 363
AA12#4 : 194 tgcncctctgtacacccatacgaccaactcttcggttaattaaa 236
Mouse MCAD: 362 tgcacccctgtacacccatacg-ccaactcttcggttaattaaa 321

B 15.3: Summary of sequence alignment of cDNA subclone AA12#4 with mouse MCAD

FluoroDD gel AA (AP1 + ARP2)					Subclone I.D.	Sequencing				
Fragment no.	PPARα (+/+)		PPARα (-/-)			FluoroDD fragment size (bp)	Size of insert after <i>Eco</i> RI cut (bp)	Primer	Gene homology to Blast search (Transcript size)	E-value (% Identity)
	CTL	Wy	CTL	Wy						
AA12	+	++	+	+	470	AA12#4	500	M13 reverse	<i>Mus musculus</i> acetyl-coenzyme A dehydrogenase, medium chain (MCAD) (1857 bp) 5e-38 100/103 (97%)	

* Sequence of primer was not completely matched with the expected sequence.

B 16.1: DNA sequence of cDNA subclone AB7#2 (AP3 & ARP3) using M13 forward (-20) primer

1	TGGGCCCTCT	AGATGCATGC	TCGAGCGGCC	GCCAGTGTGA	TGGATATCTG	CAGAATTCGC	
61	CCTTAGCGGA	TAACAATTC	ACACAGGAGA	CCATTGCAA	CCTGCTAAAC	CATTGCCTAA	ARP3
121	GGAAATGGAA	GACTTTGTTC	AGAGCTCTGG	AGAGCATGGT	GTGGTGGTGT	TTTCTCTGGG	
181	GTCAATGGTC	AGTAATATGA	CAGAAGAAAA	GGCCAATGCA	ATTGCATGGG	CTCTTGCCCA	
241	GATTCCACAA	AAGGTTCTTT	GGAGATTTGA	CGGCAAAACT	CCAGCCACCT	TAGGACCCAA	
301	TACCAGAAATC	TACAAGTGGC	TTCCCCAAAA	TGATCTTCTT	GGTCATCCAA	AAACCAAAGC	
361	CTTTATAACT	CATGGTGGCG	CGAATGGACT	CTACGAGGCG	ATCCATCATG	GAATCCCTAT	
421	GATTGGCATT	CCTTTGTTTG	GAGAACACA	TGATAACATT	GCTCACATGG	TGGCCAAAGG	
481	AGCAGCTGTT	ACATTGAATA	TCAGAACGAT	GTCCAGGTCA	GATTTGCTCA	ATGCACTGGA	
541	GGAAGTCATA	GACAATCCTT	TCTATAAAGA	GAATGCTATG	TGGTTGTCAA	CCATTACCA	
601	TGACCAGCCT	ATGAAGCCCC	TGGACAGAGC	AGTCTTCTGG	ATNGAGTTTG	TCATGCGCCA	
661	CAAAGNGCC	AAGCATCTGA	GACCACTNGC	ATACNACCTC	ACCTGGTANC	AGTACCACTC	
721	TCTGNATGTG	ATNGNATCCT	GNNGCNTTNG	TANNTNNTGT	ACCCNCATGT	AAATCTTTTG	
781	TGGTAACCAN	NNT					

B 16.2: Sequencing alignment of cDNA subclone **AB7#2** with **mouse UDP-glucuronosyltransferase 2 family, member 5 (UGT2b5)** by BLAST searching against the National Center for Biotechnology Information database

AB7#2	:	91	ccattgcaaacctgctaaccattgcctaaggaaatggaagactttgttcagagctctgg	150
Mouse UGT:	868		ccattgcaaacctgctaacccttgccctaaggatatggaagaatttgtccagagctctgg	927
AB7#2	:	151	agagcatgggtgtgggtggtgttttctctggggtcaatggtcagtaatatgacagaagaaaa	210
Mouse UGT:	928		agaccatgggtgtgggtggtcctttctctggggtcaatggttagtaacatgacagaagaaaa	987
AB7#2	:	211	ggccaatgcaattgcatgggctcttgcccagattccacaaaagggttctttggagatttga	270
Mouse UGT:	988		agccaacgcaattgcatgggcccttgcccagattccacaaaagggttctttggaaatttga	1047
AB7#2	:	271	cggcaaaaactccagccaccttaggacccaataaccagaatctacaagtggcttccccaaaa	330
Mouse UGT:	1048		tggcaaaaacccagcaactttaggacacaataaccagagtgtacaagtggctccccagaa	1107
AB7#2	:	331	tgatcttcttggtcatccaaaaaccaaagcctttataactcatgggtggcggaatggact	390
Mouse UGT:	1108		tgacctccttggtcatccaaaaaccaaagcctttgtaactcatgggtggggccaatggtgt	1167
AB7#2	:	391	ctacgaggcgatccatcatggaatccctatgattggcattcctttgtttggagaacaaca	450
Mouse UGT:	1168		ctacgaggcgatctatcatggaatccctatgattggcattcctttgtttggagaacagca	1227
AB7#2	:	451	tgataacattgctcacatggtggccaaaggagcagctgttacattgaatatcagaacgat	510
Mouse UGT:	1228		tgataacattgcccataatggtggccaaaggagcagctgttgcatgaatatcagaacaat	1287
AB7#2	:	511	gtccagggtcagatttgctcaatgcactggaggaggtcatagacaatcctttctataaaga	570
Mouse UGT:	1288		gtcaaagtcagatgtgctcaatgcactggaggaggtcatagaaaatcctttctataaaaa	1347
AB7#2	:	571	gaatgctatgtggttgtcaaccattcaccatgaccagcctatgaagcccctggacagagc	630
Mouse UGT:	1348		gaatgctatgtggttgtcaaccattcaccatgaccagcctatgaaaccccctggacagggc	1407
AB7#2	:	631	agtcttctggatngagtttgtcatgcgccacaaaaggngccaagcatctgagaccactngc	690
Mouse UGT:	1408		tgtcttctggattgagtttgttatgcgccacaaaagagccaagcacctgagaccacttgg	1467
AB7#2	:	691	atacnacctcacctgggtancagtaccactctctgnatgtgat	732
Mouse UGT:	1468		acataaccttacctgggtaccagtaccactctctggatgtgat	1509

B 16.3: Summary of sequence alignment of cDNA subclone **AB7#2 with mouse UGT2b5**

FluoroDD gel AB (AP3 + ARP3)					Subclone I.D.	Sequencing				
Fragment no.	PPARα (++)		PPARα (-/-)			FluoroDD fragment size (bp)	Size of insert after <i>EcoRI</i> cut (bp)	Primer	Gene homology to Blast search (Transcript size)	E-value (% Identity)
	CTL	Wy	CTL	Wy						
AB7	+	++	+	+	850	AB7#2	900	M13 forward (-20)	Mouse UDP- glucuronosyltransferase 2 family, member 5 (UGT2b5) (1648 bp)	0 585/642 (91%)

Appendix B. DNA sequences and sequencing alignments of FluoroDD fragments

B 17.1: DNA sequence of cDNA subclone AB7#8 (AP3 & ARP3) using M13 reverse primer

1 TAGAATACTC AAGCTATGCA TCAAGCTTGG TACCGAGCTC GGATCCACTA GTAACGGCCG
61 CCAGTGTGCT GGAATTCGCC CTTGTAATAC **GACTCACTAT AGGGCTTTT** **TTTTTGGTG** **AP3***
121 GTAAAATTTT ATTCATGTAA TGCATTATCA ATGAGTTCTA CTCATTCTTC ATTTTCTTTT
181 CTTTCTTTAC AAAGAATCGG TAAACAAACA AGAAGCACTT TACAATGAGG GCTACAATGA
241 ATGTCACAAA AGCAAGCAGG AATCCAATCA CATCCAGAGA GTGGTACTGG TACCAGGTGA
301 GGTGTATGCA AAGTGGTCTC AGATGCTTGG CCCCTTTGTG GCGCATGACA AACTCAATCC
361 AGAAGACTGC TCTGTCCAGG GGCTTCATAG GCTGGTCATG GTGAATGGTT GACAACCACA
421 TAGCATTCTC TTTATAGAAA GGATTGTCTA TGACTTCCTC CAGTGCATTG AGCAAATCTG
481 ACCTTGACAT CGTTCTGATA TTCAATGTAA CAGCTGCTCC TTTGGCCACC ATGTGAGCAA
541 TGTTATCATG TTGTTCTCCA AACAAAGGAA TGCCAATCAT AGGGATNCCA TGATGGATCG
601 CCTCGTAGAG TCCATTTCGG CCACCATGAG TNATAAAGGC TTTGGTTNTT GGATGACCAA
661 GAAGATCATT TTGGGGANGC ACTNGTANGT TCTGGTATTG GGTCTAAGGT GGCTGGAGTN
721 NNCCGTCAAA TCTCCAAGAA CCTTNGTGAA A

B 17.2: Sequencing alignment of cDNA subclone AB7#8 with **mouse UDP-glucuronosyltransferase 2 family, member 5 (UGT2b5)** by BLAST searching against the National Center for Biotechnology Information database

AB7#8 : 143 cattatcaatgagttctactcattccttcattttcttttctttcttttacaaaagaatcggt 202
Mouse UGT: 1633 cattgtcagtgagctctactcattccttcattttattttctttcttttacaaaagaatcggt 1574
AB7#8 : 203 aacaaacaagaagcactttacaatgagggtacaatgaatgtcacaaaagcaagcaggaa 262
Mouse UGT: 1573 aatgaacaagaggcactttacactaaggactatagtgggtgccacacaagagagtaggaa 1514
AB7#8 : 263 tccaatcacatccagagagtggtaggtaccaggtgaggttgatgcaagtgggtctcag 322
Mouse UGT: 1513 tccaatcacatccagagagtggtaggtaccaggtgaggttatgtccaagtgggtctcag 1454
AB7#8 : 323 atgcttggcccttttgtggcgcatgacaaactcaatccagaagactgctctgtccagggg 382
Mouse UGT: 1453 gtgcttggctcttttgtggcgcatgacaaactcaatccagaagacagccctgtccagggg 1394
AB7#8 : 383 cttcataggctgggtcatggtgaatgggtgacaaccacatagcattctctttatagaaagg 442
Mouse UGT: 1393 tttcataggctgggtcatggtgaatgggtgacaaccacatagcattctctttatagaaagg 1334
AB7#8 : 443 attgtctatgacttcctccagtgcattgagcaaactctgaccttgacatcggttctgatatt 502
Mouse UGT: 1333 attttctatgacctcctccagtgcattgagcacatctgactttgacattgttctgatatt 1274
AB7#8 : 503 caatgtaacagctgctcctttggccaccatgtgagcaatgttatcatgttgttctccaaa 562
Mouse UGT: 1273 caatgcaacagctgctcctttggccaccatgtggcaatgttatcatgttcttctccaaa 1214
AB7#8 : 563 caaaggaatgccaatcatagggatnccatgatggatcgccctcgtagagtccattcgcgcc 622
Mouse UGT: 1213 caaaggaatgccaatcatagggattccatgatagatcgccctcgtagacaccattggcccc 1154
AB7#8 : 623 accatgagtnataaaggcctttgggtnttggatgaccaagaagatcattttgggg 676
Mouse UGT: 1153 accatgagttacaaaggcctttgggttttggatgaccaaggaggtcattctgggg 1100

B 17.3: Summary of sequence alignment of cDNA subclone AB7#8 with mouse UGT2b5

FluoroDD gel AB (AP3 + ARP3)					Subclone I.D.	Sequencing				
Fragment no.	PPARα (+/+)		PPARα (-/-)			FluoroDD fragment size (bp)	Size of insert after <i>Eco</i> RI cut (bp)	Primer	Gene homology to Blast search (Transcript size)	E-value (% Identity)
	CTL	Wy	CTL	Wy						
AB7	+	++	+	+	850	AB7#8	900	M13 reverse	Mouse UDP-glucuronosyltransferase 2 family, member 5 (UGT2b5) (1648 bp)	0 482/534 (90%)

* Sequence of primer was not completely matched with the expected sequence.

Appendix B. DNA sequences and sequencing alignments of FluoroDD fragments

B 18.1: DNA sequence of cDNA subclone AB17#16 (AP3 & ARP3) using M13 reverse primer

1 CCAGACTATT TAGGTGACCT ATAGAATACT CNANNTATGC NTCAAGCTTG GTACCGAGCT
61 CGGATCCACT AGTAACGGCC GCCAGTGTGC TGGAATTCGC CCTTAGCGGA TAACAATTTC ARP3
121 ACACAGGAGA CCATTGCACA TAGGACTTAT TCTTCTTACA TGACAAAAA TTGCTCCCCT
181 ATCAATTTTA ATTCAAATTT ACCCGCTACT CAACTCTACT ATCATTTTAA TACTAGCAAT
241 TACTTCTATT TTCATAGGGG CATGAGGAGG ACTTAACCAA ACACAAATAC GAAAAATTAT
301 AGCCTATTCA TCAATTGCCC ACATAGGATG AATATTAGCA ATTCTTNCCT TACAACCCAT
361 CCCTCACTCT ACTCAACCTC ATAATCTATA TTATTCTTAC AGCCCCTATA TTCATAGCAC
421 TTATACTAAA TAACTCTATA ACCATCAACT CAATCTCACT TCTATGAAAT AAAACTCCAG
481 CAATACTAAC TATAATCTCA CTGATATTAC TATCNCTANG AGGCCTNNCA CCACTANCAN
541 GATTCTNACC CAAATGANTT ATCATCACAG AACTTATAAA AANCACTGTC TANTATAGCA
601 NACTCATAGC ANTATAGCTC TACTAACCTT CTTATCCGCC TATNANNANT ATACAATTCA
661 CACATNNCAA A

B 18.2: Sequencing alignment of cDNA subclone **AB17#16** with **mouse mitochondrion** by BLAST searching against the National Center for Biotechnology Information database

AB17#16 : 135 tgcacataggacttattcttcttacatgacaaaaaattgctcccctatcaattttaattc 194
Mouse mitochondrion: 4284 tgcacataggacttattcttcttacatgacaaaaaattgctcccctatcaattttaattc 4343
AB17#16 : 195 aaattttaccgctactcaactctactatcatTTTTaatactagcaattacttctatTTTca 254
Mouse mitochondrion: 4344 aaattttaccgctactcaactctactatcatTTTTaatactagcaattacttctatTTTca 4403
AB17#16 : 255 taggggcatgaggaggacttaaccaaacacaaatacgaaaaattatagcctattcatcaa 314
Mouse mitochondrion: 4404 taggggcatgaggaggacttaaccaaacacaaatacgaaaaattatagcctattcatcaa 4463
AB17#16 : 315 ttgcccacataggatgaatattagcaattcttnccttacaacccatccctcactctactc 374
Mouse mitochondrion: 4464 ttgcccacataggatgaatattagcaattctt-ccttacaacccatccctcactctactc 4522
AB17#16 : 375 aacctcataatctatattattcttacagcccctatattcatagcacttataactaaataac 434
Mouse mitochondrion: 4523 aacctcataatctatattattcttacagcccctatattcatagcacttataactaaataac 4582
AB17#16 : 435 tctataaccatcaactcaatctcacttctatgaaataaaaactccagcaataactata 494
Mouse mitochondrion: 4583 tctataaccatcaactcaatctcacttctatgaaataaaaactccagcaataactata 4642
AB17#16 : 495 atctcactgatattactatcnc tangaggcctnnccaccactancangattctnaccctaaa 554
Mouse mitochondrion: 4643 atctcactgatattactatccctaggaggccttccaccactaacaggattcttaccctaaa 4702
AB17#16 : 555 tgan ttatcatcacagaacttataaaaaanc-actgtct-antatagc-anactcatagca 611
Mouse mitochondrion: 4703 tgaattatcatcacagaacttataaaaaacaactgtctaattatagcaacactcatagca 4762
AB17#16 : 612 nt-atagctctactaa 626
Mouse mitochondrion: 4763 ataatagctctactaa 4778

B 18.3: Summary of sequence alignment of cDNA subclone AB17#16 with mouse mitochondrion

FluoroDD gel AB (AP3 + ARP3)					Subclone I.D.	Sequencing				
Fragment no.	PPARα (+/+)		PPARα (-/-)			FluoroDD fragment size (bp)	Size of insert after <i>Eco</i> RI cut (bp)	Primer	Gene homology to Blast search (Transcript size)	E-value (% Identity)
	CTL	Wy	CTL	Wy						
AB17	+	++	+	+	620	AB17#16	650	M13 reverse	<i>Mus musculus</i> clone LA9 mitochondrion, complete genome (16300 bp)	0 478/496 (96%)

Appendix B. DNA sequences and sequencing alignments of FluoroDD fragments

B 19.1: DNA sequence of cDNA subclone **AB18#4** (AP3 & ARP3) using **M13 forward (-20) primer**

1 TATACGACTC ACTATAGGGC GAATTGGGCC CTCTAGATGC ATGCTCGNAG CGGCCGCCAG
61 TGTGATGGAT ATCTGCAGAA TTCGGCTTAG CGGATA**ACAA** **TTTCACACAG** **GAGACCATTG** ARP3
121 **CACATAGGAC** TTATTCTTCT TACATGACAA AAAATTGCTC CCCTATCAAT TTTAATTCAA
181 ATTTACCCGC TACTCAACTC TACTATCATT TTAATACTAG CAATTACTTC TATTTTCATA
241 GGGGCATGAG GAGGACTTAA CCAAACACAA ATACGAAAAA TTATAGCCTA TTCATCAATT
301 GCCCACATAG GATGAATATT AGCAATTCTT CCTTACAACC CATCCCTCAC TCTACTCAAC
361 CTCATAATCT ATATTATTCT TACAGCCCTT ATATTCATAG CACTTATACT AAATAACTCT
421 ATAACCATCA ACTCAATCTC ACTTCTATGA AATAAACTC CAGCAATACT AACTATAATC
481 TCACTGATAT TACTATCCCT ANGANGCCTC CACCACTAAC AGGATNCTNA CCAANATGAA
541 TTATCATCAC AGAACTNATA AAAAACNACT GCCTAATTAT AGCANACTCA TAGCCATANT
601 AGCTCTCTAA NCTATTCTTT ATACTCNNNT ANTTATTCAC TNNNCTANNN NATNNCCACC
661 CACAATACCC AAAANAANN

B 19.2: Sequencing alignment of cDNA subclone **AB18#4** with **mouse mitochondrion** by BLAST searching against the National Center for Biotechnology Information database

AB18#4 : 119 tgcacataggacttattcttcttacatgacaaaaaattgctcccctatcaattttaattc 178
Mouse mitochondrion: 4284 tgcacataggacttattcttcttacatgacaaaaaattgctcccctatcaattttaattc 4343
AB18#4 : 179 aaatttaccgcgctactcaactctactatcattttaataactagcaattacttctattttca 238
Mouse mitochondrion: 4344 aaatttaccgcgctactcaactctactatcattttaataactagcaattacttctattttca 4403
AB18#4 : 239 taggggcatgaggaggacttaaccaaacacaaatacgaataattatagcctattcatcaa 298
Mouse mitochondrion: 4404 taggggcatgaggaggacttaaccaaacacaaatacgaataattatagcctattcatcaa 4463
AB18#4 : 299 ttgccacataggatgaatattagcaattcttccttacaacccatccctcactctactca 358
Mouse mitochondrion: 4464 ttgccacataggatgaatattagcaattcttccttacaacccatccctcactctactca 4523
AB18#4 : 359 acctcataatctatattattcttacagcccctatattcatagcacttataactaaataact 418
Mouse mitochondrion: 4524 acctcataatctatattattcttacagcccctatattcatagcacttataactaaataact 4583
AB18#4 : 419 ctataaccatcaactcaatctcacttctatgaaataaaaactccagcaataactaactataa 478
Mouse mitochondrion: 4584 ctataaccatcaactcaatctcacttctatgaaataaaaactccagcaataactaactataa 4643
AB18#4 : 479 tctcactgatattactatccctangangcc-tccaccactaacaggatnctnacnaanat 537
Mouse mitochondrion: 4644 tctcactgatattactatccctaggaggccttcaccactaacaggattcttaccaaaat 4703
AB18#4 : 538 gaattatcatcacagaactnataaaaaacnactgcctaattatagc-anactcatagcca 596
Mouse mitochondrion: 4704 gaattatcatcacagaacttataaaaaacaactgtctaattatagcaacactcatagcaa 4763
AB18#4 : 597 tantagctct 606
Mouse mitochondrion: 4764 taatagctct 4773

B 19.3: Summary of sequence alignment of cDNA subclone **AB18#4** with **mouse mitochondrion**

FluoroDD gel AB (AP3 + ARP3)					Subclone I.D.	Sequencing				
Fragment no.	PPARα (+/+)		PPARα (-/-)			FluoroDD fragment size (bp)	Size of insert after <i>Eco</i> RI cut (bp)	Primer	Gene homology to Blast search (Transcript size)	E-value (% Identity)
	CTL	Wy	CTL	Wy						
AB18	+	++	+	+	595	AB18#4	655	M13 forward (-20)	<i>Mus musculus</i> clone LA9 mitochondrion, complete genome (16300 bp)	0 477/490 (97%)

Appendix B. DNA sequences and sequencing alignments of FluoroDD fragments

B 20.1: DNA sequence of cDNA subclone **AB18#4** (AP3 & ARP3) using **M13 reverse primer**

1 NGCCAAGCTT GNGTACCGAG CTCGGATCCA CTAGTAACGG CCGCCAGTGT GCTGGAATTC
61 GGCTNGTAAT **ACGACTCACT ATAGGGCTTT TTTTTTTT****G** GGTATTGTT GGTTGGAAAT **AP3**
121 ATTGTTAGTG AAGTGAATA AATTAGGCGA GTATAAAGA ATAGGTTTAG TAGAGCTATT
181 ATTGCTATGA GTGTTGCTAT AATTAGGCAG TTGTTTTTTA TAAGTTCTGT GATGATAATT
241 CATTTTGGTA AGAATCCTGT TAGTGGTGGA AGGCCTCCTA GGGATAGTAA TATCAGTGAG
301 ATTATAGTTA GTATTGCTGG AGTTTTATTT CATAGAAGTG AGATTGAGTT GATGGTTATA
361 GAGTTATTTA GTATAAGTGC TATGAATATA GGGGCTGTAA GAATAATATA GATTATGAGG
421 TTGAGTAGAG TGAGGGATGG GTTGTAAGGA AGAATNGCTA ATATTCATCC TATGTGGGCA
481 ATTGATGAAT ANGCTATAAT NTNTCGTATN TGTGTTTGGT NAAGTCCTCC TCATGCCCCCT
541 ATGAAAATAG AAGTAATTGC TAGTATNAAA ATGATAGTAG AGTTGAGTAG CNGGTAAATT
601 TGAATTAAAT TGATANNGGA GCANTTTTGT TCATGTAGAG ATAGTCTATG TGCATGTCTC
661 GTGTAATGTA TCGTAGCGAT CGCNAT

B 20.2: Sequencing alignment of cDNA subclone **AB18#4** with **mouse mitochondrion** by BLAST searching against the National Center for Biotechnology Information database

AB18#4 : 102 gttattggtggttggaatatattgtagtggaagtggaataaattagcgaggtataaaagaa 161
Mouse mitochondrion: 4843 gttattggtggttggaatatattgtagtggaagtggaataaattagcgaggtataaaagaa 4784
AB18#4 : 162 taggttttagtagagctattattgctatgagtggtgctataaattagcgaggtgttttttat 221
Mouse mitochondrion: 4783 taggttttagtagagctattattgctatgagtggtgctataaattagcgaggtgttttttat 4724
AB18#4 : 222 aagttctgtgatgataaattcatttttggaagaatcctgtagtggtggaaggcctcctag 281
Mouse mitochondrion: 4723 aagttctgtgatgataaattcatttttggaagaatcctgtagtggtggaaggcctcctag 4664
AB18#4 : 282 ggatagtaatatcagtgagattatagttagtagtattgctggagttttatttcatagaagtga 341
Mouse mitochondrion: 4663 ggatagtaatatcagtgagattatagttagtagtattgctggagttttatttcatagaagtga 4604
AB18#4 : 342 gattgagttgatggttatagagttatttagtataagtgctatgaatataggggctgtaag 401
Mouse mitochondrion: 4603 gattgagttgatggttatagagttatttagtataagtgctatgaatataggggctgtaag 4544
AB18#4 : 402 aataatatagattatgaggttgagtagagtgagggatgggttgtaaggaagaatngctaa 461
Mouse mitochondrion: 4543 aataatatagattatgaggttgagtagagtgagggatgggttgtaaggaagaatngctaa 4484
AB18#4 : 462 tattcatcctatgtgggcaattgatgaatangctataatntnctgatntgtgtttggt 521
Mouse mitochondrion: 4483 tattcatcctatgtgggcaattgatgaatangctataatntnctgatntgtgtttggt 4424
AB18#4 : 522 aagtcctcctcatgccctatgaaaatagaagtaattgctagtatnaaaatgatagtaga 581
Mouse mitochondrion: 4423 aagtcctcctcatgccctatgaaaatagaagtaattgctagtatnaaaatgatagtaga 4364
AB18#4 : 582 gttgagtagcnggtaaatttgaatt-aaattgatannggagc-antttttgtcatgta 637
Mouse mitochondrion: 4363 gttgagtagcnggtaaatttgaattaaattgtaggggagcaattttttgtcatgta 4306

B 20.3: Summary of sequence alignment of cDNA subclone **AB18#4** with **mouse mitochondrion**

FluoroDD gel AB (AP3 + ARP3)					Subclone I.D.	Sequencing				
Fragment no.	PPARα (+/+)		PPARα (-/-)			FluoroDD fragment size (bp)	Size of insert after <i>EcoRI</i> cut (bp)	Primer	Gene homology to Blast search (Transcript size)	E-value (% Identity)
	CTL	Wy	CTL	Wy						
AB18	+	++	+	+	595	AB18#4	655	M13 reverse	<i>Mus musculus</i> clone LA9 mitochondrion, complete genome (16300 bp)	0 524/538 (97%)

Appendix B. DNA sequences and sequencing alignments of FluoroDD fragments

B 21.1: DNA sequence of cDNA subclone AB19#2 (AP3 & ARP3) using M13 forward (-20) primer

1 TGGGCCCTCT AGATGCATGC TCGAGCGGCC GCCAGTGTGA TGGATATCTG CAGAATTCGC
61 CCTTGTATAC **GACTCACTAT AGGGCTTTTT TTTTTTTGGG** TGAATAAAT TAGGCGAGTA **AP3**
121 TAAAAGAATA GGTTTAGTAG AGCTATTATT GCTATGAGTG TTGCTATAAT TAGACAGTTG
181 TTTTTTATAA GTTCTGTGAT GATAATTCAT TTTGGTAAGA ATCCTGTTAG TGGTGAAGG
241 CCTCCTAGGG ATAGTAATAT CAGTGAGATT ATAGTTAGTA TTGCTGGAGT TTTATTTTCAT
301 AGAAGTGAGA TTGAGTTGAT GGTTATAGAG TTATTTAGTA TAAGTGCTAT GAATATAGGG
361 GCTGTAAGAA TAATATAGAT TATGAGGTTG AGTAGAGTGA GGGATGGGTT GTAAGGAAGA
421 ATNGCTAATA TTCATCCTAT GTGGGCAATT GATGAATAGG CTATAATTTT TCGTATNTGT
481 GTNNNGGTTA AGTCCTCCTC ATGCCCTAT GAAAATAGAA GTAATTGCTA GTATTAAAAT
541 GATAGTAGAG TTGAGTAGCG GGTAAATTTG AATTAAAATT GATANGGGAG CAATTTTTTTG
601 TCATGTAAGA AGAATAAGTC CTATGTGCAA TGGTCTNCTG TGTGAANTNG TNATCCGCTA
661 AGGGCGAATN CCAGCACACT GGCGNCCGTA ACTAGTGGAT CGAGCTCNGT ACCANGCCTG
721 ATGCATAGCN TGANNNTTCT ATAGTGTNAN CTAATA

B 21.2: Sequencing alignment of cDNA subclone AB19#2 with mouse mitochondrion by BLAST searching against the National Center for Biotechnology Information database

AB19#2 : 100 gtggaataaattaggcgagtataaaagaatagggttagtagagctattattgctatgagt 159
Mouse mitochondrion: 4812 gtggaataaattaggcgagtataaaagaatagggttagtagagctattattgctatgagt 4753
AB19#2 : 160 gttgctataaattagacagttgttttttataagttctgtgatgataaattcatttttggttaag 219
Mouse mitochondrion: 4752 gttgctataaattagacagttgttttttataagttctgtgatgataaattcatttttggttaag 4693
AB19#2 : 220 aatcctgttagtggtggaaggcctcctagggatagtaatatcagtgagattatagttagt 279
Mouse mitochondrion: 4692 aatcctgttagtggtggaaggcctcctagggatagtaatatcagtgagattatagttagt 4633
AB19#2 : 280 attgctggagttttatttcatagaagttagattgagttgatggttatagagttatttagt 339
Mouse mitochondrion: 4632 attgctggagttttatttcatagaagttagattgagttgatggttatagagttatttagt 4573
AB19#2 : 340 ataagtgcctatgaatataggggctgtaagaataatatagattatgaggttgagtagagtg 399
Mouse mitochondrion: 4572 ataagtgcctatgaatataggggctgtaagaataatatagattatgaggttgagtagagtg 4513
AB19#2 : 400 agggatgggttgtaaggaagaatngctaataattcatcctatgtgggcaattgatgaatag 459
Mouse mitochondrion: 4512 agggatgggttgtaaggaagaatngctaataattcatcctatgtgggcaattgatgaatag 4453
AB19#2 : 460 gctataatttttcgtatntgtgtnnnggttaagtcctcctcatgccctatgaaaataga 519
Mouse mitochondrion: 4452 gctataatttttcgtatntgtgt-ttgggttaagtcctcctcatgccctatgaaaataga 4394
AB19#2 : 520 agtaattgctagtattaaaatgatagtagagttgagtagcgggtaaatattgaattaaaat 579
Mouse mitochondrion: 4393 agtaattgctagtattaaaatgatagtagagttgagtagcgggtaaatattgaattaaaat 4334
AB19#2 : 580 tgatangggagcaattttttgtcatgtaagaagaataagtcctatgtgca 629
Mouse mitochondrion: 4333 tgataggggagcaattttttgtcatgtaagaagaataagtcctatgtgca 4284

B 21.3: Summary of sequence alignment of cDNA subclone AB19#2 with mouse mitochondrion

FluoroDD gel AB (AP3 + ARP3)					Subclone I.D.	Sequencing				
Fragment no.	PPARα (+/+)		PPARα (-/-)			FluoroDD fragment size (bp)	Size of insert after <i>EcoRI</i> cut (bp)	Primer	Gene homology to Blast search (Transcript size)	E-value (% Identity)
	CTL	Wy	CTL	Wy						
AB19	-	+	-	-	575	AB19#2	620	M13 forward (-20)	<i>Mus musculus</i> clone LA9 mitochondrion, complete genome (16300 bp)	0 523/530 (98%)

Appendix B. DNA sequences and sequencing alignments of FluoroDD fragments

B 22.1: DNA sequence of cDNA subclone AB19#10 (AP3 & ARP3) using M13 reverse primer

1 TAGANTACTC AAGCTATGCA TCAAGCTTGG TACCGAGCTC GGATCCACTA GTAACGGCCG
61 CCAGTGTGCT GGAATTCGCC CTTAGCGGAT **AACAATTTCACACAGGAGAC CATTGCACAT** ARP3
121 AGGACTTATT CTTCTTACAT GACAAAAAAT TGCTCCCCTA TCAATTTTAA TTCAAATTTA
181 CCCGCTACTC AACTCTACTA TCATTTTAAT ACTAGCAATT ACTTCTATTT TCATAGGGGC
241 ATGAGGAGGA CTTAACCAAA CACAAATACG AAAAATTATA GCCTATTCAT CAATTGCCCA
301 CATAGGATGA ATATTAGCAA TTCTTCCTTA CAACCCATCC CTCACTCTAC TCAACCTCAT
361 AATCTATATT ATTCTTACAG CCCCTATATT CATAGCACTT ATACTAAATA ACTCTATAAC
421 CATCAACTCA ATCTCACTTC TATGGAATAA AACTCCAGCA ATACTAACTA TAATCTCACT
481 GATATTACTA TCCCTAGGAG GCCTTCCACC ACTAACAGGA TTCTTACCAA AATGAATTAT
541 CATCACAGAA CTTATAAAAA ACAACTGTCT AATTATAGCA ACACTCATAG CAATAATAGC
601 TCTACTAAAC CTATTCTTTN ATACTCGCCC CAAAAAATAA AAGCCCTATA GTGAGTCGTA
661 TNACAAGGGC GAATTCTGCA GATATCATCA CACTGNCGGG CGCTCGAGCA TGCATNNANA
721 GGCCNCATTT CNCCNTATAG TGAGNTTGTA TNACNATNCA CNGCCNGNTG NTNAACANCG
781 GTGTGACNNG NNAACNNNGC C

B 22.2: Sequencing alignment of cDNA subclone AB19#10 with **mouse mitochondrion** by BLAST searching against the National Center for Biotechnology Information database

AB19#10 : 114 tgcacataggacttattcttcttacatgacaaaaattgctcccctatcaattttaattc 173
Mouse mitochondrion: 4284 tgcacataggacttattcttcttacatgacaaaaattgctcccctatcaattttaattc 4343
AB19#10 : 174 aaattttaccgcgtactcaactctactatcatttttaatactagcaattacttctattttca 233
Mouse mitochondrion: 4344 aaattttaccgcgtactcaactctactatcatttttaatactagcaattacttctattttca 4403
AB19#10 : 234 taggggcatgaggaggacttaaccaaacacaaatagcaaaaattatagcctattcatcaa 293
Mouse mitochondrion: 4404 taggggcatgaggaggacttaaccaaacacaaatagcaaaaattatagcctattcatcaa 4463
AB19#10 : 294 ttgccccacataggatgaatattagcaattcttcttacaacccatccctcactctactca 353
Mouse mitochondrion: 4464 ttgccccacataggatgaatattagcaattcttcttacaacccatccctcactctactca 4523
AB19#10 : 354 acctcataatctatattatttcttacagcccctatattcatagcacttataactaaataact 413
Mouse mitochondrion: 4524 acctcataatctatattatttcttacagcccctatattcatagcacttataactaaataact 4583
AB19#10 : 414 ctataaccatcaactcaatctcacttctatggaataaaaactccagcaataactataactaa 473
Mouse mitochondrion: 4584 ctataaccatcaactcaatctcacttctatggaataaaaactccagcaataactataactaa 4643
AB19#10 : 474 tctcactgatattactatccctaggaggccttcaccactaacaggattcttaccaaaat 533
Mouse mitochondrion: 4644 tctcactgatattactatccctaggaggccttcaccactaacaggattcttaccaaaat 4703
AB19#10 : 534 gaattatcatcacagaacttataaaaaacaactgtctaattatagcaaacactcatagcaa 593
Mouse mitochondrion: 4704 gaattatcatcacagaacttataaaaaacaactgtctaattatagcaaacactcatagcaa 4763
AB19#10 : 594 taatagctctactaaacctattcttttatactcgcc 629
Mouse mitochondrion: 4764 taatagctctactaaacctattcttttatactcgcc 4799

B 22.3: Summary of sequence alignment of cDNA subclone AB19#10 with mouse mitochondrion

FluoroDD gel AB (AP3 + ARP3)					Subclone I.D.	Sequencing				
Fragment no.	PPARα (+/+)		PPARα (-/-)			FluoroDD fragment size (bp)	Size of insert after <i>Eco</i> RI cut (bp)	Primer	Gene homology to Blast search (Transcript size)	E-value (% Identity)
	CTL	Wy	CTL	Wy						
AB19	-	+	-	-	575	AB19#10	610	M13 reverse	<i>Mus musculus</i> clone LA9 mitochondrion, complete genome (16300 bp)	0 513/516 (99%)

Appendix B. DNA sequences and sequencing alignments of FluoroDD fragments

B 23.1: DNA sequence of cDNA subclone AB22#9 (AP3 & ARP3) using M13 forward (-20) primer

1 CANTTGGGCC CTCTAGATGC NTGCTCGAGC GGCCGCCAGT GTGATGGATA TCTGCAGAAT
61 TCGCCCTTGT AAT**ACGACTC ACTATAGGGC TTTTTTTTC TTGG**CACTAC CAGAGTCAGG **AP3***
121 TTTATTAGAG AAGAGGGGCT TGGGGGAAC TGGAGGGCTGA GGGGCCCTGC CCAGAGCAGC
181 AGAGCACAGC ACATGGCCCT CTGCCCCAGC TCCCTCATGG CTGTCAGCCC CAACTGTAGA
241 AATAGATTTT CTGCCAGGAG GGCAAGTAGT CCATGAGCGG CCTTGCCACC AGACCCACGC
301 CAGGGATGTG GTCTGTAAGC AGCTGGAGCA GGAAGAGGAT CTTGGCTTCA GAGAAGCGGT
361 NATAAGAACC GGTGAGCGTA GCAGGTANTA TAGCAGCAGG ATTGTGCGAC CGCCTCAGTT
421 CTAGCCGCTC CCTCCGGGTC AAGTTCTTCC TGTNCNTCAG GAANACTCAG GCTATTNTA
481 TTTACCACAC CANANNGTTN NCCAGGGTGT NNNACGATCG CTGACCCCTC AAGCNANCTG
541 ACCNAGTGCA CAGGGGGCCNN GGCGATGTAC AAAANANTTG CCATGGTTTT CNTGTTGTNA
601 AAATTGTATC NGCTTANGGG NNANTNNGGG CNGCNTNNTN TGATCCACNN NNNNNTNNTN
661 ANTTTTNNT

B 23.2: Sequencing alignment of cDNA subclone **AB22#9** with **mouse peroxisome biogenesis factor 16 (Pex16)** by BLAST searching against the National Center for Biotechnology Information database

AB22#9 : 105 cactaccagagtcaggtttattagagaagaggggcttgggggaactggagggctgagggg 164
Mouse Pex16: 1196 cactaccagagtcaggtttattagagaagaggggcttgggggaactggagggctgagggg 1137
AB22#9 : 165 ccctgccagagcagcagagcacagcacatggccctctgccccagctccctcatggctgt 224
Mouse Pex16: 1136 ccctgccagagcagcagagcacagcacatggccctctgccccagctccctcatggctgt 1077
AB22#9 : 225 cagccccaaactgtagaaatagattttctgccaggagggcaagtagtccatgagcggcctt 284
Mouse Pex16: 1076 cagccccaaactgtagaaatagattttctgccaggagggcaagtagtccatgagcggcctt 1017
AB22#9 : 285 gccaccagacccacgccagggatgtggtctgtaagcagctggagcaggaagaggatcctt 344
Mouse Pex16: 1016 gccaccagacccacgccagggatgtggtctgtaagcagctggagcaggaagaggatcctt 957
AB22#9 : 345 gcttcagagaagcggtcataaagaacccggtgagcgtagcaggtantatagcagcaggattg 404
Mouse Pex16: 956 gcttcagagaagcggtcat-agaa-cggtgagcgtagcaggtagtatagcagcaggattg 899
AB22#9 : 405 tgcgaccgcctcagttctagccgctccctcgggtcaagttcttctgtncntcaggaan 464
Mouse Pex16: 898 tgcga-cgcctcagttctagccgctccctcgggtcaagttcttctgtcactcagg-ag 841
AB22#9 : 465 actcaggctattcntatattaccacaccananngttnnccagggtgtnnnacgatcgctga 524
Mouse Pex16: 840 actcaggctagtcatatctaccacaccagacag-tagccagggtgt-ccacgatcgctga 783
AB22#9 : 525 cccctaagc 534
Mouse Pex16: 782 ccccataagc 773

B 23.3: Summary of sequence alignment of cDNA subclone AB22#9 with mouse Pex16

FluoroDD gel AB (AP3 + ARP3)					Subclone I.D.	Sequencing				
Fragment no.	PPARα (+/+)		PPARα (-/-)			FluoroDD fragment size (bp)	Size of insert after <i>Eco</i> RI cut (bp)	Primer	Gene homology to Blast search (Transcript size)	E-value (% Identity)
	CTL	Wy	CTL	Wy						
AB22	+	++	+	+	530	AB22#9	580	M13 forward (-20)	<i>Mus musculus</i> peroxisome biogenesis factor 16 (Pex16) (1221 bp)	e-178 405/430 (94%)

* Sequence of primer was not completely matched with the expected sequence.

Appendix B. DNA sequences and sequencing alignments of FluoroDD fragments

B 24.1: DNA sequence of cDNA subclone AB22#9 (AP3 & ARP3) using M13 reverse primer

1 AATACTCAAG CTATGCATCA AGCTTGGTAC CGAGCTCGGA TCCACTAGTA ACGGCCGCCA
61 GTGTGCTGGA ATTCGCCCTT AGCGGATAAC **AATTTACAC** **AGGAGACCAT** **TGCAGAGTCT** ARP3
121 TTGTACATCG CCCGGCCCCT GCTGCACTTG CTCAGCCTGG GCTTATGGGG TCAGCGATCG
181 TGGACACCCT GGCTACTGTC TGGTGTGGTA GATATGACTA GCCTGAGTCT CCTGAGTGAC
241 AGGAAGAACT TGACCCGGAG GGAGCGGCTA GAAGTGAGGC GTCGCACAAT CCTGCTGCTA
301 TACTACCTGC TACGCTCACC GTTCTATGAC CGCTTCTCTG AAGCCAAGAT CCTCTTCCTG
361 CTCCAGCTGC TTACAGACCA CATCCCTGGC GTGGGTCTGG TGGCAAGGCC GCTCATGGAC
421 TACTTGCCCT CCTGGCAGAA AATCTATTTT TACAGTTGGG GCTGACAGCC ATGAGGGAGC
481 TGGGGCAGAG GGCCATGTGC TGTGCTCTGC TGCTCTGGGC AGGGCCCCCTC AGCCCTCCAG
541 TTCCCCCAAG CCNCTCTTCT CTAATAAACC CTGACTCTGG TAGTGCCAAG ANAAAAAAG
601 CCCTATAGTG AGTNTTATNA CAAGNCGAA TTCTGCAAAT ATCCATCACA CTGGCGGCCG
661 CTCNANCCTG CATTTAGAGG GCCCNATCCC CCTATAGTGA GTNNTATNAC NNNNNCTGGC
721 CGTTTTTTAC ATCTTNTTGA CTGGAANCN CTGGGTTA

B 24.2: Sequencing alignment of cDNA subclone **AB22#9** with **mouse peroxisome biogenesis factor 16 (Pex16)** by BLAST searching against the National Center for Biotechnology Information database

AB22#9 : 100 caggagaccattgcagagtcctttgtacatcgcccgccctgctgcacttgctcagcctg 159
Mouse Pex16: 712 caggagaccattgcagagtcctttgtacatcgcccgccctgctgcacttgctcagcctg 771
AB22#9 : 160 ggcttatggggtcagcgatcgtggacaccctggctactgtctggtgtggtagatatgact 219
Mouse Pex16: 772 ggcttatggggtcagcgatcgtggacaccctggctactgtctggtgtggtagatatgact 831
AB22#9 : 220 agcctgagtcctcctgagtgacaggaagaacttgacccggaggagcggtagaactgagg 279
Mouse Pex16: 832 agcctgagtcctcctgagtgacaggaagaacttgacccagaggagcggtagaactgagg 891
AB22#9 : 280 cgtcgcacaaatcctgctgtatactacctgctacgctcaccgttctatgaccgcttctct 339
Mouse Pex16: 892 cgtcgcacaaatcctgctgtatactacctgctacgctcaccgttctatgaccgcttctct 951
AB22#9 : 340 gaagccaagatcctcttctgctccagctgcttacagaccacatccctggcgtgggtctg 399
Mouse Pex16: 952 gaagccaagatcctcttctgctccagctgcttacagaccacatccctggcgtgggtctg 1011
AB22#9 : 400 gtggcaaggccgctcatggactacttgccctcctggcagaaaatctatttctacagttgg 459
Mouse Pex16: 1012 gtggcaaggccgctcatggactacttgccctcctggcagaaaatctatttctacagttgg 1071
AB22#9 : 460 ggctgacagccatgagggagctggggcagagggccatgtgctgtgctctgctgctctggg 519
Mouse Pex16: 1072 ggctgacagccatgagggagctggggcagagggccatgtgctgtgctctgctgctctggg 1131
AB22#9 : 520 cagggccctcagccctccagttcccccaagcncctcttctctaataaacctgactctg 579
Mouse Pex16: 1132 cagggccctcagccctccagttcccccaagcncctcttctctaataaa-ctgactctg 1190
AB22#9 : 580 gtagtg 585
Mouse Pex16: 1191 gtagtg 1196

B 24.3: Summary of sequence alignment of cDNA subclone AB22#9 with mouse Pex16

FluoroDD gel AB (AP3 + ARP3)					Subclone I.D.	Sequencing			
Fragment no.	PPARα (+/+)		PPARα (-/-)			Size of insert after <i>Eco</i> RI cut (bp)	Primer	Gene homology to Blast search (Transcript size)	E-value (% Identity)
	CTL	Wy	CTL	Wy					
AB22	+	++	+	+	530	AB22#9	580	<i>Mus musculus</i> peroxisome biogenesis factor 16 (Pex16) (1221 bp)	0 482/486 (99%)

Appendix B. DNA sequences and sequencing alignments of FluoroDD fragments

B 25.1: DNA sequence of cDNA subclone **AB24#9** (AP3 & ARP3) using M13 forward (-20) primer

1 CCNCAACTAT AGGGCAATTG GGCCCTCTAG ATGCNTGCTC GAGCGGCCGC CAGTGTGATG
61 GATATCTGCA GAATTCGCCC TTAGCGGATA **ACAATTTTCAC ACAGGAGACC ATTGCACTGA** ARP3
121 CAGAGGAAGA TATATTTTAG AGGGAGACAC TTGTACCTTT CTCTCCCTTC AGTTATTAGA
181 CTCTTGGGAC AATGGACATC ATGAATTAAA ACGTTCTTAG AAATCACATG CTGGGAGAAA
241 ATTAACACTA AAATCTGGTA CCAGCCAGAG GAAGGAACTT GACTCAAAAT AAGAGATTTT
301 TAGATATTTT TGTCTGTCTC ATAGTTAAAA TTAATGTTCT CCTGCTTTCT GGCATATGCC
361 TCATCTTTTC TATGAAGTAG TAATACTGAT ACAGAAAGGT AGAGAGAAAT GAATAGTTTT
421 TGCTACTTTG GGCCAAACTG TGAAAAATC CATTTTATTT CACCAAAAAA AAAAAAGCCC
481 TATAGTGAGT CGTATTACAA GGGCGAATNC CAGCACACTG GCGGCCGTTA CTAGTGATC
541 CGAGCTCGGT ACCAAGCTNG ATGCATAGCT TGAGTATTCT ATAGTGTCAC CTAAATAGCT
601 TGGCGTAATC ATGGTAATAG CTGTTTCCTG TGTGAAATNG TNATCCGCTC ACNATTCCAC
661 ACAACATACG ANCCNGANCC NTAANGTGTA AAGCNTGGGG TGCCTAATGA GTGANCTACT
721 CACATANNTG CGTGCNCTAC TGCCGNNTCA GTNGGNAACT GTNTCNNCNG CNTATANNNC
781 CACCCGNGGA AGCGGTGNNT TGGCCCTTCC TTNNNTAAAT GNGCCGGTTT TGGGGGAG

B 25.2: Sequencing alignment of cDNA subclone **AB24#9** with **mouse Cyp4a14** by BLAST searching against the National Center for Biotechnology Information database

AB24#9 : 108 accattgcactgacagaggaagatatatttttagagggagacacttgtaacctttctctccc 167
Mouse Cyp4a14: 1823 accattgcactgacagaggaagatatatttttagagggagacacttgtaacctttctctccc 1882
AB24#9 : 168 ttcagttatttagactcttgggacaatggacatcatgaattaaaacgttctttagaaatcac 227
Mouse Cyp4a14: 1883 ttcagttatttagactcttgggacaatggacatcatgaattaaaacgttctttagaaatcac 1942
AB24#9 : 228 atgctgggagaaaaattaacactaaaatctggtaccagccagaggaaggaacttgactcaa 287
Mouse Cyp4a14: 1943 atgctgggagaaaaattaacactaaaatctggtaccagccagaggaaggaacttgactcaa 2002
AB24#9 : 288 aataagagattttttagatatcttctgtctgtctcatagttaaaattaatgtttctctgctt 347
Mouse Cyp4a14: 2003 aataagagattttttagatatcttctgtctgtctcatagttaaaattaatgtttctctgctt 2062
AB24#9 : 348 tctggcatatgcctcatcttttctatgaagtagtaataactgatacagaaaggtagagaga 407
Mouse Cyp4a14: 2063 tctggcatatgcctcatcttttctatgaagtagtaataactgatacagaaaggtagagaga 2122
AB24#9 : 408 aatgaatagtttttgctacttttgggccaaactgtgaaaaaatccattttattttca 462
Mouse Cyp4a14: 2123 aatgaatagtttttgctacttttgggccaaactgtgaaaaaatccattttattttca 2177

B 25.3: Summary of sequence alignment of cDNA subclone **AB24#9** with **mouse Cyp4a14**

FluoroDD gel AB (AP3 + ARP3)					Subclone I.D.	Sequencing				
Fragment no.	PPARα (+/+)		PPARα (-/-)			FluoroDD fragment size (bp)	Size of insert after <i>EcoRI</i> cut (bp)	Primer	Gene homology to Blast search (Transcript size)	E-value (% Identity)
	CTL	Wy	CTL	Wy						
AB24	-	+	-	-	420	AB24#9	460	M13 forward (-20)	<i>Mus musculus</i> cytochrome P450, family 4, subfamily a, polypeptide 14 (Cyp4a14) (2547 bp)	0 354/355 (99%)

Appendix B. DNA sequences and sequencing alignments of FluoroDD fragments

B 26.1: DNA sequence of cDNA subclone AB24#9 (AP3 & ARP3) using M13 reverse primer

1 AANNNTATTT AGGTGACACT ATAGAATACT CAAGCTATGC ATCAAGCTTG GTACCGAGCT
61 CGGATCCACT AGTAACGGCC GCCAGTGTGC TGGAAATTCGC CCTTGTAATA **CGACTCACTA** **AP3**
121 **TAGGGCTTTT TTTTTTTTGG** TGAAATAAAA TGGATTTTTT CACAGTTTGG CCCAAAGTAG
181 CAAAAACTAT TCATTTCTCT CTACCTTTCT GTATCAGTAT TACTACTTCA TAGAAAAGAT
241 GAGGCATATG CCAGAAAGCA GGAGAACATT AATTTTAACT ATGAGACAGA CAGAAATATC
301 TAAAAATCTC TTATTTTGAG TCAAGTTCCT TCCTCTGGCT GGTACCAGAT TTTAGTGTTA
361 ATTTTCTCCC AGCATGTGAT TTCTAAGAAC GTTTTAATTC ATGATGTCCC ATTGTCCCAA
421 GANTTATTAA TAACTGAAGG GAGAGAAAGG TACAAGTGTC TCCCCCTCTA AAATATATCC
481 TTCCCTCCTG TCAGTGCNAA TGGGTCTCCT GTGTGNAAAT TGTATCCGC TAAGGGCGAA
541 TTNTGCAGAT ATCCAATNNA AACAAAATAA AACAAACAAG CCNTGCNNTT TAGANNGGGC
601 CCAATTGGC CCNTATAGTT GANGTNGTAT TACAAATNNA NNTGGGCCGT TGTTTTNANN
661 ANNTNNNTGA ATGGNAAAAC CCTGGCNGTN ACNNNNNTNA ATGNCNNTNG NNGCNNNTTC
721 CCTTTTNNCN NCTGGGNTNN TANNAAAAAG NCCNCCCGAA TGCCTTTCCA ACANTTGGCC
781 NCCTGAATGN NNNTNGNCCN CCNNNTTNNN GCCNNTNNNN NNGNNGGTG NTTNNNNNTN
841 NNNT

B 26.2: Sequencing alignment of cDNA subclone AB24#9 with mouse Cyp4a14 by BLAST searching against the National Center for Biotechnology Information database

AB24#9 : 141 tgaaataaaatggattttttcacagtttggcccaaagtagcaaaaactattcatttctct 200
Mouse Cyp4a14: 2177 tgaaataaaatggattttttcacagtttggcccaaagtagcaaaaactattcatttctct 2118
AB24#9 : 201 ctacctttctgtatcagtattactacttcatagaaaagatgaggcatatgccagaaaagca 260
Mouse Cyp4a14: 2117 ctacctttctgtatcagtattactacttcatagaaaagatgaggcatatgccagaaaagca 2058
AB24#9 : 261 ggagaacattaatttttaactatgagacagacagaaatatctaaaaatctcttattttgag 320
Mouse Cyp4a14: 2057 ggaaaacattaatttttaactatgagacagacagaaatatctaaaaatctcttattttgag 1998
AB24#9 : 321 tcaagttccttcctctggctgggtaccagattttagtgtaattttctcccagcatgtgat 380
Mouse Cyp4a14: 1997 tcaagttccttcctctggctgggtaccagattttagtgtaattttctcccagcatgtgat 1938
AB24#9 : 381 ttctaagaacgtttttaattcatgatgtccattgtcccaaganttattaataactgaagg 440
Mouse Cyp4a14: 1937 ttctaagaacgtttttaattcatgatgtccattgtcccaagagt--ctaataactgaagg 1881
AB24#9 : 441 gagagaaaggtacaagtgtctccccctctaaaatatatc 479
Mouse Cyp4a14: 1880 gagagaaaggtacaagtgtct--ccctctaaaatatatc 1844

B 26.3: Summary of sequence alignment of cDNA subclone AB24#9 with mouse Cyp4a14

FluoroDD gel AB (AP3 + ARP3)					Subclone I.D.	Sequencing				
Fragment no.	PPARα (+/+)		PPARα (-/-)			Size of insert after <i>Eco</i> RI cut (bp)	Primer	Gene homology to Blast search (Transcript size)	E-value (% Identity)	
	CTL	Wy	CTL	Wy						
AB24	-	+	-	-	420	AB24#9	460	M13 reverse	<i>Mus musculus</i> cytochrome P450, family 4, subfamily a, polypeptide 14 (Cyp4a14) (2547 bp)	e-165 331/339 (97%)

Appendix B. DNA sequences and sequencing alignments of FluoroDD fragments

B 27.1: DNA sequence of cDNA subclone **AB25#6** (AP3 & ARP3) using **M13 forward (-20)** primer

1 AACTCACTCA TACGGGNCAN TCNGGGCCCN CTAGNATGCN TGCTCGAGCG GCCGCCAGTG
61 TGATGGATAT CTGCAGAAATN CNGCCCTTAG CGGATA**ACAA** **TTCTCACACA** **GGAGACCATT** ARP3
121 **GCA**CTGACAG AGGAAGATAT ATCCTNCAGA GGGAGACACT TGTACCTTTC TCTCCCTTCA
181 GTTATTANCA CTCTTGGGAC AATGGACATC ATGAATTAAA ACGTNCNTTA GAAATCACCA
241 TGCTGGGAGA AAATTAACCA CCTAAAATCT GGTACCCAGC CCAGCAGGNA AGGGAACCTG
301 CACCTCACAA ATAANGAGNA TTNNTTANCA TATTNCCTGT CNTGGTCTCA TAGTTAAAGT
361 TAATGTTTTT CCTGCCTTTC TGGGCATATG CCCCTCATCT TTTTCNTATN NAAGNTAANT
421 TAANTAACCT GNANTAACNA AGAAAAAGGG TTAAAAAGAA GNAAAAAATG NAANTTANGN
481 TTTTTTTTGGN CCNNNCTTTT NGGGGNCCCA AAANNNTGGT NAAAAAAAAT TCCATNTTTN
541 ATTTCTAACC AAAAAAAAAA AAAAGCCCCT ATNAGTGNAG CTCNNTTATT AAAAAGGGGG
601 CGAAAATNNC CCANCCCACC NCNTGGGGNC NNGGGGCNCG TTTAAANNNT AAANTTGGGG
661 NGATTCNCCC GGAAAAGNCN TCCCNNGNGG GTTNAACCNC NAAAAAACA ANCANAGAA
721 AATNTNTGNN CCNNTTNANN CCACCCCTTT GNGNNAAGNG TTTNATTTTT TCCTTTCNTT
781 TTTATNTNNG TTTNGTGTNT TNTTCANANN CNNTTTNAAN AAAANNNTTA TNNNGNCNNT
841 TTTNTGGGGG NGNNNGNNGN NTTNNNAAA TTTTTAAANT TNTGGGGGGN NTTTNCNNTT
901 TNNNTANNCC CTNNNNGGTT TTNTTNNCCN TTNGGTGTTG GTGTTNGAAN AAAATNTNTN
961 GGTTTTNNNN NN

B 27.2: Sequencing alignment of cDNA subclone **AB25#6** with **mouse Cyp4a14** by BLAST searching against the National Center for Biotechnology Information database

AB25#6 : 115 accattgcactgacagaggaagatatatcctncagagggagacacttgtagcttttctctc 174
Mouse Cyp4a14: 1823 accattgcactgacagaggaagatatat--ttagagggagacacttgtagcttttctctc 1880

AB25#6 : 175 ccttcagttattancactccttgggacaatggacatcatgaattaaaacgtncnttagaaa 234
Mouse Cyp4a14: 1881 ccttcagttattag-actccttgggacaatggacatcatgaattaaaacgttc-ttagaaa 1938

AB25#6 : 235 tcaccatgctgggagaaaattaaccacctaataatctggtacc 276
Mouse Cyp4a14: 1939 tca-catgctgggagaaaattaac--actaaaatctggtacc 1977

B 27.3: Summary of sequence alignment of cDNA subclone **AB25#6** with **mouse Cyp4a14**

FluoroDD gel AB (AP3 + ARP3)					Subclone I.D.	Sequencing				
Fragment no.	PPARα (+/+)		PPARα (-/-)			FluoroDD fragment size (bp)	Size of insert after <i>Eco</i> RI cut (bp)	Primer	Gene homology to Blast search (Transcript size)	E-value (% Identity)
	CTL	Wy	CTL	Wy						
AB25	-	+	-	-	405	AB25#6	450	M13 forward (-20)	<i>Mus musculus</i> cytochrome P450, family 4, subfamily a, polypeptide 14 (Cyp4a14) (2547 bp)	7e-47 150/162 (92%)

Appendix B. DNA sequences and sequencing alignments of FluoroDD fragments

B 28.1: DNA sequence of cDNA subclone AB26#17 (AP3 & ARP3) using M13 forward (-20) primer

1 TAATACGACT CACTATAGGG CGAATTGGGC CCTCTAGATG CATGCTCGAG CGGCCGCCAG
61 TGTGATGGAT ATCTGCAGAA TTCGGCTTAG CGGATAACAA **TTTCACACAG GAGACCATTG** ARP3
121 **CA**CTGACAGA GGAAGATATA TTTTAGAGGG AGACACTTGT ACCTTTCTCT CCCTTCAGTT
181 ATTAGACTCT TGGGACAATG GACATCATGA ATTAACACGT TCTTAGAAAT CACATGCTGG
241 GAGAAAATTA AACTAAAAT CTGGTACCAG CCAGAGGAAG GAACTTGACT CAAAATAAGA
301 GATTTTCTAG TATTTCTGTC TGTCTCATAG TTAAATTTAA TGTTTTCCTG CTTTCTGGCA
361 TATGCCTCAT CTTTCTATG AAGTAGTAAT ACTGATACAG AAAGGTAGAG AGAAATGAAT
421 AGTTTTTGCT ACTTTGGGCC AAAGTGTGAA AAAATNCATT TTATTTTACC AAAAAAAG
481 CCCTATAGTG AGTCGTATTA CAAGCNGAAT NCCAGCACAC TGGCGCCGT AACTAGTGNA
541 TNCGAGCTCN GTANCAAGCT GGGCGTAATC ATGGTCAAGC TGTTTCTGTG TGAANTGTAT
601 CGCTCNCANT CCCACAATA CGANCCGANC TAAGTGTAAG CNNNNNNGCTA TNNACTACTC
661 ATANTGNNCC CTACGCGNTC GTNGAACGG

B 28.2: Sequencing alignment of cDNA subclone AB26#17 with **mouse Cyp4a14** by BLAST searching against the National Center for Biotechnology Information database

AB26#17 : 114 accattgcactgacagaggaagatatatttttagagggagacacttgtacctttctctccc 173
Mouse Cyp4a14: 1823 accattgcactgacagaggaagatatatttttagagggagacacttgtacctttctctccc 1882

AB26#17 : 174 ttcagttatttagactcttgggacaatggacatcatgaattaaaacggttcttagaaatcac 233
Mouse Cyp4a14: 1883 ttcagttatttagactcttgggacaatggacatcatgaattaaaacggttcttagaaatcac 1942

AB26#17 : 234 atgctgggagaaaatttaacactaaaatctggtaccagccagaggaaggaacttgactcaa 293
Mouse Cyp4a14: 1943 atgctgggagaaaatttaacactaaaatctggtaccagccagaggaaggaacttgactcaa 2002

AB26#17 : 294 aataagagatttttagatatcttctgtctgtctcatagttaaaattaatgttttctgctt 353
Mouse Cyp4a14: 2003 aataagagatttttagatatcttctgtctgtctcatagttaaaattaatgttttctgctt 2062

AB26#17 : 354 tctggcatatgcctcatcttttctatgaagtagtaatactgatacagaaaggtagagaga 413
Mouse Cyp4a14: 2063 tctggcatatgcctcatcttttctatgaagtagtaatactgatacagaaaggtagagaga 2122

AB26#17 : 414 aatgaatagtttttgcacttttgggcccactgtgaaaaaatncattttatttca 468
Mouse Cyp4a14: 2123 aatgaatagtttttgcacttttgggcccactgtgaaaaaatccattttatttca 2177

B 28.3: Summary of sequence alignment of cDNA subclone AB26#17 with mouse Cyp4a14

FluoroDD gel AB (AP3 + ARP3)					Subclone I.D.	Sequencing				
Fragment no.	PPARα (+/+)		PPARα (-/-)			FluoroDD fragment size (bp)	Size of insert after <i>Eco</i> RI cut (bp)	Primer	Gene homology to Blast search (Transcript size)	E-value (% Identity)
	CTL	Wy	CTL	Wy						
AB26	-	+	-	-	390	AB26#17	450	M13 forward (-20)	<i>Mus musculus</i> cytochrome P450, family 4, subfamily a, polypeptide 14 (Cyp4a14) (2547 bp)	0 354/355 (99%)

Appendix B. DNA sequences and sequencing alignments of FluoroDD fragments

B 29.1: DNA sequence of cDNA subclone **AB26#30** (AP3 & ARP3) using **M13 reverse primer**

1 TACCAAGCTT GAGTACCGAG CTCNGATCCA CTAGTAACGG CCGCCAGTGT GCTGGAATTC
61 GGCTTGATAA **TACGACCCAC** **TATAGGGCTT** **TTTTTTTTTG** GTGAAATAAA ATGGATTTTT **AP3***
121 TCACAGTTTG GCCCAAAGTA GCAAAAAC TAACATTTCTC TCTACCTTTC TGTATCAGTA
181 TTACTACTTC ATAGAAAAGA TGAGGCATAT GCCAAAAGC AGGAAAACAT TAATTTTAAC
241 TATGAGACAG ACAGAAATAT CTAAAAATCT CTTATTTTGA GTCAAGTTCC TTCCTCTGGC
301 TGGTACCAGA TTTTAGTGTT AATTTTCTCC CAACATGTGA TTTCTAAGAA CGTTTTAATT
361 CATGATGTCC ATTGTCCCAA AGAGTCTAAT AACTGAAGGG AGAGAAAGGT ACAAGTGTCT
421 CCCTCTAAAA TATATCTTCC TCTGTCAGTG CAATGGTCTC CTGTGTGAAA TTGTNATCCG
481 CTAAGCCGAA TTCTGCAGAT ATNCATCACA CTGGCGGCCG CTCGAGCATG CATCTAGAGG
541 CCCAATNCGC NNTATAGTGA GTCGTATTAC AATTCAGTGC CNGTCGTNTN ACAACGTCGT
601 GACTGGNANA ACCCNGGCGT NANCCACCNT ANTCGCNTGC AGCNCANTCC CTTTTCGCNA
661 CTGNGTNNNA CGAGANGCNN NNGATNCCC TCCACAGTGC CNNCGTG

B 29.2: Sequencing alignment of cDNA subclone **AB26#30** with **mouse Cyp4a14** by BLAST searching against the National Center for Biotechnology Information database

AB26#30 : 102 tgaataaaaatggattttttcacagtttggcccaaagtagcaaaaactattcattttctct 161
Mouse Cyp4a14: 2177 tgaataaaaatggattttttcacagtttggcccaaagtagcaaaaactattcattttctct 2118
AB26#30 : 162 ctacctttctgtatcagattactacttcatagaaaagatgaggcatatgccaaaaagca 221
Mouse Cyp4a14: 2117 ctacctttctgtatcagattactacttcatagaaaagatgaggcatatgccagaaagca 2058
AB26#30 : 222 ggaaaacattaattttaactatgagacagacagaaatatctaaaaatctcttattttgag 281
Mouse Cyp4a14: 2057 ggaaaacattaattttaactatgagacagacagaaatatctaaaaatctcttattttgag 1998
AB26#30 : 282 tcaagttccttcctctggctggtaccagatttttagtggttaattttctcccaacatgtgat 341
Mouse Cyp4a14: 1997 tcaagttccttcctctggctggtaccagatttttagtggttaattttctccagcatgtgat 1938
AB26#30 : 342 ttctaagaacgttttaattcatgatgtccattgtcccaaagagtctaataactgaagggga 401
Mouse Cyp4a14: 1937 ttctaagaacgttttaattcatgatgtccattgtccc-aagagtctaataactgaagggga 1879
AB26#30 : 402 gagaaaggtacaagtgtctccctctaaaaatatatcttcctctgtcagtgcaatggt 457
Mouse Cyp4a14: 1878 gagaaaggtacaagtgtctccctctaaaaatatatcttcctctgtcagtgcaatggt 1823

B 29.3: Summary of sequence alignment of cDNA subclone **AB26#30** with **mouse Cyp4a14**

FluoroDD gel AB (AP3 + ARP3)					Subclone I.D.	Sequencing				
Fragment no.	PPARα (+/+)		PPARα (-/-)			FluoroDD fragment size (bp)	Size of insert after <i>Eco</i> RI cut (bp)	Primer	Gene homology to Blast search (Transcript size)	E-value (% Identity)
	CTL	Wy	CTL	Wy						
AB26	-	+	-	-	390	AB26#30	450	M13 reverse	<i>Mus musculus</i> cytochrome P450, family 4, subfamily a, polypeptide 14 (Cyp4a14) (2547 bp)	0 353/356 (99%)

* Sequence of primer was not completely matched with the expected sequence.

Appendix B. DNA sequences and sequencing alignments of FluoroDD fragments

B 30.1: DNA sequence of cDNA subclone AB29#7 (AP3 & ARP3) using M13 forward (-20) primer

1 NCNNTCACNT ATAGGGCGAA TTGGGCCCTC TAGATGCNTG CTCGAGCGGC CGCCAGTGTG
61 ATGGATATCT GCAGAATTCG CCCTTGTAAT **ACGACTCACT ATAGGGCTTT TTTTTTTTGG** **AP3***
121 GACAGGGTTT CTCGGTGCAG CCCTGGCTGT CCTGGAAGTC ACTGTGTAGA CCAGGCTGGC
181 CTCGAAGTCA GAGATCACCT GCCTCTGCCT CTGGACTGCT AAGATTAAAG GTGTACAACA
241 CCACCACCTG ATTAAATAGT TTAAACAAAC AAACAACAAC AACAAAAACC AGAAGAAAAAG
301 AGAGCTGGAG AGATGGCTCA GCAGTTAAGA GCACCAACTG CTCTTCCAGA GGTCTTGAGT
361 TCAATTCCCA GCAACCACAT GGTGGCTCCC AACCATCTGC AATGGTCTCC TGTGTGAAAT
421 GGTTATCCGC TAAGGGCGAA TTCCAGCACA CTGGCGGCCG TTAGTAGTGG ATCCGAGCTC
481 GGTACCAAGC TTGATGCATA GCTTGAGTAT NCTATAGTGT CACCTAAATA GCTTGGCGTA
541 ATCATGGTCA TAGCTGTTTC CTGTGTGAAA TTGTNATCCG CTCACAATTN CACACAACAT
601 ACGAGCCGGA AGCATAAAGT GTAAAGCCTG GGGTGCCTAA TGAGTGAGCT AACTCACATN
661 AATNGCGTNG CGCTCACTGC CCGCTTTCCA GTCNGGAAAC CTGTCGTGCA GCTGCATTAA
721 TGAATNNCCA CGCGCGGGAN NNCGGNNGCG TNTNGGCNCT CTCCNCTCCC GCTCCTGACT
781 GCTGCCTNNT GTTGGNNNNC NNN

B 30.2: Sequencing alignment of cDNA subclone AB29#7 with mouse catalase by BLAST searching against the National Center for Biotechnology Information database

AB29#7 : 439 aattccagcacactggcgccggttactagtggatccgagctcgggtaccaagct-tgatgc 497
Mouse catalase: 31 aattccagcacactggcgccggttactagtggatccgagctcgggtaccaaggtgtgatgc 90
AB29#7 : 498 atagcttgagtatnctatagtgtcacctaaatagcttggcgtaatcatgggtcatagctgt 557
Mouse catalase: 91 atagcttgagtattctatagtgtcacctaaatagcttggcgtaatcatgggtcatagctgt 150
AB29#7 : 558 ttcctgtgtgaaattgtatccgctcacaattncacacacatacagagccggaagcataa 617
Mouse catalase: 151 ttcctgtgtgaaattgtatccgctcacaattccacacacatacagagccggaagcataa 210
AB29#7 : 618 agtgtaaagcctgggggtgcctaataatgagttagcttaactcacatnaatngcgtnngcgctcac 677
Mouse catalase: 211 agtgtaaagcctgggggtgcctaataatgagttagctatttctcatnaatngcgtnngcgctcac 270
AB29#7 : 678 tgcccgcctttcca 690
Mouse catalase: 271 tgcccgcctttcca 283

B 30.3: Summary of sequence alignment of cDNA subclone AB29#7 with mouse catalase

FluoroDD gel AB (AP3 + ARP3)					Subclone I.D.	Sequencing				
Fragment no.	PPARα (+/+)		PPARα (-/-)			FluoroDD fragment size (bp)	Size of insert after <i>Eco</i> RI cut (bp)	Primer	Gene homology to Blast search (Transcript size)	E-value (% Identity)
	CTL	Wy	CTL	Wy						
AB29	-	+	-	-	335	AB29#7	380	M13 forward (-20)	if84a04.x1 Kaestner ngn3 - - subtracted <i>Mus musculus</i> cDNA 3' similar to SW:CATA_CAMJE Q59296 CATALASE (283 bp)	e-114 242/253 (95%)

* Sequence of primer was not completely matched with the expected sequence.

Appendix B. DNA sequences and sequencing alignments of FluoroDD fragments

B 31.1: DNA sequence of cDNA subclone AC1#1 (AP2 & ARP19) using M13 forward (-20) primer

1 ACCCTNACTA TAGGGCGAAT TGGGCCCTCT AGATGCATGC TCGAGCGGCC GCCAGTGTGA
61 TGGATATCTG CAGAATTCGC CCTTGTAATA **CGACTCACTA TAGGGCTTTT TTTTTTGCCC** AP2*
121 GGCCCATTC A TTCTTTATTC AGGTGGCATA AAAATCACTA CAAAACTTT ACAAAGAGT
181 CTTGGGAGCT AAAGGGTCCC TTCCTTGCCT CAGTCCCCAA GATTCTTGGC AGGGGAGGAC
241 AAGAGAGAGA AGAAGGAGGA AGACTCCTGG CAGTGTGGC ATCTCCAAAT ACCAGAGGGG
301 TGACTTGGGT GACAGGACAC AGGTNNGGGA CCTGAATGTC TTCAGCAAGG GACACTCTTG
361 TAGGGTAGGT CAGCCTCCAA CCATGAAGTA TAACACCCAA GGCCAGTCTA AGCTTGGGAG
421 ACCAACACTT GTCTCTCCTT TTCCCCACCC AGGGTGTCTG GAATATGTCT AAAGATGGCC
481 TCTCCAGCCT CTGCTTACAA ATGTGGAGGN NCCCTAAGTT AGGGACTTGC CTAACCTACC
541 TCTAGCCCAA ACTGTGTNCA CAAGTGCCAG CCCACAAAAG ATCACCCCCT GAGCCCCTTG
601 GGNAAGAAAT GAAGATTCCT CATGNCCTGC CNNNCCTCCA GGCCCCCACC CCCNCCTGGC
661 TGCNNANAAA ACNNGNTTNT ANNACTGNTG NATGGTTCNT TCCNGNTCCC ACCCTTATCC
721 CCCCAAAAGCN GGNTAAAAAA GAGTTNNAGG AGCNGAAAGN TGGTCAGGTN GACTAAGAT
781 TTNNTGNNGG NCNNTNNNNT GGGGGANNNG AATGGGNNNN

B 31.2: Sequencing alignment of cDNA subclone AC1#1 with **mouse serine (or cysteine) proteinase inhibitor (SPI)** by BLAST searching against the National Center for Biotechnology Information database

AC1#1 : 122 gcccattcattctttattcaggtggcataaaaaatcactacaaaaactttacaaaagagtc 181
Mouse SPI: 2166 gcccattcattctttattcaggtggcataaaaaatcactacaaaaactttacaaaagagtc 2107
AC1#1 : 182 ttgggagctaaagggtcccttccttgctcagtccccaagattcctggcaggggaggaca 241
Mouse SPI: 2106 ttgggagctaaagggtcccttccttgctcagtccccaagattcctggcaggggaggaca 2047
AC1#1 : 242 agagagagaagaaggaggaagactcctggcagtggtggcatctccaaataccagaggggt 301
Mouse SPI: 2046 agagagagaagaaggaggaagactcctggcagtggtggcatctccaaataccagaggggt 1987
AC1#1 : 302 gacttgggtgacaggacacaggtnggggacctgaatgtcttcagcaagggacactcttgt 361
Mouse SPI: 1986 gacttgggtgacaggacacaggttggggacctgaatgtcttcagcaagggacactcttgt 1927
AC1#1 : 362 agggtaggtcagcctccaacatgaagtataaacaccaaggccagtcctaagcttgggaga 421
Mouse SPI: 1926 agggtaggtcagcctccaacatgaagtataaca-ccaaggccagtcctaagcttgggaga 1868
AC1#1 : 422 ccaacacttgctctctccttttccccaccagggtgtctggaatatgtctaaagatggcct 481
Mouse SPI: 1867 ccaacacttgctctctcctttt-cccaccagggtgtctggaatatgtctaaagatggcct 1809
AC1#1 : 482 ctccagcctctgcttacaaatgtggaggnnccctaagttagggacttgccctaacctacct 541
Mouse SPI: 1808 ctccagcctctgcttacaaatgtggagggaccctaagttagggacttgccctaacctacct 1749
AC1#1 : 542 ctagcccaaaactgtgtncacaaagtccagcccaaaaagatcacccctgagccctctgg 601
Mouse SPI: 1748 ctagcccaaaactgtgtccacaaagtccagcccaaaaagatcacccctgagccctctgg 1689
AC1#1 : 602 gnaagaaatgaagattcccatg 624
Mouse SPI: 1688 g-aagaaatgaagattcccatg 1667

B 31.3: Summary of sequence alignment of cDNA subclone AC1#1 with mouse SPI

FluoroDD gel AC (AP2 + ARP19)						Subclone I.D.	Sequencing			
Fragment no.	PPARα (+/+)		PPARα (-/-)		FluoroDD fragment size (bp)		Size of insert after <i>Eco</i> RI cut (bp)	Primer	Gene homology to Blast search (Transcript size)	E-value (% Identity)
	CTL	Wy	CTL	Wy						
AC1	+	-	+	+	1800	AC1#1	1830	M13 forward (-20)	<i>Mus musculus</i> serine (or cysteine) proteinase inhibitor, clade F, member 2 (Serpinf2) (2187 bp)	0 495/503 (98%)

* Sequence of primer was not completely matched with the expected sequence.

Appendix B. DNA sequences and sequencing alignments of FluoroDD fragments

B 32.1: DNA sequence of cDNA subclone AC1#1 (AP2 & ARP19) using M13 reverse primer

1 CNTATTTAGG TGACACTATA GAATACTCAA GCTATGCATC CAAGCTTGGT ACCGAGCTCG
61 GATCCACTAG ATAACGGCCG CCAGTGTGCT GGAATTCCGC CCTTAGCGGA TA**ACAATTTC** ARP19
121 **ACACAGGATT TTGGCTCCCG** CATCTACTGA GCCATTCTA CCAGAACCTA GGCCCAGGGA
181 CAATCCGGCT GGCTGCCAGA ATATACCTGC AGAAAGGATT TCCCATCAA GACGATTTC
241 TGGCANGCCA CTCGGAACNG GCTCTTTGGT GCGAAGCCN GTGNNNNACC TGACTGGACA
301 AGCAGGACGG AAGACCTGGC GACNCNNTCN CNCAATGGGT GAAGGANGGC NNAGAGGGGA
361 CAGATTGANG GATTTCTNTC TGAGCCTGCC GGATNGCCCG TGCTGTTTNT CTCACGCATC
421 CTTNANGTTT NTGGAGGANN NGTTNGACCC NNNNTNNNNN ATNNNNNTGG CTGANNNGTN
481 TGTNGTGGNT GNTNNNNGTG GTNTTNTTNT GGGTCTGNTG NNNNNNTNG TGNNNNNNNN
541 NNNNTNNNN TGGTNNTNNN NTNNNTNNNT TNGTNNNNNN NTNNNNNNNN NNNGGTNNNN
601 NNN

B 32.2: Sequencing alignment of cDNA subclone AC1#1 with **mouse serine (or cysteine) proteinase inhibitor (SPI)** by BLAST searching against the National Center for Biotechnology Information database

AC1#1 : 121 acacaggattttggctcccgcatctactgagccatttctaccagaacctaggcccagggg 180
Mouse SPI: 439 acacaggatcctgcctcccgcatctactgagccatttctaccagaacctaggcccagggg 498

AC1#1 : 181 caatccggctggctgccagaatatacctgcagaaaggatttcccatcaaagacgatttcc 240
Mouse SPI: 499 caatccgactggctgccagaatatacctgcagaaaggatttcccatcaaagacgatttcc 558

AC1#1 : 241 tgg 243
Mouse SPI: 559 tgg 561

B 32.3: Summary of sequence alignment of cDNA subclone AC1#1 with mouse SPI

FluoroDD gel AC (AP2 + ARP19)					Subclone I.D.	Sequencing				
Fragment no.	PPARα (+/+)		PPARα (-/-)			Size of insert after <i>Eco</i> RI cut (bp)	Primer	Gene homology to Blast search (Transcript size)	E-value (% Identity)	
	CTL	Wy	CTL	Wy						
AC1	+	-	+	+	1800	AC1#1	1830	M13 reverse	<i>Mus musculus</i> serine (or cysteine) proteinase inhibitor, clade F, member 2 (Serpinf2) (2187 bp)	7e-52 119/123 (96%)

Appendix B. DNA sequences and sequencing alignments of FluoroDD fragments

B 33.1: DNA sequence of cDNA subclone AC1#2 (AP2& ARP19) using M13 forward (-20) primer

1 GGGCCCTCTA GATGCATGCT CGAGCGGCCG CCAGTGTGAT GGATATCTGC AGAATTTCGCC

61 CTTGTAATAC **GA**CTCACTAT **AG**GGCTTTTT **TT**TTGCTGTA GCATCAGGCA CGAGCCAGGC **AP2***

121 CAGCCTGTGT TTAATGGAAG GAACCCAATT CAGAAGGAAG GATGACATTT TAGGGTGGTC

181 ATTTATGTGT GGGATCTACC ACTTTTCCCA CAAAGATGGG GCTCTGAGTG TGTCTTCAA

241 ATATTATGAA AAGGAAAGGG TGGTCNAAGC GCAGGATAGG GGGCATAGAC ATAGGAACCA

301 TTTGTAAGAC TGTAAGTCTG GCAGCTTCTG TTCCTGTCTC ATCGATGGTC AGCACAGCCT

361 TATGCACAGC CCTGGCTGAG CTTTCCAGGG GAGCATTCTT CCCTCTGTGA TTCCGGAGAG

421 GTCAGCCCCC ATTGTTGAAG ATCCGGGTGA TGCCCCAGTN GGACTNATGA GTGTTTTNAA

481 GNNATATTCT CCAGAGATGG GACAGTCTGG GGAAGTTNGA TNNTGGGGGC TNCCCCTTTN

541 TGNGNCNTGN TNNNAGCNGG GAACNTTAAA ANNATGAAGC CTCNTTNGNN TGAAAAGTTT

601 TGGCTCCAAN ATGCTGCCTT TTTCCNNTNT TNNTTGGGGC CAAAANNGAA NNNCAGCACT

661 TGGGTTTNNN NTTGCNNTNN TTCCTTTTCC CCGCCAACCC ACCCTGNAAC GGCTTTCTGTG

721 ACCNTGGNTT CNNCNTTCNC CCCTTNCACC GAAAANGGTN NNNNNNNNNN NNNNNNNNNN

781 NNNN

B 33.2: Sequencing alignment of cDNA subclone AC1#2 with **mouse serine (or cysteine) proteinase inhibitor (SPI)** by BLAST searching against the National Center for Biotechnology Information database

AC1#2 : 95 gctgtagcatcaggcacgagccaggccagcctgtgtttaatggaaggaacccaattcaga 154

Mouse SPI: 1376 gctgtagcatcaggcacgagccaggccagcctgtgtttaatggaaggaacccaattcaga 1317

AC1#2 : 155 aggaaggatgacatttttaggggtggtcatttatgtgtgggatctaccacttttccacaaa 214

Mouse SPI: 1316 aggaaggatgacatttttaggggtggtcatttatgtgtgggatctaccacttttccacaaa 1257

AC1#2 : 215 gatggggctctgagtgtgttcttcaaataattatgaaaaggaaaggggtggtcnaagcgag 274

Mouse SPI: 1256 gatggggctctgagtgtgttcttcaaataattatgaaaaggaaaggggtggtcgaagcgag 1197

AC1#2 : 275 gatagggggcatagacataggaaccatttgaagactgtaactgctgcagcttctgttcc 334

Mouse SPI: 1196 gatagggggcatagacataggaaccatttgaagactgtaactgctgcagcttctgttcc 1137

AC1#2 : 335 tgtctcatcgatggtcagcacagccttatgcacagccctggctgagctttccaggggagc 394

Mouse SPI: 1136 tgtctcatcgatggtcagcacagccttatgcacag-cctggctgagctt--caggggagc 1080

AC1#2 : 395 attcntccctctgtgattccggagaggtcagccccattgttgaagatccgggtgatgcc 454

Mouse SPI: 1079 attct--cctctgtgattccggagaggtcag-ccccattgttgaagatccgggtgatg-c 1024

AC1#2 : 455 ccagtnggactnatgagtgttttnaagnnatattctccagagatgggacagtctggggaa 514

Mouse SPI: 1023 ccagt-ggactcatgagtgtcttcaagttatattctccagagat-ggacagtctggggaa 966

AC1#2 : 515 gt 516

Mouse SPI: 965 gt 964

B 33.3: Summary of sequence alignment of cDNA subclone AC1#2 with mouse SPI

FluoroDD gel AC (AP2 + ARP19)					Subclone I.D.	Sequencing				
Fragment no.	PPARα (+/+)		PPARα (-/-)			FluoroDD fragment size (bp)	Size of insert after <i>Eco</i> RI cut (bp)	Primer	Gene homology to Blast search (Transcript size)	E-value (% Identity)
	CTL	Wy	CTL	Wy						
AC1	+	-	+	+	1800	AC1#2	1600	M13 forward (-20)	<i>Mus musculus</i> serine (or cysteine) proteinase inhibitor clade A, member 1a (SPI) (1393 bp)	0 406/422 (96%)

* Sequence of primer was not completely matched with the expected sequence.

Appendix B. DNA sequences and sequencing alignments of FluoroDD fragments

B 34.1: DNA sequence of cDNA subclone AC1#2 (AP2& ARP19) using M13 reverse primer

1 GATACTCAAG CTATGCNTCA AGCTTGGTAC CGAGACTCGG ATCCACTAGT AACGGCCGCC
61 AGTGTGCTGG AATTCGCCCT TAGACGGATA ACAATTCAC ACAGGATTTT GGCTCCTACT ARP19
121 GCTTAAATAC AGACTAGGAC AGGGCTCTGT CTCCTCAGCC TCGGTCACCA CCCAGCTCTG
181 GGACAGCAAG CTGAAAATGA CTCCCTCCAT CTCATGGGGT CTA CTGCTTC TGGCAGGCCT
241 GTGTTGCCTG GTCCCCAGCT TTCTGGCTGA GGATGTTTCTG GAGACAGACA CCTCCCAGAA
301 GGATCAGTCC CCCAGCCTC CCATGAGATC GCCTACAAAC CCTGGGAGAC TTTGCAATCA
361 GCCTATACCG GGAGCTGGTC CATCAGTNCN AACACTTTCC AACCATNNTT CTTCTCCCN
421 AGTGAGCCAT NNGCNACACC CNTTGCNTA TGCTCTCCCT ANGGGANN CN AGGGTGACNN
481 TNCNNNCCGA TCTAAGGGCT GANTNNNNNN NNTNNNGTNN NNTNTNNNCT NNNNNNANNN
541 NCNNNNNNNT GGNTNNTNNN NNCNNTNNNN NNNNNNNNNN NN

B 34.2: Sequencing alignment of cDNA subclone AC1#2 with **mouse serine (or cysteine) proteinase inhibitor (SPI)** by BLAST searching against the National Center for Biotechnology Information database

AC1#2 : 147 ctgtctcctcagcctcggtcaccacccagctctgggacagcaagctgaaaatgactccct 206
Mouse SPI: 1 ctgtctcctcagcctcggtcaccacccagctctgggacagcaagctgaaaatgactccct 60
AC1#2 : 207 ccattctcatgggggtctactgcttctggcaggcctgtgttgctgctgggtccccagctttcttg 266
Mouse SPI: 61 ccattctcatgggggtctactgcttctggcaggcctgtgttgctgctgggtccccagctttcttg 120
AC1#2 : 267 ctgaggatgttcaggagacagacacctcccagaaggatcagtcccccagcctcccatga 326
Mouse SPI: 121 ctgaggatgttcaggagacagacacctcccagaaggatcagtc--ccccagcctcccatga 178
AC1#2 : 327 gatcgctacaaacctgggagactttgcaatcagcctataccgggagctgggtccatcag 386
Mouse SPI: 179 gatcg-ctacaaa-cctgggagactttgcaatcagcctataccgggagctgggtccatcag 236
AC1#2 : 387 t 387
Mouse SPI: 237 t 237

B 34.3: Summary of sequence alignment of cDNA subclone AC1#2 with mouse SPI

FluoroDD gel AC (AP2 + ARP19)					Subclone I.D.	Sequencing			
Fragment no.	PPARα (+/+)		PPARα (-/-)			Size of insert after <i>EcoRI</i> cut (bp)	Primer	Gene homology to Blast search (Transcript size)	E-value (% Identity)
	CTL	Wy	CTL	Wy					
AC1	+	-	+	+	1800	AC1#2	1600	<i>Mus musculus</i> serine (or cysteine) proteinase inhibitor clade A, member 1a (SPI) (1393 bp)	e-116 237/241 (98%)

Appendix B. DNA sequences and sequencing alignments of FluoroDD fragments

B 35.1: DNA sequence of cDNA subclone AC2#2 (AP2 & ARP19) using M13 reverse primer

1 ANGCTATTT AGGTGACNCT ATAGAATACT CNAGACTATG CATCAAGCTT GGTACCGAGC
61 TCGGATCCAC TAGTAACGGC CGCCAGTGTG CTGGAATTCG CCCTTAGCGG **ATAACAATTT** ARP19
121 **CACACAGGAT TTTGGCTCCC** CTATTACAAC CAGGGCTATT TCTTGATAGA GGAAGGTAGT
181 AAGCCAGAGG ATGTAGATGG GGTCTTAGAA GAGTNTGGTT TTAGAATGGG ACCCTTCAGG
241 GTGTCTGACC TCGCAGGGCT AGATGTGGGT TGGAAAGTNC GCAAAGGGCA AGGCCTTACT
301 GGACCGTCCT TACCTCCAGG AACCCCCACC CGAAAGAGGG GCAATACCAG GTATCCCCCA
361 ATTGCTGATA TGCTCTGTGA AGCTGGGCGA TTTGGTCAGA AGACAGGTAA GGGCTGGTAT
421 CAGTATGACA AGCCACTGGG TCGCATCCAC AAACCTGATC CCTGGCTTTC TGAGTTTCTG
481 TCACAGTATA GAGAAACCCA TCACATCAAG CAGCGCTCCA TCAGCAAGGA GGAAATCCTG
541 GAGCGTNGCT TATATTCCTT TATCAACGAG GCATCCCGCA TNTNGGANGA GGGGATGGCC
601 GCTAGCCCAG AGCACANNAT GTCATCTACT GCATGGGTAT NGNTGGCCAN GCACGTGGTG
661 GGCCATGTAC TATGCTGCNC AGTGGGCTGC CACAGNNTAA GANNTGCAGA ATATANCACC
721 NACTCCGACN NCCACNCTG ACCCNGACN CNNGANGAGG GGNTNNCINN GANNCCCCC
781 TGANNANGGA AAGNTGNNGA ANNATAT

B 35.2: Sequencing alignment of cDNA subclone AC2#2 with **mouse bifunctional enzyme (PBFE)** by BLAST searching against the National Center for Biotechnology Information database

AC2#2 : 139 ccctattacaaccagggctatcttctgatagaggaaggtagtaagccagaggatgtagat 198
Mouse PBFE: 1469 ccctattacaaccagggctatcttctgatagaggaaggtagtaagccagagggtgtagat 1528
AC2#2 : 199 ggggtcttagaagagntgggttttagaatgggacccttcagggtgtctgacctcgagg 258
Mouse PBFE: 1529 ggggtcttagaagagntgggttttagaatgggacccttcagggtgtctgacctcgagg 1588
AC2#2 : 259 ctatagtggtggttggaaagntcgcgaagggaaggccttactggaccgtccttacctcca 318
Mouse PBFE: 1589 ctatagtggtggttggaaagntcgcgaagggaaggccttactggaccgtccttacctcca 1648
AC2#2 : 319 ggaacccccacccgaaagaggggcaataaccaggtatcccccaattgctgatatgctctgt 378
Mouse PBFE: 1649 ggaacccccacccgaaagaggggcaataaccaggtactcccccaattgctgatatgctctgt 1708
AC2#2 : 379 gaagctggggcgatttgggtcagaagacaggttaagggctggatcagtatgacaagccactg 438
Mouse PBFE: 1709 gaagctggggcgatttgggtcagaagacaggttaagggctggatcagtatgacaagccactg 1768
AC2#2 : 439 ggtcgcattccacaaacctgatccctggctttctgagtttctgtcacagtatagagaaacc 498
Mouse PBFE: 1769 ggtcgcattccacaaacctgatccctggctttctgagtttctgtcacagtatagagaaacc 1828
AC2#2 : 499 catcacatcaagcagcgctccatcagcaaggaggaaatcctggagcgtngcttatattcc 558
Mouse PBFE: 1829 catcacatcaagcagcgctccatcagcaaggaggaaatcctggagcgtngcttatattcc 1888
AC2#2 : 559 cttatcaacgaggcatcccgcatntnggangaggggatggccgctagcccagagcacac-n 617
Mouse PBFE: 1889 cttatcaacgaggcatcccgcatntnggangaggggatggccgctagcccagagcacatt 1948
AC2#2 : 618 natgtcatctac-tgcatgggtatngntggcc-angcacgt-ggtggg-ccatgtactat 673
Mouse PBFE: 1949 gatgtcatctacttgcattgggtatgggtggccaaggcacgtgggtgggcccatgtactat 2008
AC2#2 : 674 gctgc 678
Mouse PBFE: 2009 gctgc 2013

B 35.3: Summary of sequence alignment of cDNA subclone AC2#2 with mouse PBFE

FluoroDD gel AC (AP2 + ARP19)					Subclone I.D.	Sequencing				
Fragment no.	PPARα (+/+)		PPARα (-/-)			FluoroDD fragment size (bp)	Size of insert after <i>EcoRI</i> cut (bp)	Primer	Gene homology to Blast search (Transcript size)	E-value (% Identity)
	CTL	Wy	CTL	Wy						
AC2	-	+	-	-	1600	AC2#2	1630	M13 reverse	<i>Mus musculus</i> peroxisomal bifunctional enzyme (PBE) (PBFE) [includes: enoyl-coA hydratase (EC 4.2.1.17); 3,2-trans_ enoyl-coA isomerase(EC 5.3.3.8); 3-hydroxyacyl-coA dehydrogenase (EC 1.1.1.35)] (2979 bp)	0 525/545 (96%)

Appendix B. DNA sequences and sequencing alignments of FluoroDD fragments

B 36.1: DNA sequence of cDNA subclone AC2#5 (AP2 & ARP19) using M13 reverse primer

1 ACTATTTAGG TGACACTATA GAATACTACA AGACTATGAC ATACAAGACT TGGTACCGAG
61 ACTCGGATCC ACTAGTAACG GCCGCCAGTG TGCTGGAATT NCGCCCNNTTA GACGGATA**AC** ARP19
121 **AATTTACAC** **AGGATTTTG** **CTCCAGGGAC** ACTNNATGCA TGATATGGCA AATANNNNAG
181 CAGGGAGGCA CTCCTGTGGG CTTAAGCACC TAAACCTTTT CAAATTCTCT ATGGACACAC
241 TGATGAGATA CTGAAGCGTG GGTATCAGCA CTGAACTCCA CNNGNNANNA TCAGGGGTCN
301 AGGNNTGGCA CTGTGATNNT CCATACCGTT CAGAAAGGTC NGTACNTGAG ANCCCTACGA
361 CTGCCTTGNG AGAGTTCNNT GTTCCTGACA ATTCCCAGGT TTGGGCCCTN TTCCGGGGAA
421 AANACCCNT TGGTTGTTNT AATTCCCGNC NTGGGNNAGN AGGAANNNGTC CGNTTCCCN
481 CAAAGGGAAT NNAAGAAANN CNNNAATTTA NCACATTTTG GNNTTTTTTT NNTTANTTAA
541 ANATGNGGNN NAAAGGTTAA TNNNTGGGGG GGGGGGTNTT TCCNANNGTT TTCCCCTGAA
601 AGCTGTGNN NCACAAANAT TNNTTNNANN NCCNNTGGTT GGCCNNTNNA NNTNGGGAAA
661 NAAACCACAA NNTTAATNNA AANNNNNNNN NNNAGNNCTT AAAANNAAG GGGGGGNNCC
721 NNNTNNCNG NNTTTTAA NNTNNNNNAN NNAAGACCN TNNACCANN GGCNTNNNA
781 ANAAGCNNNN NNNNTTTTNN TNNNTTTTNN NNNNNNNNN NNNANANNNN NNNNNNTATA
841 TTNTTANNNN NNNNGNNNN

B 36.2: Sequencing alignment of cDNA subclone **AC2#5** with **mouse catalase** by BLAST searching against the National Center for Biotechnology Information database

AC2#5 : 2 ctatttaggtgacactatagaataactacaagactatgacatacaagacttgggtaccgaga 61
Mouse catalase: 123 ctatttaggtgacactatagaataact-caag-ctatg-cat-caag-cttgggtaccgag- 70
AC2#5 : 62 ctcggatccactagtaacggccgccagtgctggaatt 100
Mouse catalase: 69 ctcggatccactagtaacggccgccagtgctggaatt 31

B 36.3: Summary of sequence alignment of cDNA subclone AC2#5 with mouse catalase

FluoroDD gel AC (AP2 + ARP19)					Subclone I.D.	Sequencing				
Fragment no.	PPARα (+/+)		PPARα (-/-)			FluoroDD fragment size (bp)	Size of insert after <i>Eco</i> RI cut (bp)	Primer	Gene homology to Blast search (Transcript size)	E-value (% Identity)
	CTL	Wy	CTL	Wy						
AC2	-	+	-	-	1600	AC2#5	1620	M13 reverse	if84h05.x1 Kaestner ngn3 - - subtracted <i>Mus musculus</i> cDNA 3' similar to SW:CATA_CAMJE Q59296 CATALASE (280 bp)	4e-19 93/99 (93%)

Appendix B. DNA sequences and sequencing alignments of FluoroDD fragments

B 37.1: DNA sequence of cDNA subclone AC2#6 (AP2 & ARP19) using M13 forward (-20) primer

1 NCNTCACTNN AGGGCGAATT GGGCCCTCTA GATGCATGCT CGAGCGGCCG CCAGTGTGAT
61 GGATATCTGC AGAATTCGCC CTTGTAATAC GACTCACTAT AGGGCTTTTT TTTTTGCCCA AP2*
121 TTCATTCTTT ATTCAAGTGG CATAAAAATC ACTACAAAAA CTTTACAAAA GAGTCTTGGG
181 AGCTAAAGGG TCCCTTCCTT GCCTCAGTCC CCAAGATTCC CGGCAGGGGA GGACAAGAGA
241 GAGAAGAAGG AGGAAGACTC CTGGCAGTGT TGGCATCTCC AAATACCAGA GGGGTGACTT
301 GGGTGACAGG ACACAGGTTG GGGACCTGAA TGTCTTCAGC AAGGGACACT CTTGTAGGGT
361 AGGTCAGCCT CCAACCATGA AGTATAACAC CAAGGCCAGT CTAAGCTTGG GAGACCAACA
421 CTTGTCTCTC CTTTTCCCAC CCAGGGTGTC TGGAAATATGT CTAAAGATGG CCTCTCCAGC
481 CTCTGCTTAC AAATGTGGAG GGACCCTAAG TTAGGGACTT GCCTAACCTA CCTCTAGCCA
541 AACTGTGTGC CACAAGTGCC AGCCCACAAA AGATCACCCC CTGAGCCCTT TGGGAAGAAA
601 TGAAGATTCC CCATGCCTGC CTTCTCCAG GCCCACCCCC ACCTGCTGCA AGAGANCAGC
661 TTCTACACTG GTGATGGTCN NTCNGTCCC ACCCTATCCC ACAAAGCTGG TTAGANAGAG
721 TNACAGGAGC TGAGAGGCTG ATNCAGGTGG GGACTCNNA G

B 37.2: Sequencing alignment of cDNA subclone AC2#6 with **mouse serine (or cysteine) proteinase inhibitor (SPI)** by BLAST searching against the National Center for Biotechnology Information database

AC2#6 : 116 gcccatttcattctttatttcaggtggcataaaaaatcactacaaaaactttacaaaagagtc 175
Mouse SPI: 2166 gcccatttcattctttatttcaggtggcataaaaaatcactacaaaaactttacaaaagagtc 2107
AC2#6 : 176 ttgggagctaaagggtcccttccttgccctcagtcaccaagattcccggcaggggaggaca 235
Mouse SPI: 2106 ttgggagctaaagggtcccttccttgccctcagtcaccaagattcccggcaggggaggaca 2047
AC2#6 : 236 agagagagaagaaggaggaagactcctggcagtgttggcatctccaaataccagaggggt 295
Mouse SPI: 2046 agagagagaagaaggaggaagactcctggcagtgttggcatctccaaataccagaggggt 1987
AC2#6 : 296 gacttgggtgacaggacacaggttggggacctgaatgtcttcagcaagggaactcctgt 355
Mouse SPI: 1986 gacttgggtgacaggacacaggttggggacctgaatgtcttcagcaagggaactcctgt 1927
AC2#6 : 356 agggtaggtcagcctccaacatgaagtataaacaccaaggccagtctaagcttgggagac 415
Mouse SPI: 1926 agggtaggtcagcctccaacatgaagtataaacaccaaggccagtctaagcttgggagac 1867
AC2#6 : 416 caacacttgtctctccttttccacccagggtgtctggaatatgtctaaagatggcctct 475
Mouse SPI: 1866 caacacttgtctctccttttccacccagggtgtctggaatatgtctaaagatggcctct 1807
AC2#6 : 476 ccagcctctgcttacaaatgtggagggaccctaagttagggaacttgccctaacctacctct 535
Mouse SPI: 1806 ccagcctctgcttacaaatgtggagggaccctaagttagggaacttgccctaacctacctct 1747
AC2#6 : 536 agccaaaactgtgtccacaagtgccagcccacaaaagatcacccctgagcccttggga 595
Mouse SPI: 1746 agccaaaactgtgtccacaagtgccagcccacaaaagatcacccctgagcccttggga 1687
AC2#6 : 596 agaaatgaagattcccatgcctgccttcctccaggccccacccacctgctgcaagaga 655
Mouse SPI: 1686 agaaatgaagattcccatgcctgccttcctccaggccccacccacctgctgcaagaga 1627
AC2#6 : 656 ncagcttctacactggtgatggctcnntccngtcccaccctatcccacaaagctgggttaga 715
Mouse SPI: 1626 acagcttctacactggtgatggctccttcgggtcccaccctatcccacaaagctgggttaga 1567
AC2#6 : 716 nagagtnacaggagctgagaggtgatncaggtggggactc 756
Mouse SPI: 1566 aagagtcacaggagctgagaggtgatccaggtggggactc 1526

B 37.3: Summary of sequence alignment of cDNA subclone AC2#6 with mouse SPI

FluoroDD gel AC (AP2 + ARP19)					Subclone I.D.	Sequencing				
Fragment no.	PPARα (+/+)		PPARα (-/-)			FluoroDD fragment size (bp)	Size of insert after <i>Eco</i> RI cut (bp)	Primer	Gene homology to Blast search (Transcript size)	E-value (% Identity)
	CTL	Wy	CTL	Wy						
AC2	-	+	-	-	1600	AC2#6	1800	M13 forward (-20)	<i>Mus musculus</i> serine (or cysteine) proteinase inhibitor, clade F, member 2 (Serpintf2) (2187 bp)	0 633/641 (98%)

* Sequence of primer was not completely matched with the expected sequence.

Appendix B. DNA sequences and sequencing alignments of FluoroDD fragments

B 38.1: DNA sequence of cDNA subclone AC4#3 (AP2 & ARP19) using M13 forward (-20) primer

1 CNACNTCACT ATAGGGCGAA TTGGGCCCTC TAGATGCATG CTCGAGCGGC CGCCAGTGTG
61 ATGGATATCT GCAGAATTCG CCCTTGTAAT **ACGACTCACT ATAGGGCTTT TTTTGGCCAT** AP2*
121 AAATAATATC TACTTTTATT ATTTTATTAT CCCTATAGAC AACATAGTAT AAATTTCCCT
181 CTTCTTTGGC TACCTTTGAA ATATCCTCTG CAAGTCTACT CTGTGTNCCT CTNNTTCTTC
241 TGTACCTTTG ACCTTTTCTA AGTTTCAACC CCTGNACTTG GTCTGNNCTC AATCATTCCC
301 TTTAACCTCA TGCAGCCCAG GNTCAACGGG ACNAGAAACT CNTAGTGTAG GTTGGTGGGN
361 TCCTGGCCAA GCCCACNANT CTAANNAACN CNTCGATGTT CCGGGGTGCC CGTGTGGATT
421 TGAAGTGGAA GTTCTGCATN ATGTNNGTNA AGGAGNNAAG AATTCCTCC TAACCAGTNC
481 TTCTNCCAAA CCATACCGNN TCCCATNGAA AANGGCCNAA AGNCNTCATT CTTCCNNAAN
541 NGGTTCNNN TCAATTTAAG GAAGTGCCTT NGGGTNGAAT TTTTGGNGT NGGAAAANAC
601 CTGGGGGTCT TTCACCAAAA AACCACACNN AAGGANCCCN TTAATAACCC TGGGGGAGAA
661 GGAATTTCCA AAACNNGGGT CCTGNNTGAC CCTNAANCCC GCCCCAGGN ATTGGNTTTA
721 NNTACCTTGC TCCTNNNAAC TCAAGCGGA ATGCT

B 38.2: Sequencing alignment of cDNA subclone AC4#3 with mouse Cyp2a5 by BLAST searching against the National Center for Biotechnology Information database

AC4#3 : 116 gccataaataatatctactttttattattttattatccctatagacaacatagtataaatt 175
Mouse Cyp2a5: 1688 gccataaataatatctactttttattattttattatccctattgacaacatagtataaatt 1629
AC4#3 : 176 tcctctctcttttgctacctttgaaatatcctctgcaagtctactctgtgtncctctnnt 235
Mouse Cyp2a5: 1628 tcctctctcttttgctacctttgaaatatcctctgcaagtctactctgtgt-cctctgtt 1570
AC4#3 : 236 tcttctgtacctttgaccttttctaagtttcaacccctgnacttggtctggnctcaatca 295
Mouse Cyp2a5: 1569 tcttctgtacctttgaccttttctaagtttcaacccctg-actt-gtctggtctcaatca 1512
AC4#3 : 296 ttccctttaacctcatgcagcccaggntcaacgggacnagaaactcntagtgtaggttgg 355
Mouse Cyp2a5: 1511 ttccctttaacctcatgcagcccaggctcaacgggacaagaaactcatagtgtaggttgg 1452
AC4#3 : 356 tgggntcctggccaagccacnancntaannaacnctcgatgttcgggggtgccgtgt 415
Mouse Cyp2a5: 1451 tgggatcgtggcaaagcccacgagtctaggagacacatcgatgtcctgggggtgcctgtgt 1392
AC4#3 : 416 ggatttgaagtggaagttctgcatnatgt 444
Mouse Cyp2a5: 1391 ggatttgaagtggaagttctgcatgatgt 1363

B 38.3: Summary of sequence alignment of cDNA subclone AC4#3 with mouse Cyp2a5

FluoroDD gel AC (AP2 + ARP19)					Subclone I.D.	Sequencing				
Fragment no.	PPARα (+/+)		PPARα (-/-)			FluoroDD fragment size (bp)	Size of insert after <i>Eco</i> RI cut (bp)	Primer	Gene homology to Blast search (Transcript size)	E-value (% Identity)
	CTL	Wy	CTL	Wy						
AC4	++	+	++	++	1100	AC4#3	1050	M13 forward (-20)	<i>Mus musculus</i> cytochrome P450, family 2, subfamily a, polypeptide 5 (Cyp2a5) (1720 bp)	e-121 302/329 (91%)

* Sequence of primer was not completely matched with the expected sequence.

Appendix B. DNA sequences and sequencing alignments of FluoroDD fragments

B 39.1: DNA sequence of cDNA subclone AC4#3 (AP2 & ARP19) using M13 reverse primer

1 CNCCNGANCA TTTAGGTGAC CTATAGAATA CTCAAGCTAT GCATCAAGCN TTGGTACGAC
61 TCGGATCCAN NTAGTANGGC CNCCAAGTGT GCATGGNAAN NGCCCTTACN GGNT**ACAATT** ARP19
121 **TCACACAGGA TTTTGGCTCC** CACTGCTTAA ATACAGACTA GGACAGGGCT CTGTCTCCTC
181 AGCCTCGGTC ACCACCCAGC TCTGGGACAG CNAAGCTGAA AATGACTCCC TCCATCTCAT
241 GGGGTCTACT GCTTCTGGCA GGCCTGTGTT GCCTGGTCCC CANGCNTTTC TGGCTGAGGA
301 TGTTTCAGGAN ACAGACACCT CCCNAGAAGG ATCCAGCCCC CAGCCTCCCA TGAGATCGCT
361 ACAAACCTGG GNANACTTTG CAATCNAGCC TATACCGGGN AGCNGGGTCC ATCCAGNNCC
421 AACACNTCC CAACATNCCC TCCTTCCTCC CCCCAGGTGG AGNCANTTTG NCCCACCAGC
481 CCNNNTTGN CNTTATTGNC CTCCCTCCCC CNTNAGNGGG NAGNCCAAAG GGGNNTTGNA
541 CAANCCTTCC ACCANCCGGC CCAAGAATCC CCCCCCATTT GGGGGGCCCC CTGGGGGCNC
601 TTTTCGAAAN NGGNNTNCC ACCCCCAAAA GGGGGACCAA CNNCAAAAAG GTTTTTCCGN
661 NAAAGNAAAT TTTTNTNCC TTTTCCCCTC CCCCCCCCC AAAAAGNNGG GNTNNANNAT
721 TTGGGAAAAAN GTTGGGGTTT TTTCCNNTCN AATNTGCGNN TTGGGGGGGC CTTTTTTTGN
781 TGTTTGNNNN TTGGNAAAAA AAGANAACNN CNNCCCCCAA AAAGGTTNTT TTTNTNTTTT
841 TTTNNNNNNN NCNNNNNNNN

B 39.2: Sequencing alignment of cDNA subclone **AC4#3** with **mouse serine (or cysteine) proteinase inhibitor (SPI)** by BLAST searching against the National Center for Biotechnology Information database

AC4#3 : 171 ctgtctcctcagcctcggtcaccacccagctctgggacagcnaagctgaaaatgactccc 230
Mouse SPI: 1 ctgtctcctcagcctcggtcaccacccagctctgggacagc-aagctgaaaatgactccc 59
AC4#3 : 231 tccatctcatggggtctactgcttctggcaggcctgtgttgctggtccccangcntttc 290
Mouse SPI: 60 tccatctcatggggtctactgcttctggcaggcctgtgttgctggtcccc-gc-tttc 117
AC4#3 : 291 tggctgaggatgttcagganacagacacctcccnagaaggatccagccccagcctccca 350
Mouse SPI: 118 tggctgaggatgttcaggagacagacacctccc-agaaggat-cagtccccagcctccca 175
AC4#3 : 351 tgagatcgctacaaacctgggnanactttgcaatcnagcctataccggg 399
Mouse SPI: 176 tgagatcgctacaaacctggg-agactttgcaatc-agcctataccggg 222

B 39.3: Summary of sequence alignment of cDNA subclone AC4#3 with mouse SPI

FluoroDD gel AC (AP2 + ARP19)					Subclone I.D.	Sequencing				
Fragment no.	PPARα (+/+)		PPARα (-/-)			Size of insert after <i>Eco</i> RI cut (bp)	Primer	Gene homology to Blast search (Transcript size)	E-value (% Identity)	
	CTL	Wy	CTL	Wy						
AC4	++	+	++	++	1100	AC4#3	1050	M13 reverse	<i>Mus musculus</i> serine (or cysteine) proteinase inhibitor clade A, member 1a (SPI) (1393 bp)	4e-85 219/229 (95%)

Appendix B. DNA sequences and sequencing alignments of FluoroDD fragments

B 40.1: DNA sequence of cDNA subclone AC7#5 (AP2& ARP19) using M13 forward (-20) primer

1 AACNCTCACG TATAGGGCGA ATTGGGCCCT CTAGATGCAT GCTCGAGACG GCCGCCAGTG
61 TGATGGATAT CTGCAGAATT CGCCCTTGTA AT**ACGACTCA** **CTATAGGGCT** **TTTTTTTTTT** **AP2**
121 **TGCTGTAGCA** TCAGGCACGA NGNCCAGGCC AGCCTGTGTT TAATGGAAGG AACCCAATTC
181 AGAAGGAAGG ATGACATTTT AGGGTGGTCA CTTTATGTGT GGGATCTACC ACTTTTCCCA
241 CAAAGATGGG GCTCTGAGTG TGTTCTTCAA ATATTATGAA AAGGAAAGGG TGGTCGAAGC
301 GCAGGATAGG GGGCATAAGA CATAGGAACC ATTTGTAAGA CTGTAAGTGC TGCAGCTTCT
361 GTTCCTGTCT CATCGATGGT CAGCACAGCC TTATGCACAG CCTGGCTGAG CTTCAGGGGA
421 GCATTCTCCC TCTGTGATTC CGGAGAGGTC AGCCCCATTG TTGAAAATCC NGGGTGATGC
481 CCACTGGACT CATGAGTGTN CTTCNANGTT ATATTCTCCA AAGATGGGAC AGTNNGGGNG
541 AAGTGGATTT GNGGCTAACT GGTGGGTNGG TAANANTNTN NTNNGAGTNN TGGGGATNNG
601 GNTTTGNTNA NNNNGTNGAN TNNTNNNTG GNTCTNNNTG TNNTNGNNTN NNNNNNNNGN
661 NNNNGNNNNN NNT'TNN

B 40.2: Sequencing alignment of cDNA subclone AC7#5 with **mouse serine (or cysteine) proteinase inhibitor (SPI)** by BLAST searching against the National Center for Biotechnology Information database

AC7#5 : 122 gctgtagcatcaggcacgangnccaggccagcctgtgtttaatggaaggaacccaattca 181
Mouse SPI: 1376 gctgtagcatcaggcacgag--ccaggccagcctgtgtttaatggaaggaacccaattca 1319
AC7#5 : 182 gaaggaaggatgacatttttaggggtggtcactttatgtgtgggatctaccacttttccac 241
Mouse SPI: 1318 gaaggaaggatgacatttttaggggtggtca-tttatgtgtgggatctaccacttttccac 1260
AC7#5 : 242 aaagatggggctctgagtggttcttcaaataattatgaaaaggaaagggtggtcgaagcg 301
Mouse SPI: 1259 aaagatggggctctgagtggttcttcaaataattatgaaaaggaaagggtggtcgaagcg 1200
AC7#5 : 302 caggatagggggcataaagacataggaaccatttgtaagactgtaactgctgcagcttctg 361
Mouse SPI: 1199 caggatagggggcata-gacataggaaccatttgtaagactgtaactgctgcagcttctg 1141
AC7#5 : 362 ttctgtctcatcgatggtcagcacagccttatgcacagcctggctgagcttcaggggag 421
Mouse SPI: 1140 ttctgtctcatcgatggtcagcacagccttatgcacagcctggctgagcttcaggggag 1081
AC7#5 : 422 cattctccctctgtgattccggagaggtcagcccccattgttgaaaatccnggggtgatgcc 481
Mouse SPI: 1080 cattct-cctctgtgattccggagaggtcagcccccattgttgaaatcc-ggggtgatgcc 1023
AC7#5 : 482 cagtggactcatgagtgtncttcnangttatattctccaaagatgg 527
Mouse SPI: 1022 cagtggactcatgagtggt-cttc-aagttatattctccagagatgg 979

B 40.3: Summary of sequence alignment of cDNA subclone AC7#5 with mouse SPI

FluoroDD gel AC (AP2 + ARP19)					Subclone I.D.	Sequencing				
Fragment no.	PPARα (+/+)		PPARα (-/-)			FluoroDD fragment size (bp)	Size of insert after <i>Eco</i> RI cut (bp)	Primer	Gene homology to Blast search (Transcript size)	E-value (% Identity)
	CTL	Wy	CTL	Wy						
AC7	+	-	+	+	770	AC7#5	790	M13 forward (-20)	<i>Mus musculus</i> serine (or cysteine) proteinase inhibitor clade A, member 1a (SPI) (1393 bp)	0 394/406 (97%)

Appendix B. DNA sequences and sequencing alignments of FluoroDD fragments

B 41.1: DNA sequence of cDNA subclone AD6#4 (AP2 & ARP18) using M13 reverse primer

1 AGACTATTTA GGTGACACTA TAGAATACTA CNAGACTATG ACNTNCAAGA CTTGGTACCG
61 AGACTCGGAT CNCTAGTANN GGCCGCCAGT GTGCTGGAAT TCGCCCTTAG ACGGATACAA ARP18
121 **TTTCACACAG GATGATGCTA** CCACTTGTCA CATTGTAGTC CTGAGACATA CAGGAAATGG
181 GGCAACCTGC CTGACACATT GTGATGGATC TGACACCAAA GCTGAAGTCC CTTTGATAAT
241 GAGCTCCATA AAATCCTTCT CTGAACATGC TGAGTGTGGA AGGCTGGAAG TACATCTTGT
301 GGGAGGCTTC AGTGATGACA GGCAGCTGTC ACAGAAACTT ACTCATCAGC TTCTCAGTGA
361 ATTTGACAAA CAGGATGATG ACATTCACTT AGTGACATTA TGTGTAACAG AGTTAAATGA
421 CCGTGAAGAN AAATGAAAAT CACNTTCCA ATCATTATATG GCATCGCCTG TCAACATNAA
481 AACTGCCAGA GATTTACAGA GCTNCCCTTT CAAGATCGTG GTCCCAGAGG AGCAACTGCG
541 TGCTGCAAGA GCTTTAGCAC GANGCCCAAT GATTAGCATT TATGATGCCA NGACAGNNCA
601 CCTCCGANNA GGCNCGTGTT CCTGNACCNN ATTCCCCACA AAGTGGATCN TCTGGGTTGC
661 CGCAAAGAAT GACNNNGCCN ANTTTCNTAA NANAAGNCCT TTTCCNACGN TNNTTCTCT
721 GGNNCCNCGC CCCCCCCCCC CTNTNGGTTG AANTCTTAAA CTCCTNNCCC TGATTNTTNN
781 TNNNTNNNTT TTTNNNNNNN TTTCTCTNT TTGGAATTTC CCCNCCNNN NCCNNNCTNT
841 NNNTGNTGTN GTGTNNNNNN NTNNTTCGG

B 41.2: Sequencing alignment of cDNA subclone AD6#4 with **mouse N-terminal Asn amidase (Ntanl)** by BLAST searching against the National Center for Biotechnology Information database

AD6#4 : 131 gatgatgctaccacttgtcacattgtagtcctgagacatacaggaaatggggcaacctgc 190
Mouse Asn: 285 gatgatgctaccacttgtcacattgtagtcctgagacatacaggaaatggggcaacctgc 344
AD6#4 : 191 ctgacacattgtgatggatctgacaccaaagctgaagtccccttgataatgagctccata 250
Mouse Asn: 345 ctgacacattgtgatggatctgacaccaaagctgaagtccccttgataatgagctccata 404
AD6#4 : 251 aaatccttctctgaacatgctgagtggtggaaggctggaagtacatcttgtgggaggcttc 310
Mouse Asn: 405 aaatccttctctgaacatgctgagtggtggaaggctggaagtacatcttgtgggaggcttc 464
AD6#4 : 311 agtgatgacaggcagctgtcacagaaacttactcatcagcttctcagtgaatttgacaaa 370
Mouse Asn: 465 agtgatgacaggcagctgtcacagaaacttactcatcagcttctcagtgaatttgacaaa 524
AD6#4 : 371 caggatgatgacattcacttagtgacattatgtgtaacagagttaaatgaccgtgaagan 430
Mouse Asn: 525 caggatgatgacattcacttagtgacattatgtgtaacagagttaaatgaccgtgaaga- 583
AD6#4 : 431 aaatgaaaatcacntttccaatcatttatggcatcgctgtcaacatnaaaactgccaga 490
Mouse Asn: 584 aaatgaaaatcac-tttccaatcatttatggcatcg-ctgtcaacattaaaactg-caga 640
AD6#4 : 491 gatttacagagctnccctttcaagatcgtggtcccagaggagcaactgcgtgctgcaaga 550
Mouse Asn: 641 gatttacagagctt-cctttcaagatcgtggt-ccagaggagcaactgcgtgctgcaaga 698
AD6#4 : 551 gcttttagcacgangcccaatgattagcatttatgatgccangacagnncacctccganna 610
Mouse Asn: 699 gcttttagcaggaggcccaatgattagcatttatgatgcaaagacagaacaactccgaata 758
AD6#4 : 611 ggencgtgttcctg 624
Mouse Asn: 759 ggcccgtgttcctg 772

B 41.3: Summary of sequence alignment of cDNA subclone AD6#4 with mouse Ntanl

FluoroDD gel AD (AP2 + ARP18)					Subclone I.D.	Sequencing				
Fragment no.	PPARα (+/+)		PPARα (-/-)			FluoroDD fragment size (bp)	Size of insert after <i>Eco</i> RI cut (bp)	Primer	Gene homology to Blast search (Transcript size)	E-value (% Identity)
	CTL	Wy	CTL	Wy						
AD6	+	++	+	+	840	AD6#4	860	M13 reverse	<i>Mus musculus</i> N-terminal Asn amidase (Ntanl) (1184 bp) 0 476/494 (96%)	

Appendix B. DNA sequences and sequencing alignments of FluoroDD fragments

B 42.1: DNA sequence of cDNA subclone AD6#10 (AP2 & ARP18) using M13 forward (-20) primer

1 AACNNAACCN NTANNGGCGA ATNNGGCCCT ACTAGATGCT GACTCAGACN NCCGNCACGN
61 TNGAATNGA NTNTCNGACG AANTTCGACC CTGANNANNT **ACGACTCACT ATAGGGCTTT** **AP2**
121 **TTTTTTTTTTG** CATGAACACT TGGAACCTTT ATTGNCAGAA AGGAGGGAAG ATGGAGAAAA
181 CTTGTGTGAG GATTAATAGG GTAGAGAGAG ACTATGACAG GGTAGATTTA GATGAACANA
241 TTAGGTAATT GTCATGTGAA AATGATACTA GGCTGAATAA TGGCTTCACA ATGACATTNC
301 AGGCCTTGGG TTTGGAGNCC CATGGTACAT ATTGAATAAT TCCTCATAAT TCAAAAGGAA
361 CTTAGTAGGT TAGATTGAAT AAGATATATT TAGATGAAGA AAATATCTTG GAGCTTTTAG
421 GGATCTTGAT GATGTCATAA GCATTTGTAA AAGGGAAGGA GATTAGAAGA GACAGGACGA
481 GGAGGTGGT GGCATTGAAG CAGGGGAATA TTCCAGTGCC CAAGGAATGA TGATCTATAC
541 TGAACAGAGG ATGAGAGGAC TCCTCTGGAG TACTCTTCTG AAGAANGTNG GTCACACCAA
601 CAACTTAGNN TTCTGCCAGT GANACTCATC TCAGACNTGG AGCTCCACAA CTGTAAGATA
661 ACCACTNCAA ATTATNCAAA NNNCCANGGT GNGACAATGA TATTGTAAAT GANNAGNNTG
721 TNGAAAATA GATGTAGAGT GAAGCANGAA ATGNNGAGAG NNANGTTTAT NGTTNGTNNN
781 NTNGTTAATG TNCGGTGGCN NTCNNNNNNG CGTNTNANNG

B 42.2: Sequencing alignment of cDNA subclone AD6#10 with **mouse Cyp4a10** by BLAST searching against the National Center for Biotechnology Information database

AD6#10 : 147 ctttattgncagaaaggaggggaagatggagaaaacttggtgaggattaatagggtagag 206
Mouse Cyp4a10: 2054 ctttattg-cagaaaggaggggaagatggagaaa-ctcgtgaggattaatcaggtagaa 1997
AD6#10 : 207 agagactatgacagggtagatttagatgaacanattaggtaattgtcatgtgaaaatgat 266
Mouse Cyp4a10: 1996 agagactatg-cagggtagatttagatgaacacattaggtaactgtcatgtgaaaatgat 1938
AD6#10 : 267 actaggctgaataatggcttcacaatgacattncaggccttgggttt-ggagncccatgg 325
Mouse Cyp4a10: 1937 actaagctgaataatgtcttcacaatgatggt-caggccttggattttggagacc-atgg 1880
AD6#10 : 326 tacatattgaataattcctcataattcaaaaggaacttagtaggttagattgaataagat 385
Mouse Cyp4a10: 1879 tacatattgaatgattcctcataattcagaaggaacttagtaggttagattgaataagat 1820
AD6#10 : 386 atatttagatgaagaaaatatcttggagcttttagggatcttgatgatgtcataagcatt 445
Mouse Cyp4a10: 1819 acatttagatgggaaaactatcttggagcttttagggatcttaatgatgtcataagcatc 1760
AD6#10 : 446 tgtaaaaggggaaggagattagaagagacaggacgaggagggtggtggcattgaagcaggg 505
Mouse Cyp4a10: 1759 tgtaaaaggtgaaggacattagaagagaggggatgaggagggtgctggctttgaagcaggg 1700
AD6#10 : 506 gaatattccagtgcccaaggaatgatgatctatactgaacagaggatgagaggactctc 565
Mouse Cyp4a10: 1699 gaatattccagtg-ccaaggaatgatgatctatactgaacagaggatgagaggact-ctc 1642
AD6#10 : 566 tggagtactcttctgaagaangtnggtcacaccaacaactagnnttctgccagtganac 625
Mouse Cyp4a10: 1641 tggagtattcttctgaaaaaggtaggtcacaccaacaacttagctttct-ccagtgaaac 1583
AD6#10 : 626 tcattctcagac-ntggagctccacaac 651
Mouse Cyp4a10: 1582 tcttctcagacattggagctccacaac 1556

B 42.3: Summary of sequence alignment of cDNA subclone AD6#10 with mouse Cyp4a10

FluoroDD gel AD (AP2 + ARP18)					Subclone I.D.	Sequencing				
Fragment no.	PPARα (+/+)		PPARα (-/-)			FluoroDD fragment size (bp)	Size of insert after <i>EcoRI</i> cut (bp)	Primer	Gene homology to Blast search (Transcript size)	E-value (% Identity)
	CTL	Wy	CTL	Wy						
AD6	+	++	+	+	840	AD6#10	850	M13 forward (-20)	<i>Mus musculus</i> cytochrome P450, family 4, subfamily a, polypeptide 10 (Cyp4a10) (2085 bp)	e-159 460/507 (90%)

Appendix B. DNA sequences and sequencing alignments of FluoroDD fragments

B 43.1: DNA sequence of cDNA subclone AD6#10 (AP2 & ARP18) using M13 reverse primer

1 AGCCTATTTA GGTGACACTA TAGAATACTC AAGCTATGCA TCAAGCTTGG TACCGAGCTC
61 GGATCCACTA GTAACGGCCG CCAGTGTGCT GGAATTCGCC CTTAGCGGAT **AACAATTTCA** ARP18
121 **CACAGGATGA TGCTACCTAT** ACCTGATCAT GAACCTTCTC CCTCCTCCAG CCATCTCTCC
181 TTGCCTCTCA CTTCTACCA TCTTATTTTT CCCTACATGA CTTCTTCATT TTACAAATAA
241 TCAATTGTCA CAACCTTGGT GGTCTGAAAT AATTGAAAGT TGTTATCTTA CAGTTGTGGA
301 GCTCCATGTC TGAGATGAGT TTCCTGGCA GAAAGCTAAG TTGTTGGTGT GACCAACCTT
361 CTTCAGAAGA GTACTCCAGA GAGTCCTCTC ATCCTCTGTT CAGTATAGAT CATCATTCCT
421 TGGCACTGGA ATATTCCCCT GCTTCAATGC CACCACCCTC CTCGTCTGT CTCTTCTAAT
481 CTCCTTCCCT TTTACAAATG CTTATGACAT CATCAAGATC CCTAAAAGCT CCAAGATATT
541 TTCTTCATCT AAATATATCT TATTCAATCT AACCTACTAA GTNCCTTTTG AATTATGAGG
601 AATTATTCAA TATGTACCAT GGGCTCCAAA CCCCAGGCC TGAATGTCAT AGNCACCCCA
661 TAATACAGCC TAGTATCATT TCCACATGAC AATNNNCTAA TGTGTNCATC TAAATCTACC
721 CTGCATAGTC TCTCTCTACC CTATTAATCC TCACACAAGT NNCTCATCNT CCCTCCTTCT
781 GCANNAAAGG TCNNNGTGNT ATGCAAAAAA ANNANNCCCN NATAGTGAA

B 43.2: Sequencing alignment of cDNA subclone **AD6#10** with **mouse Cyp4a10** by BLAST searching against the National Center for Biotechnology Information database

AD6#10 : 293 gttgtggagctcca-tgtctgagatgagtttactggcagaaagctaagttggtggtgtg 351
Mouse Cyp4a10: 1556 gttgtggagctccaatgtctgagaagagtttactgg-agaaagctaagttggtggtgtg 1614
AD6#10 : 352 accaaccttcttcagaagagtactccagagagtcctctcatcctctgttcagtatagatc 411
Mouse Cyp4a10: 1615 acctacctttttcagaagaatactccagagagtcctctcatcctctgttcagtatagatc 1674
AD6#10 : 412 atcattccttggcactggaatattcccctgcttcaatgccaccaccctcctcgtcctgtc 471
Mouse Cyp4a10: 1675 atcattccttggcactggaatattcccctgcttcaaagccagaccctcctcatcccctc 1734
AD6#10 : 472 tcttctaatactccttcccttttacaaatgcttatgacatcatcaagatccctaaaagctc 531
Mouse Cyp4a10: 1735 tcttctaatagtccttaccttttacagatgcttatgacatcattaagatccctaaaagctc 1794
AD6#10 : 532 caagatattttcttcatctaaatatatttcaatctaactactaagtncccttttga 591
Mouse Cyp4a10: 1795 caagatagttttcccatctaaatgtatcttattcaatctaactactaagttccttctga 1854
AD6#10 : 592 attatgaggaattattcaatatgtaccatgggctccaaacccaaggcctgaatgtcata 651
Mouse Cyp4a10: 1855 attatgaggaatcattcaatatgtaccatgggtctccaaatccaaggcctgaacatcatt 1914
AD6#10 : 652 gncaccccataatacacgcctagtagtatttccacatgacaatnnnctaagtgtgncatct 711
Mouse Cyp4a10: 1915 gtgaagacattattcagcttagtagtatttccacatgacagttacctaagtgttcatct 1974
AD6#10 : 712 aaatctaccctgcatagtctctctctaccctattaatcctcacacaagtnnct-catcnt 770
Mouse Cyp4a10: 1975 aaatctaccctgcatagtctctttctacctgattaatcctcacacgagtttctccatctt 2034
AD6#10 : 771 ccctcctt 778
Mouse Cyp4a10: 2035 ccctcctt 2042

B 43.3: Summary of sequence alignment of cDNA subclone AD6#10 with mouse Cyp4a10

FluoroDD gel AD (AP2 + ARP18)					Subclone I.D.	Sequencing				
Fragment no.	PPARα (+/+)		PPARα (-/-)			FluoroDD fragment size (bp)	Size of insert after <i>Eco</i> RI cut (bp)	Primer	Gene homology to Blast search (Transcript size)	E-value (% Identity)
	CTL	Wy	CTL	Wy						
AD6	+	++	+	+	840	AD6#10	850	M13 reverse	<i>Mus musculus</i> cytochrome P450, family 4, subfamily a, polypeptide 10 (Cyp4a10) (2085 bp) e-155 437/488 (89%)	

Appendix B. DNA sequences and sequencing alignments of FluoroDD fragments

B 44.1: DNA sequence of cDNA subclone AD8#2 (AP2 & ARP18) using M13 forward (-20) primer

1 TGGGCCCTCT AGATGCATGC TCGAGCGGCC GCCAGTGTGA TGGATATCTG CAGAATTCGC
61 CCTTGTAATA **CGACTCACTA TAGGGCTTTT TTTTTCATG** ACACTTGGAC CTTTATTGCA **AP2***
121 GAAGGGAGGG AAGATGGAGA AACTTGTGTG AGGATTAATA GGGTAGAGAG AGACTATGCA
181 GGGTAGATTT AGATGAACAC ATTAGGTAAT TGTCATGTGA AAATGATACT AGGCTGAATA
241 ATGGCTTCAC AATGACATTC AGGCCTTGGG TTTGGAGCCC ATGGTACATA TTGAATAATT
301 CCTCATAATT CAAAAGGAAC TTAGTAGGTN AGATTGAATA AGATATATTT AGATGAAGAA
361 AATATCTTGG AGCTTTTAGG GATCTTGATG ATGTCATAAG CATNTGTAAA AGGGAAGGAG
421 ATNAGAAGAG ACAGGACGAG GAGGGTGGTG GCATNGAAGC AGGGGAATAT TCCAGTGCCA
481 AGGAATGATG ATCTATACTG AACAGAGGAT GAGAGGACTC TCTGGAGTAC TCTTCTGAAG
541 AAGGTTGGTC ACACCAACAA CTTAGCTTTC TGCCAGTGAN ACTCATCTCA GACATGGAGC
601 TCCACAACCTG TAAGATAACA NCTTTCAATT ATNNCAACCA CCAGGGTGTG ACANTGATAT
661 TGTNAATAGA GTNGTNGGAA ATAGATGTAG AGGAAGCAGA AATCNGAGAG NAAGTATATC
721 GTTNGTCCTN TCGGTANGNN CCAGNCA

B 44.2: Sequencing alignment of cDNA subclone AD8#2with **mouse Cyp4a10** by BLAST searching against the National Center for Biotechnology Information database

AD8#2 : 96 gcatgacacttggacctttattgcagaagggaggggaagatggagaaacttgtgtgaggat 155
Mouse Cyp4a10: 2069 gcatgacactgggaactttattgcagaagggaggggaagatggagaaactcgtgtgaggat 2010
AD8#2 : 156 taatagggtagagagagactatgcagggtagattttagatgaacacattaggtaattgtca 215
Mouse Cyp4a10: 2009 taatcaggtagaaagagactatgcagggtagattttagatgaacacattaggtaactgtca 1950
AD8#2 : 216 tgtgaaaatgatactaggctgaataatggcttcacaatgacattcaggccttgggttt-g 274
Mouse Cyp4a10: 1949 tgtgaaaatgatactaagctgaataatgtcttcacaatgatgttcaggccttggattttg 1890
AD8#2 : 275 gagcccatggtacatattgaataattcctcataattcaaaaggaacttagtaggttagat 334
Mouse Cyp4a10: 1889 gagaccatggtacatattgaatgattcctcataattcagaaggaacttagtaggttagat 1830
AD8#2 : 335 tgaataagatatatttagatgaagaaaatatcttggagcttttagggatctttagatgt 394
Mouse Cyp4a10: 1829 tgaataagatacatatttagatgggaaaactatcttggagcttttagggatcttaatgatgt 1770
AD8#2 : 395 cataagcatntgtaaaaggggaaggagatnagaagagacaggacgaggaggggtggtggcat 454
Mouse Cyp4a10: 1769 cataagcatctgtaaaaggtgaaggacattagaagagaggggatgaggaggggtgctggctt 1710
AD8#2 : 455 ngaagcaggggaatattccagtgccaaaggaatgatgatctatactgaacagaggatgaga 514
Mouse Cyp4a10: 1709 tgaagcaggggaatattccagtgccaaaggaatgatgatctatactgaacagaggatgaga 1650
AD8#2 : 515 ggactctctggagtactcttctgaagaaggttggtcacaccaacaacttagctttctgcc 574
Mouse Cyp4a10: 1649 ggactctctggagtattcttctgaaaaaggttaggtcacaccaacaacttagctttct-cc 1591
AD8#2 : 575 agtganactcatctcagaca-tggagctccacaac 608
Mouse Cyp4a10: 1590 agtgaaactcttctcagacattggagctccacaac 1556

B 44.3: Summary of sequence alignment of cDNA subclone AD8#2 with mouse Cyp4a10

FluoroDD gel AD (AP2 + ARP18)					Subclone I.D.	Sequencing				
Fragment no.	PPARα (+/+)		PPARα (-/-)			FluoroDD fragment size (bp)	Size of insert after <i>Eco</i> RI cut (bp)	Primer	Gene homology to Blast search (Transcript size)	E-value (% Identity)
	CTL	Wy	CTL	Wy						
AD8	+	++	+	+	720	AD8#2	780	M13 forward (-20)	<i>Mus musculus</i> cytochrome P450, family 4, subfamily a, polypeptide 10 (Cyp4a10) (2085 bp)	0 474/515 (92%)

* Sequence of primer was not completely matched with the expected sequence.

Appendix B. DNA sequences and sequencing alignments of FluoroDD fragments

B 45.1: DNA sequence of cDNA subclone AD8#7 (AP2 & ARP18) using M13 reverse primer

1 ACTATTTAGG TGACACTATA GAATACTACA AGACTATGNC ATNCAAGACT TGGTACCGAG

61 ACTCGGATCN ACTAGTAACG GCCGCCAGTG TGCTGGAATT CGCCCTTAGC GGATA**ACAAT** ARP18

121 **TTCACACAGG ATGATGCTAC** CTATACCTGA TCATGAACCT TCTCCCTCCT CCAGCCATCT

181 CTCCTTGCCT CTCACTTCCT ACCATCTTAT TTTTCCCTAC ATGACTTCTT CATTTTACAA

241 ATAATCAATT GTCACAACCT TGGCGGTCTG AAATAATTGA AAGTTGTTAT CTTACAGTTG

301 TGGAGCTCCA TGTCTGAGAT GAGTTTCACT GGCAGAAAGC TAAGTTGTTG GTGTGACCAA

361 CCTTCTTCAG AAGAGTACTC CAGAGAGTCC TCTCATCCTC TGTTCAAGTAT AGATCNATCA

421 TTCCTTGGCA CTGGAATATT CCCCTGCTT CAATGCCACC ACCCTCCCTC GTCCTGTCTC

481 TTCTAATCTC CTCCCCCTT TACAAATGCT TAGACATCA TCAAGNATCC CTAAAAGCTC

541 CAAGATATTT TCTTCATCTA AATATATCTT ANNCAATCTA ACCTACTAAG TTCCTTTTGA

601 NTTATGANGA ATTATTCAAT ATGTACCATG GGCTCCAAAC CCAAGGGCCT GAATGTGATT

661 GTGANGCCAT TATCCAGCCC TAGTATCATT TNNACANTGA CAAATTACCC TAANTGTGNT

721 TCATCTAAAN NNCTACCCNT GCCATAGNTT TTCTNTTCTT ACNCCNTANT NNANTTTNCN

781 TCACANNAN GTTNNTCTC CNANTNTNC CCNNTNCNTT TTTCNTGCAA

B 45.2: Sequencing alignment of cDNA subclone AD8#7 with **mouse Cyp4a10** by BLAST searching against the National Center for Biotechnology Information database

AD8#7 : 297 gttgtggagctcca-tgtctgagatgagtttcactggcagaaagctaagttggtggtgtg 355

Mouse Cyp4a10: 1556 gttgtggagctccaatgtctgagaagagtttcactgg-agaaagctaagttggtggtgtg 1614

AD8#7 : 356 accaaccttcttcagaagagtactccagagagtcctctcatcctctgttcagtagatagatc 415

Mouse Cyp4a10: 1615 acctacctttttcagaagaataactccagagagtcctctcatcctctgttcagtagatagatc 1674

AD8#7 : 416 natcattccttggcactggaatatcccccgttcaatgccaccacccctccctcgctcct 475

Mouse Cyp4a10: 1675 -atcattccttggcactggaatatccccc-tgcttcaaagccagcacctcc-tcatccc 1731

AD8#7 : 476 gtctcttctaatactccttcccttttacaaatgcttatgacatcatcaagnatccctaaa 535

Mouse Cyp4a10: 1732 ctctcttctaatactccttacc-ttttacagatgcttatgacatcattaag-atccctaaa 1789

AD8#7 : 536 agctccaagatattttcttcatctaaatatatcttanncaatctaacctactaagttcct 595

Mouse Cyp4a10: 1790 agctccaagatagttttcccatctaaatgtatcttattcaatctaacctactaagttcct 1849

AD8#7 : 596 tttganttatgangaattattcaatatgtaccatgggctccaaacccaagggcctgaatg 655

Mouse Cyp4a10: 1850 tctgaattatgaggaatcattcaatatgtaccatggtctccaaaatccaaggcctgaaca 1909

AD8#7 : 656 tcattgtgangccattatccagccctagtagatcattt 691

Mouse Cyp4a10: 1910 tcattgtgaagacattattcag-cttagtagatcattt 1944

B 45.3: Summary of sequence alignment of cDNA subclone AD8#7 with **mouse Cyp4a10**

FluoroDD gel AD (AP2 + ARP18)					Subclone I.D.	Sequencing				
Fragment no.	PPARα (+/+)		PPARα (-/-)			FluoroDD fragment size (bp)	Size of insert after <i>Eco</i> RI cut (bp)	Primer	Gene homology to Blast search (Transcript size)	E-value (% Identity)
	CTL	Wy	CTL	Wy						
AD8	+	++	+	+	720	AD8#7	780	M13 reverse	<i>Mus musculus</i> cytochrome P450, family 4, subfamily a, polypeptide 10 (Cyp4a10) (2085 bp)	e-105 353/396 (89%)

Appendix B. DNA sequences and sequencing alignments of FluoroDD fragments

B 46.1: DNA sequence of cDNA subclone AD9#2 (AP2 & ARP18) using M13 forward (-20) primer

1 CCCTCACTAT AGGGCGAATT GGGCCCTCTA GATGCNTGCT CGAGCGGCCG CCAGTGTGAT
61 GGATNTCTGC AGAATTCGCC CTTGTAATAC **GACTCACTAT** **AGGGCTTTTT** **TTTTTTGCAT** **AP2***
121 GACACTGGGA ACTTTATTGC AGAAAGGAGG GAAGATGGAG AAACTCGTGT GAGGATTAAT
181 CAGGTAGAAA GAGACTATGC AGGGTAGATT TAGATGAACA CATTAGGTAA TTGTCATGTG
241 AAAATGATAC TAGGCTGAAT AATGGCTTCA CAATGACATT CAGGCCTTGG GTTTGGAGCC
301 CATGGTACAT ATTGAATAAT TCCTCATAAT TCAAAAGGAA CTTAGTAGGT TAGATTGAAT
361 AAGATATATT TAGATGAAGA AAATATCTTG GAGCTTTTAG GGATCTTGAT GATGTCATAA
421 GCATTTGTAA AAGGGAAGGA GATTAGAAGA GACAGGACGA GGAGGNNGGT GGCATTGACG
481 CAGGGGAATA NNCCAGTGCC AAGGAATGAT GATCTATACT GAACAGAGGA TGAGAGGACT
541 CTCTGGAGTA CTCTTCTGAA GAGGGTNGGT CACACCACCA ACTTAGNNTT NTGCCAGTGA
601 NACTCATCTC AGACATGGAG CTCCACACTG TAAGATAACNC CTTTNTATAA TNTAAANCAN
661 CNANNTGTGA CAANNATTAT NNGTAAATGA AANNTTTGTA NNNANNATAG ATGNTAGANT
721 TAAAGCCAGG AAAATNNTGA AGAGGNNAG TCNTNATNGT TTNGTNTTN GGGTANTTTT

B 46.2: Sequencing alignment of cDNA subclone AD9#2 with **mouse Cyp4a10** by BLAST searching against the National Center for Biotechnology Information database

AD9#2 : 117 gcatgacactgggaactttattgcagaaaggaggggaagatggagaaactcgtgtgaggat 176
Mouse Cyp4a10: 2069 gcatgacactgggaactttattgcagaaaggaggggaagatggagaaactcgtgtgaggat 2010
AD9#2 : 177 taatcaggtagaaagagactatgcagggtagatntagatgaacacattaggttaattgtca 236
Mouse Cyp4a10: 2009 taatcaggtagaaagagactatgcagggtagatntagatgaacacattaggttaactgtca 1950
AD9#2 : 237 tgtgaaaatgatactaggctgaataatggcttcacaaatgacattcaggccttgggttt-g 295
Mouse Cyp4a10: 1949 tgtgaaaatgatactaagctgaataatgtcttcacaatgatgttcaggccttggattttg 1890
AD9#2 : 296 gagcccatggtacatatattgaataatcctcataattcaaaaggaacttagtaggttagat 355
Mouse Cyp4a10: 1889 gagaccatggtacatatattgaatgattcctcataattcagaaggaacttagtaggttagat 1830
AD9#2 : 356 tgaataagatatatttagatgaagaaaatatcttggagcttttagggatccttgatgatgt 415
Mouse Cyp4a10: 1829 tgaataagatacatatttagatgggaaaactatcttggagcttttagggatccttaatgatgt 1770
AD9#2 : 416 cataagcatctgtaaaagggaaggagattagaagagacaggacgaggaggnngtgccat 475
Mouse Cyp4a10: 1769 cataagcatctgtaaaaggtaaggacattagaagagaggggatgaggagggtgctggctt 1710
AD9#2 : 476 tgacgcaggggaatanncagtgccaaggaatgatgatctatactgaacagaggatgaga 535
Mouse Cyp4a10: 1709 tgaagcaggggaatatccagtgccaaggaatgatgatctatactgaacagaggatgaga 1650
AD9#2 : 536 ggactctctggagtactcttctgaagagggtnngtcacaccaccaacttagntntngcc 595
Mouse Cyp4a10: 1649 ggactctctggagtattcttctgaaaaaggtaggtcacaccaacaacttagctttct-cc 1591
AD9#2 : 596 agtganactcatctcagaca-tggagctccaca 627
Mouse Cyp4a10: 1590 agtgaaactcttctcagacattggagctccaca 1558

B 46.3: Summary of sequence alignment of cDNA subclone AD9#2 with mouse Cyp4a10

FluoroDD gel AD (AP2 + ARP18)					Subclone I.D.	Sequencing				
Fragment no.	PPARα (+/+)		PPARα (-/-)			FluoroDD fragment size (bp)	Size of insert after <i>Eco</i> RI cut (bp)	Primer	Gene homology to Blast search (Transcript size)	E-value (% Identity)
	CTL	Wy	CTL	Wy						
AD9	+	++	+	+	710	AD9#2	765	M13 forward (-20)	<i>Mus musculus</i> cytochrome P450, family 4, subfamily a, polypeptide 10 (Cyp4a10) (2085 bp)	0 472/513 (92%)

* Sequence of primer was not completely matched with the expected sequence.

Appendix B. DNA sequences and sequencing alignments of FluoroDD fragments

B 47.1: DNA sequence of cDNA subclone AD9#3 (AP2 & ARP18) using M13 reverse primer

1 CCNTATNTAG GTGACACTAT AGAATACTCA AGCTATGCAT CAAGCTTGGT ACCGAGCTCG
61 GATCCACTAG TAACGGCCGC CAGTGTGCTG GAATTCGCCC TTAGCGGATA ACAATTTAC ARP18
121 ACAGGATGAT GCTACCTTATA CCTGATCATG AACCTTCTCC CTCCTCCAGC CATCTCTCCT
181 TGCCTCTCAC TTCCTACCAT CTTATTTTTC CCTACATGAC TTCTTCATT TACAAATAAT
241 CAATTGTCAC AACCTTGGTG GTCTGAAATA ATTGAAAGTT GTTATCTTAC AGTTGTGGAG
301 CTCCATGTCT GAGATGAGTT TCACTGGCAG AAAGCTAAGT TGTGGTGTG ACCAACCTTC
361 TTCAGAAGAG TACTCCAGAG AGTCCTCTCA TCCTCTGTTC AGTATAGATC ATCATTCTTC
421 GGCACTGGAA TATNCCCCTG CTTCAATGCC ACCACCTCC TCGTCCTGTC TCTTCTAATC
481 TCCTTCCCTT TTACAAATGC TTATGACATC ATCAAGATCC CTAAAAGCTC CAAGATATTT
541 TCTTCATCTA AATATATCTT ATTCAATCTA ACCTACTANG TTCCTTTTGA ATTATGAGGA
601 ATTATTCATT ATGTACCATG GGCTNCAAAN CCCAAGGCCT GAATGTCATT GTGAAGCCAT
661 TATTTCAGCCT AGTATCATNN TCACATGACA ATNANNTAAT GTGTCCATCT ANATCTACCC
721 TGCATAGTCC NNCTCTANNC NATTAATCCC CCACCAAGTT TCTCCNNTCT NCCCNCNNNN
781 CTGCAAATAA NNGG

B 47.2: Sequencing alignment of cDNA subclone AD9#3 with **mouse Cyp4a10** by BLAST searching against the National Center for Biotechnology Information database

AD9#3 : 292 gttgtggagctcca-tgtctgagatgagtttctactggcagaaagctaagttggtggtgtg 350
Mouse Cyp4a10: 1556 gttgtggagctccaatgtctgagaagagtttctactgg-agaaaagctaagttggtggtgtg 1614
AD9#3 : 351 accaaccttcttccagaagagtactccagagagtcctctcatcctctgttcagtatagatc 410
Mouse Cyp4a10: 1615 acctacctttttccagaagaatactccagagagtcctctcatcctctgttcagtatagatc 1674
AD9#3 : 411 atcattccttggcactggaatatnccctgcttcaatgccaccaccctcctcgctcctgtc 470
Mouse Cyp4a10: 1675 atcattccttggcactggaatatnccctgcttcaaagccagaccctcctcatccccctc 1734
AD9#3 : 471 tcttctaatactccttccctttttacaaatgcttatgacatcatcaagatccctaaaagctc 530
Mouse Cyp4a10: 1735 tcttctaatactccttccctttttacagatgcttatgacatcattaagatccctaaaagctc 1794
AD9#3 : 531 caagatattttcttcatctaaatatatcttattcaatctaacctactangttccttttga 590
Mouse Cyp4a10: 1795 caagatagttttcccatctaaatgtatcttattcaatctaacctactaagttccttctga 1854
AD9#3 : 591 attatgaggaattattcattatgtaccatgggctncaaancccaaggcctgaatgtcatt 650
Mouse Cyp4a10: 1855 attatgaggaatcattcaatatgtaccatggtctccaaaatccaaggcctgaacatcatt 1914
AD9#3 : 651 gtgaagccattattcagcctagtagtcatnntcacatgacaatnanntaatgtgtccatct 710
Mouse Cyp4a10: 1915 gtgaagacattattcagcttagtagtcatnntcacatgacagttacctaagtgtgttcatt 1974
AD9#3 : 711 anatctaccctgcatagtc 729
Mouse Cyp4a10: 1975 aaatctaccctgcatagtc 1993

B 47.3: Summary of sequence alignment of cDNA subclone AD9#3 with mouse Cyp4a10

FluoroDD gel AD (AP2 + ARP18)					Subclone I.D.	Sequencing				
Fragment no.	PPARα (+/+)		PPARα (-/-)			FluoroDD fragment size (bp)	Size of insert after <i>EcoRI</i> cut (bp)	Primer	Gene homology to Blast search (Transcript size)	E-value (% Identity)
	CTL	Wy	CTL	Wy						
AD9	+	++	+	+	710	AD9#3	765	M13 reverse	<i>Mus musculus</i> cytochrome P450, family 4, subfamily a, polypeptide 10 (Cyp4a10) (2085 bp)	e-153 398/439 (90%)

Appendix B. DNA sequences and sequencing alignments of FluoroDD fragments

B 48.1: DNA sequence of cDNA subclone AF1#8 (AP10 & ARP13) using M13 forward (-20) primer

1 ACTNNCTATA GGGCNAATTG GGCCCTCTAG ATGCTGCTCG AGNCGGCCGC CAGTGTGATG
61 GATATCTGCA GAATTCGCCC TTAGCGGATA ACAATTTTCAC ACAGGAGTTG CACCATTTAT ARP13
121 TGGCTATGCT GGAGGAAAGA CCCAGACAGA GAAGAAAAAA CTCAGAGATG TCTTTAAGAA
181 AGGCGACATC TACTTCAACA GCGGAGACCT CCTGATGATC GACCGTGAGA ACTTCGTCTA
241 CTTTCACGAC AGGGTTGGAG ATACTTTCCG GTGGAAAGGA GAGAACGTAG CTACCACAGA
301 AGTCGCTGAC ATCGTGGGAC TGGTAGATT TGTGAAGAA GTGAATGTGT ATGGCGTGCC
361 TGTGCCAGGT CATGAGGGTC GAATTGGGAT GGCTCCCTC AAGATCAAAG AAAACTACGA
421 GTTCAATGGA AAGAAACTCT TTCAACACAT CGCGGAGTAC CTGCCCCAGT TACGCGAGGC
481 CTCGGTTCCT GAGGATACAA GATACCATTG AGATCACTGG GACTTTTAAA CACCGCAAAG
541 TGACCCTGAT GGAAGAGGGC TTCAATCCCA CAGTCATCAA AGATACCTTG TATTTCATGG
601 ATGATGCAGA GAAAAATTT GTGCCATGAC TGAGAACNNT TATAATGCCT AATTGATAAA
661 AATCTGANGC TNTGAATATT CCCTGGTGGN TTAAGCTNAT GACATNNCCA AAAAGAANCT
721 CNATANACCT CCCANANCAC TTNNCTCGTN NAATCAATTT NNNTGGATNG AGGNTTTANG
781 TGNNTTTATT TNNGAATAT TNTTNAG

B 48.2: Sequencing alignment of cDNA subclone AF1#8 with **mouse very-long-chain acyl-coA synthetase (VLACS)** by BLAST searching against the National Center for Biotechnology Information database

AF1#8 : 111 caccattttattggctatgctggaggaaagaccagacagagaagaaaaaactcagagatg 170
Mouse VLACS: 1310 caccattttattggctatgctggaggaaagaccagacagagaagaaaaaactcagagatg 1369
AF1#8 : 171 tctttaagaaaggcgacatctacttcaacagcggagacctcctgatgatcgaccgtgaga 230
Mouse VLACS: 1370 tctttaagaaaggcgacatctacttcaacagcggagacctcctgatgatcgaccgtgaga 1429
AF1#8 : 231 acttcgtctactttcacgacagggttgagatactttccggtggaaggagagaaacgtag 290
Mouse VLACS: 1430 acttcgtctactttcacgacagggttgagatactttccggtggaaggagagaaacgtag 1489
AF1#8 : 291 ctaccacagaagtcgctgacatcgctgggactggttagattttgttgaagaagtgaatgtgt 350
Mouse VLACS: 1490 ctaccacagaagtcgctgacatcgctgggactggttagattttgttgaagaagtgaatgtgt 1549
AF1#8 : 351 atggcgtgcctgtgccagggtcatgagggtcgaattgggatggcctccctcaagatcaaag 410
Mouse VLACS: 1550 atggcgtgcctgtgccagggtcatgagggtcgaattgggatggcctccctcaagatcaaag 1609
AF1#8 : 411 aaaactacgagttcaatggaagaaactctttcaacacatcgcgagtagacctgccccagt 470
Mouse VLACS: 1610 aaaactacgagttcaatggaagaaactctttcaacacatcgcgagtagacctg-cacctg 1668
AF1#8 : 471 tacgcgaggcctcggttcctgaggatacaagataccattgagatcactgggactttttaa 530
Mouse VLACS: 1669 tacgcgaggcctcggttcctgaggatacaagataccattgagatcactgggactttttaa 1728
AF1#8 : 531 caccgcaaagtgacctgatggaagagggttcaatcccacagtcacaaagataccttg 590
Mouse VLACS: 1729 caccgcaaagtgacctgatggaagagggttcaatcccacagtcacaaagataccttg 1788
AF1#8 : 591 tatttcattgatgatgcagagaaaacattttgtg-ccatgactgagaacnnttataatgcc 649
Mouse VLACS: 1789 tatttcattgatgatgcagagaaaacattttgtgcccactgactgagaacatttataatgcc 1848
AF1#8 : 650 -taattgataaaaaatctgangctntgaatatccctgggtgnttaagctnatgacatnnc 708
Mouse VLACS: 1849 ataattgataaaaactctgaagctctgaatatccctgggtgntt-agctcatgacatttc 1907
AF1#8 : 709 caaaaagaanctcnatanacctc 731
Mouse VLACS: 1908 cagaaagaaactcgatagacctc 1930

B 48.3: Summary of sequence alignment of cDNA subclone AF1#8 with mouse VLACS

FluoroDD gel AF (AP10 + ARP13)					Subclone I.D.	Sequencing				
Fragment no.	PPARα (+/+)		PPARα (-/-)			FluoroDD fragment size (bp)	Size of insert after <i>Eco</i> RI cut (bp)	Primer	Gene homology to Blast search (Transcript size)	E-value (% Identity)
	CTL	Wy	CTL	Wy						
AF1	+	++	+	+	945	AF1#8	990	M13 forward (-20)	<i>Mus musculus</i> very-long-chain acyl-coA synthetase (VLACS) (2209 bp)	0 606/623 (97%)

Appendix B. DNA sequences and sequencing alignments of FluoroDD fragments

B 49.1: DNA sequence of cDNA subclone **AF1#8** (AP10 & ARP13) using **M13 reverse primer**

1 AGCNTATTTA GGTGACACTA TAGAATACTC AGNCTATGCT NAAGNCTTGG TACCGAGNCN
61 CGATCCACTA GTAACGGCCG CCAGTGTGCT GGAATNCGCC CTTGTAAT**AC GACTCACTAT** **AP10**
121 **AGGGCTTTTT TTTTTTAGT** GTTAATATAG TTTATTATGT CTTTAAAAAA ATAAGGCCCT
181 CTCTCCAAGA AGCTTAGTTT GCAAGGACAA ATGGCAGGTG CACATTGAAA AATAATTGTT
241 TCTAAATCTT TTTACTTGNA AAGGNTCAGG TGTACTCCA AAAAAAACA AACAACTAT
301 CCTTTTAATG AATAATTTCC TAAAAATAAA ATCGCACCTT ATAGCCCTCA NNCAAGTTAA
361 AGTTGNNTTC NACGTATGAA GTGGCTCTGC GAGGTCTATC GAGTTTCTTT CTGGANATGT
421 CATGAATAA ACCCCCCAGG NANNATTCAG ACCTTCAGAN TTTTATCCAN TNATGGCATN
481 ATAAATGTCC TCAGTCATGG NCACAAANGT NTCNTCTGCA TCANCATGAN ATCCAAGTAT
541 CTTGATAACT GGGGGATGAN CCCCCTTCAT CAGGGTCCCT TCGGGTGTTA AAAGTCCAGT
601 GATCCAATGG ATTTNNNTCC CAAGACCGAG GCNCCCCTAC NGNNNGGTCC CCCGAGTGTG
661 AANANTNNTT CCATGACCTT ATTTCTGATT GANGAGCATC ATTNAACTAT ACNGCCAGCA
721 CCATANATNN TTAAATANT TCCGAGTNA TTTGACCCTC TNCTTCCG

B 49.2: Sequencing alignment of cDNA subclone **AF1#8** with **mouse very-long-chain acyl-coA synthetase (VLACS)** by BLAST searching against the National Center for Biotechnology Information database

AF1#8 : 294 aaactatccttttaatgaataatttcctaaaaataaaatcgcaccttatagccctcannc 353
Mouse VLACS: 2027 aaactatccttttaatgaataatttcctaaaaataaaatcgcaccttatggtctccaatc 1968
AF1#8 : 354 aagttaaagttgnnttcnacgtatgaagtggctctgcgaggtctatcgagtttctttctg 413
Mouse VLACS: 1967 aagttaaagtgggtttctacgtttgaagtgggtctgcgaggtctatcgagtttctttctg 1908
AF1#8 : 414 ganatgtcatgaactaaacccccaggnannattcagaccttcaganttttatccantna 473
Mouse VLACS: 1907 gaaatgtcatgagctaaa-ccaccaggaatattcagagcttcagagttttat-caatta 1850
AF1#8 : 474 tggcatnataaatgtcctcagtcatggncacaaangtntcntctgcatca 523
Mouse VLACS: 1849 tggcattataaatgttctcagtcatgggcacaaatgttttctctgcatca 1800

B 49.3: Summary of sequence alignment of cDNA subclone **AF1#8** with **mouse VLACS**

FluoroDD gel AF (AP10 + ARP13)					Subclone I.D.	Sequencing				
Fragment no.	PPARα (+/+)		PPARα (-/-)			FluoroDD fragment size (bp)	Size of insert after <i>Eco</i> RI cut (bp)	Primer	Gene homology to Blast search (Transcript size)	E-value (% Identity)
	CTL	Wy	CTL	Wy						
AF1	+	++	+	+	945	AF1#8	990	M13 reverse	<i>Mus musculus</i> mRNA for very-long-chain acyl-coA synthetase (VLACS) (2209 bp)	1e-56 119/230 (86%)

Appendix B. DNA sequences and sequencing alignments of FluoroDD fragments

B 50.1: DNA sequence of cDNA subclone AF21#5 (AP10 & ARP13) using M13 reverse primer

1 AAGACTATTT AGGTGACCTA TAGAATACTC AAGCTATGCA TCAAGCTTGG TACCGAGCTC
61 GGATCCACTA GTAACGGCCG CCAGTGTGCT GGAATTCGCC CTTAGCGGAT **AACAATTTCA** ARP13
121 **CACAGGAGTT GCACCAT**CAG GCTTGGGGTC TGCAGTGTAC CCTAGGTAAC CAAGCTGACT
181 CCATCCTAAC AGATCTGTAC ACTGCCCTGT TCCTCTGGCC TGTACATCTT CCTGAAGAAT
241 GCTACCTGTC TTCCCTCCAC TCCTGCCCTC CACATAACCCT GCAGAACCAC AGCCTTNNCC
301 CCTGCATNCC TGATNCCAC CGTAATCGCT GCTTCATCTA GGTTCCTACT GACGCCTACC
361 CCTAAGATNC TGCATACCAA CGGGCCACTG TCCCTAGCTT TACTACAAGA TAACTTTCCC
421 CTAACAAAAA AAAAGCCCTA TAGTGAGTCG TATTACAAGG GCCAATTCCTG CAGATATCCA
481 TCACACTGGN CGGCCGCTCC AGCATGCATC NNGAGGGCCC AAATTCGCCC CTATAGTGAG
541 NTCGNNTTAC CAATTCACTG GNCCGTCGGT TTTTANAACC GTCGGTGACT GGGGAAAAAC
601 CCNTGGGCGT TAACCCAANC CTAAATCGGC CTTGGCAGCA AAATTCCCCC TTTTGCCAAG
661 CGGGCGTAAT AGCGANGAGN NCCCACCGAT GCCCTTNCAA CAGTTGCNCN GCCTNNTTGC
721 GNATGGACCC CCCCNGTANG CGCCCCATAA GCGCCNGNCG GNNGGTGGTG GNTACCGCNC
781 NGCGGTGACC GCCTACNNTT NGGCAGCGNC CCCTAGCGNC CCNNNNNTCC TTNNGCTTTT
841 TTTCTTTTCT TTTTNNCCAN NNNNN

B 50.2: Sequencing alignment of cDNA subclone AF21#5 with **mouse cell death-inducing DNA fragmentation factor, alpha subunit-like effector B (Cideb)** by BLAST searching against the National Center for Biotechnology Information database

AF21#5 : 131 gcaccatcaggcttggggctctgcagtgtaccctaggtaaccaagctgactccatcctaac 190
Mouse Cideb: 850 gcaccatcaggcttggggctctgcagtgtaccctaggtaaccaagctgactccatcctaac 909
AF21#5 : 191 agatctgtacactgccttggttcctctggcctgtacatcttcctgaagaatgctacctgtc 250
Mouse Cideb: 910 agatctgcacactgccttggttcctctggcctgtacatcttcctgaagaatgctacctgtc 969
AF21#5 : 251 ttccctccactcctgccttccacataccctgcagaaccacagccttnnccccctgcatncc 310
Mouse Cideb: 970 ttccctccactcctgccttccacataccctgcagaaccacagccttgctccctgcat-cc 1028
AF21#5 : 311 tgatnccccaccgtaatcgctgcttcatctaggttcttactgacgcctacccttaagatnc 370
Mouse Cideb: 1029 tgat-ccccaccgtaatcgctgcttcatctaggttcttactgacgcctacccttaagatcc 1087
AF21#5 : 371 tgcataccaacgggccaactgtccctagctttactacaagataaactttcccct 422
Mouse Cideb: 1088 tgcataccaac-gggccaactgtccctagctttactacaagataaactttcccct 1138

B 50.3: Summary of sequence alignment of cDNA subclone AF21#5 with mouse Cideb

FluoroDD gel AF (AP10 + ARP13)					Subclone I.D.	Sequencing				
Fragment no.	PPARα (+/+)		PPARα (-/-)			FluoroDD fragment size (bp)	Size of insert after <i>Eco</i> RI cut (bp)	Primer	Gene homology to Blast search (Transcript size)	E-value (% Identity)
	CTL	Wy	CTL	Wy						
AF21	+	++	+	+	340	AF21#5	370	M13 reverse	<i>Mus musculus</i> cell death-inducing DNA fragmentation factor, alpha subunit-like effector B (Cideb) (1182 bp)	e-140 285/292 (97%)

Appendix B. DNA sequences and sequencing alignments of FluoroDD fragments

B 51.1: DNA sequence of cDNA subclone AF25#6 (AP10 & ARP13) using M13 forward (-20) primer

1 NNTNNCTCAT ATGGGCNAAT TGGGCCCTAC TAGATGCATG CTCGAGACGG CCGCCAGTGT

61 GATGGATATC TGCAGAATTC GCCCTTAGCG GATA**ACAATT TCACACAGGA GTTGCA**CCAT ARP13

121 CATCCCTTCC TATCCATACA GCATCCCCAG TATAAATTCT GTGATCTGCA TNCCATCCTG

181 TCTCACTGAG AAGTCCAATT CCCAGTCTAT CCACATGTTA CCNTAGGATA CCTCATCAAG

241 AATCAAAGAC TTCTTTAAAT TTCTCTTTGN ATATACCCAT NACAATTTT CATGAATTC

301 TTCCTCTTCC TGTTCAATAA ATGATTACCC TTGCACTAAA AAAAAAGCC CTTATAGTGA

361 GTCGTATTAC AAGGGGCGAA TTCCAGCCAA CCTGGGCGGG CCGTTNACTT AGGTGGGATC

421 CGAAGCCTTC GGGTAACCCC AGCCNTTTGG NTGGCAATNN ACCTTTGGGA AGGTANTTTC

481 CNTANTNAAG GTGGGTTTCA CCCCCTAAAN AATNAGNNCC NTTGTGGNCN NGTTATNAAT

541 TCAAATTGGG NTTCAATTAA GGCCCTTGGT TTTCCCNTNN GGTTNGGTTG NAAAAANTNT

601 GGNTNNNNNT TCCCGCCTCC CACACNCAA NTTTNTCCCA ACACANACCA AACAAATTN

661 ACCGNNANGN GCCNCGGNN NAAGANNCAA NTAAAAAAG

B 51.2: Sequencing alignment of cDNA subclone AF25#6 with **mouse major urinary protein 2 (MUP II)** by BLAST searching against the National Center for Biotechnology Information database

AF25#6 : 115 caccatcatcccttcctatccatacagcatcccagatataaattctgtgatctgcatncc 174

Mouse MUP: 652 caccatcatcccttcctatccatacagcatcccagatataaattctgtgatctgcattcc 711

AF25#6 : 175 atcctgtctcactgagaagtccaattcccagtcctatccacatgttacntagtagacctc 234

Mouse MUP: 712 atcctgtctcactgagaagtccaatt-ccagtcctatccacatgttacc-tagtagacctc 769

AF25#6 : 235 atcaagaatcaaagacttctttaaatttctctttgnatatacccatnacaatttttcatg 294

Mouse MUP: 770 atcaagaatcaaagacttctttaaatttctctttg-atatacccatgacaatttttcatg 828

AF25#6 : 295 aatttcttcctcttctctgttcaataaatgattacccttgact 337

Mouse MUP: 829 aatttcttcctcttctctgttcaataaatgattacccttgact 871

B 51.3: Summary of sequence alignment of cDNA subclone AF25#6 with mouse MUP II

FluoroDD gel AF (AP10 + ARP13)					Subclone I.D.	Sequencing				
Fragment no.	PPARα (+/+)		PPARα (-/-)			FluoroDD fragment size (bp)	Size of insert after <i>Eco</i> RI cut (bp)	Primer	Gene homology to Blast search (Transcript size)	E-value (% Identity)
	CTL	Wy	CTL	Wy						
AF25	++	+	++	++	275	AF25#6	310	M13 forward (-20)	<i>Mus musculus</i> major urinary protein 2 (MUP II) (891 bp)	e-103 218/223 (97%)

Appendix B. DNA sequences and sequencing alignments of FluoroDD fragments

B 52.1: DNA sequence of cDNA subclone AF25#7 (AP10 & ARP13) using M13 reverse primer

1 AGAATACTCA AGCTATGCAT CAAGCTTGGT ACCGAGCTCG GATCCACTAG TAACGGCCGC
61 CAGTGTGCTG GAATTCGCCC TTAGCGGATA ACAATTCAC ACAGGAGTTG CACCATCATC ARP13
121 CCTTCCTATC CATAACAGCAT CCCAGTATA AATTCTGTGA TCTGCATTCC ATCCTGTCTC
181 ACTGAGAAGT CCAATTCCAG TCTATCCACA TGTTACCTAG GATACCTCAT CAAGAATCAA
241 AGACTTCTTT AAATTTCTCT TTGATACACC CTTGACAATT TTTCATGAAT TTCTTCCTCT
301 TCCTGTTCAA TAAATGATTA CCCTTGACACC TAAAAAAAAA AAGCCCTATA GTGAGTCGTA
361 TTACAAGGGC GAATTCTGCA GATATCCATC ACGTGGCGG CCGCTCGAGC ATGCATCTAG
421 AGGGCCCAAT TCGCCCTATA GTGAGTCGTA TNACAATTCA CTGGCCGTCG TTTTACAACG
481 TCGTGACTGG GAAAAACCTT GGCCGTNACC CAACTTAATC GCCTTGACAG CACATCCCCC
541 TTTNGCCAGC TGGCGTAATA GCGAAGAGGC CCGCACCGAT CGCCCTTCCN NACAGTTGCC
601 GCAGCCTGAA TGGCGAATGG ACGCNCNCCT GTAGCGGGNG CATTAAAGNGC GGGGGGGTGT
661 GGTGGTNACC NNCAGNGTGA NNGNTANNTT GCCAGNNCNC TAACGCCGGT CTTTNNNTTT
721 TTTTCCTNNT TTTTGCCAGT TGNNGTNCC NNTNACTTTA NNNGGGGNNN NN

B 52.2: Sequencing alignment of cDNA subclone AF25#7 with **mouse major urinary protein 2 (MUP II)** by BLAST searching against the National Center for Biotechnology Information database

AF25#7 : 111 caccatcatcccttcctatccatacagcatccccagtagataaattctgtgatctgcattcc 170
Mouse MUP: 652 caccatcatcccttcctatccatacagcatccccagtagataaattctgtgatctgcattcc 711
AF25#7 : 171 atcctgtctcactgagaagtccaattccagtcctatccacatgttacctaggatacctcat 230
Mouse MUP: 712 atcctgtctcactgagaagtccaattccagtcctatccacatgttacctaggatacctcat 771
AF25#7 : 231 caagaatcaaagacttctttaatttctcttgatacacccttgacaatttttcatgaat 290
Mouse MUP: 772 caagaatcaaagacttctttaatttctcttgatacacccttgacaatttttcatgaat 831
AF25#7 : 291 ttcttcctcttctctgttcaataaatgattacccttgac 329
Mouse MUP: 832 ttcttcctcttctctgttcaataaatgattacccttgac 870

B 52.3: Summary of sequence alignment of cDNA subclone AF25#7 with mouse MUP II

FluoroDD gel AF (AP10 + ARP13)					Subclone I.D.	Sequencing				
Fragment no.	PPARα (+/+)		PPARα (-/-)			FluoroDD fragment size (bp)	Size of insert after <i>EcoRI</i> cut (bp)	Primer	Gene homology to Blast search (Transcript size)	E-value (% Identity)
	CTL	Wy	CTL	Wy						
AF25	++	+	++	++	275	AF25#7	310	M13 reverse	<i>Mus musculus</i> major urinary protein 2 (MUP II) (891 bp)	e-114 217/219 (99%)

Appendix B. DNA sequences and sequencing alignments of FluoroDD fragments

B 53.1: DNA sequence of cDNA subclone AF30#4 (AP10 & ARP13) using M13 forward (-20) primer

1 GACTCACTAT AGGGCGAATC GGGCCCTCTA NATGCATGCT CGAGCGGCCG CCAGTGTGAT
61 GGATATCTGC AGAATCGCCC TTGTATAGAC **TCACTATAGG GCTTTTTTTT TTAGTATCGG** AP10*
121 GGGTGATCAT AGAGGTCCTC TTCTAATNNT GTGTGCTTAA TTATNATGAT GAAGNTNGGA
181 GTAATCAATC CTCGATGGTC CGGGACATCG GTCGATGTAT GAGGTCGATG ATGTTNGGAG
241 TNATGTNCGG AAGGNAGGGA TNNGGGGTAC CCGGCCAATA TATTAGTTNG TGCCTACCTT
301 NNNAANNGGT GCCAACNTCC CTGGTGGTGN AAANTTGGTT AATCCCGCTT AAAGGGGCNN
361 TANTNCCCAG CCACANCTGG GCNNGCCCGT TAAACTAGTT GGGATCCGAG CCTNNGGTAC
421 CAAGCCCTTG AATGGCATTN NCTTGAAGTT ATNNTTATNA NNTGTTCAAC NNAAANTTAG
481 NCTTGGGCGT TTAATTNNTN GGGTNNNTTA ANNNGGTTTT CNNGGTTGGT TTGAAAATTT
541 GGTTTATAAA AAAAAAAAAA AAANNCCCAA AAAAAAAAAA ANNAAAAAAG CCCNGGGAAA
601 CCCTTTTTTNA GTTTGTTTAA ANNNNTTGGG GGGGGTGGCC CTTAANTTTG AAANTGGAAC
661 CCTAACTTTT CAACTTTTTA ATTNGCGTTN GGGCCCCNTT NNNTGNCCN NATTTTTCTC
721 AATTTTGGGG NNAAANNCTN GNTTNCNTNC CACAACNNG CCTTTTAANT TTAANNNTG
781 GGCCCAANNC CCCCCNGGGG GGAAAANGGC NGNNTTNGGC GNTNTTNNNN NNNNNNNNNN
841 NNNNNNNNNN NNNNNN

B 53.2: Sequencing alignment of cDNA subclone AF30#4 with **mouse mRNA for suppressor of actin mutations (SAC1 gene)** by BLAST searching against the National Center for Biotechnology Information database

AF30#4 : 1 gactcactatagggcgaatcgggccctctanatgcatgctcgagcggccgccagtgtgat 60
Mouse SAC1: 4 gactcactatagggcgaattgggccctctagatgcatgctcgagcggccgccagtgtgat 63
AF30#4 : 61 ggatatctgcagaa-tcgcccttgt 84
Mouse SAC1: 64 ggatatctgcagaattcgcccttgt 88

B 53.3: Summary of sequence alignment of cDNA subclone AF30#4 with mouse SAC1

FluoroDD gel AF (AP10 + ARP13)					Subclone I.D.	Sequencing				
Fragment no.	PPARα (+/+)		PPARα (-/-)			FluoroDD fragment size (bp)	Size of insert after <i>Eco</i> RI cut (bp)	Primer	Gene homology to Blast search (Transcript size)	E-value (% Identity)
	CTL	Wy	CTL	Wy						
AF30	+	++	+	+	240	AF30#4	290	M13 forward (-20)	<i>Mus musculus</i> mRNA for suppressor of actin mutations (SAC1 gene) (2029 bp)	1e-29 82/85 (96%)

* Sequence of primer was not completely matched with the expected sequence.

Appendix B. DNA sequences and sequencing alignments of FluoroDD fragments

B 54.1: DNA sequence of cDNA subclone AF30#5 (AP10 & ARP13) using M13 reverse primer

1 ANNTNNTNTT ANNGTGANAN NCATAGAAAT ANCTACAAGN NCTNATGCAT CAAGCNTTGN
61 GNTACAGCAN CANCNGGCAT NCACAATNAN NTNACAAGGC CNGNCAANNT GTGCATGGCA
121 ANNAGCCCAT TNNCAGGCAT **ANCCAATTTT** **AACAACAAGG** **NAGTNGCNAN** **CCAAT**CNATT ARP13*
181 CNAAGTAGNN CAACTATATA TTGCCGCTAC CCAATCCCT CCTTCCAACA TAACTCCAGC
241 ATCATCAACC TCATACATCA ACCAATCTCC CAAACCATCA AGATTAATTA CTCCAACCTC
301 ATCATAATAA TTAAGCACAC AAATTAATAA AACCTCTATA ATCACCCCCA ATAC**CTAAAA** AP10
361 **AAAAAAGCCC** **TATAGTGAGT** **CGTATTACAA** GGGCCAATTC TGCAGATATC CATCANACTG
421 GCGGCCGCTC NAGAATGCAT TTAAGAGGNN CCAATNCCG CCCCNNNNNG TGGANGTTNG
481 NTATNNACAA ATTTTCAANN TNGGGCCCGG TTTGGTNTTT TTAACANAAA CCGTNTTNGG
541 TNGGAAACNT TGGGGGNAAA AAAAAACCCC CCTNGGGNAC CGTTTTAAAC CCCCCAAAAN
601 NCCTTTTAAA ATTTTNCGGC CCCNTTTGGG NNANGGACAA AAANANTTNT TCCCCCCCCA
661 NTTTTNTTTA GGGCNCNCAA GGCCNNTTGG GGNNCNGNNT ATAANTTNAA NNNCCNGGNA
721 NNNANAANNN GGNGCCCCC CGGGCAAAAA CCNCNGGNNN ATTTTCGGGG CCCACCCCTT
781 GTNNNNNNNN AAAAAANAG GNNTTTTGGG GGNNNNNNNN NNNNNNNNTN GGNNAAANNNT
841 NGNNGGGGGG NNNNNANNNN NTTNNGNGGG NNNNNNNNNN NNNCCNNNNN NNNNCCTTNT
901 NTTGTNNNTN TTAA

B 54.2: Sequencing alignment of cDNA subclone AF30#5 with **mouse mitochondrion** by BLAST searching against the National Center for Biotechnology Information database

AF30#5 : 183 aagtagnncaactatatattgccgctaccccaatccctccttccaacataactccagcat 242
Mouse mitochondrion: 13624 aagtagcacactatatattgccgctaccccaatccctccttccaacataactccaacat 13683
AF30#5 : 243 catcaacctcatacatcaaccaatctcccaaacatcaagattaattactccaacttcat 302
Mouse mitochondrion: 13684 catcaacctcatacatcaaccaatctcccaaacatcaagattaattactccaacttcat 13743
AF30#5 : 303 cataataattaagcacacaaaatnnnnnnnccctctataatcacccccaatact 355
Mouse mitochondrion: 13744 cataataattaagcacacaaaattaaaaaacctctataatcacccccaatact 13796

B 54.3: Summary of sequence alignment of cDNA subclone AF30#5 with **mouse mitochondrion**

FluoroDD gel AF (AP10 + ARP13)					Subclone I.D.	Sequencing				
Fragment no.	PPARα (+/+)		PPARα (-/-)			FluoroDD fragment size (bp)	Size of insert after <i>Eco</i> RI cut (bp)	Primer	Gene homology to Blast search (Transcript size)	E-value (% Identity)
	CTL	Wy	CTL	Wy						
AF30	+	++	+	+	240	AF30#5	290	M13 reverse	<i>Mus musculus</i> clone LA9 mitochondrion, complete genome (16300 bp)	1e-72 170/173 (98%)

* Sequence of primer was not completely matched with the expected sequence.

Appendix B. DNA sequences and sequencing alignments of FluoroDD fragments

B 55.1: DNA sequence of cDNA subclone AH1#6 (AP11 & ARP19) using M13 forward (-20) primer

1 CCTCACTATA GGGCGAATNG GGCCCTCTAG ATGCATGCTC GAGCGGCCGC CAGTGTGATG
61 GATNTCTGCA GAATTCGCCC TTAGCGGATA **ACAATTTTAC** **ACAGGATTTT** **GGCTCCCCTG** ARP19
121 CAGAAATCCC AAGCCCTGAT GTGTACTGCC TGCTCTTTAG CTCTCCTGAT TTAGTGATTT
181 ATGAGGACCT CGGGAGCATG ACACTTGCTG TATGACTCCT ACATCCATAG ATCCTTAAAA
241 TCACATCTCA TGATGCTGAT AGAAGATTTT AAGAAAGATA TTAATAACCC CCTTGAAAAA
301 ATACAGGAGA ACAGATTTAA AAGGGAGAAG GTTTTAAAGA GAAAAACACAA AAATCCATTA
361 AAAAATTACA AGAAAACACA ACCAAACAGG TGAAGGAATT GAACAAAACCT ATCCAGGATC
421 TAAAAATGGA AGTAGAAACA ATACAGGAAT CACAATGGGA GAAAACTTCA GAGATATAAA
481 TCCTAGGAAA GAGATCAGAA GTCATAGATT CAGGCATCAC CAAAAGAATA CAAGAAATAG
541 AAGAGAGACT TTCATGTACA GAAGATACCA TAGAAAACAT TGACACAACA GTCAAAGAAA
601 GTGCAAAATG CAAAAACTTT CTAAC TCAA ACATCCAAGC AATCCAGAAC GCAATGAGAA
661 GAACAACCTT AAGGATAACA NGNATAGANA AGANCAAAAA TNCCNAACTN AANNGGCCAG
721 TAAATATTNN CAACAAAANT AGAAAAANANA ACATT CNGAN NNTAAANGAT AAAAAAAAAG
781 CCTANNGTGA GTNNNTACA GGGCNAATNC ANCCANNGGC GCCGTTACTN TNNATCNANC
841 TNGGNNC

B 55.2: Sequencing alignment of cDNA subclone **AH1#6** with **mouse EST** by BLAST searching against the National Center for Biotechnology Information database

AH1#6 : 237 aaaatcacatctcatgatgctgatagaagattttaagaaagatattaataaccccccttga 296
Mouse EST: 16 aaaatcacttctcatgatgatgatagaggaatttaaaaaggacataaataaactccttta 75
AH1#6 : 297 aa-aaatacaggagaacagattttaa-agggagaaggttttaagagaaaacacaaaaat 354
Mouse EST: 76 aagaaatacaggagaacacaggttaaacagctagaagcccttaagaggaaacacaaaaat 135
AH1#6 : 355 ccattaaaaaattacaagaaaacacaaacacaggtgaaggaattgaacaaaactatcc 414
Mouse EST: 136 cccttaagagttacaggaaaacacaatcaaacaggtgaaggaaatgaacaaaaccatcc 195
AH1#6 : 415 aggatctaaaaatggaagtagaaacaatacaggaatcacatgggagaaaacttcagaga 474
Mouse EST: 196 aagatctaaaaatggaactagaaacaataaagaaatcacaaaggagacaaccctggagt 255
AH1#6 : 475 tataaatcctaggaaagagatcagaagtcatagatcaggcatcaccaaaagaataacaag 534
Mouse EST: 256 tagaaaacctaggaaagagatcaggagtcatagatgcaagcatcaccaacagaataacaag 315
AH1#6 : 535 aaatagaagagagacttttca---tgtacagaagataccatagaaaacattgacacaacag 591
Mouse EST: 316 acatagaagagagaatctcagagggtgcggaagataccatagaaaacattgacacaacag 375
AH1#6 : 592 tcaaagaaagtgcaaaatgcaaaaactttctaactcaaaacatccaagcaatccagaacg 651
Mouse EST: 376 tcaaagaaaatgcaaaaacaaaaagctcctaaccctaaacatctgggaaatccaggaca 435
AH1#6 : 652 caatgagaagaacaaccctaaggataa 678
Mouse EST: 436 caatgagaagaccaaacctaaggataa 462

B 55.3: Summary of sequence alignment of cDNA subclone AH1#6 with mouse EST

FluoroDD gel AH (AP11 + ARP19)					Subclone I.D.	Sequencing			
Fragment no.	PPARα (+/+)		PPARα (-/-)			Size of insert after <i>Eco</i> RI cut (bp)	Primer	Gene homology to Blast search (Transcript size)	E-value (% Identity)
	CTL	Wy	CTL	Wy					
AH1	+	-	+	+	720	AH1#6	750	vm09c03.r1 Knowles Solter mouse blastocyst B1 <i>Mus musculus</i> cDNA clone IMAGE:989668 5' similar to gb:U15647_cds1 <i>Mus musculus</i> (624 bp)	2e-82 377/447 (84%)

Appendix B. DNA sequences and sequencing alignments of FluoroDD fragments

B 56.1: DNA sequence of cDNA subclone **AI1#5** (AP6 & ARP4) using **M13 forward (-20)** primer

1 GGGCCCTCTA GATGCATGCT CGAGCGGCCG CCAGTGTGAT GGATATCTGC AGAATTCGCC
61 CTTAGCGGAT **AACAATTTCA CACAGGAGCT AGCAGACCCA** GGAATGATC AAGGAACTCA **ARP4**
121 TCTCAGAACT GGATGAGAGG ACATTGATGG TGCTGGTGAA TTACATCTAC TTAAAGGCA
181 AATGGAAGAT ATCCTTTGAC CCCCAGGACA CATTGAGTC TGAGTTCTAC TTGGATGAGA
241 AGAGATCTGT GAAGGTNCCC ATGATGAAAA TGAAGTTACT GACCACNACG CCACTTCCGT
301 GATGAGGAGC TATCGGTGCT CTGTGTTGGA GCCGAAGTAC ACAGGAANAT GCCAGCGNNC
361 TGCTNCATCC TCCCTGACCA GGGCAGGATG CANNNCAGGT GGAAGCCAGC TTACAACCAG
421 NAGACCCTGA GGAAATGGAN GGAAACTNT TGTCNTCCCA NCCAAATATG AGGATNCTAA
481 ACCTGCCCCCT AGTNCNNCAN CGCCTATTAA CTTCAGGNTT GGANGACGAT TTCCTNNNAN
541 ANGTGTGGAT TAAGGAANNT NNCANNGATA CATTCTGACC CATCTGTGGA TCTCATGAAA
601 CCGGGGATNC TTGTGNTGNT GTCTCAANGT GGTCCCAATC GTGNCTATTN CATTGCATGT
661 GGTAATGNAC ACNNNTCTCN CNANCCTAGT TTGGTTGCTA CNNAGGGTAA TTGNATNNNC
721 NTTTCATAAG GGGCNCNTANT ACCNANGCA

B 56.2: Sequencing alignment of cDNA subclone **AI1#5** with **mouse serine (or cysteine) proteinase inhibitor (SPI)** by BLAST searching against the National Center for Biotechnology Information database

AI1#5 : 93 cagacccaggggaatgatcaaggaactcatctcagaactggatgagaggacattgatggtg 152
Mouse SPI: 610 cagacccaggggaatgatcaaggaactcatctcagaactggatgagaggacattgatggtg 669
AI1#5 : 153 ctggtgaattacatctactttaaggcaaatggaagatatcctttgacccccaggacaca 212
Mouse SPI: 670 ctggtgaattacatctactttaaggcaaatggaagatatcctttgacccccaggacaca 729
AI1#5 : 213 tttgagtctgagtttctacttggatgagaagagatctgtgaaggtncccatgatgaaaatg 272
Mouse SPI: 730 tttgagtctgagtttctacttggatgagaagagatctgtgaaggttcccatgatgaaaatg 789
AI1#5 : 273 aagttactgaccacnacgccacttccgtgatgaggagctatcggtgctctgtgttggagc 332
Mouse SPI: 790 aagttactgaccac-acgccacttccgtgatgaggagctatc-gtgctctgtgttggagc 847
AI1#5 : 333 cgaagtacacaggaanatgccagcgnnctgctncatcctccctgaccagggcaggatgca 392
Mouse SPI: 848 tgaagtacacaggaa-atgccagcgccttgcct-catcctccctgaccagggcaggatgca 905
AI1#5 : 393 nnncaggtggaagccagcttacaaccagnagaccctgaggaaatgganggaaaact 448
Mouse SPI: 906 --gcaggtggaagccagcttacaaccag-agaccctgaggaaatgga-ggaaaact 957

B 56.3: Summary of sequence alignment of cDNA subclone **AI1#5** with **mouse SPI**

FluoroDD gel AI (AP6 + ARP4)					Subclone I.D.	Sequencing				
Fragment no.	PPARα (+/+)		PPARα (-/-)			Size of insert after <i>Eco</i> RI cut (bp)	Primer	Gene homology to Blast search (Transcript size)	E-value (% Identity)	
	CTL	Wy	CTL	Wy						
AI1	+	-	+	+	1100	AI1#5	1110	M13 forward (-20)	<i>Mus musculus</i> serine (or cysteine) proteinase inhibitor clade A, member 3K (Spi2) (1645 bp)	0 343/356 (96%)

Appendix B. DNA sequences and sequencing alignments of FluoroDD fragments

B 57.1: DNA sequence of cDNA subclone AI1#5 (AP6 & ARP4) using M13 reverse primer

1 GGNCNTATTT AGGTGACACT ATAGAATACT CAAGCTATGC ATCAAGCTTG GTACCGAGCT
61 CGGATCCACT AGTAACGGCC GCCAGTGTGC TGAATTCGC CCTTGTAATA **CGACTCACTA** AP6
121 **TAGGGCTTTT TTTTTTTTCC** CGGTATTGGA ACTCTGTGTA TTTGCAAATG CCTAGGTTTG
181 GGGTACAGAC ACATAAAGAG GAGTCACCCG GGAAGAAGAA TAAAGGCAGA TTCCAGGTNC
241 AGAAATATGC ACAGATGCTC CCAAGACAAC CGAGAGCCTG ACACTGAGAG TCCAAAGTCT
301 TATGTGCATG TGGGATCACA GAGATAGTTA ANTGTACCTG TCTAAGNCCA ACTTTGCAAC
361 AGCCAANTCA GAGCTTGAAT GACAGGATGT ATATNNGAGA TCCACATGCA NNACTTTGTN
421 NCCACAGCCC TGNNACAGNA ACCCATGAGN AACTTGGNTG AGCTTTTNGG TNNTACTTGG
481 GNGTNATTCT ACTTTGGCCC NTANAANGAG NGATACTCTT TATCCATCTT NGNNGTGTAT
541 AATNANTAAT TCANNAACAT TGTAANTGG GCCCCCNNGT AGAAAAATTN GNNATCAGNC
601 NTATNNGGTN AANNTTNGTT CCCCTTACCC AAATTGNCNT TTCCCTTTNT TCCCCNTTT
661 GGTTANGNTC ATTCTGCCAT NNNNTNGNN TTGNTNNATN NNTTTNNTNT TTNNNNNCTC
721 NNNNNNTTTT TTNNNANNCA TCCTTNATTA TCNANNCGNN CANCTTTNTT NTCGGNGNTT
781 TCTNCGGGNN GGANTCCCN NAAATNNNTT NNNTNNNTAN GNANTNNNA ATNNTNN

B 57.2: Sequencing alignment of cDNA subclone **AI1#5** with **mouse serine (or cysteine) proteinase inhibitor (SPI)** by BLAST searching against the National Center for Biotechnology Information database

AI1#5 : 142 ggtattggaactctgtgtatttgcaaatgcctaggtttggggtacagacacataaagagg 201
Mouse SPI: 1629 ggtattggaactctgtgtatttgcaaatgcctaggtttggggtacagacacataaagagg 1570
AI1#5 : 202 agtcaccccggaagaagaataaaggcagattccaggtncagaaatatgcacagatgctcc 261
Mouse SPI: 1569 agtcaccccggaagaagaataaaggcagattccaggttcagaaatatgcacagatgctcc 1510
AI1#5 : 262 caagacaaccgagagcctgacactgagagtccaaagtcttatgtgcatgtgggatcacag 321
Mouse SPI: 1509 caagacaaccgagagcctgacactgagagtccaaagtcttatgtgcatgtgggatcacag 1450
AI1#5 : 322 agatagttaantgtacctgtctaagnccaactttgcaacagccaantcagagcttgaatg 381
Mouse SPI: 1449 agatagttaa-tgtagctgtctaag-ccaactttgcaacagccaa-tcagagcttgaatg 1393
AI1#5 : 382 acaggatgtatatnngagatccacatgca 410
Mouse SPI: 1392 acaggatgtatata-gagatccacatgca 1365

B 57.3: Summary of sequence alignment of cDNA subclone AI1#5 with mouse SPI

FluoroDD gel AI (AP6 + ARP4)					Subclone I.D.	Sequencing				
Fragment no.	PPARα (+/+)		PPARα (-/-)			FluoroDD fragment size (bp)	Size of insert after <i>Eco</i> RI cut (bp)	Primer	Gene homology to Blast search (Transcript size)	E-value (% Identity)
	CTL	Wy	CTL	Wy						
AI1	+	-	+	+	1100	AI1#5	1110	M13 reverse	<i>Mus musculus</i> serine (or cysteine) proteinase inhibitor clade A, member 3K (Spi2) (1645 bp)	e-123 262/269 (97%)

Appendix B. DNA sequences and sequencing alignments of FluoroDD fragments

B 58.1: DNA sequence of cDNA subclone AI18#6 (AP6 & ARP4) using M13 forward (-20) primer

1 CCNTCCACTA TNNGGCGAAT NNCGGGGCCCT ACTAGATGCT GCTCAGACGG CCGCNNGNGT
61 GAATGGATTT CTGNNGAANT TCGNCCCTTG NTAAAT**ACGA CCTCACTATA GGGCTTTTTT** AP6
121 **TTTTTTCCT** GTTCTTTCAG GGACTTCACC TTTATTGGGG ACGACCGCTT TGGGTGGGAC
181 GGGATCTAGG GCTCCTGGGC TTGCCAAGTA GGGCCCGCAC CTGCCTGATC TGCCATTCTGA
241 CACTGGATTT CGCTGTGCCA CCCAAGGCAC TGTACTGTTT CACGCTGTGA CTGTAGTCCC
301 ACACGTGACT CACATCACCT GAGAACAGGG GACTGATGGT CTGCTAGCTC CTGTGTGAAA
361 TTGTATCCGC TAAGGGCGAA TTCCAGACAC ACTGGCGGCC GTTACTAGTG GATCCCGAGC
421 TCCGGTACCC AAGCTTGATG CATAAGCTTG AGTATCCCTA TAGTGTACAC TAAATAGCT
481 GGGCGTAATC ATGGTCATAG CTGTNNCTTG TGTGAAATTG TTATCCGCTC ACAATNCCAC
541 ACAACATACG AGCCGGAAGC ATAAAGTGTA AAGCCTGGGG NGCCTAATGA GTGACCTAAA
601 CTTNAATTAA TNGCGTTGCG CTCCCTGCCC GCTTCCCAGT NNGGAAACC TGTTGTGCCA
661 GCTGCATTAN TGAATTGGGC ANNGCGCGGG GAGAGGCGGT TNGGNTNTGG GNCNNNTTTC
721 GNTTNTNNT NNTGANNTGC TGNGCTNGNT NTTNGGTGNG NNANGGTNTT NNTNNTTNNN
781 GGTAATNNGT NTNNNNAATN NNNATNNNCC GAAATTNTNA CCAGGGNCA AGGCAAACCTT
841 ANNGNGNNTN TT

B 58.2: Sequencing alignment of cDNA subclone AI18#6 with **mouse argininosuccinate lyase (Asl)** by BLAST searching against the National Center for Biotechnology Information database

AI18#6 : 167 gcttttgggtgggacgggatctagggctcctgggcttgccaagtagggcccgacactgcct 226
Mouse Asl: 1494 gcttttgggtggg-cgggatctagggctcctgggcttgcc--agtagggcccgacactgcct 1438
AI18#6 : 227 gatctgccattcgacactggatttcgctgtgccacccaaggcactgtactgttccacgct 286
Mouse Asl: 1437 gatctgccattcgacactggatttcgctgtgccacccaaggcactgtactgttccacgct 1378
AI18#6 : 287 gtgactgtagtccacacgtgactcacatcacctgagaaacaggggactgatggtctgccta 346
Mouse Asl: 1377 gtgactgtagtccacacgtgactcacatcacctgagaaacaggggactgatggtctgc-a 1319
AI18#6 : 347 gctcctgt 354
Mouse Asl: 1318 gctcctgt 1311

B 58.3: Summary of sequence alignment of cDNA subclone AI18#6 with mouse Asl

FluoroDD gel AI (AP6 + ARP4)					Subclone I.D.	Sequencing			
Fragment no.	PPARα (+/+)		PPARα (-/-)			Size of insert after <i>Eco</i> RI cut (bp)	Primer	Gene homology to Blast search (Transcript size)	E-value (% Identity)
	CTL	Wy	CTL	Wy					
AI18	++	+	++	++	270	AI18#6	300	M13 forward (-20)	<i>Mus musculus</i> argininosuccinate lyase (Asl) (1589 bp) 6e-84 184/188 (97%)

Appendix B. DNA sequences and sequencing alignments of FluoroDD fragments

B 59.1: DNA sequence of cDNA subclone AI18#6 (AP6 & ARP4) using M13 reverse primer

1 NCNTATTTAG GTGACACTAT AGAATACTCA AGCTATGCAT CAAGCTTGGT ACCGAGCTCG
61 GATCCACTAG TAACGGCCGC CAGTGTGCTG GAATTCGCCC TTAGCGGATA **ACAATTTCAC** ARP4
121 **ACAGGAGCTA GCAGACC**ATC AGTCCCCTGT TCTCAGGTGA TGTGAGTCAC GTGTGGGACT
181 ACAGTCACAG CGTGGAACAG TACAGTGCCT TGGGTGGCAC AGCGAAATCC AGTGTGGAAT
241 GGCAGATCAG GCAGGTGCGG GCCCTACTGC AAGCCCAGGA GCCCTAGATC CCGCCCACCC
301 AAAGCTGCTC CCCAATAAAG TGAAGCCCTG AAGAAACAGG **AAAAAAAAAA AAGCCCTATA** AP6
361 **GTGAGTCGTA** TCACAAGGGC GAATNNCTGC AGATATCCAT CACAACCTGGC GGCCGCTCGA
421 GCATGCCATC TAGAGGGCCC CAATTNCCGC CCTATAGTGA GTCGTATTAC AATTCCTGCTG
481 NCCGTCGTTT TACAACGTGG TGAAGTGGNGA AAACCCCTGGC GTTACCCAAC TTAATTGCTCT
541 TGCAGCACAT CCCCCTTNCG CCAGCTGGCG TAATAACGAA GAGGCNNGAA CCGATCGCCC
601 TTNCCAACAG TNGGCCNCG TGAATGGCGA ATGGACCCCC CCTGTAGNNC CCCATTAAGC
661 GCNGGNGGTG GTGGTGGTAA CCCCNNNNNT GAACGTTNNA CTTNGCCAAG GNNNNTANNC
721 NNNNNTTTCT TTTTTTTTTT TCCCCNTTCT TTTTNNNCAA NNNTTGGCGG GCTTTCACAC
781 TTNNNCCNNT TNNNTTGGGG GCTCCNTTTN NGNNNNNTNT NNNNNNNNAN NNNCTNACTN
841 NNNNNNTGN NN

B 59.2: Sequencing alignment of cDNA subclone AI18#6 with **mouse argininosuccinate lyase (Asl)** by BLAST searching against the National Center for Biotechnology Information database

AI18#6 : 121 acaggagctagcagaccatcagtcacctgttctcaggtgatgtgagtcacgtgtgggact 180
Mouse Asl: 1311 acaggagct-gcagaccatcagtcacctgttctcaggtgatgtgagtcacgtgtgggact 1369
AI18#6 : 181 acagtcacagcgtggaacagtcacagtcgcttgggtggcacagcgaaatccagtgctgaat 240
Mouse Asl: 1370 acagtcacagcgtggaacagtcacagtcgcttgggtggcacagcgaaatccagtgctgaat 1429
AI18#6 : 241 ggcagatcaggcaggtgcgggccctactgcaagcccaggagccctagatcccggccaccc 300
Mouse Asl: 1430 ggcagatcaggcaggtgcgggccctactgcaagcccaggagccctagatcccggccaccc 1489
AI18#6 : 301 aaagctgctccccaataaaagtgaagccctgaagaaac 337
Mouse Asl: 1490 aaagctgctccccaataaaagtggagccctgaagaaac 1526

B 59.3: Summary of sequence alignment of cDNA subclone AI18#6 with mouse Asl

FluoroDD gel AI (AP6 + ARP4)					Subclone I.D.	Sequencing				
Fragment no.	PPARα (+/+)		PPARα (-/-)			FluoroDD fragment size (bp)	Size of insert after <i>Eco</i> RI cut (bp)	Primer	Gene homology to Blast search (Transcript size)	E-value (% Identity)
	CTL	Wy	CTL	Wy						
AI18	++	+	++	++	270	AI18#6	300	M13 reverse	<i>Mus musculus</i> argininosuccinate lyase (Asl) (1589 bp)	e-110 215/217 (99%)

Appendix B. DNA sequences and sequencing alignments of FluoroDD fragments

B 60.1: DNA sequence of cDNA subclone AJ1#4 (AP6 & ARP14) using M13 forward (-20) primer

1 CNTCACTATA GGGCGAATTG GGCCCTCTAG ATGCNTGCTC GAGCGGCCGC CAGTGTGATG
61 GATATCTGCA GAATTCGCCC TTGTAAT**ACG ACTCACTATA GGGCTTTTTT TTTTTTCCTC** AP6
121 TGAAGAGCTT TATTAATGTG CTGGACTGTA CCATACAGCA AGGGTNCAAG TCACTTTAGG
181 AAGAAACAGC AGTATGTTCA ATGATCAAGA AGTAGAAACC AGATTGGTAA CATNTAGTGG
241 TCCACCATAC TGGTCTTNNa GGGGCTGACG ATTTAAGAAA CATGGGCTCA CAGCAGCATG
301 GTCCAAGCTA AAGTCTCTGA ACAGAAACCA AAAGANGTGG TAGTTGCCCT GCTTGGGATC
361 CTACTANNCT TGGGNNNGCC CCAGTCAAGG ANGGTNCAAG TTANGTCTGG CCCTCANAGC
421 TCCTCTGGGA ACTTNCCTGC TTCTCTGCTC TCCGTGCCAT TCTGANNNTT CTTGGCAGTN
481 TCTCTGTCCA NACTGTACCC GACCCTCTTT NNCTCACCCC ATCCGTGTNN TAAACATCTC
541 CAGTATGTNC TACTGTNNAT NGGCCAAGAG CACCCTGCCT GGGATNCCGG CTGCACTGCC
601 CTTGGGCATA TGTTAGCCAC TGCTNCTCCC TGTNNCCGGN ANGCCAGAGG ACCTCTCANT
661 GAGAAGACCC AAAACANNCT TNCNGAGATG TCACNTCCCA GCGCTGACT

B 60.2: Sequencing alignment of cDNA subclone AJ1#4 with **mouse carboxylesterase** by BLAST searching against the National Center for Biotechnology Information database

AJ1#4 : 117 cctctgaagagctttattaatgtgctggactgtaccatacagcaagggttcaagtcactt 176
Mouse carboxylesterase: 2005 cctctgaagagctttattaatgtgctggactgtaccatacagcaagggttcaagtcactt 1946
AJ1#4 : 177 taggaagaaacagcagtatgttcaatgatcaagaagtagaaaccagattggtaacatnta 236
Mouse carboxylesterase: 1945 taggaagaaacagcagtatgttcaatgatcaagaagtagaaaccagattggtaacattta 1886
AJ1#4 : 237 gtggtccaccatactgggtctttnaggggctgacgatttaagaaacatgggctcacagcag 296
Mouse carboxylesterase: 1885 gtggtccaccatactgggtctttnaggggctgacgatttaagaaacatgggctcacagcag 1826
AJ1#4 : 297 catggtccaagctaaagtctctgaacagaaacaaaaagangtggttagttgccttgcttg 356
Mouse carboxylesterase: 1825 catggtccaggctaaagtctctgaacagaaacaaaaagaagttgtagttgccttgctt-g 1767
AJ1#4 : 357 gatcctactanncttgggnnngcccagtcagganggttcaagttangtctggccctca 416
Mouse carboxylesterase: 1766 gatgctactattcttgggttg-cccagtc-aggaaggtcc-aggtaggtctgg-gctca 1711
AJ1#4 : 417 nagctcctctgggaacttncctgcttctctgctctccgtgccattct--gannnttcttg 474
Mouse carboxylesterase: 1710 gagctcctct-ggaactttctgcttctctgctctcggtgccattcttgaatttttcttg 1652
AJ1#4 : 475 gcagtnctctgtcca-nactgtacccgaccct 506
Mouse carboxylesterase: 1651 gcagtgctctgtgccagaactgtagccgaccct 1619

B 60.3: Summary of sequence alignment of cDNA subclone AJ1#4 with mouse carboxylesterase

FluoroDD gel AJ (AP6 + ARP14)					Subclone I.D.	Sequencing				
Fragment no.	PPARα (+/+)		PPARα (-/-)			FluoroDD fragment size (bp)	Size of insert after <i>Eco</i> RI cut (bp)	Primer	Gene homology to Blast search (Transcript size)	E-value (% Identity)
	CTL	Wy	CTL	Wy						
AJ1	++	+	++	++	1200	AJ1#4	990+220	M13 forward (-20)	Mouse carboxylesterase (Carboxylesterase) (2006 bp)	e-123 354/393 (90%)

Appendix B. DNA sequences and sequencing alignments of FluoroDD fragments

B 61.1: DNA sequence of cDNA subclone AJ1#5 (AP6 & ARP14) using M13 reverse primer

1 GNNCATTTAG GTGANCCTAT AGAATACTCA AGACTATGCA TCAAGCTTGG TACCGAGCTC
61 GGATCCACTA GTAACGGCCG CCAGTGTGCT GGAATTCGCC CTTAGCGGAT **AACAATTTCA** ARP14
121 **CACAGGATCC ATGACTC**CTT CTTCCCACAA AGGCCCCAGA AGCTCCTAGN CAAACAAGNC
181 AATTCCCCAC TGTGCCCTAC CTCTTGGGAG TCACCAACCA TGAGTTTGGC TGGCCTTCTA
241 NCTCAAATTC TGGAATATCC TGGATAAGAT GGAACCATTT GAGACCAGGA AGACCTGTTG
301 GAGAATTCAA GGCCCTTATT AGACCNCATA TGCCACTGCC CCCTGAGATC ATGCCCNCC
361 GTCATAGATG ANNACCTAGA CAATGGCTCA NGATGAATCA GCTACCAGGT ATGCCCTCCA
421 GGAATTGCTG GGTGATATCA CATNGGTCAT TCCTACCCTN GNNCTTCTCA AAATACCCTN
481 AAAGATGCTG GGNTGCCCCCT GTTTTCTTGG TAACGANGTN NCANGCATAC ANCCCANGTT
541 NCTTTTTTGNC AAAGGTTNCA AGCCCAAGCC TGGGGNTGAA AGGNCTGAAC CATTCCCTCN
601 TGAGNAATGN CCTTTGTTTT TTGGGAANNT TCNTTTTCCT NNCTGATTGA GANNTTTCCC
661 CTCCTGGCCC TTCCCNAGAN GGCCAACNGA AGNNAAAAAA AANGCANNT NGAGCCCTGA
721 CCCNTTGANT GGGNCNCAAT TGGGNNACCN NNTNTNTTGG ACNNCCCCCN NGGGAAAAAA
781 TTNACAACAA AANAGNNNA AAANNNGGG GNGNGTGGGG CCNTTNCNC TTTGNGGG

B 61.2: Sequencing alignment of cDNA subclone AJ1#5 with **mouse carboxylesterase** by BLAST searching against the National Center for Biotechnology Information database

AJ1#5 : 131 atgactccttcttccacaaaggccccagaagctcctagncaaacaagncaattccccac 190
Mouse carboxylesterase: 947 atgactccttcttccacaaaggccccagaagctcctag-caaacaag-caattccccac 1004
AJ1#5 : 191 tgtgccctacctcttgggagtcaccaaccatgagtttggtggccttctanctcaaattc 250
Mouse carboxylesterase: 1005 tgtgccctacctcttgggagtcaccaaccatgagtttggtggc-ttcta-ctcaaattc 1062
AJ1#5 : 251 tggaaatatcctggataagatggaaccatttgagaccaggaagacctgttgagaattcaa 310
Mouse carboxylesterase: 1063 tggaaatatcctggataagatggaac-atttgag-ccaggaagacctgttgagaattcaa 1120
AJ1#5 : 311 ggcccttatttagaccncatagccactgccccctgagatcatgcccnnccgtcatagatg 370
Mouse carboxylesterase: 1121 ggcccttatttag--cccatatgcaactgccccctgagatcatgccc-a-cggtcatagatg 1177
AJ1#5 : 371 annacctagacaatggctcangatgaatcagctaccaggtatgcctccaggaattgctg 430
Mouse carboxylesterase: 1178 aatacctagacaatggctca-gatgaatcagctacaaggtatgcctccaggaattgctg 1236
AJ1#5 : 431 ggtgatatcacatnggtcattcctaccctngncttctcaaaataacctnaaagatgctg 490
Mouse carboxylesterase: 1237 ggtgatatcacattggtcattccta-ccttgatcttctcaaaata-ccttcaagatgctg 1294
AJ1#5 : 491 ggntgccccctgttttcttg 509
Mouse carboxylesterase: 1295 gg-tg-ccctgttttcttg 1311

B 61.3: Summary of sequence alignment of cDNA subclone AJ1#5 with **mouse carboxylesterase**

FluoroDD gel AJ (AP6 + ARP14)					Subclone I.D.	Sequencing				
Fragment no.	PPARα (+/+)		PPARα (-/-)			Size of insert after <i>Eco</i> RI cut (bp)	Primer	Gene homology to Blast search (Transcript size)	E-value (% Identity)	
	CTL	Wy	CTL	Wy						
AJ1	++	+	++	++	1200	AJ1#5	990+220	M13 reverse	Mouse carboxylesterase (Carboxylesterase) (2006 bp)	e-127 353/379 (93%)

Appendix B. DNA sequences and sequencing alignments of FluoroDD fragments

B 62.1: DNA sequence of cDNA subclone **AJ2#10** (AP6 & ARP14) using M13 forward (-20) primer

1 NNATAGGGCG AATNGGGCCT CTAGATGCAT GCTCGAGACG GCCGCCAGTG TGATGGATAT

61 CTGCAGAATN NCGCCCTTAG CGGATA**ACAT** **TTCACACAGG** **ATCCATGACT** **CCACTTCCTG** ARP14

121 ACACAGCTAA GTTGCTTGTC TTTACCTCCA GGCTTTCGGC CGTTGCCTGG ACTTCAATCA

181 TGGTGGCTGA CCTTCCCTTT CTTGCTTTGC TTCTCCTCAA AGAGATAATA GAGACAATGA

241 CCAGTCTTTC CTCATAGATC AAGTATGGGG AGAGCCCTCA GCTATGGTAT TCCTGTATTT

301 TGGTGACTTA TTTAAGTAAA TTTCTGGGGA CAATCCAGAT TTGAAAGATT CTGTCTTCTT

361 GTNGTCATAA ACTATTAAAA TGCTTGGTGG TCACCAAAGT ATTTGACATA AAAATAAATA

421 AATAAATCAT TCAGGCCACC TTTTACACCA GAAATCACAG GAAAGCCCTG GGCCCCAGCC

481 ATCTGCTGAG TGTTAGTNGA GAAGATGGAT CCTAAGCCAG CTGAAGACTG AGTGCAGGCT

541 GTGGGGAGGT TCTTGCTGAG TAGCTGGCTT TGTGGTAAGC TGCTAGCAGC CTTACAGNGG

601 TGGCGAAGCA GCCCCCCTT NGGATGCAGA GCAGCCNTCT ACAATNATTN NTGACCNTNA

661 AAGGTAGANN ATNGNACNTT TTTGTNGGTA TGTGTGTGNT NTGCNTCTCT NCTATTNNAG

721 NTGANTTTTT TTTTNNNTGA GAACNNNGNC CCCAGAGNTN GGCCNTGNAN CTNNTGANTN

781 CNTCAGNNNT NCCANANGNN NNNNGGTTAA NNGNTTNGNN CTGANNNNNN NGNNTAGNTG

841 GNACCTTTNG NTTTAANGAC AAGNTAAGAA ATTTGTGANC NTTT

B 62.2: Sequencing alignment of cDNA subclone **AJ2#10** with **peroxisomal acyl-coA oxidase (AOX)** by BLAST searching against the National Center for Biotechnology Information database

Mouse AOX: 111 ccacttcctgacacagctaagttgcttgtctttacctccaggctttcgccggttgccctgg 170

AJ2#10 : 2732 ccacttcctgacacagctaagttgcttgtctttacctccaggctttcgccggttgccctgg 2791

Mouse AOX: 171 acttcaatcatggtggctgaccttccctttcttgctttgcttctcctcaaagagataata 230

AJ2#10 : 2792 acttcaatcatggtggctgaccttccctttcttgcttgccttgcttctcctcaaagagataata 2851

Mouse AOX: 231 gagacaatgaccagtctttcctcataga-tcaagtatggggagagccctcagctatggta 289

AJ2#10 : 2852 gagacaatgaccagtctttcctcatagactcaagtatggggagagccctcagctatggta 2911

Mouse AOX: 290 ttcct--gtatfff-ggtgacctatftaagtaaatftcctgggacaatccagatttgaaa 346

AJ2#10 : 2912 ttcgtagtaatfttaggtgaccttgttaagtaaat--cctgggacaatccagatttgaa- 2969

Mouse AOX: 347 gattct-gtcttcttgngtcataaactattaaatgcttggtggtcaccaaagtatttg 405

AJ2#10 : 2970 gactatcgtcttgttgtgtgcataaactattaaatgcttggtcgctaacaaagtatttg 3029

Mouse AOX: 406 acataaaaaataaataaataaatcattcaggccaccttttacaccagaaatcacaggaaag 465

AJ2#10 : 3030 acataaaaaataaataaataaatcattcaggccaccttttacaccaggaatcacaggaaag 3089

Mouse AOX: 466 ccctgggccccagccatctgctgagtggttagtngagaagatggatcctaagccagctgaa 525

AJ2#10 : 3090 ccctgggccccagccatctgctgagtggttagttgagaagatggatcctaagccagctgaa 3149

Mouse AOX: 526 gactgagtgaggtgtg-ggggaggttcttgct-gagtagctggctttg-tggtaagctg 582

AJ2#10 : 3150 gaatgagtgaggtgtg-gggggaggttcttgctggagtagctggctttgttgtaagctg 3209

Mouse AOX: 583 ctagcagccttacagnggtggcgaagcag 611

AJ2#10 : 3210 -tagcagccttacag-ggtggcgaagcag 3236

B 62.3: Summary of sequence alignment of cDNA subclone **AJ2#10** with **mouse AOX**

FluoroDD gel AJ (AP6 + ARP14)					Subclone I.D.	Sequencing				
Fragment no.	PPARα (+/+)		PPARα (-/-)			FluoroDD fragment size (bp)	Size of insert after <i>Eco</i> RI cut (bp)	Primer	Gene homology to Blast search (Transcript size)	E-value (% Identity)
	CTL	Wy	CTL	Wy						
AJ2	+	++	+	+	1100	AJ2#10	1130	M13 forward (-20)	<i>Mus musculus</i> peroxisomal acyl-coA oxidase (AOX) (3778 bp)	0 481/509 (94%)

Appendix B. DNA sequences and sequencing alignments of FluoroDD fragments

B 63.1: DNA sequence of cDNA subclone AJ2#10 (AP6 & ARP14) using M13 reverse primer

1	AATAGAATAC	TCAAGCTATG	CATCAAGCTT	GGTACCGAGC	TCGGATCCAC	TAGTAACGGC	
61	CGCCAGTGTG	CTGGANTTCG	CCCTTGTAAT	<u>ACGACTCACT</u>	<u>ATAGGGCTTT</u>	<u>TTTTTTTTTC</u>	AP6
121	<u>CAGTCATTTA</u>	AATTTATTGG	CTATTTTCCA	GAATATGAAT	TACTGTCAAA	TAGAAACCCC	
181	ACAGGTGACA	TGCTGCTTAC	TGTCAATCTT	CAGGGATTAT	CAGTCATTCC	AGGAGAAAGG	
241	TTAAGACTGT	GTCAGCAAAT	CTGATGGCTT	TGACTTGATG	TCATTTCCAC	TCCATTAATA	
301	CTGTGTTCTC	AGAACTGCTC	TGAAAGAACT	GTTCTCACGA	TGCCAATGCC	ACAGACACAG	
361	ACTTAATAGG	TCACAATGAT	CTCTCTCACT	GTGCTTTTAA	GAACAAAGAG	TTCCAAC TAG	
421	CCAGGCATGT	CAGCGCAAAC	CTGTAACCCC	AGCATCTGGG	AGGCTGAGGA	TCAGANGTCA	
481	AGGCCACTCT	GGGCCCTGTC	TCAAGAAAAA	AAAATCACTA	CATAGAAAAA	AGCATACACA	
541	CACATACCAC	AANNNNNTCC	ATACTCTANC	TTTANNGTCA	GAATGATTGT	AGAGGCTGCT	
601	CTGCATCCNA	AGGGGGGCTG	CTCCCCCACC	CTGNTANNGG	CTGCNTAGCC	AGCNTNANCC	
661	ACAAAAGCCC	NAGCCNTACC	TCAGNCNNAN	GAANN CNNNN	CCCCCACA A	GCCCC	

B 63.2: Sequencing alignment of cDNA subclone **AJ2#10** with **peroxisomal acyl-coA oxidase (AOX)** by BLAST searching against the National Center for Biotechnology Information database

Mouse AOX:	122	agtcattttaaat	tatttggtat	tttt-ccagaat	atgaattact	gtcaaata	gaaacccc	180
AJ2#10	:	3744	agtcattttaaat	tatttggtat	ttttccagaat	atgacttact	gtcaaata	3685
Mouse AOX:	181	acaggtgacat	gctgcttact	gtcaatctt	cagggattat	cagtc----	attccaggaga	236
AJ2#10	:	3684	acaggtgacat	gctgcttact	gtcaatctt	cagggattat	cagacctt	3625
Mouse AOX:	237	aaggttaagact	-gtgtcagc	aaatctgat	ggctttgact	tgat--gtc	atttcactcc	293
AJ2#10	:	3624	aaggttaagact	tgtgtcagc	aaatctgat	ggctttgact	tgaatagt	3565
Mouse AOX:	294	attaatact	gtgttctc	agaactgct	ctgaaaga	actgttct	cacgatgcca	353
AJ2#10	:	3564	attaatact	gtgttctc	agaactgct	ctgaaaga	actgttct	3505
Mouse AOX:	354	gacacagact	ttaataggt	cacaatgat	ctctctact	gtgctttta	aagaacaa	413
AJ2#10	:	3504	gacacagact	ttaataggt	cacaatgat	ctctct-act	gtgctttta	3446
Mouse AOX:	414	caactagcc	aggcatgt	cagcgcaa	acctgtaac	cccagcat	ctgggagg	473
AJ2#10	:	3445	cgactagcc	aggcatgt	cagcgcaa	acctgtaac	cccagcat	3386
Mouse AOX:	474	gangtcaag	gccca-ct	ctgggccc	ctgtctcaag			505
AJ2#10	:	3385	gaggtcaag	gcccaact	ctgggccc	ctgtctcaag		3353

B 63.3: Summary of sequence alignment of cDNA subclone AJ2#10 with mouse AOX

FluoroDD gel AJ (AP6 + ARP14)					Subclone I.D.	Sequencing			
Fragment no.	PPARα (+/+)		PPARα (-/-)			Size of insert after <i>EcoRI</i> cut (bp)	Primer	Gene homology to Blast search (Transcript size)	E-value (% Identity)
	CTL	Wy	CTL	Wy					
AJ2	+	++	+	+	1100	AJ2#10	1130	M13 reverse	<i>Mus musculus</i> peroxisomal acyl-coA oxidase (AOX) (3778 bp) e-170 376/393 (95%)

Appendix B. DNA sequences and sequencing alignments of FluoroDD fragments

B 64.1: DNA sequence of cDNA subclone AJ9#1 (AP6 & ARP14) using M13 forward (-20) primer

1 CCCACNNTAA TNNAGANNGG AGTANNNGGC GCCTCTANAN NNNCNTNNGC TNCNGCANNC
61 GGNCNGCCCA GTGTGATGGA TATNCGNNNN NAATTNCACC CTGATAATAA CACCTNN**ACT** **AP6**
121 ATAGGGCTTT TTTTTTTTTC CCTACTTAAA AAGGAATTAA GTTTATTCTT TCACAGTTAT
181 ACCCACAGAT ACAGTTATGA GCTCATACAT TACAGGGAAT TTTGTTCCAT TTTACAGGG
241 TACACATCCA GTAAAACCAG CTTCCAGATC AGGAACTAGC CTTACGAACA TCTCTGCCGT
301 TACCCACAG CATCCTTTTG CTTTGCTGAT ACCCAGCACT TCTTCACACC AGAGTAGTTA
361 GGTTCGATTA GTCTTTGACT GTTGCTGACC TTTCTACAAA TGGAGTCATG GATCCTGTGT
421 GAAATTGNNA TCCGCTAAGG GCGAATTCCA GCACACTGGC GGCCGTACT AGTGGATCCG
481 AGCTCGGTAC CAAGCTTGAT GCATAGCTTG AGTATTCTAT AGTGTCACCT AAATAGCTTG
541 GCGTAATCAT GGTCATAGCT GTTTACTGTG TGAAATTGTT ATCCGCTCAC CATTCCACAC
601 AATATTACGA GCCGGGAAGC ATAAAGTGTA AAGCCTGGGG GTGCCTAATG AGTGAGGCTA
661 ANTCACATTT AATTGCGTTT GCGCCTCAAN TGGCCCCGCT TNCNAGTTNG GGNANACCTT
721 GTNNNGTGCC ANNCTNNNNA TNNTNTGANN TNNNGGNAA CCGCCNCCGG GGNANANGCN
781 NGNTTNNNNN NTANTNNGGG CGCTTTTTC GCTTTTTTTG CATTNNTGN ANNTTCCTTG
841 NNNCTNNGNT TTTTNGGNN TGNNGNNNAN CNNNTNTTG GTTTNNTN NNNNGNNNT
901 NTTGNNNAT

B 64.2: Sequencing alignment of cDNA subclone AJ9#1 with **mouse catalase** by BLAST searching against the National Center for Biotechnology Information database

AJ9#1 : 444 aattccagcacactggcgccggttactagtggatccgagctcggtagccaagcttgatgca 503
Mouse catalase: 31 aattccagcacactggcgccggttactagtggatccgagctcggtagccaagcttgatgca 90
AJ9#1 : 504 tagcttgagtattctatagtgtcacctaaatagcttggcgtaatcatggcatagctgtt 563
Mouse catalase: 91 tagcttgagtattctatagtgtcacctaaatagcttggcgtaatcatggcatagctgtt 150
AJ9#1 : 564 tactgtgtgaaattgttatccgctcaccattccacacaatattacgagccgggaagcata 623
Mouse catalase: 151 tcctgtgtgaaattgttatccgctcacaattccacacaaca-tacgagcc-ggaagcata 208
AJ9#1 : 624 aagtgtaaagcctgggggtgcctaataatgagtga 655
Mouse catalase: 209 aagtgtaaagcct-ggggtgcctaataatgagtga 239

B 64.3: Summary of sequence alignment of cDNA subclone AJ9#1 with mouse catalase

FluoroDD gel AJ (AP6 + ARP14)					Subclone I.D.	Sequencing				
Fragment no.	PPARα (+/+)		PPARα (-/-)			FluoroDD fragment size (bp)	Size of insert after <i>Eco</i> RI cut (bp)	Primer	Gene homology to Blast search (Transcript size)	E-value (% Identity)
	CTL	Wy	CTL	Wy						
AJ9	+	-	+	+	320	AJ9#1	360	M13 forward (-20)	if84h05.x1 Kaestner ngn3 - - subtracted <i>Mus musculus</i> cDNA 3'similar to SW:CATA_CAMJE Q59296 CATALASE (280 bp)	1e-93 206/212 (97%)

Appendix B. DNA sequences and sequencing alignments of FluoroDD fragments

B 65.1: DNA sequence of cDNA subclone AJ9#1 (AP6 & ARP14) using M13 reverse primer

1 CNCANNTTAN GGTGNNCNCT ATANGAATAC TACAAGNCTA TGCATCAAGC NTTGGTANCN
61 GNACATCGGC ATNCNATCAN TCACAGGCCG CCAANTGTGC NTGGCAATNC GCCCTTCACG
121 GCAN**ACAATT TCACACAGGA TCCATGACTC** CATTTGTAGA AAGGTCAGCA ACAGTCAAAG **ARP14**
181 ACTAATGCAA CCTAACTACT CTGGTGTGAA GAAGTGCTGG GTATCAGCAA AGCAAAAGGA
241 TGCTGTGGGG TAACGGCAGA GATGTTTCGTA AGGCTAGTTN CCTGATCTGG AAGCTGGTTT
301 TACTGGATGT GTACCCTGTG AAAATGGAAC AAAATTC CCTTGTATG AGCTCATAAC
361 TGTATCTGTG GGTATAACTG TGAAAGAATA AACTTAATTC CTTTTTAAGA GGAAAAAAA
421 AAAAGCCCTA TAGTGAGTGT ATTACAAGGG CGAATNNTGC AGATATNCAT CACACTGGCG
481 GCCGNTCGAG CATGCTTNTA GAGGGCCCAA TTAGCCCTAT AGTGAGTNTA TNACATTNCT
541 GCGTCGTTT TNNNGTCTGN TGGGAANCCT GGNGTNNNT NNTNTTGACC TCCCTNNNT
601 GGNTNNTCAN AGCGNNTNNT NNTGNCCNNA TGNNTNGNC NNGTNNNCTN NNNNGGTNTG
661 GTNTNNTNNN NNNNNNNNTT

B 65.2: Sequencing alignment of cDNA subclone AJ9#1 with **mouse suppressor of actin mutations (SAC1 gene)** by BLAST searching against the National Center for Biotechnology Information database

AJ9#1 : 444 acaagggcggaatnntgcagatatncatcacactggcgccgntcgagcatgcttntagag 503
Mouse SAC: 88 acaagggcggaattctgcagatatccatcacactggcgccgctcgagcatgcatctagag 29
AJ9#1 : 504 ggcccaattagccctatagtgagt 527
Mouse SAC: 28 ggcccaattcgccctatagtgagt 5

B 65.3: Summary of sequence alignment of cDNA subclone AJ9#1 with mouse SAC1

FluoroDD gel AJ (AP6 + ARP14)					Subclone I.D.	Sequencing				
Fragment no.	PPARα (+/+)		PPARα (-/-)			FluoroDD fragment size (bp)	Size of insert after <i>Eco</i> RI cut (bp)	Primer	Gene homology to Blast search (Transcript size)	E-value (% Identity)
	CTL	Wy	CTL	Wy						
AJ9	+	-	+	+	320	AJ9#1	360	M13 reverse	<i>Mus musculus</i> suppressor of actin mutations (SAC1 gene) (2029 bp)	2e-24 77/84 (91%)

Appendix B. DNA sequences and sequencing alignments of FluoroDD fragments

B 66.1: DNA sequence of cDNA subclone AL2#8 (AP7 & ARP15) using M13 forward (-20) primer

1 CCTCACTATA GGGCGAATTG GGCCCTCTAG ATGCATGCTC GAGCGGCCGC CAGTGTGATG
61 GATATCTGCA GAATTCGCCC TTGTAAT**ACG ACTCACTATA** **GGGCTTTTTT** **TTTTTCGAGT** **AP7***
121 CATTGATTTT CTTTTTATTT AAAGGTCAAG CCATGGTCTC TGCAGCAGAT GGAGACACTG
181 AGCGTGAGAT TTGGTCCATT TATTATTTCT GTCTGTCCAT CTGTCCGCGT GTTTTCCAGT
241 ACGCAGACTG CAATCCCACA GACGCTTTTC CTCCAAGCTC CCTTGGGCTG GTATCTCAGG
301 AAATAGCGCT GATCCACGGA ATGGAACGTT ACAGAGCACA TGACTCCGCT GTGAAATGAC
361 ACTACACTCA GTCCTTCATT CCACCGTGAG AGGTTAAGGT TTCTAATTTT ATATGGGGTA
421 GAAAGTCCTG TGTGAAATNG TTATCCGCTA AGGGCGAATN CCAGCACACT GGCGGCCGTT
481 ACTAGTGGAT CCGAGCTCGG TACCAAGCTT GATGCATAGC TTGAGTATTC TATAGTGTCA
541 CCTAAATAGC TTGGCGTAAT CATGGTCATA GCTGTTTNCT GTGTGANNTN GTNATCCGCT
601 CACAANNCCA CACAACATAC GAGCCNGANG CATAANNTGT AAAGCCTGGG NNGCCTANTG
661 AGTGAGCTAA CTCACATTAA TTGCGTNGCN CNCACTGNCC GCCTTTCAGT NNGNACACCT
721 GTCGTGCAGC TGCATNAATG AATNGCCAAC GCNCGNGGAA GGCGGGTTGC GTTTNGGNNC
781 NNTCCGNNNT CNCTAATGAN NNNGGCCNNG NTNTG

B 66.2: Sequencing alignment of cDNA subclone AL2#8 with **mouse hydroxysteroid (17-beta) dehydrogenase 11 (Hsd17β11)** by BLAST searching against the National Center for Biotechnology Information database

AL2#8 : 116 cgagtcattgatttttccttttattttaaaaggtcaagccatggtctctgcagcagatggaga 175
Mouse Hsd17b11: 1685 cgagtcattgatttttccttttattttaaaaggtcaagccatggtctctgcagcagatggaga 1626
AL2#8 : 176 cactgagcgtgagatttgggtccattttatttttctgtctgtccatctgtccgctgtttt 235
Mouse Hsd17b11: 1625 cactgagcgtgagatttgggtccattttatttttctgtctgtccatctgtccgctgtttt 1566
AL2#8 : 236 ccagtacgcagactgcaatccacagacgcttttccctccaagctcccttgggctggtatc 295
Mouse Hsd17b11: 1565 ccagtacgcagactgcaatccacagacgcttttccctccaagctcccttgggctggtatc 1506
AL2#8 : 296 tcaggaaatagcgctgatccacggaatggaacgttacagagcacatgactccgctgtgaa 355
Mouse Hsd17b11: 1505 tcaggaaatagcgctgatccacggaatggaacgttacagagcacatgactccgctgtgaa 1446
AL2#8 : 356 atgacactacactcagtccttcattccaccgtgagaggttaaggtttctaattttatatg 415
Mouse Hsd17b11: 1445 atgacactacactcagtccttcattccaccgtgagaggttaaggtttctaattttatatg 1386
AL2#8 : 416 gggtagaa 423
Mouse Hsd17b11: 1385 gggtagaa 1378

B 66.3: Summary of sequence alignment of cDNA subclone AL2#8 with mouse HSD17β11

FluoroDD gel AL (AP7 + ARP15)					Subclone I.D.	Sequencing				
Fragment no.	PPARα (+/+)		PPARα (-/-)			Size of insert after <i>Eco</i> RI cut (bp)	Primer	Gene homology to Blast search (Transcript size)	E-value (% Identity)	
	CTL	Wy	CTL	Wy						
AL2	+	++	+	+	350	AL2#8	390	M13 forward (-20)	<i>Mus musculus</i> hydroxysteroid (17-beta) dehydrogenase 11 (HSD17β11) (1713 bp)	e-171 308/308 (100%)

* Sequence of primer was not completely matched with the expected sequence.

Appendix B. DNA sequences and sequencing alignments of FluoroDD fragments

B 67.1: DNA sequence of cDNA subclone AL3#3 (AP7& ARP15) using M13 forward (-20) primer

1 ANCNTCACTA TACGGGCAAT CGGGCCCTNC TAGATGCTGC TCGAGACGGC CGCCAGTGTG
61 ATGGATATCT GCAGAAATTCG CCCTTAGCGG **ATAACAATTT CACACAGGAC TTTCTACCCC** ARP15
121 ATATAAAATT AGAAACCTTA ACCTCTCACG GTGGAATGAA GGACTGAGTG TAGTGTCAAT
181 TCACAGCGGA GTCATGTGCT CTGTAACGTT NCCATTCCGT GGATCAGCGC TATTTCTCTGA
241 GATACCAGCC CAAGGGAGCT TGGAGGAAAA GCGTCTGTGG GATTGCAGTC TGCGTACTGG
301 AAAACACGCG GACAGATGGA CAGACAGAAA TAATAAATGG ACCAAATCTC ACGCTCAGTG
361 TCTCCATCTG CTGCAGAGAC CATGGCTTGA CCTTTAAATA AAAGGAAAAT CAATGACTCG
421 AAAAAAAAAA AGCCCTATAG TGAGTCGTAT TACAAGGGCG AATNNCCAGC ACACCTGGCG
481 GCCGTTACTA TTGGATCCGA GCTCGGTACC AAGCTTGATG CATAACCTNN GAGTATNCTA
541 TNNTGTNACC TAAATAGCTT GCGTAATCN NTGGTCATAG CCTGTTNTNC TGTNGTGAAA
601 ATTNGTNACC NNCNCTCNC AATTTTACAC NNCNACNNT ANCNANCNNC GGAAANNCAT
661 AAAANNTGTA NACCNCNTG GGGGTGCCNT NNTGNAANN AGNCTANCTC ANNTTTAATT
721 GGCTTTGCC CTANTGCC GCCTTTACAT TTTNGGGANN ACTTGTNCTT NCCATCTGCT
781 TTTAATTAAA TTCGGCENNA CCCCCGGGN ANAGGNCNT NNNTT

B 67.2: Sequencing alignment of cDNA subclone AL3#3 with **mouse hydroxysteroid (17-beta) dehydrogenase 11 (Hsd17β11)** by BLAST searching against the National Center for Biotechnology Information database

AL3#3 : 114 ctaccccatataaaattagaaaccttaacctctcacggtggaatgaaggactgagtgtag 173
Mouse Hsd17b11: 1380 ctaccccatataaaattagaaaccttaacctctcacggtggaatgaaggactgagtgtag 1439
AL3#3 : 174 tgtcattttcacagcggagtcagtgtgctctgtaacggttccattccgtggatcagcgctat 233
Mouse Hsd17b11: 1440 tgtcattttcacagcggagtcagtgtgctctgtaacggttccattccgtggatcagcgctat 1498
AL3#3 : 234 ttcctgagataccagcccaaggagcttggaggaaaagcgctctgtgggattgcagctctgc 293
Mouse Hsd17b11: 1499 ttcctgagataccagcccaaggagcttggaggaaaagcgctctgtgggattgcagctctgc 1558
AL3#3 : 294 gtactggaaaacacgcggacagatggacagacagaaataataaatggaccaaattctcacg 353
Mouse Hsd17b11: 1559 gtactggaaaacacgcggacagatggacagacagaaataataaatggaccaaattctcacg 1618
AL3#3 : 354 ctcagtgtctccatctgctgcagagaccatggcttgacctttaataaaaaggaaaatcaa 413
Mouse Hsd17b11: 1619 ctcagtgtctccatctgctgcagagaccatggcttgacctttaataaaaaggaaaatcaa 1678
AL3#3 : 414 tgactcg 420
Mouse Hsd17b11: 1679 tgactcg 1685

B 67.3: Summary of sequence alignment of cDNA subclone AL3#3 with mouse HSD17β11

FluoroDD gel AL (AP7 + ARP15)					Subclone I.D.	Sequencing			
Fragment no.	PPARα (+/+)		PPARα (-/-)			Size of insert after <i>EcoRI</i> cut (bp)	Primer	Gene homology to Blast search (Transcript size)	E-value (% Identity)
	CTL	Wy	CTL	Wy					
AL3	+	++	+	+	345	AL3#3	380	<i>Mus musculus</i> hydroxysteroid (17-beta) dehydrogenase 11 (HSD17β11) (1713 bp)	e-166 306/307 (99%)

Appendix B. DNA sequences and sequencing alignments of FluoroDD fragments

B 68.1: DNA sequence of cDNA subclone AL3#3 (AP7& ARP15) using M13 reverse primer

1 GNCNTATTTA NGTGACACTA TAGAATACTC NAGACTATGC NTCAAGCTTG GTACCGAGAC
61 TCGGATCCAC TAGTAACGGC CGCCAGTGTG CTGGAATTCG CCCTTGTAAT **ACGACTCACT** AP7
121 **ATAGGGCTTT TTTTTTTTTC** GAGTCATTGA TTTTCCTTTT ATTTAAAGGT CAAGCCATGG
181 TCTCTGCAGC AGATGGAGAC ACTGAGCGTG AGATTGGGTC CATTATTAT TTCTGTCTGT
241 NCATCTGTCC GCGTGTTTTC CAGTACGCAG ACTGCAATCC CACAGACGCT TTTCTCCAA
301 GCTCCCTTGG GCTGGTATCT CAGGAAATAG CGCTGATCCA CGGAATGGAA CGTTACAGAG
361 CACATGACTC CGCTGTGAAA TGACACTACA CTCAGTCCTT CATTCCACCC GTGAGAGGTT
421 AAAGGTTTCT AATNTTTATA TGGGGTANAA AAGTCCTGTG TGAAATTGTT ATCCGCTAAN
481 GGGCCGAATT CTGCAAATAT CNATCACACT NGGNGGNNGN TNNANCNTGN NNTNTTANAG
541 GGNNTNNNC TATNNTNANT NTANNNTNTG GGCNTCNNNN ATNTNTNTGN AAACCTNNNT
601 NNNTATNNNN NTNNNTNNN NTNTNNNNNG NNTNNNNNT NNNNNN

B 68.2: Sequencing alignment of cDNA subclone AL3#3 with **mouse hydroxysteroid (17-beta) dehydrogenase 11 (Hsd17β11)** by BLAST searching against the National Center for Biotechnology Information database

AL3#3 : 140 cgagtcattgatttttccttttattttaaaaggtcaagccatggtctctgcagcagatggaga 199
Mouse Hsd17b11: 1685 cgagtcattgatttttccttttattttaaaaggtcaagccatggtctctgcagcagatggaga 1626
AL3#3 : 200 cactgagcgtgagatttggtccatttattatttctgtctgtncatctgtccgcgtgtttt 259
Mouse Hsd17b11: 1625 cactgagcgtgagatttggtccatttattatttctgtctgtccatctgtccgcgtgtttt 1566
AL3#3 : 260 ccagtacgcagactgcaatcccacagacgcttttcctccaagctcccttgggctggtatc 319
Mouse Hsd17b11: 1565 ccagtacgcagactgcaatcccacagacgcttttcctccaagctcccttgggctggtatc 1506
AL3#3 : 320 tcaggaaatagcgctgatccacggaatggaacggttacagagcacatgactccgctgtgaa 379
Mouse Hsd17b11: 1505 tcaggaaatagcgctgatccacggaatggaacggttacagagcacatgactccgctgtgaa 1446
AL3#3 : 380 atgacactacactcagtccttcattccaccgtgagaggttaaagggtttctaanttttat 439
Mouse Hsd17b11: 1445 atgacactacactcagtccttcattccacc-gtgagaggttaa-gggtttctaant-tttat 1389
AL3#3 : 440 atggggta 447
Mouse Hsd17b11: 1388 atggggta 1381

B 68.3: Summary of sequence alignment of cDNA subclone AL3#3 with mouse HSD17β11

FluoroDD gel AL (AP7 + ARP15)					Subclone I.D.	Sequencing				
Fragment no.	PPARα (+/+)		PPARα (-/-)			FluoroDD fragment size (bp)	Size of insert after <i>Eco</i> RI cut (bp)	Primer	Gene homology to Blast search (Transcript size)	E-value (% Identity)
	CTL	Wy	CTL	Wy						
AL3	+	++	+	+	345	AL3#3	380	M13 reverse	<i>Mus musculus</i> hydroxysteroid (17-beta) dehydrogenase 11 (HSD17β11) (1713 bp)	e-155 304/308 (98%)

Appendix B. DNA sequences and sequencing alignments of FluoroDD fragments

B 69.1: DNA sequence of cDNA subclone AO1#2 (AP5 & ARP10) using M13 forward (-20) primer

1 CCNCNCACNT ATANGGCAAT TGGGCCCTCT AGATGCATGC TCGAGACGGC CGCCAGTGTG

61 ATGGATATCT GCAGAATTCG CCCTTAGCGG **ATAACAATTT CACACAGGAG ATCTCAGACT** ARP10

121 ACATGCCAGA CTGTCTTGGT CAACGCCCAA GGGTTACCAC AGAACATTCA AGATCAGGCC

181 AGACACTTGG GGGTGATGGC AGGCGACATC TACTCCGTAT TCCGCAATGC TGCCTCCTTT

241 AAGGAAGTGT CCGATGGCGT CCTCACATCT AGCAAGGGGC AGCTGCAGAA AATGAAGGAA

301 TCCTTAGATG AAGTTATGGA TTACTTTGTT AACAAACNACG CCCCTCAACT GGCTGGTAGG

361 TCCCTTTTAT CCTCAGTCTA CCGAGGTGAA CAAGGCCAGC CNTGAAGGTC CCAGCAGTCT

421 GAGGTCNAAN GCTCAGTANA CCCCTCCCTT GTCACCAGAG CATGATGTTG CTGGCCCAGA

481 TGACCCCTT TTGCTGCATT GAAATNAACT TGGTAGATGG CTTTAGCTTA GAAAAGCAGC

541 TTNTNNAGAN CCCAGGGCCT CATTATGGTC CCTCACCGCT CAGTTATGGT CTTGCCCCAG

601 CTGNNCCTGG CACANGAGTT TCTTACCCTG GCTNGTGAGT GGCCTGTGTN AGTTTNNNTGA

661 NGANCTGNAN GAACCTATAC GCTNGATGCN CTTAAGTTTN GTNTGTNGCC TTTGTTTTGT

721 NNTGGGNTGT ACAGTTTGTC TGGANNGANT AAGATNCTTT NNNNGNNAAA AAAAAGNNCT

781 NTNNTNNNTN TTTTTCGGGG GGGANTTCAC ANNNNGNNN

B 69.2: Sequencing alignment of cDNA subclone **AO1#2** with **mouse adipose differentiation related protein (ADFP)** by BLAST searching against the National Center for Biotechnology Information database

AO1#2 : 115 cagactacatgccagactgtcctgggtcaacgcccagggttaccacagaacattcaagat 174

Mouse ADFP: 1036 cagactacatgccagactgtcctgggtcaacgcccagggttaccacagaacattcaagat 1095

AO1#2 : 175 caggccagacacttgggggtgatggcaggcgacatctactccgtattccgcaatgctgcc 234

Mouse ADFP: 1096 caggccaaacacttgggggtgatggcaggcgacatctactccgtattccgcaatgctgcc 1155

AO1#2 : 235 tcctttaaggaagtgtccgatggcgctcctcacatctagcaaggggcagctgcagaaaatg 294

Mouse ADFP: 1156 tcctttaaggaagtgtccgatggcgctcctcacatctagcaaggggcagctgcagaaaatg 1215

AO1#2 : 295 aaggaatccttagatgaagttatggattactttgttaacaacnacgcccctcaactggct 354

Mouse ADFP: 1216 aaggaatccttagatgaagttatggattactttgttaacaac-acgcctctcaactggct 1274

AO1#2 : 355 ggtaggtcccttttatcctcagtctaccgaggtgaacaaggccagccntgaaggtcccag 414

Mouse ADFP: 1275 ggtaggtcccttttatcctcagtctaccgaggtgaacaaggccagcc-tgaaggt-ccag 1332

AO1#2 : 415 cagtctgaggtcnaangctcagtanaccctcccttgtcaccagagcatgatgttgctgg 474

Mouse ADFP: 1333 cagtctgaggtc-aaagctcagtaaacctcccttgtcaccagagcatgatgttgctgg 1390

AO1#2 : 475 cccagatgaccccttttgctgcattgaaatnaacttggtagatggctttagcttagaaa 534

Mouse ADFP: 1391 -ccagatga-ccccttttgctgtattgaaattaacttggtagatggctttagcttagaaa 1448

AO1#2 : 535 agcagcttntnnagancccagggcctcattatgggtccctcaccgctcagttatggctctg 594

Mouse ADFP: 1449 agcagcttct-tagaaccaagggcctcattatgggtcactcacagctcagttatggctctg 1507

AO1#2 : 595 ccccagctgnnccctggcacangagtt-tcttaccctggctngtgagtggcctgtgtngt 653

Mouse ADFP: 1508 ccccagctggccctggcacaggagttctctta-cctggctgggtgagtggcctgtgttagt 1566

AO1#2 : 654 ttnntganganctgnangaaccta 677

Mouse ADFP: 1567 cttgtgaggacctggaggaaccta 1590

B 69.3: Summary of sequence alignment of cDNA subclone AO1#2 with mouse ADFP

FluoroDD gel AO (AP5 + ARP10)					Subclone I.D.	Sequencing				
Fragment no.	PPARα (+/+)		PPARα (-/-)			FluoroDD fragment size (bp)	Size of insert after <i>EcoRI</i> cut (bp)	Primer	Gene homology to Blast search (Transcript size)	E-value (% Identity)
	CTL	Wy	CTL	Wy						
AO1	+	++	+	+	700	AO1#2	720	M13 forward (-20)	Mouse adipose differentiation related protein (ADFP) (1680 bp)	0 530/564 (93%)

Appendix B. DNA sequences and sequencing alignments of FluoroDD fragments

B 70.1: DNA sequence of cDNA subclone AO1#5 (AP5 & ARP10) using M13 reverse primer

1 ACCC>NNNTAG TAGNATACAC ATATAANATC ATCAGACATG TNACATCAGA CTGNGNNANN
61 CCAGACTNGA ATNACCNAGN NNAACGGNCC GCNNGTGTGC TGGAAATNCN CCCTTAGACG
121 GANTAA**ACAAT** **TTCACACAAG** **GAGATCTCAG** **ACAANAANNG** ANNNATAGAA AACCTTG GTA ARP10
181 ACNAAGAGTA GGATGGTGAT GTGAACNTGG AAGGAATGTT GACCTTAAAG GAAGACCTGT
241 TAATGTAGGG TTAGGAGAGT GATGACTCTA CTAGAGTTAT TACTAACNCT TAAAGTCTNN
301 CTGTGTTNNA AACCANCAAT GNCAAAGTCA GATATAGTGA ATAGAAACTA TGNCAATGTT
361 TAAGACCNTC AANAAAGCAA ATCTATATAT CTTAANCAAT CCTACTTAAC AAGNCCTCAA
421 TCAAAGNCAA ATCCTACTCT GATGTTAAAA TAGTTTTGTT GGCACATGTG TAGGCTGCAA
481 GTCCTCTGTG AANCATGATT ATAGAGTCTA TTTCTCAANG CACTTTAATA CTTTCTAATT
541 GCCAGAGGGA TAAAGCACAC GGTTAGAAGC TAATNTCTCT GACCNTCAGT GCCTTCCACA
601 CCCAGCACAG GAGTACAGCC TGTGAGAGTN ATGGGNNACC ACTATTGTAC CATAGTGATC
661 TAAATAGCT CCTTTGAGCC ANGCCNNMNG ATCCAGTTGT ATANNAAATT NTTACCCCCC
721 CCCNNANNAG AATTTTNCAN NCTTNNTATG ATTGTTGAAT NATTTGTGAA TTAAATAAGA
781 TNCNTTGAAA AAAANAAGC

B 70.2: Sequencing alignment of cDNA subclone **AO1#5** with **mouse carnitine O-octanoyltransferase (Crot)** by BLAST searching against the National Center for Biotechnology Information database

AO1#5 : 184 aagagtaggatggtgatgtgaacntggaaggaatggtgaccttaaaggaagacctgttaa 243
Mouse Crot: 2052 aagagtaggatggtgatgtga-catggaaggaatggtgac-ttaaaggaag-cctgttaa 2108
AO1#5 : 244 tgtagggttaggagagtgatgactctactagagttattactaacncttaaagtctnnctg 303
Mouse Crot: 2109 tgtagggttaggagagtgatg-ctct-ctagagttatt-cta--ccttaaagtctc-ctg 2162
AO1#5 : 304 tgttnnaaacancaatgncaaagtcagatatagtgaatagaaactatgncaatgtttaa 363
Mouse Crot: 2163 tgttgcaa-cca-caatg-caaagtcagatatagtgaatag-aactatg-caatgtttaa 2217
AO1#5 : 364 gacctcaanaaagcaaacttatatatcttaancaatcctacttaacaagnctcaatca 423
Mouse Crot: 2218 g--cctcaacaaagcaaacttatatatcttaa-caatcctacttaacaag-cctcaatca 2273
AO1#5 : 424 aagncaaactcctactctgatgttaaaatagttttgttggtggacatgtgtaggctgcaagtc 483
Mouse Crot: 2274 aag-caaactcctactctgatgttaaaatagttttgttggtggacatgtgtaggctgcaagtc 2332
AO1#5 : 484 ctctgtgaancatgattatagagtcctatttctcaangcactttaatactttctaattgcc 543
Mouse Crot: 2333 ctctgtgaa-catgattatagagtcctatttctcaa-gcactttaatactttctaattgcc 2390
AO1#5 : 544 agagggataaagcacacggttagaagctaanttctctgacctcagtccttccacaccc 603
Mouse Crot: 2391 agagggataaagcacacggttagaagctaanttctctga-catcagtcgcttccacaccc 2449
AO1#5 : 604 agcacaggagtacagcctgtgagag-tnatggg-nnaccactattgtaccatagtgatct 661
Mouse Crot: 2450 agcacaggagtacagcctgtgagagttcatgggaaaaccactattgtacaatagtgatct 2509
AO1#5 : 662 aaaatagctccttttgagc 679
Mouse Crot: 2510 aaaatagctccttttgagc 2527

B 70.3: Summary of sequence alignment of cDNA subclone AO1#5 with mouse Crot

FluoroDD gel AO (AP5 + ARP10)					Subclone I.D.	Sequencing				
Fragment no.	PPARα (+/+)		PPARα (-/-)			FluoroDD fragment size (bp)	Size of insert after <i>Eco</i> RI cut (bp)	Primer	Gene homology to Blast search (Transcript size)	E-value (% Identity)
	CTL	Wy	CTL	Wy						
AO1	+	++	+	+	700	AO1#5	720	M13 reverse	<i>Mus musculus</i> carnitine O-octanoyltransferase (Crot) (2804 bp)	e-152 461/498 (92%)

Appendix B. DNA sequences and sequencing alignments of FluoroDD fragments

B 71.1: DNA sequence of cDNA subclone AO2#6 (AP5 & ARP10) using M13 forward (-20) primer

1 ACCNNCACTA TACGGGCNAA TNTGGGCCCT CTAGATGCNT GCTCGAGACG GCCGCCAGTG
61 TGATGGATAT CTGCAGAATT CGCCCTTAGC GGATA**ACAAT TTCACACAGG AGATCTCAGA** ARP10
121 **CAAAAATCCA** ACTGGACAGG CTACTCACAA AAGGTGTTAC CCACTTCGTT ATATATACTN
181 CCCTGTCNAT CCCAAAATGT CATCATTAGG GAAGCCACTA AGAGTTTGGA AATAGGGGCT
241 GGAGAGATGC CTCTGTGGTT AAGAGCATTG GCTGCTCCTC TAGAGGACCC AGGTTCAATT
301 CCCCAGTGCC CACACATCAG CTCACAACCTG TCTGTAACCC AGTTCTAGGT GATTTTGATAC
361 CCTCACACAG ACATACATGT AGACAGATCC ACCAATACAT ATAAAATTAA AATAAAGATT
421 TTGGAAATAA CATATTGCCA AAATGAGAAT TACTTGGTAT TATTTTGGTC TGTGGCTTCT
481 AAGATTTTTT AAAATACATG AAAAATGTAG TAAATCACTA AAATTCATTT ATCTTTCTTT
541 GAAAGANNTC AATATTTTAG TATAATAAAG AGCTGTATGT NGAGCCATCT GTGTCGGGAT
601 TTGTGNNTCC TGCTCTTTTT CAGTNCCTCT CTAGTCTATG AACTCTCATG TNCCTTAGTG
661 TCCCTATACC TTCTGGTCNA ATACAAATGC CCATNANATC CATCATGTGA AAAAAAAAAA
721 GCCNTATAGT GAGGTNTTAT NACNAGGNCC NAATCCAGCC ACNCTGGGCG GNNGTNAATA
781 NNTGNATCCN ANCTCGGTA CCANGCTTGA NNCNNTNNNT

B 71.2: Sequencing alignment of cDNA subclone **AO2#6** with **mouse RNase A family 4 (Rnase4)** by BLAST searching against the National Center for Biotechnology Information database

AO2#6 : 111 agatctcagacaaaaatccaactggacaggctactcacaaaaggtgttaccacttcgtt 170
Mouse Rnase4: 944 agatctcagacaaaaatccaactggacaggctactcacaaaaggtgttaccacttcgtt 1003
AO2#6 : 171 atatatactnccctgtcnatcccaaatgtcatcattagggagccactaagagtttggga 230
Mouse Rnase4: 1004 atatatactttc-tgt-tattccaaatgtcatcattagggagccactaagagtttggga 1061
AO2#6 : 231 aataggggctggagagatgcctctgtggttaagagcattggctgctcctctagaggaccc 290
Mouse Rnase4: 1062 aataggggctggagagatgcctctgtggttaagagcattggctgctcctctagaggaccc 1121
AO2#6 : 291 aggttcaattccccagtgcccacacatcagctcacaaactgtctgtaacccagttctaggt 350
Mouse Rnase4: 1122 aggttcaattccc-agtgcccacacatcagctcacaaactgtctgtaacccagttctaggt 1180
AO2#6 : 351 gatttgataccctcacacagacatacatgtagacagatccaccaatacatataaaattaa 410
Mouse Rnase4: 1181 gatttgataccctcacacagacatacatgtagacagatc-accaatgcatataaaattaa 1239
AO2#6 : 411 aataaagattttggaaataacatattgccaaaatgagaattacttggattatttttggtc 470
Mouse Rnase4: 1240 aataaagattttggaaataacatattgccaaaatgagaattacttggattatttttggtc 1299
AO2#6 : 471 tgtggcttctaagattttttaaaatacatgaaaaatgtagtaaactactaaaattcattt 530
Mouse Rnase4: 1300 tgtggcttctaagattttttaaaatacatgaaaaatgtagtaaactactaaaattcattt 1359
AO2#6 : 531 atctttctttgaaaga-nntcaatattttagtataataaagagctgtatgt 580
Mouse Rnase4: 1360 atccttctttgaaagattttcaatattttagtataataaagagctgtatgt 1410

B 71.3: Summary of sequence alignment of cDNA subclone AO2#6 with mouse Rnase4

FluoroDD gel AO (AP5 + ARP10)					Subclone I.D.	Sequencing				
Fragment no.	PPARα (+/+)		PPARα (-/-)			Size of insert after <i>Eco</i> RI cut (bp)	Primer	Gene homology to Blast search (Transcript size)	E-value (% Identity)	
	CTL	Wy	CTL	Wy						
AO2	+	++	+	+	695	AO2#6	760	M13 forward (-20)	<i>Mus musculus</i> ribonuclease, RNase A family 4 (Rnase4) (1412 bp)	0 458/471 (97%)

Appendix B. DNA sequences and sequencing alignments of FluoroDD fragments

B 72.1: DNA sequence of cDNA subclone AO2#6 (AP5 & ARP10) using M13 reverse primer

1 AGCTATTTAG GTGACACTAT AGAATACTCA AGCTATGCAT CAAGCTTGGT ACCGAGCTCG
61 GATCCACTAG TAACGGCCGC CAGTGTGCTG GAATTCGCCC TTGTAAT**ACG ACTCACTATA** AP5
121 **GGGCTTTTTT TTTTTTCACA** TGATGGATCT AATGGCCATT TGTATTTGAC CAGAATGTAT
181 AGGGACACTA AGGGACATGA GAGTTCATAG ACTAGAGAGG AACTGAAAAA GAGCAGGAGA
241 ACACAAATCC CGACACAGAT GGCTCAACAT ACAGCTCTTT ATTATACTAA AATATTGAAA
301 ATCTTTCAAA GAAAGATAAA TGAATTTTAG TGATTTACTA CATTTTTTCAT GTATTTTAAA
361 AAATCTTAGA AGCCACAGAC CAAAATAATA CCAAGTAATT CTCATTTTGG CAATATGTTA
421 TTTCCAAAT CTTTATTTTA ATTTTATATG TATTGGTGAT CTGTCTACAT GTATGTCTGT
481 GTGAGGGTAT CAAATCACCT AGAACTGGGT TACAGACAGT TGTGAGCTGA TGTGTGGGCA
541 CTGGGAATTG AACCTGGGTC CTCTAGANGA GCAGCCCATG CTCTTAANCA CACNCGCATC
601 TCTCCAGCCC CTATTNNCAA ACTCTTAGTG GCTTCCCTAA TGATGACANT TNTGGAATAA
661 CAGANNGTAT ATATAACGAN NTGGNTAACA CCTTNGTGA GTAGCCTGTN CAGTTGGANT
721 NNTTGTNTGA NANCCTCNTG TGTGAACNTT GTNATCCCC TAAGNGGCAA NNTNTTGNCA
781 GATTTCNTT

B 72.2: Sequencing alignment of cDNA subclone AO2#6 with **mouse RNase A family 4 (Rnase4)** by BLAST searching against the National Center for Biotechnology Information database

AO2#6 : 265 caacatacacgctctttattatactaaaatattgaaaatctttcaaagaagataaatgaa 324
Mouse Rnase4: 1412 caacatacacgctctttattatactaaaatattgaaaatctttcaaagaaggataaatgaa 1353
AO2#6 : 325 ttttagtgatttactacatTTTTcatgtattttaaaaaatcttagaagccacagacaaaa 384
Mouse Rnase4: 1352 ttttagtgatttactacatTTTTcatgtattttaaaaaatcttagaagccacagacaaaa 1293
AO2#6 : 385 ataataccaagtaattctcatTTTggcaatatgttatttccaaaatctttattttaattt 444
Mouse Rnase4: 1292 ataataccaagtaattctcatTTTggcaatatgttatttccaaaatctttattttaattt 1233
AO2#6 : 445 tatatgtattggtgatctgtctacatgtatgtctgtgtgaggggatcaaatacctagaa 504
Mouse Rnase4: 1232 tatatgcattggtgatctgtctacatgtatgtctgtgtgaggggatcaaatacctagaa 1173
AO2#6 : 505 ctgggttacagacagttgtgagctgatgtgtgggcactgggaattgaacctgggtcctct 564
Mouse Rnase4: 1172 ctgggttacagacagttgtgagctgatgtgtgggcactgggaattgaacctgggtcctct 1113
AO2#6 : 565 agangagcagcccatgctcttaancacacnccatctctccagcccctattnncaaactc 624
Mouse Rnase4: 1112 agaggagcagccaatgctcttaaccacagaggcatctctccagcccctatttccaaactc 1053
AO2#6 : 625 ttagtggttccctaataatgatgacantntggaataacaganngtatatataacganntgg 684
Mouse Rnase4: 1052 ttagtggttccctaataatgatgaca-ttttggaataacagaaagtatatataacgaagtgg 994
AO2#6 : 685 ntaacacctttngtgagtagcctgtncagttgga 718
Mouse Rnase4: 993 gtaacaccttttgtagtagcctgtccagttgga 960

B 72.3: Summary of sequence alignment of cDNA subclone AO2#6 with mouse Rnase4

FluoroDD gel AO (AP5 + ARP10)						Sequencing				
Fragment no.	PPARα (+/+)		PPARα (-/-)		FluoroDD fragment size (bp)	Subclone I.D.	Size of insert after <i>Eco</i> RI cut (bp)	Primer	Gene homology to Blast search (Transcript size)	E-value (% Identity)
	CTL	Wy	CTL	Wy						
AO2	+	++	+	+	695	AO2#6	760	M13 reverse	<i>Mus musculus</i> ribonuclease, RNase A family 4 (Rnase4) (1412 bp)	0 435/454 (95%)

Appendix B. DNA sequences and sequencing alignments of FluoroDD fragments

B 73.1: DNA sequence of cDNA subclone **AO2#8** (AP5 & ARP10) using **M13 reverse primer**

1 AGNCNTATTT AGGTGACACT ATAGAATACN NAGACNATGN CTNCNAGNCT TGGTACCNAG
61 ACNNGGATCA CCTAGTAACG GCCGCCAGTG TGCTGGAATT CGCCCTTGTA AT**ACGACTCA** AP5
121 **CTATAGGGCT** **TTTTTTTTTT** **TCAAATGGAA** ATGCTTTAAT TTTATATTCA CAAAATGAAT
181 TGCAACATAT CATAATGAAT TTTGCTAATA TTCTTTTCTG TGGTAGTGTA AAAATTTCTA
241 ATACAACCTG ATCCTTTTGC CTGCTCAAAG GAGCTATTTT AGATCACTAT TGTACAATAG
301 TGGTTTTTCCC ATGAACTCTC ACAGGCTGTA CTCCTGTGCT GGGTGTGGAC TTTTCTGAA
361 CCCTTCCATC TTCCTTCTGT CTCTAGGACT CTCTCATCAA CATAATGTGC AATGTTCACC
421 ATGACCATTG CATCGTAAGG AGCATGATCA CAGCAACAGC CAAATATCCC ATTAGCAAAG
481 GAAATCAAAT TATAGGACTT GTCACCCAG CGTACTGATG GATCTCCACC AAGAAGCATT
541 TCAAAGACCT GAGAATATCC TNCTGGGGTN GCATGTGGAC TGCTATCTTC TATGGAATAC
601 ACAAATAAAC TGGTTNGAAT TTTNTCTAAT AAAGTTAAGT TCTCTGGATC NAGANCTAAT
661 CAGATATNCT CTNGCCCTTN GNCNNCCGA GTCCGCTNCC CCCCTAGTNA NNGCNGCTAT
721 ACTGGCTCCA ACAGNTCNGT CCGACCCNNC CTGCTGCATT NTNTAACTNG NNGCACCTCN
781 GCTCTNAAAT GTTATCNNTA NNNNCNAAAT NTGNNANNTC NATNNNNNNG G

B 73.2: Sequencing alignment of cDNA subclone **AO2#8** with **mouse carnitine O-octanoyltransferase (Crot)** by BLAST searching against the National Center for Biotechnology Information database

AO2#8 : 347 ggactttttctgaacccttccatcttccttctgtctctaggactctctcatcaacataat 406
Mouse Crot: 1253 ggactttttctgaacccttccatcttccttctgtctctaggactctctcatcaacataat 1194
AO2#8 : 407 gtgcaatgttcaccatgaccattgcatcgtaaggagcatgatcacagcaacagccaaata 466
Mouse Crot: 1193 gtgcaatgttcaccatgaccattgcatcgtaaggagcatgatcacagcaacagccaaata 1134
AO2#8 : 467 tccattagcaaaggaaatcaaattataggacttgtcaccccagcgtactgatggatctc 526
Mouse Crot: 1133 ttccattagcaaaggaaatcaaattataggacttgtcaccccagcgtactgatggatctc 1074
AO2#8 : 527 caccaagaagcatttcaaagacctgagaatatcctnctggggtngeatgtggactgctat 586
Mouse Crot: 1073 caccaagaagcatttcaaagacctgagaatatcctnctggggtngeatgtggactgctat 1014
AO2#8 : 587 cttctatggaatacacaaataaaactggttngaattttntctaataaagttaagttctctg 646
Mouse Crot: 1013 cttctatggaatacacaaataaaactggttngaattttntctaataaagttaagttctctg 954
AO2#8 : 647 gatcnaganctaatacagatatnctctngcc 676
Mouse Crot: 953 gatcaaga-ctaatacagatatnctctngcc 925

B 73.3: Summary of sequence alignment of cDNA subclone **AO2#8** with **mouse Crot**

FluoroDD gel AO (AP5 + ARP10)					Subclone I.D.	Sequencing				
Fragment no.	PPARα (+/+)		PPARα (-/-)			FluoroDD fragment size (bp)	Size of insert after <i>Eco</i> RI cut (bp)	Primer	Gene homology to Blast search (Transcript size)	E-value (% Identity)
	CTL	Wy	CTL	Wy						
AO2	+	++	+	+	695	AO2#8	740	M13 reverse	<i>Mus musculus</i> carnitine O-octanoyltransferase (Crot) (2804 bp)	e-160 319/330 (96%)

Appendix B. DNA sequences and sequencing alignments of FluoroDD fragments

B 74.1: DNA sequence of cDNA subclone AO8#2 (AP5 & ARP10) using M13 forward (-20) primer

```

1 TCANNATAGG GGCNAATTGG GCCCTNCTAG ATGCNTGCTC GAGACGGCCG CCAGTGTGAT
61 GGATATCTGC AGAATTTCGCC CTTAGNCGGA TAACAATTTT ACACAGGAGA TCTCAGACAA ARP10
121 AAATCCAACCT GGACAGGCTA CTCACAAAAG GTGTNACCCA CTTCGTTATA TATACTTTCT
181 GTTATCNCAA AATGTCATCA TTAGGGAAGC CACTAAAGAG TNTGGGAAAT AGGGGGCTGG
241 AGAGATGCCT CTGTGGTTAA GAGCATNGNN NTGCTCCTCT AGAGNNCCCA GGTTCANNTC
301 CCAGTGCCCA CACATCAGCT CACAACCTGTC TGTAACCCAG TTCTAGGTGA TTTGATACCC
361 TCACACAGNA CATACATGTA AAAAGATCAC CAATNNATAT AAAATTANAA TAAAGATTTT
421 GGGAAATGAA AAAAAAAGC CCCTATAGTG AGNTCNTATN NCAAGGGGCG ANANNCCAGC
481 CACACTGGGC GGGCCGTTTA CTANGTGGGA TTCCGAGCCT CGGGTACCCA ACCNNGATGC
541 CATAGCCTNG AGTAANNCTA TAGTGTAACC TAAATAGCTN GGCGTANTCA TGGTNATANA
601 AGNNAAANAT NCCCNCAAG GANNNCCGCC TCACAAATTC CCAACANNAC AATACCGAAN
661 CCNGGGANNN CACNTAAAG NNGTNAAG GCCCNNGGG GNTGNCCTNA ANNTGGANNN
721 TGAGNCCNCA ACCNCACACA NNTTAATTTG NNGTNGCNC CCTACANTGN NCNNNNTTTC
781 CAAGTNNNGN ANCCCTGTNN TGCCCANCTG NNTNATTGAT TCGGCCACGC CCGGGANNGG
841 NNGTTGGNNN TGGNNCCTTT TCGCCTNNNC CCTANTGACT NNNNGCCTG GGTGTGGG

```

B 74.2: Sequencing alignment of cDNA subclone AO8#2 with **mouse RNase A family 4 (Rnase4)** by BLAST searching against the National Center for Biotechnology Information database

```

AO8#2      : 108 agatctcagacaaaaatccaactggacaggctactcacaaaaggtgtnacccacttcgtt 167
Mouse Rnase 4: 944 agatctcagacaaaaatccaactggacaggctactcacaaaaggtgttaccacttcgtt 1003
AO8#2      : 168 atatatactttctgttatcncaaatgtcatcattaggaagccactaaagagtntggga 227
Mouse Rnase 4: 1004 atatatactttctgttatcccaaatgtcatcattaggaagccact-aagagttt-gga 1061
AO8#2      : 228 aataggggctggagagatgcctctgtggttaagagcatngnnntgctcctctagagnnc 287
Mouse Rnase 4: 1062 aata-ggggctggagagatgcctctgtggttaagagcatg-gctgctcctctagaggac 1119
AO8#2      : 288 ccaggttcannntcccagtgccacacatcagctcacaactgtctgtaacccagttctagg 347
Mouse Rnase 4: 1120 ccaggttcaattcccagtgccacacatcagctcacaactgtctgtaacccagttctagg 1179
AO8#2      : 348 tgatttgataccctcacacagnacatacatgtaaaaagatcaccaatnnatataaaatta 407
Mouse Rnase 4: 1180 tgatttgataccctcacacag-acatacatgtagacagatcaccaatgcatataaaatta 1238
AO8#2      : 408 naataaagattttgg 422
Mouse Rnase 4: 1239 aaataaagattttgg 1253

```

B 74.3: Summary of sequence alignment of cDNA subclone AO8#2 with **mouse Rnase4**

FluoroDD gel AO (AP5 + ARP10)					Subclone I.D.	Sequencing				
Fragment no.	PPARα (+/+)		PPARα (-/-)			Size of insert after <i>EcoRI</i> cut (bp)	Primer	Gene homology to Blast search (Transcript size)	E-value (% Identity)	
	CTL	Wy	CTL	Wy						
AO8	+	-	+	+	400	AO8#2	400	M13 forward (-20)	<i>Mus musculus</i> ribonuclease, RNase A family 4 (Rnase4) (1412 bp)	e-121 294/315 (93%)

Appendix B. DNA sequences and sequencing alignments of FluoroDD fragments

B 75.1: DNA sequence of cDNA subclone **AP4#4** (AP12 & ARP2) using **M13 forward (-20)** primer

1 CCNCCTATAC GGATCGCGCN NACATCGTCG CCANNNGCCC ANTGTATNAT TTNANAATCC
61 CCTGTAATAC **GACTCACTAT AGGGCTTTTT TTTTTTCTA** ATANCCTCTC TAGGTNCAGG **AP12**
121 GTGTACGTAT ATATCTTATC CACATCCNNA TNCATAAATC AAGTCGACAC CGCTTATCTG
181 TAAGGTGGCT CTATTTCTCT TGTCTTCNC NNTACNCGGG ACANNACTCN NTCAACATAC
241 ATACAACNCC GACCTGCCAT CGCTCCGGTC TGAANCTCAC ATCCACCCTN ACGACTTTAA
301 TCGTTGAACA AACAAACCAT TAATACCCTT CTACACCATT GGGATGTCCT GATCCAACCA
361 TCGAGGTNNT AAACCCTAAT TGTNATATGA ANCTCTTAAA TAGGATCGCG CTGTNATNCT
421 ANGGTANNTN GGTCGTGATC ATTTNGGGTN TANATTGTNA TNNNTGTNT NGTNTNTNNN
481 GATTNGTNT NTNNNNNNNN

B 75.2: Sequencing alignment of cDNA subclone **AP4#4** with **mouse mitochondrion** by BLAST searching against the National Center for Biotechnology Information database

AP4#4 : 293 gactttaatcggtgaacaaacaaaccattaatacccttctacaccattgggatgtcctga 352
Mouse mitochondrion: 2498 gactttaatcggtgaacaaacgaaccattaatagc-ttctacaccattgggatgtcctga 2440
AP4#4 : 353 tccaaccatcgaggtntaaaccctaattgt-natatgaanctcttaaataggatcgcg 411
Mouse mitochondrion: 2439 tccaa-catcgaggtcgtaaaccctaattgtcgatatgaa-ctcttaaataggattgcgc 2382
AP4#4 : 412 tgt 414
Mouse mitochondrion: 2381 tgt 2379

B 75.3: Summary of sequence alignment of cDNA subclone **AP4#4** with **mouse mitochondrion**

FluoroDD gel AP (AP12 + ARP2)					Subclone I.D.	Sequencing				
Fragment no.	PPARα (+/+)		PPARα (-/-)			FluoroDD fragment size (bp)	Size of insert after <i>Eco</i> RI cut (bp)	Primer	Gene homology to Blast search (Transcript size)	E-value (% Identity)
	CTL	Wy	CTL	Wy						
AP4	+	++	+	+	680	AP4#4	720	M13 forward (-20)	<i>Mus musculus</i> clone LA9 mitochondrion, complete genome (16300 bp) 7e-30 113/123 (91%)	

* Sequence of primer was not completely matched with the expected sequence.

Appendix B. DNA sequences and sequencing alignments of FluoroDD fragments

B 76.1: DNA sequence of cDNA subclone AP4#4 (AP12 & ARP2) using M13 reverse primer

1 CNNNTATTTA GGTGACACTA TAGAATACTA CAAGACTATN NATNCAAGAC TTGGTACCGA
61 GACTACGGAT CCACTAGTAA CGGCCGCCAG TGTGCTGGAA TTNCGCCCTT AGACGGATAA ARP2
121 CAATTT**CACA** CAGGAGCTAG CATGGACGGC TAAACGAGGG TCCAAC**TGTC** TACTTATCTA
181 TAATCAGTGA AATTGACCTT TNCAGTGAAG AGGCTGAAAT ATAATAATAA GACGAGAAGA
241 CCCTATGGAG CTTAAATTAT ATAAC**TTATC** TATTTAATNT ATAAACCTA ATGGCCCAAA
301 GACTATAGTA TAAGTTTGAA ATTTNGGTTG GGGTGACCTC GAGAATAAAA AATCNTCAGA
361 ATGATTATAA CTAATACACN NNNTNATCCT NTNTATGANA TTTTNATNNA NTCTGNATGC
421 CTTTNCANNT ANANTNNANT NNNNTNNNNN NNNNNANAA AAAAAAAAAAN NNNNNGNANN
481 NNNNNANANA ANAACAAANA AAAAAAAAAA NNCAAACAA AAAAAANAA CANANAACNC
541 ACNNAAAANN AAAAAACA CAA

B 76.2: Sequencing alignment of cDNA subclone **AP4#4** with **mouse mitochondrion** by BLAST searching against the National Center for Biotechnology Information database

AP4#4 : 141 catggacggcctaaacgaggggtccaactgtctacttatctataatcagtgaaattgacctt 200
Mouse mitochondrion: 2065 catgaacggcctaaacgaggggtccaactgtct-cttatctttaatcagtgaaattgacctt 2123
AP4#4 : 201 tncagtgaagagggctgaaatataataataagacgagaagaccctatggagcttaaattat 260
Mouse mitochondrion: 2124 t-cagtgaagagggctgaaatataataataagacgagaagaccctatggagcttaaattat 2182
AP4#4 : 261 ataacttatctattttaatntataaaacctaataggcccaaagactatagtataagtttgaa 320
Mouse mitochondrion: 2183 ataacttatctattttaatttattaaacctaataggcccaaaaactatagtataagtttgaa 2242
AP4#4 : 321 atttnggttgggggtgacctc-gagaataaaaaatcntcagaatgattataac 371
Mouse mitochondrion: 2243 atttcggttgggggtgacctcggagaataaaaaatcctccgaatgattataac 2294

B 76.3: Summary of sequence alignment of cDNA subclone AP4#4 with mouse mitochondrion

FluoroDD gel AP (AP12 + ARP2)					Subclone I.D.	Sequencing				
Fragment no.	PPARα (+/+)		PPARα (-/-)			FluoroDD fragment size (bp)	Size of insert after <i>Eco</i> RI cut (bp)	Primer	Gene homology to Blast search (Transcript size)	E-value (% Identity)
	CTL	Wy	CTL	Wy						
AP4	+	++	+	+	680	AP4#4	720	M13 reverse	<i>Mus musculus</i> clone LA9 mitochondrion, complete genome (16300 bp)	7e-95 221/232 (95%)

CUHK Libraries



004306827